Sustainable Forests & Livelihoods (SUFAL) Project
Forest Department
Ministry of Environment, Forest and Climate Change

Compendium of Forestry Research under the SUFAL Innovation Grant

Volume I

SUFAL

THE WORLD BANK
IBRD • IDA | WORLD BANK GROUP

Sustainable Forests & Livelihoods (SUFAL) Project
Forest Department
Ministry of Environment, Forest and Climate Change

Compendium of Forestry Research under the SUFAL Innovation Grant

Volume I

SUFAL

THE WORLD BANK
IBRD • IDA | WORLD BANK GROUP

This publication is an output from the Sustainable Forests & Livelihoods (SUFAL) Project implemented by Bangladesh Forest Department (BFD) under the Ministry of Environment, Forest and Climate Change.

Published by : Sustainable Forests and Livelihoods (SUFAL) Project

Citation : Bangladesh Forest Department. (2025). Compendium of forestry research under the SUFAL Innovation Grant (Vol. 1). Dhaka, Bangladesh.

Layout, Graphics
and Illustrations : Md. Mehedi Hasan Khan

Design and Printing : Tithy Printing and Packaging

Cover Page Design : Narayan Sarker

Date of Publication : June 2025

Dr. Farhina Ahmed
Secretary
Ministry of Environment, Forest and Climate Change
Government of the People's Republic of Bangladesh

Message

I am pleased to share this volume of research outputs generated under the SUFAL Innovation Grant (SIG) Program, an integral component of the Sustainable Forests and Livelihoods (SUFAL) Project of the Bangladesh Forest Department under Ministry of Environment, Forest and Climate Change. This compilation reflects a significant step forward in our collective efforts to ground forest management and wildlife conservation in robust scientific evidence.

Bangladesh is endowed with a remarkable diversity of flora and fauna, yet this heritage is under mounting pressure from rapid land-use change, habitat fragmentation, climate-induced stresses, and the growing interface between people and wildlife. These complex challenges cannot be addressed through traditional management practices alone. They require interdisciplinary inquiry, empirical data, and context-specific solutions that link ecological integrity with human wellbeing.

The SIG program was conceived precisely with this vision in mind. By offering competitive grants to researchers, universities, and specialized institutions, the program has created space for innovative ideas, rigorous fieldwork, and analytical research on Forestry, wildlife and biodiversity issues.

The findings presented here do not remain confined to academic discussion; they generate clear, actionable recommendations for managers, planners, and policymakers. They provide insights that can inform zoning and management plans, improve conflict mitigation measures, strengthen community participation, and enhance the resilience of forest, wildlife and ecosystems to climate and other anthropogenic pressures.

I wish to acknowledge the dedication of the researchers and their teams, the guidance provided by the various review committees, and the support of partner organizations and development partners who have contributed to the success of the SIG program. Their combined efforts have ensured that the studies uphold scientific rigor while remaining closely aligned with national conservation priorities and international commitments.

It is my expectation that this publication will be used widely by conservation practitioners, government agencies, academia, development partners, and civil society to inform decision-making and to inspire further research and innovation. As we strive to conserve Bangladesh's forest, wildlife, biodiversity and ecosystems for present and future generations, evidence-based knowledge such as that contained in this volume will remain one of our most valuable assets.

Dr. Farhina Ahmed

Md. Amir Hosain Chowdhury
Chief Conservator of Forests
Bangladesh Forest Department

Message

Forests and wildlife in Bangladesh play a vital role in maintaining ecological balance, supporting livelihoods, and contributing to national development. To manage these resources wisely, we need a clear understanding of forest dynamics, species ecology, ecosystem services, and the social context of resource use.

This publication represents significant research on both forestry and wildlife supported by the SUFAL Innovation Grant (SIG) Program of the Sustainable Forests and Livelihoods (SUFAL) Project. The studies compiled here reflect a strong commitment to grounding conservation and forest management in scientific evidence, practical field experience, and the realities faced by forest-dependent communities in Bangladesh.

The research presented in this volume responds to that need. It includes work on forest restoration and productivity, co-management and collaborative forest management, biodiversity assessment, species conservation, human–wildlife interaction, and climate-resilient management practices. Together, these studies demonstrate how well-designed research can guide more sustainable and inclusive management of forests and wildlife.

The importance of this publication lies in its ability to translate research findings into practical guidance. The results offer concrete suggestions for improving forest management plans, enhancing protection and restoration measures, designing and managing Reserved Forests and Protected Areas, and supporting communities that depend on forests and wildlife for their livelihoods. As such, this volume is intended to serve not only researchers and academics but also policymakers, forest managers, conservation practitioners, and development partners.

I hope that the insights and recommendations contained here will be widely used to strengthen evidence-based decision making in the forestry and biodiversity sectors of Bangladesh. This publication will help to formulate our future policies, improve field practices, and inspire further research and innovation. It will make a long lasting contribution to the conservation of our forests, biodiversity and wildlife for present and future generations.

Md. Amir Hosain Chowdhury

Gobinda Roy
Project Director
Sustainable Forests and Livelihoods (SUFAL) Project
Forest Department
Government of the People's Republic of Bangladesh

Foreword

Sustainable Forests and Livelihoods (SUFAL) Project has supported research and innovation through its Innovation Grant Program, designed to strengthen forestry and biodiversity knowledge in Bangladesh. SUFAL Innovation Grant (SIG) is one of the unique features of SUFAL Project guided by the Innovation Grant Manual. This mechanism was designed to promote scientific and applied research on forestry, wildlife, and biodiversity conservation, while also ensuring transparency, accountability, and quality in both the selection and implementation of research initiatives.

Through this competitive process, 34 research grants were awarded to researchers and institutions after rigorous evaluation. Each proposal and subsequent deliverable was carefully reviewed by the Deliverable Review and Comments Committee, the Research Proposal Evaluation Committee, and the Forestry and Wildlife Research Review Council. This multi-tiered scrutiny ensured that the work undertaken met high professional standards and directly addressed the needs and challenges in forestry and wildlife management.

SUFAL Project also organized result dissemination workshops, where researchers shared their findings with policymakers, practitioners, academics, and other stakeholders. These events served not only as a platform for knowledge exchange but also as an opportunity to foster collaboration and dialogue around future research priorities. Following this, the researchers submitted their final reports, marking the successful completion of all 34 studies under the SIG program.

To make these findings widely accessible, SUFAL is now publishing four volumes of research summaries: two focusing on forestry and two on wildlife. These volumes present the essence of the research in a concise and structured manner, allowing stakeholders, decision-makers, and development partners to draw practical lessons and insights. The outcomes documented here will help shape evidence-based policies, strengthen conservation practices, and guide further research and innovation in the forestry and biodiversity sector of Bangladesh.

I would like to extend my sincere gratitude to the dedicated researchers, the review committees, partner institutions, and the World Bank for their valuable support. Their commitment and contributions have made it possible to generate a body of knowledge that will serve the sector for years to come. This publication will not only enrich our understanding but also support Bangladesh for achieving its national priorities and international commitments related to forest, biodiversity and wildlife conservation.

Gobinda Roy

Table of Content

Research Title

Identifying the Factors and Spatial Variability of Carbon Stocks in the Selected Sites of Mangrove Plantations of Bangladesh.

by
Dr. M. Nazrul Islam
Professor, Department of Geography and Environment, Jahangirnagar University, Savar, Dhaka-1342

INTRODUCTION

1.1 Background and Context of the Research

Forests play a vital role in global carbon flux and act as carbon sink by storing large quantities of carbon for a longer period of time (Salunkhe, et. al., 2018). Estimating forest carbon stocks has drawn extensive attention in the field of global climate change. The negative effect of climate change, which is presently unbalancing the environment is visible to all. The world today is facing major challenges by increasing atmospheric CO2 causing global warming (IPCC, 2013). It has been predicted that the average global temperature will increase by 2.42°C by the year 2050 (Anderson and Bows 2011). To limit global average temperature, rise to below 2°C, emissions must be reduced and excess greenhouse gases removed from the atmosphere (Macreadie et. al., 2021). There is growing evidence that the conservation or restoration of carbon ecosystems such as mangroves, saltmarshes, or seagrass meadows offer effective nature-based solutions to climate change impacts (Alongi et al., 2015). The government of Bangladesh has already taken some steps to increase the coastal plantation not only to save the country form multifarious natural hazards but also to make some contribution in world stage by sequestrate carbon in mangroves which have been identified as carbon ecosystems that are natural carbon sinks (Donato et al., 2011; Lovelock et al., 2019; Murray et al., 2011).

High-density carbon that accumulates in oceans and coastal ecosystems as a result of their high productivity and sediment trapping ability. Coastal habitats, predominantly vegetated habitats, such as mangroves, seagrasses and saltmarshes, have a disproportionate capacity to sequester carbon dioxide (CO^2) from the atmosphere and incorporate it into biomass, which ultimately becomes buried as organic matter within the sediments (Strong, et. al., 2021). Mangroves, saltmarshes, etc., are known to be the hotspots of carbon storage, in many instances containing considerably higher amounts of carbon per unit area than terrestrial systems (McLeod et al., 2011; Bauer et al., 2013). Carbon stock in mangrove ecosystem varies with species (Laffoley and Grimsditch 2009), vegetation types (Adame et al. 2013; Cero´n-Breto´n et al. 2011; Mitra et al. 2011; Sapit et al. 2011; Laffoley and Grimsditch 2009) and salinity (Adame et al. 2013). Identifying these factors and understanding the different roles they play in carbon burial is critical to implement management efforts to conserve or restore mangrove forests for climate change mitigation and adaptation or to increase the resilience of mangrove forests to climate change impacts, such as sea level rise (Mackenzie, et. al, 2021). In this context, this research project is designed to figure out the key factors, which are influencing the spatial variability, and which species does accumulate the most carbon stocks and which accumulate the least carbon stocks in the coastal areas of Bangladesh.

Accurate estimation of carbon storage is a major issue which has drawn attention to the researcher (Sun and Liu, 2020). Incomparable data sources and various estimation methods have led to significant differences in the estimation of forest carbon storage at large scales (Sun and Liu, 2020). Countries with advanced technologies also face the issues as they follow different estimation methods. According to Piao, et.al, (2009), forest carbon storage estimation can be mainly three types: inventory, satellite based and process based. Following the research goal, both inventory and satellite-based approaches has been followed as the DBH, mean tree height, forest type, forest age, etc. includes inventory approaches and remotely sensed satellite imagery data implies with latest technology works as satellite-based approach and will produce more accurate result at large scale (Wulder, et. al., 2012; Tang et. al., 2018; Sun and Liu, 2020). In recent past, the application of satellite imagery like Landsat ETM+, Landsat TM data have increased to estimate forest biomass as well as carbon stocks. That's why, this research project is an attempt to integrate the allometric equations with remotely sensed satellite data, to estimate the carbon stocks with large scales; and establish a general approach which will be cost effective and time consuming. Five forest sites have been selected for the requirement of the project and extensive field survey has been conducted in the selected mangorve forest sites of Bangladesh; such as: Haringhata Eco Park (HEP) and Tengragiri Wildlife Sanctuary (TWS) of Barguna, Char Kukri-Mukri Wildlife Sanctuary (CKmWS) of Bhola, Char Kashem (CK) of Patuakhali and Nijhum Dwip National Park (NNP) of Hatiya, Noakhali.

1.2 Project Justification and Management Implications

Bangladesh is among the most vulnerable countries affected by global warming and climate change. Forests play an important role in mitigating global climate change through sequestering atmospheric carbon (Adame et al., 2013). Organisms living in the seas can capture more than half the amount of carbon captured in forested lands. Coastal wetlands, including saltmarshes, mangroves, store more carbon per unit area than terrestrial forests, and represent a globally significant carbon sink (Duarte et. al., 2005; Nellemann and Corcoran, 2009; Mcleod et. al., 2011; Temmink et. al., 2022). Mangroves are particularly efficient sinks, sequestering four times carbon per unit area compared with terrestrial forests in the tropics (Khan et al. 2007; Donato et al. 2011). In addition to their climate change mitigation capacities (via carbon capture and subsequent burial), coastal wetlands provide numerous other ecosystem services and benefits, including fisheries support, coastal flood protection, and biodiversity enhancement (Barbier et al., 2011; Möller et al., 2014; Unsworth et al., 2019).

Globally the assessment of carbon stocks is comparatively new and insufficient number of research works have been done on it. In the recent past, scientists discoursed the increased importance of terrestrial carbon in climate change adaptation and mitigation (e.g. Nellemann and Corcoran, 2009; Sun, et. al., 2022). Due to global warming, carbon sequestration is very crucial, which could be done mostly in the coastal plantation area as coastal mangroves can sequestrate carbon three times greater than any other major forest domain. The coast of Bangladesh is very fertile and have the favorable condition of mangroves, having different species of forest (e.g. Keora, Baen, Gewa), which sequestrating carbons at different levels. As the carbon sequestration/stock assessment procedures are introduced very recently, therefore, very limited attention has been paid on the spatial variation of carbon stocks. Furthermore, different forest contains different species and have the variations to sequestrate/stock different levels of blue carbons, therefore, this research work will give importance on the key factors and spatial variability of carbon stocks in the selected sites of mangrove plantation of Bangladesh.

1.3 Objectives and Research Questions

The key factors which are influencing the carbon stocks along with the spatial variability of species to accumulate the carbon stocks in the selected sites of mangrove plantation of Bangladesh will be the main focus of this research project.

Specific Objectives: The specific objectives of this research are:

1) To identify the key factors of carbon stocks in the selected sites of mangrove plantation of Bangladesh;
2) To estimate carbon stocks (above and below ground) for different species; and
3) To find out the spatial variability of species in accumulating the most and least carbon stocks in the selected sites.

Research Questions: The following research questions will be able to fulfill the project objectives:

1) Which site-specific local and climatic factors drive carbon stock in the mangrove plantation?
2) How do carbon stocks vary among different coastal plantations?
3) What is the amount of carbon accumulated in different mangrove species?

2.0 APPROACHES AND METHODS

2.1 Research Approach

This research adopted a mixed-method approach that combined field surveys with remote sensing analysis and literature review to study carbon stock variability in selected mangrove ecosystems of Bangladesh. The methodology was structured to address both spatial distribution and the key ecological factors influencing carbon stock. Primary data were collected directly from the field through detailed measurements of tree species, including their Diameter at Breast Height (DBH) and tree height. This was done at five different sites: Haringhata Eco Park (HEP), Tengragiri Wildlife Sanctuary (TWS), Char Kukri-Mukri Wildlife Sanctuary (CKmWS), Char Kashem (CK), and Nijhum Dwip National Park (NNP). At the same time, secondary data from scientific literature and satellite imagery supported the broader spatial analysis.

To map and analyze vegetation cover, the study used very high-resolution satellite imagery from Maxar (0.5-meter resolution), which provided detailed visuals of mangrove density and structure. Landsat ETM+ imagery was also used for historical and time-series analysis, aiding in model calibration. GIS-based remote sensing techniques helped estimate carbon stocks and identify spatial patterns in vegetation. Algorithms were applied to determine which species held higher or lower carbon values, and these results were cross-checked through field verification to ensure accuracy.

The research design included both qualitative and quantitative methods. Qualitative analysis involved interpreting existing studies, expert insights, and spatial maps, helping to set the background and support the first objective. Quantitative methods focused on analyzing numerical field data and satellite images, aligning with the study's second and third objectives. This combination provided a well-rounded understanding of how different environmental and spatial factors influence carbon storage in mangrove forests.

Sampling was carried out using a gridded systematic method that ensured representation of all vegetation types and spatial variability. Based on mangrove coverage detected from satellite data, the five sites were divided into 1 km² grids (**Fig. 01**). Estimated mangrove areas included 15.60 km² in HEP, 22.54 km² in TWS, 43.19 km² in CKmWS, 4.71 km² in CK, and 52.11 km² in NNP, summing to 138.15 km² (**Table. 01**). From these, 78 grids were selected, and 312 cluster plots were designed for field sampling.

Each cluster contained four 10 m × 10 m sample plots, laid out systematically within each grid (**Fig. 02**). The first plot was placed in the southwest corner, and the remaining three were distributed across the southeast, northeast, and northwest corners, each 50 meters apart to maintain uniform spacing. Field data were successfully collected from 222 plots. Inaccessible plots, often blocked by flooding or dense growth, were mapped using GPS and pre-survey tools such as Google Earth Pro to maintain the quality of spatial data.

Overall, this integrated approach enabled a reliable assessment of carbon stocks across different sites and species. It provided the basis for analyzing spatial patterns and supported the development of site-specific strategies for carbon conservation in Bangladesh's coastal mangrove forests.

Table 01: Selected grids and expected number of sampling plots at the Study Sites of Bangladesh.

Study Sites	Area (km^2)	Selected Grids (1 km^2)	Sampling Plots (10 m x 10 m)
Haringhata Eco Park (HEP)	15.60	10	40
Tengragiri Wildlife Sanctuary (TWS)	22.54	14	56
Char Kukri-Mukri Wildlife Sanctuary (CKmWS)	43.19	25	100
Char Kashem (CK)	4.71	3	12
Nijhum Dwip National Park (NNP)	52.11	26	104
Total	**138.15**	**78**	**312**

Note: HEP = Haringhata Eco Park, TWS = Tengragiri Wildlife Sanctuary, CKmWS = Char Kukri-Mukri Wildlife Sanctuary, CK = Char Kashem, NNP = Nijhum Dwip National Park, Km² = Square kilometers, m= meters

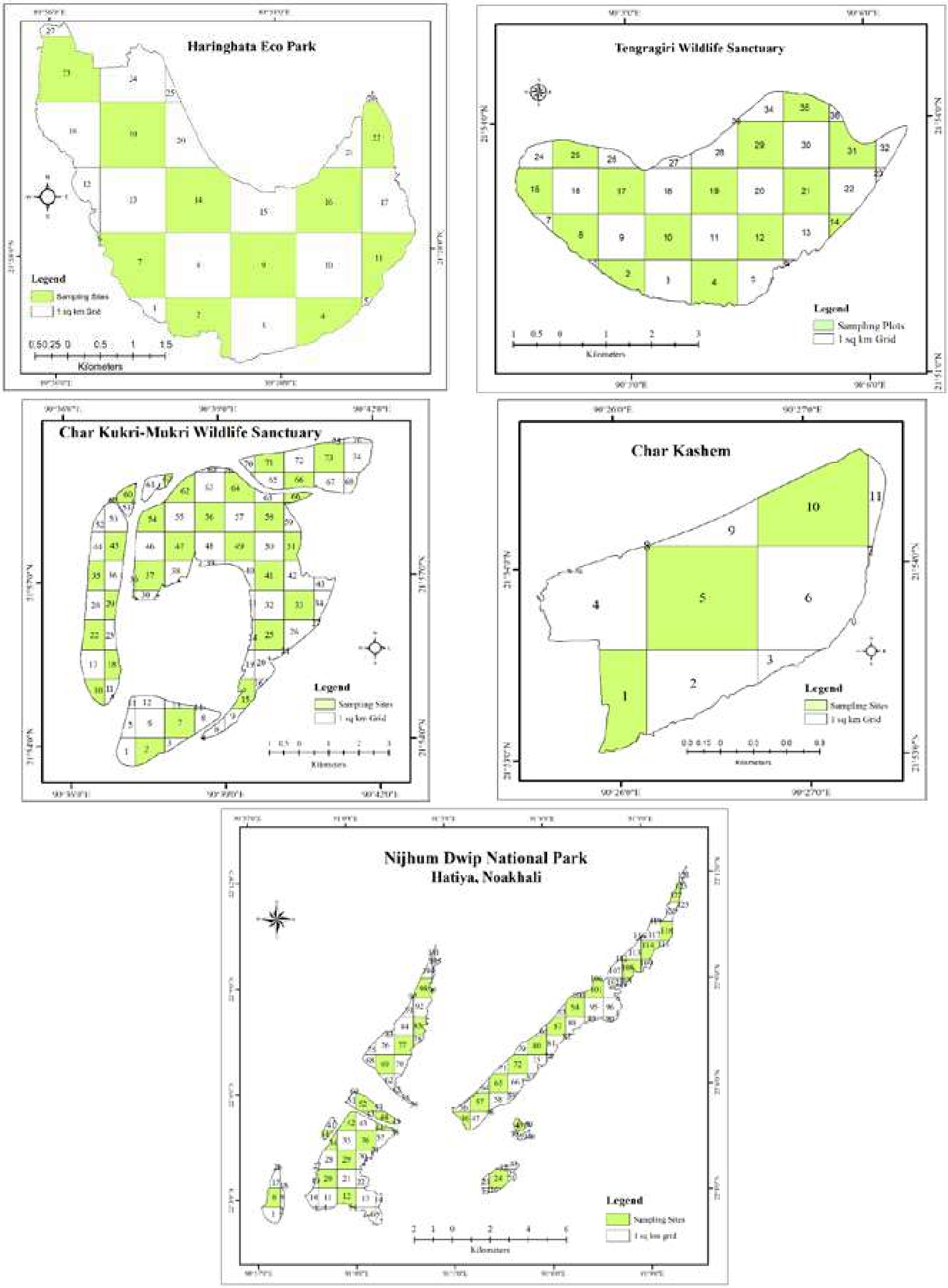

Figure 01: Grids (each grid size: 1 km^2) with accent green color represents the sampling sites of the selected study sites of Bangladesh.

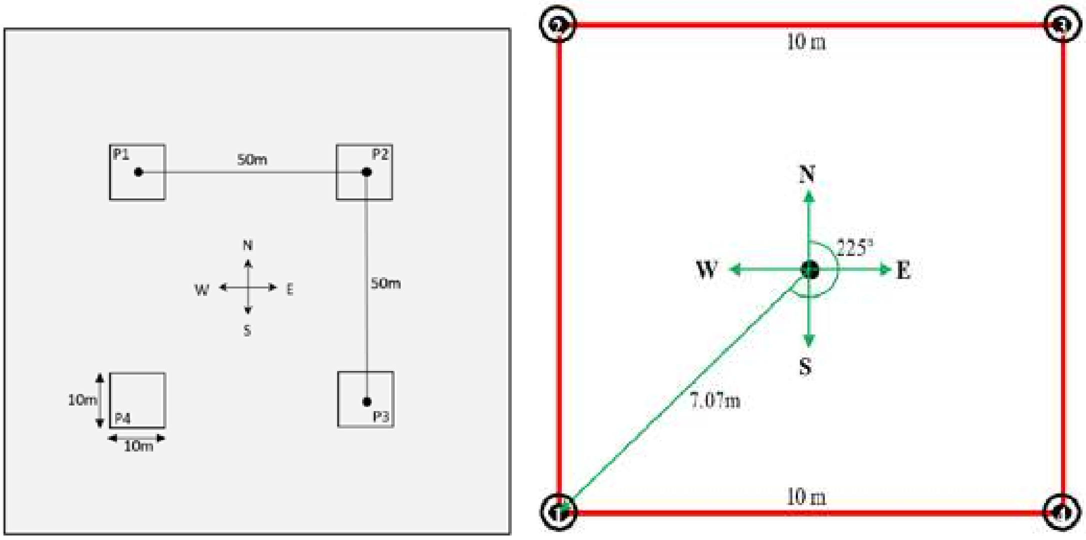

Figure 02: Schematic diagram showing cluster sample plots distributed systematically in a selected grid (1 km^2) (P1 to P4 clockwise plot no.) with a 10 m x 10 m sampling plot in the field.

2.2 Methods

Five coastal mangrove sites in Bangladesh: Haringhata Eco Park (HEP), Tengragiri Wildlife Sanctuary (TWS), Char Kukri Mukri Wildlife Sanctuary (CKmWS), Char Kashem (CK), and Nijhum Dwip National Park (NNP)—were selected for investigation. Each site was divided into 1 km × 1 km grids using georeferenced vegetation maps, and 78 alternate grids were systematically chosen. In each grid, four 10 m × 10 m sample plots were laid out in a cluster with 50 m spacing, resulting in 312 planned plots, of which 222 were accessible. In each plot, vegetation was classified into trees (DBH ≥ 5 cm), saplings, and seedlings. GBH was measured at 1.37 m, converted to DBH, and height was measured using a clinometer. Species were identified in the field with local assistance and verified with floristic keys. Dominant species included *Sonneratia apetala* and *Excoecaria agallocha*. High-resolution Maxar imagery (0.5 m) and Landsat ETM+ supported the delineation of land cover, NDVI mapping, and ground verification of 222 plots. These data were used to drive the InVEST carbon model and assess forest health. All field data were digitized and analyzed using Excel, SPSS, and R. Two-sample t-tests and one-way ANOVA assessed differences in structural variables, and cluster analysis with NMDS was used to examine floristic similarity. GIS processing and mapping were performed using ArcGIS and QGIS. Biomass was estimated using species-specific and generic allometric equations, converting DBH and height data into above- and below-ground biomass, with a carbon fraction of 0.47 applied to estimate carbon stocks per tree and scaled to plot and hectare levels. InVEST model outputs were calibrated against field estimates to understand spatial patterns of carbon storage. Species-specific equations developed for Bangladeshi mangroves (Rahman et al., 2021) were used, along with generic models from Komiyama et al. (2005) for unlisted species. Due to restrictions on destructive sampling in the Sundarbans since 1989, semi-destructive models based on stem volume, wood density, and foliage biomass (Mahmood et al., 2019) were applied, justified by the Sundarbans' ecological similarity to the study sites.

In addition to that, Rahman et al., 2021 has been developed a total of nine species-specific allometric model for *Aglaia cucullata, Avicennia sp., Bruguiera sp., Excoecaria agallocha, Heritiera fomes, Lumnitzera racemosa, Rhizophora sp., Sonneratia apetala, and Xylocarpus sp.* which has been adopted for this research.

Moreover, some species may be identified beyond the selected species during field data collection. In this case, the generic model of south-east Asian mangrove species will be used (Komiyama et. al., 2005).

$$AGB = 0.251 \times WD \times DBH^{2.46}$$

To estimate the carbon stock of the below-ground biomass (BGBC), the equation from Mokany and Yousuf will be used, which mainly depends on the above ground biomass carbon (Mokany et. al., 2006; Kumar & Barik, 2018; and Yusuf, et. al., 2019). The equation is:

$$BGBC = 0.235 \times AGB \text{ if } AGBC > 62.5tC\ ha$$

$$BGBC = 0.205 \times AGB \text{ if } AGBC \leq 62.5tC\ ha \qquad \text{(Yusuf, et. al., 2019)}$$

where, BGBC = belowground biomass carbon, AGB = aboveground biomass (kg)

In the recent past, due to development of digital satellite technology, to estimate the volume and changes of carbon stocks and carbon sequestration, satellite images and remote sensed data are widely used (e.g. Maanan, et. al., 2019; Sun et. al., 2022). Therefore, to verify the reliability and accuracy of the allometric models, a recently practiced InVEST (Integrated Valuation of Ecosystem Services and Tradeoff) model (**Fig. 03**) has been considered for this study, where LULC (Land Use and Land Cover) map and table with carbon values per LULC (which is a table with carbon stock values for each land use line cover class) are two important parameters (Kaur, et. al., 2022; Pijathilake, et. al., 2022; Sun, et. al., 2022). To run the model, the four carbon pools (aboveground biomass, belowground biomass, soil, and dead organic matter) will be taken to estimate (Chan et al. 2006; Eggleston et al. 2006; Nelson et al. 2009; Goldstein et al. 2012; Qiu and Turner 2013; Tao et al. 2015; He et al. 2016; Cabral et al. 2016; Zhang et al. 2017) the amount of carbon currently stored in the landscape or sequestered over time. By using the satellite images, the LULC map has been produced through raster data analysis in ERDAS Imagine and Arc GIS software. The carbon value of per LULC has been collected from the aboveground and belowground biomass carbon density data of the NASA's Earth Observing System Data and Information Systems (EOSDIS). The carbon storage Cm,i,j for a given grid cell (i,j) with LULC type map can be calculated as (after Eggleston et al. 2006; Maanan, et. al., 2019; Tallis et al., 2013):

$$C_{m,i,j} = A \times (AGC_{m,i,j} + BGC_{m,i,j} + SOC_{m,i,j} + DOC_{m,i,j})$$

where, A denotes the area of the cell; $AGC_{m,i,j}$, $BGC_{m,i,j}$, $SOC_{m,i,j}$ and $DOC_{m,i,j}$ are the aboveground carbon density, belowground carbon density, soil organic carbon density and dead organic matter carbon stock for the given cell (x, y) with LULC type map, respectively and at a given time.

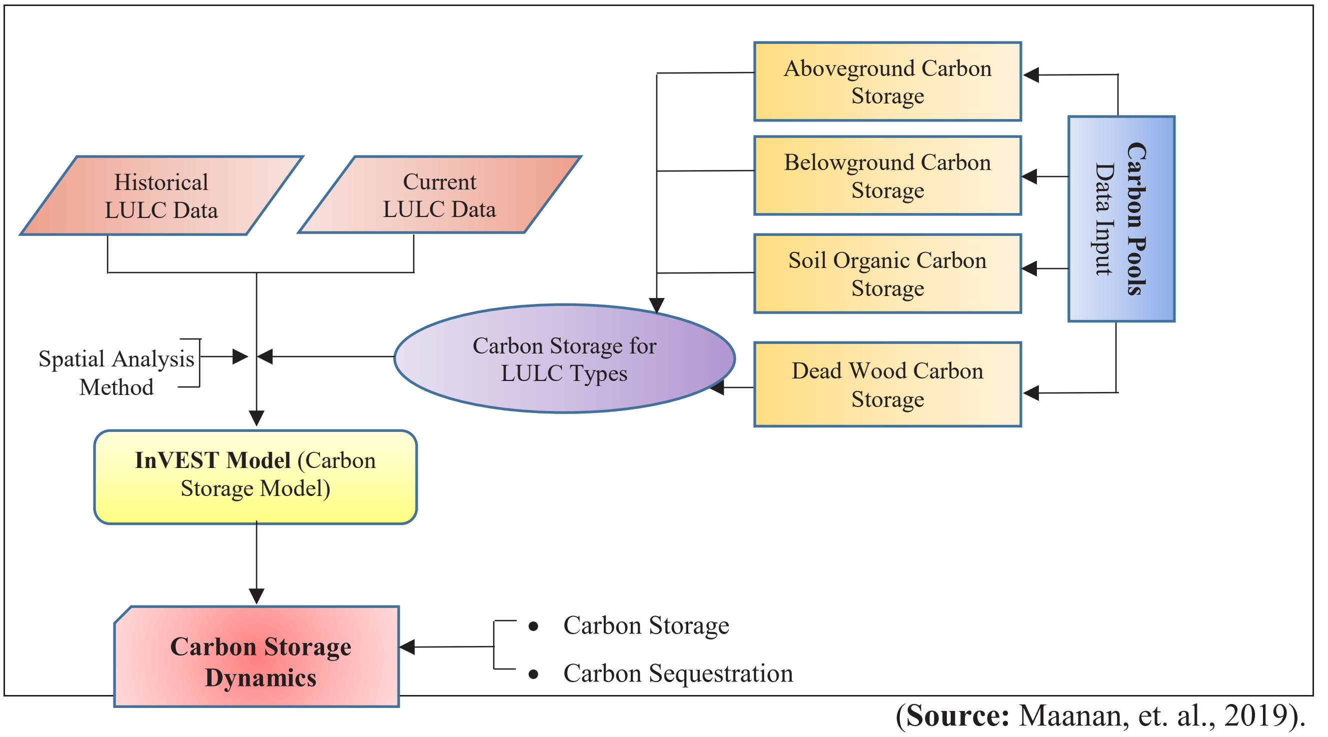

(**Source:** Maanan, et. al., 2019).

Figure. 03: Hierarchical Structure of the InVEST Carbon Storage and Sequestration Model.

2.3 InVEST (Integrated Valuation of Ecosystem Services and Tradeoff) Model

The InVEST (Integrated Valuation of Ecosystem Services and Tradeoffs) model is a spatially explicit tool used to map and quantify ecosystem services, including carbon storage and sequestration, in both biophysical and economic terms. It uses land use/land cover (LULC) data and carbon stock values to estimate carbon stored in aboveground biomass, belowground biomass, soil organic carbon, and dead organic matter. To validate the accuracy of allometric models in this study, the InVEST carbon model was applied using inputs such as classified LULC maps and carbon density tables derived from remote sensing and global datasets (NASA EOSDIS, ESDAC, IPCC). The carbon stock per cell was calculated using:

Cm,i,j = A × (AGCm + BGCm + SOCm + DOCm), where *A* is the cell area and *AGCm*, *BGCm*, *SOCm*, and *DOCm* represent the densities of carbon in respective pools.

The analysis followed a three-step integration of remote sensing, GIS, and modeling approaches. High-resolution Maxar satellite images were processed and classified using supervised methods to generate accurate LULC maps. These were reclassified into carbon-relevant categories and analyzed in GIS using zonal statistics to compute spatially distributed carbon stocks (**Fig. 04**). The InVEST model synthesized these inputs to simulate carbon dynamics, producing carbon storage maps that reveal spatial variability and identify zones with high sequestration potential in the studied mangrove plantations.

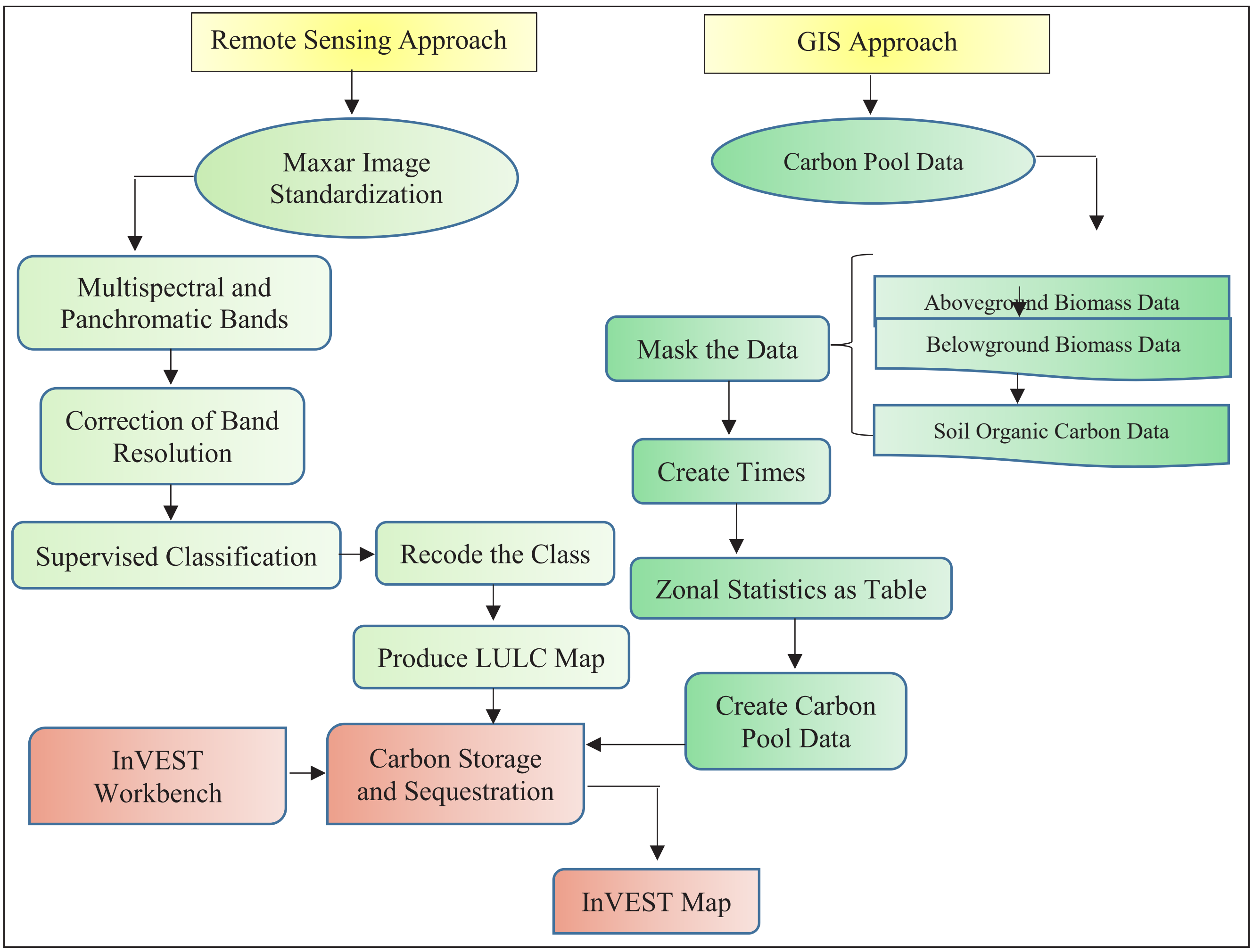

(Source: Compiled by Author, 2025).

Figure. 04: Workflow of InVEST Carbon Storage and Sequestration Model.

2.4 Research Framework/Process Flow

To achieve the anticipated results, a series of methods and steps has been followed on a constant basis. For the identification of research gaps, limitations and alternatives, relevant literature from several published and unpublished sources was reviewed. After the completion of problem identifications and finding research and policy gaps, a comprehensive research design has been finalized starting with data collection approaches. At first, literature review and satellite imagery data from secondary sources has been analyzed to figure out the drivers of carbon stocks. At the same time, collection/purchasing of satellite images is in progress to calculate and estimate the amount of carbon stocks. To identify the species and forest types (mono stand or mixed stand) an in-depth field survey has been conducted to find out the species variability of carbon stocks. And finally, the field level data has been analyzed, synthesized for report writing.

3.0 STUDY AREA

This project was conducted across five coastal mangrove sites: Haringhata Eco Park (HEP) and Tengragiri Wildlife Sanctuary (TWS) in Barguna, Char Kukri-Mukri Wildlife Sanctuary (CKmWS) in Bhola, Char Kashem (CK) in Patuakhali, and Nijhum Dwip National Park (NNP) in Hatiya, Noakhali (**Fig. 05**). Throughout the research period, an extensive field survey was undertaken at all sites to achieve the research objectives.

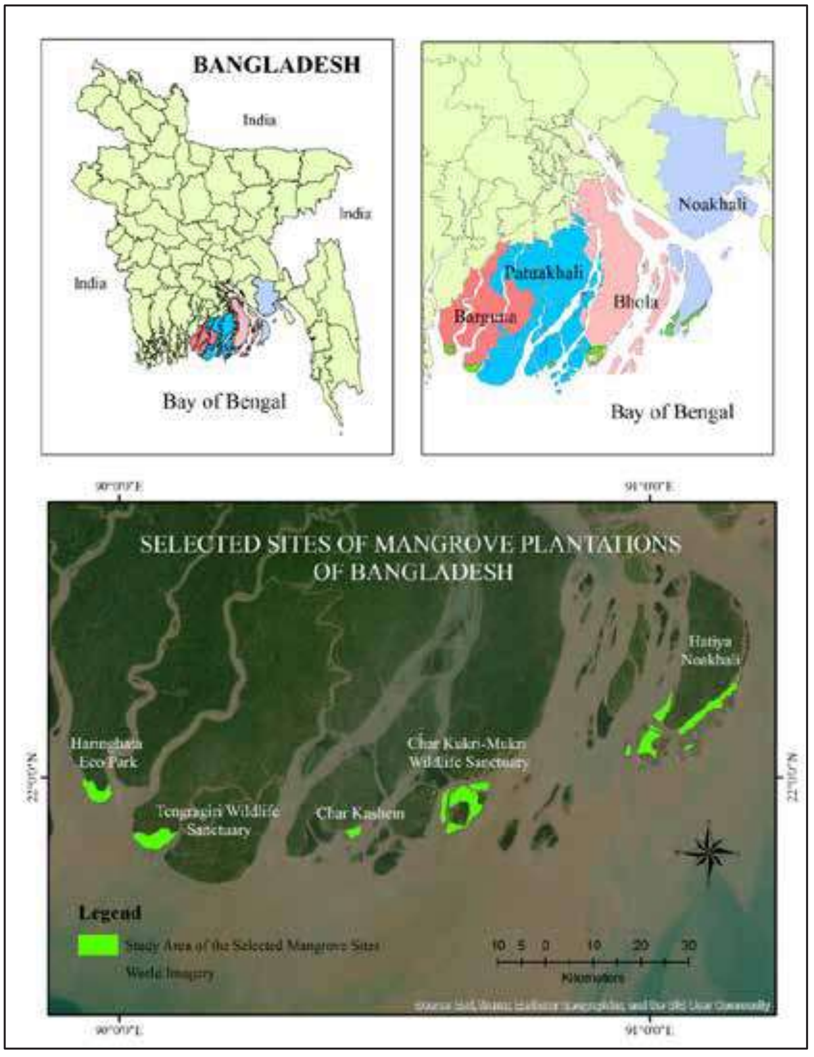

(Source: ESRI, Compiled by Author, 2025).

Figure. 05: Map of the Selected Sites of Mangrove Plantations of Bangladesh for Field Survey.

4.0 RESULTS AND DISCUSSION

4.1 Tree Species

Based on the comprehensive survey on the selected mangrove sites of Bangladesh like Haringhata Eco Park (HEP), Tengragiri Wildlife Sanctuary (TWS), Char Kukri-Mukri Wildlife Sacntuary (CKmWS), Char Kashem (CK) and Nijhum Dwip National Park (NNP), a total of 2898 trees were recorded from the selected 78 grid points, representing a diverse range of mangrove and associated species. From the 312 sampling points of the selected grids, 222 sampling points data has been collected to analyze the species composition, distribution, and dominance across the sites, which plays a crucial role in influencing the carbon stock variability among the different mangrove plantations of Bangladesh.

Dominant Species

Analysis reveals that Gewa (*Excoecaria agallocha*) is the most dominant species, contributing 56.14% (1,627 trees) of the total tree count (**Table:02**). This significant presence suggests its adaptability and extensive plantation in these mangrove areas. Gewa is widely known for its high biomass accumulation and carbon sequestration potential, making it a key species for carbon stock assessment in these regions. The second most abundant species is Keora (*Sonneratia apetala*), which accounts for 30.61% (887 trees). This species is frequently planted in mangrove afforestation programs due to its rapid growth and resilience to saline environments. Its substantial presence highlights its importance in maintaining ecosystem stability and enhancing carbon sequestration.

The combined dominance of Gewa and Keora, together constituting nearly 87% of the total recorded tree population, indicates that afforestation programs in these study sites have largely focused on these two species due to their fast-growing nature, resilience, and high carbon sequestration potential. However, the limited presence of other native mangrove species suggests that these plantations may lack the species diversity typically found in natural mangrove ecosystems, which could have long-term implications for biodiversity conservation, ecosystem resilience, and carbon storage capacity.

Minor Species

In stark contrast to the overwhelming dominance of Keora (Sonneratia apetala) and Gewa (Excoecaria agallocha), several tree species were recorded in remarkably low numbers, indicating their limited establishment and distribution within the surveyed sites. While these minor species contribute to the overall species richness of the ecosystem, their minimal representation suggests possible ecological constraints, competition, or plantation strategies that favor the more dominant species.

A very small percentage of Sundari (Heritiera fomes), Boloi (Hibiscus tiliaceus), Choila (Buchanania lanzan), Jhau (Casuarina equisetifolia), Baen (Avicennia officinalis Li), Raintree (Samanea saman), Hental (Phoenix paludosa), Kakra (Sicyos angulatus), Karanja (Pongamia pinnata), Passur (Xyclocarpus moluccensis), Shingra (Cynometra ramiflora), and Goran (Ceriops decandra) was recorded across the selected study sites, indicating their limited presence in the surveyed mangrove plantation areas.

Among these minor species, Boloi (Hibiscus tiliaceus) was the most abundant, with 116 trees (4.00%), followed by Choila (Buchanania lanzan) at 59 trees (2.04%), and Hental (Phoenix paludosa) at 66 trees (2.28%) (Table:02). These species, though limited in number, are known for their resilience in saline environments and their potential contribution to coastal ecosystem stability. Sundari (Heritiera fomes), a flagship mangrove species of the Sundarbans ecosystem, was recorded in only 35 individuals (1.21%), which is significantly low compared to its natural dominance in undisturbed mangrove forests. This suggests that afforestation efforts in these sites may not prioritize Sundari, possibly due to its slow growth rate and sensitivity to changing environmental conditions.

Other species, including Jhau (Casuarina equisetifolia) with 29 trees (1.00%), Karanja (Pongamia pinnata) with 27 trees (0.93%), and Kakra (Sicyos angulatus) with 16 trees (0.55%), were observed in moderate numbers (Table:02). Jhau, though not a true mangrove species, is often planted in coastal areas for dune stabilization and windbreak purposes. Similarly, Karanja, which has nitrogen-fixing properties, is known for its adaptability in degraded coastal lands.

Several other species exhibited extremely low representation, raising concerns about their ability to establish and thrive in these plantations. These include: Baen (Avicennia officinalis) with 15 trees (0.52%), Passur (Xyclocarpus moluccensis) with 3 trees (0.10%), Shingra (Cynometra ramiflora) with 4 trees (0.14%), Goran (Ceriops decandra) with 4 trees (0.14%), Raintree (Samanea saman) with 4 trees (0.14%), Ghoma (Lannea coromandelica) with 2 trees (0.07%), Amur (Ficus amurensis), Banyan (Ficus benghalensis), Jal Dumur (Ficus carica), and Shonajhuri (Albizia procera) with Each recorded only 1 tree (0.03%) (**Table:02**). The presence of such a low number of individuals for these species indicates that they may not be naturally regenerating in these areas, or that they were only introduced in small quantities as part of past afforestation initiatives.

The data collected from the field survey reflects the structure of the mangrove ecosystem in the selected mangrove sites of Bangladesh. The dominance of Keora and Gewa highlights their critical roles in carbon dynamics and ecological stability, while the minimal presence of other species raises concerns about biodiversity and ecosystem resilience. Understanding these dynamics is essential for informing effective conservation and management strategies aimed at preserving the ecological integrity of mangrove habitats in Bangladesh.

Table 02: Dominant Tree Species found in the Selected Mangrove Forest of Bangladesh (from 222 sampling points_10m x 10m).

Tree Species (Scientific Name)	No. of Trees					Total Trees	Percentage
	HEP	TWS	CKmWS	CK	NNP		
Amur (Ficus amurensis)	-	-	1	-	-	1	0.03
Baen (Avicennia officinalis Li)	-	13	-	-	2	15	0.52
Banyan Tree (Ficus benghalensis)	-	1	-	-	-	1	0.03
Boloi (Hibiscus tiliaceus)	-	39	77	-	-	116	4.00
Choila (Buchanania lanzan)	-	-	58	-	1	59	2.04
Gewa (Excoecaria agallocha)	433	356	214	113	511	1627	56.14
Ghoma (Lannea coromandelica)	-	-	1	1	-	2	0.07
Goran (Ceriops decandra)	-	4	-	-	-	4	0.14
Hental (Phoenix Paludosa)	-	65	1	-	-	66	2.28
Jal Dumur (Ficus carica)	-	-	-	-	1	1	0.03
Jhau (Casuarina equisetifolia)	-	29	-	-	-	29	1.00
Kakra (Sicyos angulatus)	-	-	16	-	-	16	0.55
Karanja (Pongamia Pinnata)	-	22	1	4	-	27	0.93
Keora (Sonneratia apetala)	102	25	187	23	550	887	30.61
Passur (Xyclocarpus molucceniss)	-	3	-	-	-	3	0.10
Raintree (Samanea saman)	-	-	-	4	-	4	0.14
Shingra (Cynometra ramiflora)	-	4	-	-	-	4	0.14
Shonajhuri (Albizia procera)	-	-	-	-	1	1	0.03
Sundari (Heritiera fomes)	-	34	1	-	-	35	1.21
Total	**535**	**595**	**557**	**145**	**1066**	**2898**	**100.00**

(**Source:** Field Survey, 2024).

4.2 Distribution of Trees at the Study Sites

Analysis illustrates the varying abundance of different tree species across the selected mangrove study sites: Haringhata Eco Park (HEP), Tengragiri Wildlife Sanctuary (TWS), Char Kukri-Mukri Wildlife Sanctuary

(CKmWS), Char Kashem (CK), and Nijhum Dwip National Park (NNP); have certain species which has dominate the specific areas. For example, Gewa (Excoecaria agallocha) appears in significant numbers at Haringhata Eco Park (HEP), Tengragiri Wildlife Sanctuary (TWS), and Nijhum Dwip National Park (NNP), highlighting its prevalence in these habitats. Keora (Sonneratia apetala) is also a prominent species, particularly at NNP, where it forms a large part of the mangrove population. Species such as Baen (Avicennia officinalis) and Raintree (Samanea saman) are observed in smaller numbers across all the sites, indicating their more limited presence (**Table: 02 and Fig. 06**). This distribution emphasizes the dominant role of a few species in shaping the mangrove ecosystems at the study sites, with Gewa and Keora emerging as critical contributors to the carbon sequestration potential of these regions.

At the selected study sites, Gewa (Excoecaria agallocha) is by far the most dominant species, accounting for a total of 1627 trees across all locations. Following closely is Keora (Sonneratia apetala), with 887 trees (**Fig. 07)**, confirming its significant presence in the mangrove ecosystems. This figure demonstrates that a limited number of species, specifically Gewa and Keora, make up the majority of the tree population in the study areas. In contrast, species such as Amur (Ficus amurensis), Banyan Tree (Ficus benghalensis), and Passur (Xylocarpus moluccensis) are represented in much smaller numbers, further emphasizing their secondary ecological role in the forests. This distribution underscores the dominance of a few species in the mangrove forests, which is crucial for understanding the species composition and the carbon sequestration potential of the study areas.

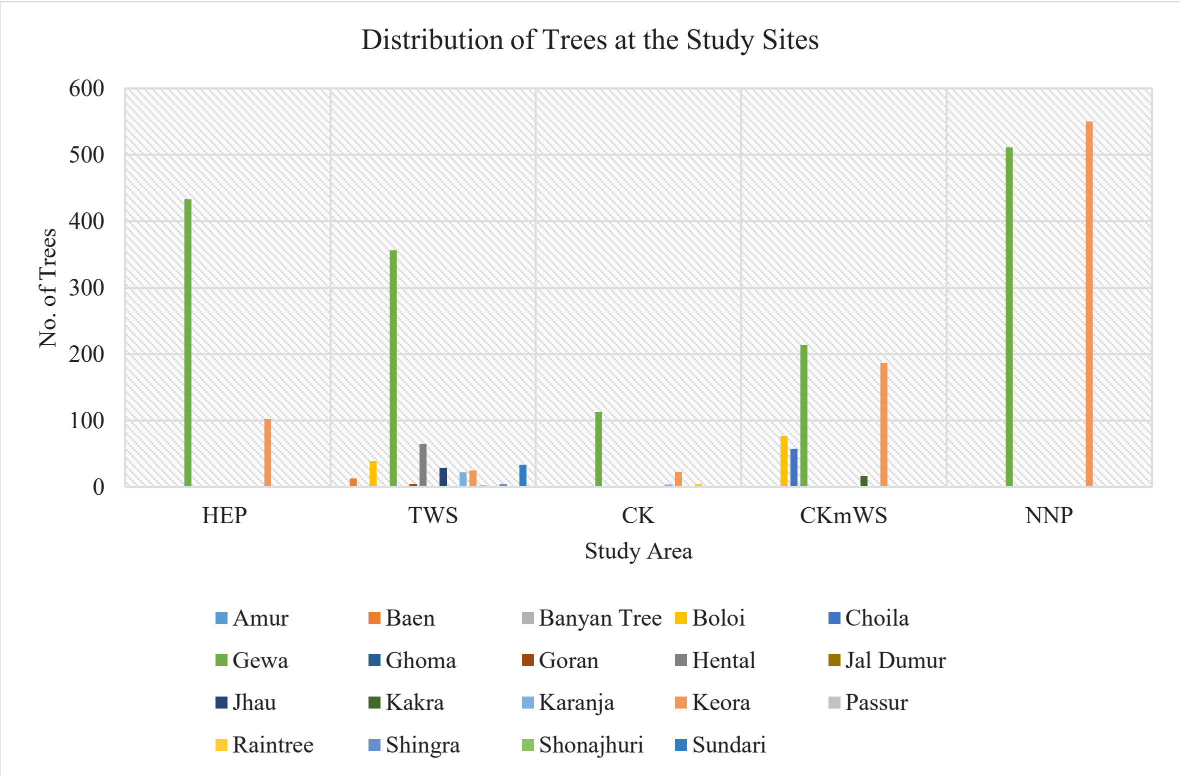

Figure 06: Distribution of Trees at the Study Sites.

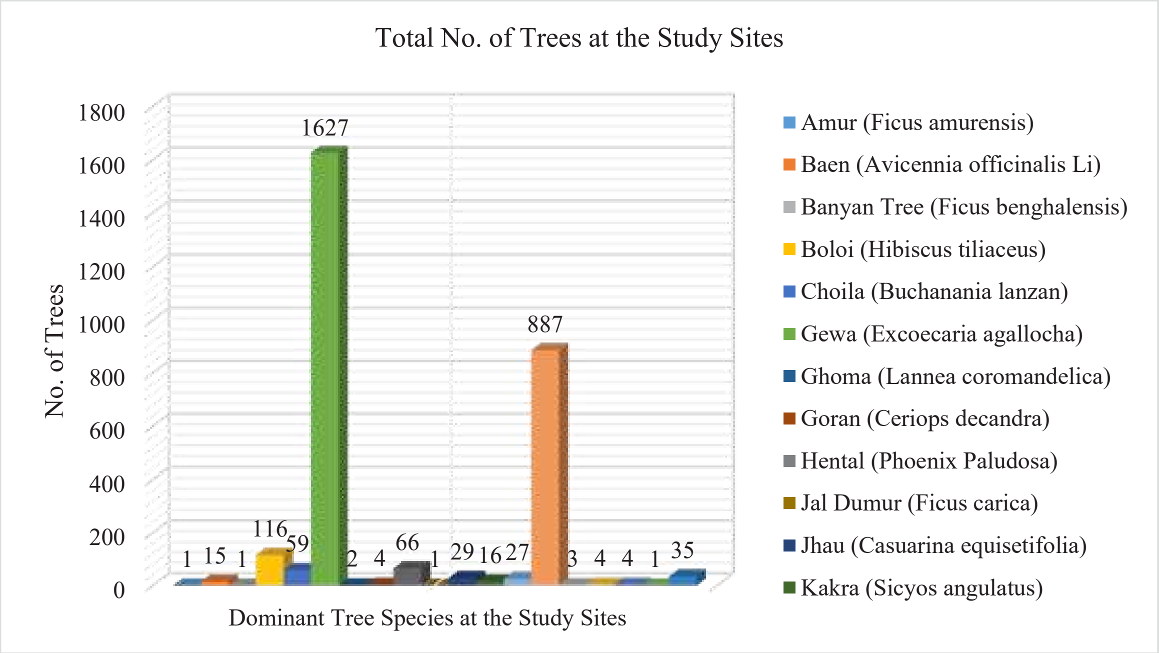

Figure 07: No. of Trees at the Study Sites.

At Haringhata Eco Park (HEP), Gewa (Excoecaria agallocha) is the clearly dominant species with 433 trees recorded, significantly outnumbering Keora (Sonneratia apetala), which accounts for only 102 trees, indicating that Gewa thrives exceptionally well in the ecological conditions of this park. In Tengragiri Wildlife Sanctuary (TWS), Baen (Avicennia officinalis) dominates with 356 trees, while Gewa is present but much less abundant with only 65 trees; other species like Banyan Tree (Ficus benghalensis), Boloi (Hibiscus tiliaceus), and Goran (Ceriops decandra) contribute to the biodiversity, though none surpass Baen in abundance. In Char Kukri-Mukri Wildlife Sanctuary (CKmWS), Gewa again takes the lead with 214 trees, closely followed by Keora with 187 trees, and other species such as Amur (Ficus amurensis) and Boloi are present in small numbers, making Gewa and Keora the dominant species at this location. At Char Kashem (CK), Gewa continues its dominance with 113 trees, while Keora is represented by 23 trees and species like Ghora (Lannea coromandelica) and Karanja (Pongamia pinnata) appear in smaller numbers, suggesting that Gewa is particularly well-suited to this site's conditions. At Nijhum Dwip National Park (NNP), Gewa stands out once again with 550 trees, slightly more than Baen, which has 511 trees, demonstrating that the park supports both species well; species like Choila (Buchanania lanzan), Jal Dumur (Ficus carica), and Keora occur in lower numbers, indicating their lesser prominence in the ecosystem. Across all study sites, Gewa consistently emerges as the most dominant species, while Baen, Keora, and other species add to the overall biodiversity but do not surpass Gewa's widespread abundance.

4.3 Radial Plot Analysis

At Haringhata Eco Park (HEP), the radial plot shows a clear dominance of Gewa (Excoecaria agallocha), which accounts for 81% of the tree population (433 trees), while Keora (Sonneratia apetala) makes up only 19% (102 trees), highlighting Gewa's overwhelming prevalence. In Tengragiri Wildlife Sanctuary (TWS), Gewa also leads with 60% dominance, but a greater diversity is present with Jhau (Casuarina equisetifolia) comprising 29% and Keora 25%, as reflected in the radial plot. Char Kukri Mukri Wildlife Sanctuary (CKmWS) exhibits a more balanced composition, with Gewa at 39% and Keora at 25%, while species like Boilo (Hibiscus tiliaceus) and Choiola (Buchanania lanzan) also contribute, suggesting a relatively even species distribution (**Fig. 08**). In Char Kashem (CK), Gewa once again dominates at 78%, whereas Keora and Karanja (Pongamia pinnata) appear in much smaller proportions, as depicted in the radial plot. Nijhum Dwip National Park (NNP) stands out for its near-equal distribution of Keora and Gewa, with Keora slightly ahead at 52% (550 trees) and Gewa at 48% (511 trees), and the additional presence of Baen (Avicennia officinalis) and Jal Dumur (Ficus carica) indicating greater species diversity compared to other sites.

In conclusion, the box plots for HEP and radial plots for TWS, CKmWS, CK, and NNP visually represent the distributions and proportions of dominant tree species in each area. The plots illustrate that Gewa (Excoecaria agallocha) is the most dominant species across all sites, although the degree of dominance varies. Other species like Keora (Sonneratia apetala), Jhau (Casuarina equisetifolia), and Boilo (Hibiscus tiliaceus) also contribute significantly but not to the same extent as Gewa.

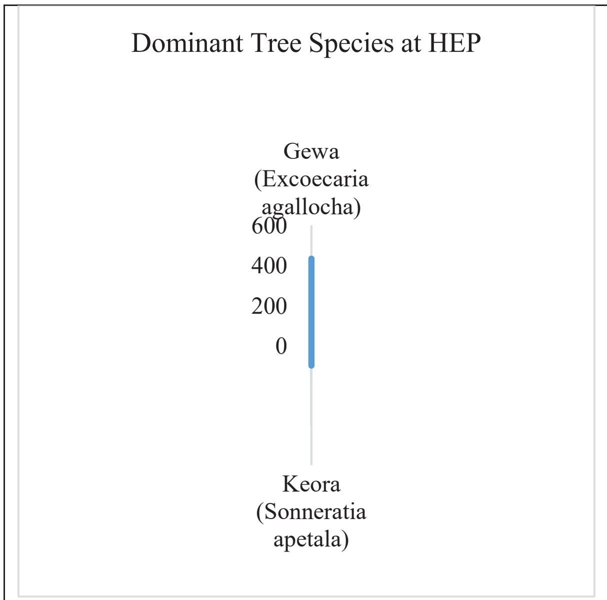

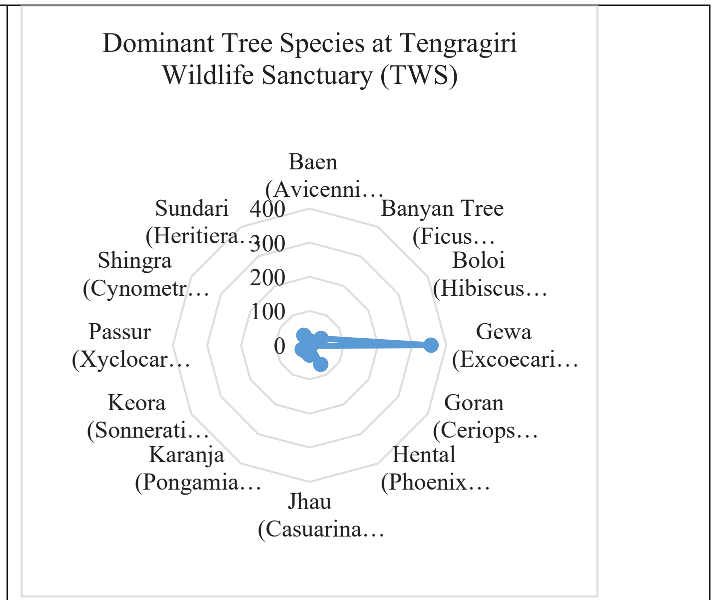

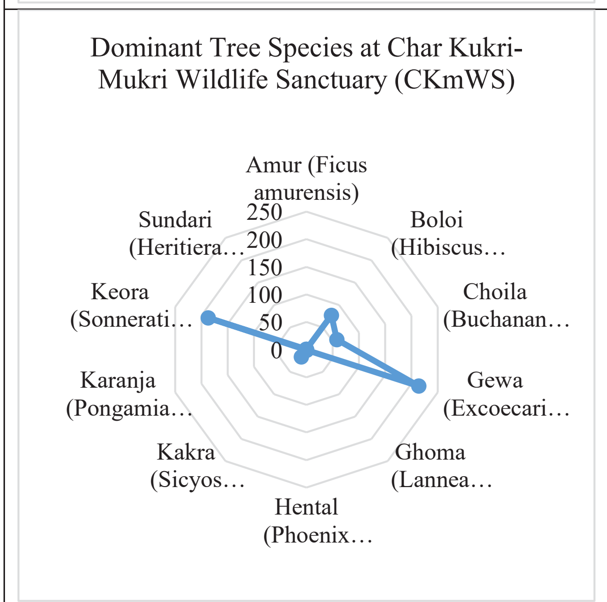

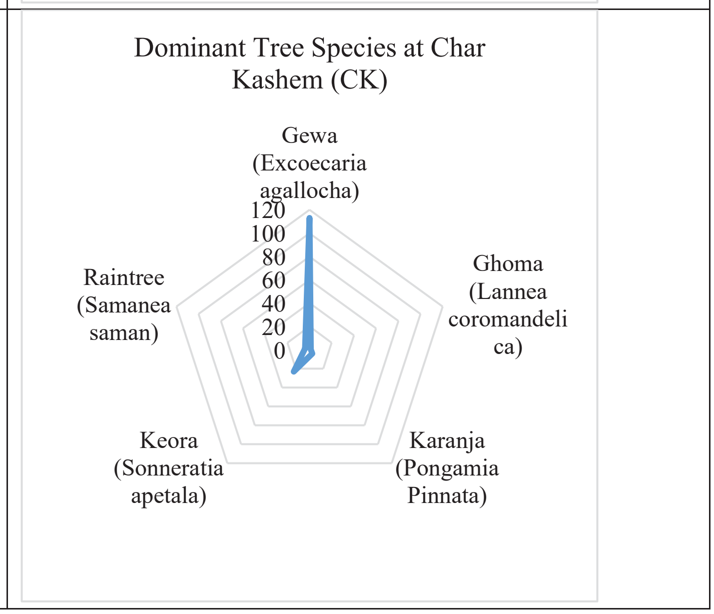

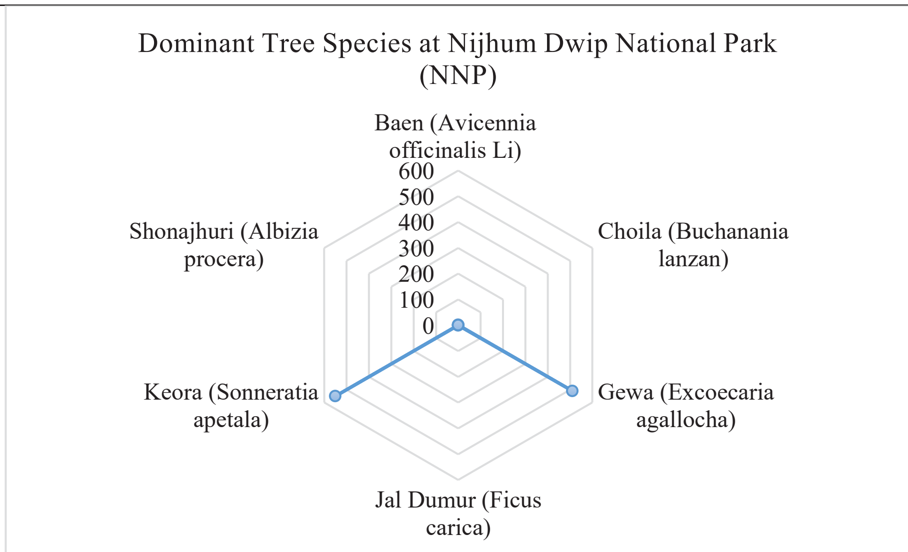

Figure 08: Dominant Tree Species at the Study Sites.

4.4 Shrubs and Seedlings

The field survey data analysis indicates that all the study area exhibits a significant presence of dominant shrubs and seedlings, particularly Gewa (Excoecaria agallocha). In few parts of several sites, Arjuree *(Acanthus ilicifolius)* was found to be the dominant shrubs. A very high density of these shrubs and seedlings has been observed throughout all the study areas. As previously noted, the selected study sites are characterized by its dense planted forests, featuring a variety of shrubs, including Gewa and Arjuree. Additionally, Gewa and Arjuree are prevalent in many areas of the forest. Notably, a high percentage of Gewa seedlings is found all over the forest regions of the selected mangrove sites, further emphasizing its status as a planted mangrove forest.

4.5 Diameter at Breast Height (DBH) and Tree Height

The diameter at breast height (DBH) and tree height are key parameters for calculating both aboveground and belowground biomass carbon, and these were measured through field surveys conducted in the selected mangrove sites of Bangladesh. Trees were defined as those having a DBH of at least 5 cm, measured at 1.37 meters above ground level, with observed DBH values ranging from 5 cm to 82.73 cm. The largest Keora (Sonneratia apetala) tree, recorded in Tengragiri Wildlife Sanctuary, had a DBH of 82.73 cm and exceeded 36 meters in height. Trees with DBH greater than 30 cm were mostly Keora, and those with DBH over 40 cm typically reached heights above 20 meters (**Fig. 09**). Some Baen (Avicennia officinalis) trees were found with DBH values of 53 cm and 44 cm and heights of around 13 meters and 22 meters, respectively. Other notable species like Raintree (Samanea saman), Karanja (Pongamia pinnata), and Choila (Buchanania lanzan) reached heights of approximately 16, 14, and 18 meters. Meanwhile, species such as Jaldumur (Dolichandrone spathacea), Khaya Babla (Pithecellobium dulce), and Shonajhuri (Acacia auriculiformis) exhibited smaller DBH and heights below 4 meters.

Field data analysis identified Keora and Gewa (Excoecaria agallocha) as the dominant tree species across all study sites. On average, Keora trees that exceeded 20 meters in height typically had DBH values over 30 cm, while Gewa trees displayed DBH values below 20 cm and heights under 15 meters. The data revealed a positive correlation between DBH and tree height, with an observable trend indicating that as DBH increases, so does height. This trend is clearly demonstrated in scatter plots (Fig. 35), which show a strong positive correlation between the DBH and height of both Keora and Gewa trees. The scatter plots, featuring DBH on the x-axis (ranging from 0 to 90 cm) and height on the y-axis (ranging from 0 to 40 meters), use blue dots to represent individual trees. Most trees had DBH values between 5 to 50 cm and corresponding heights between 10 and 25 meters, supporting the general trend that larger DBH trees tend to be taller. The series of scatter plots also included logarithmic regression models that estimate tree height based on DBH, revealing that while a positive correlation is common across species, the strength of this relationship varies by species.

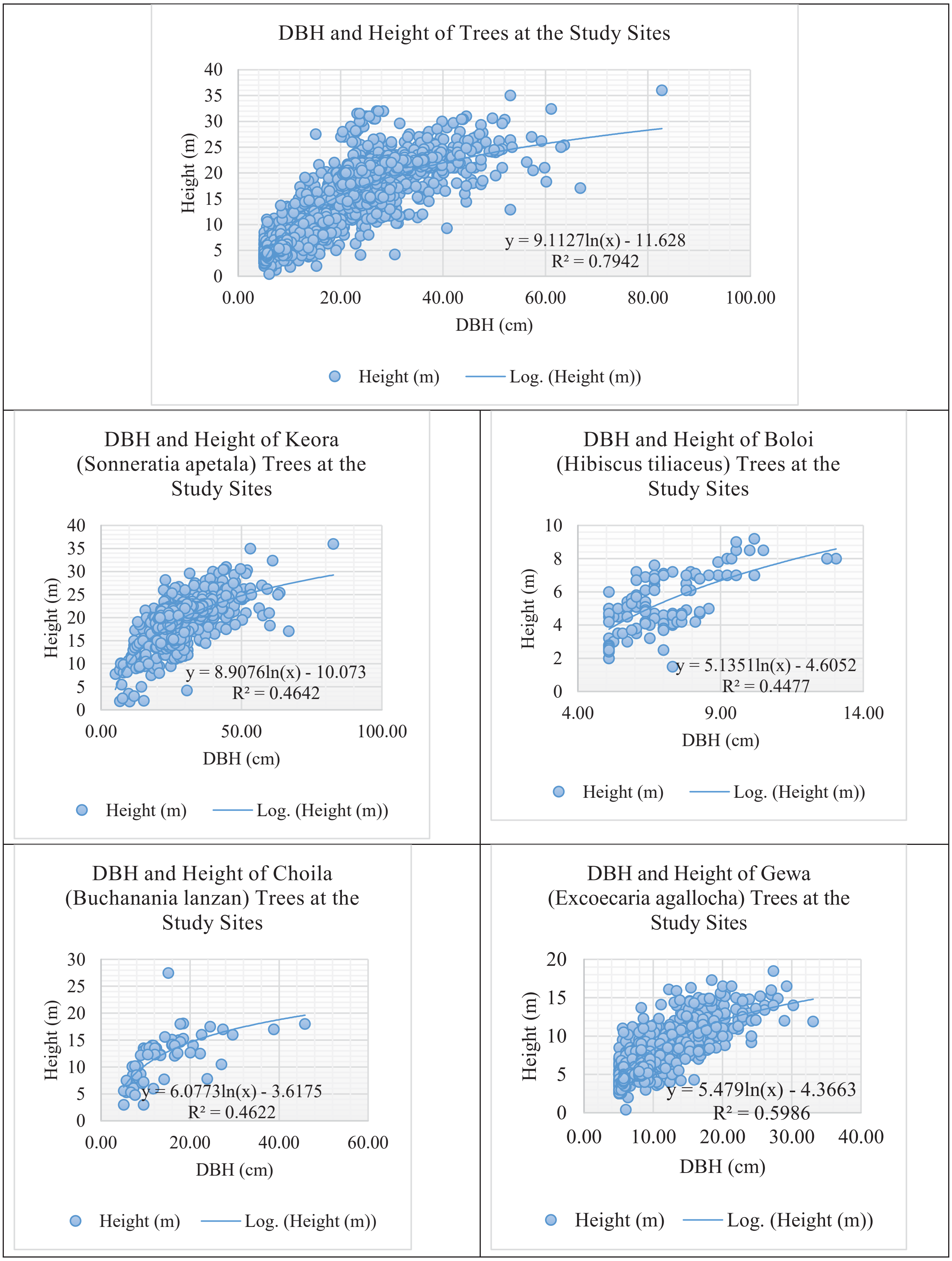

Figure 09: DBH and Height of Trees at the Study Sites.

4.6 Statistical Analysis of the Selected Forest

The structural development of a forest is reflected in the characteristics of its tree species. This study analyzed key variables for each species, including minimum, mean, maximum values, and standard deviations for diameter at breast height (DBH) and height, to understand the forest condition and structure at selected mangrove sites. The focus was on two dominant species, Keora (Sonneratia apetala) and Gewa (Excoecaria agallocha), as indicators of forest dynamics. Mean DBH varied across sites, from 11.91 cm at Tengragiri Wildlife Sanctuary to 18.39 cm at Nijhum Dwip National Park, indicating larger trees at the latter. Mean tree height followed a similar pattern, with the tallest average height at Nijhum Dwip (12.59 m) compared to 11.07 m at Haringhata Eco Park (**Table. 03**). Scatter plots revealed a generally positive correlation between DBH and height across most species, with Nijhum Dwip showing the strongest correlation ($R^2 = 0.863$). Other sites like Char Kukri-Mukri and Char Kashem showed moderate correlations, though some species such as Keora at Char Kashem exhibited weak correlation ($R^2 = 0.0716$), suggesting that DBH is not always a reliable predictor of height.

Keora emerged as the tallest and largest species overall, with an average height of 19.19 m and a maximum height of 36 m. It also had the highest mean DBH (27.92 cm at Nijhum Dwip) and showed considerable variability, indicating a structurally diverse forest where Keora acts as a canopy species. In contrast, Gewa was smaller and shorter, averaging 7.13 m in height and 8.87 cm in DBH, with less variability, suggesting it occupies a more stable, understory role. Baen (Avicennia officinalis), found only at Nijhum Dwip, showed intermediate characteristics with a mean DBH of 24.5 cm and height of 14.35 m, growing more uniformly there. Other associated species such as Raintree, Choila, Karanja, Boloi, and Kakra contributed to species diversity, each showing varied growth patterns and structural traits depending on site conditions. Overall, the data demonstrate site-specific differences in forest structure, with tree size and variability influenced by species composition and environmental factors. Nijhum Dwip hosts larger and taller trees with strong DBH-height relationships, while other sites show more moderate or variable patterns in forest development.

Table 03: Statistical Comparison of Tree Species at the Selected Mangrove Sites.

Study Sites	DBH (cm)				Height (m)			
	Min	Mean	St. Deviation	Max	Min	Mean	St. Deviation	Max
Haringhata Eco Park	5.09	13.94	11.25	61.09	3.00	11.07	6.32	32.40
Tengragiri Wildlife Sanctuary	5.09	11.91	9.09	82.73	1.20	8.46	6.29	36.00
Char Kukri-Mukri Wildlife Sanctuary	5.09	14.51	11.54	63.64	1.80	10.84	6.59	27.50
Char Kashem	5.09	12.68	11.69	49.95	2.00	10.09	6.40	26.50
Nijhum Dwip National Park	5.09	18.39	10.97	47.73	0.40	12.59	7.32	27.50

(Source: Field Survey Data Analysis, 2024-25).

4.7 Biomass and Carbon Stocks

Using established allometric equations, aboveground biomass (AGB), belowground biomass (BGB), total biomass, and carbon stock were estimated for various tree species. The total aboveground biomass recorded was 515,943.13 tons, with belowground biomass at 120,377.57 tons (**Table. 04**). The two dominant species, Gewa and Keora, together contributed over 542,527.49 tons of total biomass, with Keora being the largest contributor in both biomass and carbon storage. Among the study sites, Nijhum Dwip National Park (NNP) had the highest biomass and carbon stock, recording 226,688.35 tons of AGB and 53,078.75 tons of BGB, totaling 279,767.11 tons of biomass and 132,889.38 tons of carbon. Char Kashem had the lowest values, with 29,086.05 tons AGB, 6,786.60 tons BGB, and 17,039.51 tons of carbon stock. Char Kukri-Mukri Wildlife Sanctuary (CKmWS) and Tengragiri Wildlife Sanctuary (TWS) showed similar biomass levels, around 111,015.37 tons and 107,764.14 tons of total biomass respectively, with carbon stocks near 52,700 and 51,200 tons (**Table. 05**). Haringhata Eco Park (HEP) presented moderate biomass and carbon stock values. Overall, the five sites accounted for a total biomass of 636,320.70 tons and carbon stock of 302,252.34 tons.

Regarding dominant species, Gewa (Excoecaria agallocha) and Keora (Sonneratia apetala) together account for over 86% of the biomass, strongly influencing forest environment and carbon sequestration capacity. The carbon stock per Gewa tree is highest at Haringhata Eco Park (18.26 tons) and Tengragiri Wildlife Sanctuary (17.91 tons), suggesting favorable environmental conditions at these sites. However, carbon stock per Gewa declines significantly in Char Kukri-Mukri Wildlife Sanctuary (13.52 tons), Char Kashem (9.00 tons), and Nijhum Dwip National Park (9.78 tons), indicating site-specific factors affecting carbon storage. For Keora, Tengragiri Wildlife Sanctuary shows the highest carbon stock per tree at 478.98 tons, followed by Char Kashem at 417.24 tons. Haringhata Eco Park (397.03 tons) and Nijhum Dwip National Park (231.69 tons) exhibit relatively lower values. These differences highlight the importance of local factors such as soil type, rainfall, temperature, and forest management practices in determining biomass and carbon storage potential across mangrove ecosystems.

Table 04: Total Biomass and Carbon Stocks in the Study Sites in Selected Grids

Study Sites	Total AGB (ton)	Total BGB (ton)	Total Biomass (ton)	Total Carbon (ton)
Haringhata Eco Park	82656.87	19244.56	101901.43	48403.18
Tengragiri Wildlife Sanctuary	87464.94	20299.21	107764.14	51187.97
Char Kukri-Mukri Wildlife Sanctuary	90046.92	20968.45	111015.37	52732.30
Char Kashem	29086.05	6786.60	35872.65	17039.51
Nijhum Dwip National Park	226688.35	53078.75	279767.11	132889.38
Total	**515943.13**	**120377.57**	**636320.7**	**302252.34**

(Source: Field Survey Data Analysis, 2024-25).

Table 05: Total Biomass and Carbon Stock of Gewa and Keora Trees in the Study Area.

		Above Ground Biomass (ton)				Below Ground Biomass (ton)				Total Biomass (ton)				Carbon Stocks (ton)			
	Study Sites	Sampling Plot	Total Forest	Per sq km	Each Tree	Sampling Plot	Total Forest	Per sq km	Each Tree	Sampling Plot	Total Forest	Per sq km	Each Tree	Sampling Plot	Total Forest	Per sq km	Each Tree
Gewa	Haringhata Eco Park	13623.51	152376.30	9831.25	31.46	3021.72	33807.58	2181.25	6.98	16645.23	186183.89	12012.50	38.44	7906.48	88442.19	5706.25	18.26
	Tengragiri Wildlife Sanctuary	11005.28	143531.65	7188.37	30.91	2420.87	31576.03	1581.40	6.80	13426.15	175107.68	8769.77	37.71	6377.42	83165.70	4165.12	17.91
	Char Kukri-Mukri Wildlife Sanctuary	5005.26	151200.93	5439.53	23.39	1086.33	32838.85	1181.40	5.08	6061.59	183134.78	6588.37	28.33	2893.50	87397.89	3144.19	13.52
	Char Kashem	1771.96	56789.93	12061.54	15.68	368.46	11807.09	2507.69	3.26	2140.42	68597.02	14569.23	18.94	1016.70	32596.26	6923.08	9.00
	Nijhum Dwip National Park	8658.35	96982.43	1861.54	16.94	1847.96	20724.70	397.80	3.62	10506.31	117707.13	2259.34	20.56	4996.50	55991.04	1074.73	9.78
Keora	Haringhata Eco Park	69033.36	3278076.36	3278076.36	676.80	16222.84	770357.63	770357.63	159.05	85256.2	4048433.99	4048433.99	835.85	40496.7	1923012.20	1923012.20	397.03
	Tengragiri Wildlife Sanctuary	20412.64	3791492.29	189886.05	816.51	4796.97	891001.38	44623.26	191.88	25209.61	4682447.24	234506.98	1008.38	11974.56	2224160.12	111390.70	478.98
	Char Kukri-Mukri Wildlife Sanctuary	76806.66	2655098.75	95518.60	410.73	17998.74	622192.81	22383.71	96.25	94805.40	3277291.56	117902.33	506.98	45032.56	1556742.58	56004.65	240.82
	Char Kashem	16359.05	2576046.39	547123.08	711.26	3844.38	605385.03	128576.92	167.15	20203.43	3181431.42	675700.00	878.41	9596.63	1511162.72	320953.85	417.24
	Nijhum Dwip National Park	217230.14	2261167.70	43402.20	394.96	51043.01	531342.35	10198.90	92.81	268273.15	2792510.05	53601.10	487.77	127429.75	1326437.98	25460.44	231.69

4.8 Scatter Plot Analysis in the Selected Mangrove Sites

The scatter plot analysis (**Fig. 10**) shows the relationship between Diameter at Breast Height (DBH) and carbon stock for different mangrove species at selected sites in Bangladesh. Each plot displays individual trees with DBH on the x-axis and carbon stock in kilograms on the y-axis, along with a blue linear regression line indicating the trend. For Keora (Sonneratia apetala), there is a clear positive correlation, with carbon stock increasing steadily as DBH grows, despite one outlier at higher DBH. Gewa (Excoecaria agallocha) also shows a positive trend, though the correlation is moderate with some deviations at larger diameters. Goran (Ceriops decandra) exhibits a strong and consistent relationship between DBH and carbon stock, with a steep regression slope indicating effective carbon sequestration as the trees mature. Hental trees have a positive correlation, but their overall carbon stock is lower, with a notable outlier at high DBH values. Jhau shows a stable increase in carbon stock with DBH, though with less data variability and a moderate regression fit. Kakra demonstrates a weaker and more variable correlation, with dispersed data points, while Karanja (Pongamia pinnata) shows a strong, clear positive relationship, with tightly clustered points around the regression line. Overall, larger trees generally store more carbon across species, but the strength of the correlation and sequestration efficiency vary. Keora, Goran, and Jhau show the highest carbon sequestration potential due to steep slopes. Gewa and Kakra show positive but weaker correlations, indicating lower carbon storage. Hental and Karanja display consistent, secondary contributions to carbon stocks. These findings highlight species-specific carbon storage dynamics, providing important guidance for targeted conservation and afforestation efforts in mangrove ecosystems.

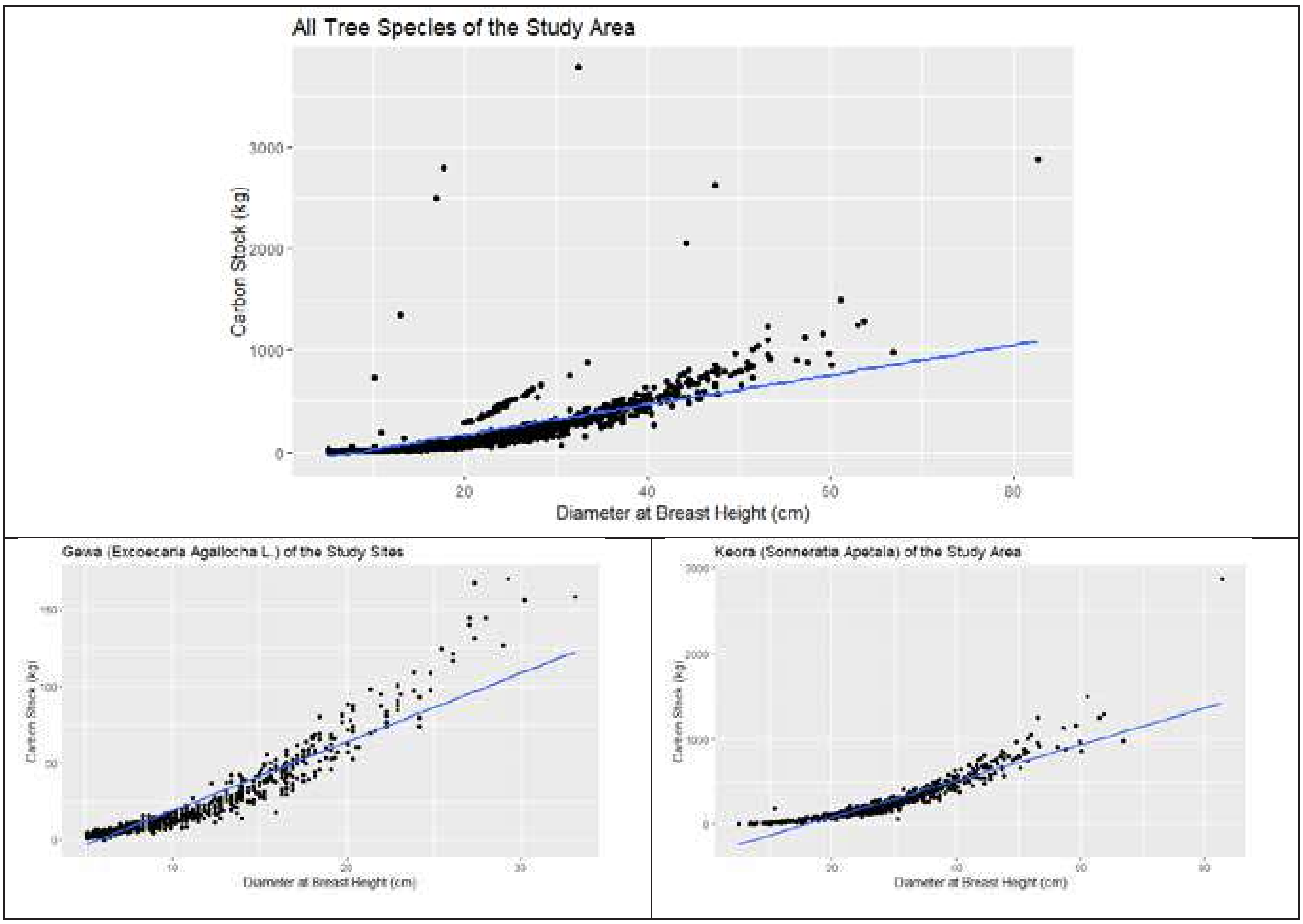

Figure 10: Scatter Plot Analysis of DBH and Carbon Stock in the Selected Sites.

4.9 Box Plot Analysis

The box plot compares carbon stock variations among different mangrove and associated tree species in the study area, showing their central tendencies, ranges, and extremes. Ceriops decandra (Goran) has the highest median carbon stock, consistently ranging from about 1,000 kg to over 3,000 kg, indicating strong and reliable carbon accumulation across tree sizes and sites (**Fig. 11**). Sonneratia apetala (Keora) also has high carbon storage capacity with greater variability, including outliers of mature trees that store significantly more carbon than average. Species like Xylocarpus moluccensis (Passur) and Samanea saman (Raintree) fall in the middle range of carbon stocks, influenced by factors like site conditions and tree age. Although they store less carbon than Goran or Keora, they still contribute meaningfully to sequestration. In contrast, Hibiscus tiliaceus (Boloi) and Excoecaria agallocha (Gewa) consistently show lower carbon stocks, generally below 50 kg, reflecting their smaller size and lower storage potential. Avicennia alba (Baen) shows a slightly wider carbon stock range but remains less effective than the top species. The presence of outliers, especially in Keora and Goran, highlights the critical role of large, mature trees in carbon storage and the importance of conserving these trees within mangrove ecosystems.

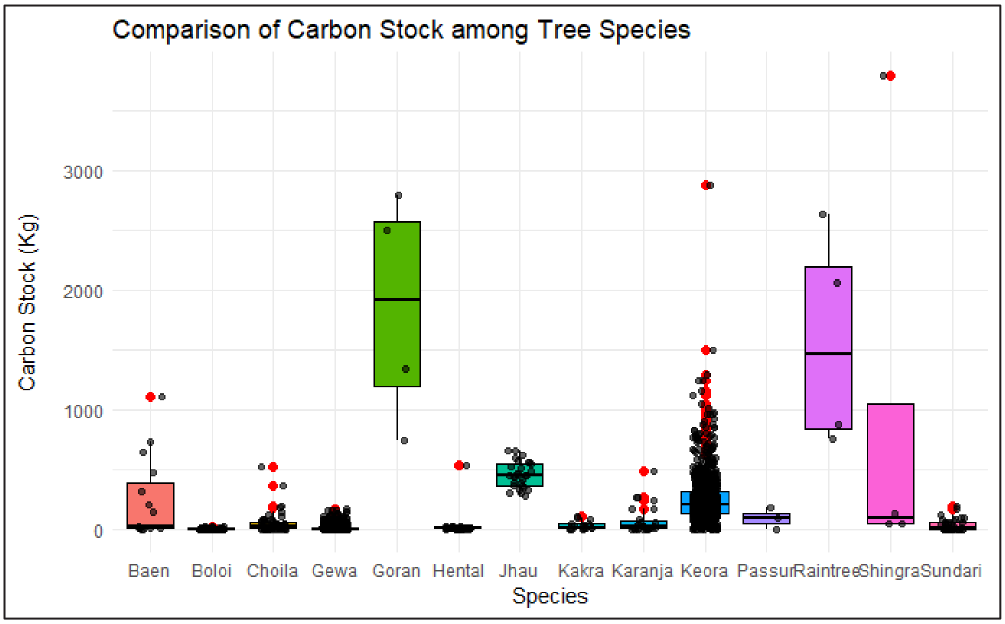

Figure 11: Box Plot Analysis of DBH and Carbon Stock in the Selected Sites.

The box plot analyses across multiple study sites consistently show significant differences in carbon stock among mangrove and associated tree species. Sonneratia apetala (Keora) stands out with much higher carbon sequestration potential compared to Excoecaria agallocha (Gewa) and other species. At Haringhata Eco Park (HEP), Keora has a notably higher median carbon stock and a wider range of values, including large outliers representing exceptionally big trees, while Gewa shows lower and less variable carbon stocks (**Fig. 12**). Statistical tests confirm these differences are highly significant, emphasizing Keora's importance in carbon storage. Similar patterns appear at Tengragiri Wildlife Sanctuary (TWS), where species like Ceriops decandra (Goran), Keora, and Cynometra ramiflora (Shingra) have higher and more variable carbon stocks, unlike species such as Xylocarpus moluccensis (Passur) and Heritiera fomes (Sundari), which show lower values. At Char Kukri-Mukri Wildlife Sanctuary (CKmWS), Keora leads again, followed by Sicyos angulatus (Kakra), while Gewa, Buchanania lanzan (Choila), and Hibiscus tiliaceus (Boloi) have lower carbon stocks with some outliers indicating inconsistency.

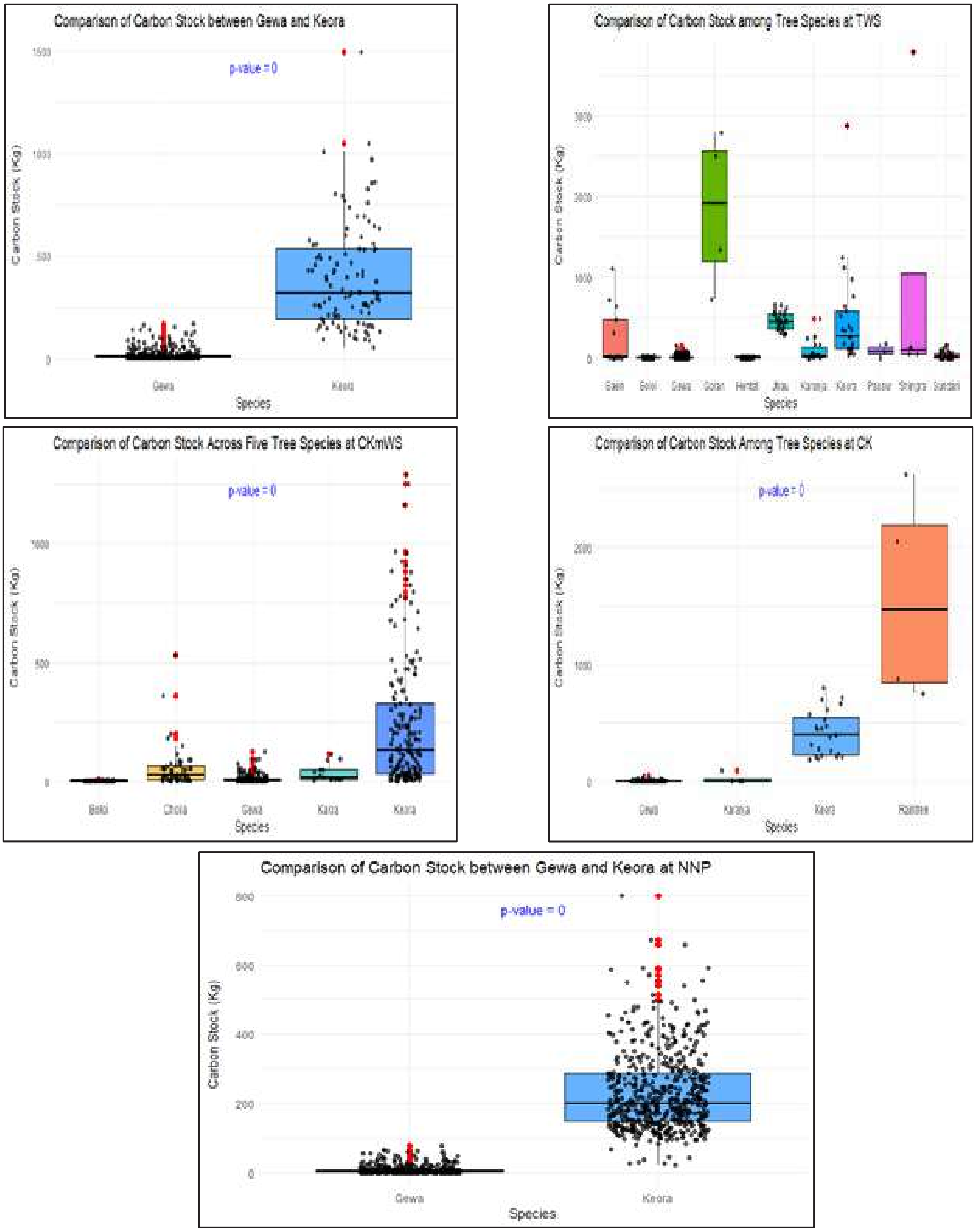

Figure 12: Box Plot Analysis of DBH and Carbon Stock at the Study Sites.

4.10 T-Test

Analysis of field survey data using R software revealed significant differences in carbon stock among tree species across multiple study sites. At the HEP site, a Welch Two Sample t-test showed a highly significant difference in mean carbon stock between Gewa (*Excoecaria agallocha*) and Keora (*Sonneratia apetala*) ($t = -14.87$, $df = 101.51$, $p < 2.2 \times 10^{-16}$). Keora had a much higher average carbon stock (397.03 units) compared to

Gewa (18.26 units), with the 95% confidence interval confirming this difference. At the TWS site, one-way ANOVA indicated significant variation in carbon stock among eleven species ($F(10, 583) = 62.98$, $p < 2 \times 10^{-16}$), showing that species identity strongly influences carbon accumulation. At CKmWS, ANOVA also revealed significant differences among five species ($F(4, 547) = 58.58$, $p < 2 \times 10^{-16}$). Tukey's HSD test found that Keora had significantly higher carbon stock than Boloi, Choila, Gewa, and Kakra ($p < 0.001$ for all comparisons). At the CK site, one-way ANOVA confirmed significant species differences in carbon stock ($F(3, 140) = 168.2$, $p < 2 \times 10^{-16}$), with Raintree (*Samanea saman*) having the highest carbon stock, followed by Keora. Gewa and Karanja showed similar, lower carbon stocks. At the NNP site, a Welch Two Sample t-test showed that Keora had a significantly higher carbon stock than Gewa ($t = -46.186$, $df = 563.15$, $p < 2.2 \times 10^{-16}$). Overall, the results indicate that species selection is an important factor for maximizing carbon sequestration in mangrove afforestation projects. Keora consistently demonstrated superior carbon storage capacity compared to other species across all sites.

4.11 Correlation Analysis

The scatter plot of Diameter at Breast Height (DBH) versus carbon stock shows a strong positive correlation ($r = 0.78$, Fig. 59): each additional centimetre of DBH raises carbon storage, and the relationship becomes steeper in larger trees, reflecting accelerated biomass accumulation (**Fig. 13**). Outliers above 3 000 kg emphasise the disproportionate contribution of very large stems. By contrast, tree-height versus carbon stock exhibits only a moderate correlation ($r = 0.66$); variability below 30 m and non-linearity among the tallest trees indicate that height alone is an inconsistent predictor. Site analyses confirm DBH as the superior indicator of carbon stock. At HEP and CKmWS, DBH correlates extremely well with carbon ($r = 0.93$ and 0.94, respectively), while height is slightly weaker ($r = 0.87$ and 0.65). TWS, CK, and NNP show the same pattern: DBH correlations of 0.61, 0.79, and 0.95 surpass height correlations of 0.54, 0.56, and 0.87. These consistent trends, coupled with steeper slopes at higher diameters, demonstrate that large-DBH trees drive ecosystem carbon storage across all five mangrove sites. Consequently, DBH should be the primary variable in carbon-stock models, with height included as a secondary predictor to capture additional variance. Integrating both metrics will improve biomass estimates and support targeted mangrove management and climate-mitigation strategies in Bangladesh's coastal forests.

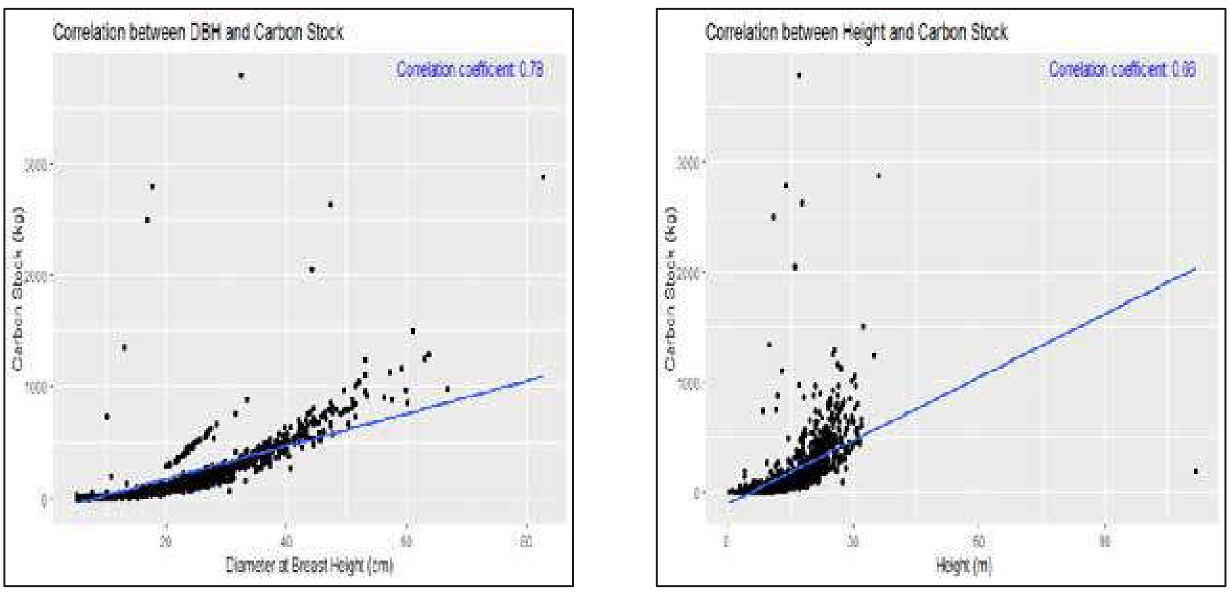

Figure. 13: Correlation Analysis between DBH and Carbon Stock at the Study Sites.

4.12 Regression Analysis

The regression analysis confirms a strong, statistically significant linear relationship between Diameter at Breast Height (DBH) and carbon stock in mangrove forests. On average, each additional centimeter in DBH corresponds to an increase of 14.62 kg of carbon. The model's negative intercept suggests near-zero carbon in very small-diameter trees, which aligns with ecological expectations. The linear model fits well overall, though some variability at higher DBH values may reflect species differences or local site effects. Tree height also shows a positive linear relationship with carbon stock, with an estimated 19.2 kg increase per additional meter. However, variability is higher among shorter trees, indicating that height alone is a less reliable predictor, particularly in younger stands. Although the model performs reasonably well, its predictive strength is weaker than that of DBH.

Site-specific regressions reinforce these findings. At HEP, DBH shows a strong correlation, though the model slightly underestimates carbon stock in the largest trees, hinting at non-linear growth. Tree height shows greater dispersion. At TWS, DBH predicts an average carbon gain of 19.53 kg/cm, while height accounts for 25.3 kg/m yet again, DBH proves more consistent. At CKmWS, the pattern holds, with DBH demonstrating a solid fit and height being more variable. In CK, carbon stock increases by 21.92 kg/cm of DBH, but tree height predictions remain less precise. NNP results are similar: DBH provides reliable estimates, while tree height contributes useful, though secondary, insight. In summary, DBH consistently emerges as the strongest and most dependable predictor of carbon stock across all sites. Tree height, while positively correlated, shows more variation and lower reliability. For accurate carbon assessments in mangrove ecosystems, DBH should be prioritized, with tree height and additional ecological variables used as complementary inputs to refine estimates and inform site-specific forest management.

4.13 Non-Linear Regression Analysis

Regression results show that Diameter at Breast Height (DBH) is the most reliable single predictor of carbon stock in Bangladeshi mangrove forests. A linear model indicates that each centimetre of DBH adds 14.6 kg of carbon, with a strong overall fit but some species-or site-specific scatter at larger diameters. Tree height is also positively related to carbon (19.2 kg m^{-1}) yet exhibits greater variability, especially among smaller trees, making it a weaker stand-alone predictor. Site-level linear regressions reinforce this hierarchy: DBH carbon correlations range from 0.79 (CK) to 0.95 (NNP), whereas height–carbon correlations are consistently lower. Non-linear (power-law) models capture the size effect more accurately, revealing accelerating carbon accumulation in large stems. At HEP, exponents of 2.31 (DBH) and 2.87 (height) confirm rapid biomass gain in mature trees; similar but slightly lower exponents occur at TWS (1.89, 1.82) (**Fig. 14**). CKmWS and CK show pronounced non-linear scaling (DBH exponents 1.06 and 2.94, respectively), again highlighting DBH's dominant influence, while NNP exhibits the steepest DBH response and a secondary height effect. Taken together, the analyses demonstrate that carbon sequestration rises disproportionately with tree size, driven mainly by DBH. Height adds complementary information but is less consistent. Therefore, DBH should be prioritised in mangrove carbon assessments, with height and site factors incorporated to refine estimates. Linear models offer convenient baselines, yet non-linear formulations are necessary for accurately representing the exponential biomass gains of large, mature mangrove trees and for avoiding underestimation of ecosystem carbon stocks.

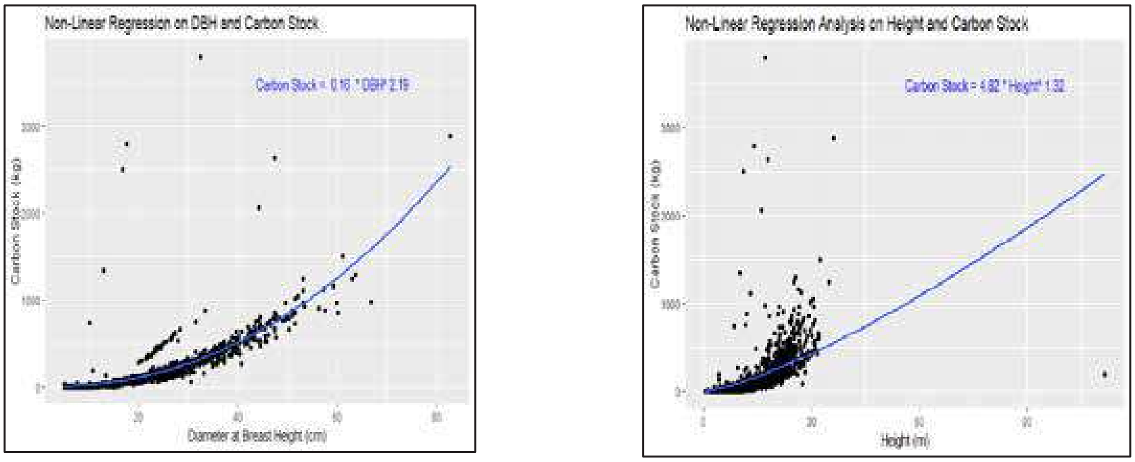

Figure. 14: Non-Linear Regression Analysis on DBH, Height and Carbon Stock at the Study Sites.

4.14 Imagery Analysis

Traditional methods for biomass and carbon stocks assessment based on field measurements are the most accurate; however, it is very difficult to conduct over large areas and also very costly, labor intensive and time consuming (Attarch and Gloaguen, 2014). That's why, currently remote sensing techniques is widely used to collect information regarding forest development, structure, health as well as to monitor and enhance the productivity on large scales. Mapping and monitoring carbon stocks in forested regions of the world, has attracted a great deal of attention in recent years (Goetz., et. al., 2009). RS data are now considered to be the most reliable method of estimating spatial biomass in tropical regions over large areas (Vicharnakorn, et., al. 2014). Forest carbon stocks mainly comprised of aboveground biomass (AGB), belowground biomass (BGB), Litter biomass, Dead wood and Soil organic carbon (SOC) pool (IPCC, 2007). Mapping carbon stocks over large areas without satellite data is clearly problematic (Houghton, et. at., 2001). Currently, multiple providers are producing the carbon pool data like: aboveground biomass, belowground biomass, soil organic carbon, etc. Here for this research, the aboveground and belowground biomass data as well as the satellite images has been taken and analysed to assess the carbon stocks of the selected mangrove sites of Bangladesh. To assess a clear perception over the selected forest sites couple of remote sensing-based forest indices is also analysed.

NDVI

Normalized Difference Vegetation Index or NDVI is generally used as a forest health index. NDVI values range from +1.0 to -1.0. Areas of barren rock, sand, or snow usually show very low NDVI values (for example, 0.1 or less). Sparse vegetation such as shrubs and grasslands or senescing crops may result in moderate NDVI values (approximately 0.2 to 0.5). A suitable NDVI range for forest cover classes by Akbar (Akbar, et. al., 2019) is followed for this research (**Table. 06**).

Table 06: Normalized Difference Vegetation Index Range for Forest.

Class	NDVI Range
Water	–0.28 – 0.015
Built-up	0.015 – 0.14
Barren Land	0.14 – 0.18
Shrub and Grassland	018 – 0.27
Sparse Vegetation	0.27 – 0.36
Dense Vegetation	0.36 – 0.74

(Source: Akbar, et. al., 2019).

The NDVI maps produced for the selected mangrove forests reveal detailed insights into forest structure and health across all study sites. At Haringhata Eco Park (HEP), the map shows predominantly healthy and dense vegetation, with large areas marked by high NDVI values (0.36 - 0.99), indicating thriving mangrove ecosystems and substantial carbon sequestration capacity. Some patches in the northern part show sparse vegetation (NDVI: 0.18 - 0.27) (**Fig. 15**), likely reflecting areas undergoing forest regeneration, but overall, the forest cover is robust.

Similarly, the NDVI map of Tengragiri Wildlife Sanctuary (TWS) displays extensive dense vegetation across most of the sanctuary, highlighting strong mangrove growth and effective conservation. However, some barren patches (NDVI: 0.14 - 0.18) near the sanctuary boundaries may result from human disturbance or environmental stressors. Despite this, the general vegetation health remains solid. At Char Kukri-Mukri Wildlife Sanctuary (CKmWS), dense vegetation dominates the landscape, showing well-preserved mangrove forests and a high potential for carbon storage. Sparse vegetation areas appear mainly around the northern edges, indicating zones of ecological recovery amidst an otherwise rich biodiversity. Char Kashem (CK) features a largely homogeneous distribution of dense vegetation across the island, signifying a well-established and healthy mangrove ecosystem. Small areas with sparse vegetation suggest ongoing plantation efforts or natural regeneration, maintaining the overall ecological balance. Nijhum Dwip National Park (NNP) shows extensive healthy, dense vegetation throughout most of the forest, with very few sparse or barren patches, reflecting a favorable ecological condition and effective conservation. The mangrove forest on Nijhum Dwip Island itself appears denser and healthier compared to the mainland part of Hatiya, where sparse to moderate vegetation is more common.

Overall, NDVI maps across all five study sites indicate a high degree of vegetation health, especially in areas classified as dense vegetation. This reflects well-established mangrove ecosystems crucial for carbon sequestration and climate change mitigation. Although some small patches of sparse or barren vegetation exist, the majority of the areas exhibit strong forest health. These findings highlight the importance of these mangrove forests as vital components of Bangladesh's coastal ecosystem network, with significant roles in carbon storage and global climate regulation. Future integration of Land Use Land Cover (LULC) and carbon stock data will provide a more comprehensive understanding of their environmental significance.

LULC

Land use and land cover (LULC) refers to the use of land, its resources, and the physical (bio) cover on the Earth's surface (e.g., water bodies, plants, forests, agricultural land, and urban areas) (Mishra, and Rai, 2016; Saputra and Lee, 2019; Arifeen, et. al., 2021). This feature of remote sensing technology is used for figure out the changes of land use over time. To figure out the changes of carbon stocks, the historical scenario as well as to predict the future scenario of carbon stocks, LULC map plays substantial role. During the analysis of aboveground and belowground biomass carbon, LULC map has been produced (**Fig. 16**) as it required to run the InVEST model as well as to figure out the carbon stocks of the study area. Like NDVI, LULC map also gives a strong perception about the forest structure.

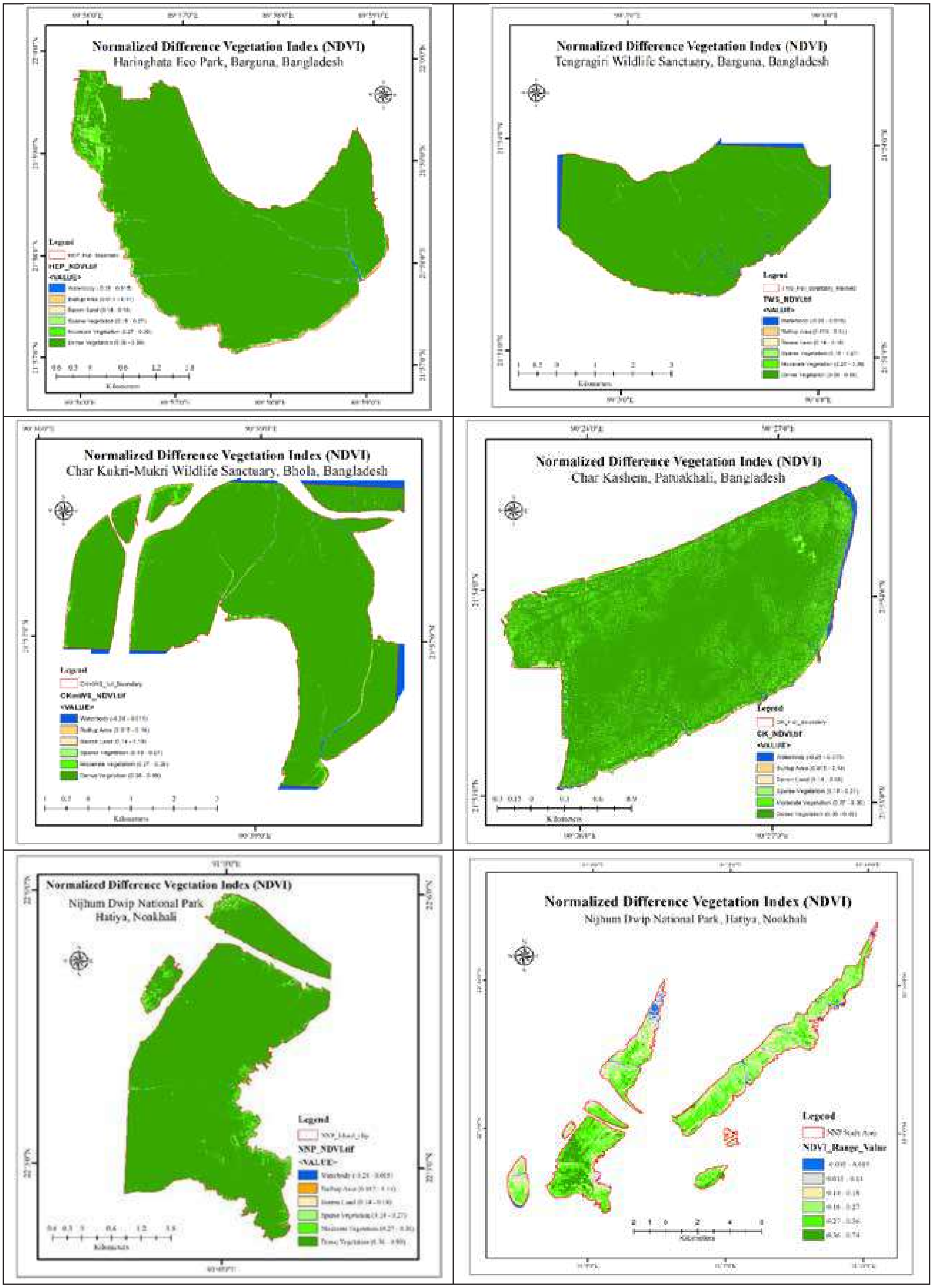

(Source: USGS, Compiled by Author, 2025).

Figure. 15: NDVI Map of the Haringhata Eco Park (HEP) of Bangladesh.

The Land Use and Land Cover (LULC) map of Haringhata Eco Park (HEP) shows a landscape mainly covered by dense mangrove vegetation, with Keora (Sonneratia apetala) and Gewa (Excoecaria agallocha) as dominant species. These species occupy large areas of the park, indicating a mature and ecologically stable mangrove system. There is very little barren land or open space, suggesting minimal human disturbance and effective conservation management. Small scattered water bodies typical of coastal and estuarine mangrove environments are present, supporting the area's ecological health and hydrological balance.

Tengragiri Wildlife Sanctuary (TWS) features extensive intact mangrove forests, also dominated by Keora and Gewa. Additional species such as Karanja (Pongamia pinnata) and Boloi add to its plant diversity. The LULC data show minimal degradation and almost no open or barren land, indicating limited human impact. Surrounded by tidal channels and estuarine waters, the sanctuary serves as an important coastal biodiversity reserve and a significant carbon sink. Char Kukri-Mukri Wildlife Sanctuary (CKmWS) displays a varied landscape with dense and moderately dense vegetation. The mangrove ecosystem is rich and diverse, dominated by Keora, Gewa, and Choila (Sonneratia caseolaris). Several water channels cross the sanctuary, with only small patches of barren land. This varied species composition and habitat complexity make CKmWS a dynamic environment crucial for biodiversity, nutrient cycling, and coastal protection. Char Kashem (CK) shows a healthy mix of mangrove vegetation dominated by Keora and Gewa, with large areas influenced by tidal water bodies. Keora's dominance aligns with natural regeneration and plantation efforts in the region. Although some patches of Rain Tree (Samanea saman) and open spaces exist, they are limited and do not affect the overall vegetation health. The low amount of barren land indicates strong ecological stability and highlights Char Kashem's potential as a site for afforestation and conservation. Nijhum Dwip National Park (NNP) is characterized by extensive dense mangrove forests, particularly Keora and Gewa, which form the core forest structure. The presence of tidal creeks and water bodies enhances habitat complexity and supports diverse fauna. Barren land is minimal, reflecting a largely undisturbed environment. The park's relative isolation has helped maintain high ecological integrity, making it a critical area for biodiversity conservation and carbon storage. The LULC maps show that the mangrove forest on Nijhum Dwip Island is very dense compared to the northern mainland part of Hatiya Island, which has sparser vegetation.

Across all five study sites, there is a consistent pattern of high-density mangrove cover dominated by Keora and Gewa, species known for rapid growth and strong carbon sequestration potential. The limited presence of barren land and open areas suggests minimal human interference and successful natural or assisted regeneration. The widespread occurrence of water bodies reflects the tidal and estuarine characteristics of these mangrove ecosystems, which are essential for nutrient exchange and sediment deposition. The lack of widespread degraded or open land indicates that these mangrove forests are not only surviving but thriving under current environmental conditions and management efforts. This consistency across different locations underscores the success of conservation strategies and plantation programs in Bangladesh's coastal zones.

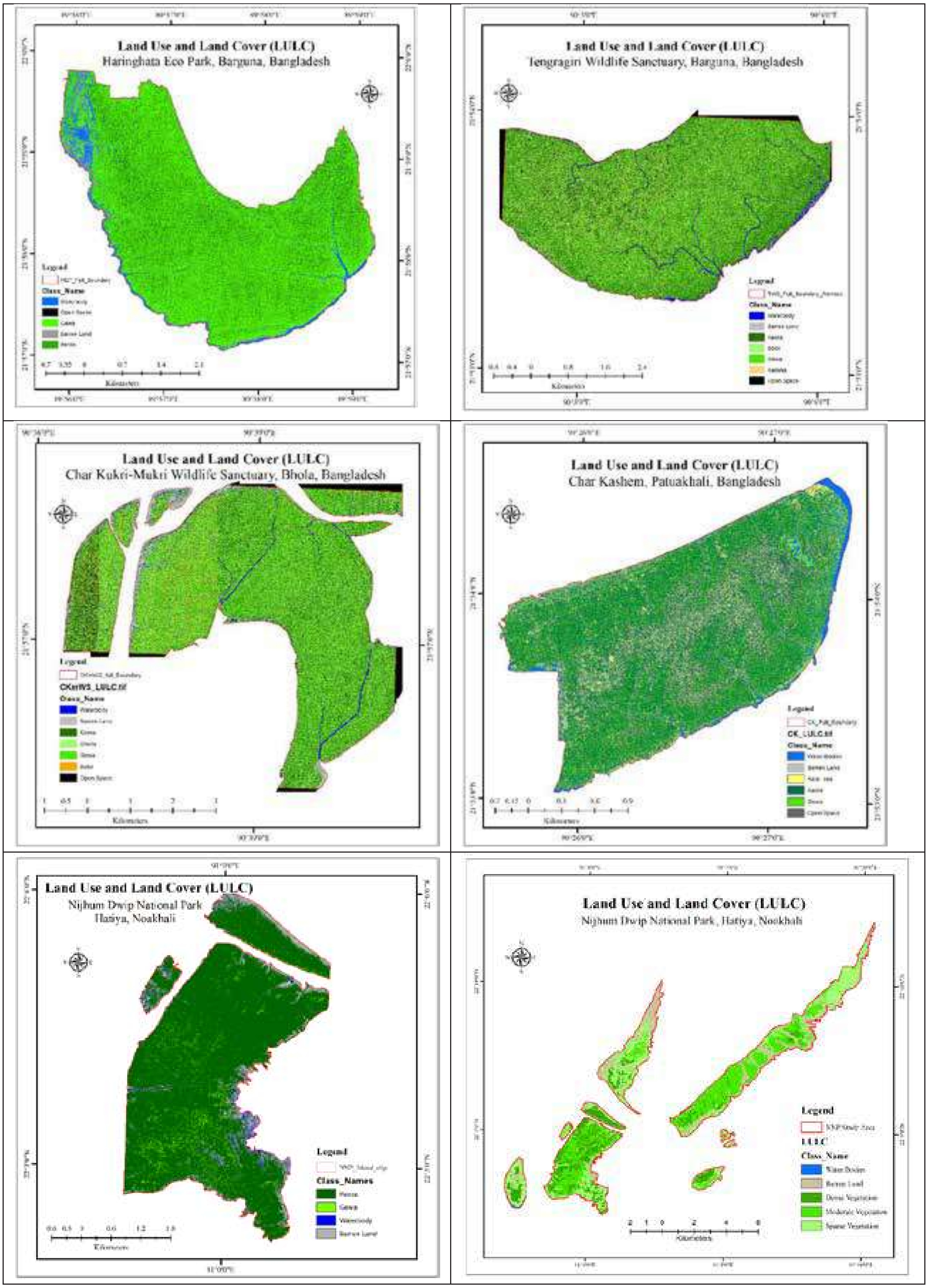

(Source: USGS, Compiled by Author, 2025).

Figure. 16: LULC Map of the Haringhata Eco Park (HEP) of Bangladesh.

4.15 InVEST Model

The InVEST (Integrated Valuation of Ecosystem Services and Tradeoffs) model necessitates specific data formats to function effectively. In this case, it requires information in .img or .tif format, which is typically generated through remote sensing techniques and Geographic Information System (GIS) applications. Additionally, information regarding carbon pools must be provided in .csv format for proper analysis.

To construct the carbon pool data, interactions between the Land Use and Land Cover (LULC) map and the three carbon pools (aboveground biomass, belowground biomass and soil organic) were performed. This integration is crucial for developing accurate carbon stock estimations. Simultaneously, field-level data collected from the study area was statistically analyzed using software such as Microsoft Excel, SPSS, and R. This analysis aimed to uncover patterns and correlations, which were then cross-referenced with ArcGIS software to determine the zonal statistics for each pixel in the dataset.

The combination of remote sensing and GIS data is essential for the InVEST model, which allows for the production of a detailed carbon stocks model. For all the selected mangrove sites, the model was developed by using aboveground biomass, belowground biomass and soil organic carbon data. The results indicate that the highest carbon stock value recorded at Nijhum Dwip National Park is 0.00279875 ton (**Fig. 17 & Table. 07**). This value is actually representing the amount of carbon per pixel (0.5 meter^2). Due to budget constraints, in this report only the Nijhum Dwip Island image has been purchased and analyzed. To have a better perspective, both the free version and purchased imagery of Nijhum Dwip Island has taken and evaluated. With aboveground, belowground and soil organic carbon pool data, the purchased imagery analysis shows that Nijhum Dwip Islands have 15.499179 km^2 area, having highest carbon stocks value of 0.00279875 ton /0.5 meter^2. Whereas, the lowest carbon stock value is 0.00243491.

The range of carbon stock values recorded at five selected mangrove plantation sites in Bangladesh (**Table. 07**), highlighting spatial variability in carbon sequestration potential across these ecosystems. Among the sites, Nijhum Dwip National Park demonstrates the highest carbon stock values, with a maximum of 0.00279875 t and a minimum of 0.00243491 t. This relatively high and narrow range suggests dense, mature plantations and possibly consistent species composition or favorable ecological conditions supporting biomass accumulation. Char Kashem also exhibits a notably high maximum carbon stock (0.00219946 t), although its lowest value (0.00032750 t) indicates greater internal variability, potentially reflecting heterogeneous plantation characteristics such as mixed species, varying stand ages, or site-specific environmental factors.

In contrast, Tengragiri Wildlife Sanctuary shows both a relatively high minimum (0.00122281 t) and maximum (0.00167497 t) carbon stock, suggesting stable carbon sequestration levels across the site with less spatial variability. Haringhata Eco Park and Char Kukri-Mukri Wildlife Sanctuary, however, show comparatively lower carbon stock values, with Haringhata recording a maximum of 0.00100478 t and a minimum of 0.00016833 t, while Char Kukri-Mukri ranges between 0.00055084 t and 0.00029550 t. These lower values may be associated with younger plantations, lower tree density, species with slower biomass accumulation rates, or environmental stress. Overall, the variation in carbon stock values across these sites underscores the influence of ecological, biological, and management factors on carbon sequestration capacity in Bangladesh's coastal mangrove ecosystems.

Table 07: Highest and Lowest Carbon Stock Value (each Pixel= 0.5 m^2) in the Selected Mangrove Forest.

Study Sites	Highest Carbon Stock (t)	Lowest Carbon Stock (t)
Haringhata Eco Park	0.00100478	0.00016833
Tengragiri Wildlife Sanctuary	0.00167497	0.00122281
Char Kukri-Mukri Wildlife Sanctuary	0.00055084	0.00029550
Char Kashem	0.00219946	0.00032750
Nijhum Dwip National Park	0.00279875	0.00243491

The Carbon Stocks model generated using the InVEST tool provides a spatial view of carbon storage across five study sites: Char Kashem, Char Kukri-Mukri Wildlife Sanctuary, Haringhata Eco Park, Tengragiri Wildlife Sanctuary, and Nijhum Dwip National Park (**Fig. 17**). The model maps carbon distribution based on land cover and vegetation density.

At Haringhata Eco Park, carbon stock varies notably, with higher storage in dense mangrove areas and lower values in degraded zones, indicating good sequestration potential in healthy forests. Tengragiri Wildlife Sanctuary shows the highest carbon stock among the sites, reflecting its dense, well-established mangrove forests, though some less vegetated areas remain. Char Kukri-Mukri Wildlife Sanctuary has generally low carbon stocks similar to Char Kashem but with some denser patches centrally, suggesting partial forest recovery. Char Kashem displays predominantly low carbon storage, with small pockets of higher values, likely due to sparse or young vegetation and possible land degradation. Nijhum Dwip National Park exhibits a broad range of carbon stocks, with many areas showing high values linked to dense mangroves like Sonneratia apetala (Keora) and Excoecaria agallocha (Gewa). This highlights the park's role as a significant carbon sink and its importance for climate change mitigation.

Overall, the InVEST carbon stocks map reveals varied carbon storage across the sites, with dense mangrove and coastal vegetation areas especially in Haringhata, Tengragiri, and Nijhum Dwip holding the greatest carbon sequestration potential. Many areas still have low carbon stocks due to sparse or disturbed forests. Enhancing and protecting mangrove and coastal ecosystems in these key areas could greatly boost carbon storage and improve coastal resilience to climate impacts like sea-level rise and storms.

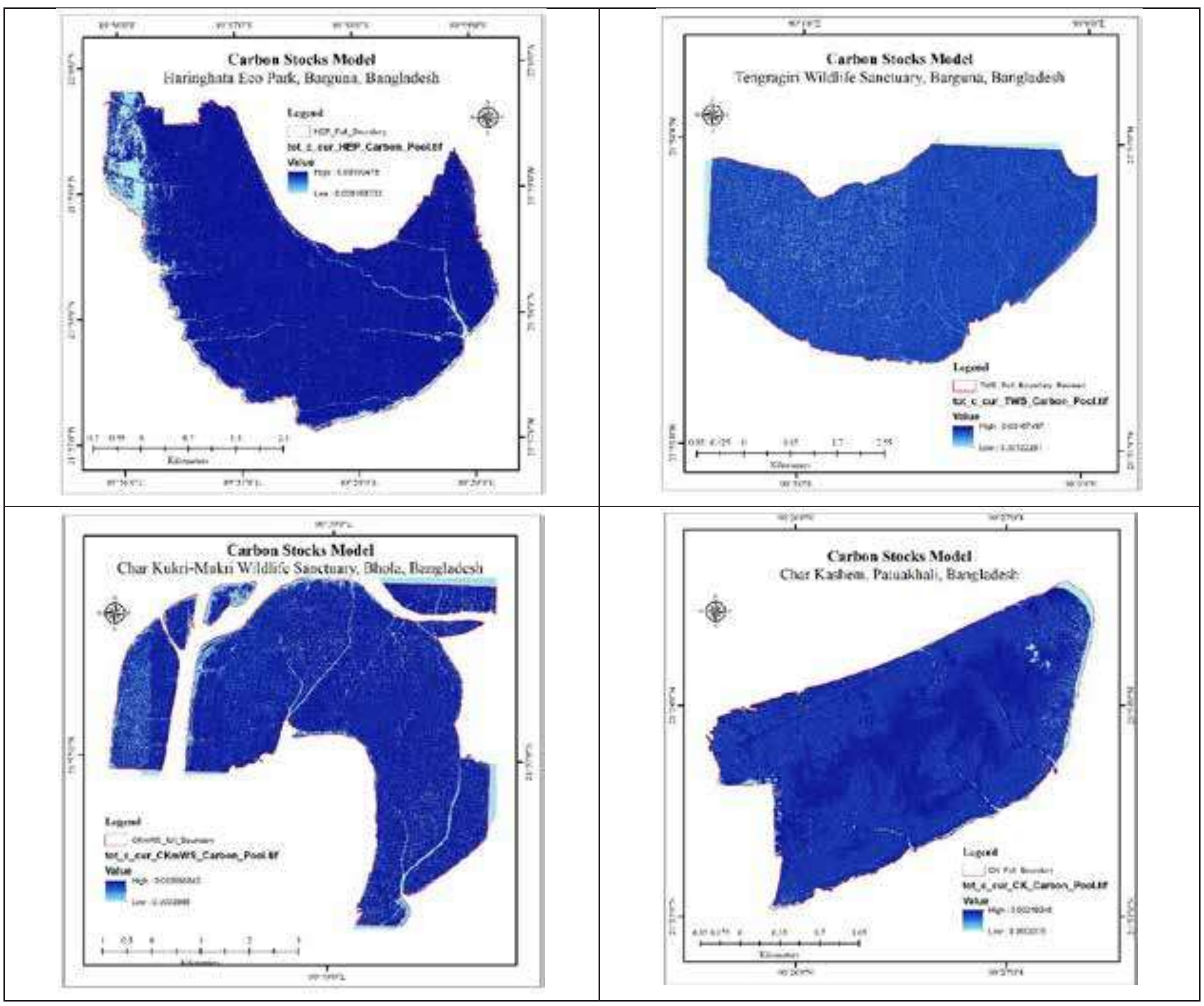

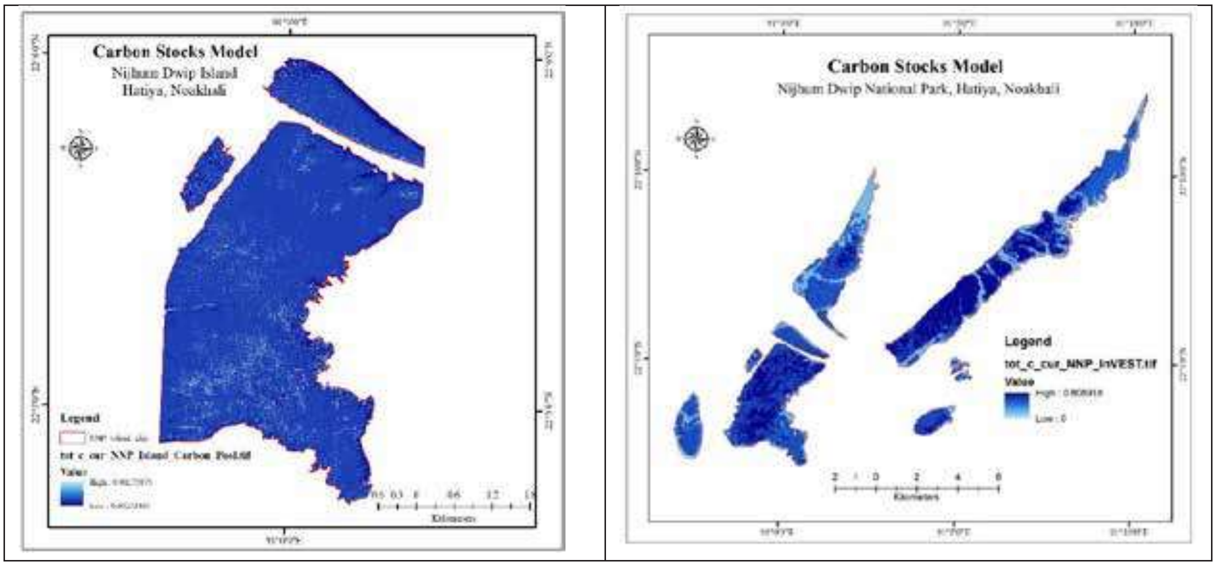

(Source: USGS, Compiled by Author, 2025).

Figure. 17: Carbon Stocks Model of the Haringhata Eco Park (HEP) of Bangladesh.

4.16 Comparative Analysis of Allometric Equations and InVEST Model Results

Estimating carbon storage and biomass is vital for effective forest management, climate change mitigation, and evaluating ecosystem services. Accurate assessments help policymakers and conservationists make informed decisions to reduce carbon emissions and promote sustainable land use. This research compares two common methods for estimating carbon storage: allometric equations and the InVEST model. Allometric equations use empirical relationships between measurable tree attributes (like diameter and height) and biomass or carbon content, providing site-specific accuracy. In contrast, the InVEST model is a GIS-based tool that estimates carbon storage by aggregating carbon pools based on land-use and land-cover maps, offering scalable, landscape-level insights.

A comparative analysis was conducted across five study sites in Bangladesh: Haringhata Eco Park, Tengragiri Wildlife Sanctuary, Char Kukri-Mukri Wildlife Sanctuary, Char Kashem, and Nijhum Dwip National Park. Total carbon stocks were estimated independently by both methods, and the ratio between allometric and InVEST estimates was calculated to assess consistency. A ratio near 1 indicates strong agreement, while lower values suggest discrepancies. Results show variability both spatially and methodologically. Char Kukri-Mukri Wildlife Sanctuary, Nijhum Dwip National Park, and Haringhata Eco Park demonstrated relatively strong agreement with ratios of 0.924, 0.863, and 0.846 respectively (**Table. 08**). Tengragiri Wildlife Sanctuary and Char Kashem showed lower agreement, with ratios of 0.405 and 0.461, likely due to differences in species composition and forest density.

Overall, the allometric method estimated a total carbon stock of 302,252 tons across all sites, while the InVEST model estimated 431,708 tons, resulting in an average ratio of 0.70. This indicates the allometric method captures about 70% of the carbon stock estimated by InVEST. These differences emphasize the need for local calibration of models and integration of field data with spatial tools to improve accuracy. In conclusion, this comparison highlights the strengths and limitations of both approaches and underscores the importance of refining spatial models like InVEST with localized data. Such efforts are essential for enhancing carbon stock assessments, supporting climate change mitigation, forest management, and carbon trading in diverse ecosystems like Bangladesh's coastal and mangrove forests.

Table 08 Comparison of Allometric Equation and InVEST Model Result.

Study Sites	Total Carbon (ton)		Ratio
	Allometric Equation	InVEST Model	
Haringhata Eco Park	48403.18	57173.557002	0.8464
Tengragiri Wildlife Sanctuary	51187.97	126475.670023	0.4047
Char Kukri-Mukri Wildlife Sanctuary	52732.30	57069.820365	0.924
Char Kashem	17039.51	36990.602428	0.4605
Nijhum Dwip National Park	132889.38	153998.817358	0.8631
Total	**302252.34**	**431708.4672**	**0.7001**

4.17 Factors of Carbon Stocks

The factors influencing carbon stocks in the selected mangrove forest can be broadly categorized into natural and anthropogenic factors, both of which contribute to the spatial variability in carbon accumulation. It is important to note that drawing definitive conclusions regarding the exact factors influencing carbon stock variability based on the allometric eqation and imagery analysis is incongruent. However, several factors stand out as notable contributors to the observed variability in carbon stocks in the selected forest.

Species Composition: Different mangrove species have distinct capacities to sequester carbon due to variations in their biomass, growth rates, and structural characteristics. For instance, in the study site, the two dominant species, Keora (Ceriops tagal) and Gewa (Excoecaria agallocha), demonstrate differing carbon storage potentials. A single Keora tree can store 264.41 tons of carbon, while a Gewa tree stores only 14.25 ton of carbon. Both allometric calculations and the InVEST model reveal that areas dominated by Keora trees tend to store significantly higher amounts of carbon compared to those dominated by Gewa trees.

Tree Age and Density: Older mangrove trees and higher tree densities generally contribute to greater carbon stocks. This is due to the increased biomass in mature trees and the extensive root systems they develop, which act as additional carbon storage. The InVEST model maps clearly demonstrate that areas with older trees and higher tree densities exhibit higher carbon storage capacities.

Soil Characteristics: Soil plays a critical role in carbon storage, especially in terms of soil organic carbon (SOC) content, soil texture, and soil depth. Clayey soils, for example, have a higher capacity for carbon retention compared to more permeable sandy soils (Rayment and Higginson, 1992; McKenzie, et. al., 2004). The composition and texture of the soil in Nijhum Dwip National Forest directly influence the carbon sequestration potential of the mangrove ecosystems.

Tidal Influence and Salinity: Mangrove ecosystems are heavily influenced by tidal cycles and salinity levels, which impact the growth and survival of mangrove species. Regular tidal flooding can deposit nutrients and organic matter in the soil, enhancing carbon storage. However, salinity fluctuations can also limit the growth of certain species, affecting overall carbon accumulation in specific areas of the forest.

Elevation and Topography: The elevation and topographic features of the land influence the flooding regime and salinity levels, which in turn affect the types of mangrove species that thrive in the area. Higher elevations might be less frequently flooded, affecting the species composition and, consequently, the carbon storage potential. Low-lying areas that are regularly inundated by tides may support more carbon-sequestering species and contribute to higher carbon stocks.

Human Activities: Anthropogenic activities, including deforestation, land-use changes, farming, and coastal development, can drastically alter the carbon stocks of mangrove ecosystems. Conversion of mangrove forests for agriculture or infrastructure development not only reduces the carbon stored in biomass but also disrupts the soil's ability to retain organic carbon. In contrast, conservation and restoration efforts can significantly enhance the carbon storage capacity of these ecosystems.

Overall, the variability in carbon stocks within the selected mangrov forest is influenced by a complex interplay of species composition, tree age and density, soil characteristics, tidal influence, elevation, and human activities. While it is premature to make conclusive statements about the exact factors influencing carbon stocks across the selected forest based on the allometric equation and imagery analysis, these factors provide valuable insights into the mechanisms driving carbon sequestration in mangrove ecosystems. Future studies encompassing multiple sites within the forest will offer a clearer understanding of these dynamics.

5.0 KEY FINDINGS

The key findings outlined below reveal important insights into species composition, carbon sequestration patterns, and the effectiveness of different assessment methods across diverse ecological settings.

- Gewa (Excoecaria agallocha) and Keora (Sonneratia apetala) dominate the study sites, with Gewa comprising 56.14% of the tree population and Keora 30.61%, making up nearly 87% of the total tree count. Native species like Sundari (Heritiera fomes) and Baen (Avicennia officinalis) are present in low numbers, indicating low species diversity in the planted mangrove areas.
- Species composition varies across sites, with Gewa and Keora being dominant in most, though TWS and CKmWS exhibit more species diversity. Haringhata Eco Park (HEP), Char Kukri-Mukri Wildlife Sanctuary (CKmWS), and Nijhum Dwip National Park (NNP) show ongoing afforestation efforts, with dense shrub and seedling populations.
- The dominance of Gewa and Keora contributes significantly to carbon stock due to their high biomass, but low species diversity may impact long-term ecosystem resilience. The correlation between Diameter at Breast Height (DBH) and tree height is positive across all sites, with DBH being a better predictor for carbon sequestration.
- Carbon storage varies by species, with Goran trees storing between 1,000 kg and 3,000+ kg of carbon, followed by Keora, which shows variable carbon stock across sites. Boloi and Gewa store less than 50 kg of carbon on average, with significant differences observed in carbon stock across sites like HEP, TWS, CKmWS, CK, and NNP.
- The study confirms that larger trees, particularly Keora and Goran, have significantly higher carbon storage due to their size and biomass. Non-linear regression models also show that both DBH and height correlate strongly with carbon stock, with mature and larger trees contributing disproportionately to carbon sequestration.
- Keora and Goran are the most effective species for afforestation and restoration due to their high carbon sequestration potential. DBH consistently correlates more strongly with carbon stock than tree height, with larger trees, particularly mature ones, storing disproportionately higher amounts of carbon.
- Despite the dominance of a few species like Gewa and Keora, mangrove forests in the study areas support biodiversity and ecosystem functions. However, the low species diversity in some areas, particularly at HEP, CK, and NNP, raises concerns about the long-term sustainability of these ecosystems if not managed properly.
- The study highlights the challenges with traditional biomass and carbon stock assessment methods, which are labor-intensive and costly. Remote sensing techniques, including satellite imagery and modeling tools

like InVEST, provide more efficient ways to estimate and monitor carbon stocks. Calibration of these models with field-based data is essential to ensure accurate carbon storage predictions.

- Remote sensing tools, including NDVI and LULC maps, are essential for large-scale monitoring of carbon stocks. These methods reveal that study sites like NNP, TWS, and HEP have healthy, dense mangrove ecosystems, indicating strong carbon sequestration potential. LULC maps also show stable mangrove cover in most sites, supporting conservation efforts.
- The study underscores the value of integrating ground-based field measurements with spatial models to improve carbon stock estimates, especially in the context of climate change mitigation, forest management, and carbon trading schemes. The InVEST model estimates higher carbon stocks than allometric equations, highlighting the importance of model calibration for improved accuracy. Differences between models were noted at sites like Tengragiri and Char Kashem, where factors like forest coverage and species composition can cause discrepancies.
- Across all sites, the Allometric Equation estimated a total carbon stock of 302,252.34 tons, whereas the InVEST model estimated 431,708.47 tons. This resulted in an average ratio of 0.7001, indicating that the Allometric Equation estimated about 70% of the carbon stock of the InVEST model.
- Carbon stock values vary significantly across sites. NNP records the highest total biomass and carbon stock, with notable contributions from species like Keora and Gewa. Sites such as Char Kashem, however, show lower carbon stock values, which may be linked to less dense vegetation or species-specific characteristics.
- The study highlights the critical importance of areas with dense mangrove cover, such as Nijhum Dwip and Tengragiri, for future conservation and restoration projects. These areas have the highest carbon sequestration potential, making them vital for long-term climate mitigation strategies.
- Ecological factors such as species composition, plantation age, and environmental stressors significantly influence carbon stock differences across sites. Sites like Nijhum Dwip and Tengragiri are identified as having the highest carbon sequestration potential, making them key targets for future conservation and restoration efforts.
- Mangrove forests play a crucial role in climate change mitigation by sequestering carbon. The study emphasizes the importance of conserving these ecosystems to ensure long-term carbon storage and supports the use of remote sensing and modeling tools for continuous monitoring and management.

These findings highlight the critical role of species composition, tree structure, and site-specific conditions in shaping carbon sequestration dynamics within mangrove ecosystems. They also emphasize the need for integrated monitoring approaches and adaptive management strategies to enhance the long-term carbon storage potential and ecological resilience of mangrove plantations in Bangladesh.

6.0 LIMITATIONS OF THE RESEARCH

While this study contributes valuable knowledge on the carbon stock capacity of the selected mangrove plantations of Bangladesh, several limitations must be considered. These limitations highlight areas for future research and refinement in methodology.

- Most of the selected sites are dominated by a few fast-growing species like Gewa and Keora, while native species such as Sundari and Baen are sparsely represented. This limited diversity may constrain the generalizability of carbon stock patterns across more diverse mangrove ecosystems.
- The accuracy of biomass and carbon stock estimations using allometric equations depends on species-specific models, many of which are generalized and not locally calibrated. This could introduce bias, especially in areas with mixed or uncommon species compositions.

- This research heavily relies on remote sensing techniques, including the use of purchased satellite imagery. However, due to budget constraints, it was not possible to acquire imagery for the entire study area.
- Differences in carbon stock estimates between the InVEST model and field-based allometric equations reveal inconsistencies due to model assumptions, input resolution, and spatial variability. These discrepancies highlight the need for further calibration and validation of remote sensing models with field data.
- The study represents a snapshot in time without incorporating multi-seasonal or long-term changes in forest structure or carbon accumulation. This limits the ability to assess trends or evaluate the impact of environmental factors such as storms, sea-level rise, or seasonal dynamics.
- While DBH and tree height were used effectively for biomass estimation, measurement errors in dense forest conditions or for irregularly shaped trees may affect the accuracy of carbon stock calculations.
- The research primarily focuses on aboveground and belowground biomass carbon; which are significant components of total carbon in mangrove ecosystems. But field level soil organic carbon data were not included due to resource, budget and time constraints.
- The study does not deeply assess human activities (e.g., cutting, grazing) or site-specific environmental stressors (e.g., salinity, erosion) that may influence forest health and carbon storage potential.
- Although the five sites (HEP, TWS, CKmWS, CK, NNP) offer ecological variety, they may not fully represent the vast heterogeneity of all mangrove regions in Bangladesh. Expanding to more diverse zones could improve the robustness of the conclusions.

Despite these constraints, the research provides a useful framework for understanding mangrove carbon stocks. Overcoming these challenges in subsequent studies will enhance the accuracy and applicability of carbon sequestration models, strengthening efforts toward effective mangrove conservation.

7.0 RECOMMENDATIONS

Based on the key findings of the research, the following recommendations have been developed to enhance carbon stock estimation, support sustainable mangrove management, and strengthen climate change mitigation efforts. These recommendations are intended to guide future afforestation practices, monitoring strategies, and policy decisions across coastal plantation sites.

- Increase species diversity in mangrove plantations by incorporating native species like Sundari and Baen alongside fast-growing species like Keora and Gewa to improve ecosystem resilience and biodiversity.
- Since DBH has the strongest correlation with carbon stock, it should be prioritized in future carbon stock estimation methods, particularly in field-based assessments, for more accurate predictions of carbon sequestration potential.
- Develop afforestation and management strategies tailored to local conditions such as salinity, tidal influence, and soil types to maximize carbon sequestration and enhance ecological health.
- Conduct long-term monitoring to track changes in carbon stock, species composition, and forest structure, ensuring that plantations continue to contribute effectively to climate change mitigation.
- Combine remote sensing tools (e.g., NDVI, LULC) with field-based measurements (e.g., DBH, tree height) for improved accuracy in carbon stock estimation and a more comprehensive landscape-level understanding.
- Use both InVEST and allometric equations for more accurate carbon sequestration assessments, especially for large-scale restoration or afforestation projects. Moreover, combining remote sensing techniques with the InVEST model offers a time and cost-efficient method for large-scale carbon stock assessments.

- Integrating UAV (Unmanned Aerial Vehicle) or drone imagery into the research could significantly enhance its scope by providing high-quality images. This would improve the accuracy of identifying tree species based on shape and color tone, and also support the creation of a DN value database to capture seasonal variations in vegetation.
- Target areas with lower carbon sequestration potential for restoration efforts, focusing on increased planting density, soil improvement, and species diversification.
- Promote community-based approaches to mangrove restoration, ensuring local communities are involved in managing and monitoring ecosystems to improve both ecological and socio-economic sustainability.

These recommendations aim to guide future initiatives toward more sustainable and scientifically informed mangrove management. Emphasizing ecological diversity, accurate carbon estimation, and inclusive participation will strengthen the role of mangrove plantations in long-term climate change mitigation.

8.0 CONCLUSION

This research project provides a detailed assessment of mangrove forest composition, structural characteristics, and carbon sequestration potential across five key sites in coastal Bangladesh. Through a combination of extensive field data, statistical modeling, and species-specific carbon estimation, the research offers valuable insights into the dynamics of these ecosystems. Dominant species such as Keora (*Sonneratia apetala*) and Gewa (*Excoecaria agallocha*) were found to contribute significantly to the overall biomass and carbon stocks, highlighting their importance in afforestation and climate mitigation initiatives. However, the limited presence of native species like Sundari (*Heritiera fomes*) and Passur (*Xylocarpus moluccensis*) raises concerns about the long-term ecological health, species diversity, and sustainability of these forests.

The project also identifies Diameter at Breast Height (DBH) as the most reliable indicator of carbon stock, demonstrating its critical role in monitoring and modeling carbon sequestration across mangrove forests. Furthermore, the variability in species composition and forest structure across the different sites underscores the need for adaptive and site-specific restoration strategies. Tailored approaches that consider local environmental conditions are essential for maximizing both carbon storage and biodiversity outcomes in mangrove ecosystems.

The findings of this project stress the importance of balancing carbon sequestration goals with biodiversity conservation. While fast-growing species with high carbon storage potential are key to achieving short-term climate objectives, the inclusion of a broader range of native species is crucial for long-term ecosystem stability and resilience. Restoration programs must therefore incorporate strategies that promote both species diversity and ecological function, in line with ecosystem-based adaptation principles.

From a policy perspective, the results offer a solid scientific foundation for informing REDD+ initiatives, national carbon inventories, and coastal resilience planning. The role of mangrove forests extends beyond carbon sequestration—they are vital buffers against climate change impacts such as sea level rise, coastal erosion, and extreme weather events. Integrating remote sensing technologies, GIS tools, and continuous field monitoring will be essential for maintaining accurate, scalable assessments of mangrove ecosystem services and their contributions to climate change mitigation.

In conclusion, this project demonstrates the power of combining empirical fieldwork with advanced modeling techniques to provide actionable insights for mangrove conservation and climate change mitigation. By bridging ecological science with practical land-use planning, the study contributes to broader efforts aimed at preserving coastal ecosystems, enhancing climate resilience, and promoting sustainable development in the face of climate change.

REFERENCES

Adame M. F., Kauffman J. B., Medina I, Gamboa J. N., Torres O, Caamal J. P., Reza M (2013) Carbon stocks of tropical coastal wetlands within the karstic landscape of the mexican caribbean. PLoS One 8(2):e56569. doi:10.1371/journal.pone.0056569.

Akhter, M., Mahmood, H., Birigazzi, L. 2013. Tree volume and biomass allometric equations of Bangladesh. FD and FAO, Dhaka, Bangladesh

Alongi, D. M. (2014) Carbon Sequestration in Mangrove Forests. *Carbon Management*, 5(3), 189-201.

Alongi, D., Murdiyarso, D., Fourqurean, J., Kauffman, J., Hutahaean, A., Crooks, S., Lovelock, C., Howard, J., Herr, D., Fortes, M., (2015) Indonesia's blue carbon: a globally significant and vulnerable sink for seagrass and mangrove carbon. Wetl. Ecol. Manag. 1-11.

Anderson K, Bows A (2011) Beyond 'dangerous' climate change: emission scenarios for a new world. Philos Trans R Soc A 369(1934):20–44. doi:10.1098/rsta.2010.0290.

Arifeen, H.M.; Phoungthong, K.; Mostafaeipour, A.; Yuangyai, N.; Yuangyai, C.; Techato, K.; Jutidamrongphan, W. (2021) Determine the Land-Use Land-Cover Changes, Urban Expansion and Their Driving Factors for Sustainable Development in Gazipur Bangladesh. Atmosphere. 12, 1353.

Attarchi, S.; Gloaguen, R. (2014) Improving of above groud biomass using dual polarimetric PALSAR and ETM+ data in the Hyrcanian fore tainnuomts (Iran). Remote Sens. 6, 3693–3715.

Banglapedia (2022) Coastal Greenbelt.https://en.banglapedia.org/index.php/Coastal_Greenbelt

Barbier, E. B., Hacker, S. D., Kennedy, C., Koch, E. W., Stier, A. C., and Silliman, B. R.(2011). The value of estuarine and coastal ecosystem services. Ecol. Monogr. 81 (2), 169– 193. doi: 10.1890/10-1510.1

Barbier, E. B., Hacker, S. D., Kennedy, C., Koch, E. W., et al. (2011) The Value of Estuarine and Coastal Ecosystem Services. *Ecological Economics*, 70(2), 201-213.

Bauer, J. E., Cai, W.-J., Raymond, P. A., Bianchi, T. S., Hopkinson, C. S., and Regnier, P. A.

G. (2013) The changing carbon cycle of the coastal ocean. Nature 504, 61–70. doi: 10.1038/nature12857.

Cabral P, Feger C, Levrel H, Chambolle M, Basque D. (2016) Assessing the Impact of Land- Cover Changes on Ecosystem Services: A First Step Toward Integrative Planning in Bordeaux, France. Ecosyst Ser. 22:318–327.

Cero´n-Breto´n R. M, Cero´n-Breto´n J. G, Sa´nchez-Junco R. C, Damia´n-Herna´ndez D. L, Guerra-Santos JJ, Muriel-Garcia M,Cordova-Quiroz AV (2011) Evaluation of carbon sequestration potential in mangrove forest at three estuarine sites in Campeche Mexico. Int J Energy Environ 5(4):487–494.

Chan KM, Shaw MR, Cameron DR, Underwood EC, Daily G.C. (2006) Conservation Planning for Ecosystem Services. PLoS Biol. 4(11):e379.

Chaturvedi, A.N., Khanna, L.S. (2002) *Forest Mensuration*. Periodical Expert Book Agency, Delhi, India.

Chowdhury, M. A. K., Rhaman, M. M., & Talukder, M. H. (2018) Biodiversity Assessment of Nijhum Dwip National Park, Bangladesh. *Journal of Biodiversity and Conservation*, 7(4), 123-134.

Dahdouh-Guebas, F., Verneaux, V., & Koedam, N. (2005) An Evaluation of the Carbon Stock of Mangrove Forests in the Indian Ocean. *Journal of Coastal Research*, 21(6), 962-974.

Dharmawan I. W. E., Ulumuddin Y. I., (2020) Mangrove Community Structure Data Analysis a guidebook for mangrove health index (MHI) training. Tiago Ferreira, Wayne Rasband, 2012, ImageJ User Guide, http://imagej.nih.gov/ij/docs/guide

Donato D, Kauffman JB, Murdiyarso D, Kurnianto S, Stidham M, Kanninen M (2011) Mangroves among the most carbon-rich forests in the tropics. Nat Geosci 4:293– 297. doi:10.1038/ngeo1123

Duarte, C. M., Middelburg, J. J., and Caraco, N. (2005) Major role of marine vegetation on the oceanic carbon cycle. Biogeosciences 2 (1), 1–8. doi: 10.5194/bg-2-1-2005.

Eggleston HS, Buendia L, Miwa K, Ngara T, Tanabe K; IPCC. (2006) IPCC Guidelines for National Greenhouse Gas Inventories. Institute for Global Environmental Strategies, Hayama, Japan. 2:48–56.

FAO (1994) Mangrove Forest Management Guidelines. FAO Forestry Paper 117.

GOB (2019) Tree and forest resources of Bangladesh: report on the Bangladesh forest inventory. Forest

Department, Ministry of Environment, Forest and Climate Change. Government of the People's Republic of Bangladesh, Dhaka, Bangladesh.

Goetz, S.J., Baccini, A., and Laporte, N. T. (2009). Mapping and monitoring carbon stocks with satellite observations: a comparison of methods. Carbon Balance Manage **4**, 2. https://doi.org/10.1186/1750-0680-4-2.

Goldstein JH, Caldarone G, Duarte TK, Ennaanay D, Hannahs N, Mendoza G, Polasky S, Wolny S. and Daily G.C. (2012) Integrating Ecosystem-Service Tradeoffs into Land-use Decisions. Proc Natl Acad Sci. 109(19):7565–7570.

Hadjimitsis, D.G., Papadavid, G., Agapiou, A., Themistocleous, K., Hadjimitsis, M.G., Retalis, A., Michaelides, S., Chrysoulakis, N., Toulios, L., Clayton. C.R.I. (2010) Atmospheric correction for satellite remotely sensed data intended for agricultural applications: impact on vegetation indices.

He C, Zhang D, Huang Q, Zhao Y. (2016) Assessing the Potential Impacts of Urban Expansion on Regional Carbon Storage by Linking the LUSD-urban and InVEST Models. Environ Model Softw. 75:44–58.

Henry M et al 2021 A multi-purpose National Forest Inventory in Bangladesh: design, operationalisation and key results For. Ecosyst. 8-12.

Houghton, R., Lawrence, K., Hackler J, Brown S. (2001) The spatial distribution of forest biomass in the Brazilian Amazon: a comparison of estimates. Global Change Biology, 7:731-746.

IPCC (2007) Expert Meeting on Detection and Attribution Related to Anthropogenic Climate Change. Cambridge University Press, Cambridge. Pp. 540–560.

IPCC (2013) Coastal Wetlands. In: 2013 Supplement to the 2006 IPCC guidelines for National Greenhouse Gas Inventories (eds. Alongi, D, Karim, A, Kennedy, H, Chen, G, Chmura, G, Crooks, S et al.).

InVEST Software (2023) What is InVEST. Policy Support Tools. InVEST Software. Kaur, S., Babbar, D., Sarif, O., Ghatak, A. and Jaafari, A. (2022) Assessment of Carbon Sequestration Using InVEST Model in Delhi, India. Conservation, Management and Monitoring of Forest Resources in India. https://link.springer.com/chapter/10.1007/978-3-030-98233-1_2

Islam, M. R., Uddin, M. N., & Das, S. K. (2019) Ecosystem Services of Mangrove Forests in Bangladesh: A Review. *Bangladesh Journal of Botany*, 48(2), 331-342.

Khan M. N. I., Suwa R., Hagihara A. (2007) Carbon and nitrogen pools in a mangrove stand of Kandelia obovata (S., L.) Yong: vertical distribution in the soil–vegetation system. Wetl Ecol Manag 15(2):141–153. doi:10.1007/s11273-006-9020-8.

Kumar, R. K. V. G. and Barik, D. K. (2018) Assessment of Carbon Storage and Erosion using InVEST Model in Visakhapatnam District, Andhra Pradesh. Journal of Rural Development. Vol. 37 (2). Pp. 207-220.

Laffoley D. D. A., Grimsditch G (2009) The management of natural coastal carbon sinks. IUCN Gland, Switzerland.

Lillesand, T., Kiefer, R.W., Chipman, J. (2015) Remote sensing and image interpretation. John Wiley & Sons., New York.https://naturalcapitalproject.stanford.edu/software/invest

Lovelock, C. E., & Duarte, C. M. (2019). Dimensions of blue carbon and emerging perspectives. Biology Letters, 15(3), 20180781.

Maanan, M., Karim, M., Kacem, H. A., Ajrhough, S., Rueff, H., Snoussi, M. and Rhinane, H. (2019) Modelling the Potential Impacts of Land Use/Cover Change on Terrestrial Carbon Stocks in North-West Morocco. International Journal of Sustainable Development & World Ecology.

McKenzie, N.J., et al. (2004) *Soil Guide: A Handbook for Understanding and Managing Australian Soils*. CSIRO Publishing, Australia.

MacKenzie, R., Sharma, S. and Rovai, A. R. (2021) Environmental Drivers of Blue Carbon Burial and Soil Carbon Stocks in Mangrove Forests. Dynamic Sedimentary Environments of Mangrove Coasts. https://doi.org/10.1016/B978-0-12-816437- 2.00006-9.

Macreadie, P. I., Costa, M. D. P., Atwood, T. B., Friess, D. A., Kelleway, J.J., Kennedy, H., Lovelock, C. E., Serrano, O. and Duarte C. M. (2021) Blue Carbon as a Natural Climate Solution. https://doi.org/10.1038/s43017-021-00224-1.

Mahmood H, Siddique M R H, Abdullah S M R, Islam S M Z, Matieu H, Iqbal M Z and Akhter M 2020 Semi-destructive method to derive allometric aboveground biomass model for village forest of Bangladesh: comparison of regional and pantropical models J. Trop. For. Sci. 32 246–56

Mahmood H, Siddique M R H, Rubaiot Abdullah S M, Costello L, Matieu H, Iqbal M Z and Akhter M 2019 Which option best estimates the above-ground biomass of mangroves of Bangladesh: pantropical or site- and species-specific models? Wetlands Ecol. Manage. 27 553–69.

McLeod, E., Chmura, G. L., Bouillon, S., Salm, R., Björk, M., Duarte, C. M., et al. (2011) A blueprint for blue carbon: toward an improved understanding of the role of vegetated coastal habitats in sequestering CO2. Front. Ecol. Environ. 9, 552-560. doi: 10.1890/110004.

Md Saidur Rahman et al (2021) Environ. Res. Lett. 16 124002, DOI 10.1088/1748- 9326/ac31ee.

Mishra, V.N.; Rai, P.K. (2016) A remote sensing aided multi-layer perceptron-Markov chain analysis for land use and land cover change prediction in Patna district (Bihar), India. Arab. J. Geosci. 9, 249.

Mitra A, Sengupta K, Banerjee K (2011) Standing biomass and carbon storage of above-ground structures in dominant mangrove trees in the Sundarbans. For Ecol Manag 261:1325–1335. doi:10.1016/j.foreco.2011.01.012.

Mokany, K., Raison, R.J. and Prokushkin, A.S. (2006) Critical Analysis of Root: Shoot Ratios in Terrestrial Biomes. Global Change Biology, 12, 84-96. https://doi.org/10.1111/j.1365-2486.2005.001043.x.

Möller, I., Kudella, M., Rupprecht, F., Spencer, T., Paul, M., Van Wesenbeeck, B. K., et al. (2014). Wave attenuation over coastal salt marshes under storm surge conditions. Nat. Geosci. 7 (10), 727–731. doi: 10.1038/ngeo2251.

Mongabay. (2021) Mangrove Restoration and Carbon Sequestration in Bangladesh. Retrieved from mongabay.com.

Murray, B. C., Pendleton, L., Jenkins, W. A., & Sifleet, S. J. G. (2011) Green payments for blue carbon: Economic incentives for protecting threatened coastal habitats. Nicholas Institute Report.

Mueller-Dombois, D., Ellenber, H. (1974) *Aims and Methods of Vegetation Ecology*. New York, Wiley.

Nellemann, C. and Corcoran E. (Eds.) (2009) Blue carbon: In A rapid response assessment (GRID-Arendal: United Nations Environment Programme/ Earthprint).

Nelson E, Mendoza G, Regetz J, Polasky S, Tallis H, Cameron D, Lonsdorf E, Daily GC, Goldstein J, Kareiva P.M., (2009) Modeling Multiple Ecosystem Services, Biodiversity Conservation, Commodity Production, and Tradeoffs at Landscape Scales. Front Ecol Environ. 7(1):4–11.

Pearson, K. (1896) Mathematical contributions to the theory of evolution, III: Regression, heredity and panmixia. Philos. Trans. Roy. Soc. London (A) 187 253–318. Reprinted in Karl Pearson's Early Statistical Papers (1956) 113–178 Cambridge Univ. Press.

Pearson, K. (1897) Mathematical contributions to the theory of evolution. On a form of spurious correlation which may arise when indices are used in the measurement of organs. Proc. Roy. Soc. London 60 489–498.

Pijathilake, I. D. U. H., Udayakumara, E. P. N., Ranaweera, L. V. and Gunatilake, S. K. (2022) Modeling Predictive Assessment of Carbon Storage Model using InVEST model in Uva Province, Srilanka. Modeling Earth Systems and Environment. https://doi.org/10.1007/s40808-021-01207-3

Piao S, Fang J, Ciais P, Peylin P, Huang Y, Sitch S, Wang T (2009) The Carbon Balance of Terrestrial Ecosystems in China. Nature 458:1009–1013. https://doi.org/10.1038/nature07944.

Qiu J, Turner MG. (2013) Spatial Interactions Among Ecosystem Services in an Urbanizing Agricultural Watershed. Proc Natl Acad Sci. 110(29):12149–12154.

Rayment, G.E., and Higginson, F.R. (1992) *Soil Chemical Methods - Australasia*. CSIRO Publishing, Australia.

Sandeep, S., Sivaram, M., Henry, M., Birigazzi, L. 2014. Inventory of volume and biomass tree allometric equations for South Asia. KFRI, Peechi, India, Food & Agriculture Organization of the United Nations, Rome, Italy.

Sapit D., Damrong S., Ladawan P., Chongrak W., Sakhan T, Aor P et al (2011) An assessment of stand structure and carbon storage of a mangrove forest in Thailand. IUFRO World Ser 29:28–30.

Saputra, M.H.; Lee, H.S. (2019) Prediction of Land Use and Land Cover Changes for North Sumatra, Indonesia, Using an ArtificialNeural-Network-Based Cellular Automaton. Sustainability. 11, 3024.

Simson, E. H. (1949) Measurement of diversity. Nature 163: 688.

Salunkhe, O., Khare, P. K., Kumari, R. and Khan, M. L. (2018) A Systematic Reviews on the Aboveground Biomass and Carbon Stocks of Indian Forest Ecosystems.

Strong, J. A., Mazik, K., Piechaud, N., Bryant, L., Wardell, C., Hull, S., Tickle, M., Norrie, E.M., Mcllvenny, H. and Clements, A. (2021) Blue Carbon Restoration in Northern Ireland – Feasibility Study. National Oceanography Centre, UK. University of Hull. Ulster Wildlife.

Sun, W. and Liu, X. (2020) Review on Carbon Storage Estimation of Forest Ecosystem and Applications in China. Forest Ecosystems. https://doi.org/10.1186/s40663-019-0210-2

Sun, J., Zhang, Y., Qin, W. and Chai, G. (2022) Estimation and Simulation of Forest Carbon Stock in Northeast China Forestry Based on Future Climate Change and LUCC. Remote Sensing. doi.org/10.3390/rs14153653. https://doi.org/10.3390/rs14153653

Tallis H.T., Ricketts T, Guerry AD, Wood SA, Sharp R, Nelson E. and Chaplin-Kramer R. (2013) InVEST 2.6.0 user's guide. Stanford: The Natural Capital Project.

Tao Y, Li F, Wang R, Zhao D. (2015) Effects of Land Use and Cover Change on Terrestrial Carbon Stocks in Urbanized Areas: A Study from Changzhou, China. J Clean Prod. 103:651–657.

Tang, X., Zhao, X., Bai, Y., Tang, Z., Wang, W., Zhao, Y., Wan, H., Xie, Z., Shi, X., Wu, B., Wang, G., Yan, J., Ma, K., Du, S., Li, S., Han, S., Ma, Y., Hu, H., He, N., Yang, Y., Han, W., He, H., Yu, G., Fang, J. and Zhou, G. (2018) Carbon pools in China's terrestrial ecosystems: new estimates based on an intensive field survey. PNAS 115:4021–4026. https://doi.org/10.1073/pnas.1700291115

Temmink, R. J., Lamers, L. P., Angelini, C., Bouma, T. J., Fritz, C., van de Koppel, J., et al. (2022). Recovering wetland biogeomorphic feedbacks to restore the world's biotic carbon hotspots. Science 376 (6593), 1479. doi: 10.1126/science.abn1479.

Unsworth, R. K., Nordlund, L. M., and Cullen-Unsworth, L. C. (2019). Seagrass meadows support global fisheries production. Conserv. Lett. 12 (1), e12566. doi: 10.1111/conl.12566

Vicharnakorn, P., Shrestha, R. P., Nagai, M., Salam, A. P. and Kiratiprayoon, S. (2014) Carbon Stock Assessment Using Remote Sensing and Forest Inventory Data in Savannakhet, Lao PDR. Remote Sensing. ISSN 2072-4292. Doi: 10.3390/rs6065452.

Wood, G.B. (1990) Ground-sampling methods used to inventory tropical mixed moist forests. Forest Ecology and Management 35: 199-206.

Wulder, M. A., White, J. C., Nelson, R. F., Næsset, E., Ørka, H. O., Coops, N. C., Hilker, T., Bater, C. W., Gobakken, T. (2012) Lidar Sampling for Large-Area Forest Characterization: A Review. Remote Sens Environ. 121:196–209. https://doi.org/10.1016/j.rse.2012.02.001

Yusuf, H.A., Oludipe, J.J., Adeoye, O.O. and Olorunfemi, I.E. (2019) Carbon Stocks in Aboveground and Belowground Biomass of Sub-Humid Tropical Forest in Southwestern Nigeria. Open Access Library Journal, 6: e5588. https://doi.org/10.4236/oalib.1105588.

Zhang F, Zhan J, Zhang Q, Yao L, Liu W. (2017) Impacts of Land Use/Cover Change on Terrestrial Carbon Stocks in Uganda. Phys Chem Earth Parts A/B/C. 101:195–203.

Developing Habitat-Based Forest Tree Species Distribution and Diversity Models to Support Sylhet Hill Forests Conservation.

by

Dr. Swapan Kumar Sarker

Professor, Department of Forestry & Environmental Science, Shahjalal University of Science & Technology, Sylhet, Bangladesh

CHAPTER 1

INTRODUCTION

1.1 Background and context

The forests of Bangladesh are now experiencing unprecedented threat from deforestation, fragmentation and climate change (Islam, Deb and Rahman, 2017; Chow *et al.*, 2019). Thus, the issue of conserving the remaining remnant vegetations has become forefront. Bangladesh government as a Contracting Party to the Convention on Biological Diversity (CBD) has put high conservation priority on the remaining natural forests, in particular, the reserve forests and protected areas (PAs) (MoEF, 2016). The current vision of the country, particularly as envisioned under the Sustainable Development Goals (SDG) and 8th Five Year Plan (2020-2025), is to improve ecosystem quality through conservation of forests and biodiversity hotspots and to enhance multiple service benefits of ecosystems with active participation of forest dependent people (MoEF, 2016).

Bangladesh mainly comprises three distinct forest ecosystems: hill forests (evergreen to semi-evergreen), plain land Sal (*Shorea robusta*) forest and mangrove forest. Among these, hill forests are exceptionally rich in biodiversity and provide valuable ecosystem goods and services. Hill forests cover an area of 0.67 million ha and mainly located in the Chattogram, Chattogram Hill Tracts and Sylhet regions. To ensure sustainable forest management, the Bangladesh government has declared most of the hill forest areas as reserve forests. To ensure further protection and restoration of the degraded sites, most of the remaining natural patches of the hill reserves have also been brought under Protected Area Management.

Sylhet hill forests in the north-eastern Bangladesh mainly comprise five hill reserves: Tarap Hill Reserve, Raghunandan Hill Reserve, West Bhanugach Reserve, Rajkandi Reserve and Patharia Hill Reserve. A number of nationally priority protected areas (PAs) such as Rema-Kalenga Wildlife Sanctuary (RKWS), Satchari National Park (SNP) and Lawachara National Park (LNP) are located within these hill reserves. These hill reserves in Sylhet, as a whole, cover a major portion of the semi-evergreen to evergreen sub-tropical forest vegetation in Bangladesh. Most importantly, they support about 90% of the nationally declared red listed vascular plant species (Sarker *et al.*, 2013) and many critically endangered primates (e.g., *Trachypithecus phayrei*, *T. pileatus*, *Hoolock hoolock* etc.) (Uddin *et al.*, 2013).

Sylhet Hill Reserves (including the PAs) provide valuable ecosystem services and goods (Chowdhury, 2014). However, an increase in human settlements, conversion of forest lands to agricultural lands, and illegal felling have resulted in rapid fragmentation and degradation of the Sylhet hill forests, leading to loss of species, habitat and biodiversity (Biswas, Swanson and Vacik, 2012), thus threatening the ecosystem health and livelihoods of millions of people living in the north-eastern Bangladesh (Chowdhury *et al.*, 2013; Mukul, Rashid and Khan, 2017).

Modelling and mapping of forest habitat conditions (soil and topography), species habitat suitability (or preference), and tree species diversity are important for (I) pinpointing the locations or species or forest patches requiring immediate or long-term protection, conservation and restoration actions, (II) in evaluating threats to those critical forest areas and (III) in monitoring spatial and temporal changes in habitat conditions, tree species abundance and diversity under future changes in the climate (Socolar *et al.*, 2015).

Given the future effects of climate change and anthropogenic pressures on Bangladesh forests (Chowdhury and Ndiaye, 2017), successful forest management and conservation will require detail scientific knowledge on forest habitat conditions, floristic composition and biodiversity, ecology, silviculture and distribution of individual tree species, and a clear understanding on the social-ecological systems (Rashid et al. 2013, Sarker et al. 2016, 2019a). Most of the forests in Bangladesh are still lagging behind in quantitative analysis of habitat, species and biodiversity distributions and their relation to habitat conditions which is a serious impediment to design and implement much needed conservation efforts (but see Sarker et al. 2015; Sarker et al. 2013). The scenario is even more degrading for the Sylhet Hill Forests (Muzaffar *et al.*, 2011).

Previous biodiversity studies (Uddin et al. 2003, 2013, NACOM 2003, Sarker et al. 2013, 2015, Rana and Akhter 2014, Pavel et al. 2016, Steinbauer et al. 2017, Gupta et al. 2019) on Sylhet Hill Forests, have mainly used either descriptive statistics or multivariate ordination statistics to explain the vegetation distributions therein. While these works offer preliminary ideas on the relationships between forest vegetation communities and environmental variables, they gave less focus on tree species ecology and their drivers. Most importantly, they lack a model-based quantitative framework to make spatial and temporal predictions of habitat conditions, tree species distribution and biodiversity (alpha, beta and gamma) under changing environmental and anthropogenic pressures.

1.2 Problem statement

Bangladesh government enforced logging ban in 1989 and recently extended the ban on cutting of trees in reserve forests until 2030 to halt forest exploitation (Sarker et al. 2011). The government also implemented several co-management programs (NSP, IPAC, CREL) to limit forest destruction and to improve livelihoods of local communities (Uddin and John, 2012). Despite such interventions, continuous habitat degradation and biodiversity loss in Sylhet Hill Forests indicate inefficient formulation and execution of forest management plans and biodiversity conservation actions (Ahsan, Aziz and Morshed, 2016). This inefficiency is closely related to the unavailability of baseline forest information - site-specific habitat conditions, suitable sites for species, and baseline spatial tree diversity (discussed below) - to the central decision makers and field-level forest officials.

1.2.1 Site-specific habitat conditions

Beat- and range-wise spatial models can generate GIS maps of site-specific habitat conditions which can easily guide the foresters during site-specific planting and in identifying areas that require immediate habitat treatment or long-term rehabilitation or restoration programs (Bulmer, Paré and Domke, 2019). These maps will also help in long-term monitoring of the forest physical conditions under future climate change scenarios.

1.2.2 Suitable sites for species

Habitat Suitability Models (HSMs) are standard tools for determining species habitat preferences and for generating spatial maps of the distribution of species under current and future environmental conditions (Franklin, 2010; Duarte, Whitlock and Peterson, 2019). These models help to identify the suitable habitat for a species to survive and reproduce. Therefore, HSMs of tree species can have important contribution to the species-site matching scheme of the BFD while conducting plantation operations or reintroduction of a tree species in its former habitat. In fact, HSMs of forest tree species can guide BFD's Site-Specific Plan for plantation establishment, habitat restoration, protection, and future reforestation projects.

1.2.3 Baseline spatial tree diversity

Habitat-based Biodiversity Models (HBMs) are used to determine the factors responsible spatial and temporal changes in biodiversity (Socolar *et al.*, 2015). The outputs HBMs, biodiversity maps, can help in specifying the biodiversity and endangered species hotspots, identifying the species that require immediate protection, determining the forest habitats suitable for wildlife and in developing realistic spatial conservation plans (Sarker *et al.*, 2019a). Biodiversity maps can also easily detect the most homogeneous (species poor) and heterogeneous (species rich) forest areas which can guide BFD in identifying suitable species and sites for ANR (Assisted Natural Regeneration), enrichment plantation, and rare and endangered species conservation programs.

With a limited logistic support (e.g., inadequate funds and patrolling workforce), local-level forest officials of the Bangladesh Forest Department (BFD) are incapable to efficiently protect and manage the whole reserve areas. Therefore, we need to categorize the reserve areas based on biodiversity (such as maximum (i.e., biodiversity hotspots) to minimum biodiversity). Then we need to identify the areas that support rare and endangered species. This scheme will help BFD to deploy their patrolling workforces at appropriate forest areas. The BFD has recently extended the SMART (Spatial Monitoring and Reporting Tool) patrolling system in the Sylhet Hill Forests for strict forest protection. Beat- and range-wise GIS maps of tree species distribution and biodiversity can increase the patrolling efficiency of the SMART teams by identifying the critical biodiversity areas or by detecting areas (or species) that may be most affected by future human interventions. However, unavailability of species, habitat and biodiversity maps has been a key challenge for BFD in identifying the conservation priority areas and in allocating adequate patrolling workforce in the critical forest areas that require constant surveillance.

Bangladesh has signed and ratified the major conventions related to biodiversity conservation including World Heritage Convention, Ramsar Convention and the Convention on Biological Diversity (Mukul, Rashid and Khan, 2017). Bangladesh has formulated National Biodiversity Strategy and Action Plan (NBSAP), the National Conservation Strategy (2016-2031) and the Biodiversity National Assessment and Program of Action 2020 to implement sufficient measures to halt further degradation of biological resources (MoEF, 2016). For achieving the SDGs target by 2030, the government already prepared a 8th Five Year Plan (2020-2025) to increase productive forest coverage to 20% with 70% tree density (MoEF, 2016).

Sylhet Hill Forests that support a significant portion of the national biodiversity can play an important role in achieving Bangladesh's abovementioned national and international commitments, goals and targets related to sustainable development and biodiversity conservation. However, future changes in the climate and increasing human pressure are expected to have severe impacts on forest habitat conditions, species ecology, and overall biodiversity. Therefore, further unavailability of baseline knowledge on hill forest ecosystem are likely to hinder BFD's success in future plantation establishment, species, habitat and biodiversity conservation, assessment and monitoring programs in Sylhet Hill Forests and elsewhere in the country.

This study is quite in line with the above priorities of the Bangladesh government and focused on two important hill reserves in the Sylhet region: Tarap Hill Reserve (THR) and Raghunandan Hill Reserve (RHR). Two priority PAs of Bangladesh, Rema-Kalenga Wildlife Sanctuary (RKWS) and Satchari National Park (SNP) are a part of these hill reserves. The overarching goal of the project was to deliver baseline scientific knowledge on habitat conditions, species site suitability, and spatial distribution of biodiversity (alpha, beta and gamma) to assist BFD's present and future initiatives on sustainable forest management and biodiversity conservation in the Sylhet Hill Forests.

1.3 Objectives

1.3.1 Specific objectives

I. To develop:

(A) Spatially Explicit Forest Habitat Models

(B) Habitat Suitability Models (HSMs) for important indigenous and endangered tree specie

(C) Habitat-based Biodiversity Models (HBMs) for the Tarap Hill Reserve (THR) and Raghunandan Hill Reserve (RHR).

II. To develop:

(A) Digital maps of forest habitat conditions

(B) Digital maps of tree species distribution and

(C) Digital Biodiversity maps for the Tarap Hill Reserve (THR) and Raghunandan Hill Reserve (RHR).

CHAPTER 2

MATERIALS AND METHODS

2.1 Study areas

This research focused on two important hill reserves under the Sylhet Forest Division: Tarap Hill Reserve (THR) and Raghunandan Hill Reserve (RHR) (Fig. 1).

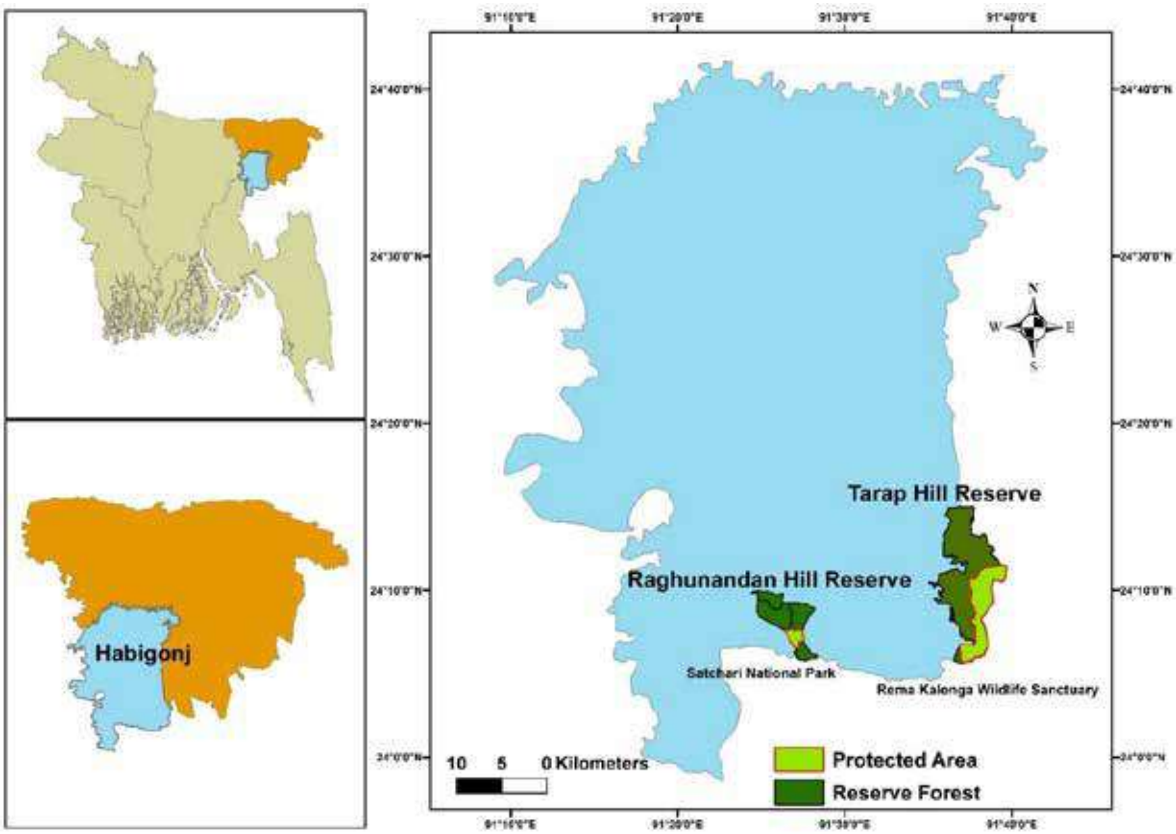

Figure 1. Tarap Hill Reserve (THR) and Raghunandan Hill Reserve (RHR) with the protected areas inside the reserves.

2.1.1 Tarap Hill Reserve

Tarap Hill Reserve [THR, 6232 ha, (24º06' to 24º14'N latitude and 91º34' to 91º41' E longitude)], a part of the Tarap Mountain System and 9b-Sylhet Hills bio-ecological zone, stretches along the Bangladesh and India borders and contains the last remaining natural patches of tropical semi-evergreen forests in the northeastern Bangladesh. The reserve encompasses numerous moderately sloped hills (maximum altitude is 70 m above mean sea level) with extended valleys and ridges. THR is divided into four forest administrative units: Rema beat, Chanbari beat, Kalenga beat and Rashidpur beat under the Sylhet Forest Division. The core zone, containing 32% area of the reserve, was declared an IUCN category IV protected area i.e., Rema Kalenga Wildlife Sanctuary (RKWS) for close monitoring and protection of the threatened animals and plants. RKWS is surrounded by reserve forests which have been heavily degraded and fragmented for illicit logging, fuelwood collection, grazing, forest land conversion to agriculture and human settlement (Sharmin & Sarker, 2020). There are Bengali and ethnic Tripura settlements (about 36 villages) located inside and outside the THR. Registered forest villagers living within the reserve get permission for paddy and lemon cultivation on the low-lying areas.

In return, they have to help local BFD offices in forest protection (IUCN, 2004; Riyad et al., 2012). The climate in the region is sub-tropical humid and the soil varies from clay loam on level ground to sandy loam on hilly ground (Sarker et al., 2013). The average annual temperature in this region is 25.8° C, with significant seasonal fluctuations. The average monthly temperature in the winter (November – February) is 10° C, while in the summer (March – June) the range is 30 to 40° C (Sarker et al., 2013). Most of the annual precipitation (2371.7 mm) typically occurs between May and July (Sarker et al., 2013).

2.1.2 Raghunandan Hill Reserve

The Raghunandan Hill Reserve (24°5' - 24°10' N and 91°25' - 91°30' E), covering 4046.86 ha in the '9b-Sylhet hill' bio-ecological zone, is located in Chunarughat upazila of Habiganj district and is under the jurisdiction of the Sylhet Forest Division. It was declared as a reserve forest in the early 19th century to protect the remaining natural vegetation patches. This reserve consists of two ranges i.e. Satchari range and Raghunandan range. Satchari range consist of two forest beats i.e. Satchari and Telmachara beat. Raghunandan range consist of three beats i.e. Jagadishpur, Shahpur and Shaltila beat. We covered three forest beats i.e. Satchari and Telmachara beat under Satchari range and Shaltila beat under Raghunandan range. The reserve comprises semi-evergreen natural patches, plantation stands, bamboo forest and grassland (Uddin *et al.*, 2013). The natural forest (243 ha) was declared as Satchari National Park in 2006. In this reserve, large deciduous trees are mixed with evergreen smaller trees and bamboos.

2.2 Sampling design and field data collection

2.2.1 Vegetation data

To have a robust representation of the vegetation and habitat conditions, we adopted a grid-based systematic sampling technique which resulted in 120 sample plots of 20 m x 20 m (0.04 ha) size for the Tarap Hill Reserve (Fig. 2A) and 100 sample plots for the Raghunandan Hill Reserve (Fig. 2B). Additional data of 60 plots were collected and measured for model validation purposes. We identified trees of diameter at breast height (d.b.h., 1.3 m) > 5 cm to species level. A representative voucher was collected from the unidentified species for identification and deposition in the Forest Ecology Laboratory, Department of Forestry & Environmental Science, Shahjalal University of Science and Technology, Bangladesh.

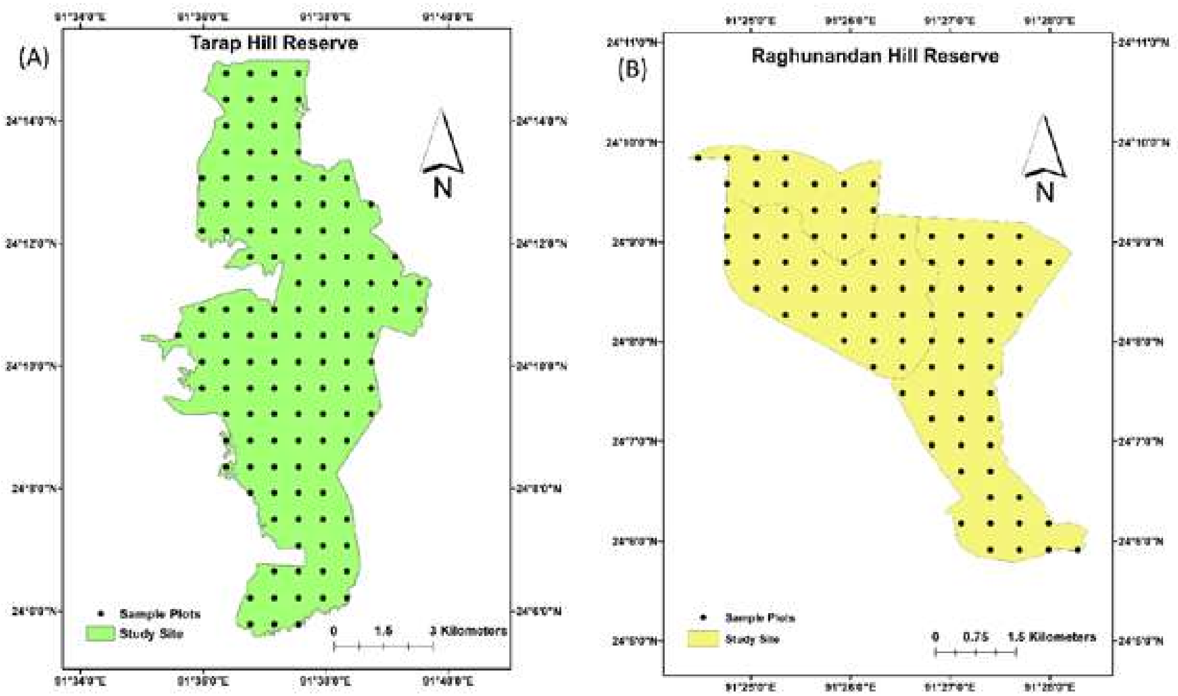

Figure 2. Sampling sites in the study areas: Tarap Hill Reserve (THR) and Raghunandan Hill Reserve (RHR) under the Sylhet Forest Division.

2.2.2 Habitat and disturbance data

Intact soil cores were collected from 3 depth layers i.e., 0-30, 30-60, 60-90cm from each plot (total 360 soil sample cores for laboratory analyses) in the THR and from top-layer (0-30 cm) in the RHR using AMS professional soil sampling kits. All the collected soil samples were then analyzed in the Soil Science Laboratory of the Department of Forestry and Environmental Science, and Chemical Engineering and Polymer Science Department of the Shahjalal University of Science and Technology, Bangladesh to quantify soil pH, sand, silt and clay percentages, soil organic carbon (SOC), and nutrients such as N, P, K, Ca, Mg, Fe, and Zn. We recorded elevation of all plots using the Garmin GPSMAP 64sc GPS meter. We also collected disturbance (number of cut trees in each plot) and canopy data from each plot to incorporate the influence of historical disturbance on species distribution and diversity. Canopy openness was measured using a Spherical Crown Densiometer.

2.2.3 Soil chemical analysis

Sand, silt and clay concentrations in the soil samples were determined using the hydrometer method (Gee & Bauder, 1986). Soil pH measurements were taken from soil water suspensions (soil to water ratio = 1:2) (Brady, 1999) using a digital pH meter (Hanna HI221 pH meter). SOC was measured using the dry combustion method (Hengl & Macmillan, 2019). The Kjeldahl method was used to measure total N content (Ali et al., 2019). P, K, Ca, Mg, Fe and Zn concentrations were measured using the tri-acid digestion method in the Induced Coupled Plasma Atomic Emission Spectroscopy (ICP-OES) system (Neubauer, 2017; Hoobin & Vanclay, 2011).

2.3 Data analysis

2.3.1 Developing spatially explicit forest habitat models and maps of forest habitat conditions

2.3.1.1 Determining soil types: Soil mechanical composition analysis

Following the USDA (United States Department of Agriculture) texture triangle and the soil textural classes (Osman, 2013) (Table 1), we quantified the mechanical composition of soil which ultimately helped us to determine the soil type in the THR and RHR.

Table 1. Soil textural classes with their particle size ranges (Osman, 2013).

Texture	Textural class name	Percentage composition		
		Sand	Silt	Clay
Coarse	Sand	80-100	0-20	0-20
	Loamy sand	70-80	0-30	10-15
	Sandy Loam	50-80	0-50	0-20
Medium	Loam	30-50	30-50	0-20
	Silt loam	0-50	50-100	0-20
	Silt	0-20	90-100	0-10
Fine	Sandy clay loam	50-80	0-30	20-30
	Clay loam	20-50	20-50	20-30
	Silty clay loam	0-30	50-80	20-30
	Sandy clay	50-70	0-20	30-50
	Silty clay	0-20	50-70	30-50
	Clay	0-50	0-50	30-10(

2.3.1.2 Quantifying variations of soil properties and their interactions across soil depths

To understand the variations of soil properties and their interactions across soil depths in the THR: 0-30, 30-60 and 60-90cm, first we checked for data normality using the Shapiro–Wilk test which showed non-normal data distribution. Therefore, we used the Kruskal Wallis test (McKight & Najab, 2010) followed by a post-hoc Dunn test to see multiple pairwise comparisons of the soil properties. Then, to determine how different soil properties interact with each other in different soil depths, we developed several Pearson correlation matrices for different soil depths in the THR.

2.3.1.3 Quantifying interactions among soil properties, topography, and community structure

We conducted Pearson correlation analysis to quantify the interactions among soil properties, topography (elevation), and community structure (species abundance) in RHR.

2.3.1.4 Assessing the effects of different forest management interventions on soil

To understand species composition and dominance across the forest types in the THR and RHR, all trees in old-growth forests (OGF), mixed plantations (MXP), and mono-specific plantations (MOP,) with diameter at breast height (d.b.h., 1.3 m) > 5 cm were identified to species level. Dominant tree species of the different forest types were identified through comparing the above ground biomass percentage of all the species within the forest type. Above ground biomass was calculated by using the generalized formula suggested for Bangladeshi forests (Mahmood et al., 2020): $Ln (TAGB) = - 6.6937+0.809 \times Ln (D^2 \times H \times W)$, where, TAGB = Total Above ground Biomass, DBH = Diameter at Breast Height, H = Total Height, and W =Wood Density). To understand the effects of different forest management interventions on soil properties in different depths (for THR), Friedman's test with repeated measures was conducted to compare how soil properties vary in different depths across the OGF, MXP, and MOP. We further performed the Wilcox post-hoc test to see multiple pairwise comparisons of the soil properties across the forest types and depth levels (0-30, 30-60 and 60-90cm).

2.3.1.5 Modeling habitat conditions

To evaluate the predictive performances of the spatial interpolation methods for different soil properties in THR and RHR, first we employed six different methods from two broad spatial interpolation approaches i.e., deterministic and geostatistical (Barrena-González et al., 2022) to make spatial prediction of the soil parameters for all depth levels (0-30, 30-60 and 60-90cm). Then we compared the predictive performances of the methods based on the normalized root mean square error (NRMSE) of the predicted versus the actual soil parameter values (Li et al., 2020). For normalization, the RMSE statistic was divided by the range of the actual soil properties values. Deterministic interpolation methods used in this study include: Inverse Distance Weighting (IDW), Local Polynomial Interpolation (LPI), Spline with tension (SWT), and Inverse Multi-quadric function (IMQF). Geostatistical interpolation methods used include: Empirical Bayesian Kriging (EBK) and Universal Kriging (UK).

2.3.1.6 Mapping habitat conditions

The interpolation methods with highest predictive ability were used to develop spatial maps (spatial resolution of 25m × 25m) for all the soil properties in the THR and RHR. All statistical analysis and visualizations were performed in the R environment (version 4.3.1) (www.cran.r-project.org). All spatial analysis and mapping were performed using the ArcGIS software (version 10.5.1).

2.3.2 Developing Habitat Suitability Models (HSMs) and Maps for important indigenous and endangered tree species

2.3.2.1 Species selection for model development in THR and RHR

A total of 3121 tree individuals of 141 species were recorded (Appendix B) from the THR. Among these species, for THR, we selected nine dominant native tree species (Table 2) which accounts for 43.55% of the total basal area and 46.41% of the total individual counts. A total of 2681 tree individuals of 140 species were recorded from the RHR. Among these species, for RHR, we selected eight dominant native tree species (Table 2) which accounts for 34% of the total basal area and 36.21% of the total individual counts.

Table 1. Taxonomy, abundances, global conservation status of the selected dominant tree species censused in the Tarap Hill Reserve (THR) and Raghunandan Hill Reserve (RHR), Bangladesh. *IUCN global population trend, NA = Not assessed for the IUCN Red List, LC = Least concern, DD = Data deficient, NT = Near threatened, VU= Vulnerable, EN = Endangered, D = Decreasing.

Forest	Scientific Name	Local Name	Family	Abundance (Presence out of 120 plots)	IUCN conservation status	IUCN Global population trend
THR	*Artocarpus chaplasha*	Chapalish	Moraceae	91 (31)	NA	NA
THR	*Dillenia pentagyna*	Hargoja	Dilleniaceae	48 (48)	NA	NA
THR	*Dipterocarpus turbinatus*	Garjan	Dipterocarpaceae	29 (29)	VU	Decreasing
THR	*Ficus roxburghi*	Dumur	Moraceae	120 (40)	NA	NA
THR	*Glochidion lanceolarium*	Kakra	Phyllanthaceae	58 (58)	NA	NA
THR	*Holarrhena pubescens*	Kurchi	Apocynaceae	44 (25)	LC	NA
THR	*Shorea robusta*	Sal	Dipterocarpaceae	16 (16)	LC	NA
THR	*Schima wallichi*	Bonak	Theaceae	200 (57)	LC	Stable
THR	*Terminalia bellerica*	Bohera	Combretaceae	194 (72)	NA	NA
RHR	*Artocarpus chaplasha*	Chapalish	Moraceae	282 (58)	NA	NA
RHR	*Ficus racemosa*	Jogga Dumur	Moraceae	79 (35)	LC	Stable
RHR	*Glochidion sphaerogynum*	Kaimola	Euphorbiaceae	63 (36)	NA	NA
RHR	*Ilex godajam*	Ludh	Aquifoliaceae	200 (57)	LC	NA
RHR	*Dillenia pentagyna*	Hargoja	Dilleniaceae	57 (19)	NA	NA
RHR	*Glochidion lanceolarium*	Kakra	Phyllanthaceae	178 (52)	NA	NA
RHR	*Terminalia bellerica*	Bohera	Combretaceae	144 (40)	NA	NA
RHR	*Bauhinia variegata*	Kanchan	Fabaceae	111 (26)	LC	Stable

2.3.2.2 Selection of predictor variables

To construct a comprehensive set of predictor variables for our Habitat Suitability Models (HSMs), we followed Franklin's (2010) conceptual models on factors influencing species distribution in tropical regions. We selected nine predictors across four key categories: soil, topography, species competition, and disturbance. Soil variables such as pH, N, P, organic carbon and sand were chosen for their recognized role in shaping tree species distribution and community composition in tropical ecosystems (Crespo-mendes et al., 2019; Kargar et al., 2015; Walthert & Meier, 2017). Soil nutrient vertical distribution varies greatly across tree species due to differences in root systems and nutrient uptake capacity; deeper layers of soil may contain nutrients that are not found on the surface (Xiong et al., 2021). The regulation of plant growth, production, and distributions is heavily influenced by essential minerals such as nitrogen and phosphorus (Guisan & Zimmermann, 2000; Mackey, 1993), which in turn affect plant physiology (Austin, 2002). Soil organic matter controls the availability of water and nutrients, while soil pH has a direct impact on plant distributions. Nutrient and moisture availability are two proximal variables impacted by soil texture, which is a distal component (Austin, 2002). To address these, we implemented a soil sampling strategy, collected and analyzed three soil samples at depths of 0-30 cm, 30-60 cm, and 60-90 cm per plot to capture vertical variations in soil parameters from the THR. We then averaged the values. For RHR, we considered only the top-soil (0-30 cm). Elevation data were recorded using GPS to account for its interaction with climate in modifying landscape conditions (Franklin, 2010b).

The relative abundance of one tree species may influence the abundance of another via biotic interactions (i.e. competition or facilitation) and such interactions are crucial in understanding plant species distribution. Incorporating community structure (CS, total tree counts in a plot) as a proxy of biotic interaction significantly enhanced the predictive power of HSMs developed for other tropical forest systems (Sarker et al., 2016; Sarker et al., 2021). Following this we used CS in our models. Historical logging (i.e., total number of cut trees in each plot) and canopy openness (CO) were included as disturbance predictors due to their influence in defining current and future species composition (Russavage et al., 2021). Canopy openness was measured using a Spherical Crown Densiometer.

To ensure predictor independence and reliability, we conducted multicollinearity checks using Variance Inflation Factors (VIF) (Robinson & Schumacker, 2009). All variables were retained as their VIF values were below the threshold of 5 (O'Brien, 2007). The final predictor set for THR models comprised soil pH, sand, elevation, SOC, N, P, CS, logging, and CO. The final predictor set for RHR models comprised soil pH, sand, silt, clay, elevation, soil organic carbon (SOC), N, P, K, Mg, Ca, Fe community structure (CS), and canopy openness (CO).

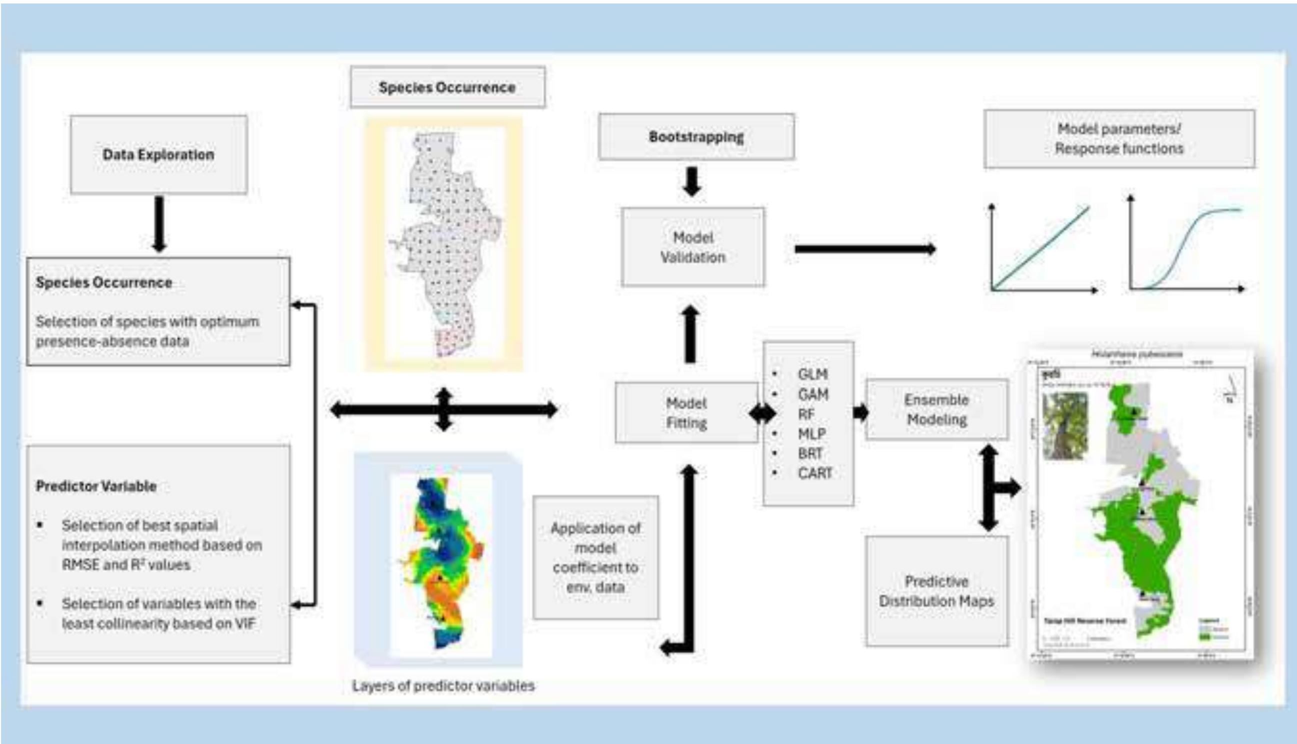

Figure 3. The methodological processes involved in species distribution modelling and prediction mapping in THR and RHR. Spatially explicit species occurrence data are linked with environmental predictors and environmental predictor values for species locations are extracted. Six models were developed to describe the link between species occurrence and environmental variables. The parameters or response functions are assessed, and the coefficients are applied onto environmental maps to produce spatial predictions of habitat suitability.

2.3.2.3 Habitat suitability modelling

We followed the conventional approach of HSM (Franklin 2010a, Sillero et al. 2021, Zurell et al., 2020 and Matthiopoulos et al., 2020) that quantifies species-habitat associations and then predicts species spatial distributions on the basis of one response (species presence-absence/abundance) and multiple explanatory variables (Fig. 3). Here, as response variable we used presence-absence data of the dominant tree species (Table 2), and as explanatory variables we used the final predictor set selected for THR (soil pH, sand, elevation, SOC, N, P, CS, logging, and CO) and RHR (soil pH, sand, silt, clay, elevation, SOC, N, P, K, Mg, Ca, Fe, CS, and CO). Various statistical methods are available to predict species distribution (Araújo & New, 2007) and the predictive performances of the models can vary for different species, study objectives, data availability, and system-specific species-environment complexity (Franklin, 2010a). Hence, first we compared the performances of different modelling approaches to determine which modelling technique performs better in predicting distribution of different tree species. Then we developed an ensemble model using the mean of the best statistical methods to ensure robust predictions.

We considered six statistical methods under three broad HSM approaches to predict suitable habitats for nine tree species: (A) Regression-based approach – generalized linear model (GLM) and generalized additive model (GAM), (B) Tree-based approach – boosted regression trees (BRT) and classification and regression trees (CART), (C) Machine learning approach – random forests (RF) and multi-layer perceptron (MLP). For each species, 600 models were built using 100 replications following bootstrapping approach for all six statistical methods. 70% of the data was selected randomly to train the model, and the remaining 30% was used to test the model. To compare and evaluate model performances, we calculated the area under the receiver operating characteristic (ROC) curve (AUC) (Sox et al., 2013), the true skill statistics (TSS) (Allouche et al., 2006) and Deviance (D) (Fenlon et al., 2016) for each model. ROC curve of a model describes its predictive ability under the whole range of probability thresholds, and the AUC represents a quantitative assessment of this ability (Iturbide et al., 2015). AUC values range from 0 (a value below 0.5 indicates random guessing) to 1.0, with higher values indicating better model performance. The TSS (sensitivity + specificity – 1) score considers both the overall accuracy of the model and the imbalance in the predicted classes. TSS value ranges from -1 to +1; -1 indicates poor classification, 0 indicates random guessing, and 1 indicates perfect classification (Elith & Leathwick, 2009). The difference between the simulated and observed values is used to calculate deviance. The lower the deviance, the better the model (Mayer & Butler, 1993).

2.3.2.4 Ensemble modelling

After developing six habitat suitability models for each species, we applied the ensemble modelling approach to create a single prediction by averaging multiple models. Ensemble modelling is desirable in circumstances where numerous candidate models have a similar level of plausibility or in which several alternative modelling approaches are available (Naimi & Araújo, 2016). Thus, this approach is useful in species distribution modelling for several reasons. First, the ensemble model helps improving the accuracy and stability of the prediction of species distribution by combining the strengths and weaknesses of different modelling techniques (Araújo & New, 2007). Second, ensemble modelling can handle uncertainty in the data and reduce the impact of outliers by averaging the models' predictions (Dietterich, 2000). For each studied species, we combined the different HSM's predictions into a single prediction by calculating the mean across selected models (hereafter referred to as the ensemble model). We selected models based on a cutoff value for both AUC and TSS. Only models with AUC > 0.7 and TSS > 0.6 were selected to retain models with satisfactory performance.

2.3.2.5 Mapping species distribution

The ensemble model-averaged predictions were used to develop the species habitat maps based on interpolated predictor surfaces. We used five different geostatistical interpolation approaches (Empirical Bayesian Kriging (EBK), Inverse Distance Weighting (IDW), Ordinary Kriging (OK), Local Polynomial Interpolation (LPI), and Spline with Tension (SWT) to see the spatial distribution of each of the predictor variables (Li et al., 2020). From these, the best approach for each predictor was selected based on values of the root mean square error (RMSE) (Al-Mamoori et al., 2021). Hence, the best interpolated layer (spatial resolution of 25m × 25m) for each predictor variable was selected for developing HSMs of the selected tree species in THR and RHR. Then, we converted the ensemble model predictions for each species into a presence-absence (binary) map by selecting a threshold value (Max (se + sp)) for the respective species that maximizes the sum of model sensitivity (se) and specificity (sp). Grid cells with a value above the threshold are classified as present (1), while those below the threshold are classified as absent (0).

2.3.2.6 Consensus map development: Multispecies habitat suitability detection

To identify multispecies habitat suitability, we combined all binary maps and created consensus maps for THR and RHR. The value of each grid cells for the consensus map ranged from 0-9 and 0-8, with 0 indicating grid cells unsuitable for any species and 9 indicating grid cells projected to be suitable for all studied species in THR, and 8 indicating grid cells projected to be suitable for all studied species in RHR. All analysis were done using the '*sdm*' package (Naimi & Araujo, 2016) and custom codes in the R programming language environment (version 4.2.1; R Core Team, 2022). ArcGIS (version 10.5.1) was used to develop the prediction maps.

2.3.3 Developing alpha, beta and gamma diversity models and maps

2.3.3.1 Quantifying tree diversity

We used the framework developed by Reeve et al. (2016) for partitioning biodiversity into alpha, beta and gamma.

2.3.3.2 Selection of variables for diversity modeling

We followed similar process as mentioned in Section 3.1.2.2 for selecting the variables for tree diversity modeling. The final predictor set for THR diversity models comprised N, P, K, Fe, pH, Sand, Silt, Clay, SOC, CS, and CO. The final predictor set for RHR models comprised soil pH, sand, silt, clay, SOC, N, P, K, Fe, CS, and CO.

2.3.3.3 Developing Tree Diversity Models

We built generalized additive models (GAMs) to quantify how tree alpha, beta and gamma diversity responded to different variables. Directed by data and using non-parametric smoothing functions, GAMs can detect response-predictors relationships without a priori knowledge of the functional form of these relationships (Guisan & Thuiller 2005). These advantageous features of GAMs are well suited for uncovering unknown biodiversity — environment linkages. All analyses were done in R and diversity GAMs were built using cubic basis splines with the Gamma error distribution using the 'mgcv' package in R (Wood 2011). Model selection and model averaging were carried out using the 'MuMIn' version 1.15.1 (Barton 2015) package.

We comprehensively fitted GAMs for each diversity index with all possible combinations of variables. Then we ranked the fitted GAMs using the second-order AIC (AICc). Models whose AIC_c had values less than 2 from the best model (ΔAIC_c <2) were retained as competing models (Burnham & Anderson 2002). The relative support for each of the competing models was then determined using their Akaike weights (AIC_{cw}, vary between 0 to 1, and the sum of all AIC_{cw} across the competing models is 1). To reduce model selection uncertainty and bias, we then conducted model averaging to predict the diversity indices. To determine the strength of the covariates, we ranked them based on their Relative Importance (RI) values. RI of each variable was calculated by adding the AIC_{cw} of the models in which the variable was included. RI values vary between 0 and 1, where 0 specifies that the target variable is not included in any of the competing models while 1 means that the variable is included in all competing models. We measured goodness-of-fit of the diversity models using the R^2 (coefficient of determination) statistic between the observed and estimated values of the diversity indices.

2.3.3.3 Developing Tree Diversity Maps

GAM-based predictions were used to develop the diversity maps based on interpolated variable surfaces. We applied the widely use geostatistical interpolation method Ordinary Kriging (OK) to see the spatial distribution of each of the predictor variables. Here we compared the predictive performances of three OK methods: Gaussian, spherical and exponential and used the best method for making variable surfaces using the normalized root mean square error (NRMSE) values. Hence, the best interpolated layer (spatial resolution of 25m × 25m) for each predictor variable was selected for developing Habitat-based Biodiversity Models (alpha, beta and gamma) for THR and RHR.

RESULTS AND DISCUSSION

CHAPTER 3

MODELS AND DIGITAL MAPS OF HABITAT CONDITIONS IN THE TARAP HILL RESERVE

3.1 Descriptive statistics of the soil physico-chemical properties

Descriptive statistics of the soil physico-chemical properties in the Tarap Hill Reserve is presented in Table 3. The coefficient of variation (CV), reflecting the degree of variability of soil properties (lower values indicate less variability where higher values indicate high variability), represents higher variability among clay, silt N, Fe and K across the soil depths while pH and sand showed least variability.

3.2 Soil type

In different soil depths in the Tarap Hill Reserve, sand, silt and clay percentages showed almost stable values (Fig. 4A). Soil mechanical composition analysis identified the soil type of the THR as Sandy Clay Loam (Fig. 4B).

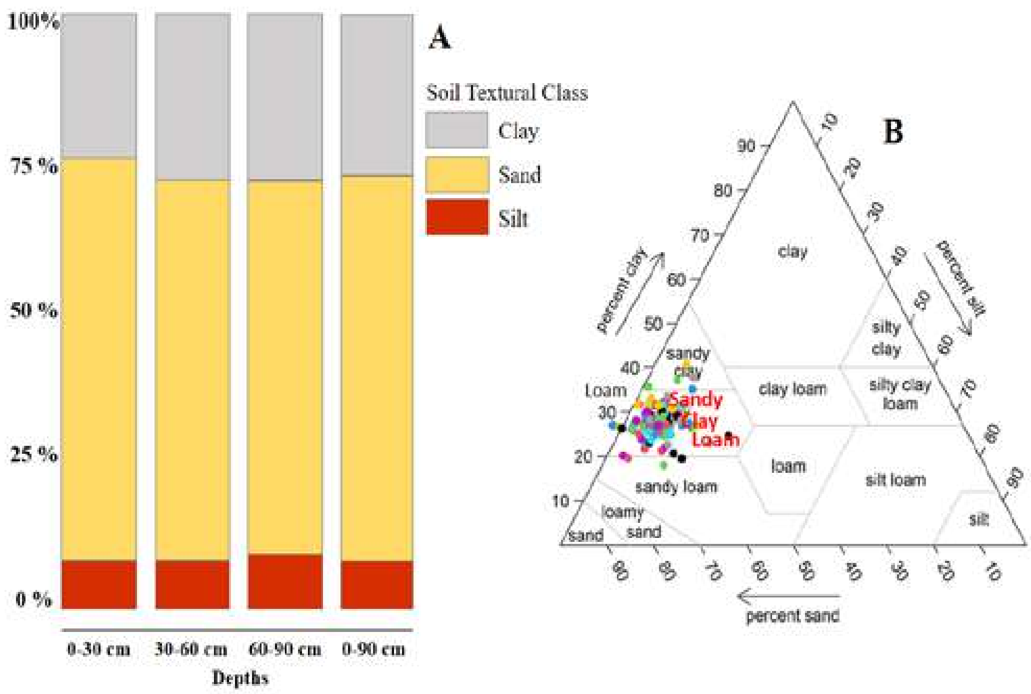

Figure 4. Soil mechanical composition in the Tarap Hill Reserve. (A) Showing % of sand, silt, and clay in different soil depth layers, and (B) showing soil type determination through a soil textural triangle devised by the United States Department of Agriculture (USDA).

Table 2. Descriptive statistics of 12 soil physico-chemical properties in the Tarap Hill Reserve, Bangladesh in different soil depths. SD = Standard deviation and CV= Coefficient of variation.

Variables	Depth (cm)	Min	Max	Range	Mean	SD	CV (%)
N (mg/L)	0-30	0.006	0.07	0.07	0.03	0.01	48.30
	30-60	0.003	0.06	0.05	0.02	0.01	59.13
	60-90	0.003	0.03	0.03	0.01	0.01	74.93
P (mg/L)	0-30	0.013	2.68	2.67	0.65	0.73	113.39
	30-60	0.002	1.6	1.60	0.30	0.35	118.33
	60-90	0.001	1.21	1.20	0.14	0.14	100.36
K (mg/L)	0-30	0.002	0.14	0.14	0.02	0.02	111.71
	30-60	0.001	0.2	0.20	0.02	0.02	136.20
	60-90	0.000	0.3	0.30	0.02	0.03	177.49
Ca (mg/L)	0-30	0.000	0.35	0.35	0.02	0.04	261.32
	30-60	0.001	0.4	0.4	0.03	0.06	211.47
	60-90	0.001	0.13	0.12	0.02	0.02	121.84
Mg (mg/L)	0-30	0.000	0.98	0.98	0.14	0.14	103.69
	30-60	0.000	0.8	0.80	0.10	0.12	117.64
	60-90	0.001	0.66	0.66	0.09	0.09	99.25
Fe (mg/L)	0-30	0.002	19.31	19.31	5.16	4.18	80.92
	30-60	0.070	22.02	21.95	4.89	4.80	98.14
	60-90	0.039	14.86	14.83	3.74	2.79	74.57
Zn (mg/L)	0-30	0.000	0.89	0.89	0.03	0.09	410.39
	30-60	0.000	1.07	1.06	0.02	0.10	522.3
	60-90	0.000	0.07	0.07	0.01	0.01	125.28
pH	0-30	3.960	5.92	1.96	4.80	0.44	9.26
	30-60	4.040	5.94	1.90	4.99	0.41	8.14
	60-90	4.090	6.51	2.42	5.00	0.42	8.40
SOC (%)	0-30	0.012	11.72	11.70	3.90	2.93	75.08
	30-60	0.024	12.35	12.33	4.60	3.48	75.75
	60-90	0.072	14.43	14.36	4.65	3.39	72.77
Sand (%)	0-30	51.740	82.74	31.00	67.28	6.48	9.63
	30-60	39.370	85.66	46.29	63.09	8.22	13.03
	60-90	40.200	78.91	38.71	63.26	7.23	11.43
Silt (%)	0-30	0.588	22.39	21.80	7.64	4.80	62.80
	30-60	0.570	19.91	19.34	7.07	4.20	59.36
	60-90	0.088	17.02	16.93	7.46	4.54	60.92
Clay (%)	0-30	10.470	40.77	30.30	25.08	5.86	23.35
	30-60	11.050	46.22	35.17	29.33	6.89	23.48
	60-90	17.230	44.40	27.17	29.11	6.29	21.61

3.3 Variation in soil properties across soil depths

The Kruskal-Wallis test showed significant variations in several soil properties across the soil depths (0-30, 30-60, and 60-90cm). Post-hoc Dunn test further specified that among the nutrients, only soil N and P concentrations significantly varied in all depths and the availability of both nutrients decreased with increasing depth (Fig. 5). Overall, N, P, Fe, Mg concentrations showed a decreasing trend with increasing soil depths while pH, SOC, and clay content exhibited the opposite pattern, rising with depth.

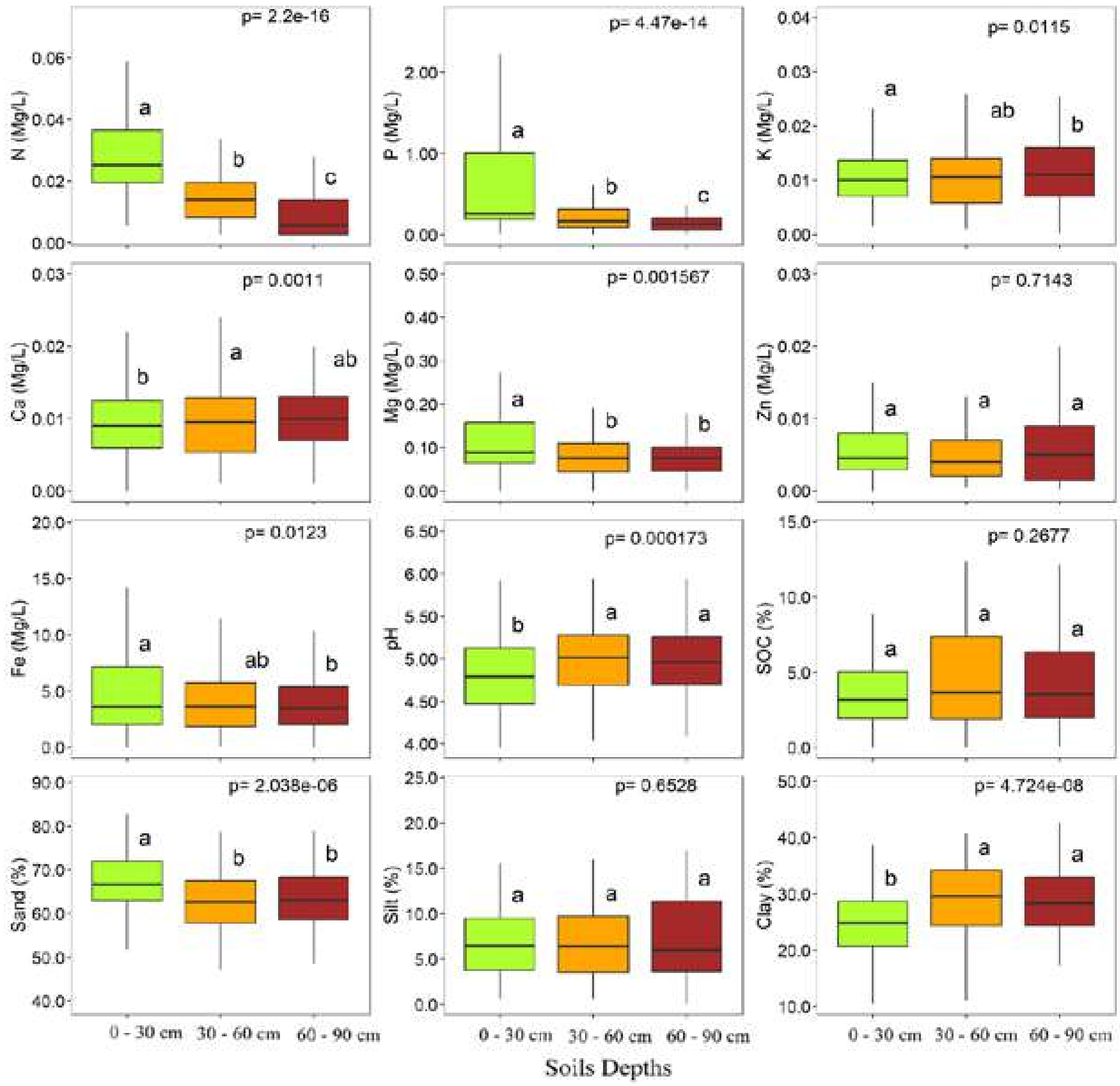

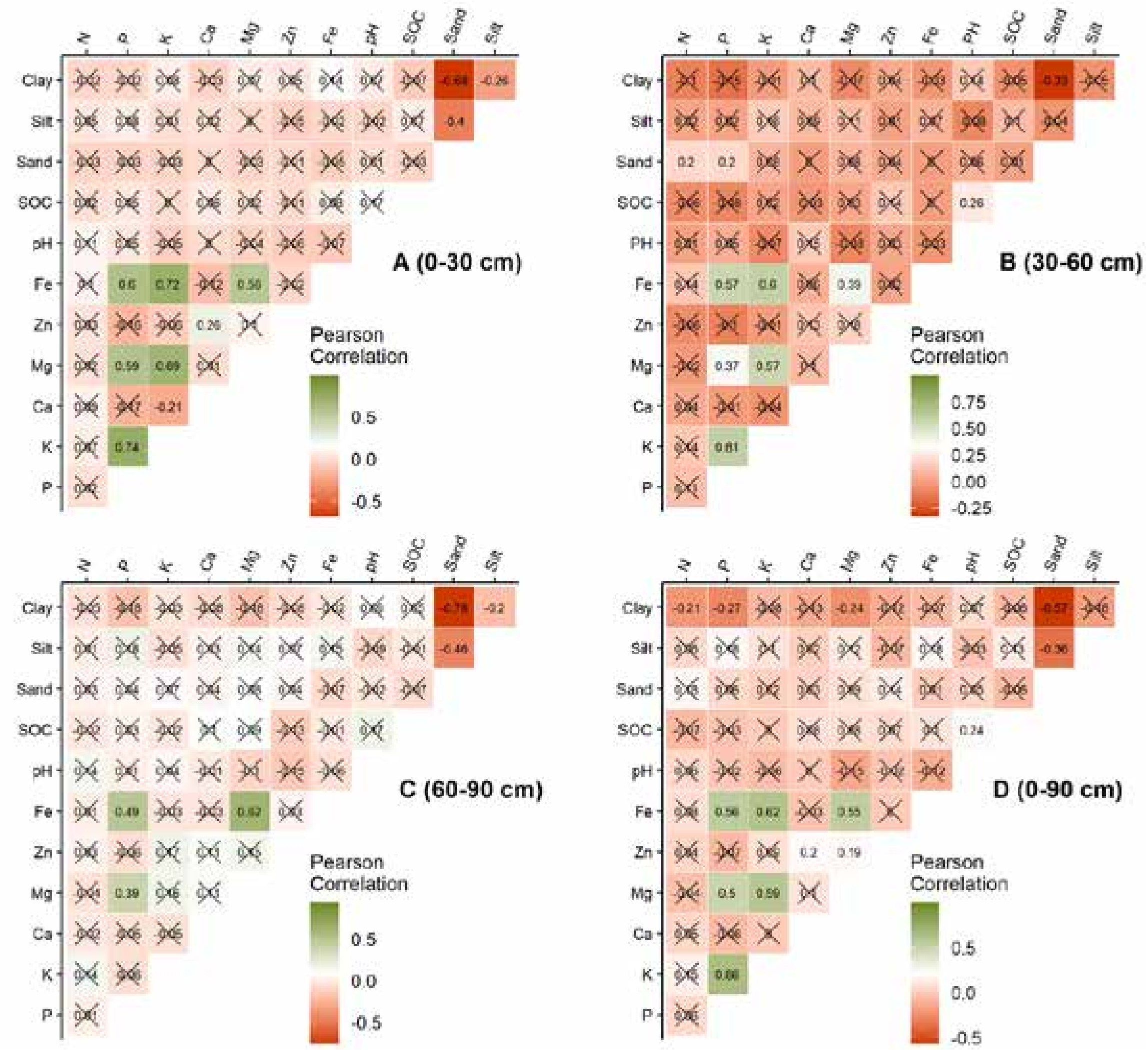

Figure 5. Pearson correlation analyses showing the relationships between soil properties across the soil depths in the THR, Bangladesh. In the correlation matrix, numbers in the green color cells represent positive correlation coefficient (*r*) values and numbers in the red color cells represent negative values at different soil depths: 0-30cm (A), 30-60cm (B), 60-90cm (C), and 0-90cm (D). Cross-marked values indicate a non-significant correlation (p>0.05).

P and Fe (r = 0.49 – 0.60, p<0.001), Mg and Fe (r = 0.56 – 0.62, p<0.001), and P and Mg (r = 0.37 – 0.59, p<0.001) showed significant positive correlations while sand and clay showed a significant negative correlation (r = -0.33 – -0.78, p<0.001) in all soil depths intervals (0-30, 30-60, 60-90, and 0-90 cm) although the strength of the relationships varied between the depth intervals. For example, the correlation coefficient value between P and Fe gradually drops from the surface layer – 0-30cm (r = 0.60, p<0.001) to deeper soils – 30-60 cm (r = 0.57, p<0.001) and 60-90 cm (r = 0.49, p<0.001). Interestingly, although a high positive correlation was observed between P and K in the surface (0-30 cm depth) and sub-surface (30-60 cm) area (r = 0.73, p<0.001, r = 0.61, p<0.001), a slightly negative correlation (r = -0.06) appeared in the deeper soil (60-90 cm).

3.5 Forest management impacts on soil properties

Our forest survey, based on the aboveground biomass contribution of each species, revealed that different species dominate different forest types in the THR. In mono plantations, Teak, Rubber, and Sal were found to be the most dominant species, while Sal, Bonak, and Bohera were the most biomass contributing species in mixed plantations. Bohera, Kakra, and Bonak were found to be the most dominating species in the old growth forest of the reserve, as illustrated in Fig. 7.

Friedman test with repeated measures test (i.e., forest management interventions have variable effects on soil properties in different soil depths) revealed significant variations in soil properties among different historically introduced forest types, i.e., OGF, MXP, and MOP, and different soil depths therein (Fig. 8). N, Ca, SOC, and clay contents varied significantly across all the forest types while N, P, K, Mg, Fe, and SOC varied significantly within the soil depths (0-30, 30-60 and 60-90cm). Our post-hoc tests further revealed significant differences in N concentrations in all forest types while, Ca and SOC concentrations only varied significantly between OGF and MOP. Overall, the availability of macro-nutrients N, P, K, and Mg was highest in the OGF and lowest in the MOP in all depth intervals. In contrast, the availability of Ca and Zn was highest in the MXP and lowest in the OGF.

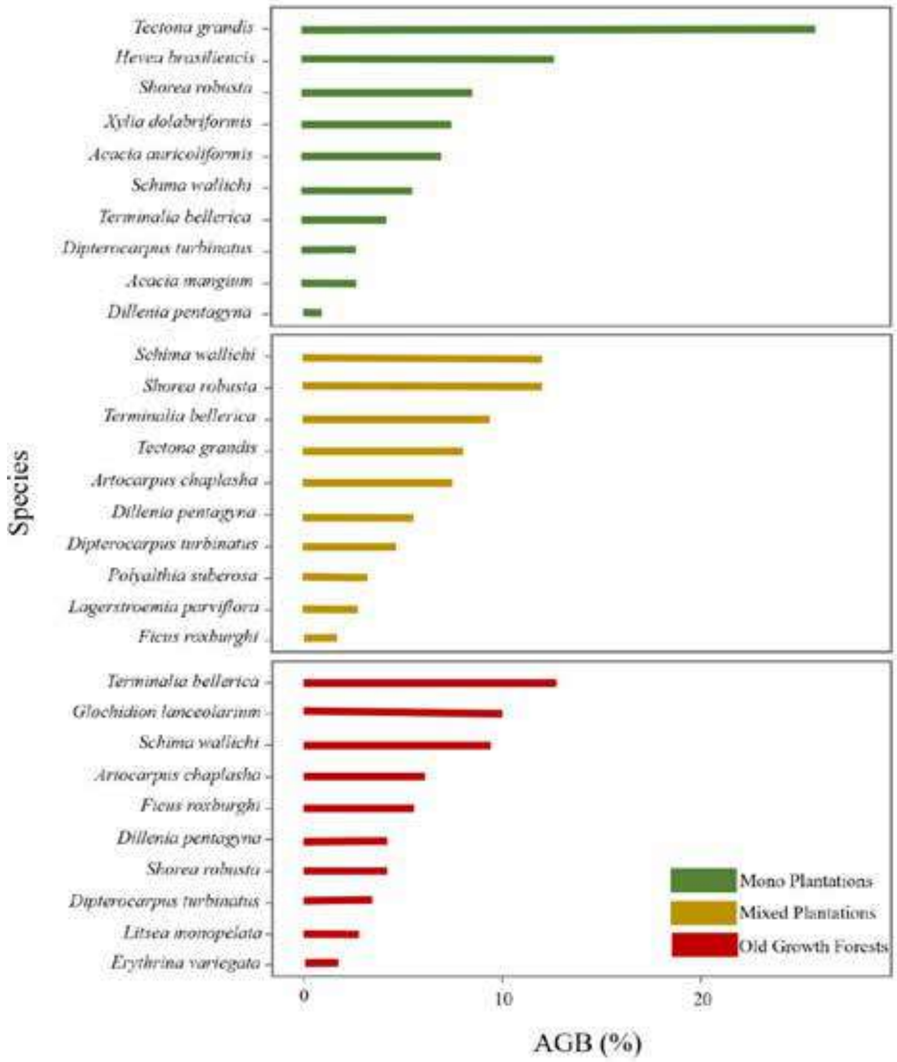

Figure 6. Dominant species of different forest types (mono plantations, mixed plantations and old growth forests) in the Tarap Hill Reserve (THR), Bangladesh based on above-ground biomass (AGB) percentage contributions.

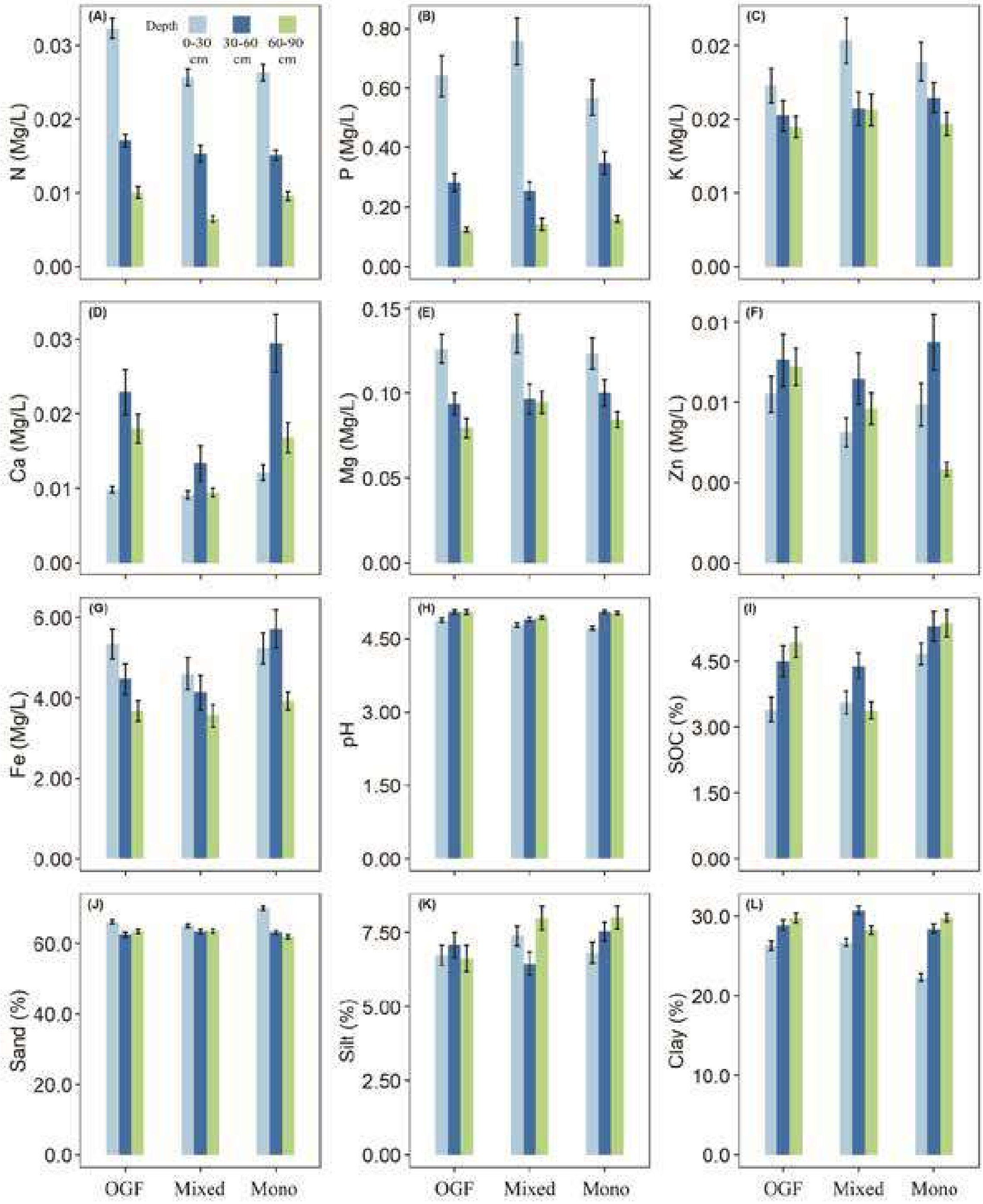

Figure 7. Bar charts showing the mean values of soil properties in three depth intervals (0-30, 30-60 and 60-90cm) in the old growth forest (OGF), mixed plantations (MXP) and mono plantations (MOP). Detailed results of Friedman test showing the variation of soil properties among forest types and Wilcox post-hoc tests looking at the multiple pairwise comparisons of the soil properties among forest types and depths are presented in Tables S4 and S5. Error bars denote mean ± standard errors.

3.6 Habitat Models

Our spatial analyses revealed that the predictive performances of the different interpolation methods varied for different soil properties in different soil depths (Table 4). Between the two geostatistical methods, EBK showed relatively higher predictive accuracy. Among the deterministic methods, LPI and IMQF showed relatively higher predictive accuracy while SWT and IDW showed least predictive ability.

Table 3. Comparison between predictive performances of the geostatistical [Empirical Bayesian Kriging (EBK) and Universal Kriging (UK)] and deterministic methods [Inverse Distance Weighting (IDW), Local Polynomial Interpolation (LPI), Spline with tension (SWT), and Inverse Multi-quadric function (IMQF)] based on normalized root mean square error (NRMSE) of the predicted versus the actual soil parameter values. NRMSE is expressed here as a percentage. Lower NRMSE values (light blue-shaded cells) indicate less residual variance (higher predictive accuracy) while higher values (grey-shaded cells) indicate higher residual variance (lower predictive accuracy).

Soil properties	**Depths**	**Geostatistical methods**		**Deterministic methods**			
		NRMSE (%)					
		EBK	**UK**	**IMQF**	**SWT**	**IDW**	**LPI**
N	0-30 cm	19.87	19.73	20.06	19.78	20.27	19.68
	30-60 cm	17.80	17.73	18.08	18.28	18.95	17.68
	60-90 cm	26.22	26.31	26.58	27.87	29.21	26.90
P	0-30 cm	25.67	25.84	25.76	26.14	26.39	26.48
	30-60 cm	23.01	22.54	22.72	24.37	25.08	22.41
	60-90 cm	12.24	12.52	12.22	13.04	13.52	12.20
K	0-30 cm	15.11	15.13	14.98	15.40	15.82	15.42
	30-60 cm	8.87	8.96	8.72	8.88	8.98	8.71
	60-90 cm	4.04	4.28	4.04	4.13	4.15	4.02
Ca	0-30 cm	2.34	2.36	2.39	2.39	2.41	2.27
	30-60 cm	10.76	11.62	10.81	11.26	13.79	13.42
	60-90 cm	15.85	15.77	15.99	16.08	15.77	15.03
Mg	0-30 cm	10.14	10.14	10.22	10.26	10.43	10.30
	30-60 cm	10.29	10.63	10.47	10.33	10.41	10.27
	60-90 cm	9.37	9.41	9.43	9.82	10.17	9.29
Fe	0-30 cm	19.90	20.68	20.02	19.88	20.08	20.46
	30-60 cm	21.37	23.07	21.43	22.44	22.59	21.36
	60-90 cm	18.02	17.98	17.61	22.99	19.72	18.04
Zn	0-30 cm	9.65	10.07	9.62	9.88	9.81	9.55
	30-60 cm	9.90	10.54	9.81	10.02	10.12	9.68
	60-90 cm	14.84	15.83	14.59	15.26	15.33	14.60
pH	0-30 cm	20.91	21.25	21.41	21.31	21.29	21.96
	30-60 cm	22.11	22.23	22.41	22.66	23.21	21.90
	60-90 cm	17.52	18.56	17.48	18.23	18.53	17.46
SOC	0-30 cm	25.09	24.34	24.49	24.51	24.68	25.23
	30-60 cm	28.06	29.09	27.76	28.92	29.61	28.35
	60-90 cm	24.22	25.23	24.58	25.45	25.79	23.92
Sand	0-30 cm	19.68	19.81	19.19	19.30	19.44	19.83
	30-60 cm	18.31	18.53	17.77	17.88	18.04	17.92
	60-90 cm	18.59	18.84	18.59	19.92	19.16	18.34
Silt	0-30 cm	17.82	17.20	17.33	17.18	17.33	17.26
	30-60 cm	21.69	21.67	21.67	21.78	21.87	21.67

	60-90 cm	27.17	27.96	27.18	27.71	27.97	27.23
	0-30 cm	18.42	18.15	18.09	17.98	18.30	18.61
Clay	30-60 cm	19.42	19.49	19.49	19.79	20.12	19.59
	60-90 cm	22.98	23.19	22.75	24.11	24.55	22.93

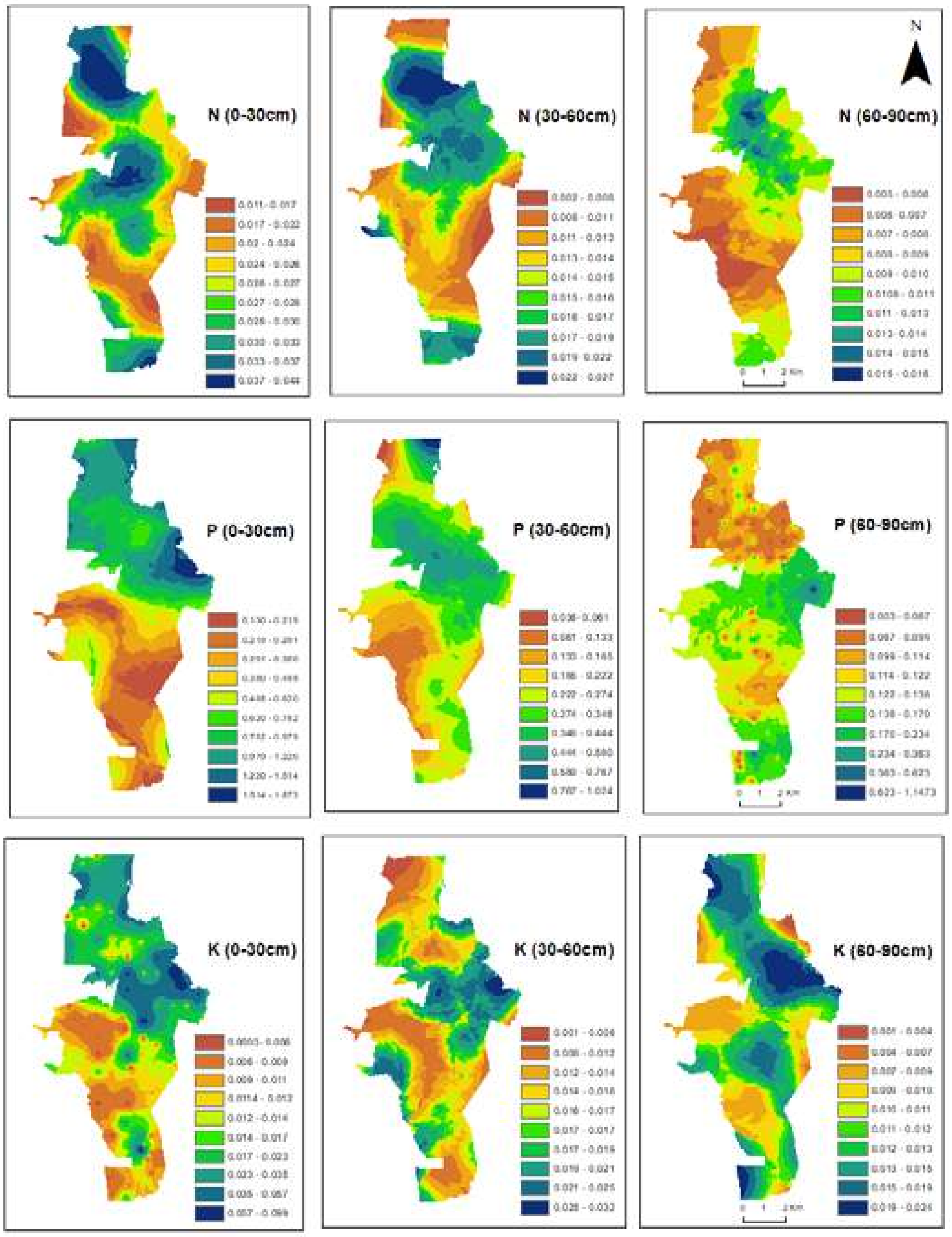

3.7 Digital Soil Maps

Figure 8. Maps showing the spatial distributions of three key soil macro-nutrients (N, P and K [mg/L]) in the Tarap Hill Reserve, Bangladesh at three soil depth levels (0-30, 30-60, 60-90cm) using the most accurate interpolation method (Table 4).

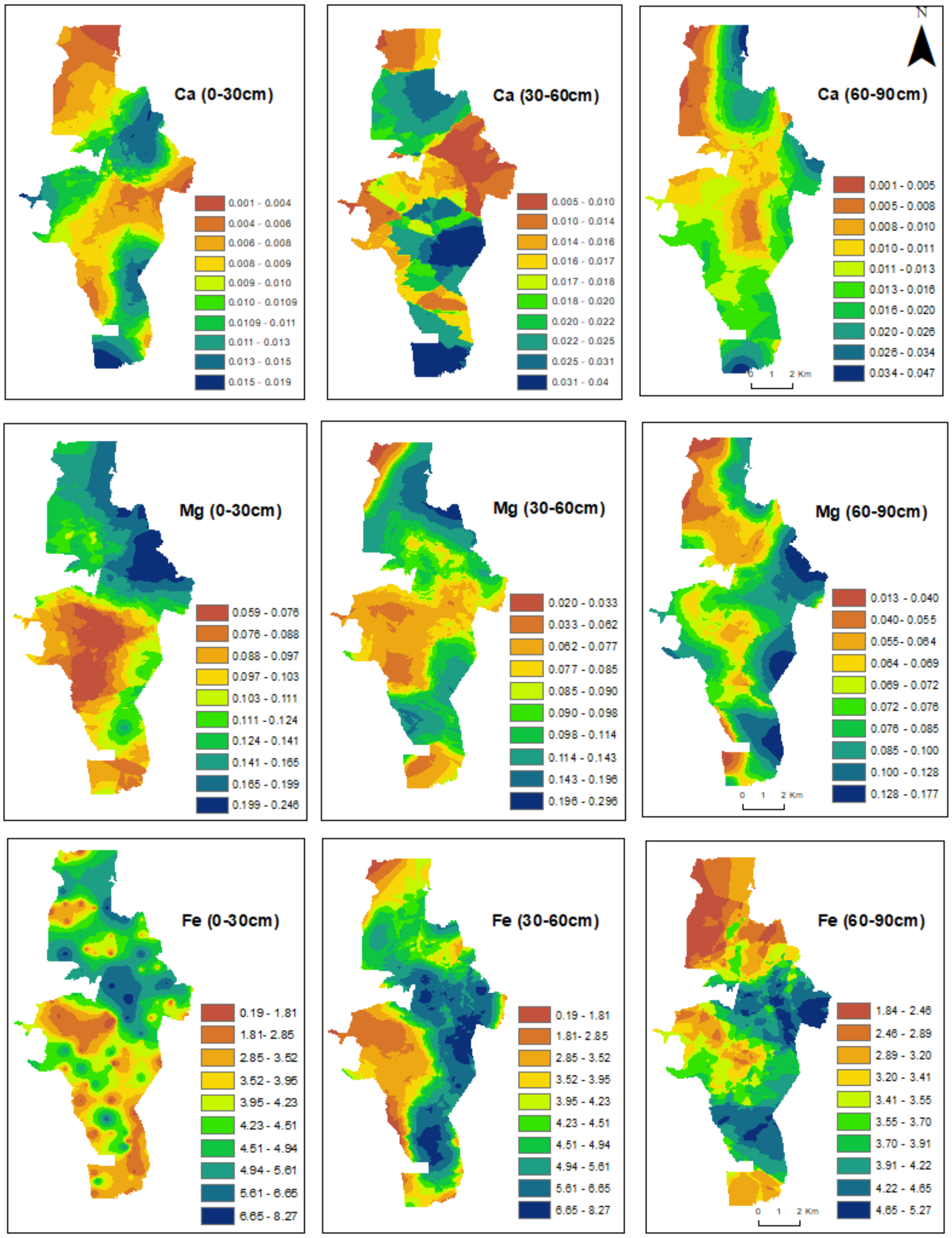

Figure 9. Maps showing the spatial distributions of three key soil nutrients (Ca, Mg and Fe [mg/L]) in the Tarap Hill Reserve, Bangladesh at three soil depth levels (0-30, 30-60, 60-90cm) using the most accurate interpolation method (Table 2).

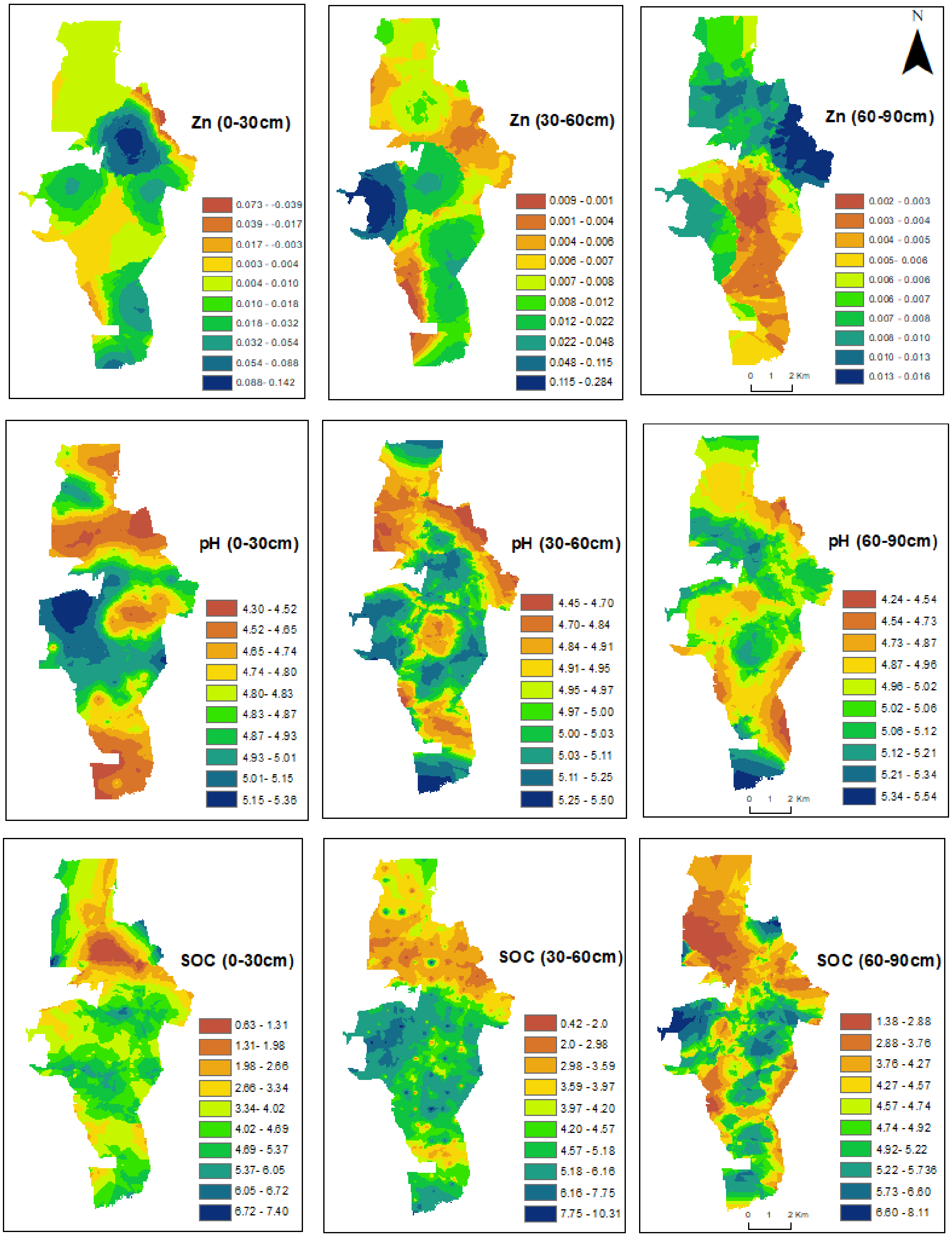

Figure 10. Maps showing the spatial distributions of three key soil nutrients (Zn [mg/L], pH and Soil organic carbon (SOC, %)) in the Tarap Hill Reserve, Bangladesh at three soil depth levels (0-30, 30-60, 60-90cm) using the most accurate interpolation method (Table 2).

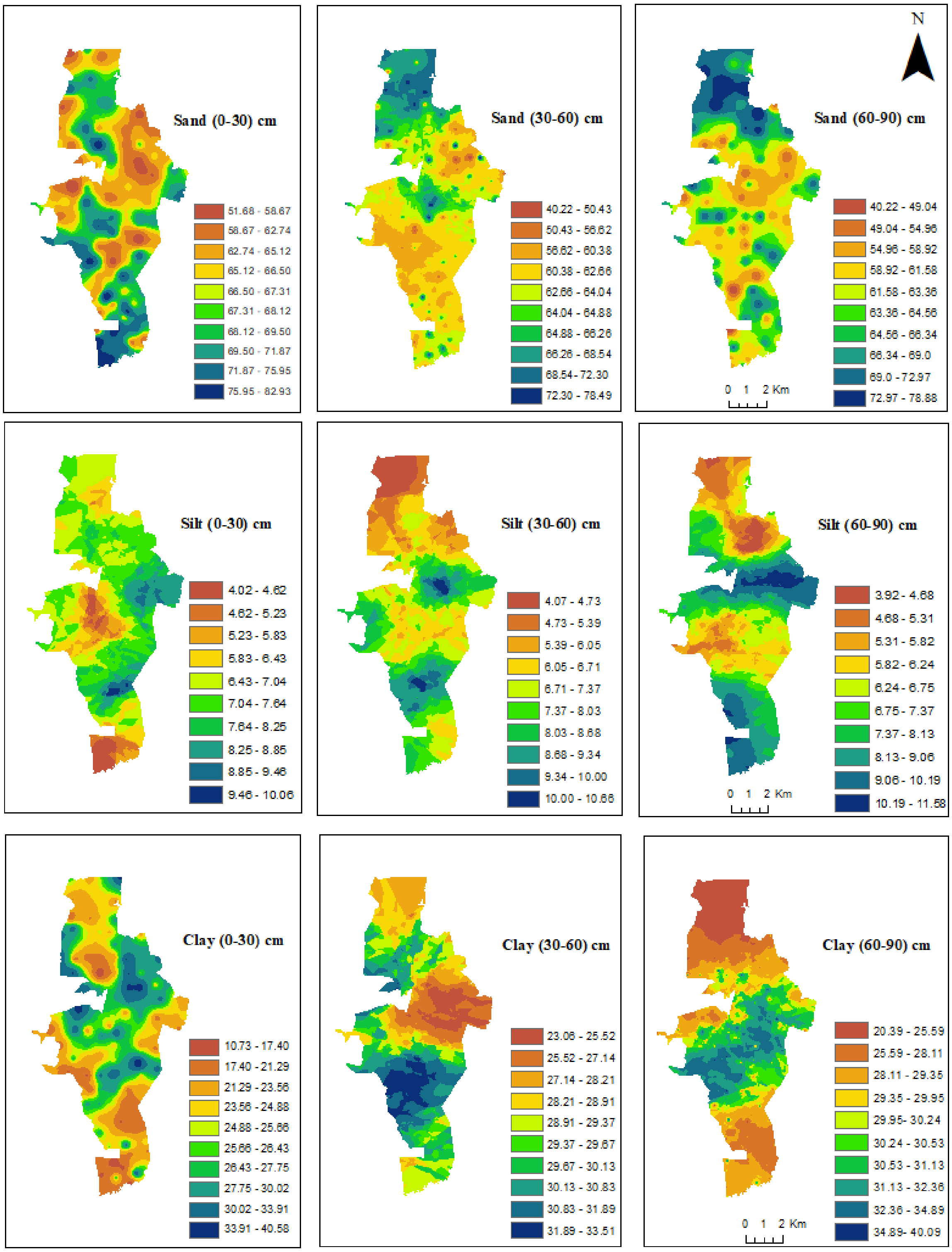

Figure 11. Maps showing the spatial distributions of sand, silt and clay percentages in the Tarap Hill Reserve, Bangladesh at three soil depth levels (0-30, 30-60, 60-90cm) using the most accurate interpolation method (Table 2).

CHAPTER 4

HABITAT SUITABILITY MODELS AND MAPS OF MAJOR TREE SPECIES IN TARAP HILL RESERVE

4.1 Model comparison and selection

Random Forest (RF) performed best for all nine species (Table 5), with AUC values ranging from 0.8 to 0.9, TSS values ranging from 0.62 to 0.81 and deviance (D) value ranging from 0.43-1.06.

4.2 Key drivers and species response

Regulatory variables*, historical* disturbance and community structure (a proxy of biotic competition) were the key predictors driving spatial distribution of the tree species. Soil nutrients and topography *were the* weak *predictors. Among* the regulatory variables, sand was the prominent predictor with higher influences on the spatial distribution of four species: *S. wallichi, T. bellerica, G. lanceolarium*, and *D. pentagyna*. Among the disturbance variables, canopy openness (CO) was the key driver (variable contribution percentage (VCP) = 11.3%) for the spatial distribution of *D. turbinatus* and the distribution of the valuable timber yielding species *A. chaplasha* was driven predominantly by historical logging (VCP = 7.6%). Among all the variables, CS showed highest influences (VCP = 11.3%) on *F. roxburghi* and *S. robusta* distributions.

Table 4. The variable contribution percentages (VCP) for fitting the species distribution model (SDM) using the random forest (RF) algorithm with fourteen predictor variables across five broad categories.

Species names	Regulatory variables (%)			Biotic competition variable (%)	Disturbance variables (%)		Soil nutrients (%)		Topographic variable (%)	Suitable Habitat (km^2)
	Sand (%)	pH	SOC	CS	CO	Logging	N	P	Elevation	
Artocarpus chaplasha	5.6	3.6	4.4	2.6	4.9	7.6	4.9	7.2	5.2	23.07
Schima wallichi	7	7	4.7	5.8	6.1	5.9	5.4	5.1	4.1	26.53
Terminalia bellerica	9.2	5.1	4.6	9.2	6.7	2.7	3	2.6	3.2	32.6
Glochidion lanceolarium	8.8	4.2	6	6.9	3.4	6.4	5.5	5.6	5.6	34.08
Holarrhena pubescens	6	4.8	2.6	8.5	2.5	4.4	3.8	3.1	4.2	30.76
Dillenia pentagyna	7.3	4.5	6.2	5.8	5.3	3.2	4.4	3.1	5.1	22.53
Shorea robusta	2.5	3	3.5	11.3	3.2	8.5	1.1	3.3	2.9	14.85
Ficus roxburghi	3.3	5.8	3	11.3	4.1	6.5	4.7	6	6	20.55
Dipterocarpus turbinatus	2.6	4.9	2.7	5.7	11.1	6.4	3.7	6.1	3.3	13.5

4.2 Key drivers and species response

Regulatory variables, historical disturbance and community structure (a proxy of biotic competition) were the key predictors driving spatial distribution of the tree species. Soil nutrients and topography were the weak predictors. Among the regulatory variables, sand was the prominent predictor with higher influences on the spatial distribution of four species: *S. wallichi, T. bellerica, G. lanceolarium*, and *D. pentagyna*. Among the disturbance variables, canopy openness (CO) was the key driver (variable contribution percentage (VCP) = 11.3%) for the spatial distribution of *D. turbinatus* and the distribution of the valuable timber yielding species *A. chaplasha* was driven predominantly by historical logging (VCP = 7.6%). Among all the variables, CS showed highest influences (VCP = 11.3%) on *F. roxburghi* and *S. robusta* distributions.

Table 4. The variable contribution percentages (VCP) for fitting the species distribution model (SDM) using the random forest (RF) algorithm with fourteen predictor variables across five broad categories.

Species names	Regulatory variables (%)			Biotic competition variable (%)	Disturbance variables (%)		Soil nutrients (%)		Topographic variable (%)	Suitable Habitat (km^2)
	Sand (%)	pH	SOC	CS	CO	Logging	N	P	Elevation	
Artocarpus chaplasha	5.6	3.6	4.4	2.6	4.9	7.6	4.9	7.2	5.2	23.07
Schima wallichi	7	7	4.7	5.8	6.1	5.9	5.4	5.1	4.1	26.53
Terminalia bellerica	9.2	5.1	4.6	9.2	6.7	2.7	3	2.6	3.2	32.6
Glochidion lanceolarium	8.8	4.2	6	6.9	3.4	6.4	5.5	5.6	5.6	34.08
Holarrhena pubescens	6	4.8	2.6	8.5	2.5	4.4	3.8	3.1	4.2	30.76
Dillenia pentagyna	7.3	4.5	6.2	5.8	5.3	3.2	4.4	3.1	5.1	22.53
Shorea robusta	2.5	3	3.5	11.3	3.2	8.5	1.1	3.3	2.9	14.85
Ficus roxburghi	3.3	5.8	3	11.3	4.1	6.5	4.7	6	6	20.55
Dipterocarpus turbinatus	2.6	4.9	2.7	5.7	11.1	6.4	3.7	6.1	3.3	13.5

4.3 Tree Species Habitat Suitability Maps

The average predicted suitable habitat area for all nine species calculated by the RF algorithm is 24.27 km^2 (SD ±7.38) (Table 6). The species with the lowest predicted suitable habitat was *D. turbinatus*, with an area of 13.50 km^2, while the species with the largest predicted suitable habitat was *G. lanceolarium* with an area of 34.08 km^2. Most of the predicted suitable habitat across all species was located in the southwest part of the reserve. However, isolated patches of suitable habitats were also observed for almost all species throughout the reserve.

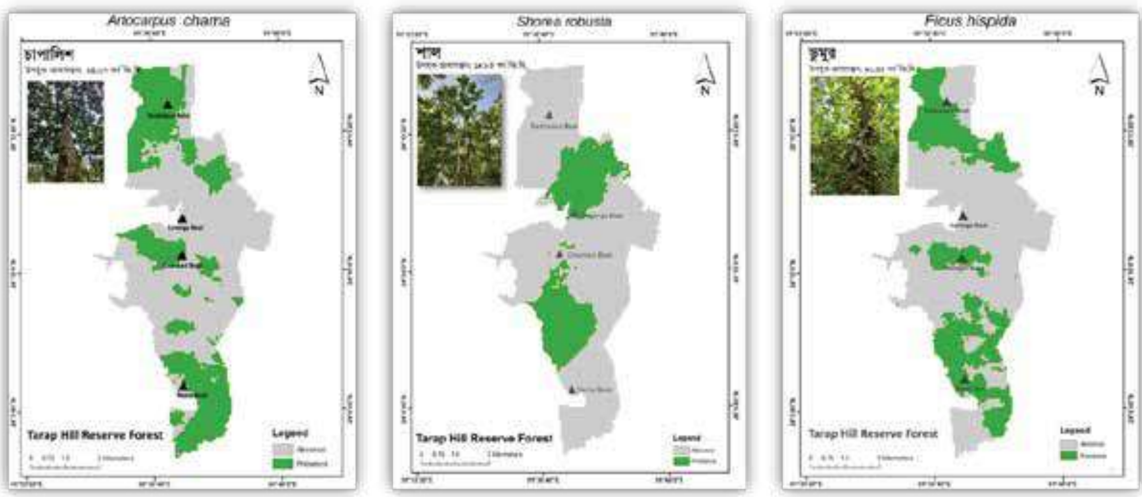

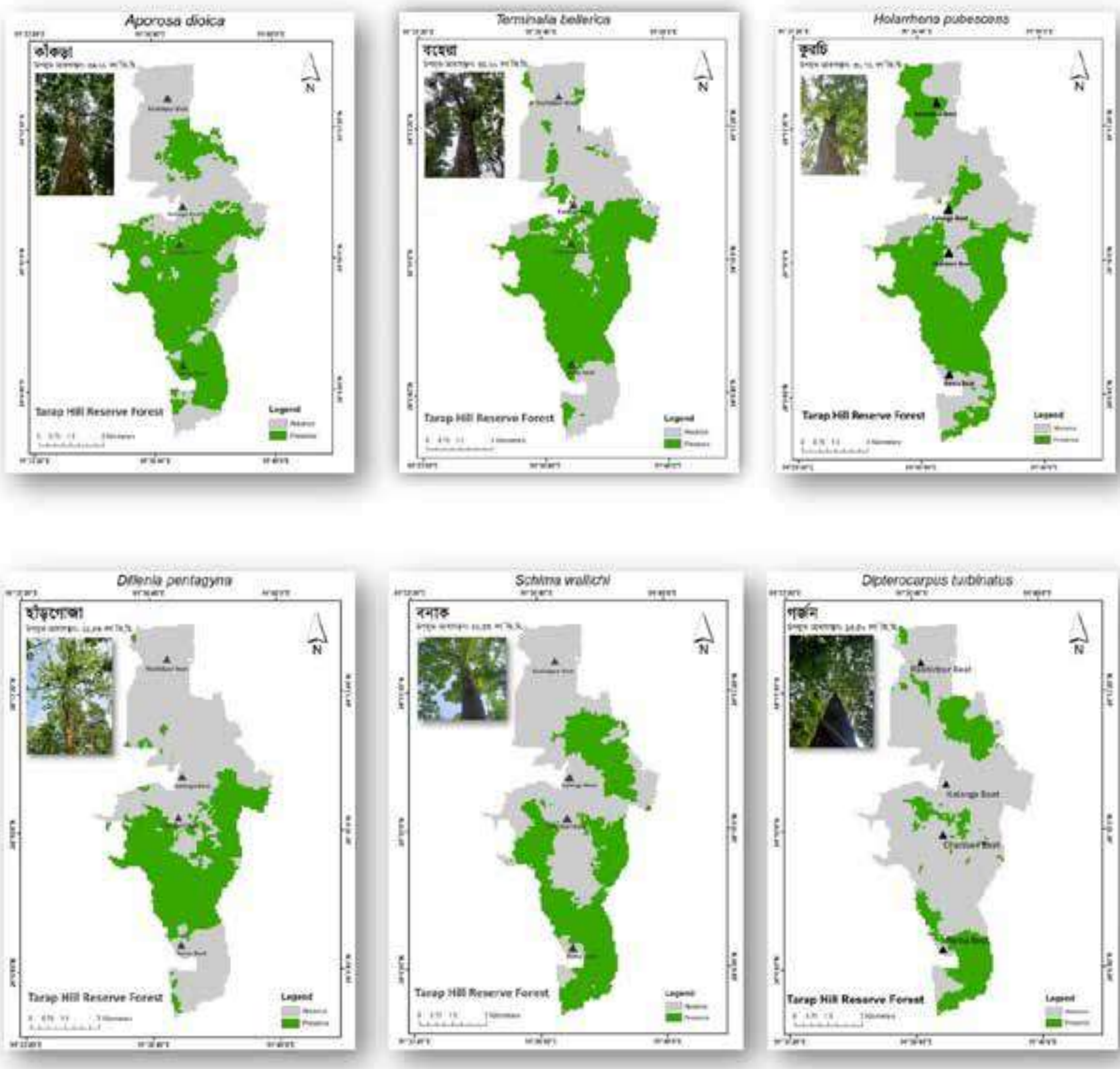

Figure 13. Spatial distribution i.e., habitat suitability map of the nine dominant species in the Tarap Hill Reserve generated from ensemble modelling. The binary (presence-absence) map was created by applying the Maximum (sensitivity + specificity) threshold. Here, green color represents areas of presence and grey color represents areas of absence.

4.4 Consensus Map: Multispecies Habitat Suitability Areas

The consensus map (combined binary maps of all species) revealed that the area coverage for multispecies habitat suitability (i.e., suitable habitat for all nine species) is only 0.47 km^2, which is 0.75% of the total THR area (**Error! Reference source not found.**7). Surprisingly, the established protected area (RKWS, Rema-Kalenga Wildlife Sanctuary) does not comprise any of this crucial multispecies habitat suitability area (Fig. 14).

Table 5. Distribution of multispecies habitat suitability areas within the protected area, RKWS (Rema-Kalenga wildlife sanctuary) and outside the RKWS (reserve forests) in the Tarap Hill Reserve forest (THR) in Bangladesh.

Number of species	Area of THR (km^2)	Number of grid cells within THR	Multispecies habitat suitability (km^2) within THR	% of THR	Aera of RKWS (km^2)	Number of grid cells within RKWS	Multispecies habitat suitability (km^2) within RKWS	% of RKWS
0	62.32	436	4.36	7.00	17.96	47	0.47	2.62
1	62.32	815	8.15	13.08	17.96	77	0.77	4.29
2	62.32	846	8.46	13.58	17.96	172	1.72	9.58
3	62.32	953	9.53	15.29	17.96	291	2.91	16.20
4	62.32	1151	11.50	18.45	17.96	566	5.66	31.51
5	62.32	1034	10.30	16.53	17.96	469	4.69	26.11
6	62.32	613	6.13	9.84	17.96	221	2.21	12.31
7	62.32	266	2.66	4.27	17.96	32	0.32	1.78
8	62.32	93	0.93	1.49	17.96	3	0.03	0.17
9	62.32	47	0.47	0.75	17.96	0	0.00	0.00

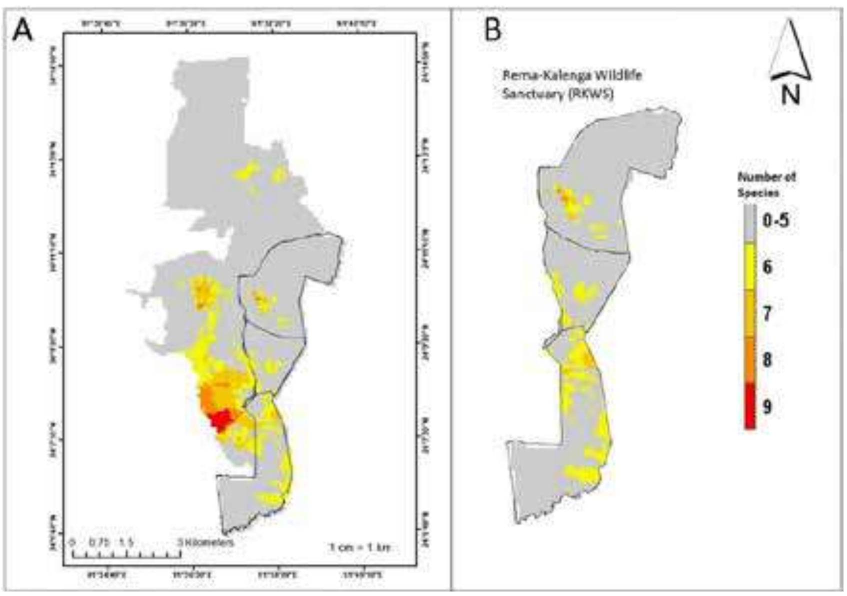

Figure 12. Consensus map of the predicted habitat suitability following Random Forest (RF) algorithm for nine dominant tree species of Tarap Hill Reserve (THR), highlighting multispecies habitat suitability for the respective number of species that fall within (A) THR, and the designated protected area within the reserve, (B) Rema-Kalenga Wildlife Sanctuary (RKWS)

CHAPTER 5

TREE DIVERSITY MODELS AND MAPS OF THE TARAP HILL RESERVE

5.1 Habitat-Based Biodiversity Model

The explanatory power and the goodness of fit of the alpha, beta, and gamma diversity GAMs varied when we increased weight on species relative abundances (q = 0, 1, and 2) in the subcommunities (SCs). $^0\overline{\alpha}$ (species richness) GAM explained more deviance (DE = 53.3%) and showed a better fit to the data (Adj. R^2 = 0.52) compared to those for $^1\overline{\alpha}$ (Shannon entropy) and $^2\overline{\alpha}$ (Simpson's concentration) (Table 8). This suggests that, for alpha diversity, the model with a moderate focus on species presence–absence (q = 0) could capture more signal compared to the models that only considered species relative abundances in the SCs (i.e., q = 1) or offered more importance to the more dominant species (q = 2) in the SCs. Similarly, the $^0\overline{\rho}$ GAM (DE = 46.9%) and the $^0\gamma$ GAM (DE = 56.5%) captured more signal than the other models (for q = 1, 2).

Table 6. Results of the generalized additive models (GAMs) for the Alpha, Beta and Gamma diversity measures. Model fit summaries, shown in the rightmost two columns, are only provided for the best model (DE = deviance explained). Numbers within the cells represent the Relative Importance (RI) of each covariate. Dashed boxes indicate that the respective variable did not participate in any of the candidate models.

Diversity	Variables										Adj. R^2	DE
	N	P	K	Fe	pH	Sand	Silt	Clay	SOC	CS	Canopy openness		
$^0\overline{\alpha}$	0.2	1	0.8	0.5	1	---	1	1	1	1	1	0.52	53.3%
$^1\overline{\alpha}$	0.4	1	---	0.6	0.7	---	0.3	0.9	1	1	1	0.28	30%
$^2\overline{\alpha}$	0.4	0.9	0.5	0.9	0.5	0.5	---	0.6	1	1	1	0.19	23.2%
$^0\overline{\rho}$	---	0.7	1	1	0.1	0.2	0.1	0.9	0.3	1	1	0.46	46.9%
$^1\overline{\rho}$	0.3	0.5	1	0.8	0.6	0.5	1	1	0.7	1	0.6	0.34	39.1%
$^2\overline{\rho}$	0.3	---	---	0.4	0.3	---	1	1	0.5	1	---	0.25	29.5%
$^0\overline{\gamma}$	0.5	0.9	0.5	0.8	0.4	0.6	---	0.5	---	0.8	1	0.45	56.5%
$^1\overline{\gamma}$	0.1	0.3	0.3	---	0.1	0.1	---	0.5	0.2	0.8	0.8	0.24	28.7%
$^2\overline{\gamma}$	---	---	---	0.51	---	---	---	0.7	0.7	1	---	0.38	30.4%

1.2 Drivers of Tree Diversity and Responses

The RI of the covariates in influencing biodiversity indices also varied when we changed the weight on species relative abundances in the SCs (Table 8). For example, while SOC did not influence $^0\gamma$, it had stronger effects on $^2\gamma$ (RI = 0.7). SC alpha diversity $^0\overline{\alpha}$ was mainly influenced by silt (RI = 1), Clay (RI = 1), SOC (RI = 1), CS (RI = 1), and Canopy openness (RI = 0.8). K (RI = 1), Fe (RI = 1), Community structure (CS, RI = 1), Canopy openness (RI = 1), and Clay (RI = 0.9) were the predominant drivers for spatial variations in SC beta diversity $^0\overline{\rho}$. SC gamma diversity $^0\gamma$ was mostly influenced by Canopy openness (RI = 1), P (RI = 0.8), Fe (RI = 0.8), and CS (RI = 0.8).

5.3 Tree Diversity Maps

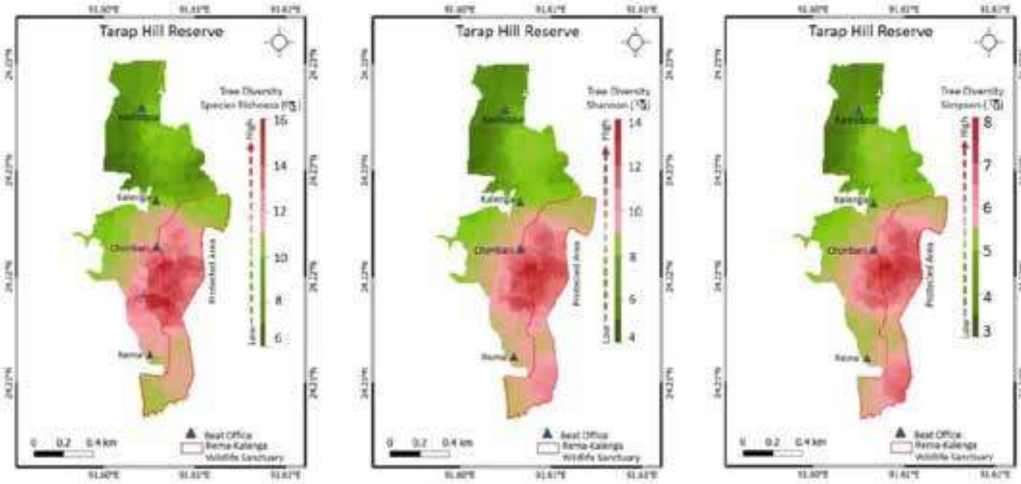

Figure 15. Spatial distributions of alpha diversity in the Tarap Hill Reserve (THR).

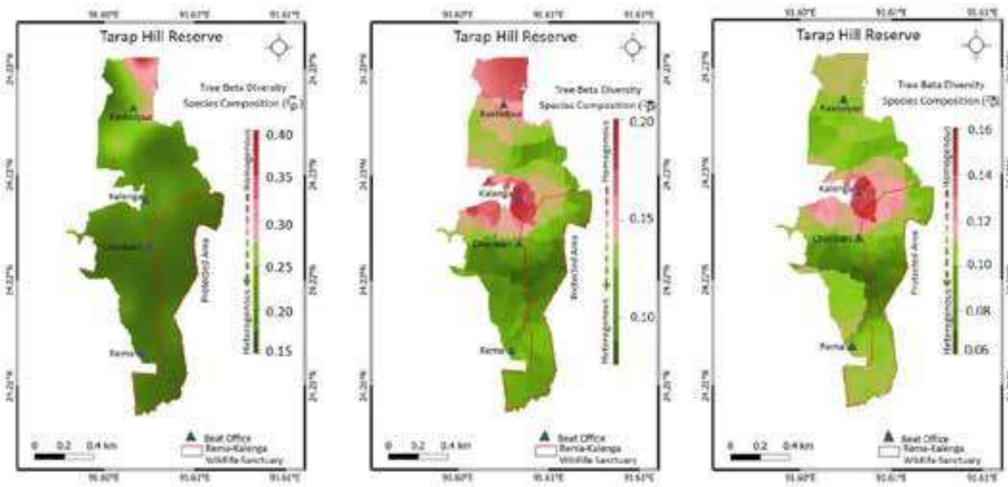

Figure 16. Spatial distributions of Beta diversity in the Tarap Hill Reserve.

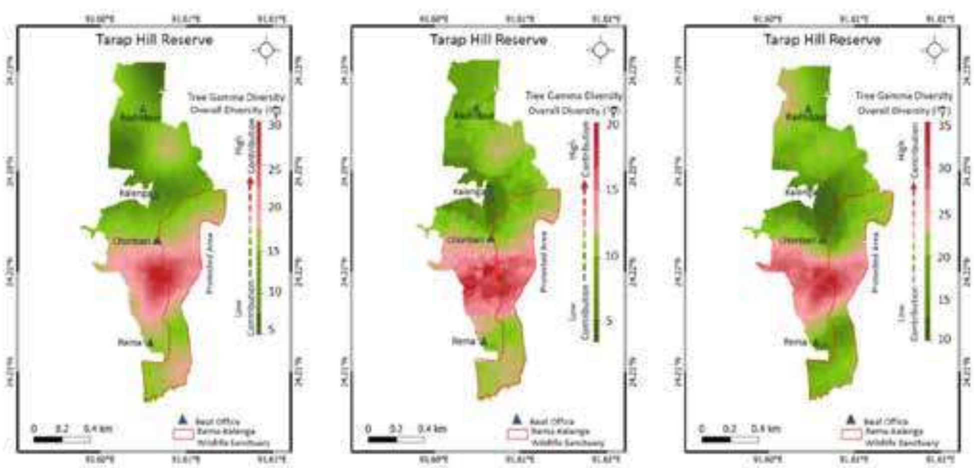

Figure 17. Spatial distributions of gamma diversity in the Tarap Hill Reserve.

CHAPTER 6

MODELS AND DIGITAL MAPS OF HABITAT CONDITIONS IN THE RAGHUNANDAN HILL RESERVE

6.1 Descriptive statistics of the soil physico-chemical properties

Descriptive statistics of the soil physico-chemical properties in the Tarap Hill Reserve is presented in Table 9. The coefficient of variation (CV), reflecting the degree of variability of soil properties (lower values indicate less variability where higher values indicate high variability), represents higher variability among Ca, P, SOC, silt and Fe across different forest management while N, pH and sand showed least variability.

6.2 Soil type

Based on our soil mechanical analysis and the soil textural triangle developed by the United States Department of Agriculture (USDA) and the soil textural classes with their particle size ranges table adopted by Osman (2013), the soil type of the Raghunandan Hill Reserve can be classified as 'Sandy Loam' (sand = 76.42%, silt = 5.71%, and clay = 17.86%) (Fig. 18).

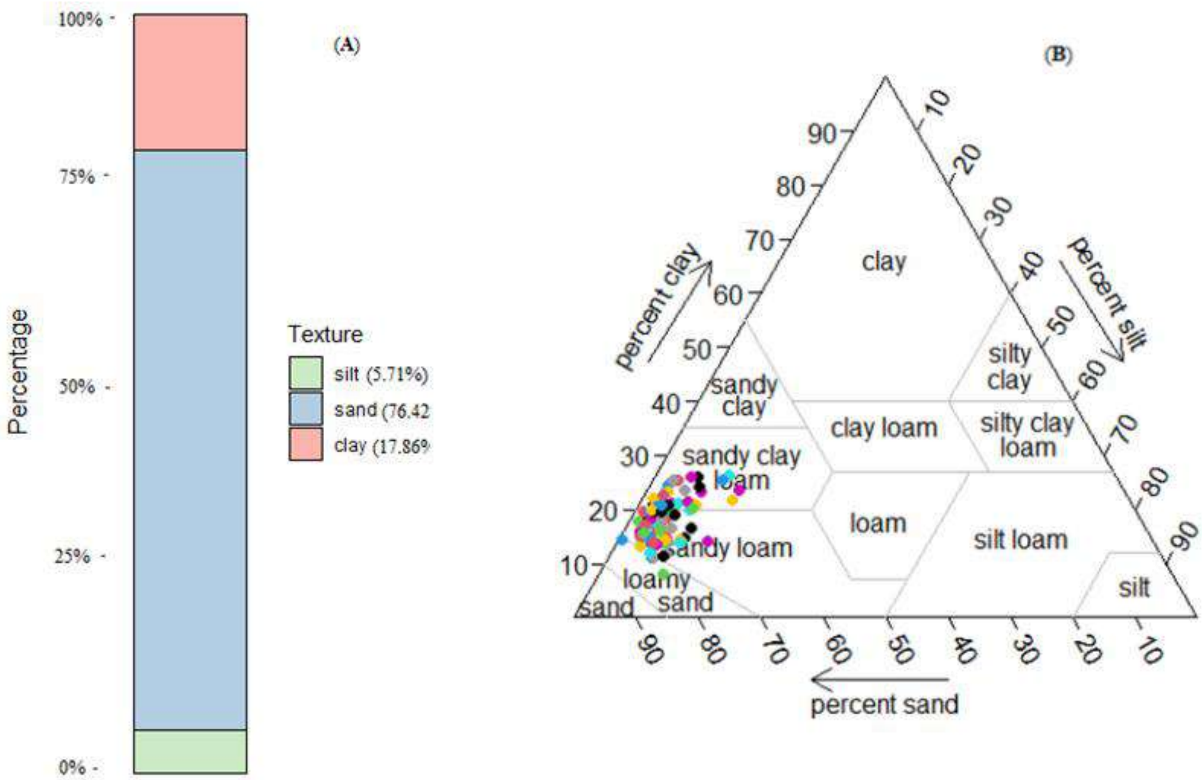

Figure 18. Soil mechanical composition in the Tarap Hill Reserve. (A) Showing % of sand, silt, and clay in different soil depth layers, and (B) showing soil type determination through a soil textural triangle devised by the United States Department of Agriculture (USDA).

Table 7. Descriptive statistics of 12 soil physico-chemical properties (top soil, 0-30 Cm) in the Raghunandan Hill Reserve, Bangladesh in different soil depths. SD = Standard deviation and CV= Coefficient of variation.

Variables	N	Min	Max	Range	Mean	SD	CV (%)
N (mg/L)	98	0.036	0.047	0.011	0.042	0.003	7.8209
P (mg/L)	98	0.001	0.012	0.011	0.004	0.002	61.472
K (mg/L)	98	0.001	0.003	0.002	0.001	0.0001	39.69
Fe (mg/L)	98	0.129	1.304	1.175	0.401	0.182	45.457
Ca (mg/L)	98	0.007	0.206	0.199	0.029	0.026	89.706
Mg (mg/L)	98	0.002	0.052	0.05	0.024	0.011	43.565
Sand (%)	98	61.531	85.189	23.659	76.421	4.683	6.128
Silt (%)	98	0.4826	14.748	14.265	5.732	2.970	51.820
Clay (%)	98	8.0171	26.298	18.282	17.847	4.041	22.641
Soc (%)	98	0.2202	5.2408	5.0217	1.825	0.989	54.195
pH	98	3.36	6.3	2.94	4.538	0.356	7.8508

6.3 Interactions between soil properties, topography, and community structure

Pearson correlation analyses revealed significant interactions (positive and negative) between several soil properties and elevation (Fig. 19). Mg and Fe (r = 0.6, p<0.001), and Ca and elevation (r = 0.42, p<0.001) showed significant positive correlations while sand and clay (r = -0.78–, p<0.001) and sand and silt (r=-0.52, p<.001) showed a significant negative correlation.

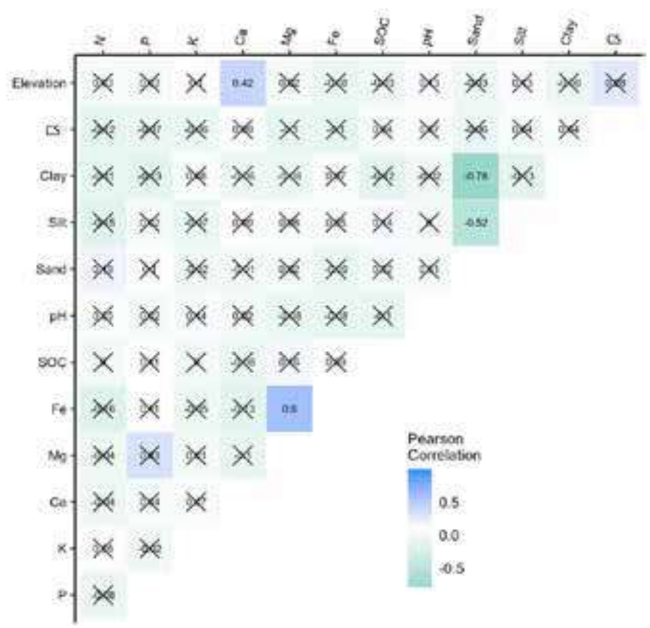

Figure 19. Pearson correlation analyses illustrating the relationships among soil properties, topography (elevation) and community structure in the RHR, Bangladesh. In the correlation matrix, numbers in the blue color cells represent positive correlation coefficient (r) values and numbers in the green color cells represent negative values. Cross marked indicates non-significance at p>0.05 level.

6.4 Effects of Forest Management Interventions on Soil Properties and Community Structure

The Kruskal-Wallis test showed significant variations in several soil properties across different management interventions (mixed plantations, mono plantations and natural forests) (Fig. 20). Post-hoc Dunn test further specified that among the nutrients, only soil Mg and SOC concentrations significantly varied in different management interventions and the availability of Mg and SOC decreased with lower species diversity.

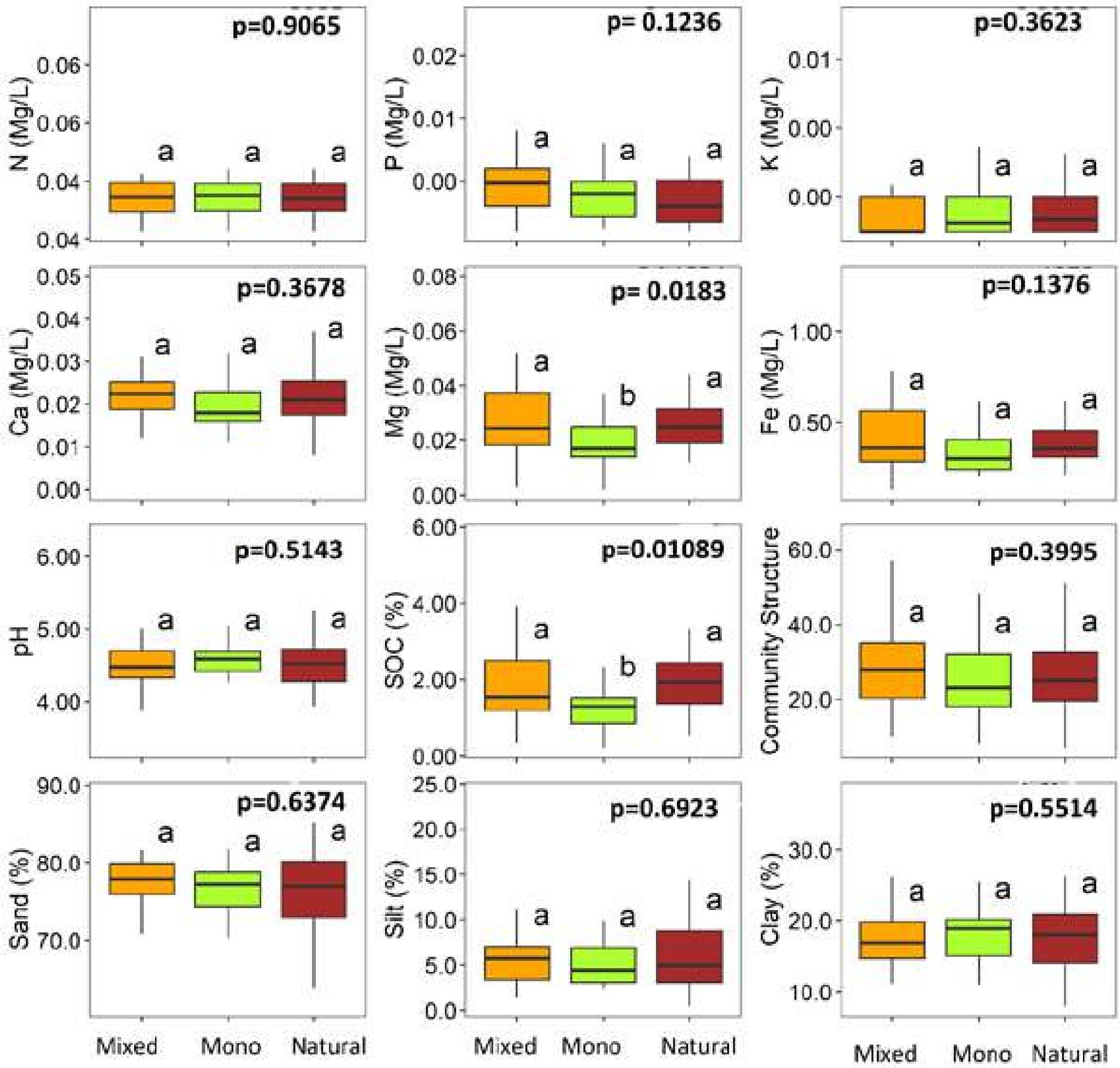

Figure 20. Boxplot representing the variations among soil physico-chemical properties (N, P, K, Ca, Mg, Fe, pH, SOC, Sand, Silt and Clay) and community structure across different forest management interventions. Different letters indicate the groups are statistically significant at $p<0.05$.

6.5 Habitat Models

Our spatial analysis showed that the predictive performances of the different interpolation methods varied for different soil properties, and community structure in the RHR (Table 10). Between the two geostatistical methods, the UK showed relatively higher predictive accuracy. Among the deterministic methods, IMQF and LPI showed relatively higher predictive accuracy while IDW showed least predictive ability. Both EBK and IDW showed least predictive ability for these properties.

Table 8. Comparison between predictive performances of the geostatistical [Empirical Bayesian Kriging (EBK), and Universal Kriging (UK)] and deterministic methods [Inverse Distance Weighting (IDW), Spline with tension (SWT), Local Polynomial Interpolation (LPI), and Inverse Multi-quadric function (IMQF)] based on normalized root mean square error (NRMSE) of the predicted versus the actual parameter values. For normalization, the root mean square error statistic was divided by the range of the actual values and NRMSE is expressed here as a percentage. Lower NRMSE values (light blue-shaded cells) indicate relatively higher predictive accuracy and higher values (grey-shaded cells) indicate lower predictive accuracy.

Variables	Geostatistical Methods		Deterministic Methods			
	EBK	UK	IDW	SWT	LPI	**IMQF**
N	30.35	30.56	32.83	33.04	30.67	**29.88**
P	20.69	20.97	20.60	20.34	21.24	**20.02**
K	28.84	29.41	29.03	29.08	**28.29**	28.80
Ca	12.41	**12.60**	12.69	12.30	12.63	13.77
Mg	19.53	19.68	19.44	19.41	19.43	**0.22**
Fe	13.30	**13.24**	13.75	13.77	13.66	13.33
Sand	20.62	**19.94**	20.65	20.53	20.35	20.27
Silt	21.42	21.56	21.76	21.61	21.51	**21.30**
Clay	23.01	23.29	22.98	23.27	**22.11**	22.32
pH	33.95	12.70	12.58	**12.53**	498.81	12.58
SOC	19.91	20.21	21.80	21.15	109.38	**19.80**
CS	1.74	**18.82**	**19.13**	18.35	93.83	18.49

6.6 Soil Maps

The spatial distributions of soil nutrients (N, P, K, Ca, Mg, Fe), soi acidity, community structure, soil organic carbon, sand, silt and clay contents in the RHR are shown in Figs. 21-22, using the interpolation method with the highest accuracy, as outlined in Table 10. These maps reveal significant spatial variability in the values of soil parameters throughout the area. Hotspots of soil N concentration in the surface soil (0-30cm) are observed in the southern and northwestern parts of the reserve, while lower N content is evident in the central region. Conversely, P exhibits opposite patterns to N, with higher content in areas of lower N and lower P content in the central part of the RHR. K content demonstrated the highest concentrations in the northern part while it gradually decreased, and the lowest K concentrations were noted towards the southern, southwestern, and eastern parts. Interestingly, the central area of the reserve exhibited higher levels of K content.

The spatial distribution of Ca within the reserve exhibits a notable concentration gradient, with higher levels observed in the northwestern and southern regions. Conversely, the lowest concentrations of Ca are evident in the northern and northeastern portions, extending towards the central zone of the reserve. Meanwhile, Mg and Fe showed analogous trends; both elements exhibit lower concentrations in the central part of the reserve, extending towards the southernmost regions. Conversely, the northern and northwestern part display the highest concentrations of Mg and Fe.

The soil pH demonstrated its highest concentration across the entire reserve from the northern to the southern regions, with the central and a portion of the northeastern area displaying the lowest pH concentrations.

Concurrently, both the northeastern and southwestern parts of the reserve exhibited elevated concentrations of SOC, while the central region displayed lower SOC content. Interestingly, the community structure exhibited considerable variability throughout the reserve, with higher species abundance observed in the central and southeastern parts, and lower species diversity in the northwestern region (specifically in Telmachara Beat and Shaltila Beat). Regarding soil textural class, the entire reserve featured higher percentages of sand, while the percentages of silt and clay displayed notable variability across the reserve. Some sections of Telmachara Beat and Shaltila Beat showed lower silt content but higher clay content. In contrast, the northeastern and southern parts of the reserve exhibited lower clay content and higher silt concentrations.

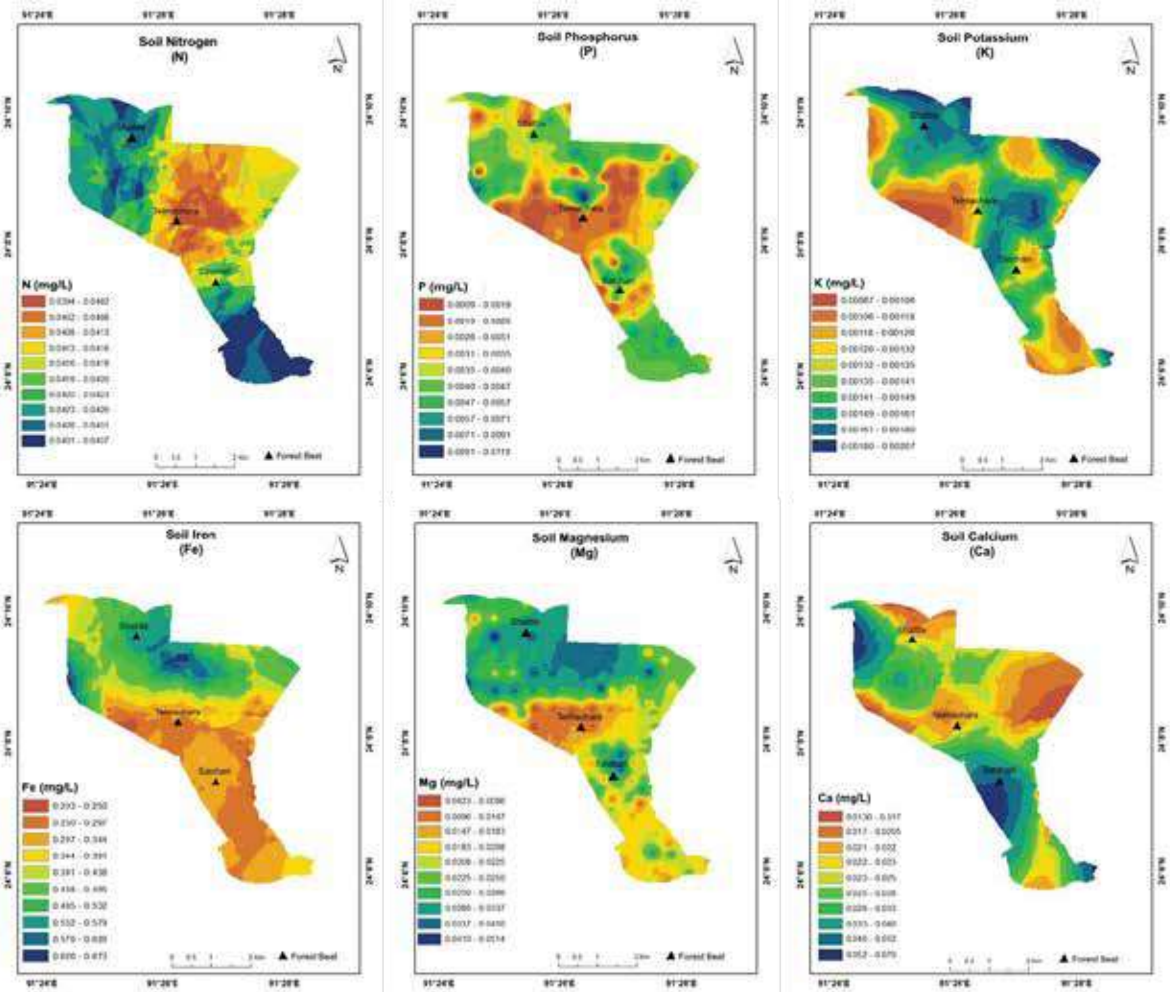

Figure 21. Maps showing the spatial distributions of soil N, P, K, Ca, Mg and Fe (mg/L) concentrations in the Raghunandan Hill Reserve, Bangladesh using the most accurate interpolation method (Table 10).

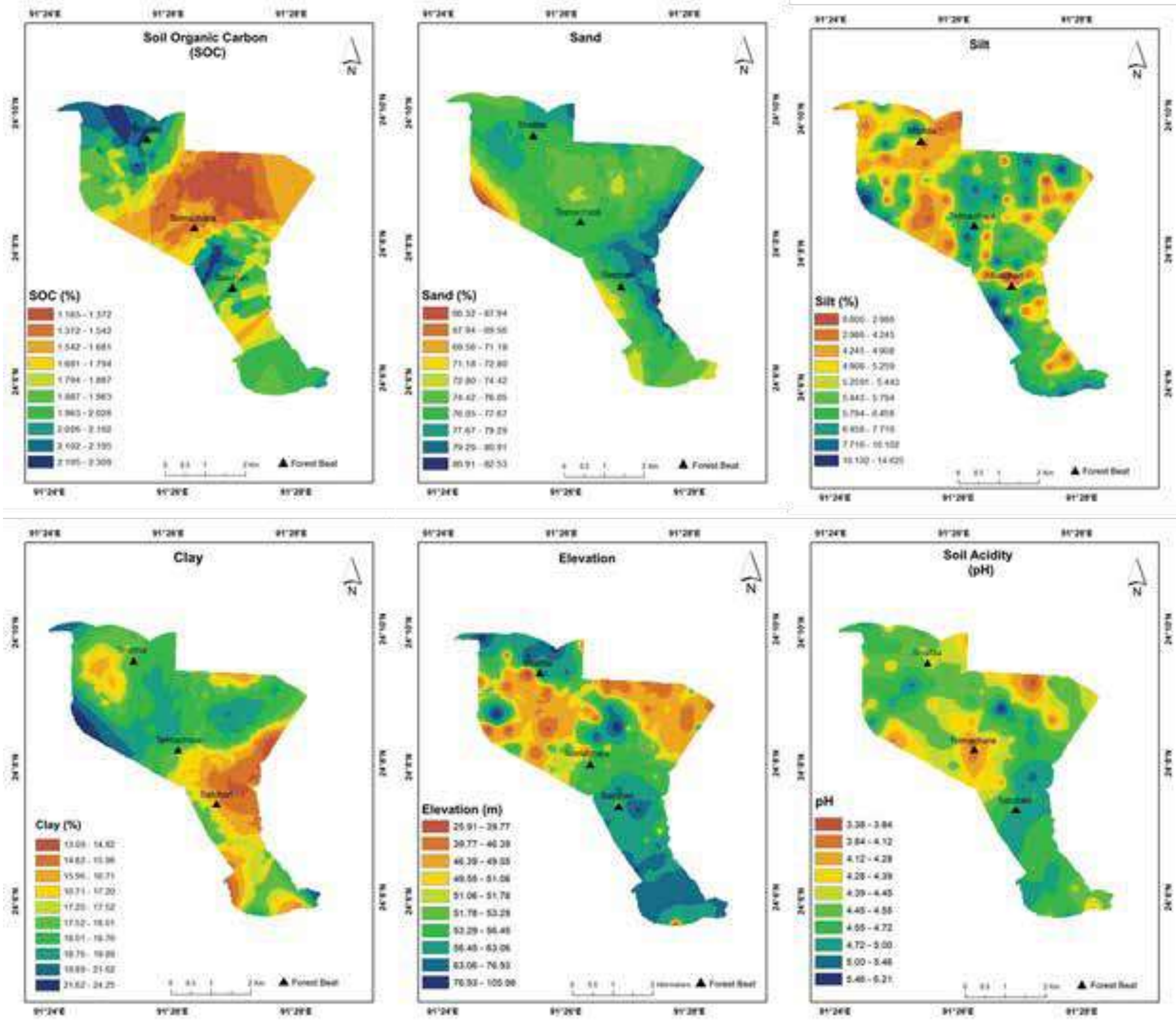

Figure 22. Maps showing the spatial distributions of SOC, sand, silt, clay, elevation and pH in the Raghunandan Hill Reserve, Bangladesh.

CHAPTER 7

HABITAT SUITABILITY MODELS AND MAPS OF MAJOR TREE SPECIES IN RAGHUNANDAN HILL RESERVE

7.1 Model comparison and selection

All eight species were successfully predicted by each of the six statistical methods falling into three broad modelling approaches: regression (GLM and GAM), tree-based classification (BRT and CART), and machine learning (RF and MLP). The only exception to this is GAM, which had a success rate of 0% because of insufficient presence data for model cross-validation. The results of the model performance evaluation are presented in Table 10. Overall, the machine learning and tree-based approaches performed better than the regression approach for most species. Specifically, RF performed the best for *A. chaplasha*, *T. bellerica*, *F. racemosa*, *G. lanceolarium*, and *I. godajam*, while BRT performed the best for *D. pentagyna*, *D. turbinatus*, and *B. variegata*.

Table 9. Model performance for each species using Generalized Linear Model (GLM), Generalized Additive Model (GAM), Random Forests (RF), Multi-Layer Perceptron (MLP), Boosted Regression Trees (BRT) and Classification and Regression Trees (CART) modelling approaches. Indices used to measure model performance are area under the receiver operating characteristic curve (AUC), the true skill statistics (TSS) and Deviance (D).

Species		Regression		Machine learning		Tree-based	
		GLM	GAM	RF	MLP	BRT	CART
Artocarpus chaplasha	AUC	0.73	NA	0.87	0.77	0.78	0.74
	TSS	0.5	NA	0.69	0.59	0.55	0.46
	Deviance (D)	3.45	NA	0.92	2.4	1.2	2.22
Glochidion sphaerogynum	AUC	0.65	NA	0.86	0.71	0.75	0.73
	TSS	0.4	NA	0.68	0.5	0.52	0.46
	Deviance (D)	2.15	NA	0.9	2.38	1.18	2.12
Terminalia bellerica	AUC	0.71	NA	0.87	0.77	0.79	0.71
	TSS	0.46	NA	0.69	0.59	0.55	0.46
	Deviance (D)	2.76	NA	0.9	2.32	1.17	2.76
Ficus racemosa	AUC	0.71	NA	0.88	0.8	0.75	0.73
	TSS	0.49	NA	0.7	0.63	0.51	0.45
	Deviance (D)	3.13	NA	0.88	1.88	1.21	2.28
Dillenia pentagyna	AUC	0.63	NA	0.82	0.72	0.74	0.71
	TSS	0.43	NA	0.65	0.57	0.55	0.44
	Deviance (D)	3.85	NA	0.73	1.65	0.88	1.6
Ilex godajam	AUC	0.78	NA	0.9	0.84	0.81	0.75
	TSS	0.6	NA	0.75	0.7	0.61	0.5
	Deviance (D)	5.28	NA	0.72	1.43	1	1.76
Bauhinia variegata	AUC	0.65	NA	0.82	0.73	0.71	0.71
	TSS	0.41	NA	0.63	0.55	0.49	0.42
	Deviance (D)	3.99	NA	0.86	2.26	1.07	2.05

7.2 Key drivers

Topographic variable is often of less importance in predicting species occurrence, with elevation being the most important variable for only two species (*A. chaplasha* and *G. sphaerogynum*) (Table 11). Disturbance variables were more important, with canopy openness ranking in the top three variables for five species. Community structure was the key driver for *D. pentagyna, G. lanceolarium*, and *B. variegata*. Soil nutrients varied in importance, with some variables (e.g., P, Ca, and Fe) being critical for several species while others (e.g., Mg, N) being less important. In general, regulatory factors were less important, with clay and silt being the most important for only one species (*F. racemosa*). A combination of disturbance and community structure variables, as well as some soil nutrient variables, are the most important predictors of the examined species' distribution.

Table 10. The variable contribution percentages for fitting the HSMs using the random forest (RF) algorithm with fourteen predictor variables across five broad categories.

Species names	Topographic variable (%)	Disturbance variables (%)	Community structure (%)	Soil nutrients (%)						Regulatory variables (%)				
	Ele	CO	CS	P	Ca	Fe	K	Mg	N	Clay	pH	Sand	Silt	SOC
Artocarpus chaplasha	2.4	2	6.6	3.9	2.3	3.3	3.1	1.7	4.3	1.8	3.2	1.8	3.8	1.8
Glochidion sphaerogynum	2.6	1.6	12.6	1.8	3.2	1.7	1.8	6.9	2.1	2.4	2.6	1.3	2.3	2.7
Terminalia bellerica	4.3	5.7	2.1	3.9	2.9	1.7	3.2	6.5	3.2	7.2	2.2	2.8	1.3	3.6
Ficus racemosa	1.6	3.3	1.9	2.3	1.8	6.7	3.5	7.4	2	2.4	3.1	6.3	1.6	3.6
Dillenia pentagyna	7	3.6	6.5	1.9	4.7	3.4	1.9	2.6	3.2	3	3.4	3.8	5.5	4.5
Glochidion lanceolarium	2.3	1.5	10.9	2.9	1.5	2.8	1.7	1.4	2.9	1.4	1.3	1.1	1.6	7.2
Ilex godajam	1.3	1.5	4.1	3.4	4.2	2	2.1	6.6	4	2.4	3.1	5.3	3.6	2.5
Bauhinia variegata	3.3	2.2	2.6	1.8	7	2	3.2	4.8	6	3	5.7	2.4	2.2	3.4

7.3 Tree Species Habitat Suitability Maps

The average predicted suitable habitat area for all eight species calculated by the RF algorithm is 11.16 km^2 (SD ±4.56). The species with the lowest predicted suitable habitat was *B. variegata*, with an area of 6.72 km^2, while the species with the largest predicted suitable habitat was *T. bellerica* with an area of 21.41 km^2. Most of the predicted suitable habitat across all species was located in the north-east part of the RHR (Figs. 23-24). However, isolated patches of suitable habitats were also observed for almost all species throughout the reserve.

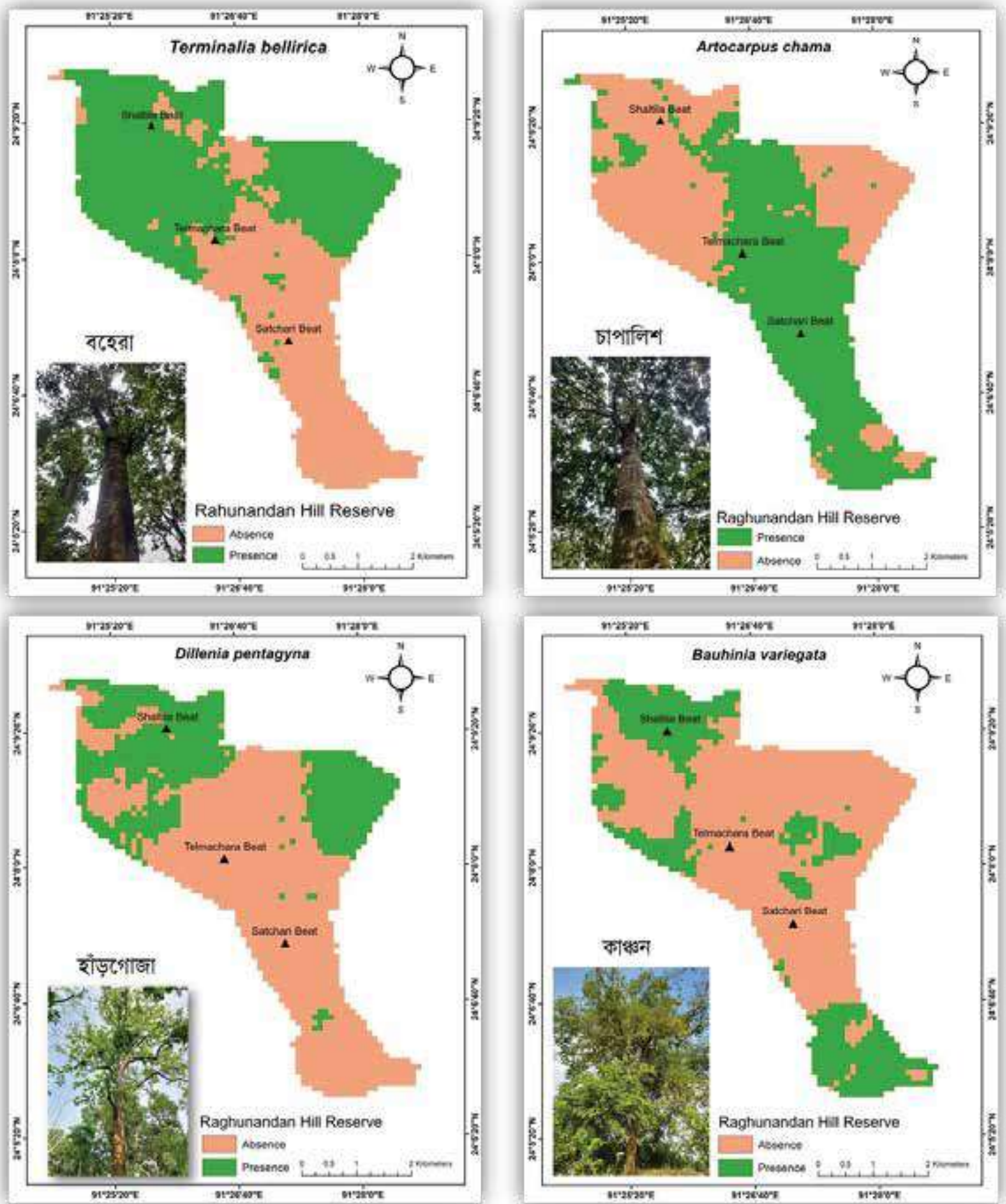

Figure 13. Spatial distribution i.e., habitat suitability of species in the Raghunandan Hill Reserve generated from ensemble modelling. The binary (presence-absence) map was created by applying the Maximum (sensitivity + specificity) threshold. Here, green color represents areas of presence and grey color represents areas of absence.

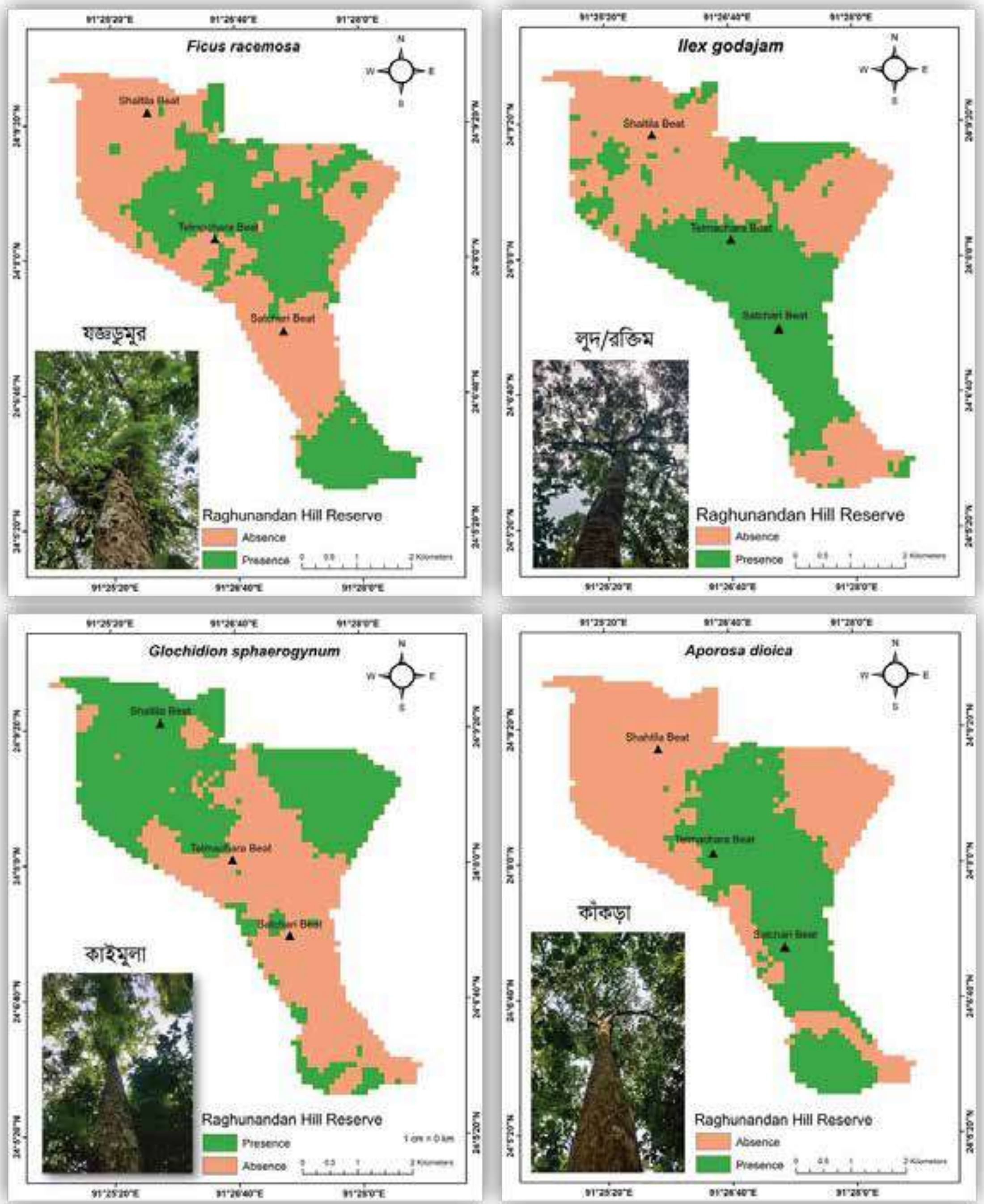

Figure 24. Spatial distribution i.e., habitat suitability of species in the Raghunandan Hill Reserve generated from ensemble modelling.

7.5 Consensus Map: Multispecies Habitat Suitability Areas

A consensus map across all studied species was developed to identify multispecies suitable habitat areas in the RHR. The result revealed that only 3.26 km^2 (multispecies suitable habitat) was projected to be suitable for five species, which is 31.17% of the total RHR area. Surprisingly, the established protected area (SNP, Satchari National Park) does not comprise any of this crucial multispecies suitable habitat. However, 0.01%, 0.1%, and 0.21% of the SNP contains the multispecies suitable habitat for 5,4 and 3 species, respectively (Table 13, Fig. 25). This multispecies suitable habitat encompasses 0.41%, 4.10%, and 8.61% of the reserve. The SNP protects

69.26% of the multispecies suitable habitat for two species, which is the highest among all multispecies suitable habitat categories.

Table 11. Distribution of species' multispecies suitable habitat areas within the protected area, SNP (Satchari National Park) and outside the RHR (reserve forests) in the Raghunandan Hill Reserve Forest (RHR) in Bangladesh.

Number of species residing in the multispecies suitable habitat	Number of grid cells within RHR	Multispecies suitable habitat area (km^2) within RHR	Area of RHR (km^2)	% of RHR	Number of grid cells within SNP	Multispecies suitable habitat area (km^2) within SNP	Aera of SNP (km^2)	% of SNP
0	2	0.02	10.45742	0.19	0	0.00	2.44	0.00
1	22	0.22	10.45742	2.10	32	0.32	2.44	13.11
2	196	1.96	10.45742	18.74	169	1.69	2.44	69.26
3	781	7.81	10.45742	74.68	21	0.21	2.44	8.61
4	756	7.56	10.45742	72.29	10	0.1	2.44	4.10
5	326	3.26	10.45742	31.17	1	0.01	2.44	0.41
6	69	0.69	10.45742	6.60	0	0.00	2.44	0.00
7	7	0.07	10.45742	0.67	0	0.00	2.44	0.00
8	93	0.00	10.45742	0.00	0	0.00	2.44	0.00

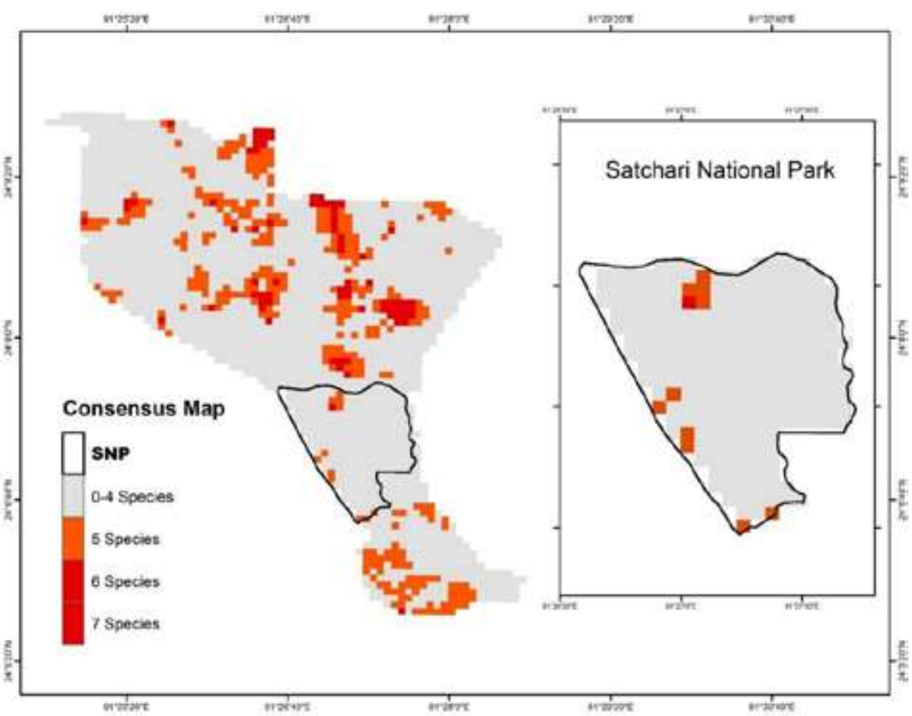

Figure 2514. Consensus map of the predicted habitat suitability following Random Forest (RF) algorithm for eight dominant tree species of RHR, highlighting multispecies suitable habitat for the respective number of species that fall within a) RHR, b) SNP.

CHAPTER 8

TREE DIVERSITY MODELS AND MAPS OF THE RAGHUNANDAN HILL RESERVE

8.1 Habitat-Based Biodiversity Model

The explanatory power and the goodness of fit of the alpha, beta, and gamma diversity GAMs varied when we increased weight on species relative abundances (q = 0, 1, and 2) in the subcommunities (SCs). ${}^{0}\overline{\alpha}$ (Species richness) GAM explained more deviance (DE = 56.1%) and showed a better fit to the data (Adj. $R^2 = 0.47$) compared to those for ${}^{1}\overline{\alpha}$ (Shannon entropy) and ${}^{2}\overline{\alpha}$ (Simpson's concentration) (Table 14).

8.2 Drivers of Tree Diversity and Responses

The relative importance (RI) of the variables in influencing biodiversity indices also varied when we changed the weight on species relative abundances in the SCs (Table 14). For example, while pH did not influence ${}^{0}\overline{\rho}$, it had stronger effects on ${}^{2}\overline{\rho}$ (RI = 0.9). SC alpha diversity (${}^{0}\overline{\alpha}$) was mainly influenced by N (RI = 0.8), Sand (RI = 1), Clay (RI = 0.9), and CS (RI = 1). Sand (RI = 0.8), Clay (RI = 0.7), SOC (RI = 1), and CS (RI = 1) were the predominant drivers for spatial variations in SC beta diversity (${}^{0}\overline{\rho}$). SC gamma diversity (${}^{0}\overline{\gamma}$) was mostly influenced by Silt (RI = 1), SOC (RI = 1), and CS (RI = 1).

Table 12. The results of the generalized additive models (GAMs) for nine diversity measures are presented. Model fit summaries, shown in the rightmost two columns, are only provided for the best model (DE = deviance explained). The numbers within the main section of the table represent the Relative Importance (RI) of each covariate. Dashed boxes indicate that the respective covariate did not participate in any of the candidate models.

Diversity	Variables											Adj. R^2	DE (%)
	N	P	K	Fe	pH	Sand	Silt	Clay	SOC	CS	CO		
${}^{0}\overline{\alpha}$	*0.8*	---	---	*0.7*	*0.3*	*1*	---	*0.9*	*0.6*	*1*	---	0.47	56.1
${}^{1}\overline{\alpha}$	*0.7*	---	---	*0.4*	---	*0.3*	---	*0.4*	*0.5*	*1*	*0.4*	0.31	41.7
${}^{2}\overline{\alpha}$	*0.7*	---	---	*0.4*	---	*0.3*	---	*0.3*	*0.4*	*1*	*0.4*	0.21	31.40
${}^{0}\overline{\rho}$	---	*0.5*	---	*0.5*	---	*0.8*	*0.5*	*0.7*	*1*	*1*	---	0.42	43.2
${}^{1}\overline{\rho}$	*0.4*	*0.4*	*0.4*	*1*	*0.5*	*0.4*	*0.4*	---	*0.9*	*1*	*0.4*	0.30	39.8
${}^{2}\overline{\rho}$	*0.6*	*0.3*	*0.4*	*0.7*	*0.9*	*0.6*	*0.5*	*0.3*	*0.7*	*1*	*0.5*	0.25	34.6
${}^{0}\gamma$	*0.4*	*0.3*	---	*0.6*	*0.7*	---	*1*	---	*1*	*1*	*0.6*	0.49	49.3
${}^{1}\gamma$	*0.3*	*0.7*	*0.4*	---	*0.4*	*0.4*	*0.7*	*0.3*	*1*	*1*	---	0.44	43.2
${}^{2}\gamma$	---	*0.7*	*0.5*	*0.5*	*0.6*	*0.5*	*0.3*	*0.3*	*1*	*1*	*0.4*	0.30	38.2

8.3 Tree Diversity Maps

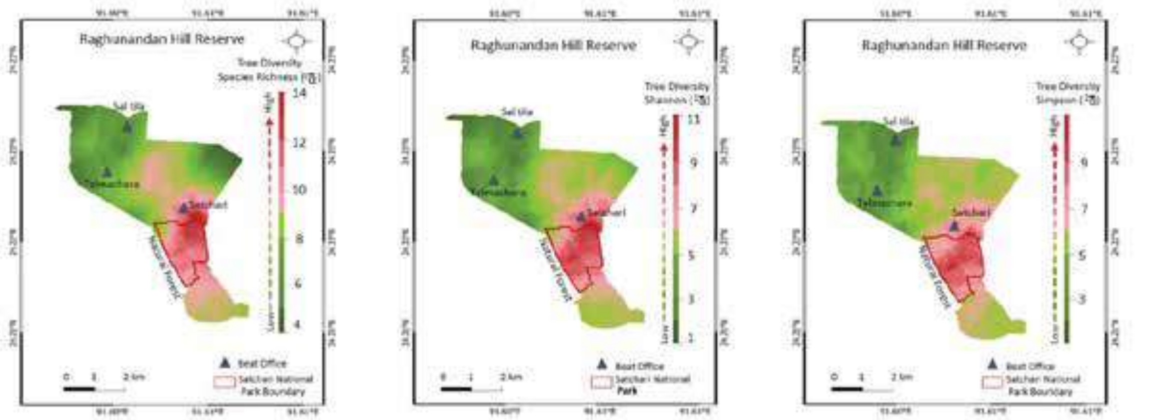

Figure 26. Spatial distributions of tree alpha diversity in the Raghunandan Hill Reserve (RHR) developed using generalized additive models.

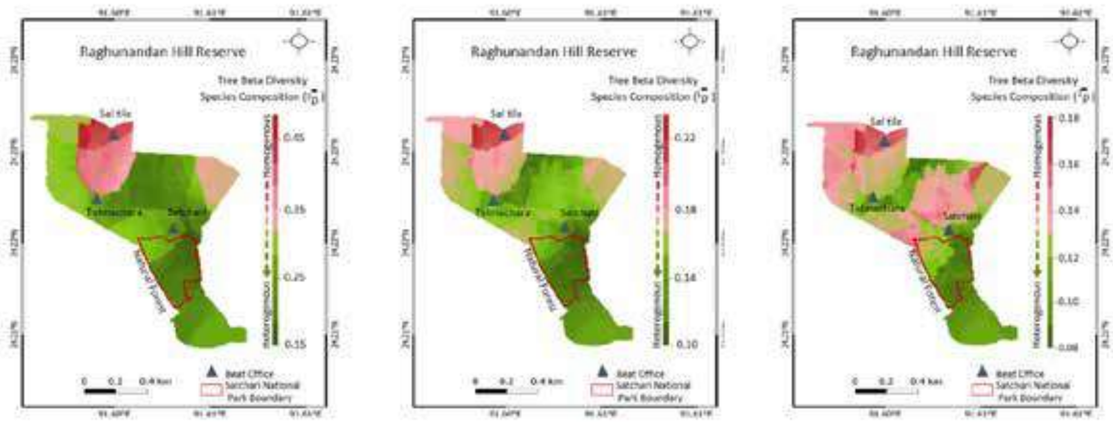

Figure 27. Spatial distributions of tree beta diversity in the Raghunandan Hill Reserve (RHR) developed using generalized additive models.

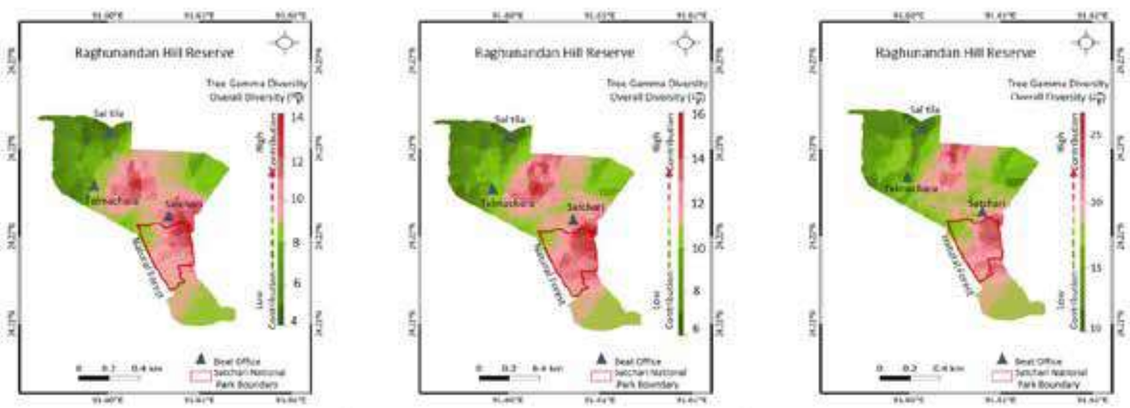

Figure 28. Spatial distributions of Gamma diversity in the Raghunandan Hill Reserve (RHR) developed using generalized additive models.

CHAPTER 9

APPLICATIONS OF RESULTS FOR FOREST MANAGEMENT AND RESTORATION

9.1 Applications of Models and Maps of Habitat Conditions

To successfully apply sustainable forest management practices, it is imperative to understand the variability in soil physicochemical properties and their spatial distribution, enabling the identification of intervention areas and the determination of intervention levels needed (Bogunovic et al., 2017; Dai et al., 2018). To understand plant nutrient requirements and optimal growing conditions for specific plant, it is important to understand soil chemistry and the interplay of elements that affect soil (Hossain et al., 2014). Here, our results (Chapter 3 and Chapter 6) on spatial variability in the values of soil properties across space and depths and their current distribution across different forest types (i.e., OGF, MXP and MOP) could help (I) designing site specific plan for new plantation establishment programs, (II) identifying appropriate sites and species for conducting Assisted Natural Regeneration, enrichment plantation, and rare and endangered species conservation programs, and (III) determining the critical areas that require constant protection measures in the THR and RHR. Our digital soil maps in combination with the species composition information generated in this study and elsewhere (Sarker et al, 2013) can be easily used by the central decision makers and field-level forest officials while conducting site-specific planting and in identifying areas that require immediate habitat treatment or long-term rehabilitation or restoration programs. These maps will also help the Bangladesh Forest Department for long-term monitoring of the forest habitats in the THR and RHR under future human pressure and climate change scenarios. Spatially explicit baseline soil information generated in this study, especially, the soil maps and the data therein could be a valuable addition to the global soil information and would guide future ecological and restoration-centric studies in degraded tropical forests.

9.2 Applications of Species Habitat Suitability Models and Maps

Our study emphasizes the significance of adopting a multi species and multi algorithm approach in habitat suitability modelling to identify areas of conservation priority (Chapter 4 and Chapter 7). By employing this approach, we successfully generated consensus maps which provides insight into the most favorable habitat areas for the dominant tree species within the THR and RHR. These maps showed that estimated habitat suitability for multiple species in the THR were located in the southwestern part which is outside the protected area i.e., Rema-Kalenga Wildlife Sanctuary. The information on multispecies habitat suitability is particularly valuable for conservation efforts (Brundrett, 2016; Qamar & Reza, 2020), as it highlights the significance of the southwestern region of the reserve. On the other hand, estimated habitat suitability for multiple species in the RHR were located within the natural forests of the Satchari National Park. This implies that the readjustment of the protected area is not currently required.

We propose that the boundaries of the Rema Kalenga Wildlife Sanctuary (RKWS) should be reevaluated, as the hotspot for dominant tree species of the reserve are not fully encompassed within the current sanctuary area. Remarkably, only 0.75% of the total THR is estimated as hotspot for all nine species, none of which falls within the sanctuary. This finding underscores the inadequacy of the current sanctuary boundaries in effectively protecting the hotspot of the most dominant species. Similar findings were also observed for Himalayan biodiversity hotspots, Sundarbans mangrove forest and Moist Tropical Forest, where the ineffectiveness of the current protected area in conserving habitats for dominant and threatened plant species were identified (Sarker et al., 2016; Spracklen et al., 2015; Zhang et al., 2012). Consequently, conservation and management strategies should consider expanding the sanctuary or creating new protected areas that encompass the multispecies habitat suitability area identified by the consensus map. Additionally, the use of ensemble models in this study, which combine the predictions of multiple individual models, improves the overall accuracy and robustness of the final prediction map. This approach can also reduce uncertainty and increase interpretability by highlighting areas of agreement and disagreement among the component models. In poorly surveyed areas, experiencing rapid habitat loss and degradation, habitat suitability modelling can be an invaluable and cost-effective instrument for conservation planning and biodiversity management. In fact, across the globe, the assessment of protected areas' effectiveness under future climate scenarios has extensively relied on the utilization of habitat suitability models (Cabeza, 2011; Reza et al., 2020; Wang et al., 2016).

Habitat Suitability Models (HSMs) developed in this study for the major indigenous tree species of the THR and RHR, have the potentials to provide valuable information for conservation and management efforts. Most importantly, it can serve as a baseline study for assessing the multispecies habitat suitability of the reserves. By identifying the factors that influence the distribution of different species in this forest, conservationists and managers can better understand the needs of different species and develop more effective management strategies (Peres & Terborgh, 1995). For example, the models could identify areas of high biodiversity that should be protected or predict how species may respond to land use or climate change. Our results also highlight the importance of considering the entire landscape, not just protected areas, in conservation and management efforts. Even if a species is present within a protected area, the hotspot of the species may be located outside of that area (Watson et al., 2014). Therefore, The Bangladesh Forest Department (BFD) can utilize the spatial distribution maps in their regular conservation and monitoring activities. These maps can be beneficial when planning, implementing, and directing programs to plant indigenous tree species in the THR and RHR.

9.3 Applications of Biodiversity Models and Maps

Chapter 5 and Chapter 8 uncovered the key drivers of tree alpha, beta and gamma diversity and provided key location specific information for THR and RHR visualized with maps that can contribute to present and future conservation plans and sustainable management measures that are\will be taken under the “National Conservation Strategy (2016–2031)”, Sustainable Development Goals, $REDD^+$ initiatives and ongoing Sustainable Forests and Livelihoods (SUFAL) Project of the Bangladesh government. Variable response graphs explained how any change in individual variable could affect the whole diversity and at what extent the change may/may not affect alpha, beta and gamma diversity. Forest managers can get information from these to make better decisions. Maps showing the biodiversity hotspots (alpha diversity), most heterogenous tree communities (beta diversity), and the most biodiversity contributing areas (gamma diversity) in the THR and RHR could be resourceful to forest managers to make location specific restoration and protections plans.

Most diversified (and hence heterogeneous) areas are located on the fringes of the RKWS and SNP and only occupy a small swath of the total reserve areas of THR and RHR. Because of their position on the periphery of the area, these habitats are particularly vulnerable to overexploitation. Therefore, protection mechanisms for these biodiversity hotspot areas need to be immediately designed, implemented, and regularly monitored.

CHAPTER 10

LIMITATIONS AND FUTURE DIRECTIVES

10.1 Models and Maps of Habitat Conditions

While this study focused on important soil physico-chemical properties, soil biological properties (e.g., microorganisms, earthworms, millipedes and microorganisms such as bacteria and protozoa) remained unnoticed. Soil biological properties represent both the direct and indirect impacts of the organisms residing in a specific soil, serving as indicators of the soil's capacity to sustain and support life (Prescott et al., 2019; Neina et al., 2023). Therefore, we suggest for its inclusion in future studies. Predictive soil mapping (PSM) can contribute to understanding the effect of soil properties in biophysical and biogeochemical functioning of a forest (Blanco Velázquez et al., 2022), which were also not addressed in this study. Future studies can expand on PSM by incorporating important abiotic and biotic factors (e.g., elevation, slope, species and functional diversity, disturbance etc.) that drive ecosystem structure and functioning in the tropical hill forests and soil physico-chemical and biological properties.

10.2 Species Habitat Suitability Models and Maps

One limitation of this study is the potential inadequacy of sample size in achieving an optimal presence-absence ratio for the response variable. A larger sample size could provide more robust results and increase the prediction accuracy. As Soultan and Safi, (2017) demonstrated, species specialism is a major factor in shaping species distribution. However, the impact of sample size and positional accuracy on species distribution modeling (SDM) still elicits differing opinions. Furthermore, this study is focused on a specific set of dominant species within THR and did not consider other species that may also be present in the area. For a broader understanding of the entire biodiversity of the forest and to make a rigorous assessment of the efficacy of protected areas, it would be beneficial to expand the scope of the study to include other species as well. Despite incorporating soil nutrient data, we could not consider other important environmental variables such as temperature and precipitation developing HSM, mostly because of the lack of variability in data due to the fine spatial scale of THR. However, incorporating other variables in future studies could provide greater insight of the factors influencing species distribution. There are, however, also some limitations of the methods we used to develop HSM. As some algorithms (RF and MLP) are more prone to overfitting, fine-tuning the model parameters could mitigate such issues. By addressing these limitations in future studies, we can advance our understanding of species distribution modeling and improve the reliability of conservation planning efforts.

10.3 Tree Diversity Models and Maps

Tree diversity models could be advanced by incorporating more data and conducting more modelling approaches (i.e., CART, Random Forest, GBM, GDM, Maxent, Bayesian hierarchical modeling etc.) to identify the best model that has most explanatory and predictive power. Inclusion of detail disturbance data (both natural and anthropogenic) in the models, when available, could be very helpful for more robust modelling with greater explanatory power and more accurate spatial predictions.

CHAPTER 11

CONCLUSIONS

Growing demand exists for spatially detailed soil and species data to help conserve human-altered tropical forests. However, due to data scarcity, many habitat restoration efforts in degraded tropical areas like Sylhet Hill Forests (in particular the Tarap Hill Reserve and the Raghunandan Hill Reserve) in Bangladesh lack this critical information. This has limited the applications of restoration actions in the degraded hill forests in Bangladesh. Soil mechanical composition analysis identified the soil type of the THR as 'Sandy Clay Loam'. We found significant variations in several soil properties across different soil depths (0-30, 30-60 and 60-90cm) and the availability of N, P, Mg and Fe decrease from surface to deeper soils while pH, SOC, and clay concentration increase with depth. Significant interactions (positive and negative) between several soil properties were also observed although the strength of the interactions varied for different depth levels. In terms of the effects of forest management interventions on soil properties, we also observed significant variations in multiple soil properties (N, Ca, SOC and clay contents) among different historically introduced forest types i.e., OGF, MXP and MOP, and different soil depths therein. Overall, the availability of essential macro-nutrients N, P, K, and Mg was highest in the *T. bellerica* dominated OGF and lowest in the *T. grandis* dominated MOP in all depth intervals while the availability of Ca and Zn was highest in the *Schima wallichi* dominated MXP and lowest in the OGF. Predictive performances of the different interpolation methods varied for different soil properties in different soil depths and among the six methods the deterministic method LPI and the geostatistical method EBK showed relatively higher predictive accuracy. However, the small margin of differences between the approaches demonstrates the utility of both deterministic and geostatistical approaches when extensive abiotic, biotic and disturbance data are unavailable for predictive soil mapping (PSM). Soil maps show high spatial variability in the values of several soil parameters across space and depths. Soil N concentration hotspots in the surface (0-30cm) and sub-surface (30-60cm) layers were located in the northern *T. grandis* dominated MOP in the THR while P hotspots were distributed in the *Glochidion lanceolarium* dominated southern OGF and *T. bellerica* dominated eastern MXP. K content was higher in the northwest OGF and MXP for the surface layer and decreased gradually from north to south for deeper layers, with the southwestern MOP having the availability of K in soil.

The soil type of the Raghunandan Hill Reserve is classified as 'Sandy Loam' (sand = 76.42%, silt = 5.71%, and clay = 17.86%). Significant interactions (positive and negative) between several soil properties and elevation were also observed. Mg and Fe (r = 0.6, p<0.001), and Ca and elevation (r = 0.42, p<0.001) showed significant positive correlations while sand and clay (r = -0.78–, p<0.001) and sand and silt (r=-0.52, p<.001) showed a significant negative correlation. Among the nutrients, only soil Mg and SOC concentrations significantly varied in different management interventions and the availability of Mg and SOC decreased with lower species diversity. The predictive performances of the different interpolation methods varied for different soil properties, and community structure in the RHR. Between the geostatistical methods, the UK showed relatively higher predictive accuracy. Among the deterministic methods, IMQF and LPI showed relatively higher predictive accuracy while IDW showed least predictive ability. Soil maps show significant spatial variability in the values of soil parameters throughout the RHR. Hotspots of soil N concentration are observed in the southern and northwestern parts of the reserve, while lower N content is evident in the central region. Conversely, P exhibits opposite patterns to N, with higher content in areas of lower N and lower P content in the central part of the RHR. K content demonstrated the highest concentrations in the northern part while it gradually decreased, and the lowest K concentrations were noted towards the southern, southwestern, and eastern parts. Interestingly, the central area of the reserve exhibited higher levels of K content.

This study provides a comprehensive understanding of the distribution and habitat preferences of total seventeen indigenous tree species growing in the THR and RHR by evaluating the performance of six widely used habitat suitability models. The findings confirm the importance of constructing HSMs as a tool to predict the abundance of a species in its preferred habitat. The HSMs and the habitat suitability maps provide spatially explicit knowledge of the distribution of the species as well as their preference for habitats. Furthermore, this study imitates the underlying mechanisms of biotic-abiotic interaction on species' circulation and contributes towards the advancement of explanatory powers of HSMs that forms the base of future studies. The species distribution maps constructed in this study can be readily useful for Bangladesh Forest Department in planning conservation initiatives for these nine species. Most importantly, the Forest Department can readily include the distribution maps in their regular monitoring program to protect these poorly studied species in the reserve. Additionally, this research also highlights the importance of the consensus map in identifying habitat suitability with a multi-species approach. The consensus map, created by combining the results of different habitat suitability models, provides a more comprehensive and accurate representation of the distribution and preferred habitats of the native tree species. This information can be used to identify areas of high conservation value within the protected areas and guide management and conservation efforts. Moreover, this research can also be used as a framework for redesigning protected areas, preserving optimal conditions for the protected species and their habitats, and ensuring the sustainable use of natural resources in the entire THR and RHR.

This study provides a baseline quantification and habitat-based modelling of all three aspects of biodiversity (alpha, beta and gamma), to determine their drivers and to make predictions about their spatial patterns in the THR and RHR. We find that several environmental drivers, biotic interactions and historical events have combined effects on the biodiversity components. Specifically, historical harvesting, increasing community size, soil pH, soil texture and several nutrients such as N and Pare the dominant stressors responsible for reducing species diversity and community distinctness. Our baseline biodiversity maps uncover that most diversified (and hence heterogeneous) areas are located on the fringes of the RKWS and SNP and only occupy a small swath of the total reserve areas of THR and RHR. Because of their position on the periphery of the area, these habitats are particularly vulnerable to overexploitation. Therefore, protection mechanisms for these biodiversity hotspot areas need to be immediately designed, implemented, and regularly monitored. We believe details on the drivers and their capacity to influence tree diversity and composition, and our baseline biodiversity maps, collectively, will contribute to designing and implementing climate-smart hill forest enhancement, restoration, reforestation and nutrient enrichment initiatives. In addition, our maps can guide the existing and future biodiversity protection, monitoring and REDD+ initiatives.

REFERENCES

1. Ahsan, M. M., Aziz, N. and Morshed, H. M. (2016) Assessment of Management Effectiveness of Protected Areas of Bangladesh. Bangladesh Forest Department, Dhaka.
2. Allouche, O., Tsoar, A., & Kadmon, R. (2006). Assessing the accuracy of species distribution models: Prevalence, kappa and the true skill statistic (TSS). Journal of Applied Ecology, 43(6), 1223–1232. https://doi.org/10.1111/j.1365-2664.2006.01214.x
3. Al-Mamoori, S. K., Al-Maliki, L. A., Al-Sulttani, A. H., El-Tawil, K., & Al-Ansari, N. (2021). Statistical analysis of the best GIS interpolation method for bearing capacity estimation in An-Najaf City, Iraq. Environmental Earth Sciences, 80(20), 1–14. https://doi.org/10.1007/s12665-021-09971-2
4. Araújo, M. B., & New, M. (2007). Ensemble forecasting of species distributions. Trends in Ecology and Evolution, 22(1), 42–47. https://doi.org/10.1016/j.tree.2006.09.010
5. Austin, M. P. (2002). Spatial prediction of species distribution: an interface between ecological theory and statistical modelling. 157.
6. Barton, K., 2015. MuMIn: Multi-model inference. R package version 1.10.5.
7. Bulmer, C., Paré, D. and Domke, G. M. (2019) 'A new era of digital soil mapping across forested landscapes', in Developments in Soil Science. Elsevier, pp. 345–371. doi: 10.1016/B978-0-444-63998-1.00014-8.
8. Chow, J. et al. (2019) 'Synthesis: A Future for Bangladesh Under a Changing Climate', in Confronting Climate Change in Bangladesh. Springer, pp. 193–203. doi: 10.1007/978-3-030-05237-9_13.
9. Chowdhury, M. R. and Ndiaye, O. (2017) 'Climate change and variability impacts on the forests of Bangladesh - a diagnostic discussion based on CMIP5 GCMs and ENSO', International Journal of Climatology, 37(14), pp. 4768–4782. doi: 10.1002/joc.5120.
10. Chowdhury, M. S. H. (2014) Forest conservation in protected areas of Bangladesh. Springer. doi: 10.1007/978-3-319-08147-2.
11. Chowdhury, M. S. H. et al. (2013) 'Community development through collaborative management of protected areas: evidence from Bangladesh with a case of Rema-Kalenga Wildlife Sanctuary', International Journal of Sustainable Development & World Ecology, 20(1), pp. 63–74. doi: 10.1080/13504509.2012.755480.
12. Crespo-mendes, N., Laurent, A., Henrik, H., & Zwicky, M. (2019). Relationships between plant species richness and soil pH at the level of biome and ecoregion in Brazil. Ecological Indicators, 98(September 2017), 266–275. https://doi.org/10.1016/j.ecolind.2018.11.004
13. Dietterich, T. G. (2000). Ensemble methods in machine learning. Lecture Notes in Computer Science (Including Subseries Lecture Notes in Artificial Intelligence and Lecture Notes in Bioinformatics), 1857 LNCS, 1–15. https://doi.org/10.1007/3-540-45014-9_1
14. Duarte, A., Whitlock, S. L. and Peterson, J. T. (2019) 'Species Distribution Modeling', in Encyclopedia of Ecology. Elsevier, pp. 189–198. doi: 10.1016/B978-0-12-409548-9.10572-X.
15. Elith, J. and Leathwick, J. R. (2009) 'Species Distribution Models: Ecological Explanation and Prediction Across Space and Time', Annual Review of Ecology, Evolution, and Systematics, 40(1), pp. 677–697. doi: 10.1146/annurev.ecolsys.110308.120159.
16. Fenlon, C., O'Grady, L., Dunnion, J., Shalloo, L., Butler, S., & Doherty, M. (2016). A comparison of machine learning techniques for predicting insemination outcome in Irish dairy cows. CEUR Workshop Proceedings, 1751, 57–67.
17. Franklin, J. (2010a) Mapping species distributions, Mapping Species Distributions: Spatial Inference and Prediction. Cambridge: Cambridge University Press. doi: 10.1017/CBO9780511810602.
18. Franklin, J. (2010b). Moving beyond static species distribution models in support of conservation biogeography. Diversity and Distributions, 16(3), 321–330. https://doi.org/10.1111/j.1472-4642.2010.00641.x
19. Guisan, A., & Thuiller, W. (2005). Predicting species distribution: Offering more than simple habitat models. Ecology Letters, 8(9), 993–1009. https://doi.org/10.1111/j.1461-0248.2005.00792.x
20. Guisan, A., & Zimmermann, N. E. (2000). Predictive habitat distribution models in ecology. Ecological Modelling, 135(2–3), 147–186. https://doi.org/10.1016/S0304-3800(00)00354-9
21. Gupta, K. K., Das, S., Sonet, S. S., Deb, S. K., Islam, N., & Sarker, S. K. (2019). Determining Tree-habitat Associations at the Raghunandan Hill Reserve Forest in Bangladesh. SUST J Sci Tech, 29(1), 1–11.
22. Islam, M., Deb, G. P. and Rahman, M. (2017) 'Forest fragmentation reduced carbon storage in a moist tropical forest in Bangladesh: Implications for policy development', Land Use Policy, 65, pp. 15–25. doi: 10.1016/j.landusepol.2017.03.025.

23. Iturbide, M., Bedia, J., Herrera, S., del Hierro, O., Pinto, M., & Gutiérrez, J. M. (2015). A framework for species distribution modelling with improved pseudo-absence generation. Ecological Modelling, 312(March 2016), 166–174. https://doi.org/10.1016/j.ecolmodel.2015.05.018
24. IUCN. (2004). Flora of Rema-Kalenga Wildlife Sanctuary. Bangladesh.
25. Kargar, M., Jutras, P., Clark, O. G., Hendershot, W. H., & Prasher, S. O. (2015). Macro-nutrient availability in surface soil of urban tree pits influenced by land use, soil age, and soil organic matter content. Urban Ecosystems, 18(3), 921–936. https://doi.org/10.1007/s11252-015-0439-7
26. Mackey, B. G. (1993). A spatial analysis of the environmental relations of rainforest structural types. Journal of Biogeography, 20(3), 303–336.
27. Manzoor Rashid, A. Z. M. et al. (2013) 'A journey towards shared governance: status and prospects for collaborative management in the protected areas of Bangladesh', Journal of Forestry Research, 24(3), pp. 599–605. doi: 10.1007/s11676-013-0391-4.
28. Matthiopoulos, J., Fieberg, J., & Aarts, G. (2020). Species-Habitat Associations: Spatial data, predictive models, and ecological insights. In Species-Habitat Associations: Spatial data, predictive models, and ecological insights. https://doi.org/10.24926/2020.081320
29. Mayer, D. G., & Butler, D. G. (1993). Statistical validation. Ecological Modelling, 68(1–2), 21–32. https://doi.org/10.1016/0304-3800(93)90105-2
30. MoEF (2016) Bangladesh National Conservation Strategy (2016 - 2031).
31. Muzaffar, S. Bin et al. (2011) 'The endangered forests of Bangladesh: why the process of implementation of the Convention on Biological Diversity is not working', Biodiversity and Conservation, 20(7), pp. 1587–1601. doi: 10.1007/s10531-011-0048-6.
32. NACOM, (Nature Conservation Management). (2003). Secondary data collection for pilot protected areas: Rema-Kalenga Wild-life Sanctuary. Bangladesh.
33. Naimi, B., & Araujo, M. B. (2016). Getting started with sdm package. April, 1–20.
34. Naimi, B., & Araújo, M. B. (2016). Sdm: A reproducible and extensible R platform for species distribution modelling. Ecography, 39(4), 368–375. https://doi.org/10.1111/ecog.01881
35. Pavel, M. A. Al, Mukul, S. A., Uddin, M. B., Harada, K., & Arfin Khan, M. A. S. (2016). Effects of stand characteristics on tree species richness in and around a conservation area of northeast Bangladesh. Journal of Mountain Science, 13(6), 1085–1095. https://doi.org/10.1007/s11629-015-3501-2
36. Rana, P., & Akhter, F. (2014). Uses of invasive alien plant species in Rema-Kalenga Wildlife Sanctuary of Uses of Invasive Alien Plant Species in Rema-Kalenga Wildlife Sanctuary of Bangladesh.
37. Reeve, R. et al. (2016) 'How to partition diversity', arXiv [q-bio.QM], 1404.6520. Available at: http://arxiv.org/abs/1404.6520.
38. Riyad, S., Chowdhury, R., & Ishtiaque, A. (2012). Integrated Protected Area Co-Management. May.
39. Russavage, E., Thiele, J., Lumbsden-Pinto, J., Schwager, K., Green, T., & Dovciak, M. (2021). Characterizing Canopy Openness in Open Forests: Spherical Densiometer and Canopy Photography Are Equivalent but Less Sensitive than Direct Measurements of Solar Radiation. Journal of Forestry, 119(2), 130–140. https://doi.org/10.1093/jofore/fvaa052
40. Sarker, S. K. et al. (2013) 'Disentangling the role of soil in structuring tropical tree communities at Tarap Hill Reserve of Bangladesh', Ecological Research, 28(4), pp. 553–565. doi: 10.1007/s11284-013-1045-x.
41. Sarker, S. K. et al. (2015) 'Tree assemblages and diversity patterns in Tropical Juri Forest, Bangladesh', Journal of Forestry Research, 26(1), pp. 159–169. doi: 10.1007/s11676-014-0006-8.
42. Sarker, S. K. et al. (2016) 'Are we failing to protect threatened mangroves in the Sundarbans world heritage ecosystem?', Scientific Reports. Nature Publishing Group, 6(October 2015), p. 21234. doi: 10.1038/srep21234.
43. Sarker, S. K., Matthiopoulos, J., et al. (2019) '1980s–2010s: The world's largest mangrove ecosystem is becoming homogenous', Biological Conservation. Elsevier, 236(August), pp. 79–91. doi: 10.1016/j.biocon.2019.05.011.
44. Sarker, Swapan K, Reeve, R., Thompson, J., Paul, N. K., & Matthiopoulos, J. (2016). Are we failing to protect threatened mangroves in the Sundarbans world heritage ecosystem? Nature Publishing Group, February, 1–12. https://doi.org/10.1038/srep21234
45. Sarker, Swapan K., Reeve, R., Thompson, J., Paul, N. K., & Matthiopoulos, J. (2016). Are we failing to protect threatened mangroves in the Sundarbans world heritage ecosystem? Scientific Reports, 6(March). https://doi.org/10.1038/srep21234
46. Sarker, Swapan Kumar, & Deb, J. C. (2011). A Diagnosis of Existing Logging Bans in Bangladesh A Diagnosis of Existing Logging Bans in Bangladesh. May 2014. https://doi.org/10.1505/146554811798811344

47. Sarker, Swapan Kumar, Nur-Un-Nabi, M., Mohasinul Haque, M., Sharmin, M., Sonet, S. S., Das, S., & Das, N. (2015). Tree assemblages and diversity patterns in Tropical Juri Forest, Bangladesh. Journal of Forestry Research, 26(1), 159–169. https://doi.org/10.1007/s11676-014-0006-8
48. Sarker, Swapan Kumar, Reeve, R., & Matthiopoulos, J. (2021). Solving the fourth-corner problem: forecasting ecosystem primary production from spatial multispecies trait-based models. Ecological Monographs, 91(3). https://doi.org/10.1002/ecm.1454
49. Sillero, N., Arenas-Castro, S., Enriquez-Urzelai, U., Vale, C. G., Sousa-Guedes, D., Martínez-Freiría, F., Real, R., & Barbosa, A. M. (2021). Want to model a species niche? A step-by-step guideline on correlative ecological niche modelling. Ecological Modelling, 456(July), 109671. https://doi.org/10.1016/J.ECOLMODEL.2021.109671
50. Socolar, J. B. et al. (2015) 'How Should Beta-Diversity Inform Biodiversity Conservation?', Trends in Ecology and Evolution. Elsevier Ltd, 31(1), pp. 67–80. doi: 10.1016/j.tree.2015.11.005.
51. Sox, H. C., Higgins, M. C., & Owens, D. K. (2013). Measuring the Accuracy of Diagnostic Information. Medical Decision Making, 93–142. https://doi.org/10.1002/9781118341544.ch5
52. Steinbauer, M. J. et al. (2017) 'Drivers for plant species diversity in a characteristic tropical forest landscape in Bangladesh', Landscape Research, 42(1), pp. 89–105. doi: 10.1080/01426397.2016.1252038.
53. Uddin, M. B. et al. (2013) 'Do environmental attributes, disturbances and protection regimes determine the distribution of exotic plant species in Bangladesh forest ecosystem?', Forest Ecology and Management. Elsevier B.V., 303, pp. 72–80. doi: 10.1016/j.foreco.2013.03.052.
54. Uddin, M. B., Steinbauer, M. J., Jentsch, A., Mukul, S. A., & Beierkuhnlein, C. (2013). Do environmental attributes, disturbances and protection regimes determine the distribution of exotic plant species in Bangladesh forest ecosystem? Forest Ecology and Management, 303, 72–80. https://doi.org/10.1016/j.foreco.2013.03.052
55. Uddin, M. S. and John, P. (2012) 'Evaluating Collaborative Management within the National Parks and Wildlife Sanctuaries of Bangladesh', Parks, 18(1). doi: 10.2305/IUCN.CH.2018.PARKS-24-1MSU.en.
56. Uddin, M. Z., Hassan, M. A. and Khan, M. S. (2003) 'An annotated checklist of Angiospermic flora of Rema-Kalenga Wildlife Sanctuary (Habiganj) in Bangladesh II.a: Magnoliopsida (Dicots)', Bangladesh Journal of Plant Taxonomy, 10(1), pp. 79–94.
57. Wood, S.N., 2011. Fast stable restricted maximum likelihood and marginal likelihood estimation of semiparametric generalized linear models. Journal of the Royal Statistical Society: Series B (Statistical Methodology), 73(1), pp.3–36.
58. Xiong, Q., Hu, J., Wei, H., Zhang, H., & Zhu, J. (2021). Relationship between plant roots, rhizosphere microorganisms, and nitrogen and its special focus on rice. Agriculture (Switzerland), 11(3), 1–18. https://doi.org/10.3390/agriculture11030234

Identifying 'Climate-smart' Tree Species (CsTree): Delivering a Nature-based Solution (NbS) for Forest Ecosystem Restoration in Bangladesh.

by

Dr. Md. Qumruzzaman Chowdhury

Professor, Department of Forestry & Environmental Science, Shahjalal University of Science & Technology, Sylhet, Bangladesh

Chapter I

1. Introduction

Climate change is anticipated to worsen the forest health in the coming decades, with a probable increase occurrence of heatwaves and droughts. Trees, being among the planet's longest-living organisms, offer one of the best biological examples of adjusting to constantly shifting weather patterns (Aranda et al., 2012). Because trees have a longer life span, their adaptations have been imprinted for millennia by previous climatic changes and experiences with climatic disturbances such as droughts (Dudney et al., 2023). Therefore, restoration of forests is now one of the best options to recover and adapt to climate change. In this context, it is important to assess how different tree species' cope with the varying drought events. In order to understand how tree species will respond to future drought events, we need to improve our understating of how species have responded to historical drought events. Analyzing retrospective growth patterns alongside climate data from recent events enables an in-depth exploration of the intricate relationship between climate and growth. This approach provides invaluable insights into how ecosystems might respond to future shifts in climate (Martinez del Castillo et al., 2018). However, there is a limited understanding on drought resilience of tree species growing in Bangladesh (Rahman et al., 2019). This understanding is an essential prerequisite for delivering an effective nature-based solution (NbS) for future forest restoration initiatives under climate change.

The UN Decade on Ecosystem Restoration (2021-2030) is a recent initiative of UNEP and FAO, has notably augmented national focus on restoring ecosystems, aiming to concurrently achieve biodiversity conservation, climate change mitigation, and sustainable livelihoods. Forest ecosystem restoration predominantly involves preserving forested lands for natural recovery while also employing active measures such as soil enhancement and tree planting to bolster forest stock and species diversity. Its tangible impacts on mitigating and adapting to global climate change have created significant opportunities for implementation within forestry practices. These initiatives support the conservation and management of forests, aligning with the sustainable development goals (SDGs). Furthermore, climate change mitigation efforts, such as utilizing Nature-based Solutions (NbS) like forest conservation, play a crucial role in various national strategies and plans, including the Bangladesh Climate Change Strategy and Action Plan (BCCSAP), and the National Adaptation Plan (NAP). These initiatives are also aligned with global climate change mitigation policies, such as the nationally determined contributions (NDCs) outlined in the Paris Agreement (MoEFCC, 2022). However, the escalating threat of drought resulting from climate change poses a significant challenge to the survival and development of tree species. Therefore, ecosystem restoration with climate-smart tree species is an important NbS option to enhance resilience of forests in the face of climate change.

Despite Bangladesh Forest Department's diverse nationwide restoration programs using various tree species, the dwindling of tree species in different forest ecosystems poses adverse implications for biodiversity conservation and mitigation measures. Moreover, the slowed growth rates of existing tree species signal underlying environmental stresses (Rahman et al., 2019), significantly impacting the carbon cycle. Forests in Bangladesh face increased susceptibility to climate change, primarily stemming from escalating temperature, heightened occurrences of flooding, and intensified drought events, notably impacting the northwestern and northeastern regions (Rahman and Lateh, 2016). Furthermore, Coastal forests face additional stress from escalating salinity, exacerbating physiological drought in trees. Anticipating temperature rise, shifting precipitation patterns, and escalating salinity in the coming decades, assessing how tree species respond to changing environmental conditions is crucial for effective species selection. Because climate-smart tree species exhibit low sensitivity to changes, a high adaptive capacity, or both. The implementation of climate-smart ecosystem restoration necessitates a comprehensive understanding of species' climate sensitivity, drought tolerance ranges, and habitat suitability under changing environmental conditions.

This project aims to bridge the critical knowledge gap by delivering a NbS through the identification of climate-smart tree species in distinct ecosystems across Bangladesh: the northeastern Hill forests, northwestern Sal forests, and coastal forests. The strategic selection of climate-smart tree species tailored to specific sites during changing climatic conditions is pivotal for the long-term viability of plantations and consequent carbon sequestration. Assessing the resilience of tree species to drought under predicted climate changes is essential to determine suitable climate-smart species for restoration efforts. As climate change advances, adopting climate-smart forestry could prove a viable nature-based solution, enhancing the prospects of successful restoration in Bangladesh amidst future climatic stresses. Therefore, the project objective was to identify climate-smart indigenous tree species in three distinct ecosystems to lay down a robust foundation for transitioning to climate-smart forestry practices in Bangladesh.

1.1 Problem Statement

The forests of Bangladesh face heightened vulnerability to the effects of climate change, primarily attributable to escalating temperature, shifting precipitation patterns, and consequently increase of droughts (Rahman and Lateh, 2016). Notably, the historically biodiverse semi-evergreen northeastern Hill forests, northwestern deciduous Sal forests, and coastal mangrove ecosystem are threatened under increasing drought events (Sarker et al., 2015; Rahman et al., 2019; Rashid, 2019). In addition, coastal forests bear the brunt of rising sea level, and intensifying storms, compounding the impact of physiological droughts stemming from altered precipitation and escalating salinity (Ahmed et al., 2023; Chowdhury et al., 2023). In this context, the Bangladesh Forest Department (BFD) endeavors for continuous restoration efforts in different ecosystems. Nonetheless, the persistent and severe droughts have resulted in forest degradation and tree mortality, significantly harming biodiversity and carbon sequestration (Zuidema et al., 2020).

Considering these challenges, the adoption of indigenous tree species displaying heightened climate resilience and/or drought tolerance that emerges as a promising NbS to mitigate climate change, in addition to biodiversity conservation and livelihoods. However, responses of tree species to climate change are multifaceted; while a certain degree of drought might bolster growth in specific species under moist conditions or during wet years, it could impede growth during drier periods or in different habitats. Furthermore, tree species exhibit varying responses to changing climate scenarios, with some able to recover after droughts while others face mortality due to drought-induced stress (e.g., Anderegg et al., 2013). Despite these complexities, there remains a dearth of understanding regarding the drought resilience, tolerance, or vulnerability of tree species in Bangladeshi forests, which is essential for crafting effective forest ecosystem restoration strategies in the face of climate change.

Hence, interpreting NbS, such as species-specific reaction to climate change assumes pivotal importance in formulating adaptable, site-specific climate-smart restoration initiatives in Bangladesh. While current studies often assess forest species' drought tolerance within controlled greenhouse settings using seedlings, these findings possess limited generalizability due to the intricacies of natural environment and dissimilar responses of saplings compared to mature trees (Meir et al., 2015; Tng et al., 2018). Moreover, such studies predominantly focus on individual species, emphasizing single trait-based acclimation, while comprehensive evaluations spanning various traits across multiple species remain scarce. Consequently, an integrated approach employing observations from juvenile to mature stage within natural environmental conditions presents an advantageous strategy to surmount these limitations. Functional, anatomical, or physiological characteristics, including tree-ring width (TRW) and hydraulic traits, offer a set of pertinent parameters to scrutinize tree responses to drought stress and predict their adaptability to climate fluctuations.

Therefore, this research aims to fill this knowledge gap by investigating trees across diverse forest ecosystems in Bangladesh—specifically, the Rema Kalenga Hill Reserve, Singra National Park (SNP), and Chattogram Coastal Forest Division—to compile a prospective list of climate-smart tree species as a NbS for future restoration programs in the wake of climate change.

1.2 Stipulative definition

In this project, climate-smart tree species include those with low sensitivity to climate change, and a high capacity to adapt to climate change, or both. Using such species in restoration can increase tree growth resilience to climate change which is a nature-based solution (NbS) option.

1.3 Objectives

The main objective was to identify climate-smart indigenous tree species for restoration in three major forest ecosystems (i.e., northeastern Hill forests, northwestern Sal forests and coastal forests) in Bangladesh.

1.3.1 Specific objectives

(i) To develop a resilience (Rs), resistance (Rt) and recovery (Rc) index of major indigenous tree species to drought.

(ii) To formulate a drought tolerance index assessing hydraulic architecture of tree species.

1.3.2 Research questions

(i) How do drought resilience (Rs), resistance (Rt) and recovery (Rc) vary among the species?

(ii) How does hydraulic vulnerability vary among the tree species?

(iii) Do the tree species show a trade-off between hydraulic safety and efficiency?

Chapter II

2. Methodology

2.1 Study area

In this study, major indigenous tree species were selected from three of the forest ecosystems in Bangladesh, which are northeastern Hill forests (Rema Kalenga Hill reserve), northwestern Sal forests (Singra National Park, Dinajpur Forest Division) and Coastal forests (Shitakunda Coastal Forest Division) (Fig. 1).

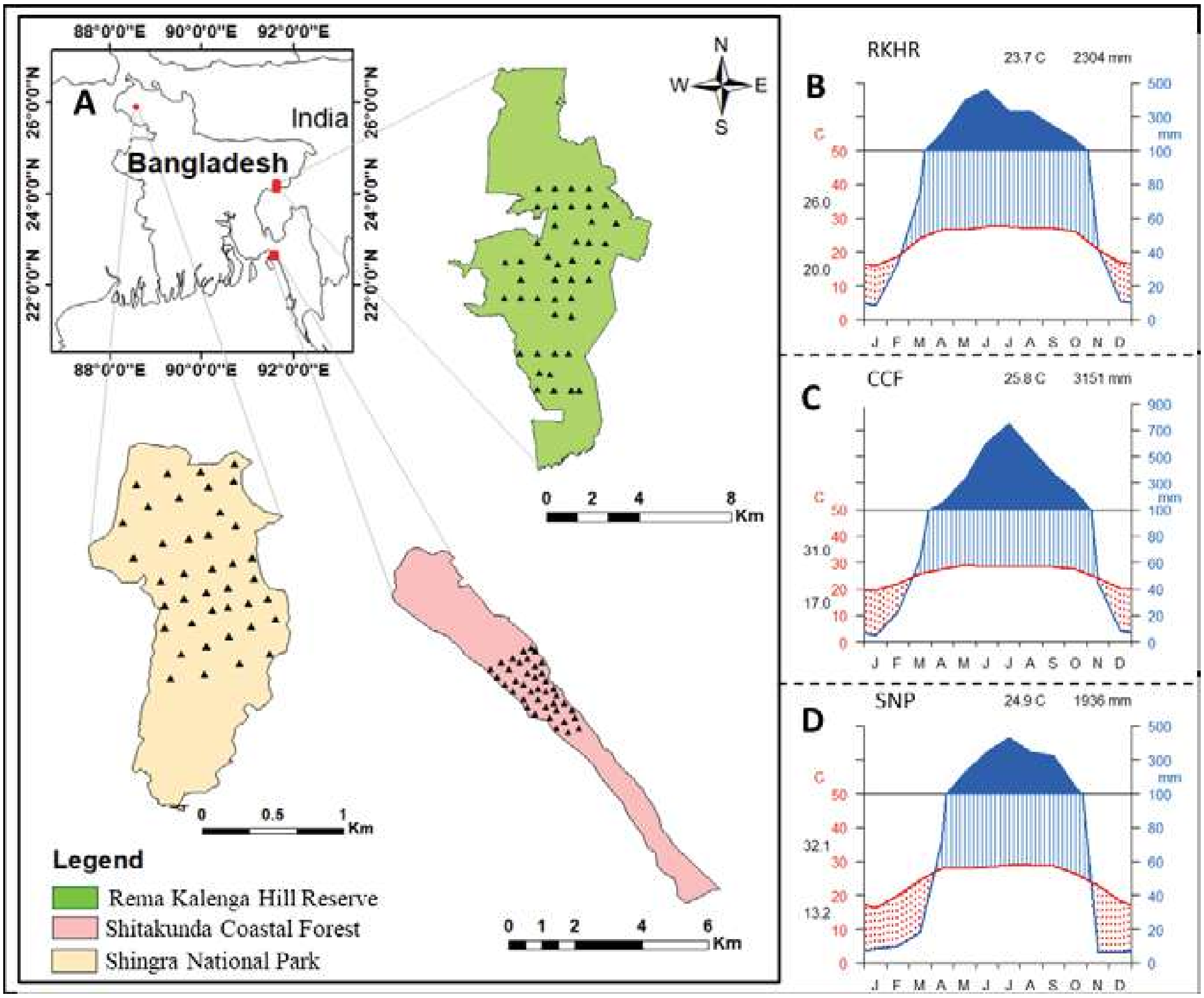

Figure 1. The map shows the distribution of sample plots (black triangles) (A) and climate diagram of Rema Kalenga Hill Reserve (RKHR) (B), Shitakunda Coastal Forest (SCF) (C) and Shingra National Park (SNP) (D).

2.1.1 Rema Kalenga Hill Reserve

The study took place within the Rema Kalenga Hill Reserve, spanning an area of 6232 hectares, recognized as one of the most crucial forest conservation sites in Bangladesh. (Uddin et. al., 2002). It is located between latitudes 24°06′–24°14′N and latitudes 91°36′–91°39′E (Rana & Akhter, 2010). This is a tropical evergreen and semi-evergreen forest (Uddin et al., 2002). The Rema Kalenga Hill Reserve is located in the north-eastern Chunarughat Upazila (sub-district; administrative entity) of Habiganj district in Sylhet division (Mollah et al., 2003; USAID, 2012). This protected area (PA) is under the authority of Sylhet Forest Division at Habigonj-2 Range, comprising three beats (i.e., Chanbari Beat, Kalenga and Rema). The core zone of the reserve comprising natural forests was declared as Rema Kalenga Wildlife Sanctuary in 1982, consisting of an area of 1095 ha and further expanded to 1795 ha in 1996 (Mollah et al., 2003). The Rema Kalenga Hill Reserve exemplifies a moist tropical climate marked by substantial rainfall, measuring at 4,162 mm annually. The mean annual temperature fluctuates between the highest recorded at 34.8 °C and the lowest at 9.6 °C (Rahman & Miah, 2017). The climate in the study area is significantly influenced by the South Asian summer monsoon. Annual rainfall totals 2363 mm, with an average yearly temperature of 24.8°C (Rahman et al., 2019) with high precipitation from May to August (main-monsoon) and four months of dry weather from November to February, the period of March-April is considered as pre-monsoon and the September to October can be referred as post-monsoon (Islam et al., 2018), this sanctuary has the most tropical characteristics. The average monthly temperature in the winter (November February) is 10 °C while in the summer (March – June) the range is 30 to 40 °C (Sarker et al., 2013).

2.1.2 Shitakunda Coastal Forest

Stretching between geographical coordinates of 22°24′ to 22°50′ N latitude and 91°28′ to 91°46′ longitude (Figure 1), the Sitakunda-Mirsarai region encompasses the area from the mouth of the Big Feni River to the newly formed coastal land adjacent to the Sandwip channel, hosting Bangladesh's largest planted mangrove forest. The Coastal Afforestation Program in Mirsarai and Sitakunda commenced in 1968 and 1976, respectively, under the administration of the Chattagram Coastal Afforestation Division (CCAD). Within the mangrove distribution framework, three coastal villages—Bagachattar in Sayedpur union, Ichakhali (ChuniMizirtake) in Ichakhali union, and Uttar kattoli adjacent to Salimpur union—were specifically chosen for survey purposes. These villages collectively accommodate 2,970 households, comprising a population of approximately 23,000 individuals, with a gender distribution of 53.7% male and 46.3% female residents. Sitakunda in Chittagong experiences a subtropical monsoon climate, marked by notable seasonal fluctuations in temperature and rainfall. Throughout the warmer months, temperature in Sitakunda typically range from approximately 23°C to 32°C (73°F to 90°F). In contrast, during the cooler months, temperatures may decrease to around 10°C to 20°C (50°F to 68°F). Sitakunda experiences substantial rainfall, particularly during the monsoon season extending from June to September. Annually, the region receives an estimated precipitation ranging from 2,000 mm to 3,000 mm (79 inches to 118 inches), with a significant portion concentrated within the monsoon period. These climatic features characterize monsoon climate, portraying discernible fluctuations in temperature and notable precipitation patterns throughout the year (BMD).

2.1.3 Shingra National Park

The research site is situated within the Birganj Upazila, spanning approximately between latitudes 25º90'N and 26º30'N, and longitudes 88º20'E and 88º50'E in the Dinajpur district. Positioned 45 kilometers southwest from Dinajpur town, it is adjacent to the Dinajpur – Panchagarh highway and encompasses Dalagram, Chaulia, Singra, Nortodangi, Gandari, Singhojani, Sator, Ganpoito, Rathinthpur, and Laskarpur Mouza. Notably, the Singrasal forest covers an area of 305.69 hectares within this region (Ali et al., 2020). The climatic conditions prevalent in the studied area denote a tropical monsoon climate. This climate is typified by a hot summer season, a warm and rainy season, and a cool and winter period. The rainy season, also referred to as the wet monsoon season, is relatively brief and occasionally delayed in certain years; however, it is conducive to robust plant growth. This phase extends from July to October, receiving an average monthly rainfall of 333 mm. The subsequent dry winter season experiences sporadic drizzles, prevailing from November to February, contributing to an average annual rainfall of 1811mm (BBS, 2010). The cool dry season, characterized by the lowest temperatures, records an average highest temperature of 34.6°C and a lowest of 9.7°C. This period is associated with the lowest relative humidity throughout the year, albeit subject to annual fluctuations.

2.2 Data collection methods

2.2.1 Sampling and sample collection

We have selected eight indigenous tree species from Rema Kalenga Hill Reserve: Awal (*Vitex pubescens* Vahl), Chapalish (*Artocarpus chaplasha* Roxb.), Hargoja (*Dillenia pentagyna* Roxb.), Chikrasi (*Chukrasia tabularis* A. Juss.), Jarul (*Lagerstroemia speciosa* (L.) Pers.), Pitraj (*Aphanamixis polystachya* (Wall.) R.N. Parker), Lal Kakra (*Pistacia integerrima* J.L. Stewart ex Brandis), and Sal (*Shorea robusta* Gaertn. f.), three from Shitakunda Coastal Forest: Baen (*Avicennia officinalis* L.), Keora (*Sonneratia apetala* Buch.-Ham.), and Gewa (*Excoecaria* *agallocha* L.), and four species from Shingra National Park: (*Shorea robusta* Gaertn. f.), Chikrashi (*Chukrasia tabularis* A. Juss.), Jarul (*Lagerstroemia speciosa* (L.) Pers.), and Gora Neem (*Melia azedarach* L.).

A total of 43, 40 and 40 sample plots (20 x 20 m) were selected in three ecosystems, respectively and a minimum of one tree sample was selected for sampling in each plot considering the abundance of the species. In each forest ecosystem, tree heights (m) were measured using Range finder, diameters (cm) at breast height (1.3 m) were measured using diameter measuring tape and canopy openness were measured using densitometer

of all individuals. A minimum of three increment cores along three transects of each tree was extracted at breast height (1.3 m) using an increment borer. Wood cores were collected from 30 sample trees for each species in each ecosystem, except *V. pubescens* and *P. integerrima* at RKHR. The third order fully expanded leaves pair from the apex of plagiotropic (lateral) branches was selected for sampling. Leaves showing clear signs of pathogen or herbivore damage, or those heavily covered with epiphylls, were excluded from our study. If any symptoms were present, we measured the fourth order of leaf in the branches. Afterward the collected leaves were preserved in polythene bags for measurement. Soil samples were collected from each tree to a depth of 30 cm using a soil auger and preserved in polythene bags for laboratory analysis.

2.2.2 Sample preparation and measurement

2.2.2.1 Growth ring measurement

Each core surface was prepared after sanding the samples using sanding paper (with a series ranging from 120 grit to 2000 grit). Afterward, the sanded wood cores were scanned using a high-resolution scanner with a 2400 dpi for ring-width measurements. Fiji ImageJ software was used to

Figure 2. A schematic diagram of the sample collection preparation and measurement: RF= range finder, DT= diameter tape, IB= increment borer, CH= core holder, SP= sanding paper, RKHR= Rema Kalenga Hill Reserve, SCF= Shitakunda Coastal Forest, SNP= Shingra National Park.

measure the rings on the scanned sanded cores (Schindelin et al., 2012). For each sample tree, rings were measured for three cores. Then, measurements were averaged for average growth-ring data.

The TRW (growth-ring width) series for individual trees underwent visual crossdating, where attempts were made to establish chronological correspondences among trees, ensuring the accurate allocation of each growth ring to its respective calendar year (Douglass, 1941). To address age-related patterns, the raw series underwent detrending using a 10-year cubic spline with a 50% frequency of smoothing, as outlined by Rahman et al. (2020). The detrended ring-width series for each salinity zone were processed using the dplR package in R software, version 4.3.1 (R Core Team, 2023), employing a bi-weight robust mean to generate growth-ring indices. Additionally, several statistical parameters, including mean inter-series correlation (Rbar), expressed population signal (EPS), mean sensitivity (MS), and autocorrelation (AR1), were utilized for cross-dating validation (Wigley et al., 1984; Wigley et al., 1990). The assessment of first-order autocorrelation (AR1) aimed to evaluate the persistence of growth variation following standardization, following the approach outlined by Blasing and Fritts (1976). An EPS threshold of 0.85, often applied in conifer studies, served to identify the reliable segment within a chronology, measuring its proximity to an idealized chronology derived from an infinite number of samples (Wigley et al., 1984).

Additionally, mean sensitivity (MS) of standardized chronologies, as per Ferguson's scale (Blasing and Fritts, 1976), provided insights into mean relative changes across adjacent ring widths (Savva et al., 2006). The signal-to-noise ratio (SNR), computed as SNR = Nr/(1-r), served as a measure of the strength and reliability of a chronology's signal, as described by Wigley et al. (1984), where 'r' denotes the average correlation among trees and 'N' indicates the total number of trees in a site chronology. These methodological approaches collectively ensured the accuracy and reliability of the derived tree ring indices while assessing growth variations and their persistence over time.

2.2.2.2 Drought years selection and measurement of resilience components

We have collected the climate data (temperature and precipitation) of these three regions from the Bangladesh Meteorological Department (BMD) to calculate the climate correlation and SPEI of the corresponding drought year. Initially, the "pointRes" tool by van der Maaten-Theunissen et al. (2015) was utilized to conduct event and point-year analyses, following methodologies delineated by Cropper (1979) and Neuwirth et al. (2007). To authenticate these selected pointer years, the SPEI values spanning 1950 to 2022 were employed, specifically scrutinizing their association with the targeted research area. Upon this scrutiny, the years 1987, 1999, and 2006 emerged as notable periods of drought from the identified pointer years for Rema Kalenga Hill Reserve (Fig 3), 1982, 1988 and 2009 for Shitakunda Coastal Forest (Fig 4) and 1982, 2006 and 2018 for Shingra National Park (Fig 5). This determination was derived from a comprehensive assessment integrating the SPEI values, bolstered by references drawn from local and regional climatic studies (Figs. 3-5) (Shahid, 2010; Miyan, 2015; Rahman and Lateh, 2016). These specific years deemed significant owing to their alignment with observed drought conditions within the region, supported by empirical data and established climatic research. To ascertain whether the radial growth of the species under investigation significantly declined during drought years compared to growth

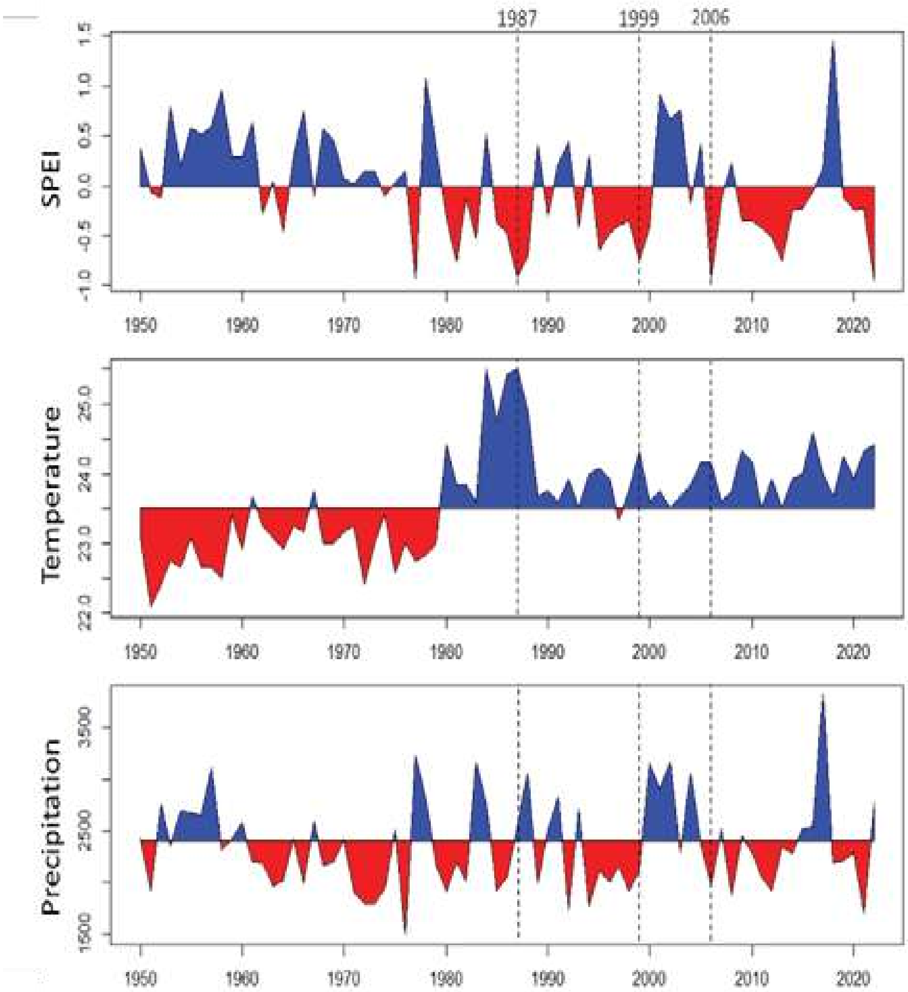

Figure 3. Annual fluctuations and extended patterns in climate parameters and drought indices are depicted. Vertical dashed lines denote the occurrence of drought years (1987, 1999, and 2006) within the Rema Kalenga Hill Reserve. SPEI, representing the Standardized Precipitation Evapotranspiration Index averaged over three months from January to March (3-month period, March).

observed two years prior and two years post the drought events, we conducted a Superposed Epoch Analysis (SEA) (Prager and Hoenig, 1989; Samson and Yeung, 1986). With 10,000 bootstrapped samples and a significant threshold of $p<0.05$, superposed epoch analysis was carried out using the "dplR" package (Bunn, 2008). These formulas were used to calculate three resilience components, such as drought resistance (Rt), recovery (Rc), and resilience (Rs), which can be used to study how severe droughts affect trees. (Lloret et al., 2011).

Resilience (Rs) = Post drg/Pre drg
Resistance (Rt) = dgr/Pre drg
Recovery (Rc) = Post drg/drg

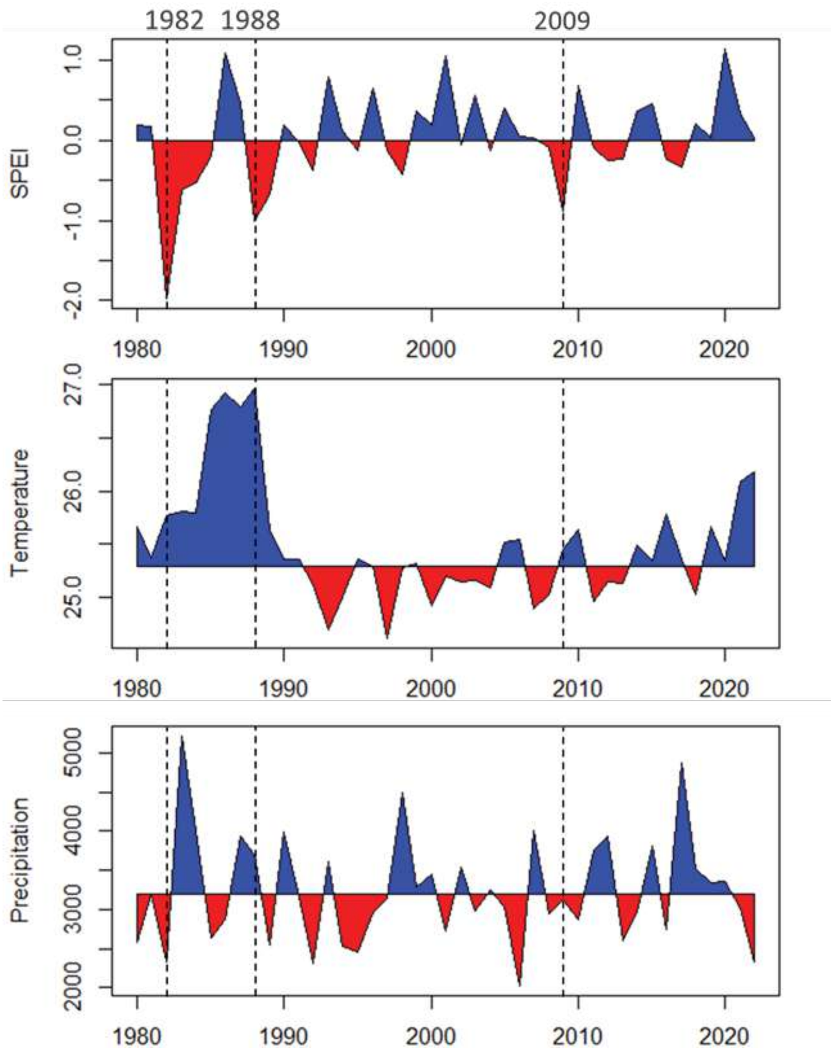

Figure 4. Annual fluctuations and extended patterns in climate parameters and drought indices are depicted. Vertical dashed lines denote the occurrence of drought years (1987, 1999, and 2006) within the Shitakunda Coastal Forest. SPEI, representing the Standardized Precipitation Evapotranspiration Index averaged over three months from January to March (3-month period, March).

In this context, "drg" represents the radial growth of each tree during the drought year, "Pre drg" signifies the radial growth observed two years before each drought event, and "Post drg" indicates the radial growth recorded two years after each drought event (Fig 6).

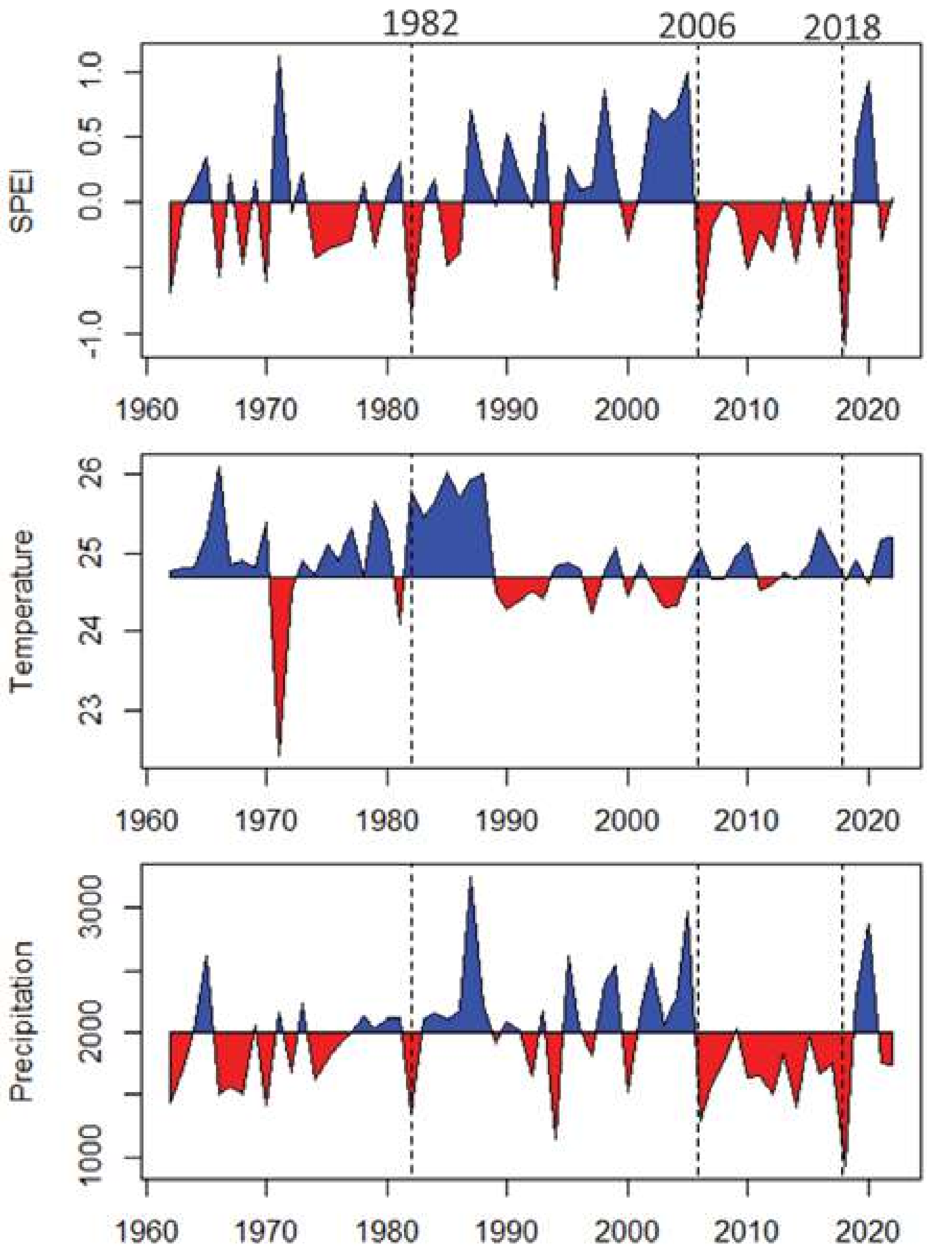

Figure 5. Annual fluctuations and extended patterns in climate parameters and drought indices are depicted. Vertical dashed lines denote the occurrence of drought years (1987, 1999, and 2006) within the Shingra National Park. SPEI, representing the Standardized Precipitation Evapotranspiration Index averaged over three months from January to March (3-month period, March).

2.2.2.3 Wood sample preparation, vessel measurement and hydraulic traits calculations

Bark and pith were removed from the core and part of sapwood was used for wood traits analysis. To produce microscopic thin sections with a thickness ranging from 10 to 20 µm, we utilized a Rotary microtome (HistoCore AUTOCUT). Subsequently, the thin sections were stained using safranin red. The microslides were examined under a digital microscope Carl Zeiss Primostar 3 which resulted in resolution of 200µm, 100µm and 20µm of Images using imaging app ZEISS Labscope. To calculate the vessel density for each tree, the number of vessels was manually counted and divided by area. The result was an average. ImageJ software was used to measure the vessel's diameter (tangential and radial) (Schneider et al., 2012). As most vessels have an elliptical shape, we determined the major (a) and minor (b) axes for each of the 100 randomly chosen vessels in each snap to be radial parallel to the ray and tangential perpendicular to the ray's length.

To calculate the safety factor for vessel implosion, denoted as $(t/b)^2$, we measured the double thickness of walls of adjacent vessels, represented as 't', and the diameter of the conduit closest to the mean diameter, denoted as 'b'. This safety factor was computed based on an average of 100 vessels per species. This metric serves to assess the theoretical ability of vessels to withstand negative pressures during periods of water deficit stress (Fig 6). Huber value also measured dividing sapwood area by leaf area. The vessel composition index, denoted as 'S', was determined by the ratio of vessel area (VA) to vessel density (VD). Additionally, the vessel lumen fraction, represented as 'F', was calculated as the product of vessel area (VA) and vessel density (VD). The index 'S' characterizes the vessel properties within the tree ring, while 'F' represents the percentage of the tree ring area occupied by water-conducting vessel lumina. Based on the Hagen–Poiseuille law, the hydraulically weighted diameter (D_{H}, µm) was calculated using a statistic that weights the vessel lumen size (Sperry et al.,1994).

$$D_H = \Sigma D^5/\Sigma D^4$$

Hagen–Poiseuille's law was also used to determine potential conductivity (K_P, kg m $^{-1}$ MPa $^{-1}$ s $^{-1}$) based on hydraulic diameter (D_H) and vessel density (VD).

$$K_P = \left(\frac{\pi\rho}{128\eta}\right) * D_H^4 * VD$$

where η = the viscosity index of water (1.002×10^{-9} MPa S at 20° C)

ρ is the density of water at 20° C (998.21 kgm^3)

D is the vessel diameter (Fig. 6)

2.2.3 Vulnerability index

The vulnerability index (VI) will be determined by employing the vessel diameter (D, µm) and vessel density (VD, mm^{-2}), offering a preliminary assessment of the plant's ability to withstand cavitation induced by drought conditions (Lens et al., 2011). VI values below 1.0 indicate a high level of xeromorphy, whereas values exceeding 3.0 would indicate mesomorphy characteristics.

$VI=D/V_D$

$MI = VI \times L_{VE}$

Where D = hydraulic diameter of vessel,

V_D = vessel density and

L_{VE} = vessel element length

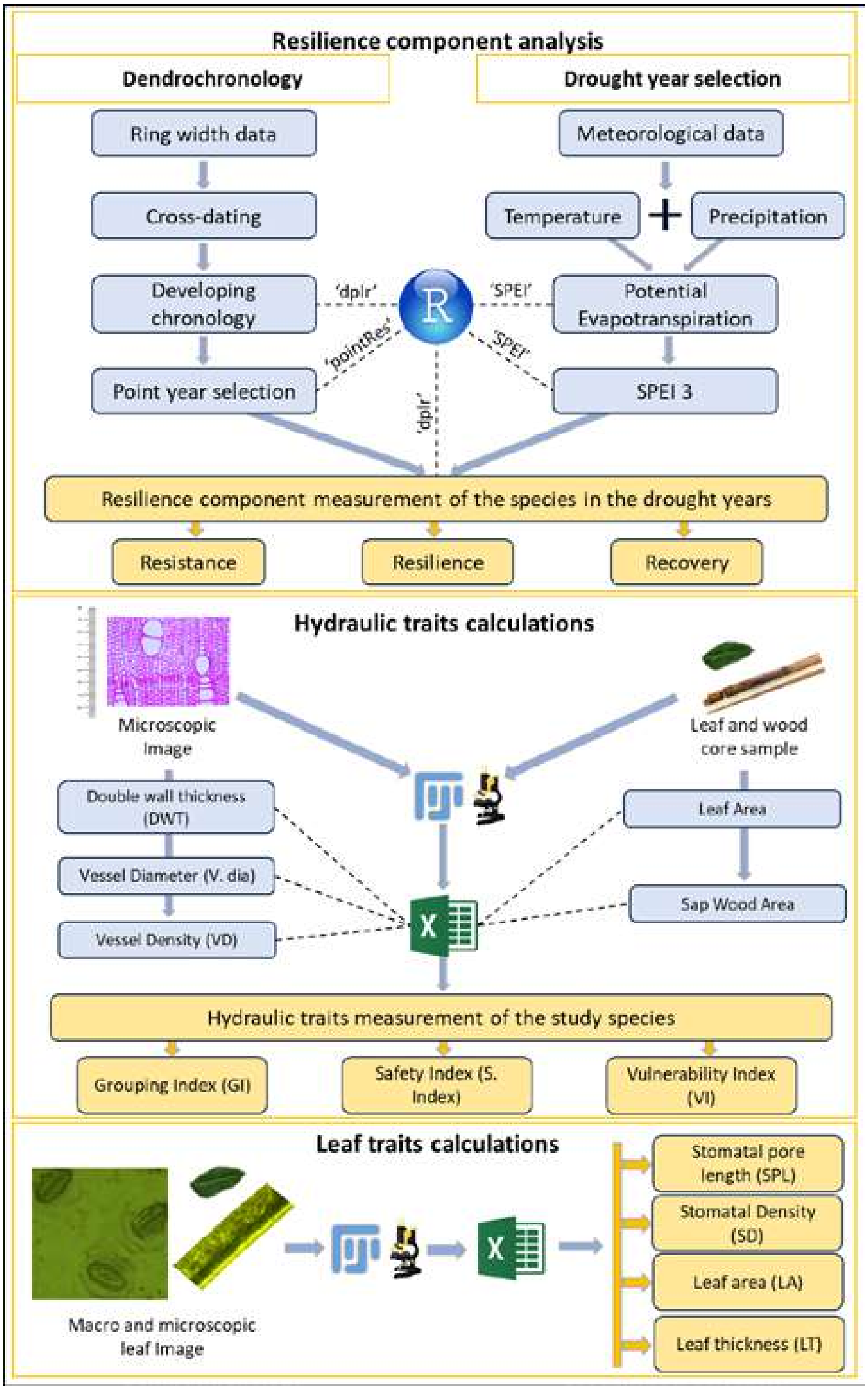

Figure 6. A schematic diagram of the method of resilience component and hydraulic traits measurements.

2.2.4 Leaf morphology and stomatal anatomy

Leaf area (LA) (include petiole) of the fresh leaves was measured using at least three leaf images of each individual tree. We thin section were taken from leaves of each individual and observed under a light microscope in the laboratory for leaf thickness (LT) measurement. Specific leaf area (SLA) was measured by the ratio of Leaf area and the dry mass of the leaf (Garnier et al., 2001). LA was measured and then fresh leaves were dried in the oven at 105 °C for 24 hours. Nail varnish peels were taken from the abaxial surface of each leaf and observed under a light microscope (AmScope, FMA050) with a camera system to capture the images (Sack et al., 2003). Afterwards the images of LA, LT and stomata were analyzed using an image analyzing (FiJi ImageJ) software (Schneider, Rasband and Eliceiri, 2012). Stomatal density (SD) (no. of stomata mm^{-2}), stomatal pore length (SPL) (µm) and guard-cell length (GL) (µm) were measured. In each leaf, 100 measurements were carried out for each parameter to have a mean value.

2.2.5 Wood density measurement

Wood density (g cm^{-3}) was determined by measuring the dry weight over the fresh weight volume. Initially, the fresh weight of each tree sample was recorded. Subsequently, the wood sample underwent drying in an oven at 105°C for a duration of 48 hours following a 1 cm section of each core being cut (Hoeber et al., 2014). To calculate the fresh volume of the wood core, the formula utilized was:

Wood core volume, V (cm^3) = $\pi r^2 h$,

where 'r' denotes the radius of the fresh wood core sample and 'h' represents the length of the fresh wood sample.

2.3 Soil analysis

2.3.1 Soil pH

Soil pH was measured using a digital pH meter (Hanna HI2211 pH/ORP meter) and a 1:2 ratio in a suspension of soil in water (Brady, 1999). At first, buffer solutions with pH levels of 7, 4, and 10 were used to calibrate the pH meter. Ten milliliters of distilled water were mixed with five grams of soil sample in a test tube. The Vortex meter was shaken irregularly for half an hour while the solution was allowed to stand. Submerging the pH meter electrode was the next step in taking the pH reading.

2.3.2 Soil texture

he hydrometer method, as outlined by Gee and Bauder (1986), was employed to ascertain the proportions of sand, silt, and clay in the soil samples. Particularly, calibrated hydrometer was used to calculate the density of suspension at a given depth after a fixed period. The following formula was used to obtain corrected hydrometer reading:

$Rcc = (R-R_L) + (t-20.0) \times 0.3$

Here, R_{cc}= Corrected Hydrometer reading, R= Hydrometer reading at different time (40 sec and 2 hour), R_L= Blank (hydrometer reading from 1000 ml distill water), and t = Temperature

It is considered that all sand particles settle down beyond the range of hydrometer reading after 40 seconds and after 2 hours all clay and silt particles settle (preferably 8 hours).

The percentage of sand, silt and clay was then measured using the following equations (Gee & Bauder, 1986):

Silt % + Clay % = (R_c at 40 sec)/ (Dry Weight of sample soil) ×100

Clay % = (R_c at 2 hrs)/ (Dry Weight of sample soil) ×100

Silt % = (Silt % + Clay %) – Clay %

2.3.3 Nutrient analysis

Total nitrogen (N) content was measured using the Kjeldahl method (Ali et al., 2019). 1 gm of oven-dried soil was first prepared with 9:1 K2SO4: $CuSO_4$, 15ml conc. H_2SO_4 (soil preparation was done in fume hood for safety issues). It was then put into a fully automatic digestion unit (Model: DKL fully programmed digestion component, VELP Scientifica) for 1.5 hours at 150°-400°. Then it rested for 30 minutes to cool down. The samples were then taken to a distillation unit (model UDK 129, VELP Scientifica), where a 30 ml indicator (a mixture of boric acid, bromocresol green, and methyl red) was used for measurement. The solution was then prepared for titration with H_2SO_4 of 2 normalities. Finally, total nitrogen content was measured using the following equation:

N (mg/L) = {(T-B) *14.007*N}/ (sample weight*1000); Where, T-B = volume of H_2SO_4 used for titration and N = normality of H2SO4.

Using the tri-acid digestion method, phosphorus (P) and potassium (K) were also assessed using induced coupled plasma atomic emission spectroscopy (ICP-OES) (Neubauer, 2017; Hoobin & Vanclay, 2011). A soil sample of 1 gram was initially dried in an oven for 24 hours. After that, 10 ml of HNO_3 was added to the soil inside the fume hood, heated for 10 to 15 minutes, and then let to cool for 10 minutes. With the addition of 5ml of HNO_3, the solution was then reheated for 30 minutes. The heated solution was left to cool for ten minutes before it was put to rest. When the brown gas appeared, 5 ml of HNO_3 was then poured over it, and heating was resumed for 10 minutes. 3ml of H_2O_2 and 2ml of distill water were added, and heat was initiated for several minutes. The solution needed 1 ml of H_2O_2 added until there were no color changes.

Following a reduction of the final volume to 5 ml, 10 ml of HCl was added to the solution, which was then heated for almost 15 minutes. Each solution was then diluted with 100ml of di-ionized water after being filtered via filter paper. Finally, each nutrient's concentration was measured using the ICP-OES equipment (Fig. 7).

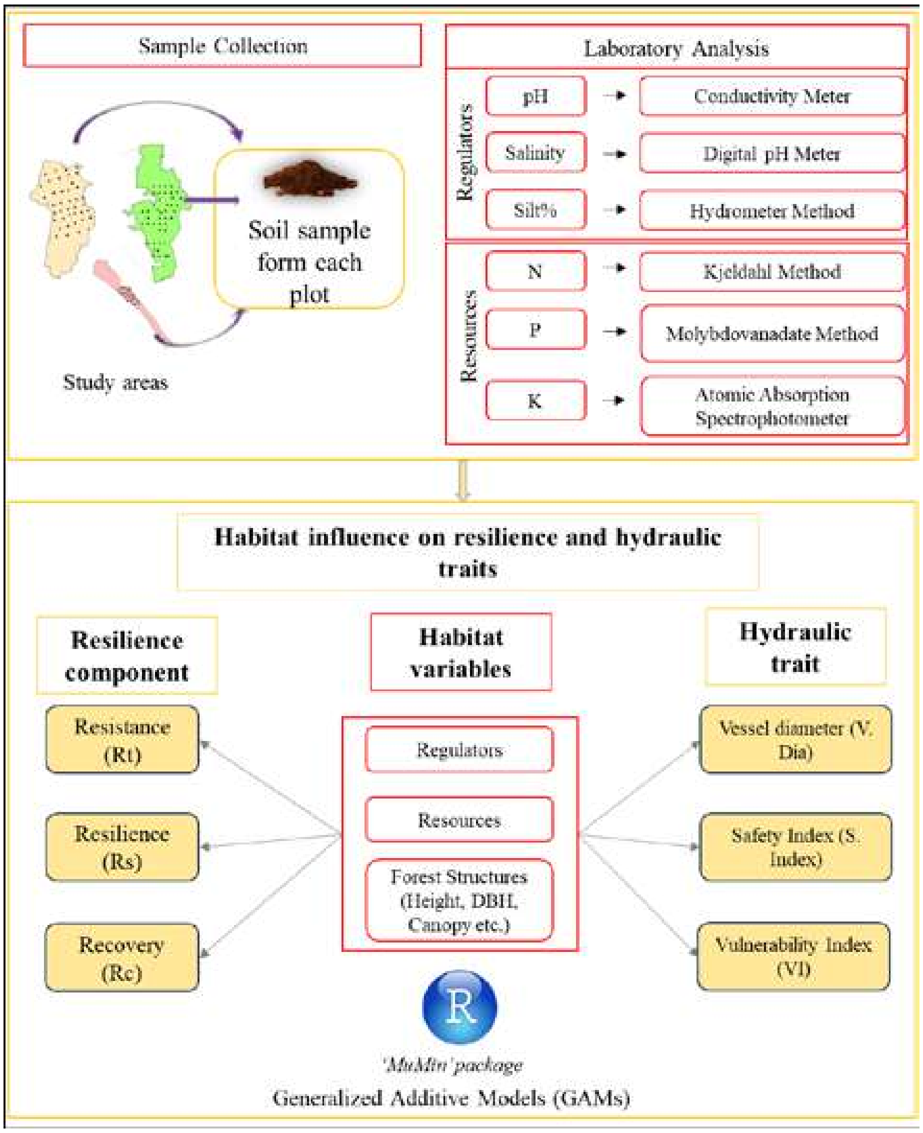

Figure 7. A schematic diagram of the method of soil properties analysis and their influence on tree variables.

2.4 Statistical analysis

Before analyzing trait interrelationship, Shapiro-wilk test was done for normality test and data which are not normal log transformed them for attaining normal distribution. The association between wood and vessel anatomical traits was investigated by a simple linear regression model. A density plot was performed to see the frequency distribution of hydraulic weighted vessels diameter. To examine the variation of resilience component in the corresponding drought years, vessel traits and leaf traits among the species species we used Kruskal Wallis test followed by Dunn test for not normal data, and Anova and post hoc Tukey HSD test for normal data. To test the association among the studied variables, Principal component analysis (PCA) was conducted. In order to depict the connections and potential trade-offs among sapwood hydraulic traits and radial growth (RW), we constructed a ternary axis plot illustrating the three key characteristics associated with mechanical support, hydraulic efficiency, and safety (WD, KLS, and $(t/b)^2$).

With 10,000 bootstrapped samples and a significant threshold of p 0.05, superposed epoch analysis and cross-dating was carried out using the "dplR" package (Bunn, 2008). The examination of growth response to drought incidents involved the calculation of four resilience components: resistance (Rt), recovery (Rc), resilience (Rs), and relative resilience (Rr) (Lloret et al., 2011).

2.5 Multi-criteria decision analysis (MCDA)

In facilitating the creation of a climate-smart species list, we employed multi-criteria decision analysis (MCDA). Such approaches typically necessitate scores across various dimensions linked to different alternatives and outcomes, as well as weights reflecting trade-offs among these dimensions. A common method involves calculating the total value score for each alternative, achieved through a linear weighted sum of its scores across multiple criteria. We have used resilience components (growth resilience (Rs), resistance (Rt) and recovery (Rc)), hydraulic traits (vessel diameter (V. dia), grouping index (GI), hydraulic conductivity (Kp), vessel wall reinforcement $(t/b)^2$ and vulnerability index (VI)), stomatal variables (stomatal pore length (SPL) and stomatal density (SD)) and leaf area (LA) as climate smart species selection criteria. Based on the importance of these criteria for tree species adaptation to drought and other climatic changes, we fixed weight values up to 5 and score them depending on their species-specific performance across these three ecosystems (Table 1). We have followed the following steps (Fig. 8):

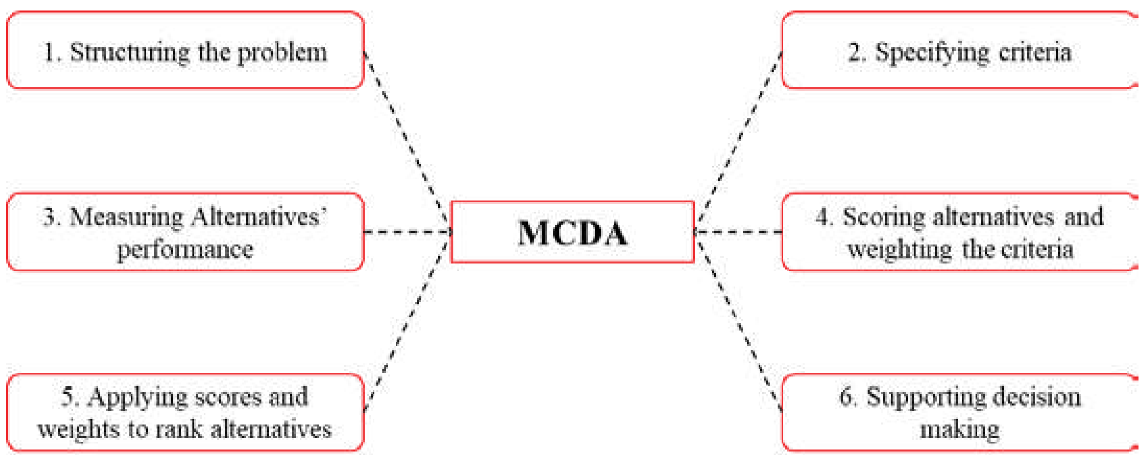

Figure 8. Steps of multi-criteria decision analysis

Chapter III

3. Result and Discussion

3.1 Rema Kalenga Hill Reserve

3.1.1 Cross-dating and growth pattern during the drought events of the species in the RKHR

The study species had distinct growth rings. Crossdating of *L. speciosa, D. pentagyna, A. chaplasha, A. polystachya, C. tabularis,* and *S. robusta* among growth-ring series of 25 out of 30 trees was successful. In the case of *V. pubescens* and *P. integerrima* 21 out of 25 and 13 out of 15 trees were successful respectively (Table 1).

Table 1. Chronological characteristics of the sampled trees (Rema Kalenga Hill Reserve).

	Variables	*D. pentagyna*	*S. robusta*	*A. chaplasja*	*A. polystachya*	*L. speciosa*	*V. pubescens*	*C. tabularis*	*P. integerrima*
Chronology	Time span (year)	1969-2022	1952-2022	1965-2022.	1941-2022	1954-2022	1968-2022	1999-2022	1968-2022
	GLK	0.61	0.638	0.64	0.64	0.62194	0.69	0.653	0.67
	EPS	0.809	0.801	0.794	0.839	0.79981	0.78	0.82	0.79
	MS	0.2499	0.26	0.21	0.2562724	0.251	0.26	0.23	0.31
	SNR	3.09	4.022	3.863	4.123	3.07	3.689	3.996	3.225
	R bar	0.34	0.401	0.386	0.407	0.33	0.381	4.02	0.383
	AR1	0.2357	0.11	0.196	0.3385667	0.29	0.11	0.29	0.13

The statistics commonly used to assess the quality of chronologies in dendrochronology indicate that all the species of Rema Kalenga Hill Reserve are of good quality. The EPS ranged from 0.79 to 0.84 for all species except P. *integerrima*, which approached the critical value of 0.85 (Wigley et al., 1984). This indicates that the samples of these seven species collectively capture approximately 79 to 84% of the interannual growth variation within the population.

The RW chronology of Crossdating of *L. speciosa, D. pentagyna, A. chaplasha, A. polystachya, S. robusta* and *V. pubescens* revealed moderate environmental sensitivity (Table 2) compared to formerly determined thresholds (low: 0.10-0.19, intermediate: 0.20-0.29 and high: ≥0.30, Respectively) (Grissino-Mayer, 2001). The mean inter-series correlation (Rbar) exhibited low values across all species, largely due to the limited time span of the series and the minimal influence of previous year's growth on the characteristics. Higher SNR values were observed for *A. chaplasha, A. polystachya, S. robusta,* and *V. pubescens*, indicating stronger signal strength relative to noise in the chronology (Table 2). Both the first-order correlation (AR1) and the mean series intercorrelation of the chronologies were generally low for all species (Table 1). Radial growth for all species notably declined during the drought events in 1987, 1999, and 2006 (Fig 9). Compared to the average radial growth of the two years preceding the drought events, growth for these six species decreased by more than 30% during the drought events (Table 2).

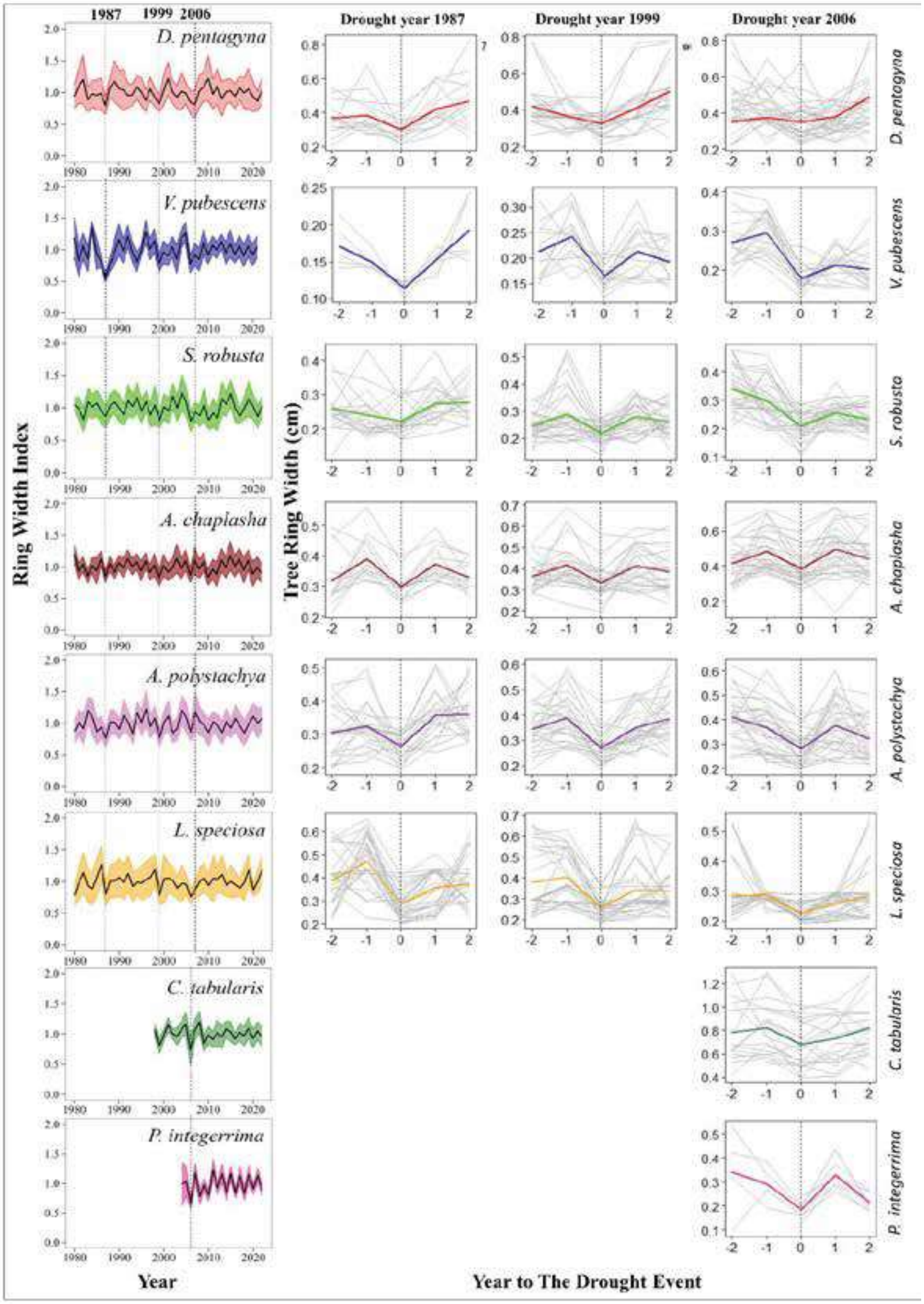

Figure 9. The chronology of the species of RKHR *(D. pentagyna, V. pubescens, S. robusta, A. polystachya, A. chaplasha, C. tabularis, P. integerrima* and *L. speciosa*) (black line). Vertical dashed lines mark the chosen drought years, while shaded areas denote standard deviations. In the right panels, grey lines represent individual trees, while bold lines depict their respective mean radial growth curves.

3.1.2 Species resistance, recovery, and resilience to drought of RKHR

Our results show that the study species were negatively affected by the drought episodes, leading to pronounced tree growth reductions compared to the previous decade (Fig 9). Drought reduced radial growth of 18–34%, varying with species and drought years. Among the species*, V. pubescens* showed the highest growth reduction to drought while the lowest was in *D. pentagyna*. We also observed a lower growth reduction in *S. robusta* to drought compared to *A. chaplasha*, *A. polystachya* and *L. speciosa*. Reduced radial growth during drought years might be related to shortening of the growing season that slowing down the cambial activity, as described for other tropical species (Rahman et al., 2019). This species-specific growth reduction is also related to physiological response to interannual variability in soil moisture availability during drought. This physiological approach allows the study species to achieve greater growth reduction, compensating for a brief growing season by maximizing CO2 uptake rates under conditions of reduced moisture (Leo et al., 2014; Obojes et al., 2018).

In general, drought reduced the growth resistance in the study species in drought years, as indicated by a lower resistance value < 1 (Fig 10). However, the growth resistance significantly varied among the study species ($p < 0.05$). *V. pubescence* exhibited the lowest growth resistance value in three drought years among the species. On the other hand, *A. chaplasha* and *D. pentagyna* exhibited the highest resistance in each drought year.

The studied species had a recovery value ≥1, indicating a faster recovery after the drought (Fig 10). Albeit the study species showed no variation in recovery in 1999 and 2006, *V. pubescence* and *D. pentagyna* had significantly higher recovery than other species only in 1987.

Tree species were resilient in 1987 ≥1. On the other hand, these species showed different resiliency in 1999 and 2006. Three species, namely *V. pubescence, L. speciosa,* and *A. polystachysa*, exhibited low resilience with values significantly below 1, suggesting that droughts had enduring adverse effects on stem growth. However, the majority of species displayed growth resilience values of ≥1, indicating that they maintained or even accelerated growth rates following the drought year. (Fig 10). However, *A. chaplasha*, *D. pentagyna* and *S. robusta* were more resilient than other species during the drought event in 1999. *D. pentagyna* showed the highest resilience while *S. robusta* showed the lowest in 2006. Moreover, these three species Among the species, *C. tabularis* showed significantly higher resilience and recovery but comparatively lower resistance in 2006 (Table 3).

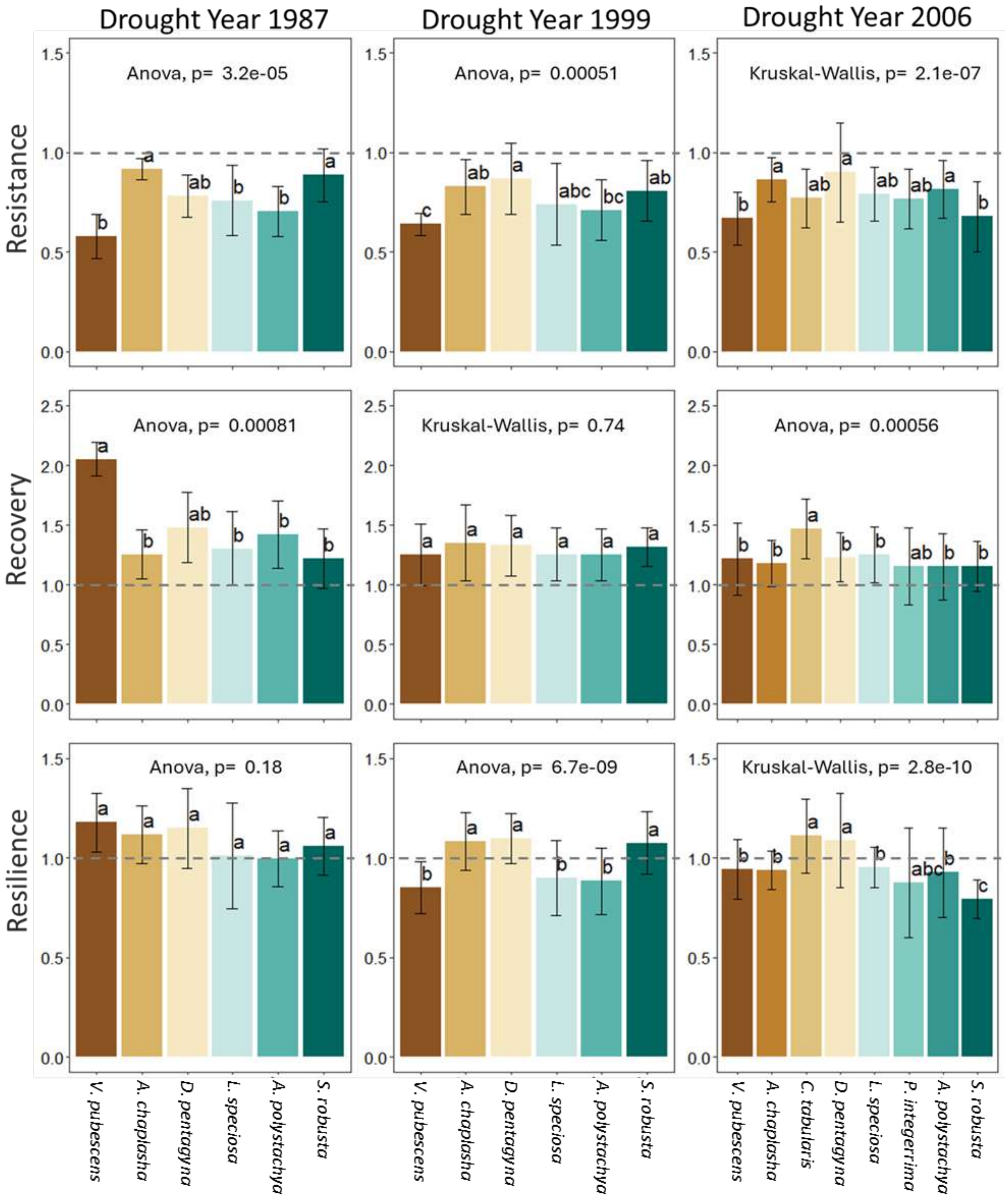

Figure 10. The studied species in the Rema Kalenga Hill Reserve exhibited varied responses to drought events. Distinct letters denote significant differences (p < 0.05) in drought responses among the species.

Table 2. Resilience component characteristics of studied species of THR during drought year.

	Variables	Year	*D. pentagyna*	*S. robusta*	*A. chaplasha*	*A. polystachya*	*L. speciosa*	*V. pubescens*	*C. tubularis*	*P. integerrima*
Resilience Component	Resistance	1987	0.84 ± 0.18	0.89 ± 0.15	0.88 ± 0.11	0.73 ± 0.16	0.78 ± 0.21	0.58 ± 0.08		
		1999	0.86 ± 0.17	0.80 ± 0.14	0.83 ± 0.13	0.72 ± 0.16	0.73 ± 0.20	0.69 ± 0.18		
		2006	0.90 ± 0.24	0.68 ± 0.17	0.88 ± 0.15	0.82 ± 0.14	0.79 ± 0.13	0.66 ± 0.18	0.85 ± 0.2	0.5 ± 0.23
	Recovery	1987	1.43 ± 0.28	1.24 ± 0.25	1.27 ± 0.19	1.40 ± 1.26	1.38 ± 0.38	2.05 ± 0.09		
		1999	1.32 ± 0.23	1.34 ± 0.28	1.31 ± 0.31	1.26 ± 0.21	1.25 ± 0.22	1.31 ± 0.28		
		2006	1.31 ± 0.37	1.23 ± 0.36	1.19 ± 0.22	1.15 ± 0.27	1.26 ± 0.26	1.22 ± 0.29	1.26 ± 0.23	1.03 ± 0.26
	Resilience	1987	1.22 ± 0.31	1.07 ± 0.18	1.09 ± 0.13	0.99 ± 0.14	1.01 ± 0.26	1.18 ± 0.10		
		1999	1.13 ± 0.25	1.07 ± 0.15	1.09 ± 0.16	0.88 ± 0.16	0.89 ± 0.19	0.85 ± 0.13		
		2006	1.11 ± 0.28	0.79 ± 0.11	1.00 ± 0.17	0.93 ± 0.22	0.97 ± 0.14	0.94 ± 0.15	1.03 ± 0.18	0.72 ± 0.08

3.1.3 Variation in xylem hydraulic traits among the Species of RKHR Forest

Based on the difference between vessel diameter distribution (Fig 14), it can be inferred that the hydraulic transport systems are highly different among the study species. For example, light-demanding *V. pubescence, S. robusta,* and *C. tabularis* had a left-skewed vessel distribution where most of the vessels were narrow. On the other hand, shade-tolerant *A. chaplasha, L. speciosa, D. pentagyna* had a right-skewed vessel diameter distribution with mostly wider vessels. Another shade-tolerant species, *A. polystachya*, had a vessel distribution between *V. pubescence* and *A. chaplasa*, where vessels of intermediate size were more frequent.

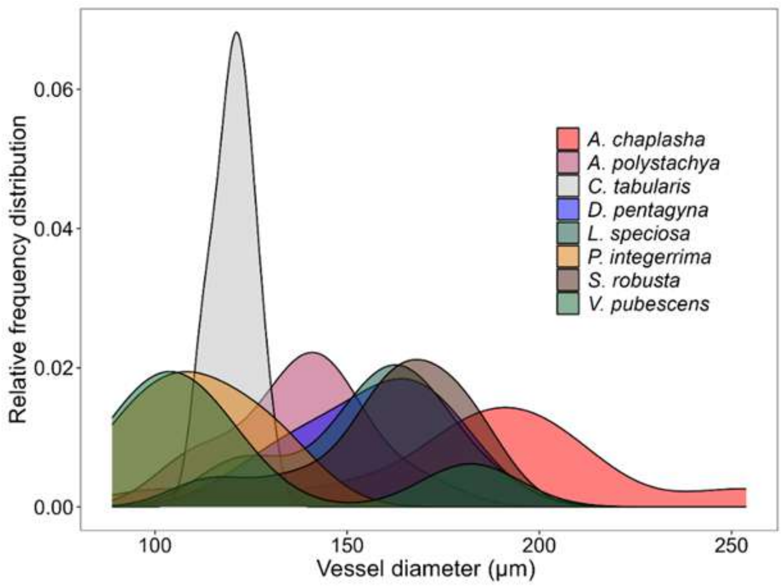

Figure 11. Vessel diameter distribution of the species of RKHR.

Furthermore, the decrease in vessel diameter from right to left skewed species indicates a lower conductive efficiency, which is related to increased conductive safety (Fig 15*). V. punescens* had not only a smaller vessel size than the other study species did but also a greater proportion of the tiniest vessels. Earlier studies (Carlquist,

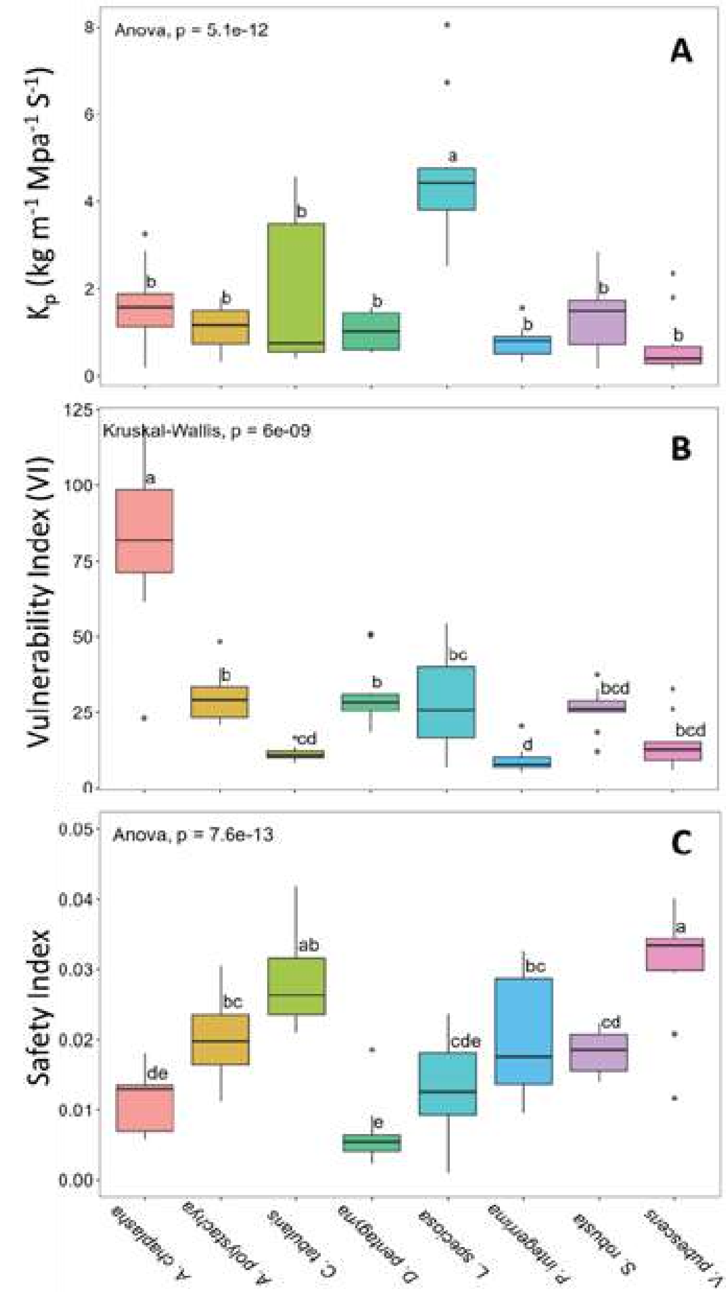

2016, 2018; Jacobsen and Pratt, 2023) reported that narrow vessels are positively related to low vulnerability to cavitation and thus indicates that *V. punescens*'s hydraulic transport system is relatively safer than the other species.

Anova and Kruskal-walis test revealed a significant difference in potential conductivity (k_p) of *L. speciosa* with other studied species (Fig 15A) and significant difference of VI among the species (Fig 15B). *A. chaplasha* showed comparatively moderate conductivity (k_p) (Fig 15A) and vulnerability (VI) to cavitation (higher efficiency) and lower safety (Fig 15C) than the other

Figure 12. Variation in hydraulic conductivity (A) and hydraulic vulnerability index (B) and Safety Index (C) among the studied species in Rema Kalenga Hill Reserve.

species. *C. tubularis, V. pubescence,* and *P. integerrima* exhibited greater resistance to cavitation, indicating lower vulnerability to this phenomenon (Fig 15C). However, this resistance is accompanied by reduced efficiency in water conduction, as observed in previous studies (Hacke et al., 2006; Islam et al., 2018a; Sperry et al., 2008). Other species Showed in between higher and lower vulnerability (in between safety and efficiency against the cavitations).

3.1.4 Stomatal traits variation among the species in Rema Kalenga Hill Reserve

Stomata were found in the abaxial surface of all the species. We found that *C. tubularis, S. robusta* and *A. polystachya* show the longer SPL, GCL (Stomatal Size) and higher Stomatal Density (SD) than other species (Fig 16). The CO_2 fixation rate may be higher in the leaf of these three species than the other as improvements in CO_2 fixation are due to increases in maximum potential stomatal conductance via higher stoma-density (SD), or due to quick stomatal responses endorsed by smaller size (S) (Harrison et al., 2020).

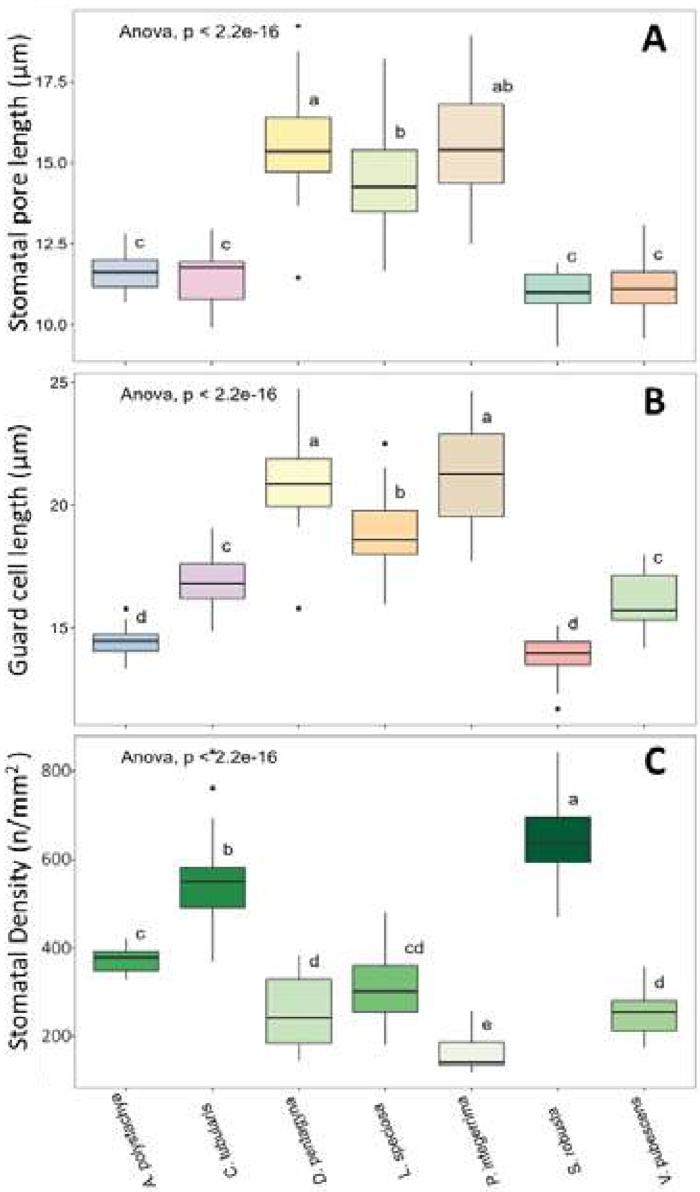

Figure 13. Variation of Stomatal pore length (SPL) (A), Guard cell length (GCL) (B) and Stomatal density (SD) (C) among the species of RKHR.

Our results are similar to the hypothesis that stomatal size and density frequently exhibit a negative association, with higher density accompanied by a decrease in size (Franks and Beerling, 2009).

3.1.5 Climate-smart species selection

Mult-criteria decision analysis revealed that *C. tabularis*, *S. robusta* and *V. pubescens* are the most suitable species for RKHR as these species showed higher resistance to the drought, lower hydraulic conductivity and vulnerability and higher safety to the cavitation compared to the other species (Fig 20 and Table 16).

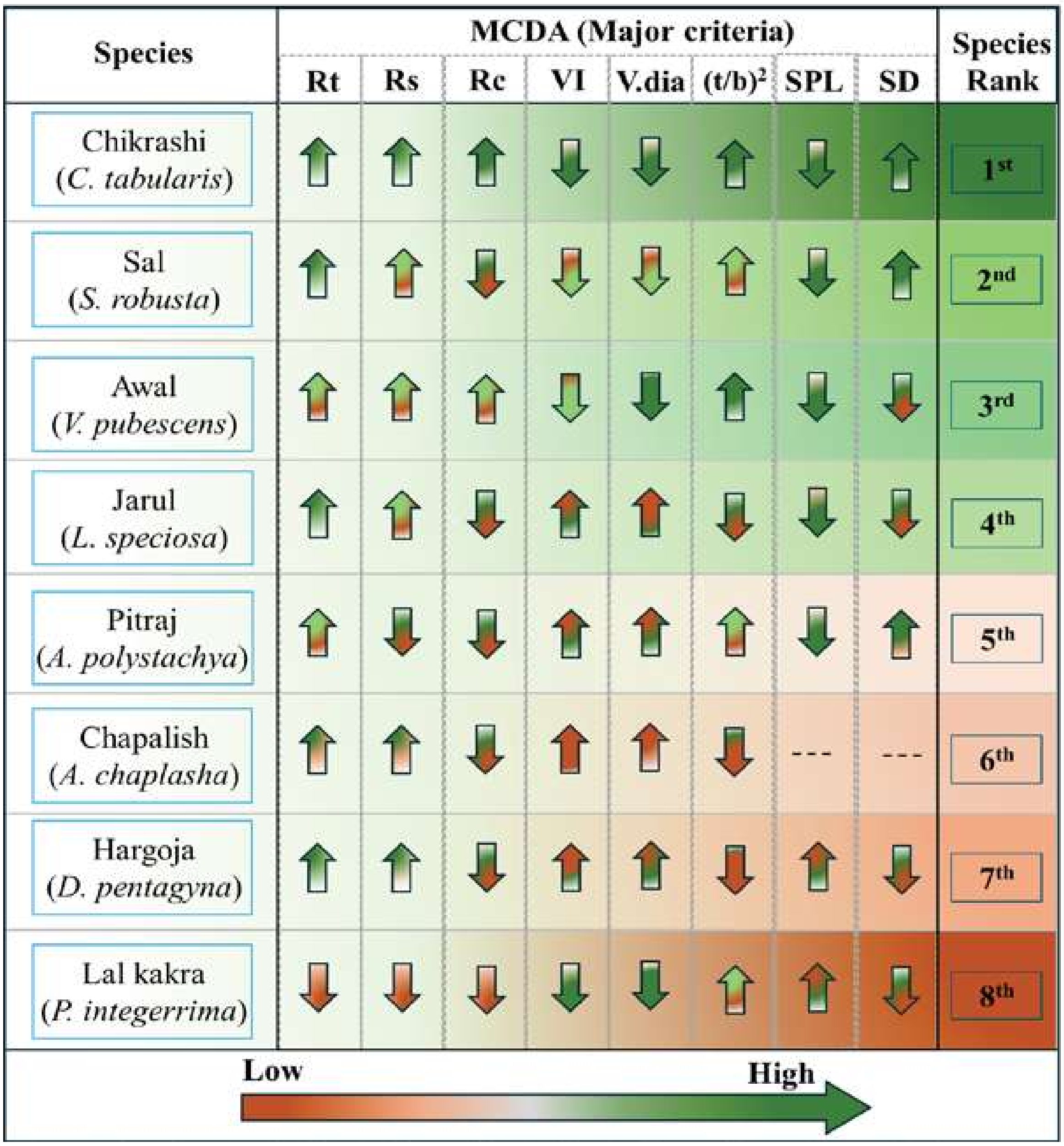

Figure 14. Executive Summary of the results of the RKHR. MCDA (Multicriteria Decision Analysis), Rt (Resistance), Rs (Resilience), Rc (Recovery), VI (Vulnerability Index), V.dia (Vessel Diameter), $(t/b)^2$ (vessel wall reinforcement), SPL (Stomatal Pore Length) and SD is the Stomatal Density.

3.2 Shitakunda Coastal Forest (SCF)

3.2.1 Crossdating and growth pattern during the drought events of the species in the SCF

Among the study species, distinct growth rings were found in *S. apetala and E. agallocha.* Crossdating among growth-ring series of 24 out of 30 trees was successful for both *S. apetala and E. agallocha*.

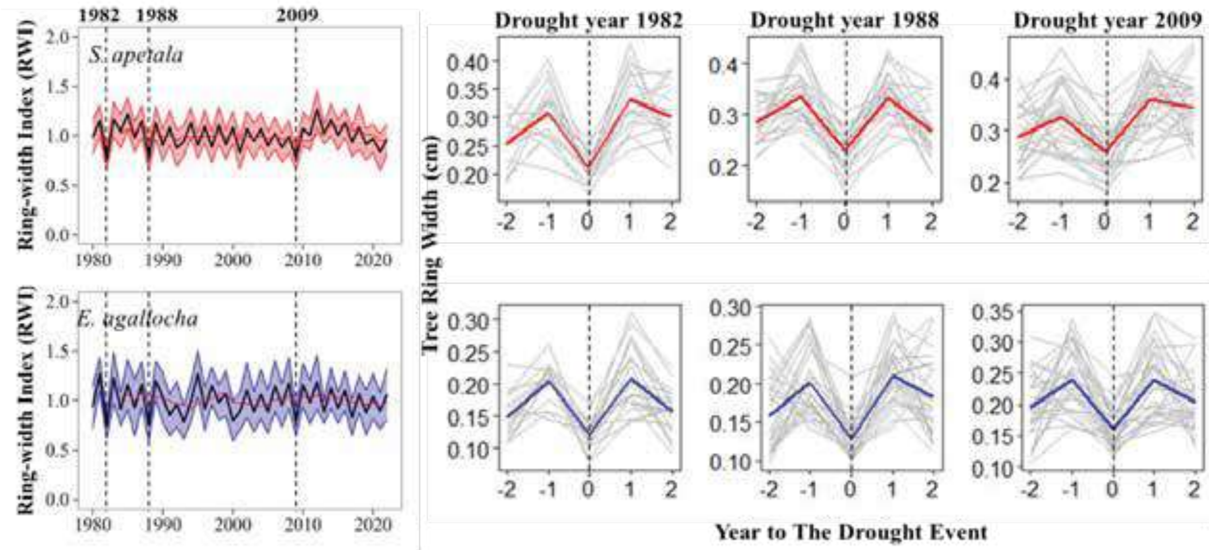

Figure 115. The chronology of *S. apetala*, and *E. agallocha* (black line) of the species of SCF. Vertical dashed lines mark the chosen drought years, while shaded areas denote standard deviations. In the right panels, grey lines represent individual trees, while bold lines depict their respective mean radial growth curves.

Table 3. Chronological characteristics of the sampled trees (Shitakunda Coastal Forest).

		S. apetala	***E. agallocha***
Chronology	Time span (year)	1966-2022	1965-2022
	GLK	0.67	0.67
	EPS	0.79	0.78
	MS	0.23	0.31
	SNR	3.68	3.442
	R bar	0.369	0.348
	AR1	0.18	0.1

The EPS values were 0.79 for S. apetala and 0.78 for *E. agallocha*, which closely approach the critical value of 0.85 (Wigley et al., 1984), suggesting that the samples of these seven species capture approximately 79% and 78% of the interannual growth variation in the population. Environmental sensitivity was moderate for *S. apetala* and high for *E. agallocha* (Table 8), as compared to established thresholds (low: 0.10-0.19, intermediate: 0.20-0.29, and high: ≥0.30) (Grissino-Mayer, 2001), indicating relatively higher year-to-year variation. The mean inter-series correlation (Rbar) was generally low for all species, primarily due to the short time span of the series and minimal influence of the previous year's growth on the characteristics. The Signal-to-Noise Ratio (SNR) value was higher, indicating a stronger signal strength than noise (Table 8). Both species exhibited very low first-order correlation (AR1) and mean series intercorrelation (Table 8). Radial growth for both species significantly declined during the drought events in 1982, 1999, and 2006 (Fig. 21). In comparison to the average radial growth of the two years preceding the drought events, growth of these species decreased by more than 40% during the drought events. (Fig 21).

3.2.2 Species resistance, recovery, and resilience to drought of SCF

Among the three drought years examined, 1982 emerged as the most severe in the study area, succeeded by 1988 and 2009 (Fig 3). The growth reactions of the tree communities within our site appeared to closely parallel the meteorological drought occurrences, with the most substantial growth reduction observed in 1982 (31-40%), followed by 1988 (15-33%) and 2009 (17-31%). Likely RKHRs' species, the species of SCF had lower resistance value (<1) in all the drought events and resilience, and recovery >1 except *S. apetala* (lower resilience) in 1988 drought year. *S. apetala* showed higher resilience, and resistance, to 1982 and 2009 drought events than that of *E. agallocha*. On the other hand, in 1988 drought event *E. agallocha* showed heigher resistance than *S. apetala.* However, these differences were not significant (Fig. 22).

Although SCF experienced severe drought in 1982 than the other drought year, species of this region showed comparatively higher recovery (>1.5) after the drought event than the other species. This suggests that species with higher drought resistance face more difficulties during the recovery period after drought.

Previous research has pointed to the fact that a trade-off between resistance and recovery may occur in forest trees during drought periods, contingent upon the availability of saved resources (Galiano et al., 2011). Our findings reveal that *S. apetala* has the higher resistance capacity to adapt to droughts than *E. agallocha*. Albeit droughts, numerous causes may be considered to describe the lower resistance, recovery, and resilience in *E. agallocha* during all the drought events, including salinity, tree age, height, DBH, canopy openness, soil gradient (i.e, pH, silt%, N, P, K etc.).

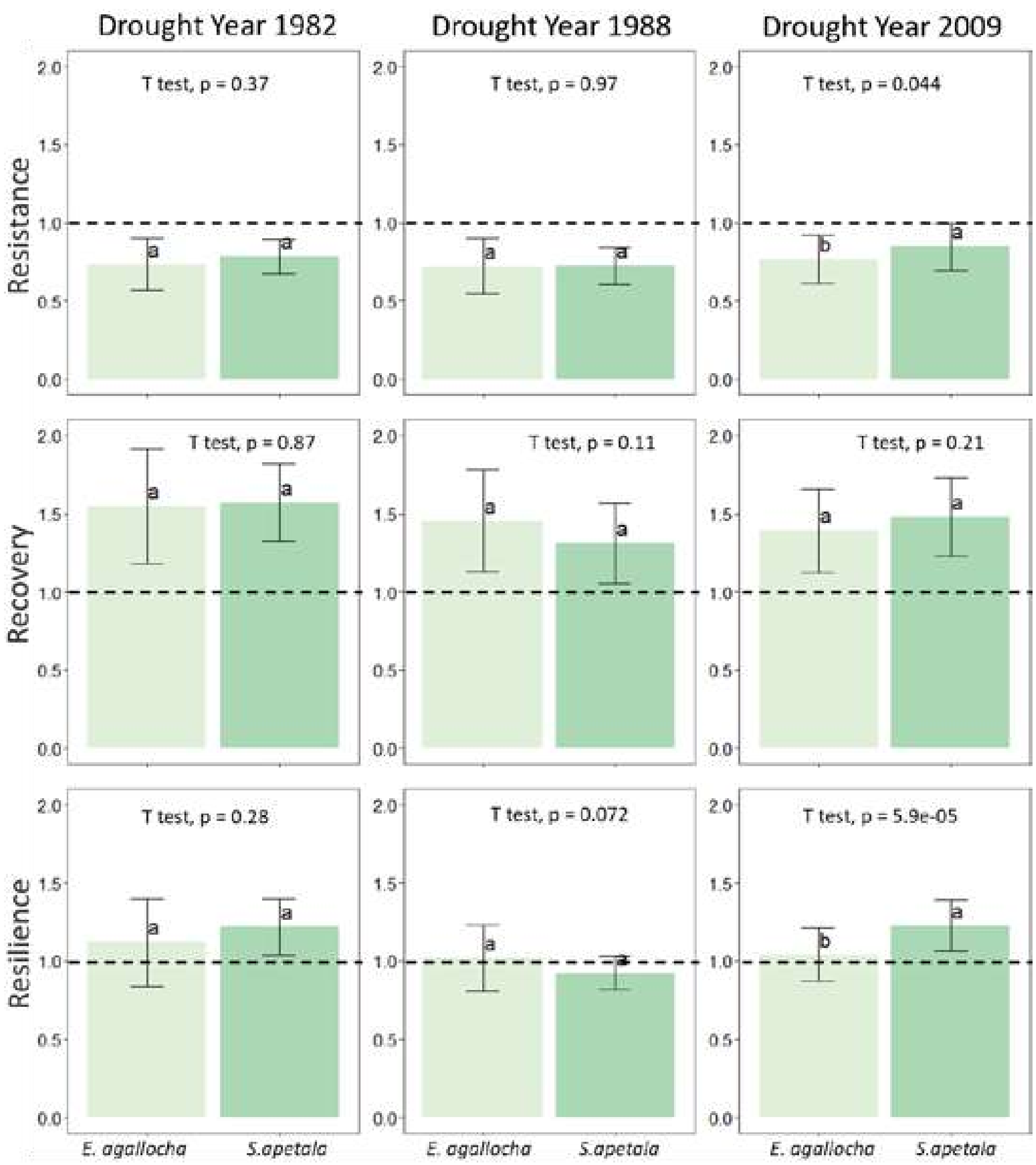

Figure 16. The studied species in the Shitakinda Coastal Forest exhibited varied responses to drought events. Distinct letters denote significant differences (p < 0.05) in drought responses among the species.

3.2.3 Variation in xylem hydraulic traits among the Species of SCF

Although vessel diameter exhibited a unimodal distribution, the patterns varied among the species. For example, most of the vessels were wider and had a right-skewed distribution in *S. apetala* (Fig 24), and conversely, *A. officinalis* had a left-skewed distribution where most of the vessels were smaller in diameter. On the other hand, the vessel distribution in *E. agallocha* was intermediate between that in the two other species. The mean vessel diameter also varied significantly among the study species, where the highest mean diameter was found in *S. apetala* and the lowest was in *A. officinalis*.

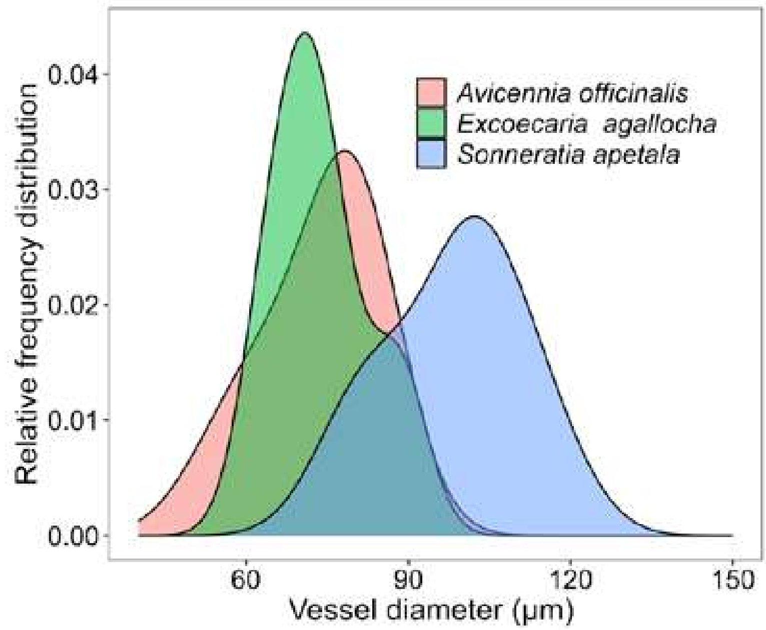

Figure 17. Vessel diameter distribution of the species of SCF

Earlier studies (Carlquist, 2016, 2018; Jacobsen and Pratt, 2023) reported that narrow vessels are positively related to low vulnerability to cavitation, and thus indicates that *A. officinalis* hydraulic transport system is relatively safer than the other species (Fig 25).

A significant variation was found in k_p (p=6.2e^{-5}), VI (p= 0.0025) and S. Index (p= 0.00014) of the species in SCF (Fig 25 A, B and C). *S. apetala* proved to be a more vulnerable species in SCF as it showed significantly higher vulnerability (Fig 25B) and lower safety (Fig 25C) along with higher conductivity (Fig 25A). Conversely, *A. officinalis* and *E. agallocha* exhibited greater resistance to cavitation, resulting in lower vulnerability. However, this resistance is accompanied by reduced efficiency in water conduction, as noted in prior studies (Hacke et al., 2006; Islam et al., 2018a; Sperry et al., 2008).

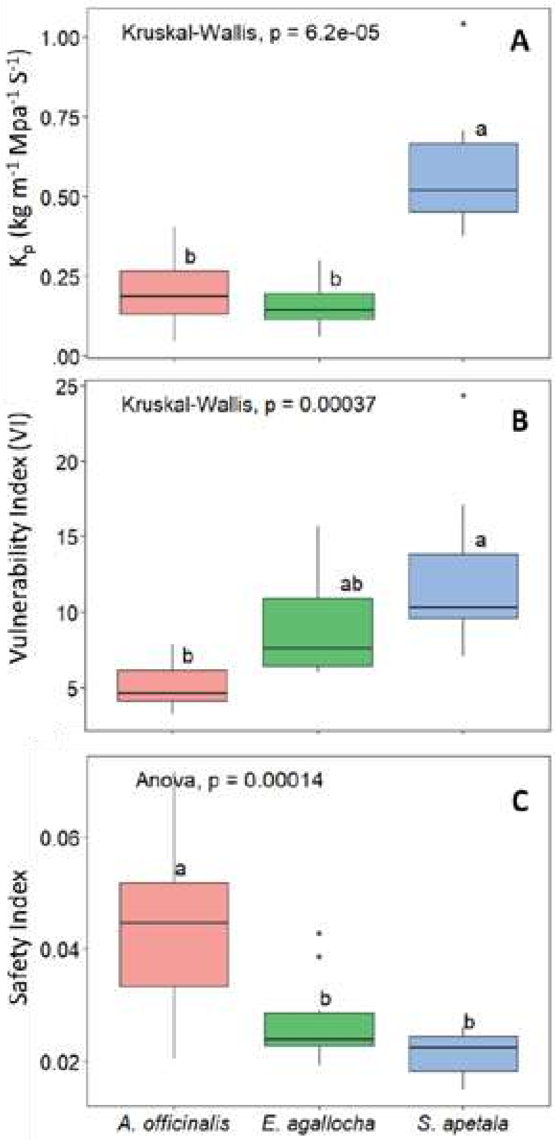

Figure 18. Variation in hydraulic conductivity (Kp), vulnerability index (VI) and safety index (SI) among the studied species in SCF.

3.2.4 Stomatal traits variation among the species in SCF

Stomata were found in the abaxial surface of *A. officinalis* and *E. agallocha* leaves but *S. apetala* had stomata both abaxial and adaxial surface of its leaves. Furthermore, we were able to measure stomatal traits (i.e., SPL and GCL) except *A. officinalis* because of the sunken nature of this species. *E. agallocha* showed significantly longer SPL and GCL and higher stomatal density than *S. apetala* (Fig 26 A, B and C). Such smaller size stomata in Bangladeshi *S. apetala* may help the species responding quickly under environmental perturbations through rapid stomatal opening and closing (Bertolino et al. 2019) and by providing a reduction in total pore area that can facilitate faster aperture response (Lawson and Blatt 2014). In addition, smaller and faster stomata of this species could minimize the effects of excessive water-potential gradients in saline environment that might help to avoid the risks of xylem embolisms (Franks and Beeerling 2009). In the case of SPL. GCL and SD our results are not similar to the hypothesis that stomatal size and density frequently exhibit a negative association, with higher density accompanied by a decrease in size (Franks and Beerling, 2009).

Figure 19. Variation of SPL (A), GCL (B) and SD (C) among the species of SCF.

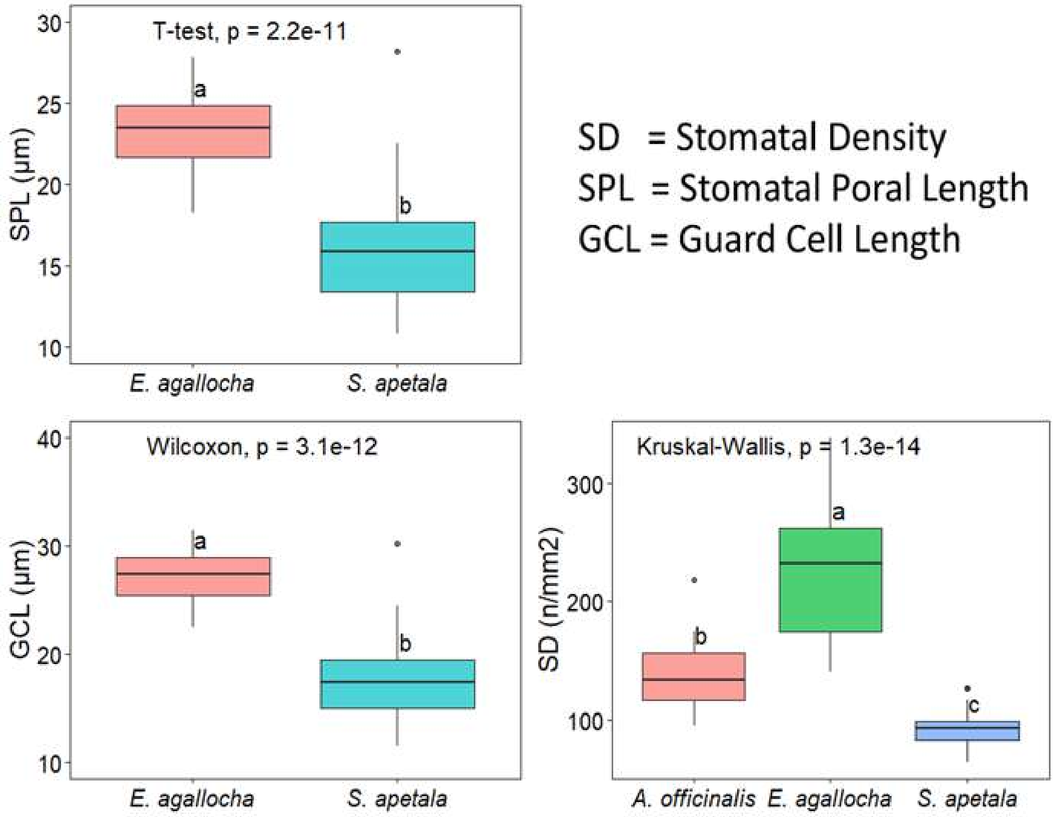

3.2.5 Climate-smart species selection

Among the species of Chattogram coastal forest we were not able to measure the resilience components and stomatal variables (SPL and GCL) of *A. officinalis* because of no annual growth ring formation and sunken type stomata in the abaxial side of leaves. So that, we divided the species selection criteria into two sections, one is with *A. officinalis* (based on hydraulic variables) and another is without *A. officinalis* (include all the selection criteria). In case of hydraulic variables multicriteria decision analysis revealed that *A. offiicinalis* and *E. agallocha* are the most suitable species for RKHR as these species showed lower hydraulic conductivity and vulnerability and higher safety (resistance) to the cavitation compared to *S. apetala* (Fig 25 and Table 9). Although it was not possible to calculate the resilience components to drought of *A. officinalis,* it shows lowest vulnerability and is relatively safer than other species in SCF.

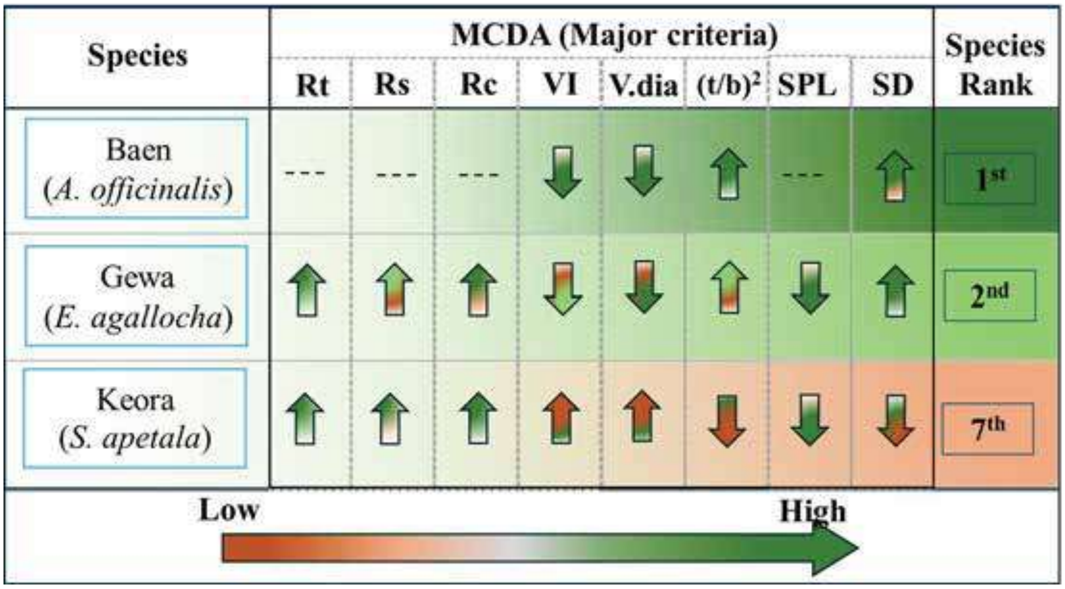

Figure 20. Executive Summary of the results of the SCF. MCDA (Multicriteria Decision Analysis), Rt (Resistance), Rs (Resilience), Rc (Recovery), VI (Vulnerability Index), V.dia (Vessel Diameter), (t/b)2 (vessel wall reinforcement), SPL (Stomatal Pore Length) and SD is the Stomatal Density

3.3 Shingra National Park (SNP)

3.3.1 Cross-dating and growth pattern during the drought events of the species in the SNP

Growth rings were distinct in the study species at SNP. Crossdating among growth-ring series of 26 out of 30 trees was successful for all the species (*S. robusta, C. tubularis, L. speciosa* and *M. azaderach*) of Shingra National Park (SNP).

Table 4. Chronological characteristics of the sampled trees (Shingra National Park).

		S. robusta	*C. tubularis*	*L. speciosa*	*M. azaderach*
Chronology	Time span (year)	1977-2022	2003-2022	2000	2000-2022
	GLK	0.66	0.69	0.69	0.67
	EPS	0.79	0.76	0.84	0.83
	MS	0.31	0.39	0.39	0.27
	SNR	3.08	3.24	4.09	3.406
	R bar	0.34	0.35	0.41	0.4
	AR1	0.11	0.23	0.31	0.1

The EPS values ranged from 0.79 to 0.84 for *S. robusta, C. tubularis, L. speciosa,* and *M. azaderach*, closely approaching the critical value of 0.85 (Wigley et al., 1984). This suggests that the samples of these seven species capture approximately 79% to 84% of the interannual growth variation in the population. Mean sensitivity was moderate for all the species (Table 12), compared to established thresholds (low: 0.10-0.19, intermediate: 0.20-0.29, and high: ≥0.30) (Grissino-Mayer, 2001), indicating relatively higher year-to-year variation.

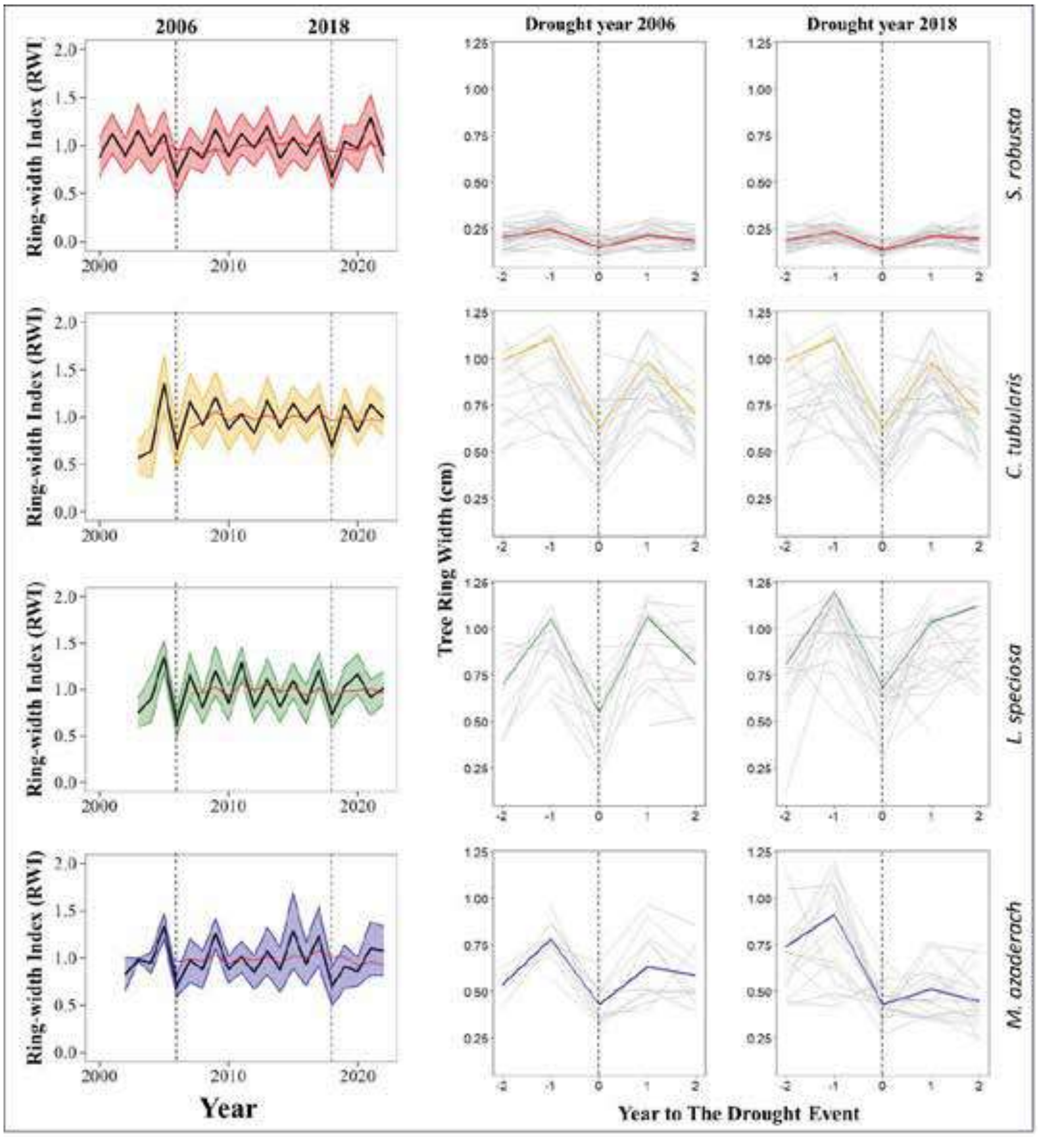

Figure 21. The chronology of *S. robusta, C. tubularis, L. speciosa,* and *M. azaderach* (black line) of the species of SNP in the left panel. Vertical dashed lines mark the chosen drought years, while shaded areas denote standard deviations. In the right panels, grey lines represent individual trees, while bold lines depict their respective mean radial growth curves.

The mean inter-series correlation (Rbar) was generally low for all species, primarily due to the short time span of the series and minimal influence of the previous year's growth on the features. Signal-to-Noise Ratio (SNR) values were higher, indicating stronger signal strength than noise (Table 12). First-order correlation (AR1) and mean series intercorrelation were very low for both species (Table 12).

3.3.2 Species resistance, recovery, and resilience to drought of SNP

The tropical dry forest (SNP) environment, characterized by the periodicity of precipitation and the prevalence of drought episodes during the wet season, imposes significant challenges on plant life (García-Oliva et al., 1991; Páramo-Pérez, 2009). Adaptability in such conditions is likely governed by two key factors: the plants' ability to sustain growth, particularly in dry periods, and their capacity to resist hydraulic failure, thereby mitigating the risk of plant cell death (plant cell environment).

All the species showed higher recovery, resilience and relative resilience value in 2006 than the drought year 2018 (Table 13). The reason behind this might be the higher intensity of drought in 2018 (SPEI=-1.1) than 2006 (SPEI=-0.89) (Fig 4).

Table 5. Resilience component characteristics of studied species of SNP during drought years.

	Variables	Year	*S. robusta*	*L. speciosa*	*C. tabularis*	*M. azedarach*
Resilience Components	**Resistance**	2006	0.61 ± 0.17	0.54 ± 0.16	0.54 ± 0.12	0.55 ± 0.14
		2018	0.58 ± 0.11	0.58 ± 0.14	0.58 ± 0.12	0.56 ± 0.30
	Recovery	2006	1.66 ± 0.65	2.18 ± 0.89	2.30 ± 0.67	1.51 ± 0.38
		2018	1.64 ± 0.49	1.61 ± 0.63	1.65 ± 0.43	1.24 ± 0.45
	Resilience	2006	0.94 ± 0.33	1.16 ± 0.39	1.21 ± 0.33	0.83 ± 0.28
		2018	0.93 ± 0.21	0.89 ± 0.26	0.93 ± 0.27	0.64 ± 0.31

In terms of drought resistance, there are no significant variations among the species (Fig. 30). Also, all the species showed approximately similar resistance value in both drought events (<.62). In the case of recovery and resilience, *C. tubularis* illustrated a higher value than the other species in both drought years. However, we can also see a higher trend in resilience and recovery in *L. speciosa* and *S. robusta* for the years 2018 and 2006 respectively. In comparison with that, the resilience and recovery capacity of *M. azedarach* were lowest for both years (Table 13). In 2006 *M. azaderach* and *S. robusta* showed the lowest recovery and higher resistance than the other two species (Table 13). This suggests that species with higher drought resistance face more difficulties during the recovery period after drought. Previous research has pointed to the fact that a trade-off between resistance and recovery may occur in forest trees during drought periods, contingent upon the availability of saved resources (Galiano et al., 2011).

Notably we found all the individual of L. speciosa beside the river. No individual was found inside the forest. This may be the reason behind the higher recovery after the drought year, as they can use the water of the river in the easier way than the other species. Therefore, the evidence from these consecutive drought years proved that *C. tubularis* and *S. robusta* is the most drought resistance species among the species of SNP.

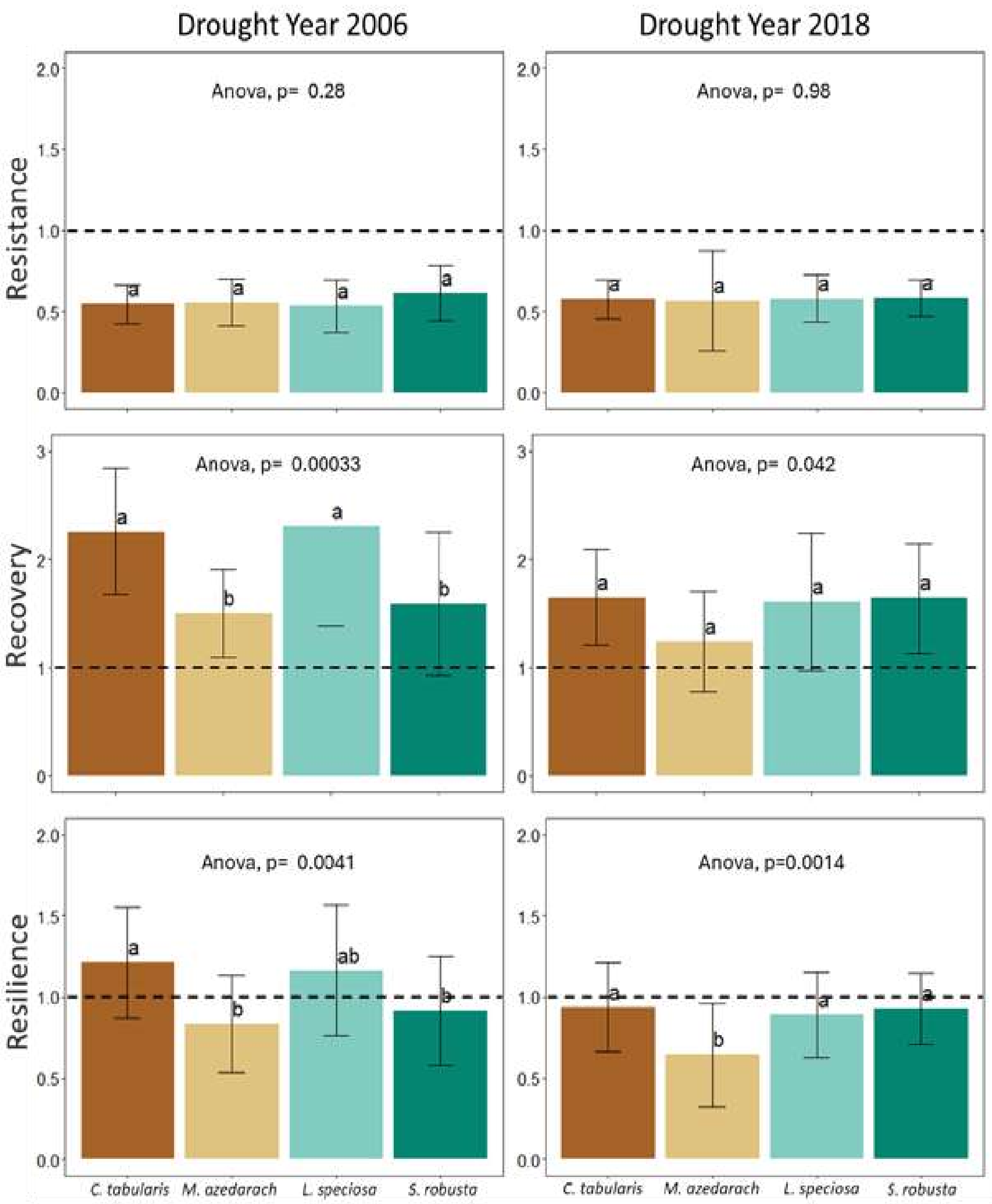

Figure 22. The studied species in the Sjingra National Park exhibited varied responses to drought events. Distinct letters denote significant differences ($p < 0.05$) in drought responses among the species.

3.3.3 Variation in xylem hydraulic traits among the Species of SNP

Although vessel diameter exhibited a unimodal distribution, the patterns varied among the species. For example, most of the vessels were wider and had a right-skewed distribution in *L. speciosa* and *M. azaderach* (Fig. 33), and conversely, *C. tabularis* had a left-skewed distribution where most of the vessels were smaller in diameter. On the other hand, the vessel distribution in *S. robusta* was intermediate between that in the three other species. The mean vessel diameter also varied significantly among the study species, where the highest mean diameter was found in *M. azaderach* and the lowest was in *C. tabularis*.

Earlier studies (Carlquist, 2016, 2018; Jacobsen and Pratt, 2023) reported that narrow vessels are positively related to low vulnerability to cavitation, and thus indicates that *C. tabilaris* and *S. robusta* hydraulic transport system is relatively safer than the other species in SNP (Fig 34).

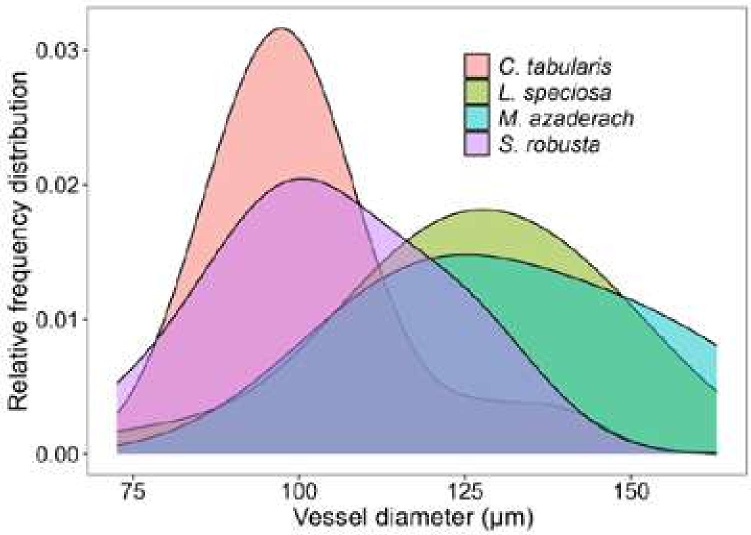

Figure 23. Vessel diameter distribution of the species in SNP

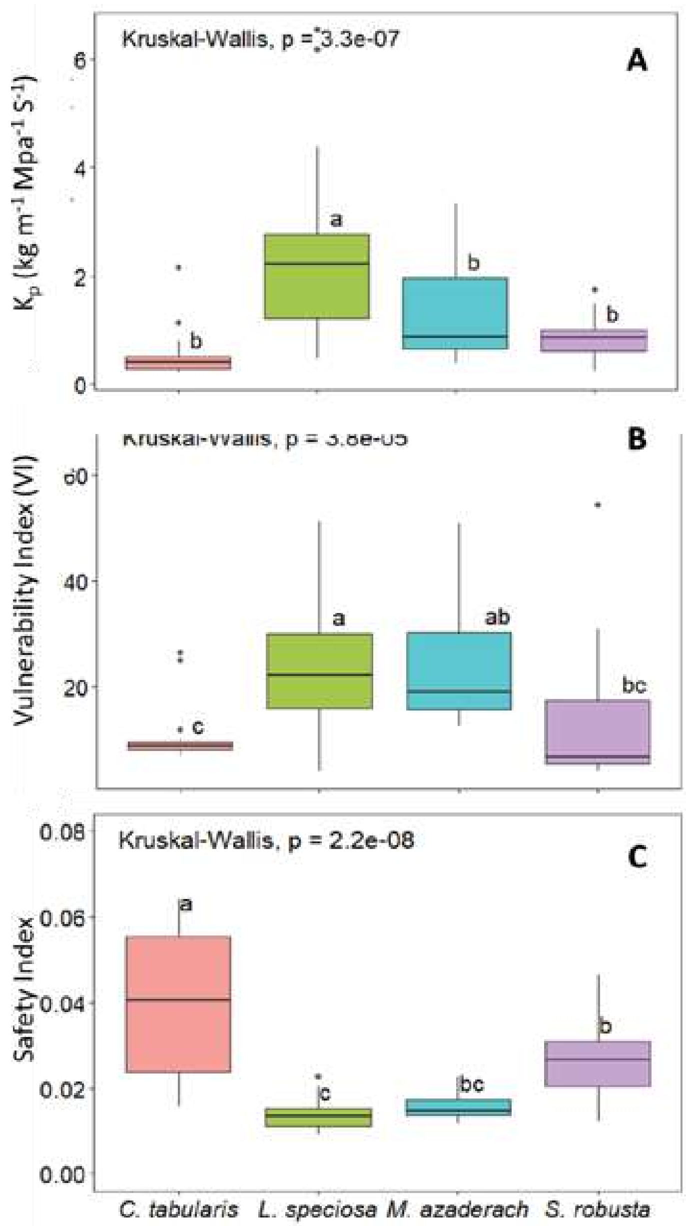

Figure 24. Variation in hydraulic conductivity (Kp), vulnerability index (VI) and safety index (SI) among the studied species in SNP.

A significant variation was found in k_p ($p=6.2e^{-5}$), VI ($p= 0.0025$) and SI ($p= 2.2^{-08}$) of the species in SNP (Fig 34 A, B and C). We found *L. speciosa* and *M. azaderach* showed significantly higher potential conductivity and vulnerability among the species of SNP (Fig 34 A, B). Conversely, *C. tubularis* and *S. robusta* demonstrated greater resistance to cavitation (Fig 34 C), resulting in lower vulnerability. However, this resistance is accompanied by reduced efficiency in water conduction, as noted in prior studies (Hacke et al., 2006; Islam et al., 2018a; Sperry et al., 2008).

3.3.4 Stomatal traits variation among the species in Shingra National Park

Stomata were found in the abaxial surface of all the species.

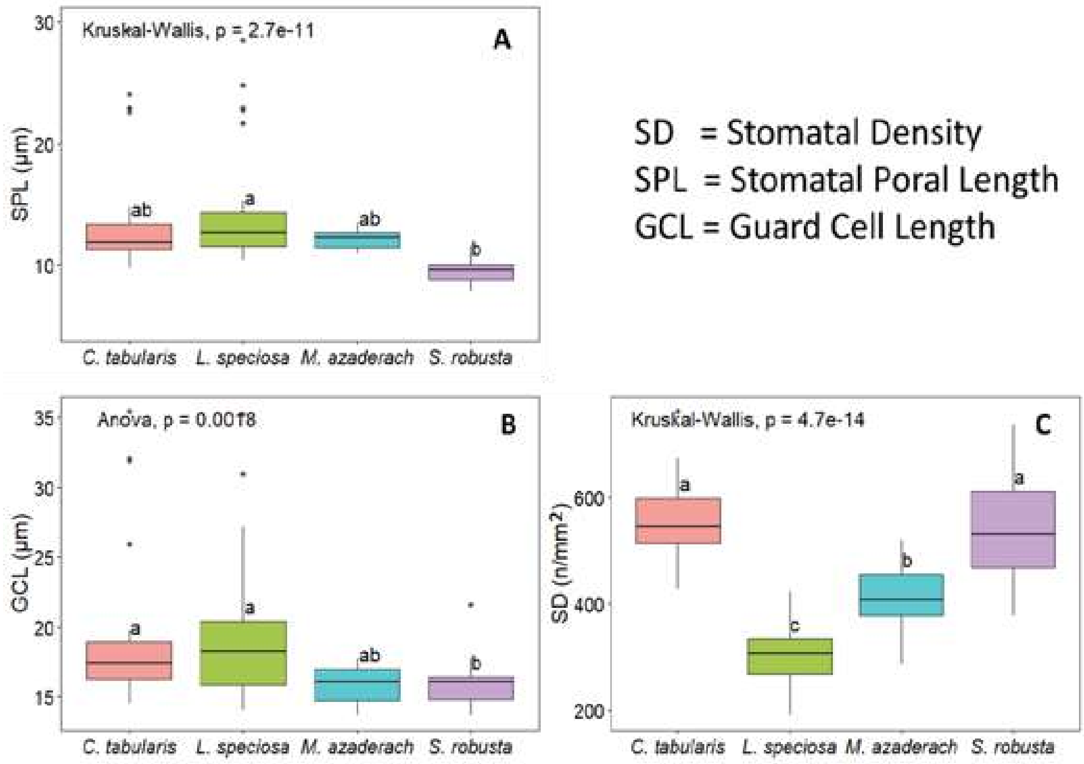

Figure 25. Variation of SPL (A), GCL (B) and SD (C) among the species of SNP .

C. tubularis and *S. robusta* portrayed comparably shorter SPL, GCL (Stomatal Size) and higher stomatal density (SD) than other species. (Fig 35 A-C). Such smaller size stomata *C. tabularis* and *S. robusta* may help the species responding quickly under environmental perturbations through rapid stomatal opening and closing (Bertolino et al. 2019) and by providing a reduction in total pore area that can facilitate faster aperture response (Lawson and Blatt 2014). In addition, smaller and faster stomata of this species could minimize the effects of excessive water-potential gradients in saline environment that might help to avoid the risks of xylem embolisms (Franks and Beeerling 2009). The CO_2 fixation rate may be higher in the leaf of these two species than the other as improvements in CO_2 fixation are due to increases in maximum potential stomatal conductance via higher density (SD), or due to quick stomatal responses endorsed by minor stoma (S) (Harrison et al., 2020). These results are similar to the hypothesis that stomatal size and density frequently exhibit a negative association, with higher density accompanied by a decrease in size (Franks and Beerling, 2009). Therefore, likely the response from resilience components to drought and hydraulic traits, from the leaf stomatal variables it is also proved that *C. tabularis* and *S. robusta* showed greater safety than the other species and more suitable specie for this region (SNP) than the other two species.

3.3.5 Climate-smart species selection

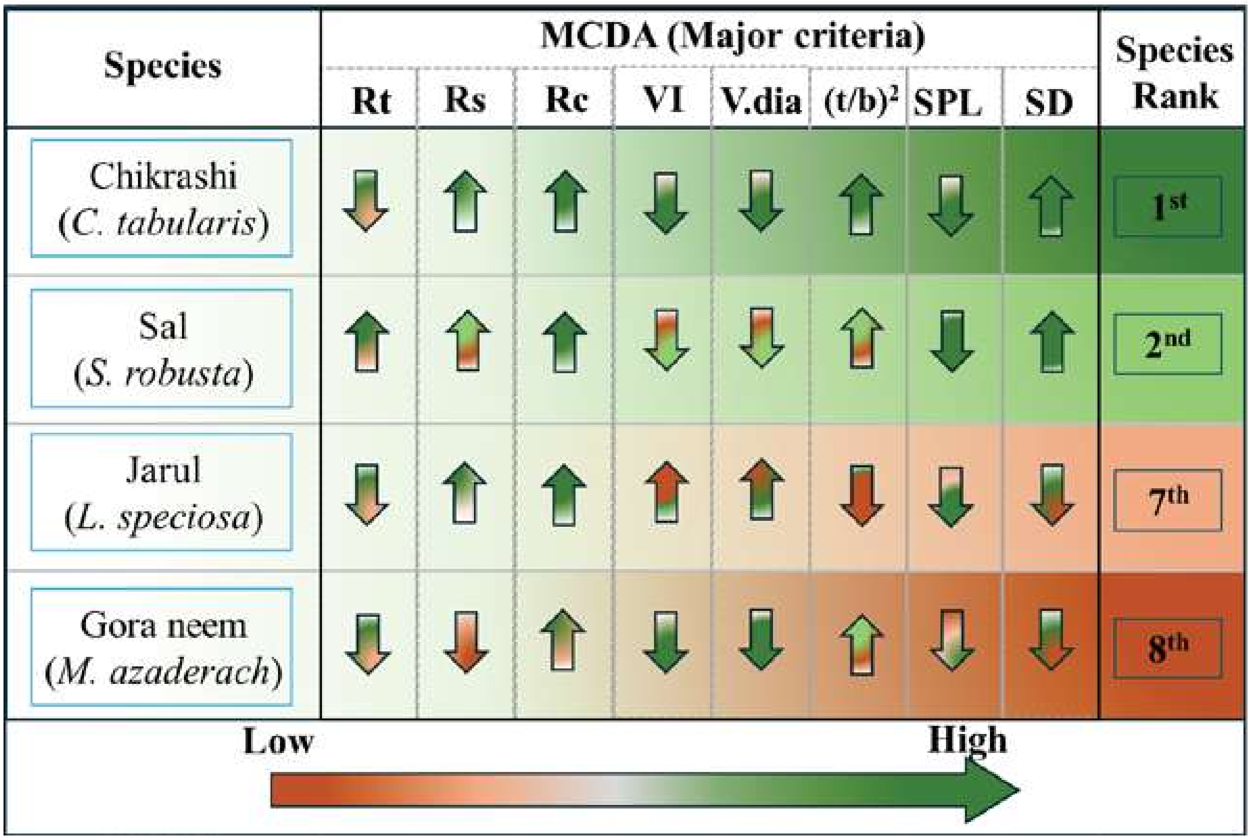

Figure 26. Executive Summary of the results of the SNP. MCDA (Multicriteria Decision Analysis), Rt (Resistance), Rs (Resilience), Rc (Recovery), VI (Vulnerability Index), V.dia (Vessel Diameter), $(t/b)^2$ (vessel wall reinforcement), SPL (Stomatal Pore Length) and SD is the Stomatal Density

Although *S. robusta* is the most dominant species in the Shingra national Park, we found another species (*C. tubularis*) which is very much suit this ecosystem with significantly high growth rate (Table 12). Depending on all the criteria (Resilience components, Hydraulic traits and Stomatal variable), multi-criteria decision analysis (MCDA) revealed that *C. tabularis* and *S. robusta* are the most suitable and adaptive species for SNP as these species showed higher resistance to the drought (Fig 31), lower hydraulic conductivity and vulnerability and higher safety to the cavitation compared to the other species (Fig 35).

Chapter IV

Conclusion and Recommendations

4.1 Conclusion

Based on the methods, this project identified climate resilient tree species that could be used for restoration in the studied ecosystems of Bangladesh. The results of the MCDA showed that *C. tabularis, S. robusta* and *V. pubescens* were the most suitable species in RKHR, as they gained the highest scores from the species selection criteria compared to the other study species in this ecosystem. During both drought events in SNP, *C. tubularis* and *S. robusta*, along with *L. speciosa* manifested superior drought tolerance and exhibit the capacity to thrive in adverse climatic conditions. In the case of hydraulic traits, both species exhibited greater vessel wall reinforcement $(t/b)^2$ and safety, and lower vulnerability. Similarly, *E. agallocha* and *S. apetala* demonstrated higher resilience, resistance, and recovery capabilities specifically in the SCF, particularly in response to drought conditions. Due to absence of distinct datable growth rings, we were not able to calculate the resilience components of *A. officinalis*. However, MCDA revealed that *A. officinalis* had the highest weight than other species because of higher hydraulic safety and lower vulnerability to cavitation. This empirical evidence underscores the significance of these species in ecological context and emphasizes their potential to ecosystem stability. This research adds additional factors to our understanding in changing adaptive capacity of forests. Such study highlights its importance since today's exceptional drought events are likely to become routine in the future. Therefore, the growth resilience to drought along with hydraulic and ecophysiological traits will help to develop the key evidences to identify the potential climate-smart tree species to cope in the extreme climatic conditions. In addition, understanding the combined influences of soil and forest structural variables on growth resilience components provides new insights into the processes underlying microhabitat constraints and will improve our ability to predict how the studied forest ecosystems could be impacted by future changes in climate and local environmental conditions.

4.2 Recommendations

The forests of Bangladesh face significant vulnerability to climate change, with extreme weather occurrences like droughts, heatwaves, and floods posing extensive impacts on biodiversity, carbon sequestration, and livelihoods. In this context, increasing climate-smart forests is a NbS to address the challenges. Selection of climate-smart planting materials such as tree species is a basic consideration to increasing smartness of the forests. The outcomes of this research emphasize the integration of climate-smart indigenous tree species into Bangladesh's forest restoration endeavors across diverse ecosystems. However, identifying climate-smart tree species is not the only practical decision to make restoration success: other considerations need to be considered in the planting strategies such as shade tolerance, habitat suitability of the selected tree species.

It is imperative for the Bangladesh Forest Department to prioritize the integration of identified climate-smart species into restoration strategies. Restoration plans should be habitat-specific in the ecosystems. Although *L. speciosa* is a priority species in both dry (SNP) and wet (RKHR) ecosystems, the habitat analysis indicates that this species should be planted in the moist areas. Other less priority species in the list such as *P. integerrima, D. pentagyna* and *A. chaplasha* are could be used in mesic conditions as their hydraulic traits are less plastic to drought stress.

Light characters of the selected tree species should also be well-thought-out. Light demanding species such as *C. tabularis* is useful for monospecific stands in both dry and wet ecosystems. However, restoring monospecific stands are vulnerable to stressful events such as insect outbreaks and storms, which need to be considered. Mixed stands are more effective in stress tolerance and biodiversity conservation. In this context, restoration of ecosystems integrating light demanding species with shade tolerance species will be useful. For example, in coastal mangroves, the moderately light demander *E. agallocha* can be used after modify the area by light demanding *S. apetala* and *A. officinalis*.

Sustained monitoring activities are essential to evaluate the performance and adaptability of climate-smart species across various ecological settings. Establishing long-term monitoring programs will facilitate the tracking of growth patterns, resilience levels, and ecological impacts of selected species, thereby providing invaluable insights for adaptive management and decision-making processes.

Advocacy efforts should be directed towards policymakers to enact supportive policies and bolster institutional frameworks for climate-smart forestry practices. This may involve incentivizing the conservation and cultivation of climate-smart species, advocating for sustainable forestry practices, and fortifying institutional capacities for ecosystem-based adaptation (EbA) as a key component of NbS. Collaborative efforts with local communities and stakeholders are pivotal for the successful implementation of forest restoration endeavors. The Bangladesh Forest Department should prioritize community engagement initiatives aimed at fostering awareness towards climate-smart forestry, enhancing capacity, and instilling local ownership of restoration projects, ensuring their long-term sustainability and effectiveness.

References

Ahmed, M., Kha, W., & Haque, M. A. (2023). Impact of salinity stress on coastal agriculture and livelihoods: evidence from the southwest coastal region of Bangladesh. Regional Environmental Change, 23(2), 455-468.

Ali, M. Z., Hassan, M. U., & Islam, S. (2019). Assessment of nitrogen availability in soil of selected forest plantations of Bangladesh. Journal of Forest and Environmental Science, 35(3), 233–243.

Ali, M.R., et al. (2020). Indigenous Knowledge of the Local Communities on the Management and Conservation of Singra National Park, Bangladesh. Journal of Biodiversity Conservation and Bioresource Management, 6(1), 1-10.

Anderegg W. R., et al. (2013). Drought's legacy: Multiyear hydraulic deterioration underlies widespread aspen forest die-off and portends increased future risk. Global Change Biology 19: 1188–1196.

Aranda, I., et al. (2012). Variation in photosynthetic performance and hydraulic architecture across European beech (Fagus sylvatica L.) populations supports the case for local adaptation to water stress. Tree Physiology, 32(2), 249-258.

Bangladesh Bureau of Statistics (BBS). (2010). Statistical Yearbook of Bangladesh. Dhaka, Bangladesh: Bangladesh Bureau of Statistics.

Bertolino, L. T., Caine, R. S., & Gray, J. E. (2019). Impact of stomatal density and morphology on water-use efficiency in a changing world. Frontiers in plant science, 10, 225.

Blasing, T. J., & Fritts, H. C. (1976). Estimating the response of ring-width chronologies to changes in atmospheric CO2 concentration. Tree-Ring Bulletin, 36, 1-11.

Brady, N. C. (1999). The nature and properties of soils (12th ed.). Prentice Hall.

Bunn, A. G. (2008). A dendrochronology program library in R (dplR). Dendrochronologia, 26(2), 115–124.

Carlquist, S. (2016). Ecological factors in wood evolution: a floristic approach. Botanical Journal of the Linnean Society, 181(3), 441-464.

Carlquist, S. (2018). Comparative wood anatomy: systematic, ecological, and evolutionary aspects of dicotyledon wood. Springer Science & Business Media.

Chowdhury, M.Q., et al. (2023). Synergistic effects of climate and salinity on radial growth of Excoecaria agallocha L. in the Sundarbans world heritage mangrove ecosystem. Estuarine, Coastal and Shelf Science, 280, p.108181.

Cropper, J. P. (1979). Tree-ring skeleton plotting by computer. Tree-Ring Bulletin, 39, 47–59.

Douglass, A. E. (1941). Crossdating in dendrochronology. Journal of Forestry, 39(10), 825-831.

Dudney, J., Barringer, S., & Martin, D. (2023). Species-specific Responses to Drought Stress: A Comprehensive Review. Environmental Research Letters, 1(1), 1-15.

Franks, P. J., & Beerling, D. J. (2009). Maximum leaf conductance driven by CO2 effects on stomatal size and density over geologic time. Proceedings of the National Academy of Sciences, 106(25), 10343-10347.

Galiano, L., Martínez-Vilalta, J., & Lloret, F. (2011). Carbon reserves and canopy defoliation determine the recovery of Scots pine 4 yr after a drought episode. New Phytologist, 190(3), 750-759.

García-Oliva, F., Ezcurra, E., & Galicia, L. (1991). Pattern of rainfall distribution in the Central Pacific Coast of Mexico. Geografiska Annaler: Series A, Physical Geography, 73(3-4), 179-186.

Garnier, E., Shipley, B., Roumet, C., & Laurent, G. (2001). A standardized protocol for the determination of specific leaf area and leaf dry matter content. Functional Ecology, 15(5), 688–695.

Gee, G. W., & Bauder, J. W. (1986). Particle-size analysis. In A. Klute (Ed.), Methods of Soil Analysis. Part 1. Physical and Mineralogical Methods (2nd ed., pp. 383–411). American Society of Agronomy.

Grissino-Mayer, H. D. (2001). Evaluating crossdating accuracy: a manual and tutorial for the computer program COFECHA. Tree-Ring Research, 57(2), 205-221.

Hacke, U. G., et al. (2006). Water transport in vesselless angiosperms: conducting efficiency and cavitation safety. International Journal of Plant Sciences, 167(6), 1113-1126.

Harrison, L.G., et al. (2020). Impact of stomatal conductance on the response of net ecosystem carbon dioxide exchange to environmental drivers in a temperate deciduous forest. Agricultural and Forest Meteorology, 284, 107895.

Hoeber, S., Leuschner, C., Köhler, L., Arias-Aguilar, D., & Schuldt, B. (2014). The importance of hydraulic conductivity and wood density to growth performance in eight tree species from a tropical semi-dry climate. Forest Ecology and Management, 330, 126–136.

Hoobin, S., & Vanclay, J. K. (2011). Assessment of potassium status in Queensland soils. Soil Research, 49(7), 596–607.

Islam, M. A., et al. (2018a). Drought stress acclimation imparts tolerance to subsequent osmotic stress in Jatropha curcas L. seedlings. Environmental and Experimental Botany, 155, 694-709.

Islam, M. S., & Rahman, M. M. (2018). Mangrove species composition and changes in Sundarbans Reserve Forest in Khulna, Bangladesh. International Journal of Fisheries and Aquatic Studies, 6(2), 415-422.

Jacobsen, A. L., & Pratt, R. B. (2023). Evolution of plant hydraulic traits across environmental gradients. In Annual Review of Ecology, Evolution, and Systematics (Vol. 54, pp. 297-319). Annual Reviews.

Lawson, T., & Blatt, M. R. (2014). Stomatal size, speed, and responsiveness impact on photosynthesis and water use efficiency. Plant physiology, 164(4), 1556-1570.

Lens, F., Sperry, J. S., Christman, M. A., Choat, B., Rabaey, D., & Jansen, S. (2011). Testing hypotheses that link wood anatomy to cavitation resistance and hydraulic conductivity in the genus Acer. New Phytologist, 190(3), 709–723.

Leo, J., et al. (2014). Physiological responses of trees to drought stress. Journal of Ecology, 102(6), 1353-1365.

Lloret, F., Keeling, E. G., & Sala, A. (2011). Components of tree resilience: Effects of successive low-growth episodes in old ponderosa pine forests. Oikos, 120(12), 1909–1920.

Martinez del Castillo, E., Canellas, I., Velasco, A. G., Serrano, L., & Sánchez, J. G. (2018a). Growth response of dominant Mediterranean tree species to drought events in past decades: The complex relationships between climate and tree growth. Agricultural and Forest Meteorology, 263, 172-183.

Meir, P., Wood, T. E., Galbraith, D. R., Brando, P. M., Da Costa, A. C., Rowland, L., ... & Mencuccini, M. (2015). Threshold responses to soil moisture deficit by trees and soil in tropical rain forests: insights from field experiments. BioScience, 65(9), 882-892.

MoEFCC 2021. Bangladesh Climate Change Strategy and Action Plan (BCCSAP). Retrieved from https://www.moef.gov.bd/sites/default/files/files/moef.portal.gov.bd/files/e19bfa7f_3d1b_4912_9274_8dd2d1b2be58/BCCSAP2019English.pdf

Miyan, M. A. (2015). The changing pattern of the monsoon in Bangladesh. Weather, 70(8), 240–245.

Mollah, A.R., et al. (2003). Forest Types of Bangladesh. Bangladesh Journal of Forest Science, 32(1), 1-11.

Neubauer, K. R. (2017). Determination of phosphorus, potassium, calcium, and magnesium in soil and plant tissue with induced coupled plasma-atomic emission spectroscopy (ICP-AES). MethodsX, 4, 153–162.

Neuwirth, B., Schweingruber, F., & Winiger, M. (2007). Spatial patterns of central European pointer years from 1901 to 1971. Dendrochronologia, 25(1), 1–19.

Obojes, N., et al. (2018). Compensation for reduced growth during droughts in European beech (Fagus sylvatica L.) forests. Trees, 32(6), 1555-1568.

Páramo-Pérez, M. (2009). Análisis temporal de los eventos de sequías cortas y su efecto en la fisiología y supervivencia de plántulas de cuatro especies arbóreas de la selva baja caducifolia (Doctoral dissertation, Msc dissertation, Universidad nacional autónoma de México, México).

Prager, M., & Hoenig, J. (1989). Superposed epoch analysis with application to environmental time series. Environmental Software, 4(1), 61–76.

R Core Team. (2023). R: A language and environment for statistical computing. R Foundation for Statistical Computing, Vienna, Austria. URL https://www.R-project.org/.

Rahman, M. M., & Lateh, H. (2016). Salinity Intrusion and the livelihoods of people: Evidence from southwest coastal Bangladesh. Regional Environmental Change, 16(8), 2195-2205.

Rahman, M. M., et al. (2019). Drought-induced tree mortality in a tropical dry forest: the role of bark functional traits and microclimate. Biotropica, 51(6), 937-947.

Rahman, M. M., Islam, M. R., & Hoque, M. A. (2020). Climate variability and tree growth in Bangladesh: a dendrochronological perspective. Climate Dynamics, 54(1-2), 931-942.

Rahman, M.M., & Miah, M.D. (2017). Seasonal Variation of Physicochemical Properties of Water in Five Ponds of Sylhet City, Bangladesh. International Journal of Ecology and Environmental Sciences, 43(1), 69-80.

Rana, S.M.M., & Akhter, S. (2010). Review of the Floristic Diversity of Bangladesh. Bangladesh Journal of Plant Taxonomy, 17(1), 71-80.

Rashid, A. (2019). A Handbook of Common Trees and Shrubs of Sundarbans (2nd ed.). Bangabandhu Sheikh Mujibur Rahman Agricultural University.

Sack, L., Cowan, P. D., Jaikumar, N., & Holbrook, N. M. (2003). The 'hydrology' of leaves: Co-ordination of structure and function in temperate woody species. Plant, Cell & Environment, 26(8), 1343–1356.

Samson, J. M., & Yeung, C. (1986). Seasonal variations in SO2 concentrations measured in the vicinity of a molybdenum mine using superposed epoch analysis. Environmental Monitoring and Assessment, 7(1), 1–10.

Sarker, S. K., Haque, M. M., & Rahman, M. A. (2015). Impact of habitat types and restoration treatments on structural parameters of vegetation in degraded Sundarbans mangrove forest, Bangladesh. Journal of Forestry Research, 26(4), 917-926.

Sarker, S. K., Rahman, M. A., & Hashem, M. A. (2013). Spatial analysis of forest distribution and its relation with geology and soil in Bhawal National Park, Bangladesh. The Bangladesh Journal of Botany, 42(2), 339-348.

Savva, Y., Oleksyn, J., Reich, P. B., Tjoelker, M. G., Vaganov, E. A., & Modrzynski, J. (2006). Interannual growth response of Norway spruce to climate along an altitudinal gradient in the Tatra Mountains, Poland. Trees, 20, 735-746.

Schindelin, J., Arganda-Carreras, I., Frise, E., Kaynig, V., Longair, M., Pietzsch, T., ... & Cardona, A. (2012). Fiji: an open-source platform for biological-image analysis. Nature methods, 9(7), 676-682.

Schneider, C. A., Rasband, W. S., & Eliceiri, K. W. (2012). NIH Image to ImageJ: 25 years of image analysis. Nature Methods, 9(7), 671–675.

Shahid, S. (2010). Rainfall variability and the trends of wet and dry periods in Bangladesh. International Journal of Climatology, 30(16), 2299–2313.

Sperry, J. S., Alder, N. N., & Eastlack, S. E. (1994). The effect of reduced hydraulic conductance on stomatal conductance and xylem cavitation. Journal of Experimental Botany, 45(1), 175–184.

Sperry, J. S., et al. (2008). Hydraulic constraints on plant gas exchange. Agricultural and Forest Meteorology, 148(2), 210-218.

Tng, D. Y., Janos, D. P., Jordan, G. J., Weber, E., Bowman, D. M., & Hoffmann, W. A. (2018). Experimental evidence of functional differentiation between seedling and sapling stages in a dominant rainforest tree. Functional Ecology, 32(2), 499-512.

Uddin, M.B., et al. (2002). Bangladesh: Sylhet District. Forest Resources Assessment Working Paper No. 66. FAO, Rome.

USAID. (2012). Bangladesh - Forests and Forestry. Available at: https://rmportal.net/library/content/asia/regional/asia/regional-documentation-centre-of-the-sustainable-land-management/forests-and-forestry-bangladesh-2013/forests-and-forestry-bangladesh-2013.pdf/view

van der Maaten-Theunissen, M., van der Maaten, E., Bouriaud, O., Hus, J., van der Maaten, J. H., & Bouriaud, L. (2015). pointRes: An R package to analyze pointer years and components of resilience. Dendrochronologia, 35, 34–38.

Wigley, T. M. L., Briffa, K. R., & Jones, P. D. (1984). On the average value of correlated time series, with applications in dendroclimatology and hydrometeorology. Journal of Climate and Applied Meteorology, 23(2), 201-213.

Wigley, T. M. L., Briffa, K. R., & Jones, P. D. (1990). On the average value of correlated time series, with applications in dendroclimatology and hydrometeorology: Reply. Journal of Climate, 3(7), 807-818.

Zuidema, P. A., Martínez-Ramos, M., & Johnson, D. M. (2020). Population dynamics, growth and demographic rates of tropical trees: A review. Global Ecology and Biogeography, 29(1), 5-14.

Appendix

Figure S1. The studied forest ecosystems.

Restoration of Biodiversity at Baraiyadhala National Park for Water Conservation, Utilization, And Eco-Tourism.

by

Md. Baktiar Nur Siddiqui

Director (rtd.), Forestry Development and Training Center (FDTC), Kaptai, Rangamati

CHAPTER I

INTRODUCTION

The hill forests of Ramgarh-Sitakundu hill ranges of Chattogram district are well-known for their rich biodiversity and other resources like *Cycas pectinata* and waterfalls (Hossain et al. 2021). It was managed from 1923 under the working plan prescriptions with different working circles. Later, it continued with different working plans in the same circles. After 1976, a Management Plan was prepared with a budgetary proposal mentioning a specific rotation period. In most of these plans, prescriptions were provided for timber and fuel wood production with little emphasis on water conservation and the daily requirements of the local people. To fulfill the requirements of fuel wood and livelihood opportunities, nearby people entered the forests and collected the forest products, disturbing the biodiversity. At the same time, illegal extraction was done, and forest land encroachment occurred in some areas. Degraded forest lands have been converted into vegetable gardens and horticultural crops sporadically. In this perspective, legal measures taken by the Forest Department could not stop them from entering the forest. In the early nineties, the Participatory approach of plantation raising activities involved the local people managing the plantation and getting a share from the sale proceeds after the rotation period. These were project-based and target-oriented approaches. Despite this participatory approach, remarkable progress or success could not be achieved in restricting the illegal extraction as well as the conversion of forest land to other agricultural uses. Considering the importance of rich biodiversity in the area, a part of this forest area (800 acres) was declared Sitakundu Eco-Park in the year 2001 and Baraiadhala National Park in 2010. This park is in the Sitakundu and Mirsarai upazila of Chittagong district. For managing this National Park, one management plan was prepared in 2015 (Hossain 2015). The co-management approach was adopted. Forest-dependent people and other concerned stakeholders were involved in one project. After the completion of the project, these activities have stopped now. The most promising water conservation/utilization and waterfall-based ecotourism issue did not get due attention in this project either.

South-East Asian countries have made their natural forest landscape to a big ecotourism industry. Whereas the natural landscape of Mirsarai and Sitakunda hill ranges is no less attractive than South-East Asian regions. Baraiyadhala National Park and its adjacent areas are a potential site and could be built as an ecotourism destination. Many waterfalls and trekking sites have already attracted tourists from different remote regions of the country. Delineation of risky locations of the waterfall was not identified, even after the deaths of several excursionists in the past couple of years. Keeping this on the priority list, research was conducted on whether and how the security, safety, and other facilities could be managed. The research could make suggestions based on the outcome of the respondent who paid or visited earlier. The heavy usage of water by the adjacent areas decreased the underground water recharge. Fuel and water are the lifeblood of all economic and social activities of the adjacent community. Before late, we must make reservoirs or lakes or any other appropriate measures that may recharge the underground water level and utilize the rainwater and help irrigation and drinkable water, industrial use, and the water shedding areas. Two organizations attempted to build structures to regulate water supplies for agricultural use in three scattered areas. Water user committees were formed at the downwards of the waterfall areas. But no coordinated approach was observed. The use of drained-out rainwater by the steel re-rolling mills established near the forest area was not brought under the management decision. The scope of developing collaborative arrangements for conserving upland forests and waters of waterfalls, strengthening eco-tourism facilities, and using rainwater for agricultural and industrial use needs to be explored and assessed.

Objectives of the study are:

1. Assess the biodiversity (flora) of the Protected Area (PA),
2. Delineate the waterfall routes and connectivity, and develop spatial maps and databases,
3. Identify the eco-tourism facilities and networks in the area,
4. Provide awareness and training to local people, tour guides, and forestry staff about the safe travel and conservation of resources, including the endangered *Cycas pectinata*, and
5. Design a restoration plan in upland forests and waterfall areas and use of the rainwater through a collaborative arrangement.

CHAPTER TWO

LITERATURE REVIEW

2.1 Biodiversity

2.1.1 Flora

Being rich in plant diversity (Harun-Ur-Rashid et al. 2018), Baraiyadhala National Park possesses a total of 553 species of angiosperms under 97 families and 3 Critically Endangered gymnosperms, while over 300 monocot species are believed to be present there (Hossain 2015, Haider et al. 2022). Out of these 553 species of angiosperms, 205 are trees, 143 shrubs, and 205 herb species, whereas the number of Endangered and Critically Endangered species is 100 and 9, respectively. As per Harun-Ur-Rashid et al. (2018), there exist 528 species of Magnolids and Eudicots under 337 genera of 73 families with 179 tree species, 174 herbs, 95 shrubs, 78 climbers, and 2 epiphytes. However, Karim et al. (2023) reported 267 plant species from the selected trails. They found Euphorbiaceae was the largest family, representing 18 species, followed by Cyperaceae with 11 species, whereas according to Harun-Ur-Rashid et al. (2018), Fabaceae is the largest family with 75 species, followed by Rubiaceae with 47 species in Baraiyadhala National Park. The number of cultivated species is 45 (Jalal et al. 2020).

2.1.2 Fauna

Baraiyadhala National Park is also blessed with faunal species equating to 102, mammals 27, reptiles 20, and amphibians 12 (Jalal et al. 2020). Karim and Ahsan (2016) found 29 mammal species under 26 genera of 17 families, with Rodentia as the biggest family, having 10 species. Though rich in animal diversity, species like Sambar (*Cervus unicolor*), Mainland Serow (*Capricornis sumatraensis*), Asiatic Black Bear (*Ursus thibetanus*), and Hoolock Gibbon (*Hylobates hoolock*) are threatened. The park has seen the extermination of some megafauna like tigers, leopards, elephants, and wild dogs because of a combination of anthropogenic factors (Hossain 2015). Some of the carnivorous mammals found in this area are *Prionailurus viverrinus*, *Aonyx cinereus*, and *Arctonyx collaris*, while *Manis pentadactyla*, *Capricornis rubidus*, and *Macaca nemestrina* are some of those who represent non-carnivorous mammals (Hasan et al. 2024).

2.2 Forest Types

The following 5 categories of forests are found in Baraiyadhala National Park (Jalal et al. 2020, Karim et al. 2023, Karim and Ahsan 2016):

1. Tropical Mixed Evergreen/ Semi-evergreen,
2. Tropical Wet Evergreen,
3. Tropical Moist Deciduous,
4. Bamboo Groves, and
5. Afforestation and/or Reforestation sites

2.3 Cycas pectinata Buch. - Ham.

Being the sole natural abode of *Cycas pectinata* in Bangladesh (Harun-Ur-Rashid et al. 2018), Baraiyadhala National Park is unique among the 53 Protected Areas of Bangladesh (Hasan et al. 2024). *Cycas pectinata*, frequently referred to as a living fossil, was first encountered in Baraiyadhala by British botanist William Griffith in 1838 (Jalal et al. 2020), and now the species is critically endangered in this area (Hossain 2015). A study by Hossain et al. (2021) reported 5 Cycas-dense hotspots in the park, viz, Dottorichora, Jambagan, Amtola, Fhulgazi, and Taraghona Hills. Based on the health of *Cycas* plants, the Jambagan area was found to be better than the other hotspots with the tallest stem height of 1.42 m, the broadest average base diameter of 13.58 cm, the widest average top diameter of 6.78 cm, and the highest average number (13) of leaves in Jambagan. On average, 5 seedlings of *Cycas pectinata* per hectare were found in Baraiyadhala National Park (Hossain et al. 2021) with the highest average of 14 in the Taraghona Hill hotspot. The population of *Cycas pectinata* in this National Park is shockingly decreasing (Jalal et al. 2020) because of forest fires, alterations in land use, illicit exploitation mainly for its leaves and megasporophylls, and habitat degradation (Hossain et al. 2021).

A total of 10 significant threats to the Cycas population in Baraiyadhala National Park have been enumerated by Hossain et al. (2021), e.g. i) human-induced habitat destruction, ii) harvesting of forest produces, iii) excess cycas harvesting, iv) fire outbreak, v) grazing, vi) hunting, vii) inefficient management, viii) inadequacy of mass awareness, ix) scarcity of political commitment, and x) landslides. Among these, fire is the most prominent, with around 5.9% of the overall Cycas population affected and an average of 0.81 (±0.61) number of Cycas plants damaged per hectare due to fire (Hossain et al. 2021).

2.4 Tourism

Though tourists' advents were few in the past (Hossain 2015), Baraiyadhala National Park is now a popular tourist destination, especially in the monsoon (Hasan et al. 2024), with a total of 62,553 visitors visiting the park (Jalal et al. 2020) from July 2018 to June 2019. Previously, there were no entry fees from the visitors (Hossain 2015), but now fee collection booths were found to be operating in some places. Similarly, Jalal et al. (2020) did not find any foreign tourists, whereas recently, data collectors have found some Chinese tourists visiting the site.

Harun-Ur-Rashid et al. (2018) emphasized the necessity for a Sustainable Management Plan with adequate and active participation of the stakeholders, as mass tourism is likely to endanger the area and its biodiversity. In Bangladesh, tourism, in general, is accompanied by picnic activities with high-decibel music and the dumping of plastic and other wastes, which necessitates the consideration of the ecosystem and its carrying capacity (Hossain 2015).

According to Jalal et al. (2020), the majority of the tourists (93%) have an educational qualification from secondary to a higher level, and most of the visitors are young (53% of tourists aged between 21 and 30 years and 40% under 20 years of age). Around three-fifths of the tourists (58%) were students, one-fifth (19%) were engaged in service provision, and nearly 10% were businessmen. Jalal et al. (2020) enlisted the following need to improve, i.e. networking of routes, security enhancement, first aid services, food stalls, hygiene, afforestation, trained travel guide, sanitation, safe hiking path, tenting facilities, facilities of consumable water, lodges, parking facilities and washing and bathing facilities.

2.5 Waterbodies

Throughout the monsoon period (May to October), Baraiyadhala National Park receives an average total precipitation of 1891 mm (Hasan et al. 2024). The park has various waterbodies (Harun-Ur-Rashid et al. 2018), including streams, gullies, etc. With receding water levels in the streams and other waterbodies, the number of visitors dwindles accordingly (Jalal et al. 2020). Some notable watercourses are Labankha Chora, Juiggya-Bil Chora, Sonai Chora I, Sonai Chora II, Napittya Chora, Bawa Chora, Doptori (Baraiyadhala) Chora, Bayezid Chora, Murali Chora, Boro Komoldoho Chora, Kanir Chora, and Hatir Dhala Chora (Hossain 2015). Depending on seasonal water levels, tourists generally get attracted to seven streams in Baraiyadhala National Park (Jalal et al. 2020), namely Khoiyya Chora, Napittya Chora, Ruposhi Jhorna, Sohosro Dhara, Bawa Chora, Sonai Chora, and Baraiyadhala Boro Chora. The following table (**Table 1**) depicts the water availability (number of months in a year) of some of the prominent streams of this National Park.

Table 1: Water availability in different waterbodies of Baraiyadhala National Park (Jalal et al. 2020)

Water availability (months in a year)	Waterbody
4-5 months	Bawa Chora, Sonaichori Jhorna
8-9 months	Napittya Chora, Ruposhi Jhorna
10-12 months	Khoiyya Chora, Sohosro Dhara

CHAPTER THREE

METHODS AND MATERIAL

3.1 Study Area

3.1.1 Location

Baraiyadhala National Park is located in Sitakunda-Mirsharai Upazilla of Chattogram district. The National Park is located approximately 207 km East-Southeast of Dhaka and 40 km North of Chattogram in both Mirsharai and Sitakunda upazila under the Chattogram district. Geographically, the area lies between 22°39' - 22°47' N latitude and 91°35' - 91°41' E longitude. It is under the jurisdiction of the Baraiyadhala range of Chittagong North Forest Division. The park is surrounded by Gobania block of Gobania beat, Mirsharai Range on North; Jungle Sitakunda mouza of Sitakunda block and beat on South; Ramgarh-Sitakunda reserve forests, Balukhali beat, Fatikchari beat, Hazarikhil beat, and Baromasia beat on East, and Gobania mouza, East Mogadia, East Khoiyachara, Wahedpur, Baro Kamaldah on West. There are signboards and indications about the location of Baraiyadhala National Park on the Dhaka-Chittagong Highways so that tourists can find their destination easily.

Figure 1: Location map of Baraiyadhala National Park

According to the Bangladesh Forest Department, Baraiyadhala National Park is composed of the Baraiyadhala and Wahedpur blocks of Baraiyadhala Sadar beat and the Kunderhat block of Bartakia forest beat under the Baraiyadhala range. The national park covers an area of 2,933,61 hectares (**Table 2**) and consists of the forests from Sadar beat and Bartakia beat.

Table 2: Distribution of land area of Baraiyadhala National Park under different forest beats

Range	Beat	Block	Area (hectares)
Baraiyadhala	Sadar	Baraiyadhala	664.78
		Wahedpur	1110.93
	Bartakia	Kunderhat	1157.90
Total			2933.61

3.1.2 Climate

BdNP has a tropical monsoon climate, characterized by basically four seasons, e.g., winter (December-February), summer (March-May), monsoon (June-September), and autumn (October-November). The southwest monsoon provides most of the annual rainfall. The average annual rainfall of the area is 3,000 mm with a range of 1,611-3,878 mm. On average, the highest rainfall occurs in July (727 mm) and the lowest rainfall in January, was 5 - 6 mm. The monthly average minimum and maximum temperature of the area ranges from 14.5°C to 32.4°C (Khatun et al. 2016), whereas the yearly minimum and maximum humidity ranges from 73 - 80% (mean 78.04%).

BdNP is frequently affected by monsoonal heavy rainfall and cyclones during May and October. Pre-monsoon north-westernly and cyclonic storms are accompanied by high-speed winds and rains, significantly damaging property and biotic life. Floods and cyclones have both direct and indirect repercussions for the forests and forest resources. This forest faced extensive damage that occurred in the cyclones of 1991, 1994, and 1997.

3.1.3 Geography

The topography of BdNP is very undulating, consisting of a linear hill range stretching North to South, reaching an altitude of up to 350 m. The soils in this area are clay to clayey loam in the valleys and sandy loam to coarse sand in hilly areas. The clayey and sandy loams are fertile, and the sandy soil is often impregnated with iron, resulting in a red or yellowish tinge. Hilly soils contain unconsolidated rocks, sandstones, shales, and siltstones. Moderately well to excessively well drainage capacity and high depth of the soil made it highly suitable for plant growth. The soil of high hills is sometimes yellowish-brown or strong brown.

The forest valleys of BdNP, comprising sandy bedded streams (*chara*), canals, and lakes, contain and carry the water to the Bay of Bengal. The national park is crisscrossed by more than 10 streams, most of which developed from the hills located in the middle of the BdNP. The small streams enable drainage water stagnation in the depressions and valleys in the hilly landscape, which serve as important habitats for flora and fauna, as well as providing drinking water for both human and animal populations. These streams are associated with a beautiful landscape and charming natural waterfalls. Water flows through some of the streams around the year, keeping the waterfalls active and attractive to people, while the remaining streams flow sufficiently only in the monsoon season.

3.2 Methodology

3.2.1 Floral Data Collection, Plant Identification, and Biodiversity Assessment

Considering the heterogeneity of the study area, the study is conducted through robust fieldwork followed by two pre-designed survey methods consisting of a transect survey and a quadrat survey. A transect survey is conducted to record the plants of all habit forms occurring throughout all sorts of habitats. The quadrat survey was designed to assess the quantitative structure of the tree species.

a. Transect Survey

Several walking trails have been followed to record the flora occurring in different habitats. The common habitats covered are hilltops, hill slopes, valleys, hill bottoms, shady places, stream banks, roadsides, marshy areas, degraded sites, landslide-prone areas, etc. All the plants that occurred within the transects were recorded by their local and scientific names in the field notebook. In cases where they are unknown, fertile parts of a plant (if available with flower, fruit, seed, etc.) were collected. If fertile portions (i.e., flower, fruit, seed, etc.) were not available, only fresh twigs were collected as a sample for the preparation of a herbarium specimen.

b. Quadrat Survey

Circular sample plots were used in the quadrat survey. All the tree individuals having ≥25 cm DBH were measured in a 19 m radius circular plot whereas the individuals having ≥10 cm DBH were measured from a nested 8 m radius circular plot. Another nested circular plot of 2.5 m radius was located at 90° bearing and 5 m distance from the centre of the 19 m radius plot. All the regenerations were recorded from the 2.5 m radius plot. In the sample plots, the species name, total height, and DBH were recorded. Besides, information on the land slope, disturbances, and canopy coverage was collected for each sample plot. In the regeneration plot, the seedlings of tree species, climbers, clumps of bamboo, and canes were identified and counted by species. In cases, the sample plots could not be reached due to inaccessibility, water body, or any other reasons, it was shifted to another location as close as possible. A total of 45 sample plots were taken

Density, $D = \frac{a}{b}$

Relative density, $RD = \frac{n}{N} \times 100$

Frequency, $F = \frac{c}{b}$

Relative frequency, $RF = \frac{F_i}{\sum_{i=1}^{S} (F_i)}$

Relative abundance, $RA = \frac{A_i}{\sum_{i=1}^{S} (A_i)}$

Importance Value Index, $IVI = Relative\ density + Relative\ frequency + Relative\ dominance$

Shannon-Wiener Diversity Index, $H = -\sum_{i=1}^{S} P_i(ln\ ln\ P_i)$

Margalef's Richness Index, $R = \frac{(S-1)}{lnln\ (N)}$

Simpson's Dominance Index, $S_D = (1 - \frac{\sum_{i=1}^{S} n_i(n_i-1)}{N(N-1)})$

$$Simpson's\ diversity\ index = \sum_{i=1}^{n} P_i^2$$

Pilou's Evenness Index, $E = \frac{H}{lnln\ (S)}$

$$Relative\ dominance = \frac{Basal\ area\ of\ one\ species}{Total\ basal\ area} \times 100$$

Here,

a = total number of individuals of a species that occurred in all the quadrats

b = total number of quadrats studied

c = total number of quadrats in which the species occurred

N = total number of individuals of all the species

n = number of individuals of i^{th} species

P_i = proportional occurrence of i^{th} species (n_i/N)

S = total number of species

3.2.2 Field Visit and Perception of Forest Officials and Locals on Cycas Management

A transect survey has been conducted, and a total of 26 points where more than two Cycas plants were found have been surveyed. The management aspect of Cycas was studied through secondary data collection, field visits, primary data collection, and interviews with forest officials and local people of different professions. Cycas-related office records of Chattogram North Forest Division and the Baraiadhala range office were collected and verified. Forest officials of different capacities, from Forester to Chief Conservator of Forests (Rtd.), were interviewed for this purpose. Semi-structured questionnaires were used for interviewing. In addition, other staff of the beats also discussed the status of Cycas in the study area. Data analysis has been accomplished by applying SPSS v25 and GraphPad Prism v8, as used in the perception survey in this study.

A total of 40 perception surveys have been conducted with local inhabitants, 25 from the vicinity of Boro Darogarhat Forest Beat Office Road and 15 from Napittachora Road. Semi-structured questionnaires were used to accumulate the perceptions of 40 respondents randomly selected from the 2 areas. Microsoft Excel and GraphPad Prism (version 8.0) have been applied for statistical data analysis.

3.2.3 Surveying Local Communities about dependency on forest resources

Generally, the most dependent people on the forest are the adjacent locals. Hence, a survey was conducted to understand the perception and to identify the dependency of the locals on the forest. A total of 100 surveys were conducted, followed by a semi-structured questionnaire. We conducted random samples for the survey. For surveying, we prefer the locals around the Jharna (waterfalls) as people are highly dependent on the water resources of the Jharna. Afterward, we compile the data by using Microsoft Excel and analyze the data using GraphPad Prism v8 software.

3.2.4 Tourist Survey

Barayardhala National Park is famous for different jharna e.g., Khoyachora, Napittachora, Shonaichori, etc. Therefore, a lot of tourists go there to find quality time with nature. So, knowing about the perception of the tourists and the facilities given or to be given to tourists is a must-know fact to facilitate ecotourism. Hence, we surveyed 100 tourists from different jharna of BDNP randomly with a semi-structured questionnaire. The data collected were subjected to different statistical analyses using Microsoft Excel.

3.2.5 GIS Data Analysis

The Curve Number (CN) method is widely used for estimating direct runoff from rainfall events. It's handy in hydrological modeling for its simplicity and effectiveness, especially when detailed data is limited. Here's an overview of how the CN method incorporates factors such as Basins, Hydrological Soil Group (HSG), and Land Use/Land Cover (LULC) to calculate water runoff:

The first step in applying the CN method is identifying the drainage basins or catchment areas within the study area. These basins are delineated based on natural topographic features like ridgelines, and they represent areas where rainfall collects and eventually flows out through a common outlet.

Soil is crucial in determining how rainfall is absorbed and subsequently contributes to runoff. The Natural Resources Conservation Service (NRCS) categorizes soils into four hydrological soil groups (A, B, C, and D) based on their infiltration characteristics. Group A soils have high infiltration rates, while Group D soils have low infiltration rates. This classification helps in understanding how quickly water will move through the soil and into the stream network.

The type of land cover influences how much rainfall infiltrates into the soil and how much becomes surface runoff. Different land uses and covers have varied degrees of permeability and a rough surface. For instance, urban areas with impervious surfaces like concrete and asphalt generate more runoff than forests or grasslands. Detailed land cover data is essential for accurately estimating runoff using the CN method. The CN is a parameter that represents the combined effects of soil, land cover, and land use on runoff generation. It typically ranges from 30 to 100, with lower values indicating higher infiltration and less runoff potential. The CN value is determined based on the soil group, land use, and antecedent soil moisture conditions.

Once the CN values are assigned to different land cover and soil types within the basin and considering the prevailing antecedent soil moisture conditions.

CN is the most influential factor within this method to determine excessive runoff. CN is also crucial for the synthesis of composed hydrograms. In general terms, this method estimates runoff based on the application of the following equation (Calvo et al., 2005; Ling et al., 2020):

Where Q is the effective precipitation,

P is the precipitation, and

S is a storage index for watershed.

It is important to note that the term 0.2 S represents the initial infiltration loss. This value was challenged by Hawkins and Hibbert (2000), who found values lower than 0.2 for agricultural sites in the United States. CN as a function of S is given by the following equation. In this study, the 2nd equation has been used because the rainfall was in millimeters. If the rainfall amount unit in inch, then it should be used the 1st equation. The CN (a dimensionless number ranging from 0 to 100) is determined from a table based on land-use /land cover (LULC), hydrological soil group (HSG), and Antecedent moisture conditions (AMC). Classification of Antecedent Moisture Conditions (AMC) categorizes soil moisture levels based on antecedent weather conditions preceding a rainfall event. The AMC classification system typically consists of several discrete classes, each representing different degrees of soil moisture. These classes are often designated numerically or descriptively, ranging from dry to wet conditions. The classification scheme aids in determining the runoff potential of a watershed or catchment area by accounting for the moisture content of the soil before rainfall occurs. This information is crucial for hydrological modeling and runoff prediction, as soil moisture significantly influences infiltration rates and surface runoff generation. According to precipitation limits for dormant and growing seasons, antecedent Moisture Condition (AMC) is expressed in three levels (AMC I, AMC II, and AMC III).

3.2.6 Vegetation Change during 2000-2024

The Normalized Difference Vegetation Index (NDVI) is the most widely used; it was proposed by (Rouse Jr. et al. 1973), which can be expressed as

$$NDVI = \frac{NIR - R}{NIR + R}$$

NDVI is derived through a normalization method, resulting in values ranging from 0 to 1. It exhibits a heightened responsiveness to green vegetation, even in areas with sparse vegetation cover. However, its sensitivity to factors like soil brightness, soil color, atmospheric conditions, cloud cover, shadows, and leaf canopy shadow necessitates remote sensing calibration for accurate interpretation. The NDVI map is a tool used to assess and quantify the density and health of vegetation in an area based on satellite imagery or remote sensing data. The higher value of NDVI indicates healthier and denser vegetation cover, while lower values represent sparse or stressed vegetation, and values around zero might indicate barren areas or water bodies. In this context, the maximum value of 1.0 suggests areas with the highest possible vegetation density and health. These regions likely have lush, dense vegetation cover, such as forests, healthy crops, or thriving plant growth.

Sentinel Hub EO browser has been used to compare/calculate the year-wise (2000-2024) NDVI. The data of NDVI has been exported in csv format from the Sentinel Hub online platform (Table-9). A total of 4628 samples have been calculated automatically by Sentinel Hub online platform for each of the date-wise NDVI raster files. The data of average NDVI min, average NDVI max, and average NDVI mean have been summarized by using pvot table in MS Excel (Table-10).

CHAPTER FOUR

RESULTS

4.1 Floral Composition of the BdNP area

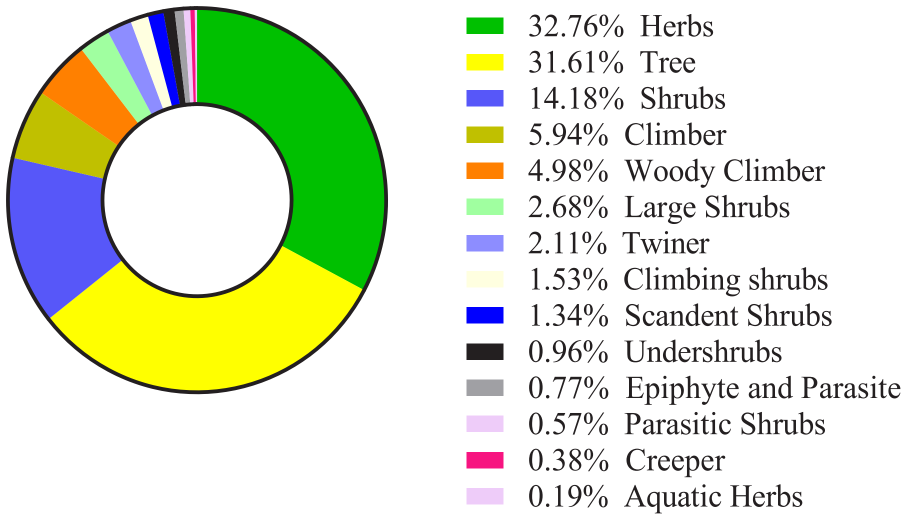

Figure 2: Floral composition of BdNP

A total of 522 plant species were recorded from Baraiyadhala National Park and categorized into 15 types. Herbs (32.76%) were dominant, followed by Trees (31.61%), shrubs (14.18%), climbers (5.94%), and woody climbers (4.98%).

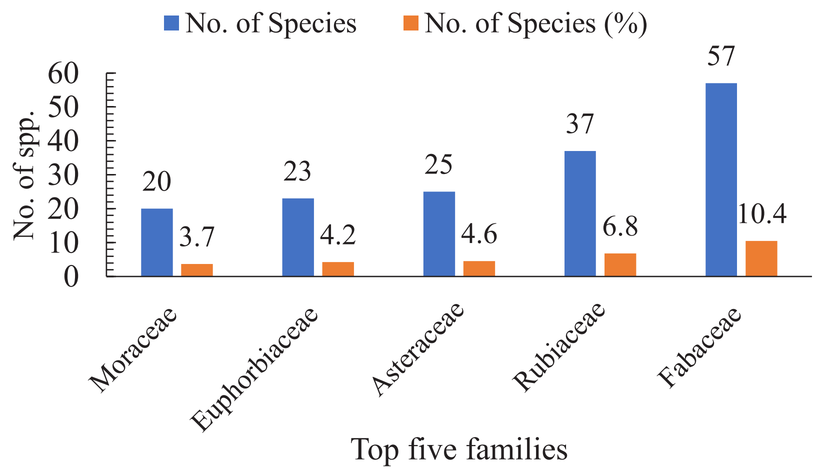

Figure 4: Top five families of the BdNP forest with species (No. & percentage)

The highest number of species was possessed by Fabaceae (57 species) which was 10.4% of the total species of the National Park, followed by Rubicaceae (37 species, 6.8%), Asteraceae 25 species, 4.6%), Euphorbiaceae (23 species, 4.2%) and Moraceae (20 species, 3.7%)

4.1.1 Tree species of BdNP

4.1.1.1 IUCN red list category of tree species recorded from BdNP

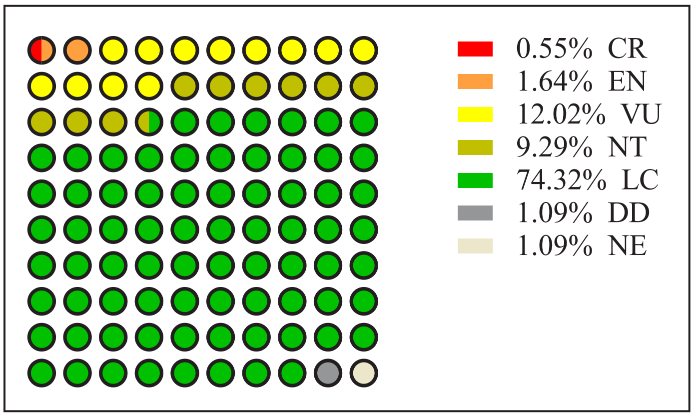

Figure 3: IUCN category of red list in Barayordhala National Park

Most of the species recorded from BdNP (74.32%) were Least Concern. 12.02% of total species were Vulnerable, 1.64% Endangered, and 0.55% were Critically Endangered. So, species that belong to VU, EN, and CR require special care for conservation **(Figure 5).**

4.1.1.2 Use of trees of Barayardhala National Park

The highest number of trees were medicinal use (29.81%) along with 20.19% timber species and 20.19% fodder species. 18.01% of trees had non-timber value (Figure 4).

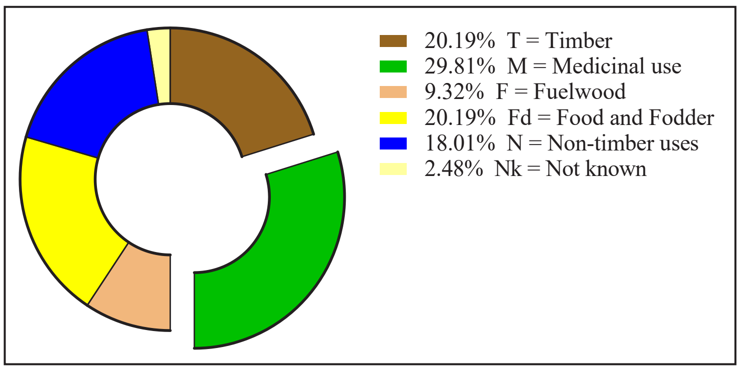

Figure 4: Use category of the tree species

4.1.1.3 Distribution of tree individuals according to height class

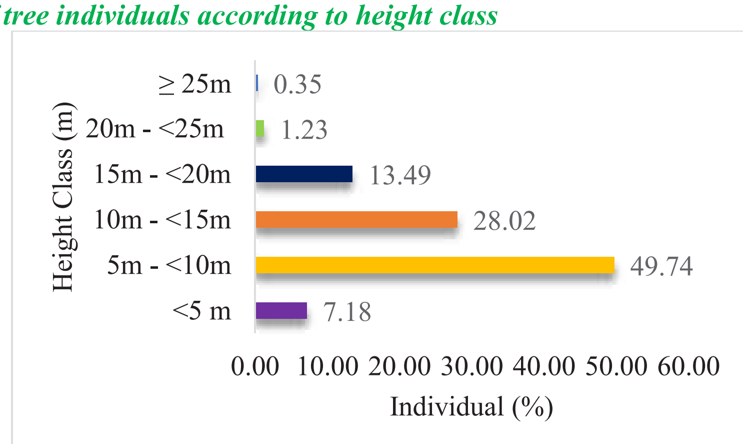

Figure 5: Distribution of tree stems according to height class

All the measured trees are further classified according to six height classes. The highest amount (49.74%) of individuals have been found under the 5m - <10m height class followed by 10 m - <15m (28.02%), whereas the lowest number of trees (0.35%) have a height ≥ 25m followed by 20m - < 25m (1.23%).

4.1.1.4 Distribution of tree individuals according to DBH class

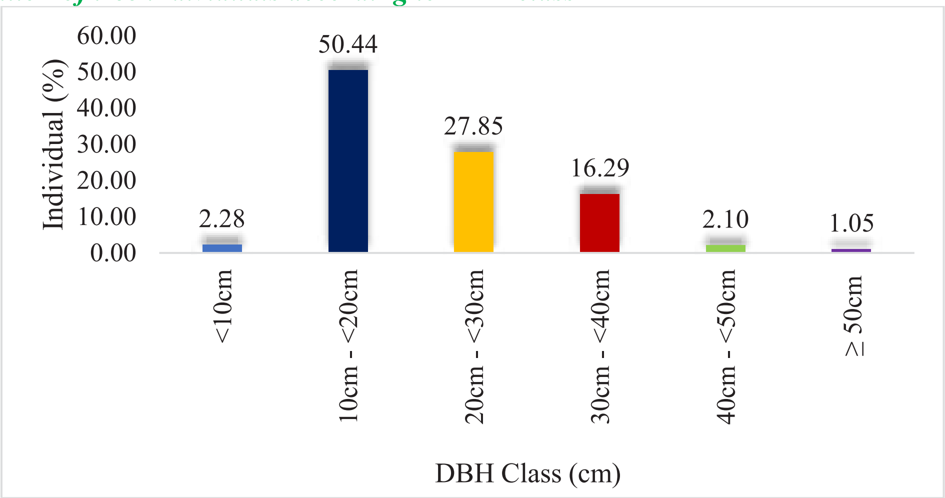

Figure 6: Distribution of tree stems according to DBH class

DBH class is another important parameter to describe the distributional structure of a forest. In Baraiyadhla National Park, almost half (50.44) of the total tree individual's DBH ranged from 10 cm - < 20cm. This is the highest number of individuals accumulated in a particular range. Only 2.1% and 1.05% of total individuals are old trees that ranged a DBH class from 40 cm to <50 cm and ≥ 50 cm respectively.

4.1.1.5 Basal Area (m^2/ha) and Volume (m^3/ha) of top five tree species

In case of the Basal area (m^2/ha) and volume/ha top five species were *A. procera, G. arbora, F. hispida, A. chama,* and *A. auriculiformis*. The highest basal area (m^2/ha) was observed in *A. procera* (0.49) with a volume of 7.69 m^3/ha. Food species for an animal like *F. hispida* and *A. chama* were also on the list with a basal area (m^2/ha) of 0.31 and 0.19 with a volume of 3.42 and 2.94 m^3/ha.

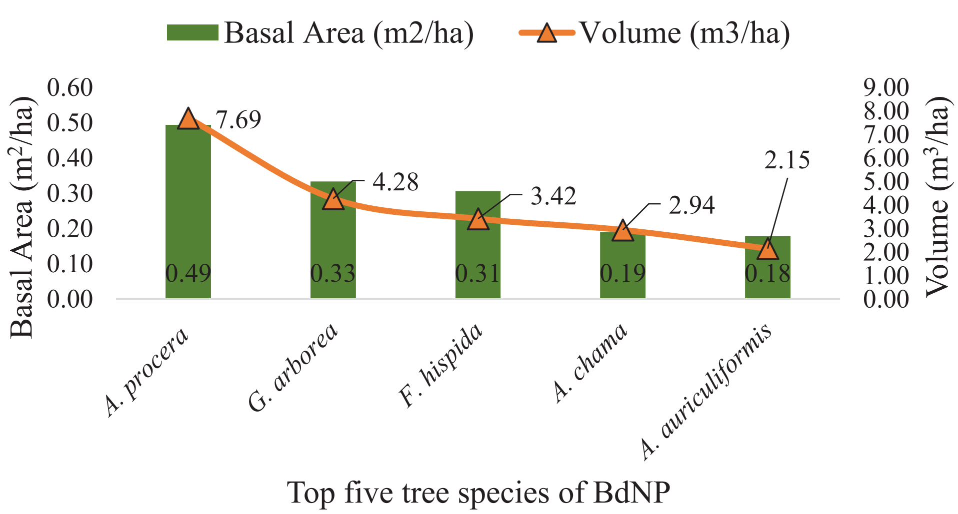

Figure 7: Basal area (m^2/ha) and volume (m^3/ha) of dominant five dominant tree species

4.1.1.6 Density (stem/ha) of top five species

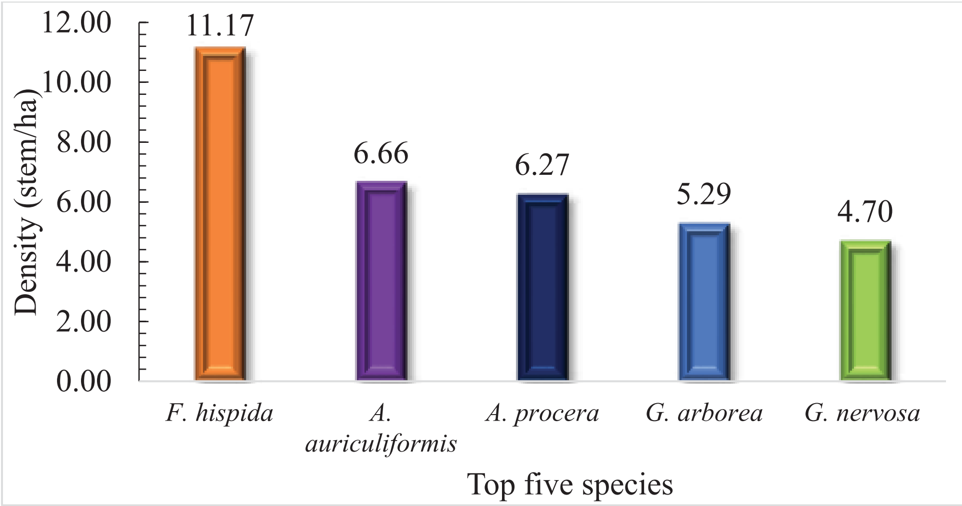

Figure 8: Density (stem/ha) of the top five tree species

The species with the highest density was *F. hispida* (11.17/ha) followed by *A. auriculiformis* (6.66/ha) and *A. procera* (6.27/ha).

4.1.1.7 Correlation Matrix among height, dbh, basal area, volume, and (stem/ha)

Most of the parameters were positively correlated with each other. Volume (m^3/ha) is strongly positively correlated with Basal area (m^2/ha), Average height (m) of species, and Average DBH (m) of species (**Table 3**).

Table 3: Correlation Matrix of the parameters

Parameters	Average Height (m)	Average DBH (m)	Basal Area (m^2/ha)	Volume (m^3/ha)	Density (stem/ha)
Average Height (m)	1	.532**	.509**	.763**	0.132
Average DBH (m)	.532**	1	.987**	.897**	0.065
Basal Area (m^2/ha)	.509**	.987**	1	.915**	0.053
Volume (m^3/ha)	.763**	.897**	.915**	1	0.110
Density (stem/ha)	0.132	0.065	0.053	0.110	1

4.1.1.8 Relation of volume/ha and Basal Area/ha

Volume/ha is strongly related to basal area/ha. A regression equation is developed from field data, where $R^2 = 0.905$. The derived equation is y = 10.19 + 14.38* x. Here, y = Volume/ha in m^3 and x = basal area/ha in m^2 (Figure 9).

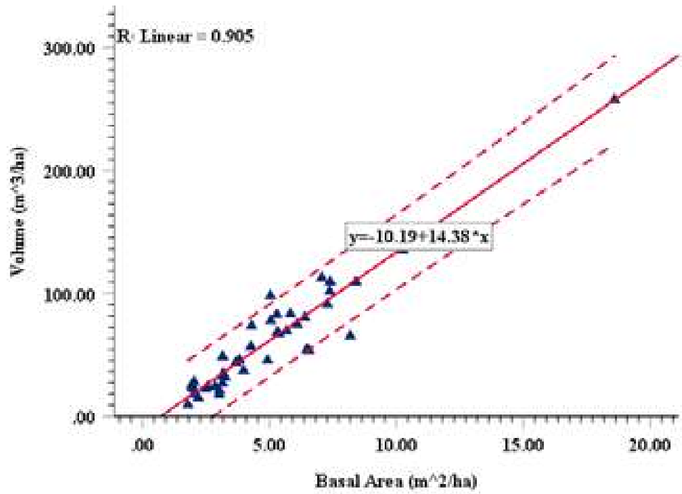

Figure 9: Relation between volume/ha and basal area/ha

4.1.1.9 Diversity Index Assessment

A total number of 572 tree individuals were measured. While assessing the diversity indexes, we find that the value of Margalef's index is 19.22, which indicates that the plant diversity of Barayiadhala National Park is rich. Simpson Index ranged from 0 – 1. Here, 0 means infinite diversity and 1 means no diversity. Our Simpson index value is 0.03, which denotes that the diversity here is quite rich. After that, we assessed the Shannon-Wiener index. The principal objective of this diversity index is to obtain a quantitative estimation of biological variety that can be used to compare biological entities at a particular time. Our value of the Shannon-Wieners index is 4.17 (**Table 4**). It denotes the high amount of diversity accumulated in that forest. Finally, we assess the species evenness index. The species evenness index indicates how even our diversity is. If the value of it is close to 1 the forest is more even. Here its value is 0.66 which means a moderate evenness exists in this forest.

Table 4: Plant diversity indexes of Barayiodhla National Park and the National values (GoB 2020)

Different Diversity indexes	Value (this study)	GoB (2020)					
		Coastal	Hill	Sal	Sundar ban	Village	National
Margalef's Richness index	19.22	9.439	24.316	11.485	2.187	20.286	29.372
Simpson's Dominance Index	0.03	0.318	0.054	0.151	0.296	0.077	0.116
Shannon-Wiener Diversity index	4.17	1.99	3.984	2.737	1.403	3.40	3.162
Pielou's Evenness Index	0.66	0.428	0.705	0.578	0.417	0.624	0.529

The relative density, relative frequency, relative dominance, and Importance Value Index (IVI) are shown in **Table 5.**

Table 5. Relative Density, Relative Dominance, Relative Frequency, and IVI of Tree species of BdNP

Local Name	Scientific Name	Relative Density	Relative Dominance	Relative Frequency	IVI
Akashmoni	*Acacia auriculiformis* A. Cunn. ex Benth. & Hook.	2.1	1.18	3.06	6.35
Mangium	*Acacia mangium* Willd.	0.18	0.51	0.28	0.97
Bon Jamir	*Acronychia pedunculata* (L) Miq.	0.18	1.49	0.28	1.94

Local Name	Scientific Name	Relative Density	Relative Dominance	Relative Frequency	IVI
Chakua koroi	*Albizia chinensis* (Osbeck) Merr.	2.1	1.48	1.95	5.53
Kalo koroi	*Albizia lebbeck* (L.) Benth.	0.18	0.85	0.28	1.31
Tetua koroi	*Albizia odoratissima* (L.f.) Benth.	2.63	0.68	2.79	6.09
Sada koroi	*Albizia procera* (L.) Benth.	5.78	1.9	2.79	10.46
Chaitan/Chatiyan	*Alstonia scholaris* (L.) R.Br.	0.53	1.22	0.84	2.58
Ata	*Annona reticulata* L.	0.18	2.34	0.28	2.8
Khudi Jam	*Antidesma ghaesembilla* Gaertn.	0.18	0.58	0.28	1.03
Shiyal Buka	*Antidesma montanum* var. *montanum* P. Hoffm.	0.35	0.52	0.56	1.43
Pat Khorulla	*Aporosa octandra (Buch.-Ham. ex D. Don) A.R. Vickery*	0.18	0.34	0.28	0.79
Khorulla	*Aporosa wallichii* Hook. F.	0.7	0.86	0.56	2.12
Chapalish	*Artocarpus chama* Buch.-Ham. *ex* Wall.	2.1	0.91	2.23	5.24
Kanthal	*Artocarpus heterophyllus* Lamk.	0.88	1.23	0.56	2.66
Dewa/Borta	*Artocarpus lacucha* Buch.-Ham.	1.93	1.08	1.39	4.4
Neem	*Azadirachta indica* A.Juss.	0.36	0.6	0.56	1.51
Deb Kanchan	*Bauhinia purpurea* L.	2.81	0.63	1.68	5.1
Rakta kanchan	*Bauhinia variegata* L.	1.05	0.89	1.11	3.05
Kanjal Bhadi	*Bischofia javanica* Blume.	1.4	0.33	1.11	2.84
Shimul Tula	*Bombax ceiba* L.	0.88	0.62	0.84	2.34
Bon shimul	*Bombax insigne* Wall.	0.18	1.47	0.28	1.92
Muss	*Brownlowia elata* Roxb.	0.18	0.39	0.28	0.84
Bormala	*Callicarpa arborea* Roxb.	2.63	0.87	2.51	6
Sonalu	*Cassia fistula* L.	1.41	1.56	1.12	4.08
Bon Sonalu	*Cassia nodosa* Buch.-Ham. *ex* Roxb.	0.35	2.71	0.56	3.61
Chikrussi	*Chukrassia tabularis* A. Juss.	2.1	0.66	2.23	4.99
Baruna	*Crateva religiosa* G. Forst.	0.18	1.64	0.28	2.1
Bhuiya	*Cryptocarya amygdalina* Nees	0.53	2	0.84	3.36
Cycus	*Cycas pectinata* Buch. -Ham.	0.53	0.94	0.84	2.3
Jhummuijja koroi	*Derris robusta* (Roxb. *ex* DC.) Benth.	0.53	0.76	0.84	2.12
Hargoza	*Dillenia pentagyna* Roxb.	0.35	0.69	0.56	1.6
Deshi Gab	*Diospyros malabarica* (Desr.) Kostel.	0.18	1.13	0.28	1.59
Bandorhola	*Duabanga grandiflora* (Roxb. *ex* DC.) Walp.	0.18	2.01	0.28	2.47
Eucalyptus	*Eucalyptus camaldulensis* Dehnh.	2.11	0.99	2.51	5.61
Boropata	*Fernandoa adenophylla* (Wall. *ex* G. Don.) van Steenis	0.18	1.2	0.28	1.65
Lal Dumur	*Ficus auriculata* Lour.	0.7	0.75	1.11	2.56
Kak dumur	*Ficus hispida* L.f.	8.41	0.92	8.08	17.4
Joggo dumur	*Ficus racemosa* L.	0.18	0.94	0.28	1.39
Chokorgula	*Ficus semicordata* Buch.-Ham. *ex* Smith	0.53	1.42	0.56	2.5
Bhadi	*Garuga pinnata* Roxb.	0.53	1.89	0.84	3.25
Kechuwa	*Glochidion multiloculare* (Rottler *ex* Willd.) Voigt.	0.18	0.67	0.28	1.13
Gamar	*Gmelina arborea* Roxb.	5.95	0.9	4.74	11.59
Assargula	*Grewia nervosa* (Lour.) Panigr.	1.4	0.43	1.39	3.23
Kala Kuruch	*Holarrhena antidysentrica* (L.) Wall. *ex* G. Don	0.88	3.06	1.11	5.05

Local Name	Scientific Name	Relative Density	Relative Dominance	Relative Frequency	IVI
Aam Berella	*Holigarna caustica* (Dennst.) Oken	0.18	1.8	0.28	2.25
Telsur	*Hopea odorata* Roxb.	1.23	1.44	1.4	4.06
Jarul	*Lagerstroemia speciosa* (L.) Pres	1.58	3.12	2.23	6.91
Jiol Bhadi/Sil Bhadi	*Lannea coromandelica* (Houtt.) Merr.	3.15	0.84	0.84	4.83
Achila	*Leea indica* (Burm.f.) Merr.	1.4	0.44	1.67	3.51
Horina gula	*Lepisanthes rubiginosa* (Roxb.) Leenhouts	0.53	1.77	0.84	3.13
Guduri gach	*Lepisanthes senegalensis* (Roxb.) Leenhouts	0.35	0.72	0.28	1.35
Lichu	*Litchi chinensis* (Gaertn.) Sonn	0.35	0.5	0.28	1.13
Kali Batna	*Lithocarpus elegans* (Blume) Hatus. ex Soepadmo	0.35	0.6	0.56	1.51
Karjuki Menda	*Litsea glutinosa* (Lour.) Robinson	0.71	0.76	0.84	2.29
Menda	*Litsea monopetala* (Roxb.) Pers.	0.7	0.61	0.56	1.87
Sada Bura	*Macaranga denticulata* (Blume.) Muell.-Arg.	1.4	0.89	2.23	4.52
Lal Bura	*Macaranga indica* Wight	1.83	1.74	1.95	5.61
Sada Moricha	*Maesa indica* (Roxb.) Sweet	0.53	0.38	0.84	1.74
Sinduri	*Mallotus philippensis* (Lamk.) Müell.-Arg.	6.48	1.14	4.18	11.8
Uriaam	*Mangifera sylvatica* Roxb.	0.53	0.48	0.56	1.56
Pesi Kao	*Miliusa longiflora* (Hook. f. & Thom.) Finet & Gagnep.	0.53	0.42	0.56	1.5
Kadam	*Neolamarckia cadamba* (Roxb.) Bosser	0.36	1.41	0.56	2.32
Kom	*Neonauclea sessilifolia* (Roxb.) Merr.	0.18	0.56	0.28	1.01
Kanaidinga/Thona	*Oroxylum indicum* (L.) Kurz.	0.36	0.96	0.56	1.86
Amloki	*Phyllanthus emblica* L.	0.53	2.04	0.56	3.11
Gutgutiya	*Protium serratum* (Wall. *ex* Colebr.) Engl.	1.75	0.87	1.67	4.3
Muchkanda	*Pterospermum acerifolium* (L.) Willd.	0.18	0.41	0.28	0.86
Lanna Assor	*Pterospermum semisagittatum* Buch. -Ham. *ex* Roxb.	0.18	0.55	0.28	1.01
Raintree	*Samanea saman* (Jacq.) Merr.	0.8	1.14	1.11	3.13
Ashok	*Saraca asoca* L.	0.71	4.12	1.12	5.93
Minjiri	*Senna siamea* (Lamk.) Irwin & Barneby	0.18	0.51	0.28	0.96
Bon Amra	*Spondias pinnata* (L.f.) Kurz	0.18	1.53	0.28	1.98
Muli Udal	*Sterculia villosa* Roxb. *ex* Smith	0.32	0.39	0.56	1.3
Dharmara	*Stereospermum colais* (Buch.-Ham. *ex* Dillw.) Mabberley	2.1	0.64	2.23	4.97
Sheora	*Streblus asper* Lour.	1.05	1.41	1.67	4.14
Kalo jam	*Syzygium cumini* (L.) Skeels	0.88	1.41	0.84	3.12
Puti jam	*Syzygium fruticosum* DC.	0.35	0.32	0.28	0.95
Teak	*Tectona grandis* L.f.	2.98	1.2	1.67	5.85
Arjun	*Terminalia arjuna* (Roxb. ex DC.) Wight & Arn.	1.41	3.43	1.95	6.78
Bohera	*Terminalia bellirica* (Gaertn.) Roxb.	2.1	1.94	2.23	6.27
Toon/Suruj	*Toona ciliata* M. Roem.	0.88	0.67	1.11	2.66
Bon pepe	*Trevesia palmata* (Roxb. ex Lindl.) Vis.	0.7	1.64	0.8	3.17
Goda	*Vitex peduncularis* Wall. *ex* Schauer	1.4	0.43	1.67	3.5

Local Name	Scientific Name	Relative Density	Relative Dominance	Relative Frequency	IVI
Dudh Kuruch	*Wrightia arborea* (Dennst.) Mabb.	1.23	2.52	1.67	5.42
Lohakath	*Xylia xylocarpa* (Roxb.) W. Theob.	0.11	0.52	0.24	0.97
Bon boroi	*Ziziphus mauritiana* Lam.	0.15	1.5	0.24	1.95

4.1.1.11 Density of seedlings (stem/ha)

The most highly dense seedling/ha was *F. hispida* (650.73 seedlings/ha) followed by *G. nervosa* (594.14 seedlings/ha), *M. philippenses* (282.93 seedlings/ha), *A. auriculiformis* (212.19 seedlings/ha) and *M. denticulata* (198.05 seedlings/ha).

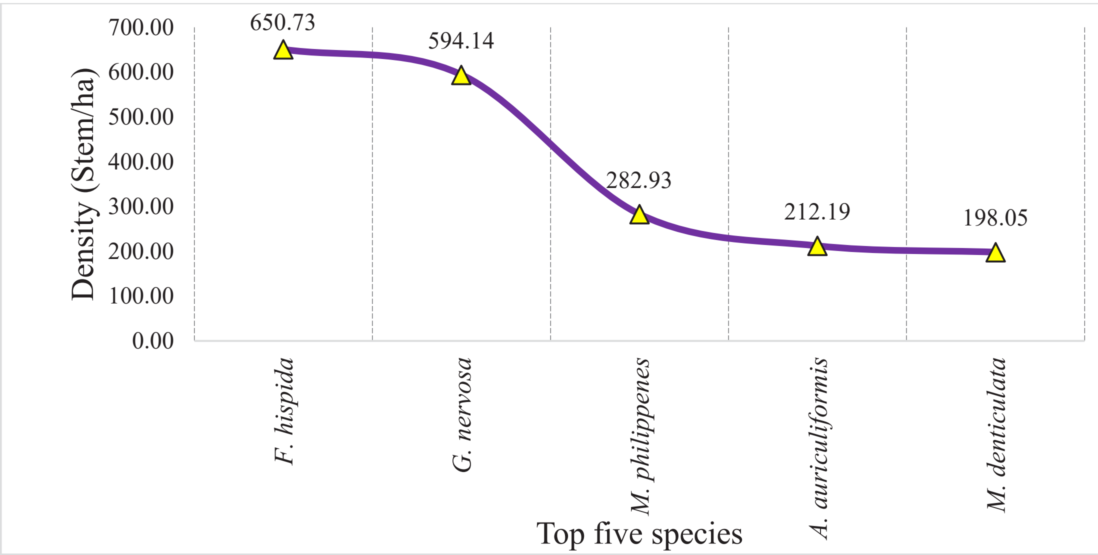

Figure 10: Density (stem/ha) of seedlings regenerated

4.1.2 Large Shrubs

14 species of 9 families were found in this study. Among all the families, the Rubiaceae family had the highest species (5 species) followed by the Fabaceae family. The rest of the families had one species each.

4.1.3 Shrubs

Under 31 families, 74 species of shrubs were found. The largest family of shrubs was Fabaceae (15 species), followed by Rubiaceae (10 species) and Euphorbiaceae (6 species). 12 families had only one species.

4.1.4 Under-shrubs

Under 3 families, 5 species of 5 genera were found in the BdNP. Among five under-shrub species, Fabaceae had 3 species of 3 genera. The rest 2 families had one species each

4.1.5 Scandent shrubs

Scandent shrubs had been found in 6 families BdNP. Under those 6 families, 7 species of 7 genera were found. Family Combretaceae with 2 species possess the highest position. The rest of the families have one species each

4.1.6 Parasitic shrubs

All the parasitic shrubs in BdNP are found under the Loranthaceae family. 3 species of 3 genera are recorded

4.1.7 Climbing shrubs

8 species of climbing shrubs were found in BdNP. The family Mimosaceae have 2 species and rest of the families have one species each 4.1.8 Twiner

Eleven (11) species of twiner have been found under 9 genera and 4 families. The largest family was Convolvulaceae (7 species).

4.1.9 Epiphyte and Parasite

3 species of epiphytes and one species of parasite were found in BdNP. All 3 epiphytes belong to the family Apocynaceae, and one parasite belongs to the Convolvulaceae family. The only parasite found in the forest was *Cuscuta reflexa* Roxb.

4.1.10 Climber

Under 11 families and 22 genera, 32 climber species were found. The highest number of species was accumulated in the family Convolvulaceae (8 species), followed by Vitaceae, Cucurbitaceae, and Fabaceae.

4.1.11 Woody climbers

26 species of woody climbers under 10 families and 22 genera were found in BdNP. The highest number of woody climbers was found in the Annonaceae family, with 6 species, followed by Fabaceae (5 species).

4.1.12 Creepers recorded from BdNP

2 species of creeper under 2 families and 2 genera were recorded. Both Piperaceae and Onagraceae families have one species each.

4.1.13 Herbs

Under 37 families in 122 genera, 171 species of herbs had been found in BdNP. The highest number of species was found in the Asteraceae family (25 species), followed by the Acanthaceae family (16 species) and the Fabaceae (15 species).

4.1.14 Aquatic Herbs

One aquatic plant of *Ipomoea aquatica* Forssk. had been recorded from BdNP, which is under the Convolvulaceae family.

4.1.15 Threats to Conserving Biodiversity

Fire outbreak:

Fire, be it natural or anthropogenic, is one of the major reasons for the destruction and deterioration of forests. In Bangladesh, winter is associated with the least or literally no rainfall. Such dry conditions facilitate the easy outbreak of fire inside the forests.

Reasons for wildfire in Bangladesh: The Following reasons are some of the major ones responsible for forest fires in Bangladesh-

(i) Malicious acts
(ii) Accumulation of excessive dry litter
(iii) High oil concentration within the leaves of some species
(iv) Thunder
(v) Unintentional ignition from cigarettes, etc.
(vi) Extreme heatwaves

Damages associated with forest fire: Forest fires bring about disastrous consequences to both the flora and fauna of a forest land. Some of the major implications of wildfires are-

a) Destruction of habitat
b) Forage shortage
c) Soil deterioration
d) Removal of cover plants
e) Hampering of the food chain and food web
f) Removal of stored carbon within trees and accumulation in the atmosphere
g) Beginning of retrogression, a process inverse to succession

Precautionary measures to stop forest fires and/or minimize the impacts thereof:

1) Regular monitoring and surveillance, especially during the dry season
2) Gradual removal of over-accumulated litter from the forest floor
3) Creation of firebreaks
4) Strict implementation of forest laws
5) Mass-awareness raising campaigns

The following are some of the photographs of the forest fire in the surveyed area taken during the conduct of vegetation surveys. Herbs, shrubs were destroyed on a massive scale, whereas trees were burnt, some partially and others fully.

Figure 11: Forest fire and damage at the Baraiadhala National Park

Illicit harvesting of bamboo and Fuelwood Collection:

Bamboos are called the "Poor man's wood". It is one of the major non-timber forest products. During the surveys, illegal harvesting of bamboo by the local inhabitants was experienced red-handed. These harvested bamboos are sold at the nearby markets. *Bambusa burmanica* (Mitinga Bans) and *Melocanna baccifera* (Paiyya) were the two species of bamboos observed being illegally harvested from the surveyed area. Most of the forest dwellers and people around the forest areas are still dependent on the forests for fuelwood.

Figure 12: Resource extraction from the Baraidhala National Park

Agriculture within the govt. forest lands:

Even though it is prohibited to convert forest lands into other land uses, agricultural practices of various extents are frequently encountered within the forest areas. This phenomenon is now an open secret in the Bangladesh context. Previously, agricultural cultivation was for subsistence, but nowadays, agriculture within the forests is much more business-oriented and has a commercial aspect.

Poaching within forest territories:

A group of four poachers, two Bengalis and two tribals, is reportedly active in the poaching of wild animals. This group is allegedly involved in the sale of animal parts to outsiders. Though their main target area is Hazarikhil Wildlife Sanctuary, the group also hunts, traps wild fauna of the study area. This information was shared by one of the Co- Co-management Committee (CMC) members.

Illegal harvesting of Cycas:

The inflorescence-like organ of Cycas pectinata is sold in the local market under the name of snake hood. Some tribal community members are reportedly involved in this activity. The occurrence of Cycas pectinata is very localized, and hence, special attention is urgently needed.

4.2 *Cycas pectinata* in BdNP

Cycas pectinata represents a significant gymnosperm that is presently restricted to the fragmented ecosystems within the Indian subcontinent, extending into certain regions of Southeast Asia. This species is categorized as a vulnerable taxon within the threatened classifications established by the IUCN. Among the 117 extant species of Cycas, only *Cycas pectinata* is recorded in Bangladesh (**Table 20**). Although *C. pectinata* is extensively recognized in Southeast Asian nations, it has not undergone a comprehensive study within the context of Bangladesh. The widespread occurrence of *Cycas pectinata* was initially documented in the Bengal region by William Griffith in the Baroiyadhala forest of Chattogram in the year 1838. The species is limited to several hills in Baroiyadhala, situated in the Sitakunda and Mirsarai upazila of the Chattogram district. In recognition of its rich biodiversity, both floral and faunal, the Baroiyadhala forests were designated as a National Park in 2010, encompassing an area of 2933.61 hectares.

Table 6. Classification of *Cycas pectinata*

Kingdom		**Phylum**	**Class**	**Order**	**Family**	**Genus**	**Species**
Plantae		Tracheophyta	Cycadopsida	Cycadales	Cycadaceae	*Cycas*	*pectinata*

Cycas pectinata Buch. - Ham. is an evergreen gymnosperm (Hossain et al. 2021) having 1-12 m in height, and 14-20 cm in diameter. The trunk is characterized by an apical crown of pinnately compound foliage, exhibiting a limited presence of spines within the petioles area. Male specimens produce substantial, cylindrical ovoid strobili, which may be yellow or green, and are distinguished by a multitude of microsporophylls adorned with elongated apical spines (Khuraijam and Singh 2015, Lindstrom and Hill 2007). Female plants bear compacts closed cones with numerous broadly subulate pectinate megasporophylls which bear 2-6 ovules. Seeds are ovoid, glabrous, and orange to red-yellow colour in its mature state (Grierson and Long 1983, Lindstrom and Hill 2007, Khuraijam and Singh 2014, 2015). A transact survey has been done and located a total of 26 points where we found more than two Cycas plants. A map is prepared of those 26 locations that are shown.

Figure 13: Cycas

Some *Cycas* population are available beside the trail of different waterfalls or around waterfalls, e.g. *Cycas* on Sohosrodhara Road, Khoyachora Trail, Khoyachora Pathway, Ruposhi Waterfall Trail, etc. The coordinates of Cycas populations are given below.

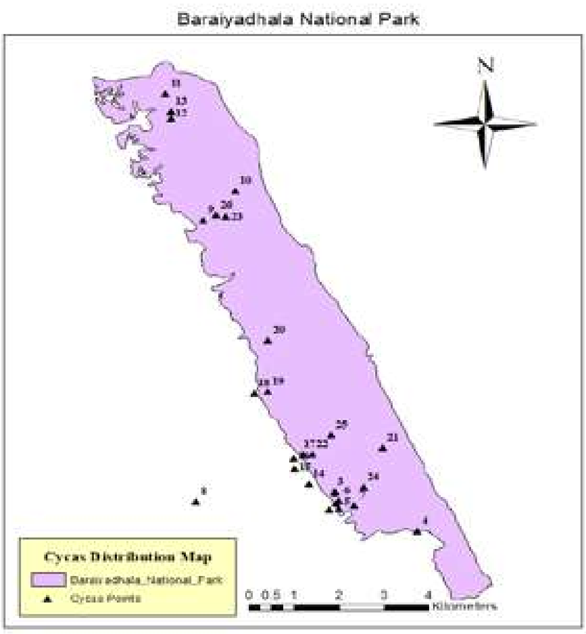

SL No	Location Name
1	Banglaa Tila
2	Hunukhola
3	Dottorichora
4	Sohosrodhara road
5	Jam Bagan
6	Moishachara
7	Amtola
8	Ujalia Pahar
9	Napittachora
10	Gorapainna
11	Khoiatali
12	Khoiyachora Waterfall
13	Khoiyachora Trail
14	Random Forest Patch 1
15	Fulgazi Village
16	Ruposhi Waterfall Pathway
17	Ruposhi Waterfall Trail
18	Bhadhala
19	Komoldoho
20	Random Forest Patch 4
21	Random Forest Patch 2
22	Ruposhi Waterfall Trail 2
23	Napittachara Waterfall
24	Random Forest Patch 3
25	Chagolkainda Waterfall
26	Harinmara Trail

Figure 14: Cycas abundance area in Baraiyadhala National Park

4.2.1 Threats of Cycas pectinata in BdNP

Frequent wildfires within the Baraiyadhala National Park (BdNP) during the dry season, particularly between January and April, are occurring. The frequency and intensity of these fires contribute to the mortality of numerous seedlings, saplings, and poles of the park. Forest fires inflict damage on the foliage and apical regions of the stems. Typically, a substantial number of the Cycas population are located on hill slopes or adjacent to aquatic bodies, rendering them vulnerable to landslides. In the 1980's due to clear felling followed by artificial regeneration, the population of Cycas reduced significantly according to the locals (outcome from individual surveys and FGD). The team documented landslide-damaged Cycas pectinata within the protected area, which adversely impacts the population size of the species in BdNP. Although the correlation is statistically insignificant, a positive relationship has been identified between the presence of *Cycas pectinata* and the associated tree species of *Bauhinia acuminata, Streblus asper,* and *Bombax ceiba* (Hossain et al. 2021). However, *C. pectinata* has been observed to thrive beneath the canopies of various other tree species, including *Phyllanthus emblica, Terminalia bellirica, Lannea coromandelica, Alstonia scholaris, Ficus hispida, Albizia procera, Gmelina arborea, Lagerstroemia speciosa, Samanea saman,* and *Tectona grandis,* indicating that *Cycas* exhibits varying degrees of symbiotic relationships with a diverse array of species (Hossain et al. 2021). The destruction of these associated species harms the habitat suitability for Cycas.

Figure 15: Cycas Cone

The cones of Cycas are used for medicinal purposes by traditional healers known as Kabiraj, who operate without formal accreditation. Findings indicate that male cones are marketed at prices ranging from BDT 2000-2500, whereas female cones are sold for BDT 350-500.

The natural ecosystems that support the growth of Cycas are increasingly under threat, having experienced significant reduction and degradation. The increasing pressures that lead to this decline are primarily linked to deforestation, intentional ignitions, escalating human populations, urban development, and the unsustainable harvesting of seeds and male reproductive structures.

Figure 16: Fire burns Cycas

4.2.2 Suggested Control Measures in Cycas Conservation

Although in urban environments, Cycas is cultivated in gardens and private nurseries for ornamental purposes, it remains relatively unpopular for plantation programs in forests. Considering the alarming decline of Cycas populations, both *in situ* and *ex-situ* conservation strategies are suggested. The suggested control measures are, i) Awareness among local communities regarding biodiversity, particularly about Cycas species, ii) Facilitate sustainable livelihood opportunities through Alternative Income Generation (AIG) initiatives, iii) Encourage afforestation efforts within residential areas and barren lands, iv) Assisted Natural Regeneration (ANR) by controlling fire, invasive species, and biotic pressures, v) Develop eco-tourism facilities that showcase waterfalls and natural forest areas, inclusive of Cycas, vi) Implement forest zoning strategies, such as core zones and buffer zones, while preserving native species within core areas, vii) Engage diverse stakeholders in the conservation framework, viii) assigning responsibilities and incentives, ix) Establish comprehensive initiatives for ex-situ conservation programs, and x) Safeguard the 26 identified Cycas hotspots with appropriate demarcation and ensure the collection of seeds for future natural regeneration.

A comprehensive conservation approach is needed to secure the conservation and maintenance of the surviving Cycas populations in Baroyardhala National Park.

4.3 Perception of local people on natural resources of BdNP

4.3.1 Demographic Indicators

During the survey of residents, we surveyed 69% of males, and 31% were female. Respondents were classified into six age ranges. Among all age ranges, 30% of our total respondents were aged between 31 to 40 years. The highest number of respondents (27%) educational level was less than PSC pass or equivalent to PSC pass, whereas 14% of respondents had a BSc pass. Among the respondents, 72% were married. Adult males in respondents' families were 55%. The income of adult males was higher than the income of adult females (**Table 7**).

Table 7. Demographic indicators of the locals

Demographic Indicators	Parameters	Percentage
Gender (%)	Male	69.00
	Female	31.00
Age Range (%)	15 – 20	5.00
	21 – 30	25.00
	31 – 40	30.00
	41 – 50	22.00
	51 – 60	12.00
	60 +	6.00
Educational Level (%)	$\geq$ PSC	27.00
	JSC	7.00
	SSC	25.00
	HSC	22.00
	BSC	14.00
	Higher than BSC	5.00
Marital status (%)	Married	72.00
	Unmarried	28.00
No. of adult family members (%)	Male	55.00
	Female	45.00
Average income of respondents (BDT)	Male	45514.00
	Female	14003.00

4.3.2 Dependency on Forest

Dependency on fuel wood is higher in BdNP. In general, a family uses 1650.40 BDT equivalent of fuel wood from the forest per month. From the forest, a family uses bamboo resources equivalent to 227 BDT/month. Grazing is less, but still, it happened in BdNP (Figure 17).

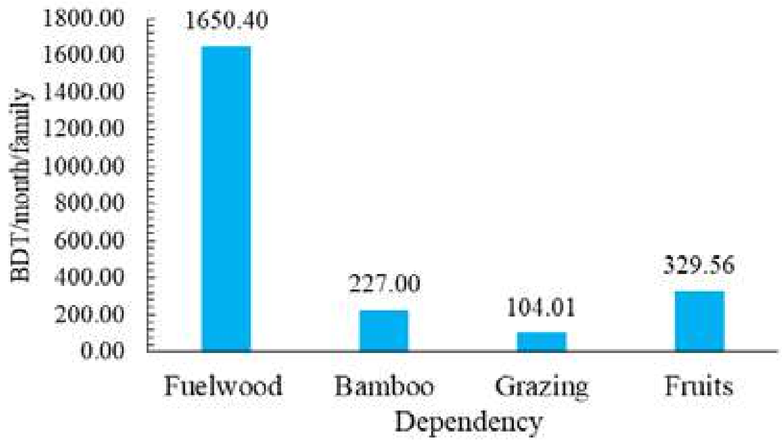

Figure 17: Dependent on forest products or services

4.3.3 Experiences of the community about different resources of the forest

Most of the people (97%) know the Jharna (waterfall) very well, whereas most of the people have no idea about wildlife, especially bears (**Table 8**). There are a lot of birds, as there are so many species of *Ficus hispida, Ficus auriculata*, etc. However, the people had less knowledge of *Cycas pectinata*.

Table 8. Experiences of the community about the resources of the forest

Knowing the Intensity	Jharna (%)	Cycas (%)	Wild Goat (%)	Monkey (%)	Bear (%)	Deer (%)	Birds (%)
Very well known	97.00	17.00	19.00	46.00	1.00	29.00	73.00
Known well	3.00	56.00	14.00	12.00	12.00	56.00	22.00
Known a little bit	0.00	12.00	55.00	38.00	17.00	12.00	5.00
No idea	0.00	15.00	12.00	4.00	70.00	3.00	0.00
Total respondents (%)	100.00	100.00	100.00	100.00	100.00	100.00	100.00

4.3.4 Distribution of respondents living near the waterfall

Most of the respondents of this survey lived about 0.5 – 2.5 km away from the waterfalls. The highest number (31%) of respondents was found in the Shonaichora within 0.5 km distances. **(Table 9)**.

Table 9. Distribution of respondents from the waterfall site

Name of the waterfall	0 - 0.5 km	0.5 - 1 km	1.0 - 1.5 km	1.5 – 2.0 km	2.0 - 2.5 km	> 2.5 km	Total Percentage
Khoiachara	12.00	30.00	22.00	29.00	3.00	4.00	100.00
Napittachara	14.00	29.00	24.00	22.00	10.00	1.00	100.00
Ruposhi	13.00	24.00	12.00	12.00	22.00	17.00	100.00
Shonaichori	10.00	25.00	35.00	15.00	7.00	8.00	100.00
Baoa chora	23.00	28.00	12.00	12.00	15.00	10.00	100.00
Shonaichora	31.00	12.00	22.00	12.00	10.00	13.00	100.00
Shahsradhara	15.00	25.00	13.00	22.00	17.00	8.00	100.00
Harin mara	12.00	26.00	12.00	15.00	17.00	18.00	100.00

4.3.5 Risk/life-threatening experiences by the visitors

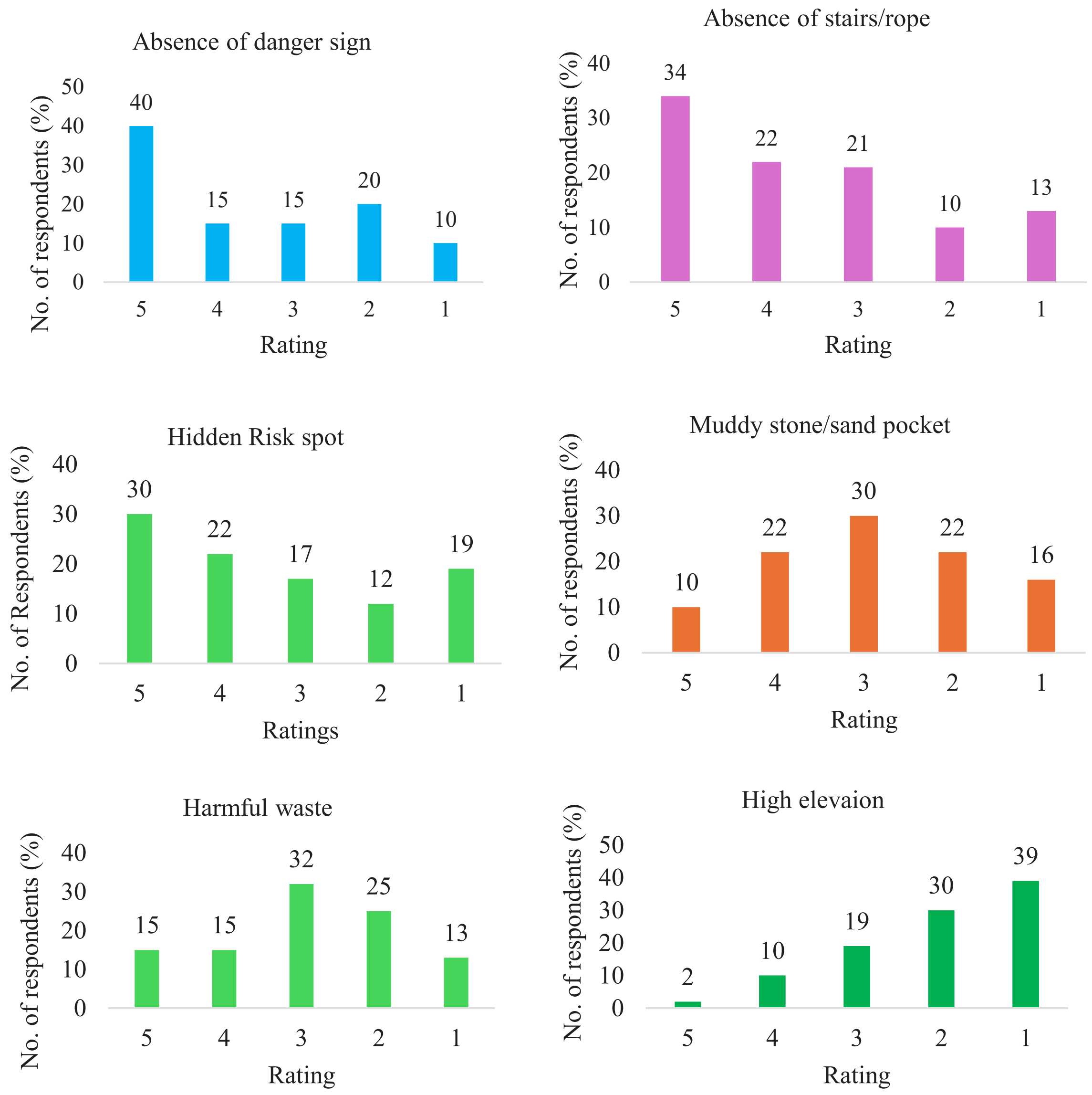

Figure 18: Risk/life-threatening experiences faced by visitors

In the waterfalls, we identified several risks for the tourists, e.g., Hidden risk spots, Absence of danger marks, High elevations, Absence of stairs/ropes to climb the hills, Harmful waste here and there, and muddy stone/sand pockets were reported by the locals.

4.3.6 Harmful activities at the waterfall/forests

The harmful activities recorded in the waterfalls, natural forests/plantations, soils, local culture, flowing water, and wildlife are mentioned in Table 10. The clean waters of the waterfalls lost their purity due to the activities of tourists and local people. Forest plantations were degraded, and the habitat of several species was lost due to fire and fuelwood extraction by the dependent locals.. Small kids learn slang from some of the tourists. The lack of knowledge due to sound pollution leads to disturbance to the wilderness and hampers wildlife.

Table 10. Harmful activity at the protected area

Components of the Protected Area	Observed activities	Nature of harm	Responsible person/agency
Waterfall/Jharna	Waste Deposition in the water body	Purity of water is lost	Tourists
			Dependent locals
Forest/Plantations	Fire	Plantation and Seedling Burn	Dependent local communities
	Fuel wood extraction	Seedlings and Poles are cut and reduce density	
Wildlife	Sound pollution	Wildlife habitat is disturbed	Mostly by tourists
Local culture	Use slang by tourists	Small kids learn slang	Tourists
	Sound pollution	Disturb the wilderness of the park	

4.3.7 Tourism development improves the area or not

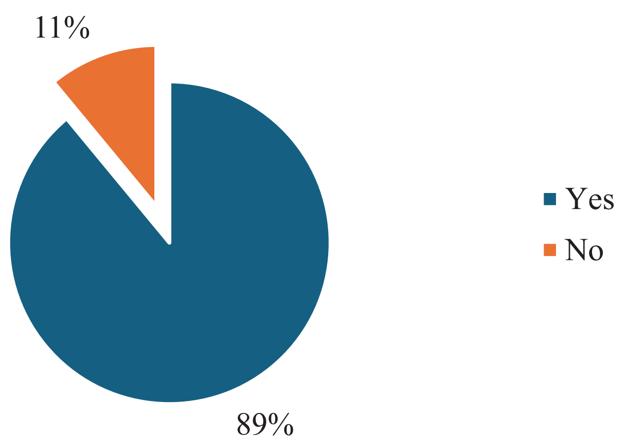

Figure 19: Development of tourism facilities improves

A question arises among the locals whether the development of tourism facilities benefits the locals more or not. The survey reported that most of the locals (89%) believe that tourism facilities may develop the area, whereas 11% still believe that it will not improve the area.

4.3.8 Perception of local communities about Cycas

Local people think that *Cycas pectinata* has some medicinal uses. According to people, anthropogenic fire, fuelwood collection, and cone/seed collection by the locals cause damage to the natural populations of Cycas. Maintaining forest health, controlling forest fires and debris, and protecting the Cycas population from the locals can be ways to conserve the natural Cycas populations in BdNP **(Table 11).**

Table 11. Local people's perception of the *Cycas* population

Importance	Causes of Deterioration	Problems in Management	Measure
Medicine	Fire	Anthropogenic fire	Maintain forest health by controlling dead & dry forest debris
Ornamental	People take the cone/seed	Some people extract cones/seeds for medicinal purposes	Protect them from illegal cutting/harvesting
	Use as fuelwood	Easy to cut for fuel wood	Regular patrolling of illegal harvesting

4.4 Perception of tourists on ecotourism and its potential management

4.4.1 Location-wise tourists

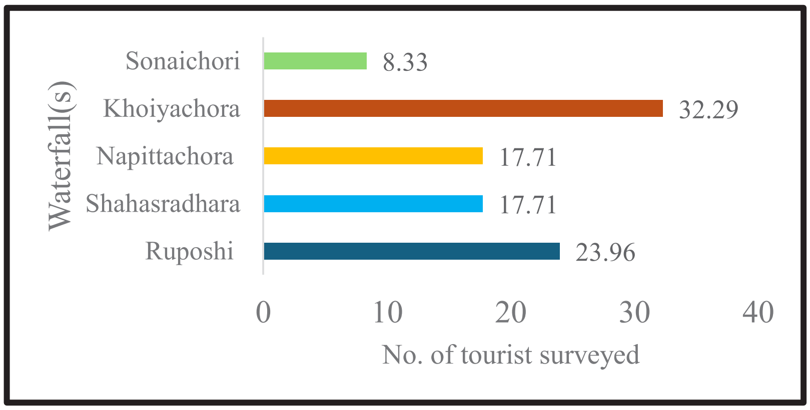

Figure 20: Distribution of tourists at different waterfall spots

A total of 32.29% of tourists were surveyed in the Khoiyachora, followed by Ruposhi (23.96%), Napittachora, and Sahasradhara.

4.4.2 Gender of tourists surveyed

The respondent's gender percentage is shown in Figure 21. About 81.25% of the surveyed visitors are male, and the females are only 18.75%. The religion-wise records reveal that Islam dominates the majority of 83.33%, followed by Hinduism at 16.67%. The fewer female tourists than male tourists indicates that possibly due to safety concerns and cultural norms. Women could feel unsafe traveling alone or with others, while men are more likely to travel for leisure.

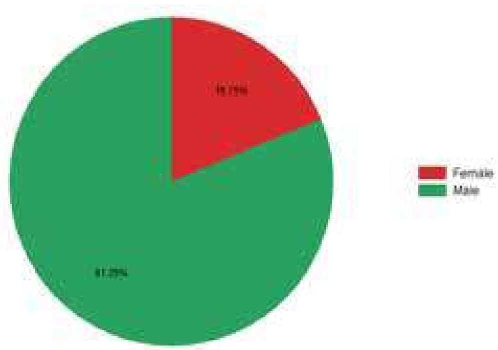

Figure 22: Respondents' distribution to gender and religion

4.4.3 Age range of tourists

Most of the tourists' age group is 21-30 (66.67%), followed by 15-20, 30-40, and 40-50 years respectively (Figure 23). Most visitors are young adults, followed by the 30-40-year age range. The tourists' main attractions are hiking and wildlife viewing. Physical demands, such as strenuous activities or challenging terrain, may attract younger, more physically active individuals.

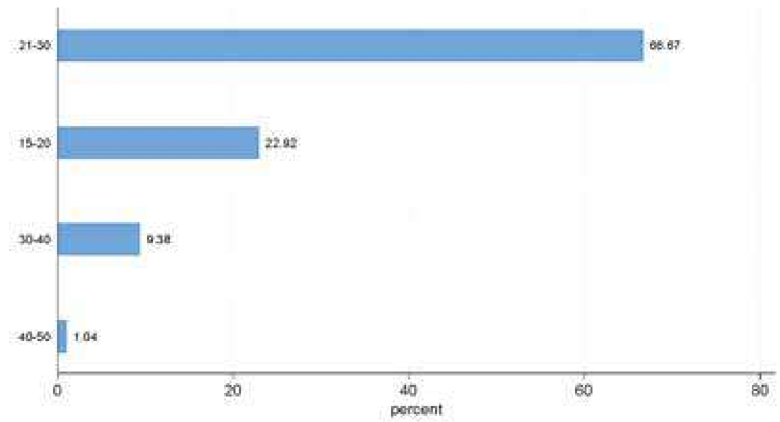

Figure 23: Age class of Tourists

4.4.4 Tourist's residential location

The percentage distribution of the visitors' origin shows that 65.62% tourists are from Chittagong, while about 34% came from outside the Chittagong (Fig. 25). This indicates that BdNP are attractive to visitors across the country. Beyond Chittagong, tourists come from Noakhali, Narayanganj, Mymensingh, Jamalpur, Feni, Cumilla, Tangail, Chandpur, Faridpur, Dhaka, Cox's Bazar, and Gaibandha (Fig. 24). Factors influencing distribution of tourists include proximity to the hill area, accessibility, targeted marketing efforts, and cultural and historical ties. Most visitors believe that easier transportation links and awareness also contribute to the high visitor percentage in Chattogram.

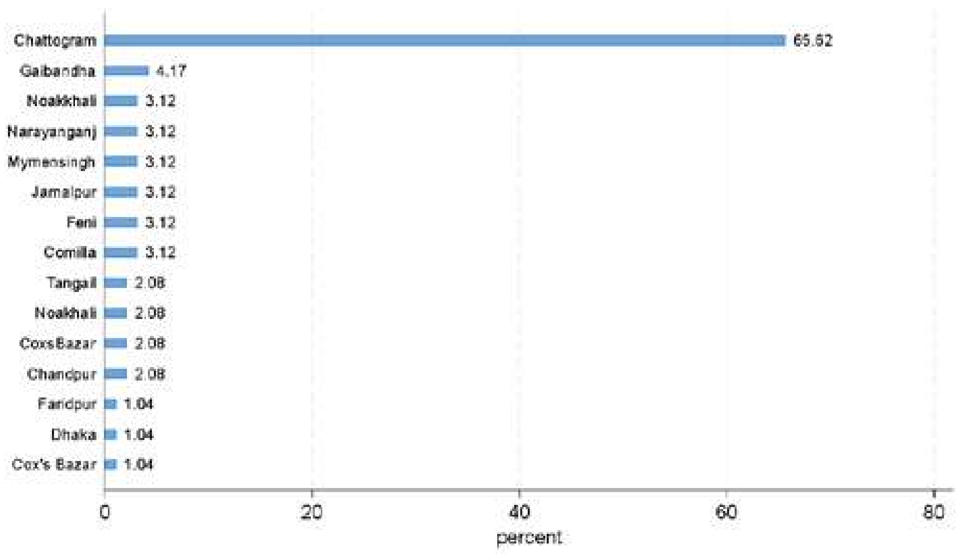

Figure 24: District-wise presence of Tourists

4.4.5 Employment status

Occupational distribution of visitors is shown in Fig. 26. BdNP is primarily visited by students (67.71%) followed by job holders (6.25%), housewives (6.25%), business workers (5.21%), freelancers (3.12%), professional overseers (2.08%), and bankers (2.08%). Shop owners and accountants have the lowest representation at 1.04% each. Factors influencing such distribution include accessibility and affordability, educational focus, recreational activities, and proximity to educational institutions. Students have flexible schedules, energy, enthusiasm, and lower financial constraints, making visiting their respective forest areas easier. The forest area may be used for educational purposes, like field trips or research projects, including recreational activities, such as hiking or camping.

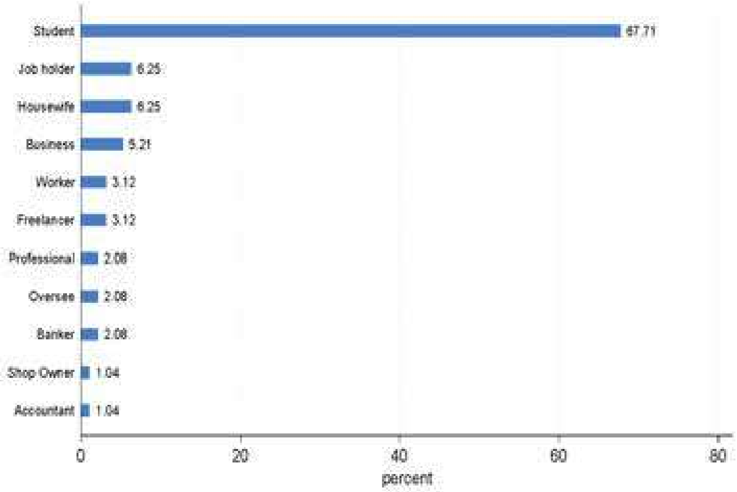

Figure 25: Occupation of tourists

4.4.6 Accompanying during Tour

Most visitors of the BdNP come with their friends (65.62%) followed by family members (22.92%), individuals (5.21%), Facebook friends (4.17%), and housing society members (2.08%). Social factors, family activities, individual interests, and group dynamics can influence the distribution of visitors. Family activities like hiking, picnicking, and nature observation suit families. Individuals may prefer exploring the forest area independently for solitude or specific interests.

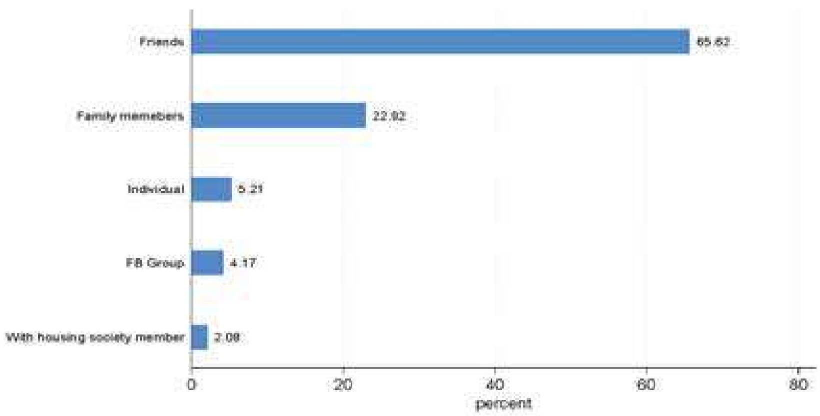

Figure 26: Distribution of accompanied tourists

4.4.7 Choosing options for the spots

Figure **27** shows the distribution of people how they choose their visitors to the spot/site in the forest area. Most tourists are primarily influenced by information from friends (62.50%) followed by Facebook group (15.62%), relatives (14.58%), and YouTube (7.29%). Social networks, personal experiences, and visual appeal are some factors that influence travel decisions. Friends and family are trusted sources of information, while social media platforms like Facebook and YouTube have increased their influence. However, social networks, personal experiences, and visual appeal are key factors in shaping travel decisions.

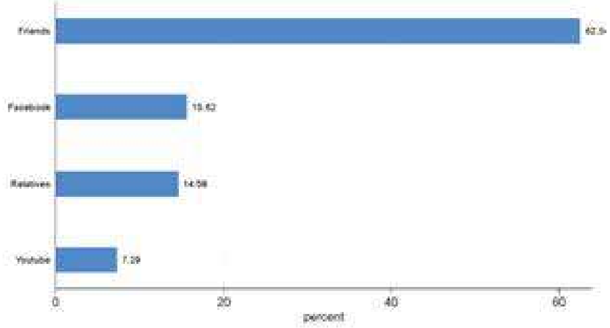

Figure 27. Sources of choosing tourist spots/sites

4.4.8 Travel motives

The primary reasons for visiting Baraiyadhala National Park are to enjoy the natural beauty, relax, and enjoy tranquility (Fig. 28). The most common motives are to see waterfalls and forests in the hill terrains, while others appreciate the natural environment. About 37.23% of tourists visited the forest area to enjoy nature, while 23.40% responded as expected highly, and 37.23% did it a moderate expectation. Overall, about 98% of people are likely to visit the site because of the waterfalls within the forest. Findings indicate that natural beauty is a popular attraction within the forest area. Entertainment and social factors also motivate visitors. About 45.83% of visitors have a moderate expectation of camping, while 39% do not. Canoeing, camping, and wild tracking are less popular, and a lack of security discourages camping. To promote wild tracking, proper track roads and danger zones should be marked, as lack of security demotivates people from staying in these areas.

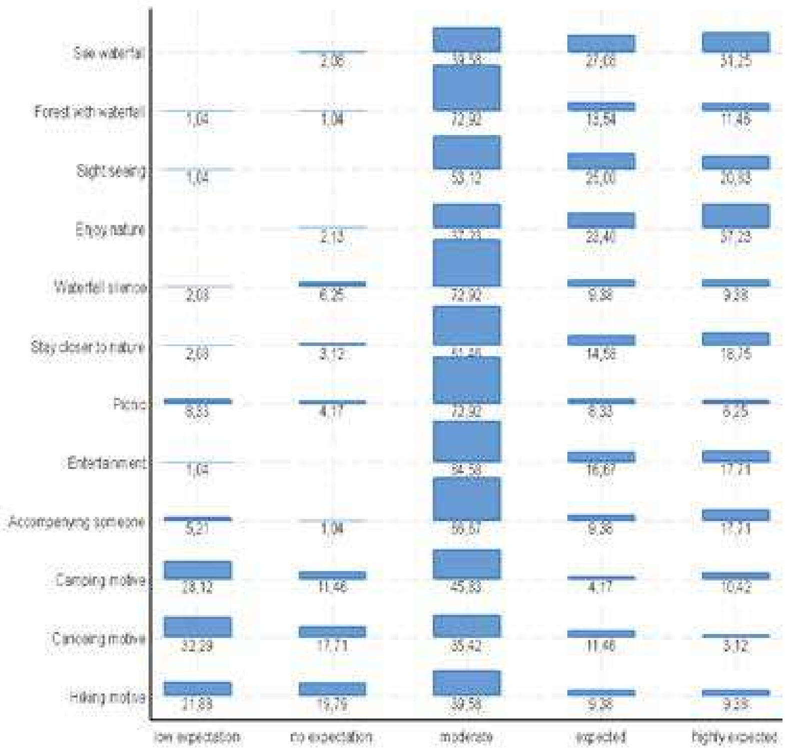

Figure 28: Tourists travel motive in BdNP

4.4.9 Use of transportation

The transport pattern shows that buses are mostly (64%) used transport, together with microbuses (27%) followed by taxis (7%), and cars (2%).

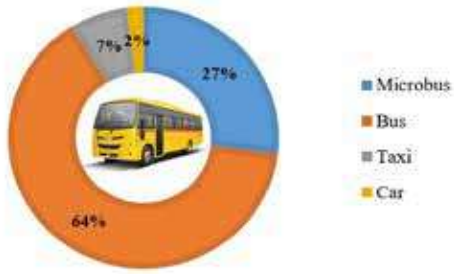

Figure 29: Transports used by the tourists

4.4.10 Average willingness to pay

Tourists express their willingness to pay to visit the waterfalls, i.e., for Khoiyachora waterfall (82.89 BDT), followed by Bawachara waterfall and Napittachora waterfall. They are interested in paying 56 BDT for Shahasradhara waterfall and the least for Shonaichora waterfall (50 BDT).

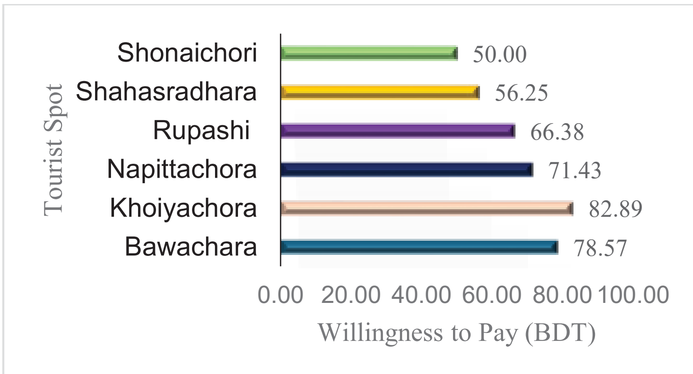

Figure 30: Tourists' average willingness to pay in BDT

4.4.11 Problem faced by Tourists during Tracking

While tracking waterfalls, tourists face several problems, e.g. absence of stairs/ropes for climbing to the top of the waterfalls, followed by hidden risk points and the absence of risk points. The percentage of risks/points are hidden risk points, steep slopes, absence of stairs/ropes, danger marks/sign boards, high elevation, connectivity GIS/route maps, theft/robbery, harmful waste, and muddy soil/sandy pockets etc. About 82% of visitors reported their concerns about theft and robbery, whereas 81% reported muddy and sandy pockets on the way to tracking.

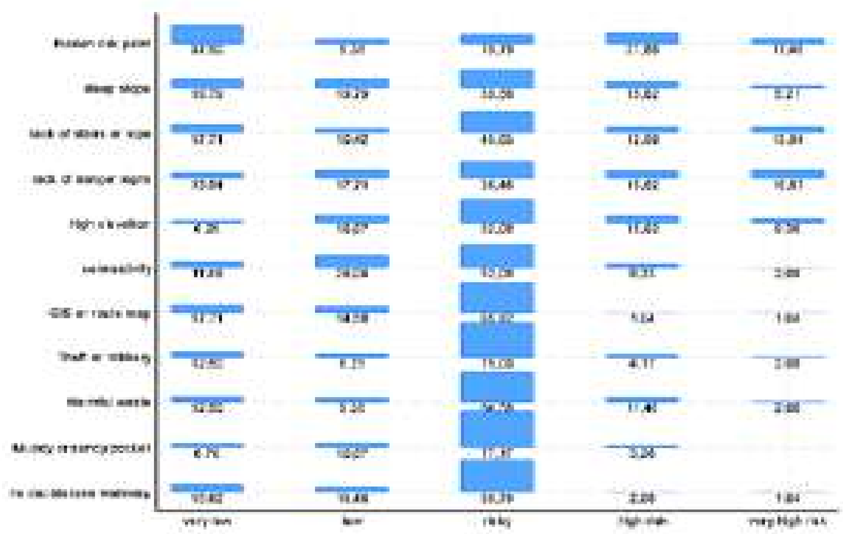

Figure 31: Risks faced by tourists during tracking in the hill areas

4.4.12 Visitors' Knowledge of ecotourism and nature-based parameters

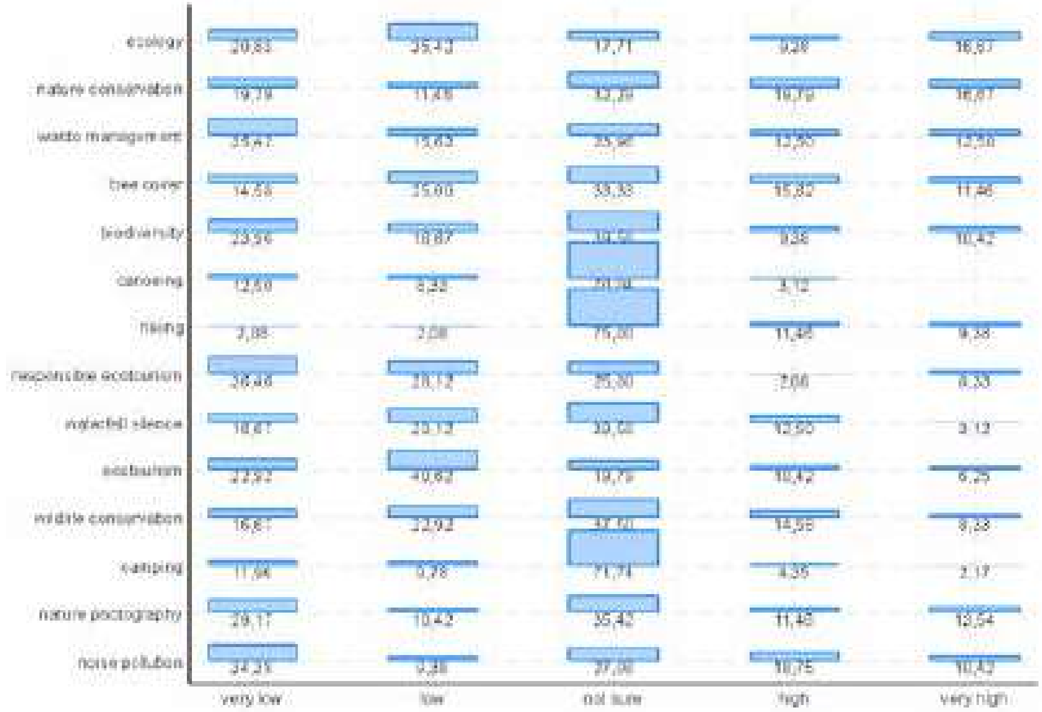

Figure 32: Perception of visitors' knowledge about ecotourism

The percentage of visitors' perceptions on ecotourism knowledge is variable, e.g, 26% of tourists have a clear idea about ecology, followed by nature conservation (37%), waste management in forest areas (24%), and tree cover (26%). In addition, 21% of tourists support biodiversity, 3.12% support canoeing, 10% support responsible tourism, and 6% support camping.

4.4.13 Ecotourism knowledge and attitudes to conservation

There is a positive correlation between ecotourism knowledge and attitudes towards nature and wildlife conservation in visiting the BdNP. The positive correlation implies that attitudes towards nature and wildlife conservation increase (from low to high), as does ecotourism knowledge. The positive correlation is also statistically significant, suggesting that ecotourism-related education programs can be initiated to increase awareness and conservation attitudes of the visitors.

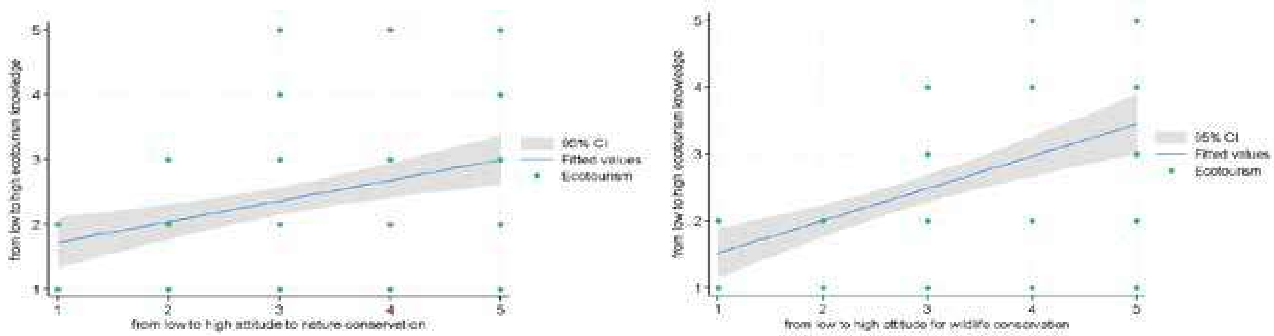

Figure 33: Correlation between ecotourism knowledge and nature conservation and Correlation between tourists' ecotourism knowledge and wildlife conservation in BdNP

4.4.14 Ecotourism knowledge and attitudes towards responsible tourism

A correlation between ecotourism knowledge and attitudes toward responsible tourism and picnic arranging is observed in BdNP. The positive correlation implies that the attitude of tourists toward responsible tourism increases with an increase in ecotourism knowledge. Conversely, the attitude towards arranging picnics in forest areas is increasing, but most visitors believe that arranging traditional picnics in forest areas is harmful to the ecosystem.

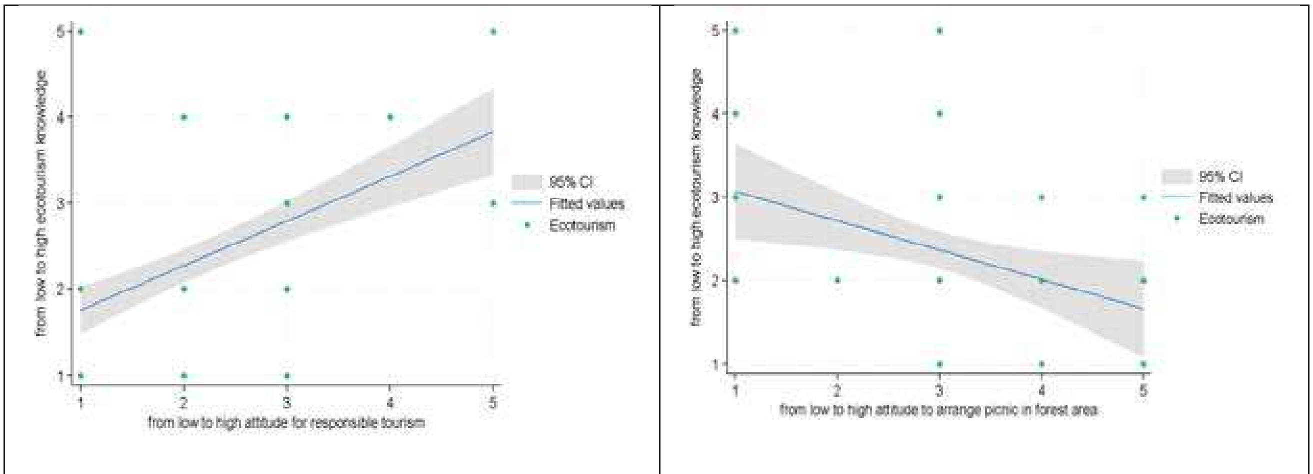

Figure 34: Ecotourism knowledge reflection

4.4.16 Problems in relation to tourism in the Protected Area (PA)

The visitors in BdNP face several hurdles in visiting BdNP forest areas despite the excellent natural beauty of this Protected Area (PA). Visitors complain about inadequate accommodation, poor road connectivity, limited food options, and inadequate night stay facilities. Visitors are concerned about the environment and safety, including cleanliness, waste management, inadequate tree cover, risk points, and poor waste management. They have privacy and security concerns, including inadequate water availability and unhygienic washroom facilities. However, they have a mixed response on building residential hotels in forest areas.

Table 12. Issues have to address visiting BdNP as a tourist site

Issues have to address visiting BdNP	**Bawachara**	**Khoiyachara**	**Napittachora**	**Rupashi**	**Shahasradhara**	**Shonaichora**
Accommodation is inadequate/disappointing?	Y*	Y	Y	Y	Y	Y
Whether behavior of local people is disappointing?	N	N	Y	N	N	N
Do you want to build more residential hotels in forest area?	N	N	Y	N	N	Y
Whether cleanliness of the park area is disappointing?	Y	Y	Y	Y	Y	Y
Whether connectivity or road network is disappointing?	N	Y	Y	Y	N	Y
Whether drinking water availability and quality is disappointing?	Y	N	Y	Y	Y	Y
Whether you have issues with eco-cottage?	N	Y	Y	Y	Y	Y
Whether you face issues with eco-trails (platforms for seeing waterfalls)?	Y	Y	Y	Y	Y	Y
Whether food facilities disappointing?	Y	Y	Y	Y	Y	Y

Is infrastructure development disappointing?	Y	Y	Y	Y	Y	Y
Are more transport facilities needed?	N	Y	Y	Y	Y	Y
Do you need to assess risk points in waterfalls?	N	Y	Y	Y	Y	Y
Want night stay facilities?	N	N	N	N	N	N
Whether the adequate tree cover is absent?	Y	N	Y	Y	Y	Y
Whether privacy and security are disappointing?	Y	Y	Y	Y	Y	Y
Whether installing ropes on the slope is needed?	Y	Y	Y	Y	Y	Y
Whether installed signboards disappointing?	Y	Y	Y	Y	Y	Y
Whether unhygienic washroom is disappointing?	N	Y	Y	N	N	N
Whether poor waste management exist?	Y	Y	Y	Y	Y	Y

* - Y= Yes, N= No

Visitors also reported their concerns about signboards, informative remarks, and hygienic washrooms. Visitors suggested that park management should be more effective in addressing the visitors' needs and requirements. Authorities should improve infrastructure, enhance safety and security, improve waste management, zoning for tourists, promote community engagement, prioritize eco-friendly development, and inform visitors about responsible tourism practices in PAs.

4.4.17 Tourists' perception of solving the problems

Most of the tourists (39%) believe that the Forest Department can solve all these problems by visiting the waterfalls, whereas 29% of visitors believe that local people can play an important positive role. About 9% of tourists believe that the Forest Department and local community jointly can solve those problems, which will be a great initiative for safe visits to the waterfalls.

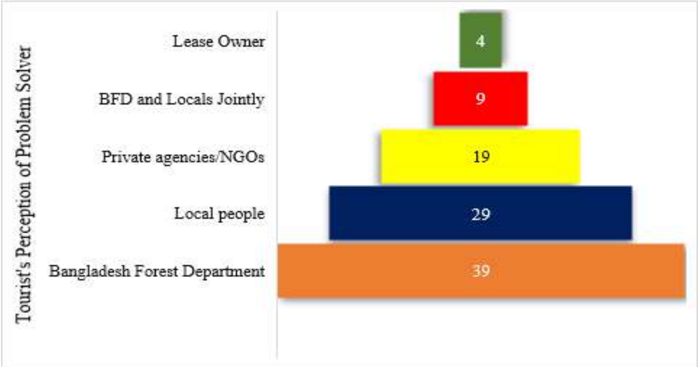

Figure 35: Tourists' perception of solving the problems

Major tourists believe that the Forest Department is the sole authority responsible for managing the waterfall resources. Others opined for the inclusion of local people, BFD, private agencies/NGOs, and lease owners. Tourists also recognize the importance of local knowledge and involvement in solving problems. Lease owners are alleged to have the least responsibility in addressing issues within the waterfall areas.

4.5 Wise use of water resources

The Forest Department has taken several projects to enhance the vegetation cover and restore the degraded forest ecosystems. However, BdNP has the scope to utilize the water resources for the purpose of the agricultural and/or industrial sectors, causing minimum harm to the forest ecosystem. Some arrangements may be made for creating water reservoirs and storing rainwater on the downstream private land. Dams are established by the Local Government Engineering Department (LGED) at three locations in the Baraiadhala National Park to store the rainwater for agricultural use, mostly for rice and vegetable cultivation (**Table 13**).

Table 13. Artificial dams constructed in BdNP for agricultural uses

Project name	**Shonaichora Hydro-project**	**Shahasradhara Hydro-project**	**Bawachora Dam**
Location	East Polmogra, Bortakia, Mirsoroi	Dharmapur, Baraiadhala, Sitakund	Baoachora
Construction status	Completed	Completed	Completed
Financial status	Govt. of Bangladesh, Asian Development Bank, Govt. of Netherlands	Govt. of Bangladesh, Asian Development Bank, Govt. of Netherlands	Govt. of Bangladesh, Asian Development Bank, Govt. of Netherlands
Project implementing body	LGRD Ministry	LGRD Ministry	LGRD Ministry
Construction year	2016-2017 fiscal year	2005 fiscal year	
Target coverage (area in acres	500 acres	1900 acres	
Construction expenditure	45,000,000/- including the excavation	45,000,000 BDT (including the expenditure of re-excavation of 4.5 kilometers of streams)	45,000,000 BDT
Achieved coverage	About 100 acres of agricultural land and two ponds.	About 1100 acres of agricultural lands and ponds	
People's perception of the dam	Positive	Positive	

4.5.1 Present uses of water from waterfalls

Local people in the BdNP depend mostly on all eight waterfalls and their water. Baoachora water reservoir is mostly used (68%) for agriculture, whereas Napittachora water is used for drinking, and Shasradhara water is used mostly for household uses. In most cases, water from waterfalls is used for baths and the rest of the household work (Table 14). Present uses of the waters from BdNP waterfalls

Table 14: Present uses of water from waterfalls

Waterfall	Agriculture (%)	Drinking water (%)	Household use (%)
Khoiachora	35	5	60
Napittachora	21	17	62
Ruposhi	53	7	40
Shonaichori	47	2	51
Baoachora	68	0	32
Shonaichara	22	12	66
Shasradhara	24	8	68
Harin mara	37	13	50

4.5.2 Want more DAMs

There is a debate about making more dams on the natural waterfall in this PA. About 52% of local people do not want more dams, and the rest, 48%, want dams, although they say it will not be convenient and will not be cost-effective.

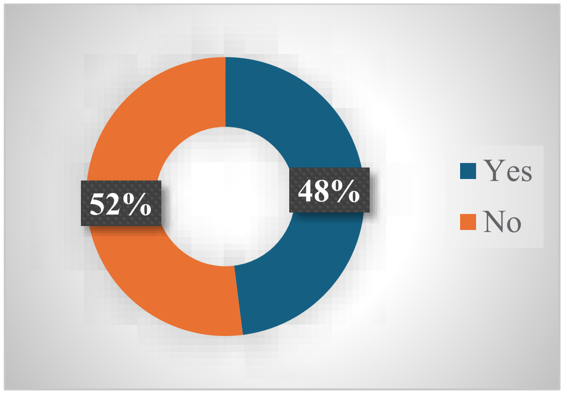

Figure 36. Comments on making more DAMs inside the forest

4.5.3 Suggestion about low-cost structure

Local people opined that low-cost-structure water storage is a solution to overcome the water problem of the locals. Local people generally store water in ponds. Most (70% of total respondents) said that a structure for rainwater harvesting would be effective for them, though 7% of people said there is no land for such a new structure. So, it will not be effective.

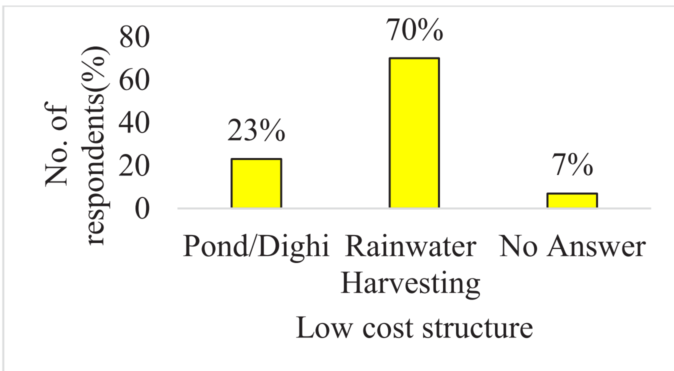

Figure 37. Low-cost structure for water storage

4.5.4 People's opinion on making DAMs inside the forest

A total of 63% of the locals do not want to pay for any project undertaken by the government. Most people give the opinion that DAMs may ease the process of irrigation, but the DAMs are not effective due to the water continuity throughout the years. A lot of people (21%) have no idea what loss may happen to the plants and the wildlife if DAMs are made inside the forest (**Table 15**).

Table 15. People's opinion on making DAMs inside the forest

Factors	Opinion of people	No. of people gave this opinion (%)
Loss of plant and wildlife	Yes	37
	No	42
	No comment	21
Loss of livelihood opportunity	Yes	8
	No	90
	No comment	2
Beneficial for irrigation	Yes	97
	No	3
	No comment	0
Pay for the reserve or not	Yes	37
	No	63

4.6 Details of Jharna (Waterfalls) of Baraiadhala National Park, Chattogram

4.6.1 Tourist Guide Map

1.	**Name**	**Khoiachara Jharna (Waterfall)**	
1	**Location**	**Mirsarai, Chattogram**	
2	**Spatial Location**	Lat. 22.769772	Long. 91.612484
3	**Brief Description of the Jharna**	Khoiyachara Waterfall is very famous in Mirsarai upazila, Chattogram. It's series of steps making it attractive and distinct from others.	
4	**Main Attraction of the Jharna**	The main attraction of Khoiyachara waterfall is its impressive waterfall surrounded by greenery, and the peaceful environment of the natural surroundings. Visitors enjoy hiking trails and attractive viewpoints that offer breathtaking views of the waterfall. Adventurists may go up to the peak of the hills to enjoy the lovely scenery of the jharna. It is an ideal destination for a day-long trip.	
5	**Travel**	**Bus** ● *From Dhaka, take a bus to Chattogram.* ● *Non-AC bus fares: 420-480 taka.* ● *AC bus fares: 800-1100 taka.* ● *Get off at Khoiyachara Ideal School near Bortakia Bazaar in Mirsarai.* ● From Sayedabad Bus Stand, take Star Line Paribahan to Feni (280 taka). ● From Feni, take a local bus to Mirsarai/Bortakia Bazar near Khoiyachara Jharna. ● From Mirsarai to Bortakia, by taxi/car	**Train** ● From Dhaka, take any intercity train to Feni station (fares: 265-909 taka). ● From Feni station, take a rickshaw/auto (10-15 taka) to Feni Mahipal bus stand. ● From there, take a local bus to Mirsarai/Boro Takia Bazaar near Khoiyachara Jharna, opposite Khoiyachara Ideal School.
6	**Time required to visit**	Tourists can visit the waterfall all year round, but it's best during the rainy season. Winter is also enjoyable for tourists of different age class.	
7	**Available Facilities**	Many tourist facilities have been developed over the years, including food stalls, resting huts, and seating areas. There are designated parking areas and affordable tour guides. Tourists can also enjoy nature while relaxing in front of the hotels.	
8	**Food Facility**	Along the way to Khoiyachara Jharna, you'll find food hotels where you can order and take your meal. These local spots offer affordable food, but check prices if necessary. Remember, they close after 5 PM. Alternatively, in Sitakunda, you can dine at Saudia Restaurant, Apon Restaurant, or Al Amin Restaurant.	
9	**Season of travel**	Tourists can visit the waterfall all year round, but it's best during the rainy season. Winter might not be as enjoyable for adventurous tourists.	
10	**Safety measures**	•Maintain the specified route. •Avoid the risk zone and spots. You can use Google Maps to avoid risk zones. • Use rope where needed.	
13	**Accommodation**	There are no accommodations near Khoiyachara Jharna or Bortakia Bazaar, but you can contact the UP chairman for special arrangements. However, in Sitakunda, you'll find some local hotels, including Saudia and Saimun, where you can stay. Prices range from 300 to 1600 taka at Saimun and Saudia.	
14	**Management of the Jharna**	The waterfall's management is somewhat active. Baskets are provided in front of every hotel, but there's no waste management system within the forest area. It's advised for tourists not to garbage in the forest area to help conserve nature.	
15	**Emergency Contact**	Beat Office/Fire Brigade Office/Police Station	
16	**Nearby Tourist Spots**	1. Ruposhi Jhorna 2. Shasradhara Jharna 3. Mohamaya Lake 4. Guliakhali Sea Beach 5. Shitakundu Eco-Park	

4.6.2 Risk Zone Identification

Figure 38. Risk zone of Khoyachara Waterfall

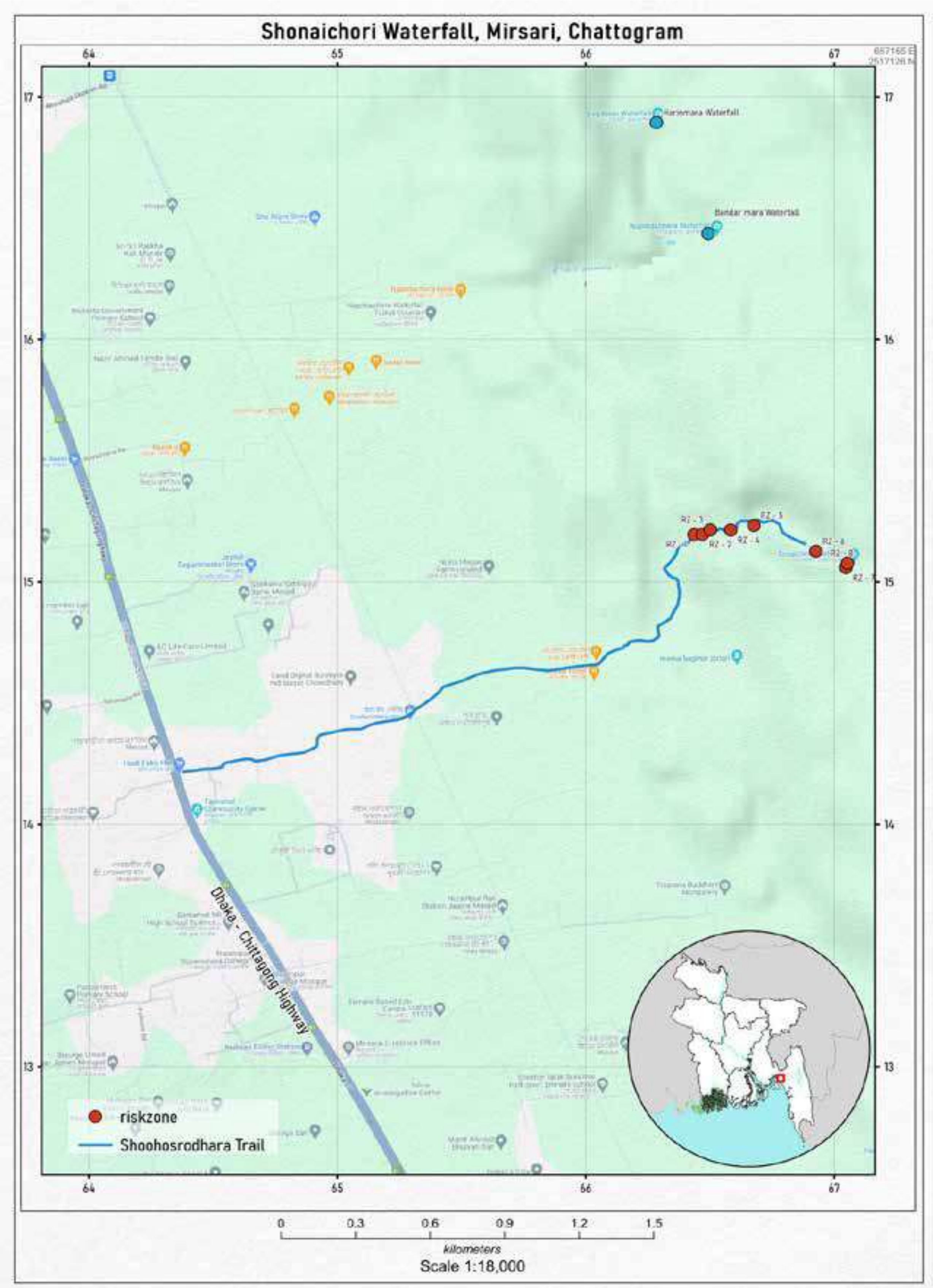

Figure 39: Risk Zone identification of Sonaichori Waterfall

Figure 40: Risk zone of Ruposhi Waterfall

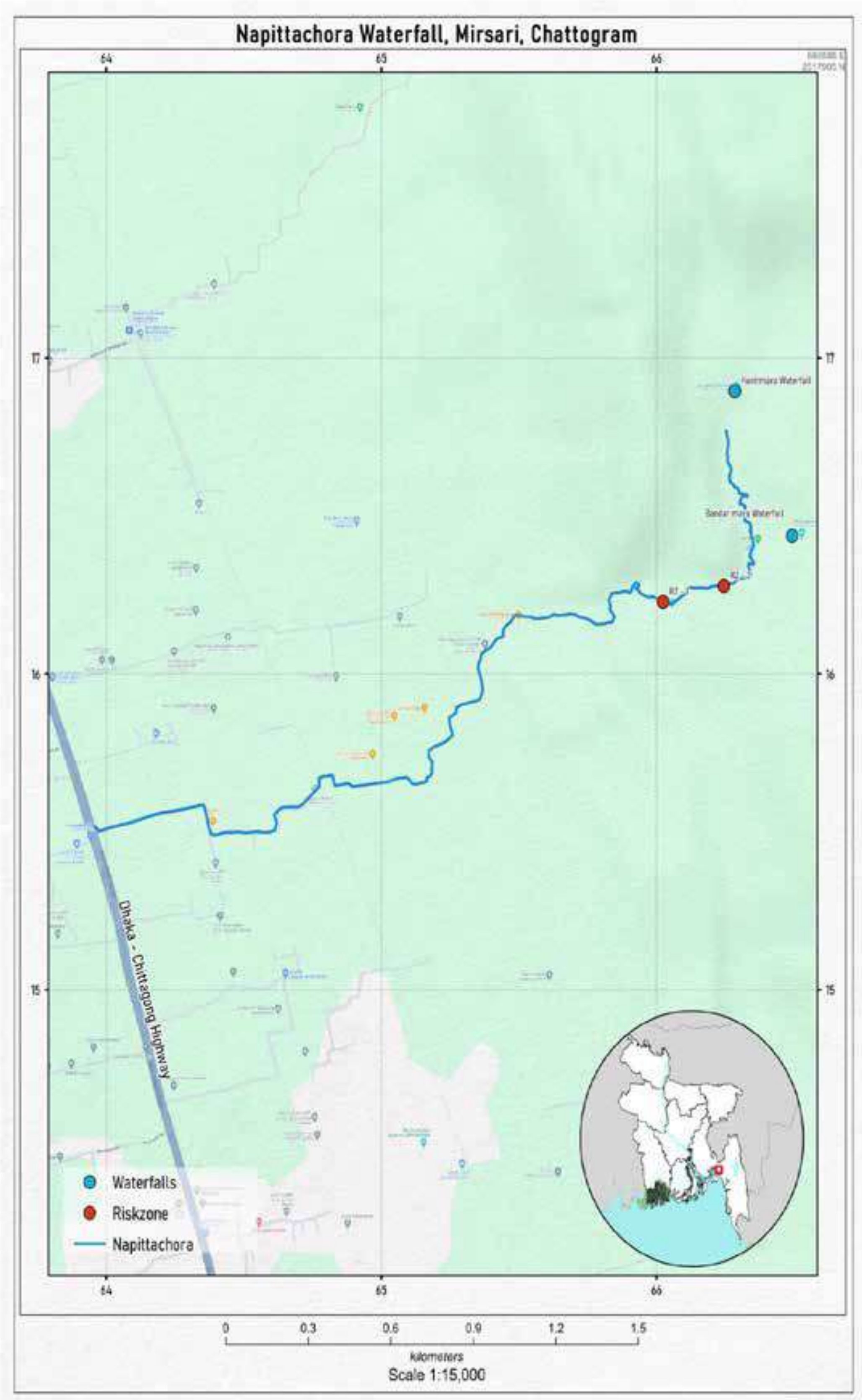

Figure 41: Risk zone of Napittachora Waterfall

Accident Information of the Waterfalls of BaNP:

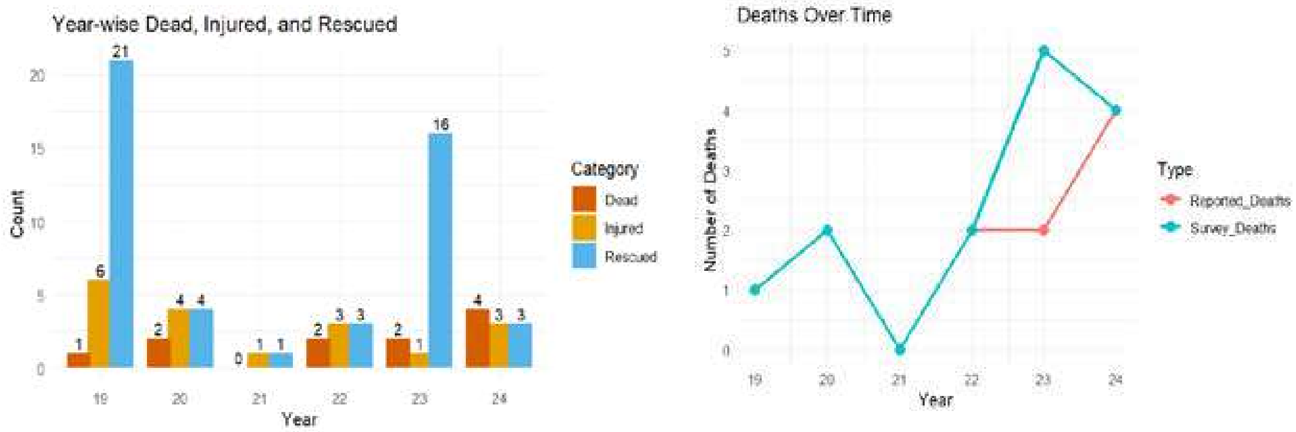

(a)

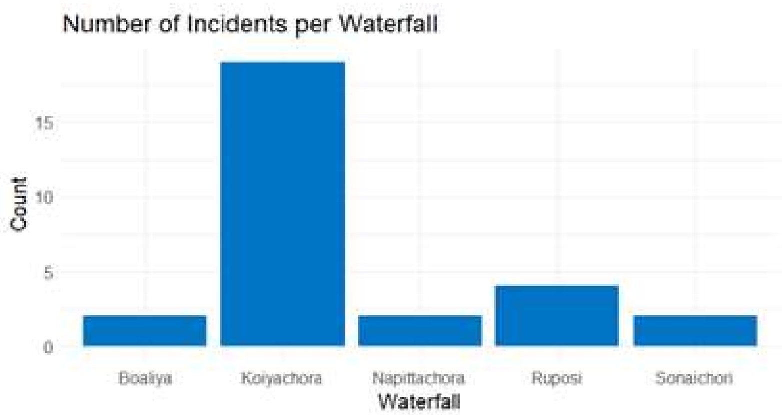

Figure 42: Death, Injury, and Rescue on the waterfalls of BaNP

Streams/ waterfalls in BdNP have several risky spots, most of which are hidden, some are along steep slopes, and some are above/around the attractive spots. Most accidents were observed frequently over the last few years, especially at the Khoiachora, Napittachora waterfall areas of Mirsari Upazila. Precautionary measures taken by the Forest Department are not enough to locate the danger points and create awareness among tourists during the rainy season. On the other hand, a few tourists are unaware of the worst situation or ignore the precautionary signal erected by the Forest Department. Most tourists do not want to be accompanied by tour guides or local people, aware of the potential threat of moving through the danger points.

Meeting with the local journalists

On Saturday, 4 May 2024, a discussion meeting was held near the Khaiyachara waterfall in Baraiyadhala National Park (BdNP), Mirsharai, Chattogram, between the research team and local journalists. The purpose was to brief the media on the park's biodiversity and water resources, and to gather insights on improving eco-tourism in this protected area. Journalists from local, regional, and national platforms participated, sharing valuable opinions on tourism development, environmental conservation, and safety. The consultation highlighted the media's role as a mirror of public perception. Journalists emphasized the need for safer tourism practices, such as banning bathing at the waterfall, constructing viewing platforms, stairways to upper levels, and assigning rescue personnel. Concerns were raised about annual casualties due to the lack of safety measures. Suggestions included limiting resorts and restaurants to prevent ecological degradation, setting up police cabins or tourist police, and establishing a single emergency contact number. Participants supported creating a reservoir or artificial lake for water storage but stressed that a thorough feasibility and environmental impact assessment must precede any development. They also discussed reforestation to prevent erosion and siltation and raised awareness about the endangered *Cycas* plant, attributing its decline to fire and illegal logging. Rare wildlife such as wild goats, small cats, snakes, and even bears were noted, with a call to protect their habitats. The Community Management Committee (CMC) was praised but recommended for strengthening. On climate change, reforestation and strict enforcement of environmental laws were advised. The session concluded with refreshments, appreciation for the journalists' engagement, and a request for future collaboration.

4.7 GIS-based Analysis

4.7.1 Delineation of hydrological Soil Group

. In Baraiadhala National Park, HSG-C was found HSG-C which is a moderately high runoff potential (<50% sand and 20-40% clay). The soil texture was Clay loam, Silty clay loam, Sandy clay loam, Loam, Silty loam, Silt, and the runoff potential is Moderately high.

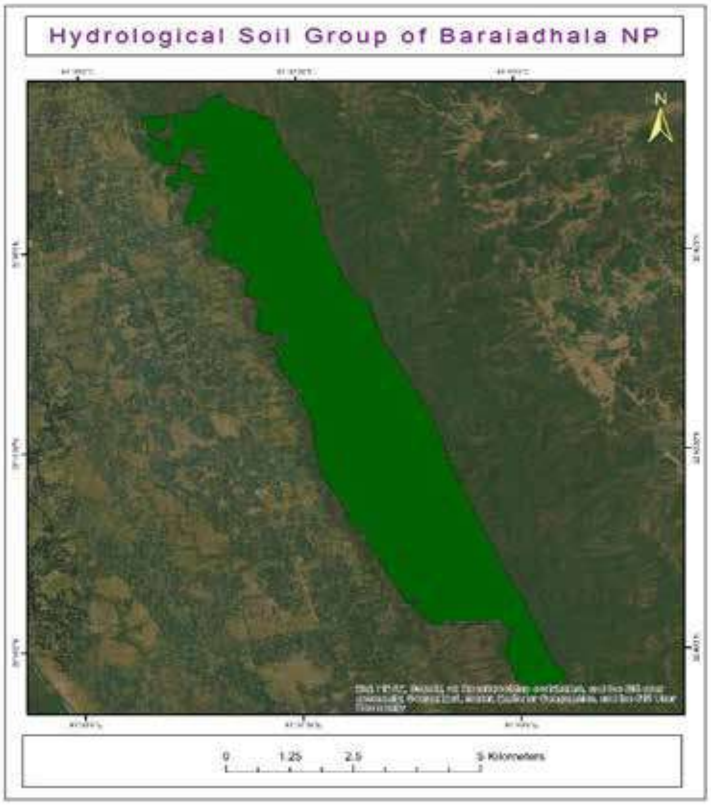

Figure 48: Hydrological Soil Group

Table 16. Identified classes of hydrologic soil groups (HSGs) in Baraiadhala National Park

HSG	Soil texture class	Runoff potential	soilGrids250m texture class value
C	Clay loam, Silty clay loam, Sandy clay loam, Loam, Silty loam, Silt	Moderately high	4, 5, 6, 7, 8, 10

4.7.2 Land Use Land Cover

The 2015 land use and land cover data of Bangladesh, derived from the last Bangladesh Forest Inventory, has been used in this study. There are five land cover classes has been identified, which were extracted by masking the study area using ArcMap 10.8 (**Table 17**).

Table 17. Land use land cover areas of BdNP

CLASS NAME	Area_SqKm	Area_SqKm (%)
Forest plantation	0.05674	0.1949
Lake/waterfall reservoir	0.01138	0.0391
Mixed hill forest	11.9453	41.0308
Shrub dominated area	16.9786	58.3194
Single crop Is it agriculture?	0.12105	0.41578
Total	**29.1131**	**100**

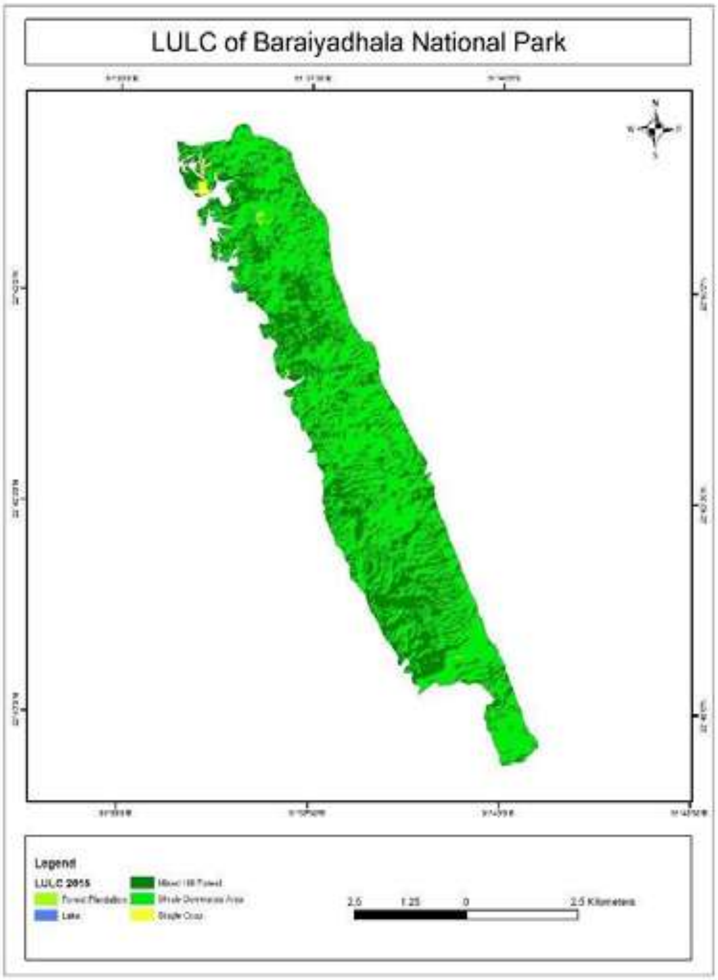

Figure 43: LULC of BdNP

4.7.3 Watershed Basin Area Delineation Digital Elevation Model (DEM)

Fill

Fills sink in a surface raster to remove small imperfections in the data.

- A "sink" denotes a cell within a digital elevation model lacking a defined drainage direction, with no surrounding cells of lower elevation. The "pour point" corresponds to the boundary cell with the lowest elevation within the contributing area of a sink, simulating the outlet where water would flow if the sink were filled.

- The "z-limit" parameter establishes the maximum allowable disparity between the depth of a sink and its pour point. This criterion dictates which sinks will undergo filling operations and which will remain unaffected. Notably, the z-limit does not determine the maximum depth to which a sink may be filled.
- To illustrate, envision a sink area where the pour point stands at an elevation of 210 feet, while the deepest point within the sink descends to 204 feet, resulting in a 6-foot discrepancy. If the z-limit is set at 8, the sink will undergo filling. However, should the z-limit be reduced to 4, the sink would remain unfilled, as its depth surpasses this designated threshold and is considered a valid sink.
- All sinks with depths less than the z-limit and situated lower than their lowest adjacent neighbor will be filled up to the elevation of their respective pour points.

When the filling process is complete, a new grid is added to the data frame in the map document. There would be a difference in the lowest elevation value between the original DEM and the filled DEM.

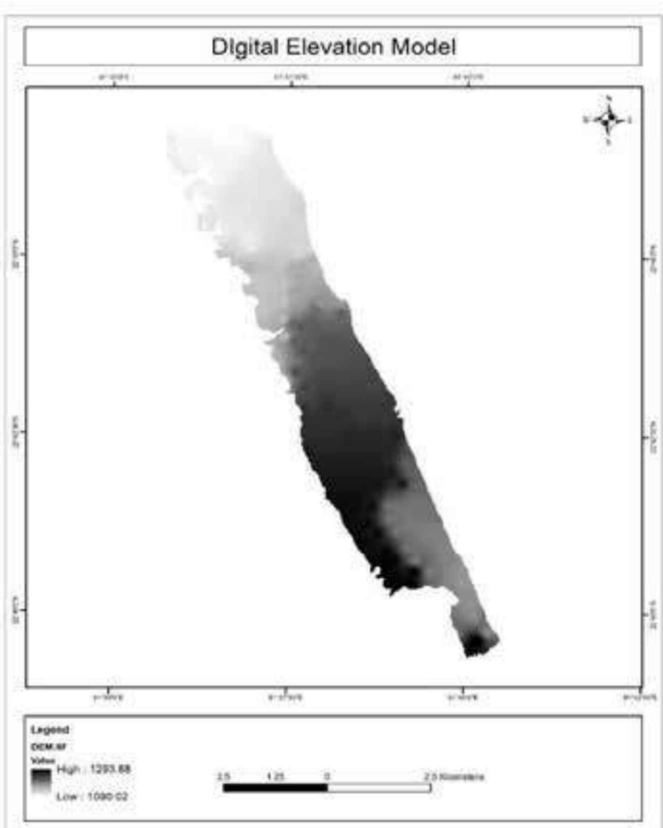

Figure 44: Digital Elevation Model (DEM)

4.7.4 Flow Direction

Understanding the direction of flow for each cell is imperative, as it dictates the trajectory of water movement across the terrain. This involves generating a raster representation of flow direction, wherein each cell is linked to its downslope neighbor(s) through methodologies such as D8, Multiple Flow Direction (MFD), or D-Infinity (DINF). In this process, a flow direction grid assigns a directional value to each cell, indicating the anticipated path of water flow based on the underlying topography. This step holds significant importance in hydrological modeling, as it determines the eventual destination of water. traversing the land surface. In this study, the D8 method has been applied**.**

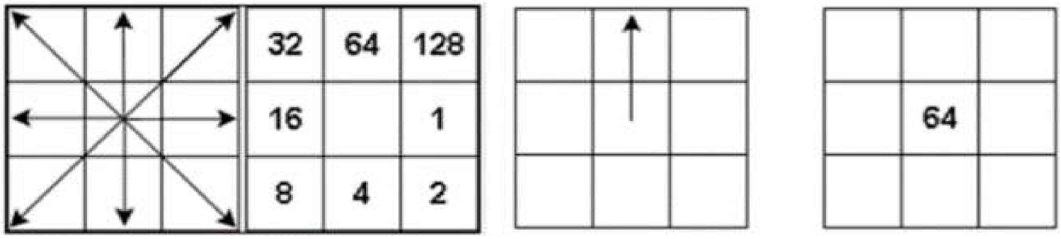

Figure 45: Flow Direction Model

4.7.5 Acquisition of rainfall data

NASA's POWER (Prediction of Worldwide Energy Resources) project provides access to various meteorological and climatological datasets, including rainfall data. The rainfall data available through NASA's POWER project typically includes gridded datasets derived from satellite observations, reanalysis data, and ground-based measurements. These datasets offer spatial and temporal coverage at different resolutions and time intervals, allowing users to analyze rainfall patterns and variations across different regions and periods. Researchers, scientists, and policymakers utilize NASA's POWER rainfall data for a wide range of applications, including hydrological modeling, drought monitoring, agriculture, and climate studies. Rainfall data of 2023 in Baraiardhala National Park has been downloaded from Access to NASA's POWER rainfall data through the POWER Data Access Viewer (https://power.larc.nasa.gov/data-access-viewer/) by taking a point in the middle of the study area. Total rainfall has been calculated as 3203.04 mm in 2023. These data are used to calculate Q.

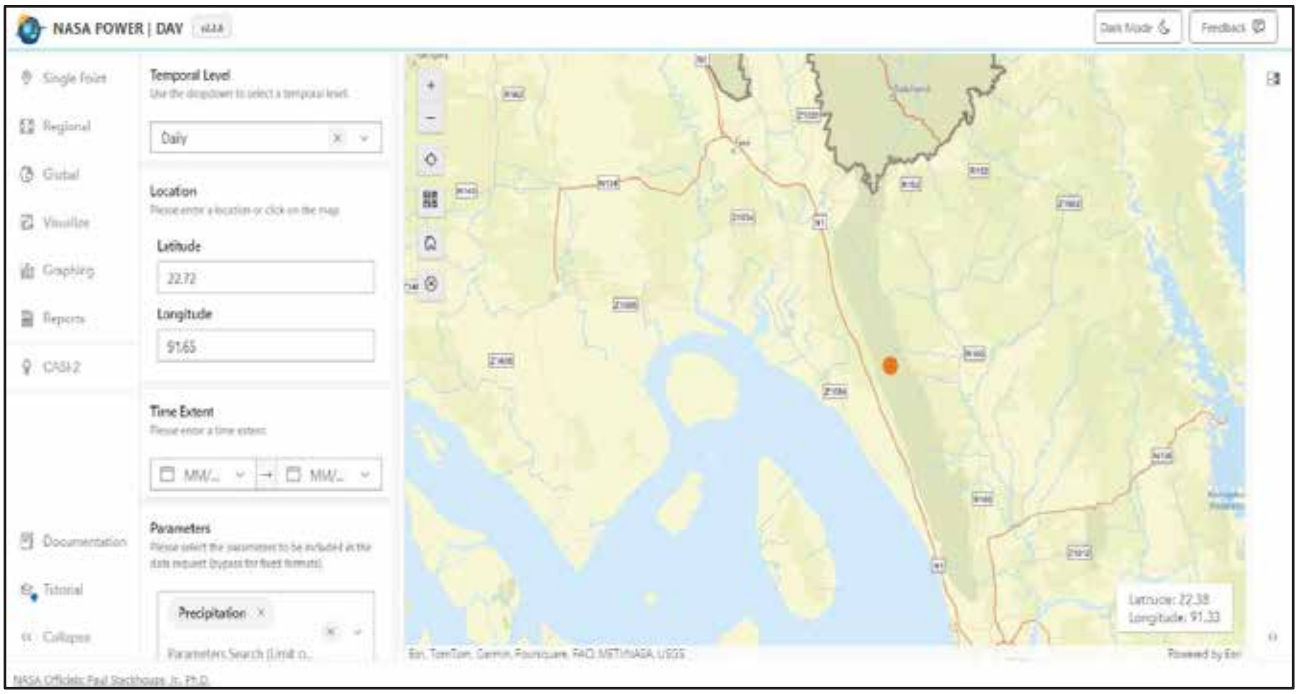

Rainfall and runoff play pivotal roles in hydrological assessments of water resources. While various methods exist for estimating runoff from rainfall, the Soil Conservation Service Curve Number (SCS-CN) method stands out as the most prevalent and widely utilized approach. The SCS-CN method hinges on the runoff curve number (CN), a critical parameter dependent on factors such as land use/land cover (LULC), soil type, and antecedent soil moisture (AMC). Additionally, essential inputs to the SCS-CN model encompass Hydrological Soil Characteristics (HSG), precipitation (P), and Weighted Curve Number (WCN). In this study, the daily runoff data for the Baraiardhala National Park basin spanning 2023. The results reveal an average annual surface runoff of 33.18 mm, followed by a Minimum of 0.004147 mm, a Maximum of 287.132869 mm, and a total of 6171.135 mm for the Baraiardhala National Park basin.

Table 18: AMC class-wise value, Total 5-day Antecedent Rainfall

AMC Class	Soil Characteristics	Total 5-day Antecedent Rainfall (mm)		
		Dormant Season	Growing Season	Average
AMC-I	Soils are dry not to wilting point, Cultivation has taken place	< 13	< 36	< 23
AMC-II	Average Condition	13-28	36-53	23-40
AMC-III	Heavy or light Rainfall and low temperatures have occurred within the last 5 days; saturated soils	> 28	> 53	> 40

4.7.6 Vegetation Change 2000 - 2024

The year-wise average of NDVI-min values presents a fluctuating pattern indicative of vegetation activity across the years. Negative values in 2001, 2006, and 2007 suggest periods of decreased vegetation cover during those years, possibly influenced by environmental stressors or land management practices. However, from 2010 onwards, there's a notable increase in the average NDVI minimum values, indicating healthier vegetation cover during the least productive periods. This upward trend suggests potential improvements in overall vegetation health and density, possibly attributed to more favorable environmental conditions or enhanced land management strategies. The peaks observed in 2022 and 2024 suggest particularly robust vegetation activity during those years, highlighting potential periods of optimal growth and ecosystem resilience. Understanding the drivers behind these fluctuations can provide valuable insights into ecosystem dynamics and inform future conservation and management efforts.

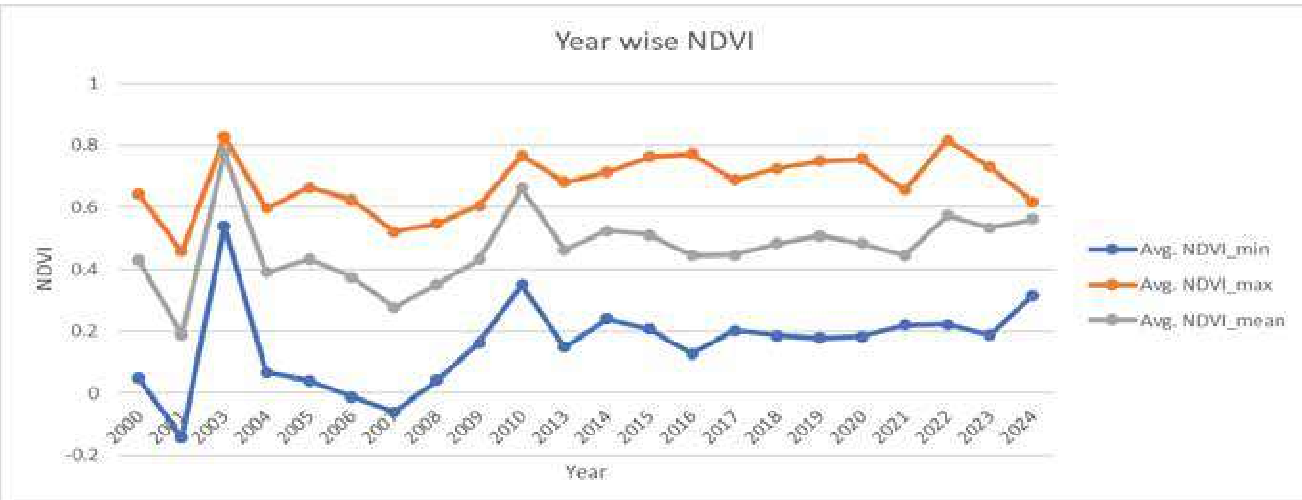

Figure 46: Year wise NDVI

The five-year average NDVI (Normalized Difference Vegetation Index) values—minimum, maximum, and mean—offer valuable insights into the trends of vegetation health and density over time. Between 2000 and 2005, the NDVI minimum averaged at a low 0.026, indicating sparse vegetation during the least productive seasons. A slight increase to 0.044 in 2006–2010 suggests modest improvement. A substantial rise occurred in 2011–2015, with a minimum of 0.207, pointing to improved vegetation cover, followed by a slight dip to 0.176 in 2016–2020. However, vegetation remained healthier than in earlier years, and the upward trend continued from 2021 to 2024 with a minimum value of 0.212. The NDVI maximum values reflect the periods of peak vegetation vigor. From 2000 to 2005, the average was 0.603, which dipped slightly to 0.581 in 2006–2010. A sharp increase followed, with values reaching 0.726 in 2011–2015 and 0.738 in 2016–2020. The latest period, 2021–2024, recorded the highest value of 0.743, indicating steadily increasing vegetation vitality. Mean NDVI values offer a balanced view of vegetation health. The average was 0.380 in 2000–2005 and slightly decreased to 0.369 in 2006–2010. A marked improvement occurred in 2011–2015 (0.505), with continued strength in 2016–2020 (0.472) and a further rise to 0.530 in 2021–2024. Overall, these NDVI trends reveal long-term improvement in vegetation conditions, likely influenced by changing environmental factors, improved land use practices, and possibly climate change adaptation measures.

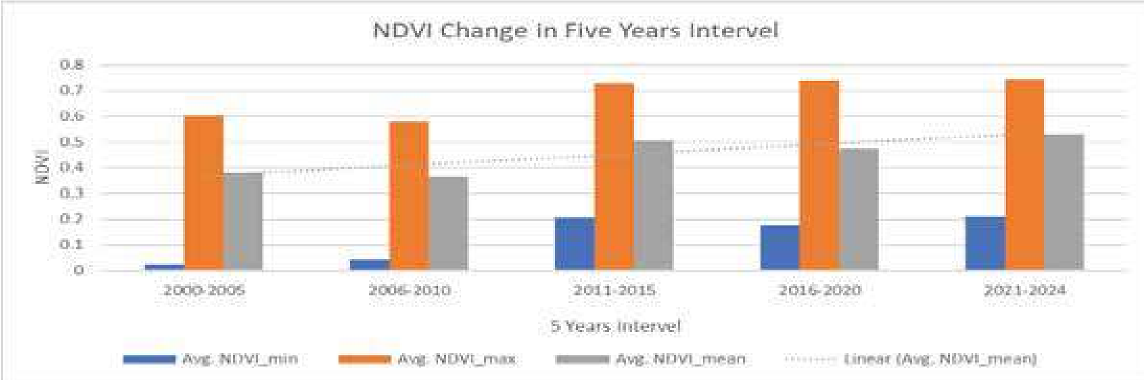

Figure 47: Change of NDVI in a five-year intervals

CHAPTER FIVE

CONCLUSIONS AND RECOMMENDATIONS

5.1 Conclusions

Baraiadhala National Park (BdNP), being a hub of diverse natural and historic resources, deserves special and immediate attention to conserve the existing flora and fauna, especially Cycas and Wild Serow habitat, natural beauty of waterfalls, as well as the safety and security of the tourists visiting the different waterfalls of the park. Hence, a Master Plan followed by a complete Development Project Proposal (DPP) for 20 years may be developed for the BdNP.

5.2 Recommendations

5.2.1 Restoration of the degraded forests of BdNP

1. Bangladesh Forest Department (BFD) has to ensure the protection of the existing forest resources of flora, fauna, soil, water, etc. of BdNP ecosystems,
2. Social forestry/Participatory Forest plantations (*Acacia auriculiformis, Eucalyptus camaldulensis*) have to be felled/replaced (due to over maturity or commitment to the participants to comply with social and legal obligations) with indigenous tree species,
3. Silvicultural operations like climber cutting and sanitation cutting only may be allowed for certain areas or individual tree populations,
4. Entrance of the tourists/visitors should be limited to tourist zones, especially along the waterfall courses, to avoid human interference in the interior forest areas. Indiscriminate movement of tourists may disturb the growth of regenerations/seedlings, suppress the undergrowth, and disturb wildlife (mammals, birds etc.).
5. Vacant or poorly stocked areas may be restored through ANR or enrichment plantations with indigenous tree species, and habitat conservation of the available wildlife.
6. Alternative Income Generation (AIG) activities may be developed to divert the forest-dependent people from extracting forest resources. CMC, CPG, and forest-dependent people may be involved in AIG activities.
7. A restoration plan with detailed activities needs to be developed for the conservation of the resources and bringing back the native species to their site. The ROAM model may be practiced considering the suitability and adaptability to the site.

5.2.2 Conservation of Threatened Plant Species in BdNP

1. Bangladesh has put in place mechanisms to ensure its resources are sustainably managed and effectively conserved through policy and legislative framework, research and development programs,
2. In the conservation of biological diversity, the combination of *in situ* and *ex-situ* conservation measures has to be given priority.
3. BdNP biodiversity may address the issues of the Global initiatives for reducing loss of biodiversity in alignment with the National Conservation Strategy 2021-2036, Biodiversity Strategy and Action Plans and Sustainable Development Goal 15.

5.2.3 Waterfall and Risk Zone Management

1. Tourists' movement should be confined to a planned route of the trail and the waterfall courses.
2. Identify and locate the risk/danger spots – with a red circle/red line, demarcate with proper signage/signboard, and update before every rainy season to avoid unexpected death/injury of the tourists.
3. Install more than one heavy barrier around/along the risk spots/routes with clear signs of indication.

4. Create/develop/maintain alternative routes/walkways as an alternative route to travel the area.
5. Excavate/dig/make steps as per requirement, even construction of RCC/PCC structures at specific areas,
6. Arrange rope lines/ rope along the steep slope, and change/maintain them in every rainy season.
7. Construct an Observation Deck closer to the waterfall to discourage the tourists from the hidden risk/death spots of the waterfall areas and enjoy the flow of water from the waterfall/sound of falling water. 8. Structures like roads, stairs, shade, changing rooms, and washrooms nearer the waterfall may also be constructed.
9. Prepare/develop a group of local tour guides and engage them as tour guides, and make it compulsory during the heavy rainfall,
10. Employ/depute watcher/guide/special caretaker at the spots on a rotation basis to help the tourists during the whole rainy season. It may be included as a condition of tender documents for the bidders,
11. Ensure some internet facilities nearer to the waterfall area. Develop Apps for the tourists and install the App on the mobile phone of the tourists during entry at the waterfall area. Provision will be made to see/hear the signal before entering/crossing the danger spots,
12. Precautionary instructions may be given during the purchasing ticket/entrance to warn the tourists about the location of the risky spot/area and the potential threat of the waterfall areas. Restrict tourists' movement at the waterfalls during the heavy rainfall period.
13. Along with the Forest Department, the Fire brigade and Police officials may be involved in ensuring security, safety, and rescue operations of tourists during emergencies, and keep the Police/Fire Brigade Officials alert and engaged during the rainy season at the center of the waterfall areas.
14. Ensure monitoring of the activities of the BFD officials/ Tenderer engaged in tour management at the waterfall areas.

5.2.4 Cycas Management

1. Ensure awareness campaigns about natural Cycas in and around the Baraiyadhala National Park area,
2. Prepare a complete spatial map of the Cycas population by counting individual populations,
3. Ensure engagement of watchers at the vulnerable sites during the dry season (December to March) to avoid the fire hazard of CYCAS.
4. Create fire lines at appropriate locations and keep them clean during dry seasons.
5. Involve the local community/CPG to assist BFD in protecting the Cycas in its native ranges, and
6. Open code for species conservation or ensure a special budget for Cycas conservation in BdNP areas,
7. Development of a local-level action plan for Cycas management.

5.2.5 Eco-tourism Facility

1. **Local people's commitment**: Measures should be adopted to encourage community involvement in ecotourism with emphasis on forest conservation. Visitors suggest community education programs, awareness material circulation, ecotourism training, and incentives for local participation in conservation efforts.
2. **Infrastructure development**: Constructing information centers, interpretation centers, gates, ticket counters, washroom facilities, souvenir shops, parking spaces, and accessible facilities for disabled individuals is a requirement of the site.
3. **Ensure security**: The Authority should ensure visitors' privacy, safety, and security. They must take required measures, including patrols, emergency response services, and raise awareness about safety precautions.
4. **Installing road map/sign board**: Most visitors want clear, informative signage for visitor orientation and safety, suggesting multilingual options, local flora and fauna information, and the installation of maps and trail guides.
5. **Ensure quality food**: Facilities for safe and healthy food with reasonable prices around the park need to be ensured.

6. **Providing tour guides**: Eco-guides can enhance the visitor's experience and promote environmental education. This provision would offer valuable information about natural heritage.
7. **Connectivity**: Visitors emphasize improving connectivity, easy and safe accessibility, e.g., improving public transportation facilities. Network and Linkage with other nearby tourist spots may be circulated to attract visitors and utilize the visitors' time.
8. **Mobile apps and tracking system**: The authorities can prepare a mobile application to track visitors' location during their stay in the park. This would also allow forest personnel to track whether visitors face any problems.
9. **Visitor management capacity**: The authority should determine the carrying capacity to prevent overcrowding. This approach also offers a quality experience for visitors and helps management minimize environmental impacts.
10. **Develop waste management facilities**: The authority must have effective waste management to minimize negative environmental impacts. They should maintain the park by providing adequate waste bins and collection points.
11. **Building eco-cottages, eco-resorts, and eco-bridges**: Visitors want eco-cottages, eco-resorts for night stay. This issue may be addressed after a thorough study.

5.2.6 Water Management

Despite Baraiadhara National Park possessing several natural waterfalls, the local community experiences significant challenges with drinking water, water for agricultural activities, and industrial development. Local communities and wildlife around the forest area could face water scarcity during dry seasons. The rapidly growing industrialization in Sitakunda and Mirsarai accelerates the immense pressure on local water resources. The authorities should think of a potential solution for the wise use of water resources.

Bawachora, Shahasradhara, and Shonaichora are the largest waterfalls, including some smaller ones that should be converted into water reservoirs. The Shonaichora Hydro project in East Polmogra has completed construction with financial assistance from Bangladesh, the Asian Development Bank, and the Netherlands. People's perception of the dam is positive, and they also pay for water use. However, there is a concern about the future benefits of these huge, invested projects.

The water demand around the area is primarily driven by agriculture, industries, domestic uses, and ecological conservation. For example, water-intensive industries like textiles, garments, food processing, chemical and pharmaceuticals, and cooling require water for various processes. Understanding these specific water demands is crucial for sustainable management and distribution. Considering these circumstances, the authorities would think about the following options.

1. The authority could assess the expected benefits of the establishment of dams. They could work to increase the utilization of the water resources from the existing dams.
2. Authorities could establish eco-friendly reservoirs around the area, and even water traps at different locations. These reservoirs and traps would save water from streams and rainy seasons and increase groundwater recharge to ensure water availability during dry seasons and minimize the risk of over-extraction and depletion.
3. Rainwater harvesting/storing mechanisms may be developed to utilize the water for agricultural as well as industrial purposes.
4. Authorities could also consider a "pay for use" scheme for community, agricultural, and industrial uses. The pay distribution could be different depending on the basic and commercial uses. In addition, industries need to stop extracting groundwater to conserve the ecology of the area.
5. A water management committee may be formed/reformed to wisely use and manage the water distribution system.

REFERENCES

GoB (Government of Bangladesh). 2020. Tree and Forest Resources of Bangladesh: Report on the Bangladesh Forest Inventory. Forest Department, Ministry of Environment, Forest and Climate Change, Government of the People's Republic of Bangladesh, Dhaka.

Haider, R., Saifullah, M., & Alam, M. S. (2022). *Ethnomedicinal plants of Chittagong Hill Tracts in Bangladesh.* Bangladesh Agricultural Research Council; Bangladesh Forest Research Institute.

Harun-Ur-Rashid, M., Islam, S., & Kashem, S. B. (2018). Floristic diversity (Magnoliids and Eudicots) of Baraiyadhala National Park, Chittagong, Bangladesh. Bangladesh J. Plant Taxon., 25(2), 273–288. https://doi.org/10.3329/bjpt.v25i2.39532

Hasan, M. K., Saha, A., Datta, A. K., Begum, S., Nahid, M. I., Roy, A., & Debbarma, P. (2024). Heterogeneous habitat supports cryptic diversity of the terrestrial mammalian community in a protected forest of Bangladesh. Community Ecology, 1–13. https://doi.org/10.1007/s42974-024-00219-0

Hossain, M. K. (2015). Protected Area Management Plan for Hazarikhil Wildlife Sanctuary and Baraiyadhala National Park 2016-2025. Bangladesh Forest Department. https://www.google.com/url?sa=t&source=web&rct=j&opi=89978449&url=http://bfis.bforest.gov.bd/library/wp-content/uploads/2018/10/HWS-BNP-Management-Plan-Final.pdf&ved=2ahUKEwjG34jAocuKAxVMW0EAHRk1B-UQFnoECBUQAQ&usg=AOvVaw23RjIQirroSApFe1Onjaur

Hossain, M. K., Hossain, M. A., Hossen, S., Rahman, M. R., Hossain, M. I., Nath, S. K., & Siddiqui, M. B. N. (2021). Status and conservation needs of *Cycas pectinata* Buch.-Ham. in its natural habitat at Baroiyadhala National Park, Bangladesh. *Journal of Threatened Taxa, 13*(8), 19070-19078. https://doi.org/10.11609/jott.5922.13.8.19070-19078.

Jalal, M. A. H. S., Haider, R., Melon, M., Rahman, M. M., Alam, S., Alam, S. M. R., Hossain, M. K., & Hossain, M. A. (2020). Valuation of ecosystem services in Baraiyadhala National Park, Bangladesh (Bulletin 05). Bangladesh Forest Research Institute. https://www.google.com/url?sa=t&source=web&rct=j&opi=89978449&url=https://bfri.portal.gov.bd/sites/default/files/files/bfri.portal.gov.bd/page/145fcf41_ef67_4402_a4a0_83e3fba112e9/2021-04-12-05-55-3b840b2ddbba55c1a7cfd76ee8037d00.pdf&ved=2ahUKEwjG34jAocuKAxVMW0EAHRk1B-UQFnoECBcQAQ&usg=AOvVaw2cIGnXPTt6xy2emQ3-opxF

Karim, M. R., Ahsan, M. F., Uddin, S. B., & Rahman, A. S. M. S. (2023). Plant diversity of the Baraiyadhala National Park in Chattogram, Bangladesh. American Journal of Plant Sciences, 14, 357–376. https://doi.org/10.4236/ajps.2023.143024

Karim, R., & Ahsan, F. (2016). Mammalian fauna and conservational issues of the Baraiyadhala National Park in Chittagong, Bangladesh. Open Journal of Forestry, 6, 123–134. https://doi.org/10.4236/ojf.2016.62011

L. Calvo, F. Ogden, J. Hendrickx. "Infiltration in the Upper Río Chagres Basin, Panamá: The Soil Conservation Service Curve Numbers". The Río Chagres: A Multidisciplinary Profile of a Tropical Watershed. R. Harmon (editor). Ed. Kluwer Acad. Pub. New York (USA). 2005. pp. 139-147.

Nguyen, H. T. (2010). *Cycas pectinata: The IUCN Red List of Threatened Species 2010*. International Union for Conservation of Nature and Natural Resources. http://dx.doi.org/10.2305/IUCN.UK.2010-3.RLTS.T42062A10617695.en

Pasha, M. K. (2012). Gymnosperms & paleobotany. Janokalyan Prokashani.

Prabhu, Nanjundi & Kumar, T M Mohan & Inayathulla, Dr. (2020). Runoff Estimation for Arkavathi Valley, Hebbala Valley, KC Valley, South Pennar Valley, Vrishabhavathi Valley by using Soil Conservation Services Curve Number Method (SCS-CN). Water and Energy International.

Pradhan, A., & Chettri, A. (2017). Identifying protected areas suitable for conservation of *Cycas pectinata* Buch. Ham. in Southeast Asia under climate change scenario. *International Journal of Ecology and Environmental Sciences, 43*(2), 129-135.

Quijano, I. P., Valenzuela, J., Carredo, R. S., Patiño, C., & Sinogaya, J. (2015, October). Vulnerability assessment of government buildings in sagay city through flood modeling and mobile GIS. In *36th Asian Conference on Remote Sensing: Fostering Resilient Growth in Asia (ACRS 2015)* (pp. 19-23).

R. Hawkins, A. Hibbert. "Initial abstraction and loss in the curve number method". Water Resour. In Arizona and the Southwest. Vol. 30. 2000. pp. 29-35.

Ross, C.W., L. Prihodko, J.Y. Anchang, S.S. Kumar, W. Ji, and N.P. Hanan. 2018. Global Hydrologic Soil Groups (HYSOGs250m) for Curve Number-Based Runoff Modeling. ORNL DAAC, Oak Ridge, Tennessee, USA. https://doi.org/10.3334/ORNLDAAC/1566

Rouse, J. W., Jr., Haas, R. H., Deering, D. W., Schell, J. A., 1973. Monitoring the vernal advancement and retrogradation (green wave effect) of natural vegetation: Progress Report RSC 1978-2. Available online: http://ntrs.nasa.gov/archive/nasa/casi.ntrs.nasa.gov/1974 0004927.pdf

Siddiqui, K. U., Islam, M. A., Ahmed, Z. U., Begum, Z. N. T., Hassan, M. A., Khondker, M., Rahman, M. M., Kabir, S. M. H., Ahmad, M., Ahmed, A. T. A., Rahman, A. K. A., & Haque, E. U. (Eds.). (2007). *Encyclopedia of flora and fauna of Bangladesh,* Vol. 5. *Bryophytes, Pteridophytes and Gymnosperms.* Asiatic Society of Bangladesh.

Singh, K. J., & Singh, R. (2014). Population assessment and distribution of *Cycas pectinata* Buchanan-Hamilton in Northeast India. *Pleione, 8*(1), 17-25.

Tobgay, S., Wangdi, T., Wangchuck, K., Dolkar, J., & Nidup, T. (2023). Assessment of population, habitat, and threats to *Cycas pectinata* Buch.-Ham. (Cycadaceae), a vulnerable cycad in Bhutan. *Journal of Threatened Taxa, 15*(3), 22866-22873. https://doi.org/10.11609/jott.7809.15.3.22866-22873

Uddin, M. S., Lee, S. W., Uddin, S. B., Oh, S.-R., Choi, S., Lee, C., Kim, J., Bae, D. Y., & Park, J. K. (Eds.). (2016). *Ethnomedicinal plants of Bangladesh.* IBMRC; KRIBB.

Uddin, S. N., & Hassan, M. A. (Eds.). (2018). *Vascular flora of Chittagong and the Chittagong Hill Tracts,* Vol. 1. *Pteridophytes, Gymnosperms & Liliopsida.* Bangladesh National Herbarium.

Providing soil macro-nutritional information to support decision making in forest management of Bangladesh.

by
Chameli Saha
Assistant Professor, Forestry and Wood Technology Discipline, Khulna University, Khulna -9208

CHAPTER 1

1. INTRODUCTION

1.1 Problem Statements

Bangladesh is a densely populated country with about 17.5% of forest cover (Arannayk Foundation, 2019). These forest areas and its' resources are under immense pressure to meet the demand of wood, fuelwood, and fibers for the society and conversion of forestland to other land use. On the other hand, the Government of Bangladesh (GoB) has taken policies and initiatives to be a middle-income country by 2021. Consequently, Bangladesh has given more emphasis on industrialization and other service-oriented business. Collectively all these issues are significantly influencing the environment and extent of forest cover. Therefore, it is very challenging for the Bangladesh Forest Department (BFD) to increase the forest cover through afforestation/ reforestation; conservation, and sustainable management of forests; reduce degradation and deforestation as stated in SDGs by 2020 to 2030. But, BFD has committed to increase the percentage of forest cover and to manage the existing forests in a sustainable way. BFD is planting indigenous and exotic tree species in the fallow and marginal land, newly accreted coastal land, degraded and denuded forest lands throughout the country since 1989 under different projects. Presently, BFD wanted to cover about 1800 ha of land under plantation with the support of SUFAL project in a different array of land types (plantation in newly accreted char lands; denuded, heavily degraded and less degraded forest land of Hill and Sal Forest). However, the selection of tree species in the potential planting sites will be challenging to ensure restoration success and sustainable production. However, BFD has little scope to select the site-specific tree species considering the soil physical and nutrient properties. Very recently, BFD has measured bulk density, soil texture, and organic carbon content of forest soil during the BFI (Bangladesh Forest Inventory) activities with the technical support of FAO. Until today, we do not have much information on the chemical/ nutrient properties of the forest soil of Bangladesh. However, planting of site-specific tree species and rotation of tree species is very important for achieving the sustainable productivity in production forestry (Kimmins, 1987). The influence of tree species on soils has been of scientific interest for decades. In the early 20th century, the influence of trees on soil development was well recognized. Conversely, ideal growth and development of trees strongly depend on the physical and chemical properties of the soils (Remezov and Pogrebnyak, 1969).

The chemical analysis of plant tissue explains that carbon (C), hydrogen (H), and oxygen (O) constitute about 90-95% of the dry weight. The other elements constitute on the average 5-10% of the dried plant material and are the soil's contribution to the growth of the plants: nitrogen (N), phosphorus (P), potassium (K), calcium (Ca), magnesium (Mg), and sulfur (S), which are considered as macronutrients, and manganese (Mn), iron (Fe), zinc (Zn), copper (Cu), boron (B), chlorine (Cl), and molybdenum (Mo), which are called micronutrients due to their requirement at lower quantities in the tissue in comparison with the macronutrients (Alvarado, 2015). Plant uptake these nutrients from the soils for its' normal growth and development. The requirements of these nutrients are not the same for all tree species. Some tree species may absorb higher or lower quantities of a nutrient or a group of nutrients compared to other tree species (Meyer, 1973; Marschner 1986). Moreover, different types of soil have different levels of nutrients. The level of soil nutrients is highly influenced by the physical and biological properties of a particular soil. This indicates that a particular soil is not able to support all tree species or a single species for a longer time (Mahendrappa et al., 1986). The plant-available/ total form of nutrients largely depends on soil texture, organic matter content, acidity (pH), salinity (EC), shallowness, stagnating water, cation exchange capacity (CEC). Therefore, available/total forms of essential nutrients and some physio-chemical properties of forest soil like (soil texture, pH, EC, OM, OC, and CEC) must be known before initiating any plantation for the production of wood, fiber, etc. In addition, the assessment of soil properties can also describe the site quality for establishing a plantation and restoration of natural forests (Alvarado, 2015). Thus, besides nutrients, a good number of soil properties may appear as the limiting factors for successful forest stand, its healthy growth, and productivity (Chanan et al., 2018). Naturally, forest productivity is seen to decrease with the decreasing level of nutrients in forest soil (Hardiwinoto et al., 2013; Chanan et al., 2018). Considering this discussion, it can be suggested that a database on soil physical and nutrients properties for the potential planting sites and BFI plots of Hill and Sal forests of Bangladesh will be helpful for decision making on species choice for afforestation/reforestation, future monitoring of the site quality for sustainable production, better management, carbon sequestration, climate change mitigation measures and biodiversity conservation.

1.2. Objectives

The specific objectives

- Develop a database of soil pH, EC (Electrical Conductivity) and soil nutrients (nitrogen, phosphorus, potassium and calcium), for the Hill, and Sal forests using BFI soil samples
- Develop a database of soil physiochemical parameters (bulk-density, soil texture and organic carbon, pH and Electrical Conductivity) and soil nutrients (nitrogen, phosphorus, potassium and calcium), for the potential planting sites under SUFAL project located in Hill, and Sal forests
- Develop nutrient maps for the Hill and Sal forests at the landscape or forest division or range level as appropriate.
- Species recommendation for the Hill and Sal zones.

1.3. Research questions

- What is the baseline information/ data on soil physiochemical and nutrient content of the Hill and Sal forests of Bangladesh to support forest management decision to ensure sustainable production of forest produces, species selection in plantation forestry, enhance carbon sequestration as climate change mitigation measures?

CHAPTER II

2. LITERATURE REVIEW

2.1 Hill Forests

Hill Forest is one of the major forest types in Bangladesh, located in hills and hilly areas (Akhtaruzzaman et al., 2014). These forests are composed of tropical evergreen and semi-evergreen vegetation. The forests are located in the Rangamati, Bandarban, and Khagrachari Hill Tracts, as well as in the districts of Chittagong, Cox's Bazar, Sylhet, Maulvi Bazar, and Habiganj (Feroz et al., 2016). These areas encompass approximately 1.40 million hectares, with 0.67 million hectares managed by the Forest Department. The remaining 0.73 million hectares consist of unclassed state forest, which is under the jurisdiction of the Hill District Councils.

2.1.1. Climatic and soil characteristics of Hill Forest

Bangladesh's hill forests, especially in the CHTs, have a subtropical monsoon climate with significant seasonal variations. The monsoon season brings heavy rainfall of 4000 mm and temperatures ranging from 15°C in winter to 33°C in summer (Moslehuddin et al., 2018). Hill forests' unique ecological dynamics, including vegetation and challenges, are influenced by this climate. Climate change, shifting cultivation, and unauthorized settlements worsen deforestation and land degradation in hill forests (Nadiruzzaman et al., 2024; Farukh, 2023). These activities have increased vulnerability to natural disasters like landslides and wildfires, especially during the dry-to-wet season (Jafrin et al., 2023; Farukh, 2023). These forests are significant carbon sinks, storing organic carbon per tree and unit area, but climate change favors low-biomass plants over slow-growing, high-density trees (Alamgir & Turton, 2013). Poor plant diversity and exotic species reduce hill forests' natural regeneration potential and climate resilience (Bhuiyan et al., 2019).

In Bangladesh's Hill Forest, especially in Cox's Bazar and the Chittagong Hill Tracts, topography, land use, and vegetation types affect soil physical and chemical properties. These hilly soils are strongly acidic with pH values of 4.44 to 5.52 and coarse, with sand fractions ranging from 38% to 73% (Akhtaruzzaman et al., 2014; Biswas et al., 2012). The soils have low exchangeable bases and base saturation and low organic carbon content (0.26% to 1.73%) (Akhtaruzzaman et al., 2014). These soils have higher bulk densities in shifting cultivation areas than in forests (Biswas et al., 2012). Forests have higher concentrations of organic matter, nitrogen, phosphorus, and potassium than agricultural or barren lands due to litter deposition and stand structure (Biswas et al., 2012). DTPA extractable micronutrients like Fe, Mn, and Cu are abundant in the soils, but Zn availability varies (Akhtaruzzaman et al., 2016). However, only 4% of sampling points have a humus layer, indicating a need for soil quality improvement (Mahmood et al., 2021). The sedimentary soils and steep slopes make them prone to erosion, which is exacerbated by deforestation and land use changes (Islam & Islam, 2018). These areas benefit from vetiver-based soil erosion and landslip mitigation (Islam & Islam, 2018). In general, sustainable land management practices are needed to maintain soil fertility and ecological balance in Bangladesh's Hill Forest (Akhtaruzzaman et al., 2014; Biswas et al., 2012).

2.2 Sal Forest

Sal (Shorea robusta) forests are an important vegetation type in Bangladesh, providing crucial ecological services and supporting numerous plant and animal species. According to a study, the Sal forests in Bangladesh are primarily located in the northwestern region and cover an area of approximately 80,000 hectares (Rahman et al., 2010). The topographical features of these forests are diverse, ranging from lowlands to hilly terrain. The species composition of the Sal forests in Bangladesh is quite rich, with the dominant species being Sal trees along with its associate species Chakua Koroi (Albizia chinensis), Koroi (Albizia lucidor), shimul (Bombax ceiba), udal (Sterculia villosa) and other three site suitable species e.g. Neem (Azadirachta indica), Teligaijan (Dipterocarpus turbinatus), Dhakijam (Syzygium firmum) forms dominant mono-specific canopies in dry deciduous and moist deciduous forests). The undergrowth of these forests is dominated by shrubs, climbers, and herbaceous plants. The vegetation structure and species composition of these forests have been influenced by natural and anthropogenic factors, including human disturbance, fire, and grazing pressure (Siddique, 2022). However, despite the ecological significance of these forests, they are facing numerous threats, including deforestation, over-exploitation of forest resources, and degradation due to various human activities (Islam et al., 2022). But, the Sal forests of Bangladesh play a crucial role in supporting biodiversity and ecological services in the region. However, it is imperative that appropriate measures are taken to address the current threats and protect these valuable ecosystems.

2.2.1. Soil characteristics of Sal Forest

The soil physical properties of the Sal Forest in Bangladesh have been studied by several researchers to better understand the conditions that support vegetation growth in this region. One study by Habibur et al. (2012) effects of land-use change on the properties of top soil of deciduous sal forest in Bangladesh. The authors found that the soil in these forests had a high proportion of sand and silt particles, with a low content of clay particles. The average bulk density was found to be 1.30 g/cm3, and the porosity of the soil ranged from 53.83% to 57.57%. Additionally, the soil moisture content was found to be within the optimal range for plant growth, with values ranging from 10.23% to 17.17%. Another study by Rahman et al. (2012) investigated the soil physical and chemical properties of the Sal Forest in Bangladesh and compared them to adjacent agricultural lands. The authors found that the soil in the Sal Forest had a higher proportion of sand and silt particles, lower bulk density, and higher porosity compared to the agricultural lands. Additionally, the soil in the Sal Forest had higher organic matter content and lower levels of heavy metals. So, the soil physical properties of the Sal Forest in Bangladesh have been thoroughly studied and characterized by multiple research groups. The findings of these studies indicate that the soil in these forests is favorable for vegetation growth, with optimal particle size distribution, bulk density, and soil moisture content. This information is valuable for forest management and conservation efforts in Bangladesh.

The soil chemical properties of the Sal Forest in Bangladesh have been studied. Research indicates that land use change significantly affects soil properties like moisture content, conductivity, pH, organic carbon, total nitrogen, and total phosphorus (Kashem et al., 2016). In the sal forest of Bangladesh, the soil is typically acidic, nutrient-poor, and low in organic matter. The soil pH ranges from 4.5 to 5.5, which is considered to be very acidic. This low pH is due to the presence of high levels of aluminum and iron in the soil, which affects the availability of nutrients for plant growth (Mondol & Wadud, 2021). In addition to the low pH, the soil in the sal forest is also low in nutrients, especially phosphorous, which is a critical element for plant growth and development. The lack of phosphorous in the soil can limit the growth and productivity of sal trees, which in turn, can affect the entire ecosystem. The low nutrient levels are also due to the slow weathering of the soil's parent material and the leaching of nutrients by heavy rainfall (Kashem et al., 2016). Organic matter is another important component of soil, as it provides a source of energy and nutrients for microorganisms, improves soil structure and water-holding capacity, and helps to regulate soil pH (Nasir et al., 2018). In the sal forest of Bangladesh, organic matter levels are low, typically ranging from 0.5 to 1.5%. This is due to the high rate of decomposition and the limited input of organic matter from fallen leaves, twigs, and branches (Islam et al., 2019). So, the soil in the sal forest of Bangladesh is characterized by low pH, low nutrient levels, and low organic matter content.

CHAPTER III

3. METHODOLOGY

3.1 Study area

The study area encompasses the diverse forest divisions of Bangladesh, which are categorized into two main types: Hill Forest and Sal Forest. The Hill Forest divisions include the Chittagong Forest Division, Cox's Bazar North Forest Division, Cox's Bazar South Forest Division, and Sylhet Forest Division. These divisions, situated primarily in the southeastern and northeastern parts of the country, feature rugged terrain, steep slopes, and dense vegetation cover. Particularly, the Chittagong Hill Tracts region, within which the Chittagong Forest Division lies, is known for its rich biodiversity and critical ecological significance. Similarly, Cox's Bazar and Sylhet Forest divisions exhibit diverse vegetation and are subject to similar environmental pressures. The Sal Forest divisions consist of the Tangail Forest Division, Mymensingh Forest Division, Dinajpur Forest Division, and Dhaka Forest Division. These divisions, located in central and northern Bangladesh, are characterized by sal-dominated forests with deciduous trees. They play a vital role in the conservation and management of forest resources, providing habitat for various flora and fauna.

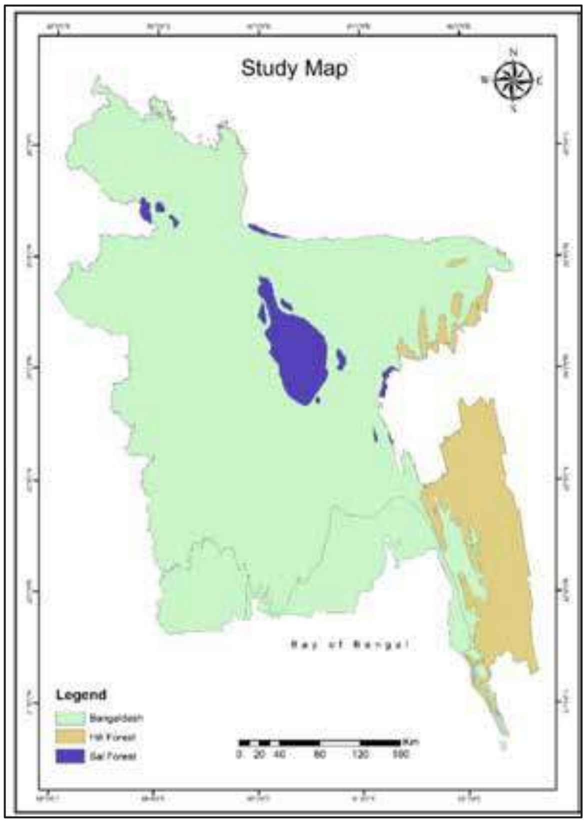

Figure 1: Study Area

3.2 Methods

3.2.1 Soil samples from BFI plots

There are soil sample of 1750 BFI plots out of 1858 plots in the soil archive that was established in Khulna University in cooperation with the Bangladesh Forest Department (BFD). Among those soil samples, a total of 1148 samples of 574 plots are included in this research project which are from the Hill and Sal zones of Bangladesh. Soil samples of Hill and Sal Forest were collected from two layers (0 to 15 cm and 15 to 30 cm) along with their land features/ land uses. BFD has measured bulk density, soil texture, and organic carbon content of forest soil during the BFI (Bangladesh Forest Inventory) activities with the technical support of FAO. Present study will analyze the soil pH, EC (Electrical Conductivity) and soil nutrients (nitrogen, phosphorus, potassium, calcium and magnesium), for the Hill, and Sal forests using BFI soil samples to develop a database and nutrient map. This deliverable had been included 152 soil samples of 76 plots from soil archives.

3.2.2 Soil sampling from the potential planting sites under SUFAL project

Stratified random sampling technique had been adopted to select the fifteen sample sites from each category of site like denuded, heavily degraded and less degraded as identified by SUFAL project in the Hill and Sal forests. Soil samples for the bulk-density, soil texture, and organic carbon had been collected according to the BFI sample collection procedure (BFD, 2016). A total of 90 sample plots [(15 samples plots x 3 category of sites (Denuded, heavily degraded and less degraded) x 2 types (Hill and Sal forest)] had been collected form the potential planting sites.

3.2.3 Specific method for each parameter

Both the physiochemical (bulk-density, soil texture, organic carbon, pH and electrical conductivity) and nutrients (nitrogen, phosphorus, potassium and calcium) properties of the soil samples of potential planting sites had been analyzed. While pH and electrical conductivity, nitrogen, phosphorus, potassium and calcium content of BFI soil samples had been measured. All the soil physical and nutrient analysis had been conducted in Nutrient Dynamic Laboratory, Forestry and Wood Technology Discipline, Khulna University.

3.2.3.1 Bulk density

Sample collection

Soil bulk density is the oven-dry weight of soil in a given unite volume. All the litter, grasses and other undergrowth will be cleared from the sample collection point. Samples for estimating the soil bulk density had been collected from two layers (0-15 cm and 15 to 30 cm) at a depth of 10-15 cm and 20-25 cm (Figure 1) respectively using metal cores.

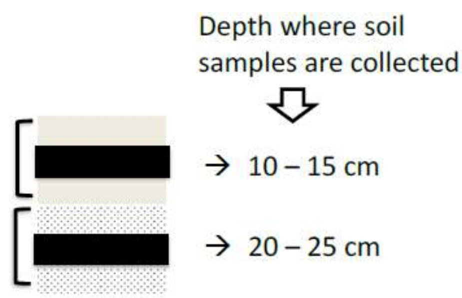

Figure 2: Depth of soil bulk density sample collection

Stainless steel metal rings with known volume had been used to collect the sample. The metal rings had been inserted into the desired depth of the soil using a handle and wooden hammer. After reaching the desired depth, the metal rings had been collected using a spade. Both end of the metal rings had been a level off using a knife (Figure 2) and finally, labeling of the sample will be done as Plot/Depth/ BD.

Push the core sampler into the soil

Extract the sample using a field knife or shovel

Level the surface of the soil sample on both sides and ensure that soil is completely level with edge of the core.

Figure 3: Steps of sample collection for soil bulk density

Sample processing

The collected samples had been oven-dried at 105 °C until constant weight. The weight of oven-dried cool samples had been measured using a high precision laboratory digital balance.

Sample analysis

Soil core of 5 cm diameter was used to collect the sample for bulk density at a depth of 5-10 cm and 20-25 cm (BFD, 2016). Finally, bulk density of the soil samples was measured according the following equation.

Bulk density (g/m^3) = dry weight (g)/sample volume (cm^3)……………............... (Equation 1)

3.2.3.2 Soil texture

Sample collection

Remove all the debris and vegetation from the sample collection point. One soil pith of 15 × 15 cm with 30 cm depth will be opened at each sample collection point. Soil samples of about 200 g had been collected from 0-15 cm and 15-30 cm depth separately. The collected sample had been stored in a leveled polybag separately according to soil depth (Figure 3). The collected samples had been labeled as Plot/Depth/ texture.

Dig a pit and measure the depth of soil	Mark the depth of sample layer and collect the sample using spade	Put the sample in plastic bag or jar

Figure 4: Steps of sample collection for soil texture analysis

Sample processing

The collected sample had been transported immediately to the laboratory for processing. The samples had been air-dried, crushed and sieved through 2 mm mesh. The sieved samples had been kept in air-tightened container for further analysis of soil texture, and determination of organic carbon and nutrients (N, P, K and Ca) content.

Texture analysis

Soil samples were collected from 0-15 cm and 15-30 cm depth from each sampling point. The soil texture was determined using the hydrometer method (Day, 1965; Allen, 1989).

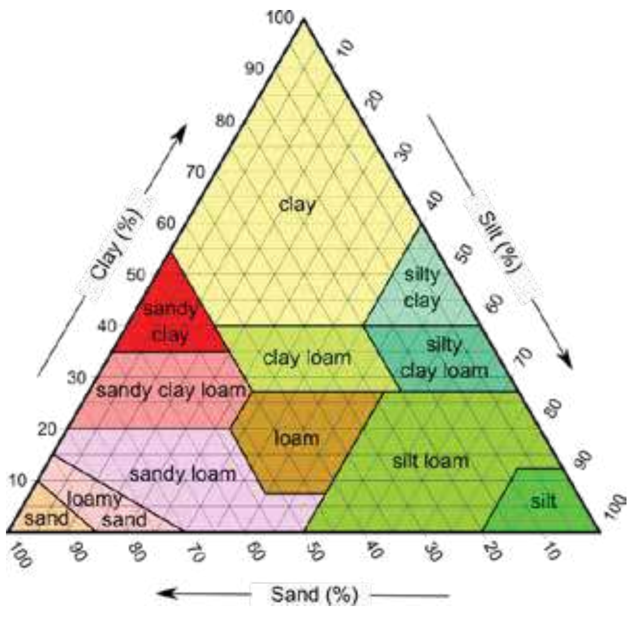

Figure 5: Triangle for soil texture determination

3.2.3.3 Soil organic carbon

Sample collection

The collected samples for the soil texture determination had been used for the determination of soil organic carbon at a depth of 0 to 15 cm and 15-30 cm depth. The sample collection procedure had been mentioned at section 3.2.3.2

Sample processing

The processed samples as described in section 3.2.3.2 had been used for organic carbon determination.

Sample analysis

Soil organic matter and organic matter had been measured using loss on ignition method (Allen, 1974). The Loss of Ignition (LOI) can be determined with the following formula

$$\text{LOI (\%)} = \frac{Loss\ of\ weight\ after\ ignition\ (g)}{Oven{-}dry\ initial\ weight\ (g)} \times 100$$

Figure 6: Porcelain cup, high precision analytical balance and muffle furnace

3.2.3.4 Soil pH

Sample collection

The collected samples for the soil texture determination had been used for the determination of soil pH at a depth of 0 to 15 cm and 15-30 cm depth. The sample collection procedure had been mentioned at section 3.2.1.

Sample processing

The processed samples as described in section 3.2.2 had been used for soil pH determination.

Sample analysis

Soil pH had been measure from the same collected sample. 1:2 soil extraction will be followed to determine soil pH using high precision pH meter (Sension 3 pH) (Allen, 1974).

3.2.3.5 Soil electrical conductivity (EC)

Sample collection

The collected samples for the soil texture determination had been used for the determination of soil conductivity at a depth of 0 to 15 cm and 15-30 cm depth. The sample collection procedure had been mentioned at section 3.2.1.

Sample processing

The processed samples as described in section 3.2.2 had been used for soil pH determination.

Sample analysis

Soil EC had been measured from the same collected sample. 1:2 soil extraction had been followed to determine soil EC using high precision EC meter (EC 215 Conductivity meter). (Allen, 1974).

3.2.3.6

3.2.3.7 Nutrients (N, P, K and Ca) concentration in soil

Sample collection

The collected samples for the soil texture determination had been used for the determination of Nitrogen, Phosphorus, Potassium and Calcium concentration at a depth of 0 to 15 cm and 15-30 cm depth. The sample collection procedure had been mentioned at section 3.2.1.

Sample processing

The processed samples as described in section 3.2.2 had been used for the determination of soil nutrient concentration.

Sample analysis

Micro Kjeldahl digestion for Nitrogen and tri-acid (H2SO4, HClO4 and HNO3) digestion for Phosphorus, Potassium, Calcium and Magnesium had been applied to the processed samples (Allen 1989) (Figure 6). Nitrogen and Phosphorus in the sample extract had been measured calorimetrically according to the Baethgen and Alley (1989) and Timothy et al. (1984), respectively, using UV–visible Recording Spectrophotometer (HITACHI, U-2910, Japan). Potassium concentration in sample's extract was measured by Flame Photometer (PFP7, Jenway LTD, England). Calcium concentration in soil extract had been analyzed using ICP of Central Laboratory of Khulna University.

Figure 7: Block digester for digestion of soil samples and filtration of soil extract for analysis

3.2.4. Nutrient maps for Hill and Sal zones

Ordinary Kriging interpolation technique in ArcGIS was used to create the spatial distribution map of soil nutrient content in the Sal zone. A spherical semi-variogram model was applied to predict nutrient concentrations. The interpolation process included defining upazila boundaries and categorizing soil nutrient levels into distinct classes for better visualization. Spatial statistics tools within ArcGIS were utilized for model generation and error estimation during the mapping process. For the Sal zone, the nutrient mapping of the central part and north part of the Sal forest had been done separately for each layer. For each map the dataset was divided into ten classes from low to high value and low values were marked as red where it turned in green for high values. For the Hill zone, the nutrient mapping of the

Sylhet and Chattogram had been done separately for each layer following the method of Salzone.

3.2.5. Statistical analysis

Simple statistical analyses were conducted, including the calculation of mean values and standard errors for each soil physical and chemical parameter at the study sites. Soil quality parameters were compared across different locations (North and Central), soil depths (0 to 15 cm and 15 to 30 cm). An unpaired t-test was performed using SAS University Edition to determine the statistical differences in soil properties between locations and depths. Visualization of the data, including bar plots with error bars and significance annotations were accomplished using the ggplot2 and ggsignif packages in R.

CHAPTER IV

4. RESULT AND DISCUSSION

4.1. Results for the Sal zone

4.1.1 Soil Texture

The soil texture across the studied locations and depths exhibited notable variations, reflecting a range of soil compositions. In the North region, the surface soil (0-15 cm) varied from clay loam to sandy loam, with sand content ranging from 34.43% to 60.55%. In the subsurface layer (15-30 cm), the texture varied between clay and sandy clay loam, with sand content ranging from 33.30% to 58.05%. In the Central region, the surface soil (0-15 cm) showed a wider variability, ranging from clay to sand and sand content ranged between 0.55% and 94.18%. The subsurface soil (15-30 cm) also ranged from clay to sand, with sand content from 0.55% to 94.18% (Table 1).

Table 1: Soil texture of Sal Forest

Zone	Depth(cm)	Texture	Sand %	Clay %	Silt %
North	0-15	Clay Loam-Sandy Loam	34.43- 60.55	13.08- 58.83	3.88-41.75
	15-30	Clay- Sandy Clay Loam	33.30-58.05	15.95-61.33	3.88-39.25
Central	0-15	Clay-Sand	0.55-94.18	0.45-76.7	1.75-67.13
	15-30	Clay-Sand	0.55-94.18	0.45-81.7	1.75-82.63

4.1.2 Soil bulk density

The bulk density of soils in the study area showed significant variations across locations and depths. At a depth of 0-15 cm, soils in the North location had a bulk density of 1.46 g/cm³, while in the Central location it was 1.36 g/cm³. At a depth of 15-30 cm, the bulk density increased to 1.52 g/cm³ in the North and 1.40 g/cm³ in the Central region. Significant differences were observed between the 0-15 cm depths in North and Central locations ($p < 0.05$) and also for 15-30 cm depth (Figure 8).

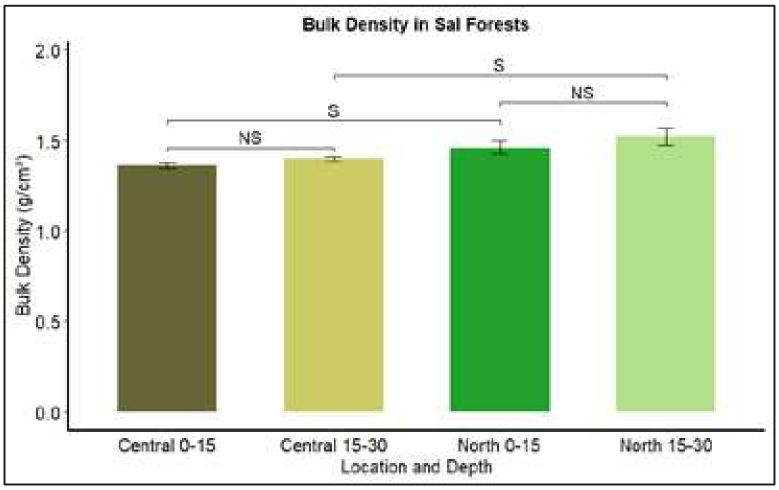

Figure 8: Soil bulk density in Sal Forests (S=significant and NS= not significant)

4.1.3. Soil organic carbon

The organic carbon content varied between depths and locations. In the North, the organic carbon content at a depth of 0-15 cm was 1.79 ± 0.11%, while it slightly decreased to 1.79 ± 0.10% at 15-30 cm. Similarly, in the Central region, organic carbon content was 2.05 ± 0.06% at 0-15 cm and 1.94 ± 0.06% at 15-30 cm. The comparison between the depths in both regions was statistically non-significant ($p > 0.05$). However, a significant difference ($p < 0.05$) was observed between the 0-15 cm depths of the North and Central locations, indicating a notably higher organic carbon concentration in the Central region (Figure 9).

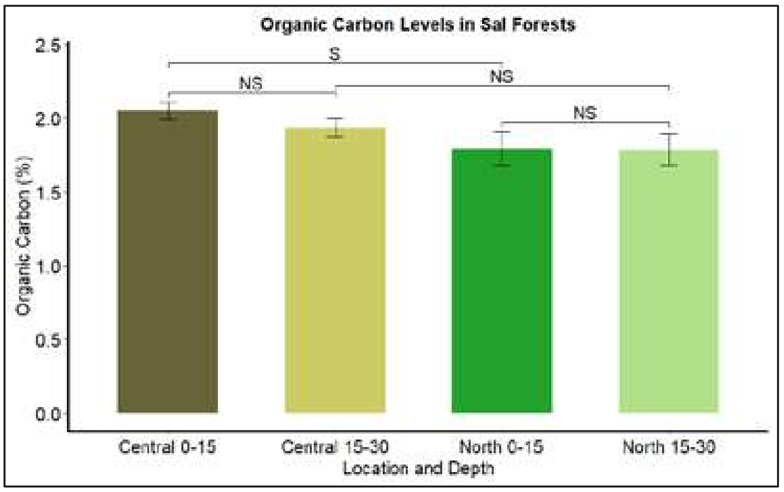

Figure 9:Soil Organic carbon in Sal Forests (S=significant and NS= not significant)

4.1.4. Soil EC

The EC values ranged from 88.74 to 135.31 µS/cm, with the highest mean observed at the Central Sal Forest (0-15 cm depth) and the lowest at the North Sal Forest (15-30 cm depth). Statistical comparisons between groups indicated no significant differences (NS) in EC values across all pairs tested, as visualized in Figure 10.

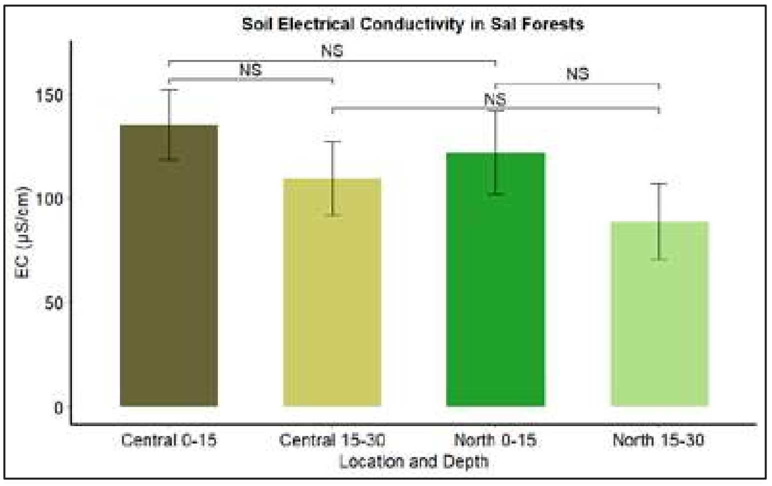

Figure 10: Soil Electrical Conductivity in Sal Forests (NS= not significant)

4.1.5. Soil pH

The study found noticeable differences in soil pH levels across different forest regions and depths. The pH values ranged from 5.57 to 6.03, with higher values observed in the North region compared to the Central region. The lowest mean pH (5.57) was recorded at Central 0-15 cm depth, while the highest mean pH (6.03) was noted at North 15-30 cm depth. Statistical comparisons revealed significant differences ($p > 0.05$) between North region and Central region at the depth of 0-15 and 15-30 cm. However, comparisons within the same location depths were not statistically significant (Figure 11).

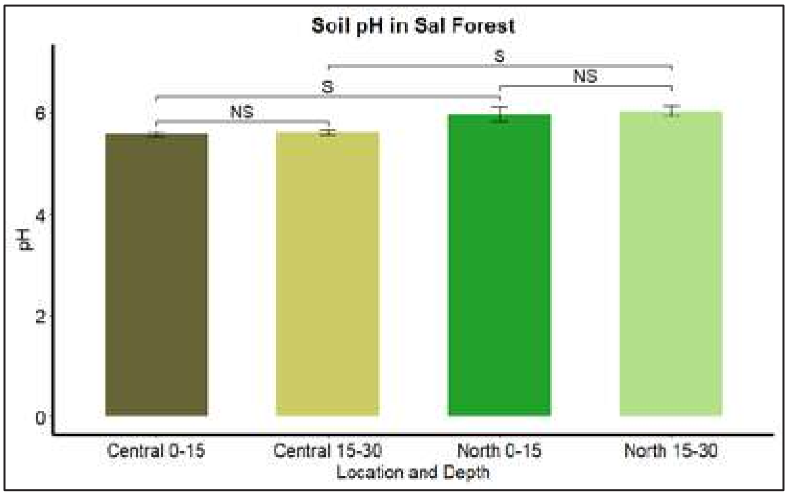

Figure 11: Soil pH in Sal Forests (S=significant and NS= not significant)

4.1.6. Soil Nitrogen

The mean value of total nitrogen ranged from 0.416 to 0.71 mg/g, with higher values observed in the Central region. Statistical analysis indicated significant differences ($p > 0.05$) between North 0-15 cm and Central 0-15 cm, while other comparisons between depths and locations were not statistically significant (Figure 12). These findings point to the potential influence of location and depth on nitrogen availability in the soil.

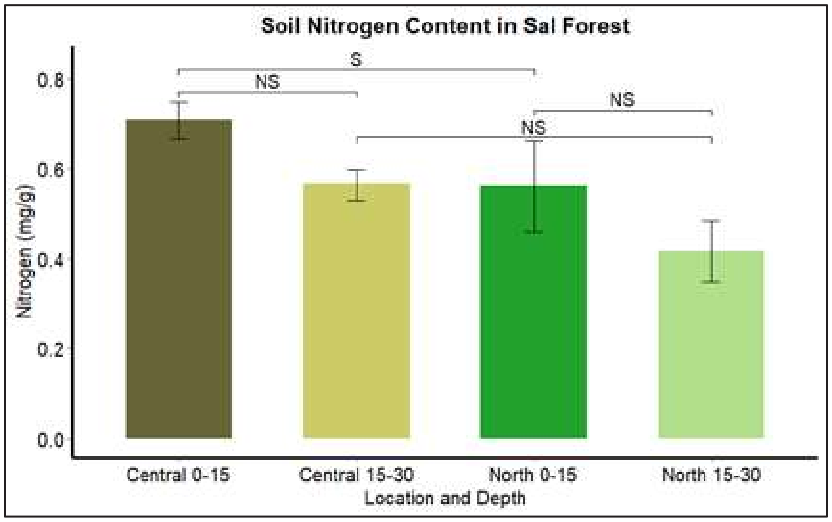

Figure 12: Soil Nitrogen in Sal Forests (S=significant and NS= not significant)

The highest (1.02-1.19 mg/g) range was observed in 0-15 cm of the North part, which indicated the Nawabgang and Fulbari upazzila under Dinajpur district. On the other hand, the lowest (0.05-0.17 mg/g) range was observed in 15-30 cm of the central part, which represented Badda, Demra, Rupganj, and Gajipur Sadar upazilla under Dhaka, Narayanganj and Gajipur district (Appendix 2).

4.1.7. Soil Phosphorus

The mean value of total phosphorus (P) was higher in the North at the 0-15 cm depth (0.36 mg/g), while the lower was recorded in the Central region at the 15-30 cm depth (0.27 mg/g). Statistical analysis shows that a significant difference ($p < 0.05$) between the Central region at the surface and subsurface depths (0-15 cm and 15-30 cm), with a notable decline in phosphorus at greater depths. However, no statistically significant differences were found in phosphorus content between depths in the North region. Comparisons between North and Central regions also showed no significant differences at either depth (Figure 13).

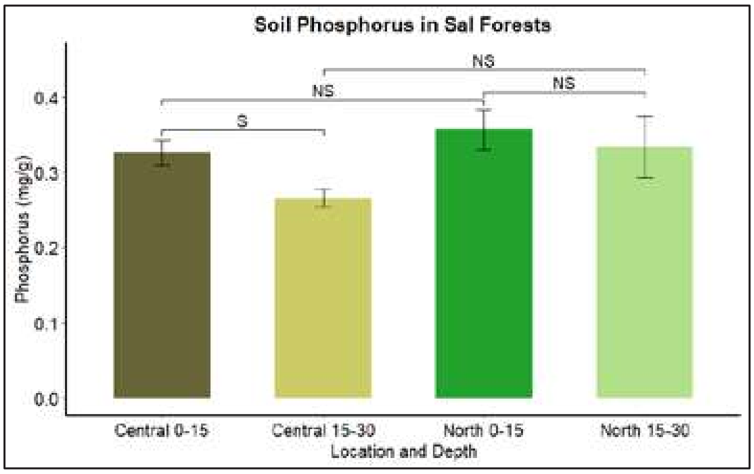

Figure 13: Soil Phosphorus in Sal Forests (S=significant and NS= not significant)

The highest (0.55-0.47 mg/g) range was observed in 15-30 cm of the North part, which indicated the Nawabgang and Birampur upazzila under Dinajpur district. On the other hand, the lowest (0.00-0.14 mg/g) range was observed in 15-30 cm of the central part, which represented Kaliakair upazilla under Gajipur district (Appendix 2).

4.1.8. Soil Potassium

The mean value of total potassium (K) was higher in the North at the 0-15 cm depth (6.34 mg/g), while the lower was recorded in the Central region at the 0-15 cm depth (5.53 mg/g). No significant differences were observed between surface (0-15 cm) and subsurface (15-30 cm) depths for either the North or Central locations. Additionally, potassium levels showed no significant differences between the North and Central regions at either depth (Figure 14).

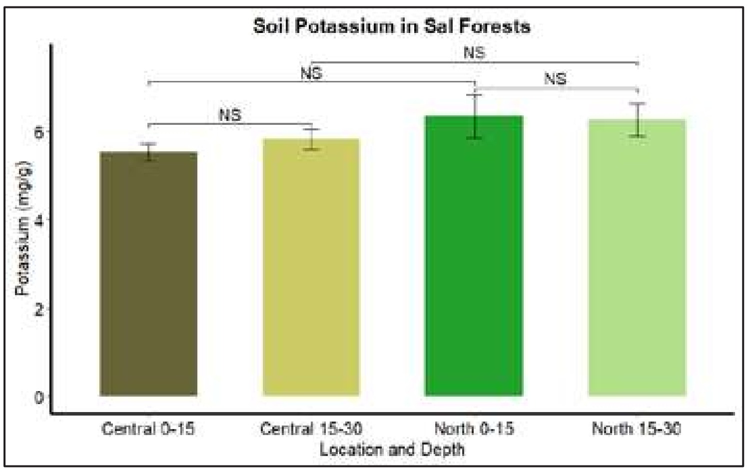

Figure 14: Soil Potassium in Sal Forests (NS=not significant).

The highest (8.59-9.77 mg/g) range was observed in 15-30 cm of the Central part, which indicated the Narsingdi Sadar and Kaliganj upazilla under Narsingdi and Gajipur districts. On the other hand, the lowest (2.87-3.60 mg/g) range was observed in 15-30 cm of the central part, which represented Mymensingh Sadar, Haluaghat, Muktagacha and Nalitabari, upazilla under Mymensingh and Sherpur district (Appendix 2).

4.1.9. Soil Calcium

The mean value of total Calcium (Ca) was higher in the North at the 0-15 cm depth (0.56 mg/g) and the lower in the Central region at the 15-30 cm depth (0.49 mg/g). Despite variations in absolute values, no statistically significant differences were observed between depths within each region or across regions for the same depth (Figure 15).

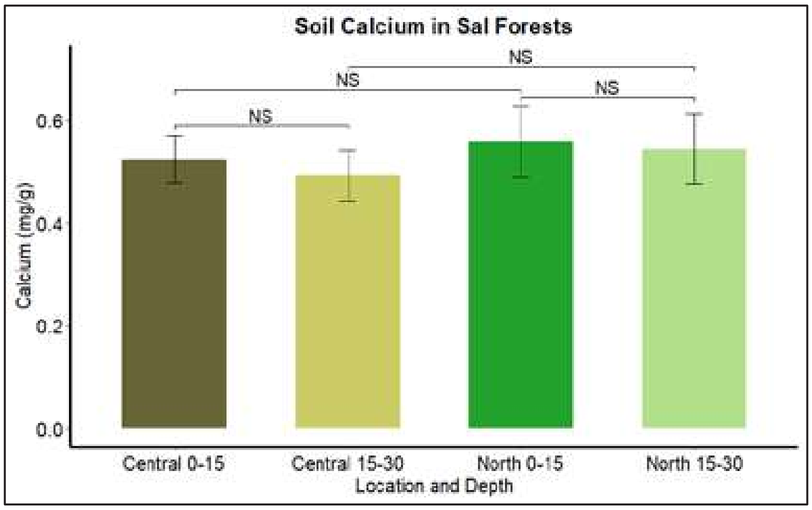

Figure 15: Soil Calcium in Sal Forests (NS = not significant).

The highest (1.86-2.08 mg/g) range was observed in 0-15 cm of the Central part, which indicated the Pallabi, Badda, Demra and Narsingdi Sadar under Dhaka and Narsingdi district. On the other hand, the lowest (0.07-0.28 mg/g) range was observed in 15-30 cm of the central part, which represented Madhupur, Ghatail, Bhaluka, Kapasia and Gajipur Sadar upazilla under Tangail, Mymensingh and Gajipur district (Appendix 2).

4.2. Results for the Hill zone

4.2.1 Soil Texture

The table presents soil characteristics for two different Forest Division, Sylhet and Cox's Bazar, with a focus on two soil depths: 0-15 cm and 15-30 cm. The information provided includes soil texture and the percentage ranges of sand, clay, and silt within each soil layer. In Sylhet, the soil texture in the 0-15 cm layer ranges from sandy clay loam to silty clay (Table 2).

Table 2: Soil texture of the collected soil samples from the Hill zone

Division	Depth	Texture	Sand %	Clay %	Silt %
Sylhet	**0-15 cm**	Sandy Clay Loam- Silty Clay	64.05-91.3	5.45-21.2	3.25-18.25
	15-30 cm	Sandy Clay Loam- Silty Clay	61.55- 91.3	2.95 - 25.2	3.25 - 18.25
Cox's Bazar	**0-15 cm**	Sandy Clay loam - Loamy Sand	48.05 - 86.3	7.95 - 26.2	3.25- 25.75
	15-30 cm	Loam - Loamy Sand	45.55 - 88.05	6.2 - 26.2	5.75 - 28.25

4.2.2. Soil Bulk density

Bulk density in the Hill Zone of collected samples was found to be 1.37 g/cm³. Bulk density represents the mass of soil per unit volume and is an indicator of how compacted or dense the soil is. Lower bulk density values suggest a less compacted soil structure, which is generally favorable for plant growth. A lower bulk density allows for better root penetration, aeration, and water movement within the soil. At the 15-30 cm depth, the bulk density in the Hill Zone collected samples are increased to 1.42 g/cm³ (Figure 16).

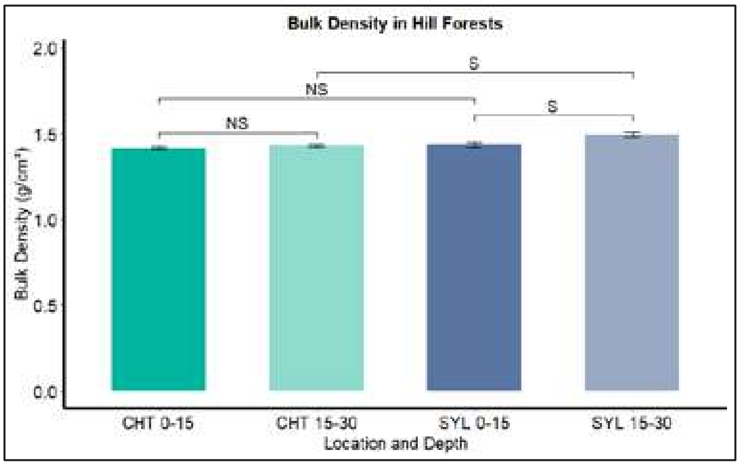

Figure 16: Soil bulk density in Hill Forests (S=significant and NS= not significant)

4.2.3. Soil organic carbon

For the 0-15 cm depth, the organic carbon content in the Hill Zone was found to be 1.77%. The 15-30 cm depth in the Hill Zone exhibited a slightly lower organic carbon content of 1.60%. While this value is slightly lower than the shallower depth, it still indicates a moderate level of organic matter in the soil Figure (17).

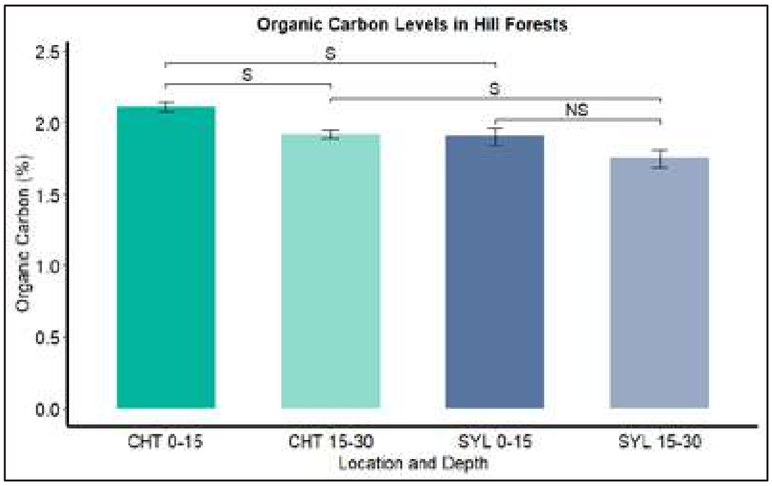

Figure 17: Soil Organic carbon in Hill Forests (S=significant and NS= not significant)

4.2.4. Soil EC

The study compared the electrical conductivity (EC) at two soil depths (0-15 cm and 15-30 cm) for two locations, CHT and SYL. At the CHT location, the mean EC at the 0-15 cm depth was 57.49 ± 3.76, showing a significant difference compared to the 15-30 cm depth, which had a mean EC of 43.97 ± 3.75 and was not significant. Similarly, at the SYL location, the mean EC at the 0-15 cm depth was 64.80 ± 4.09, indicating a significant difference, while the 15-30 cm depth had a mean EC of 47.94 ± 3.92 and was not significant (Figure 18).

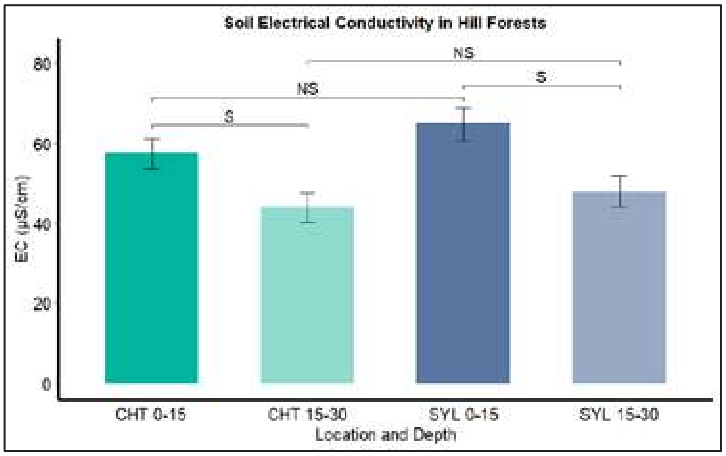

Figure 18: Soil Electrical Conductivity in Hill Forests (S=significant and NS= not significant)

4.2.5. Soil pH

The analysis of pH levels across different locations and depths reveals notable differences, particularly between the CHT and SYL regions. In the 0-15 cm depth range, CHT exhibited a significantly higher average pH (5.67) compared to SYL's average pH of 5.17, indicating a substantial variation in soil acidity. Similarly, at the 15-30 cm depth, CHT maintained a higher pH level of 5.63 versus SYL's average pH of 5.15, reinforcing the trend observed in shallower depths (Figure 19).

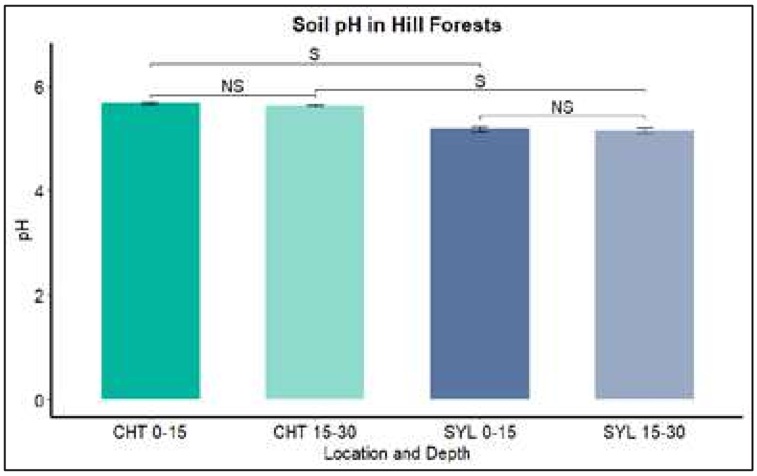

Figure 19: Soil pH in Hill Forests (S=significant and NS= not significant)

4.2.6. Soil Nitrogen

The analysis of soil nutrient availability across different depths revealed notable variations between the CHT and SYL regions. At a depth of 0-15 cm, CHT exhibited a significantly higher nutrient concentration (mean = 0.644) compared to SYL, which had a mean of 0.621. This significant difference indicates that soil management practices in CHT may be more effective at enhancing nutrient levels within this depth range. Conversely, at the 15-30 cm depth, both regions showed similar nutrient concentrations, with CHT having a mean of 0.55209 and SYL at 0.52443, indicating that the differences in nutrient availability become less pronounced as soil depth increases (Figure 20).

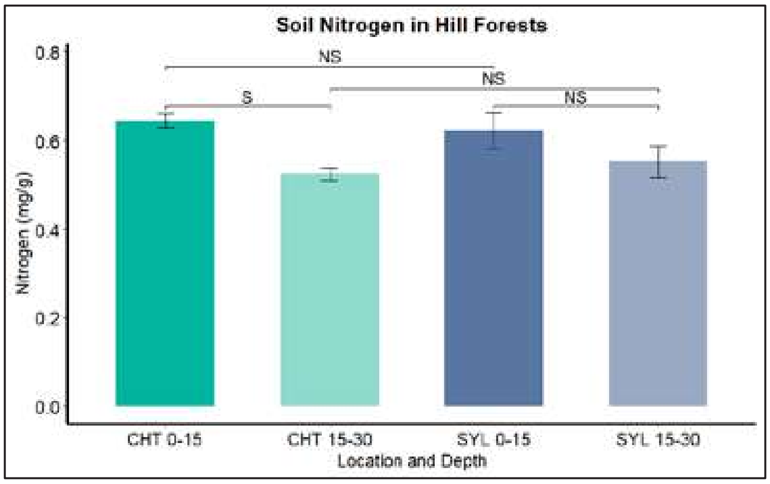

Figure 20: Soil nitrogen in Hill Forests (S=significant and NS= not significant)

4.2.7. Soil Phosphorus

The analysis of nutrient dynamics across varying soil depths revealed distinct patterns in the comparison between CHT and SYL locations. At the 0-15 cm depth, both CHT and SYL exhibited relatively high phosphorus levels, with CHT showing a significantly higher mean value (0.238396) compared to SYL (0.21578). However, as soil depth increased to 15-30 cm, there was a notable decline in phosphorus concentration for both sites, particularly at SYL, wherethe mean value dropped to 0.167602, indicating a significant reduction in available phosphorus. In contrast, CHT maintained a higher concentration of phosphorus at this depth, with a mean value of 0.218219 (Figure 21).

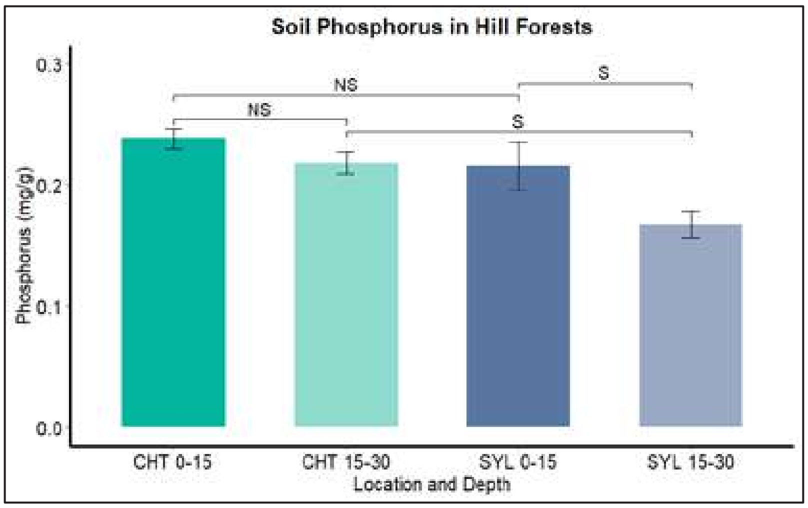

Figure 21: Soil phosphorus in Hill Forests (S=significant and NS= not significant)

4.2.8. Soil Potassium

The analysis of potassium (K) levels across different soil depths and locations revealed notable variations in nutrient availability. In the upper layer (0-15 cm), CHT exhibited significantly higher K concentrations (5.61483) compared to SYL, which recorded a lower value of 3.47294. Similarly, at the deeper layer (15-30 cm), CHT maintained a greater K concentration (5.750837) than SYL (3.454521). However, comparisons within each layer indicated that the differences in K levels between SYL and CHT were statistically significant, highlighting the influence of location on nutrient distribution (Figure 22).

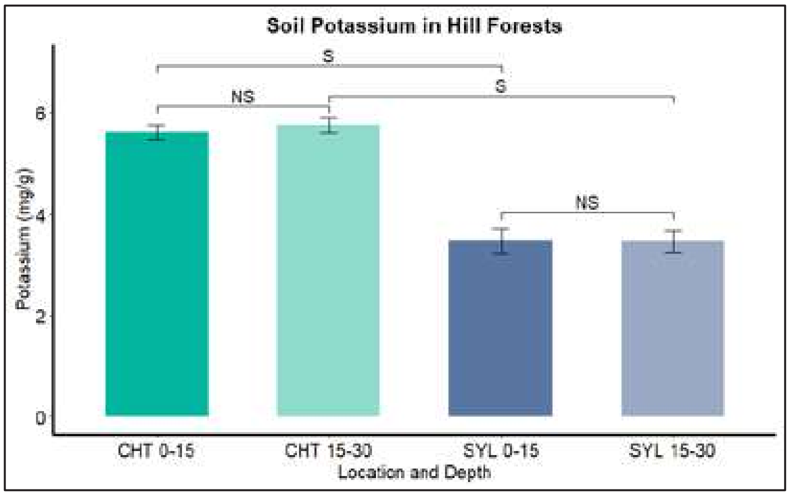

Figure 22: Soil potassium in Hill Forests (S=significant and NS= not significant)

4.2.9. Soil Calcium

The analysis of calcium levels across different depths and locations revealed notable differences in nutrient distribution. At the 0-15 cm depth, calcium concentrations were higher in SYL (0.402) compared to CHT (0.311), though this difference was not statistically significant. However, at the 15-30 cm depth, the trend continued with SYL exhibiting a calcium level of 0.392, while CHT showed a lower concentration of 0.257, indicating a significant variation between the two locations (Figure 23).

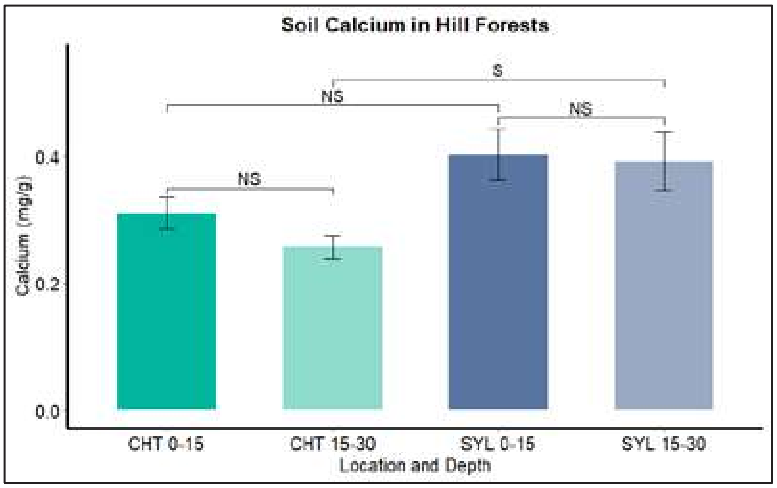

Figure 23: Soil calcium in Hill Forests (S=significant and NS= not significant)

4.3. Discussion

Forest soils influence the composition of the forest stand and ground cover, rate of tree growth, vigor of natural reproduction and other silviculturally important factors (Bhatnagar, 1965). For instance, growth of *Shorea robusta* (Sal) and other tree species, such as *Terminalia alata* and *Syzygium cumini*, in tropical forests is highly influenced by nitrogen, phosphorus, potassium, and soil pH (Bhatnagar, 1965). Physiochemical characters of forest soils vary in space and time due to variations in topography, climate, physical weathering processes, vegetation cover, microbial activities, and several other biotic and abiotic factors.

In this study, soil texture in the Sal Forest ranged from Clay Loam-Sandy Loam and Clay- Sandy Clay Loam across the two depths (0-15 cm and 15-30 cm) of North region and Clay-Sand in both the two depths (0-15 cm and 15-30 cm) of Central region, with sand content predominantly higher than clay and silt (Table 1). These findings are in line with observations made in other Sal Forest regions, such as Madhupur, where soil texture also exhibits significant variation due to factors like land use and forest management practices (Islam et al., 2024; Kashem et al., 2016). The supply of water to plants usually is greater as the texture becomes finer (Black, 1968) and again the soil texture affects the nutrient supply of the soil and thus determine the overall health and productivity of the forest ecosystem. Bulk density, which indicates soil compaction, is another critical parameter. In this study, the Central Sal Forest soils bulk density is 1.36 g/cm³ at 0-15 cm depth and 1.40 g/cm³ at 15-30 cm depth (Figure 2), which is relatively higher than the 0.48 g/cm³ observed in the Madhupur Sal forest (Rahman et al., 2012). The lower bulk density in Madhupur suggests a well-structured soil with higher organic matter and porosity, supporting better water infiltration and root penetration. The higher bulk density in the Sal Forest of this study may indicate some degree of compaction, possibly linked to human activities or natural processes affecting soil structure over time. Soil organic carbon (SOC) is a pivotal factor that regulates the physical as well as chemical qualities of soil and maintains productivity as well as sustainability on a long-term basis (Pathak and Reddy 2021). The organic carbon content in this study was 1.79% and 1.79% at depth of 0-15 and 15-30 cm in Northern region. Beside that 2.05% and 1.94% depth of 0-15 and 15-30 cm in Central region (Figure 3), which is comparable to organic matter levels found in other Sal forests. In Madhupur Sal forest, organic matter content ranged from 0.70% to 2.11% (Gomes, 2005), with higher concentrations in plantation stands (Hasan & Mamun, 2015). These similarities suggest that the organic carbon content in the Sal Forest of this study is within the expected range for tropical forest soils. Plant tissues both from aboveground litter and belowground root detritus are the main source of soil organic carbon, which influences physiochemical characteristics of soil such as pH, texture and nutrient availability (Johnston, 1986). Electrical conductivity (EC), a measure of soil salinity, showed notable differences between the two depths and between the two regions soil (North and Central). EC values were higher in Central Sal soils, particularly at the 0-15 cm depth (Figure 4). These findings align with those from Madhupur, where EC values varied across different forest stands, with the highest EC observed in mixed stands (Hasan & Mamun, 2015). The variation in EC in this study suggests that soil salinity may influence forest structure and composition, potentially affecting the types of vegetation that thrive in different parts of the Sal Forest. Soil pH is a key factor influencing nutrient availability and microbial activity. In this study, the pH of Sal Forest soils was slightly acidic, ranging from 6.03 to 5.57 (Figure 5), which is consistent with other studies in Sal forests, including those in Madhupur, where pH values ranged from 4.60 to 6.28 (Hoque et al., 2009). This may be due to local environmental factors such as aspect, rainfall, and vegetation composition. It reflects the stability of soil pH of sal forest over time and land use practices. Good sal regeneration areas have low pH in soils (Bhatnagar 1965). Soils with higher pH generally have poorer capacity for regeneration (Suoheimo 1995).

The total nitrogen content in this study was higher in Central Sal Forest soils at 0-15 and 15-30 cm depth (0.71 mg/g and 0.56 mg/g) compared to Sal soils of North at the same depth (Figure 6). These results are consistent with findings from the Madhupur Sal forest, where nitrogen content was higher in plantation stands compared to pure and mixed stands (Hasan & Mamun, 2015). The variation in nitrogen content may reflect differences in forest management practices, organic matter inputs, and microbial activity across forest types. The total phosphorus levels in this study were consistent with those found in other Sal forests, where phosphorus concentrations were observed to decrease with depth (Kashem et al., 2016). In this study, there is also decrease trend with the depth in both Central and North Sal Forest. Phosphorus content (Figure 8), which could be due to similar soil management practices or natural nutrient cycling. The findings from Madhupur, where available phosphorus was higher in pure Sal stands (Hasan & Mamun, 2015), highlight the importance of forest composition in determining soil nutrient availability. In terms of total potassium and total calcium, no significant differences were observed between the two depth intervals for both Central and North Sal Forest soils. The relatively stable calcium distribution across depths may indicate a consistent mineral input and low calcium leaching from the topsoil. However, variations in exchangeable potassium and calcium levels across forest stands in Madhupur (Hasan & Mamun, 2015) suggest that forest management practices, such as land use change, can influence these nutrient concentrations. Land use changes, including conversion to plantations or agricultural use, can affect soil moisture, pH, and nutrient availability, ultimately influencing forest health and biodiversity (Kashem et al., 2016).

The nutrient concentrations observed in the soil samples from the Bangladesh hill forests reveal significant variations across different depth ranges, particularly between 0-15 cm and 15-30 cm. The data indicate relatively high levels of nitrogen (N) and phosphorus (P), which are crucial for plant growth and ecosystem health. For instance, the total nitrogen concentration measured at 47.94 mg/kg in the 15-30 cm depth range is notably higher than findings reported by Rahman et al. (2021) who documented a total nitrogen concentration of 35.60 mg/kg in similar forest soils. This discrepancy may be attributed to variations in organic matter content and land use practices across different study sites. Additionally, phosphorus levels in the upper soil layer (0-15 cm) were recorded at 22.30 mg/kg, which aligns with the observations made by Ahmed et al. (2020), who found comparable concentrations in their research on hill forest ecosystems. However, our findings suggest that deeper soil layers may exhibit different nutrient dynamics, indicating the potential influence of root activity and microbial processes that alter nutrient availability as soil depth increases.

CHAPTER V

5. CONCLUSIONS AND RECOMMENDATIONS

5.1 Conclusion

In conclusion, this research aims to provide crucial soil macro-nutritional information to inform decision-making in forest management within Bangladesh. By developing comprehensive databases of soil pH, electrical conductivity, physiochemical parameters, and key nutrients such as nitrogen, phosphorus, potassium, and calcium, this study lays the groundwork for sustainable forest management practices. By addressing pertinent research questions regarding baseline soil data and its implications for sustainable forest production, species selection, and climate change mitigation, this research provides valuable insights to support informed decision-making processes in Bangladesh's forest management sector. The findings presented herein underscore the importance of soil health and nutrient management in promoting the long-term viability and resilience of forest ecosystems in Bangladesh.

5.2 Recommendations

5.2.1 Prescription on site specific tree species selection for plantation and soil quality improvement of Hill zone

Here we have prepared a list of 40 potential native tree species for the plantation in the hill zone of Bangladesh. This list contains scientific and local name, type, height and DBH range, distribution in Bangladesh, light requirement, preferred soil types and pH range, crown condition, growth condition and commercial use of each species. The prescribed native tree species have been categorized for the-

- Heavily degraded sites with full sunlight, sandy texture and low nutrient content (Land reclamation/ soil or site improvement)
- Sites with loamy to clayey texture and average to high nutrient content
- Sites with semi-shade
- Riparian plantation with full sunlight to partial shade and building form/ dwelling sites (fruit trees) (Box 1 to 5).

Heavily degraded sites with full sunlight, sandy texture and low nutrient content (Land reclamation/ soil or site improvement)

Box 1	
Prescribed species	
Castanopsis indica (Batna)*	*Trema orientalis* (Naricha)*
Macaranga denticulata (Bura)*	*Vitex pinnata* (Arsol)*

* Naturally occurred

Box 2		
Prescribed species		
Albizia lebbeck (Kala koroi)	*Albizia odoratissima* (Tetua Koroi)	*Albizia procera* (Sada Koroi)
Azadirachta indica (Neem)	*Gmelina arborea* (Gamar)	*Bombax ceiba* (Shimul)
Cassia fistula (Sonalu)	*Chukrasia velutina* (Chikrassi)	

Sites with loamy to clayey texture and average to high nutrient content

Box 3		
Prescribed species		
Alstonia scholaris (Chatian)	*Artocarpus chaplasha* (Chapalish)	*Calikarpa arboria* (Bormala)*
Aphanamixis polystachya (Pitraj)	*Butea monosperma* (Palash)	*Terminalia arjuna* (Arjun) *Terminalia bellirica* (Bahera)

* Naturally occurred

Sites with semi-shade

Box 4		
Prescribed species		
Aquilaria malaccensis (Agar)	*Mallotus nudiflorus* (Pitali)	*Syzygium firmum* (Dhaki-jam)
Cassia fistula (Sonalu)	*Stereospermum personatum* (Dharmara)	*Syzygium fruticosum* (Puthi Jam)*
Dipterocarpus turbinatus (Telia garjan)		*Ficus racemose* (Jog-dumur)
		Oroxylum indicum (Kanai dinga)*

* Naturally occurred

Riparian plantation with full sunlight to partial shade

Box 5		
Prescribed species		
Aphanamixis polystachya (Pitraj)	*Butea monosperma* (Palash)	*Neolamarckia cadamba* (Kadam)
Artocarpus chaplasha (Chapalish)	*Hopea odorata* (Telsur)	*Pongamia pinnata* (Karach)
Barringtonia acutangula (Hijal)	*Lagerstroemia speciosa* (Jarul)	*Terminalia arjuna* (Arjun)
		Terminalia bellirica (Bahera)

5.2.2 Prescription on site specific tree species selection for plantation and soil quality improvement of Sal zone

A list of 30 potential native tree species was recommended for the plantation in the Sal zone to restore the forest and soil quality (Annex 2).

Site condition	Recommended species
Heavily degraded sites with full sunlight	*Adina cordifolia, Albizia lebbeck, Albizia odoratissima, Albizia procera, Aphanamixis polystachya*, Bauhinia variegate*, Grewia nervosa*, Neolamarckia cadamba*, Pterocarpus indicus, Shorea robusta, Swietenia mahagoni, Tamarindus indica, Dalbergia sissoo,*
Sites with semi-shade	*Abroma agustua*, Artocarpus chama*, Azadirachta indica*, Barringtonia acutangular*, Chukrasia tabularis*, Gmelina arborea*, Lannea coromandelica*,* Alstonia scholaris*, *Phyllanthus emblica*, Sterculia villosa*, Terminalia arjuna*, Terminalia belirica*, Terminalia chebula*, Syzygium syzygioides, Syzygium firmum, Lagerstroemia speciose and Diptocarpus turbinatus*

* Naturally occurred

5.3. Social and environmental safeguard

All kinds of social and laboratory safety had been maintained properly.

6. REFERENCES

Abdullah Al Faruq, M., Zaman, S., & Katoh, M. (2016). Analysis of Forest Cover Changes Using Landsat Satellite Imagery:A Case Study of the Madhupur Sal Forest in Bangladesh. *Journal of Forest Planning*, *21*(2), 29–38. https://doi.org/10.20659/jfp.21.2_29

Ahirwal, J., & Maiti, S. K. (2016, May). Assessment of soil properties of different land uses generated due to surface coal mining activities in tropical Sal (Shorea robusta) forest, India. *CATENA*, *140*, 155–163. https://doi.org/10.1016/j.catena.2016.01.028

Akhtaruzzaman, M., Haque, M. E., & Osman, K. T. (2014). Morphological, Physical and Chemical Characteristics of Hill Forest Soils at Chittagong University, Bangladesh. *Open Journal of Soil Science*, *04*(01), 26–35. https://doi.org/10.4236/ojss.2014.41004

Allen, S.E. 1989. Chemical analysis of ecological materials. Blackwell Scientific Publications, Oxford

Alvarado, A. 2015. Plant Nutrition in Tropical Forestry. Agronomic Reseaarch Center, Costa Rica University, San Pedro Montes de Oca, Costa Rica, Springer-Verlag Berlin Heidelberg, 2015

Arannayk Foundation, 2019. Forests of Bangladesh. https://www.arannayk.org /index.php?option=com_content&view=article&id=17&Itemid=132. Accessed on 5th July 2019.

Baribault, T.W., Kobe, R.K., Finley, A.O. 2012. Tropical tree growth is correlated with soil phosphorus, potassium, and calcium though not for legumes. Ecological Monograph, 82:189–203

Beathgen, W.E., Alley, M.M. 1989. A manual colorimetric procedure for measuring ammonium nitrogen in soil and plant Kjeldahl digests. Soil Sci Plant Anal 20 (9 & 10): 961-969.

BFD, 2016. Manual for Soil Measurements for the Bangladesh Forest Inventory. Bangladesh Forest Department and Food and Agricultural Organization of the United Nations, Dhaka, Bangladesh.

BFD, 2017a. Hill forest. http://www.bforest.gov.bd/site/page/28615def-835e-4b3a-a412-da954f55a943/-. Accessed on 1 June 2020.

BFD, 2017b. Tropical Moist Deciduous Forest (Sal Forest). http://www.bforest.gov.bd/site/page/6c336d56-9484-442d-81e1-7f47bf44cab9/-. Accessed on 1 June 2020.

Bhattarai, K. P., & Mandal, T. N. (2017, January 23). Effect of altitudinal variation on the soil characteristics in sal (Shorea robusta gaertn.) forests of eastern Nepal. *Our Nature*, *14*(1), 30–38. https://doi.org/10.3126/on.v14i1.16438

Bowen, G.D., Nambiar, E.K.S. 1984. Nutrition of plantation forests. Academic.

Braimoh, A.K., Vlek, P.L.G. 2008. Land Use and Soil Resources. © Springer Science. pp 167-200.

Chanan, M., Hardiwinoto, S., Agus, C., Purwanto, R.H., Purwanta, S. 2019. The identification of macro nutrient status of superior teak plantation (Tectona grandis Lin.F) by means of DRIS norms (Diagnosis and Recommendation Integrated System) in Indonesia, Forest Science and Technology, 15(1): 7-12

Chowdhury, M., & Bashar, M. (2022, January 10). Diversity and abundance of some insect fauna in Bhawal and Madhupur Sal forests of Bangladesh. *Journal of Biodiversity Conservation and Bioresource Management*, *7*(1), 11–24. https://doi.org/10.3329/jbcbm.v7i1.57119

Das, D.K. 1990. Forest Types of Bangladesh. Bulletin 6, Plant Taxonomy Series, Bangladesh Forest Research Institute, Chittagong. 9 pp.

Hardiwinoto, S., Nakasuga, T. and Igarashi, T. 1989. Litter production and decomposition of a mangrove forest at Ohura Bay, Okinawa. Research Bulletin of the College of Experiment Forests, Hokaido University, 46(3):577–594.

Hasan, M. K., & Mamun, M. B. (2015, April 27). Influence of different stands of sal (Shorea robusta C. F. Gaertn.) forest of Bangladesh on soil health. *Research in Agriculture Livestock and Fisheries*, *2*(1), 17–25. https://doi.org/10.3329/ralf.v2i1.23025

Hossain, MK. 2016. Plantation forestry- paradign to meet the demand of the forestry resources in Bangladesh. In: T.K. Nath and Patrick O'Reily (eds.). Monoculture Farming- Global Perspectives, Ecological Impact and Benefits/Drawbacks. Edition: 1st, Chapter: 3, nova Publishers, New York.

Huq, S. I., & Shoaib, J. U. M. (2013). The Soils of Bangladesh. *World Soils Book Series*. https://doi.org/10.1007/978-94-007-1128-0

Islam, M. S., & Azijul Islam, M. (2018). Reduction of Landslide Risk and Water-Logging Using Vegetation. *E3S Web of Conferences*, *65*, 06003. https://doi.org/10.1051/e3sconf/20186506003

Islam, M. S., Roy, S., Khanom, S., & Islam, M. (2022, September 29). DEFORESTATION AND BIODIVERSITY DEGRADATION IN MADHUPUR SAL FOREST AT TANGAIL REGION. *Khulna University Studies*, 235–239. https://doi.org/10.53808/kus.2013.11and12.1201-sc

Karlen, D.L., Andrews, S.S., Wienhold, B.J., Zobeck, T.M. 2008. Soil Quality Assessment: Past, Present and Future. Journal of Integrative Biosciences 6(1):3-14.

Kashem, M. A., Ahmed, A., Hoque, S., & Hossain, M. Z. (2016, August 27). EFFECTS OF LAND-USE CHANGE ON THE PROPERTIES OF TOP SOIL OF DECIDUOUS SAL FOREST IN BANGLADESH. *Journal of Mountain Area Research*, *1*, 5. https://doi.org/10.53874/jmar.v1i0.7

Kimmins, JP. 1987. Forest ecology. Macmillan, London. 531 pp

Kumar, R., & Saikia, P. (2021, January 27). Spatio-temporal soil nutrient dynamics and plant species diversity in selected Sal forests of Ranchi, Eastern India. *Vegetos*, *34*(1), 235–248. https://doi.org/10.1007/s42535-020-00173-y

Mahendrappa, M.K., Foster, N.W., Weetman, G., Krause, H.H. 1986. Nutrient cycling and availability in forest soils.

Mahmood, H., Saha, C., Paul, N., Deb, S., Abdullah, S. R., Tanvir, M. S. S. I., Bashar, A., Roy, S., Rabby, F., Ahmed, S. N., & Ali, M. H. (2021, April). The soil quality of the world's largest refugee campsites located in the Hill forest of Bangladesh and the way forward to improve the soil quality. *Environmental Challenges*, *3*, 100048. https://doi.org/10.1016/j.envc.2021.100048.

Marschner, H. 1986. Mineral nutrition in higher plants. Academic, London.

Masum, K. M., & Hasan, Md. M. (2020). Assessment of Land Cover Changes from Protected Forest Areas of Satchari National Park in Bangladesh and Implications for Conservation. Journal of Forest and Environmental Science, 36(3), 199–206. https://doi.org/10.7747/JFES.2020.36.3.199

Md., Habibur, Rahman., M., Bahauddin., Mohammed, Abu, Sayed, Arfin, Khan., Md., Jahirul, Islam., Mohammad, Belal, Uddin. (2012). Assessment of soil physical properties under plantation and deforested sites in a biodiversity conservation area of north-eastern Bangladesh. International Journal on Environmental Sciences, 3(3):1079-1088.

Mengel K, and Kirkby, E.A. 1987. Principles of plant nutrition, 4th edn. International Potash Institute, Worblaufen-Bern

Meyer, B.S., Anderson, D.B., Bohning, R.H. and Fratiane, D.G. 1973. Introduction to plant physiology. New York: D. Van Nostrand Company.

Mondol, M. A., & Wadud, M. A. (2021, August 31). Soil, Plant Species and Encroachment Status of Sal Forest in Bangladesh. *Advances in Image and Video Processing*, *9*(4). https://doi.org/10.14738/aivp.94.10691

Rahman, H., Ishaque, F., Rashid, S., Rahman, J., & Hossain, A. (2022). An analysis of 50 years of seasonal rainfall and temperature pattern data in the Sylhet region of Bangladesh. *Multidisciplinary Science Journal*, *4*(4), 1–8. https://doi.org/10.31893/multiscience.2022019

Rahman, M. H., Bahauddin, M., Khan, M. A. S. A., Islam, M. J., & Uddin, M. B. (2012). Assessment of soil physical properties under plantation and deforested sites in a biodiversity conservation area of north-eastern Bangladesh. International Journal of environmental sciences, 3(3), 1079-1088.

Rahman, M. M., Rahman, M. M., Guogang, Z., & Islam, K. S. (2010, March). A Review of the Present Threats to Tropical Moist Deciduous Sal (Shorea Robusta) Forest Ecosystem of Central Bangladesh. *Tropical Conservation Science*, *3*(1), 90–102. https://doi.org/10.1177/194008291000300108

7. APPENDICES

Appendix 1: Nutrient maps for different nutrients (N, P, K and Ca) has also been prepared for the Hill zone.

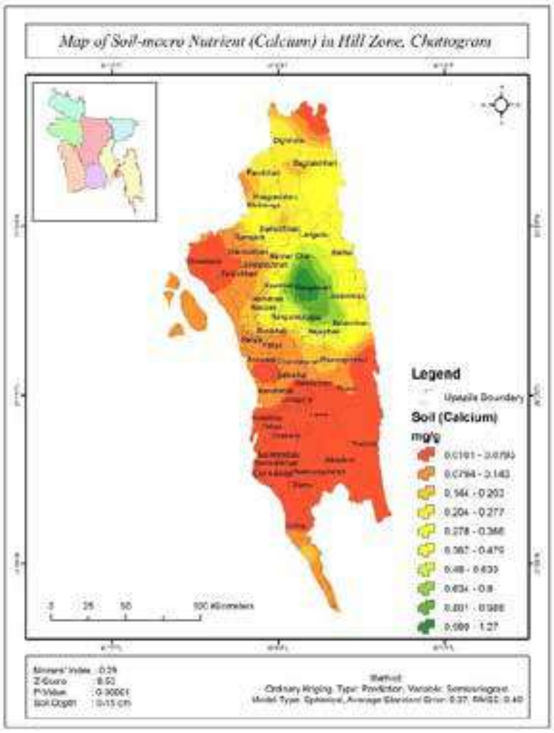

a

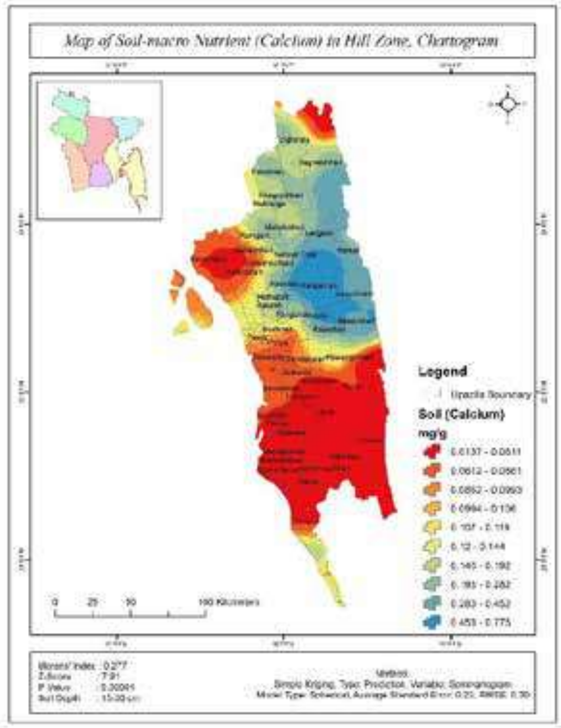

b

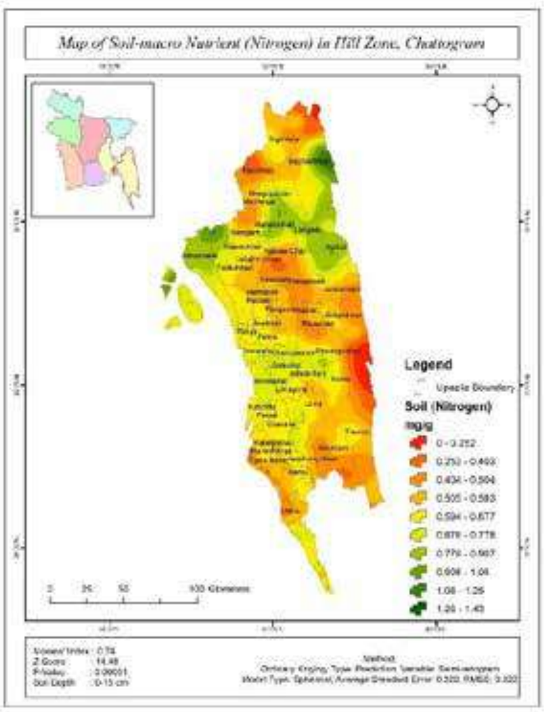

c

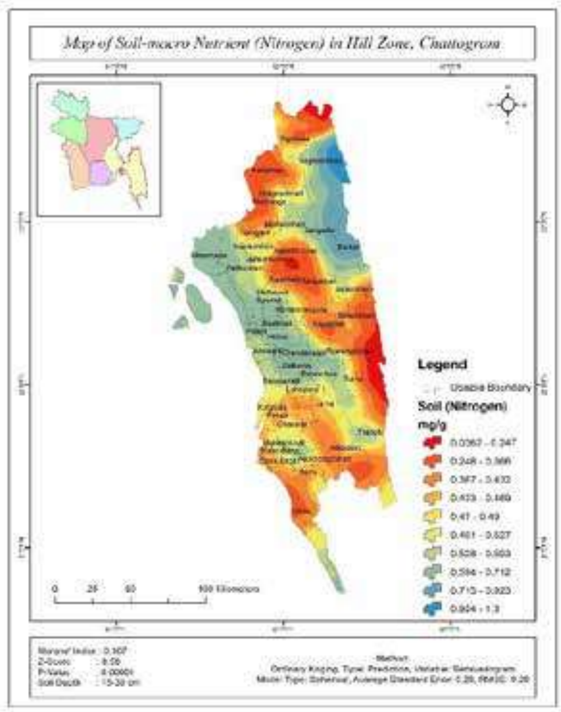

d

Nutrient maps of Calcium a) 0-15 cm, b) 15-30 cm and Nitrogen c) 0-15 cm, d) 15-30 cm for the Hill zone, Chattogram.

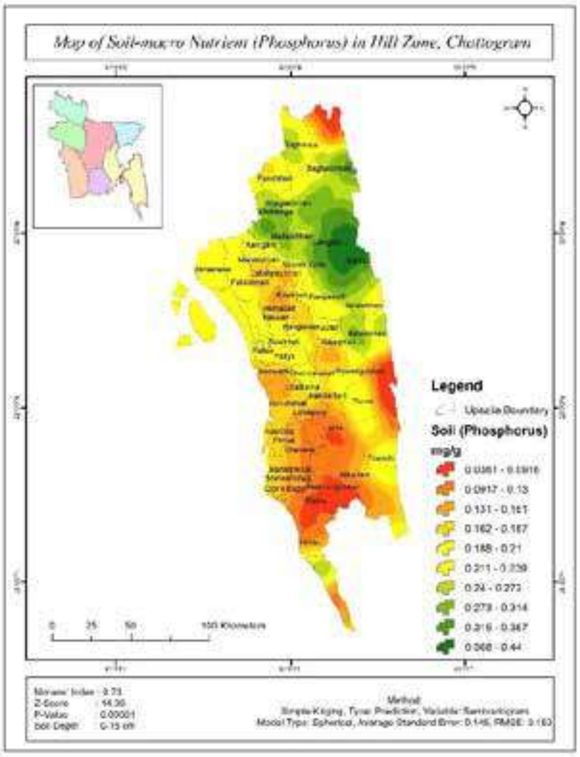

e

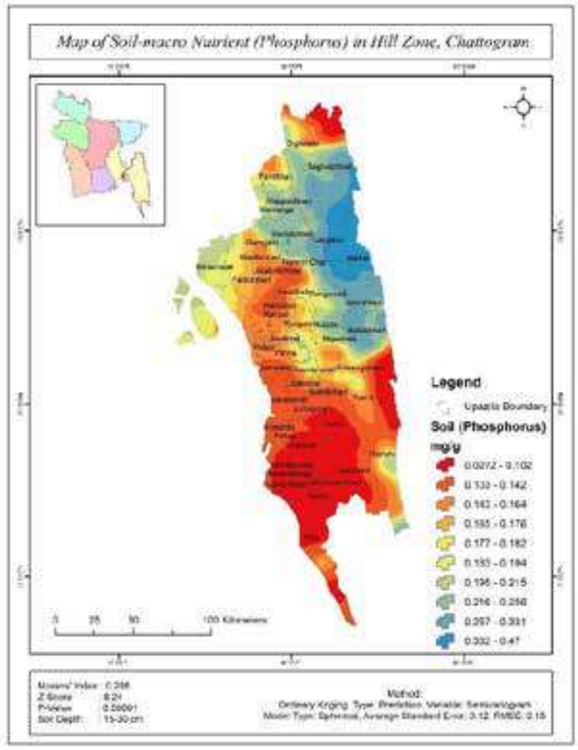

f

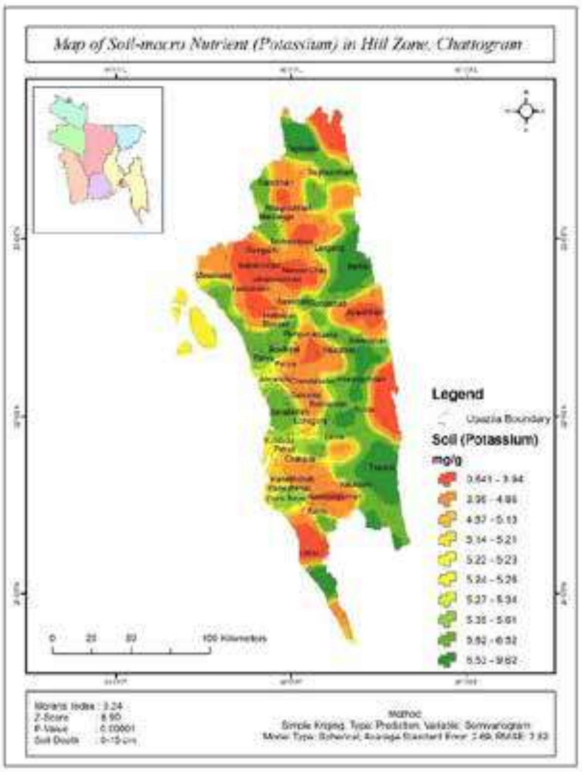

g

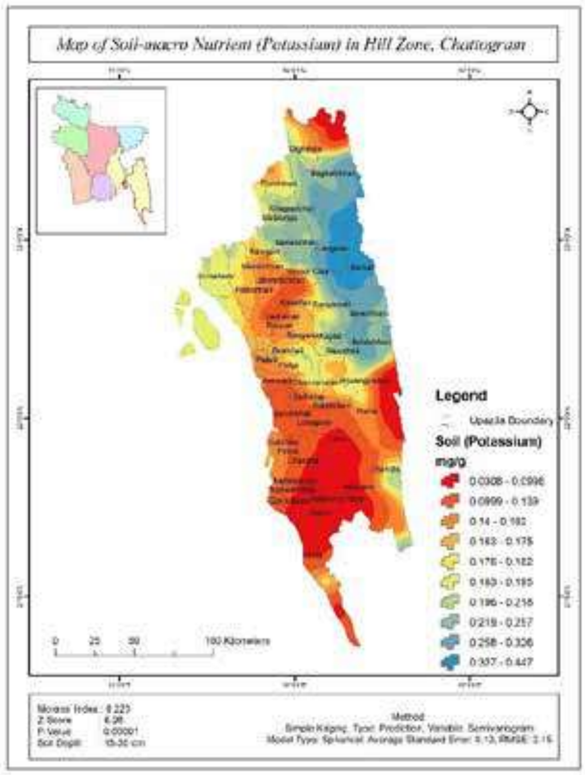

h

Nutrient maps of Phosphorus e) 0-15 cm, f) 15-30 cm and Potassium g) 0-15 cm, h) 15-30 cm for the Hill zone, Chattogram.

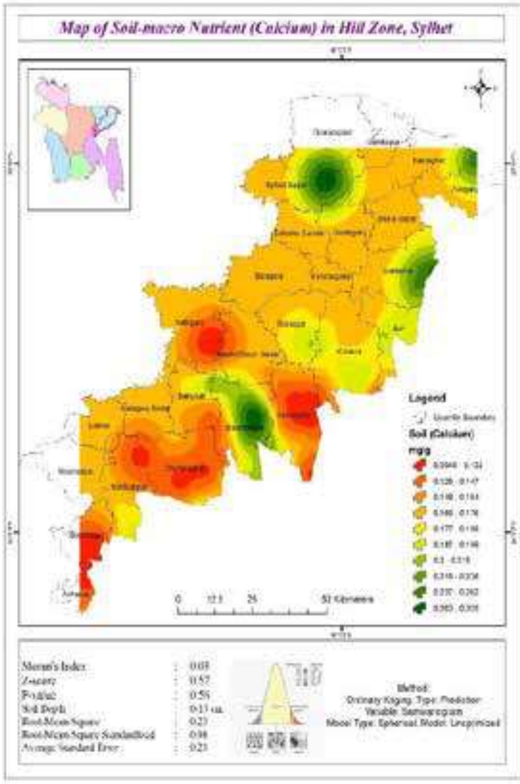

a

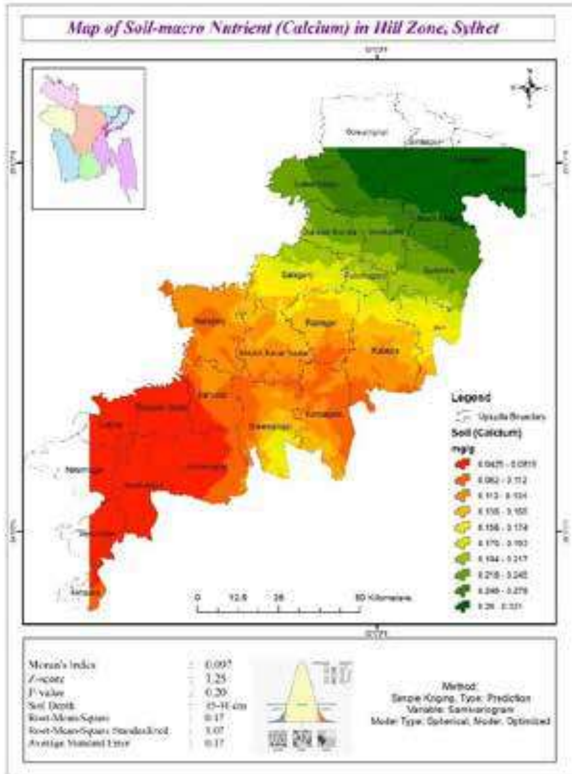

b

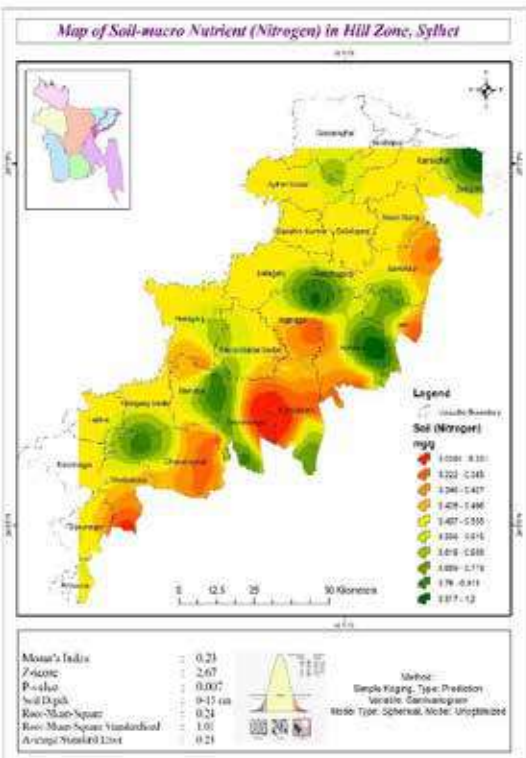

c

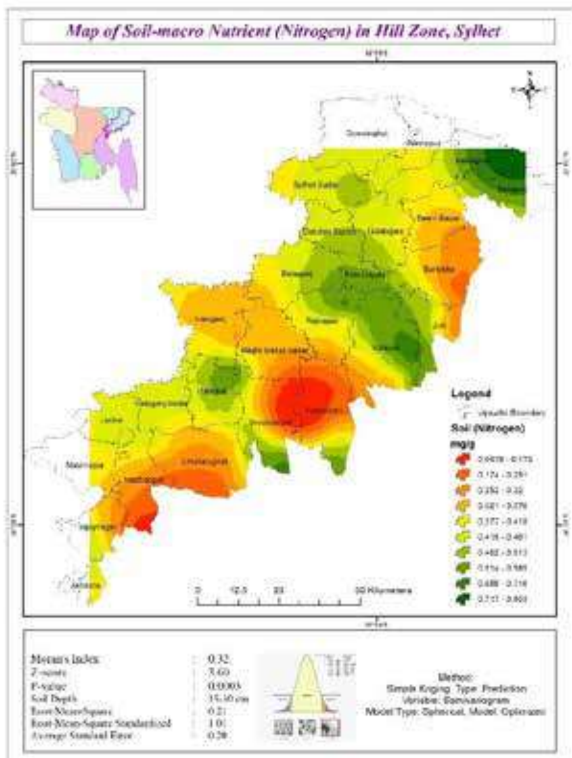

d

Nutrient maps of Calcium a) 0-15 cm, b) 15-30 cm and Nitrogen c) 0-15 cm, d) 15-30 cm for the Hill zone, Sylhet.

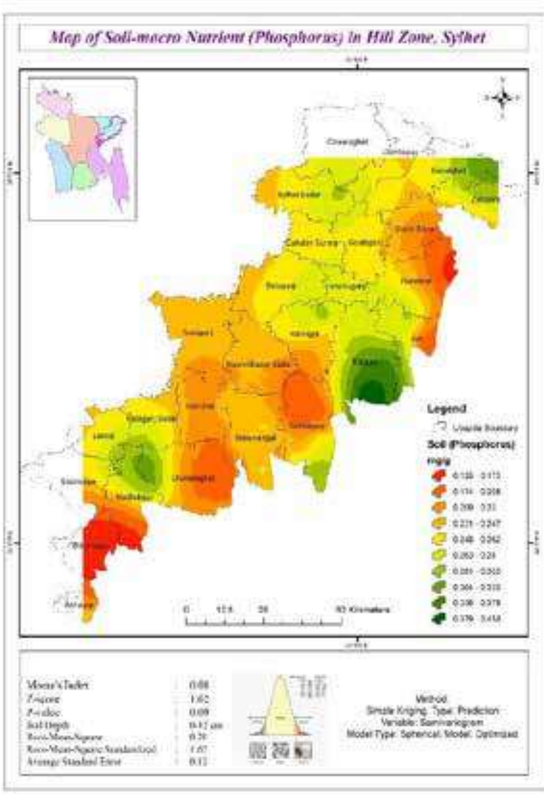

e

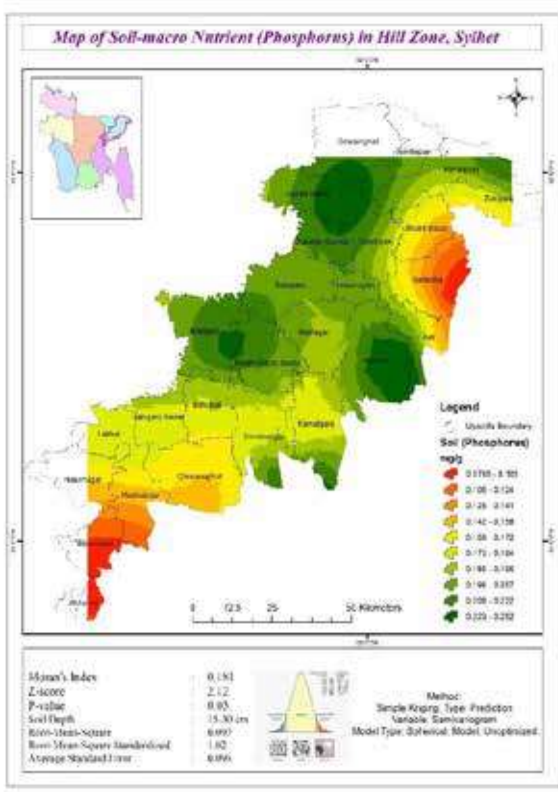

f

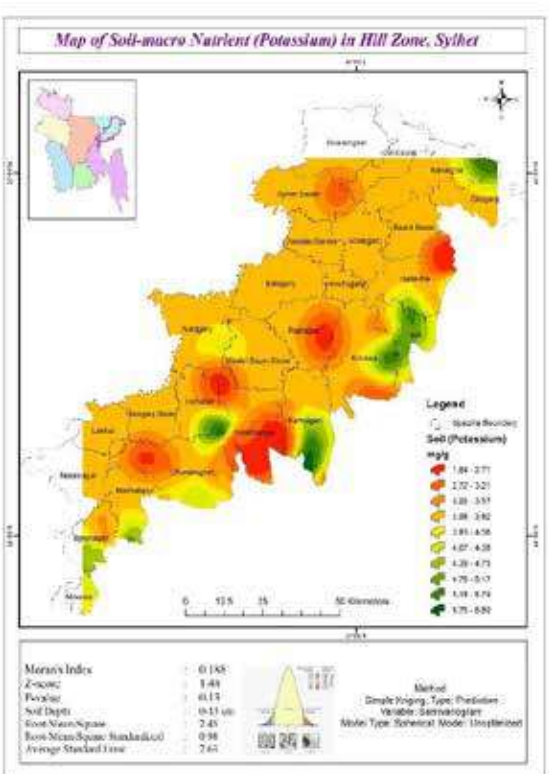

g

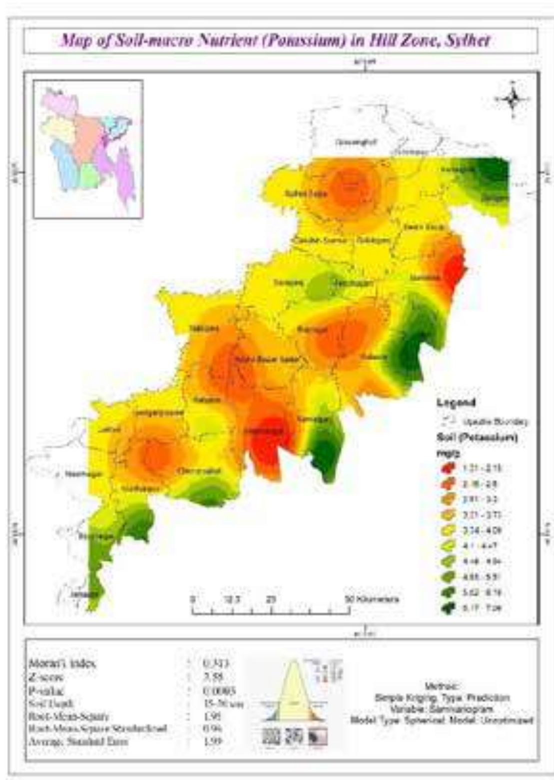

h

Nutrient maps of Phosphorus e) 0-15 cm, f) 15-30 cm and Potassium g) 0-15 cm, h) 15-30 cm for the Hill zone, Sylhet

Appendix 2: Nutrient maps for Sal zone

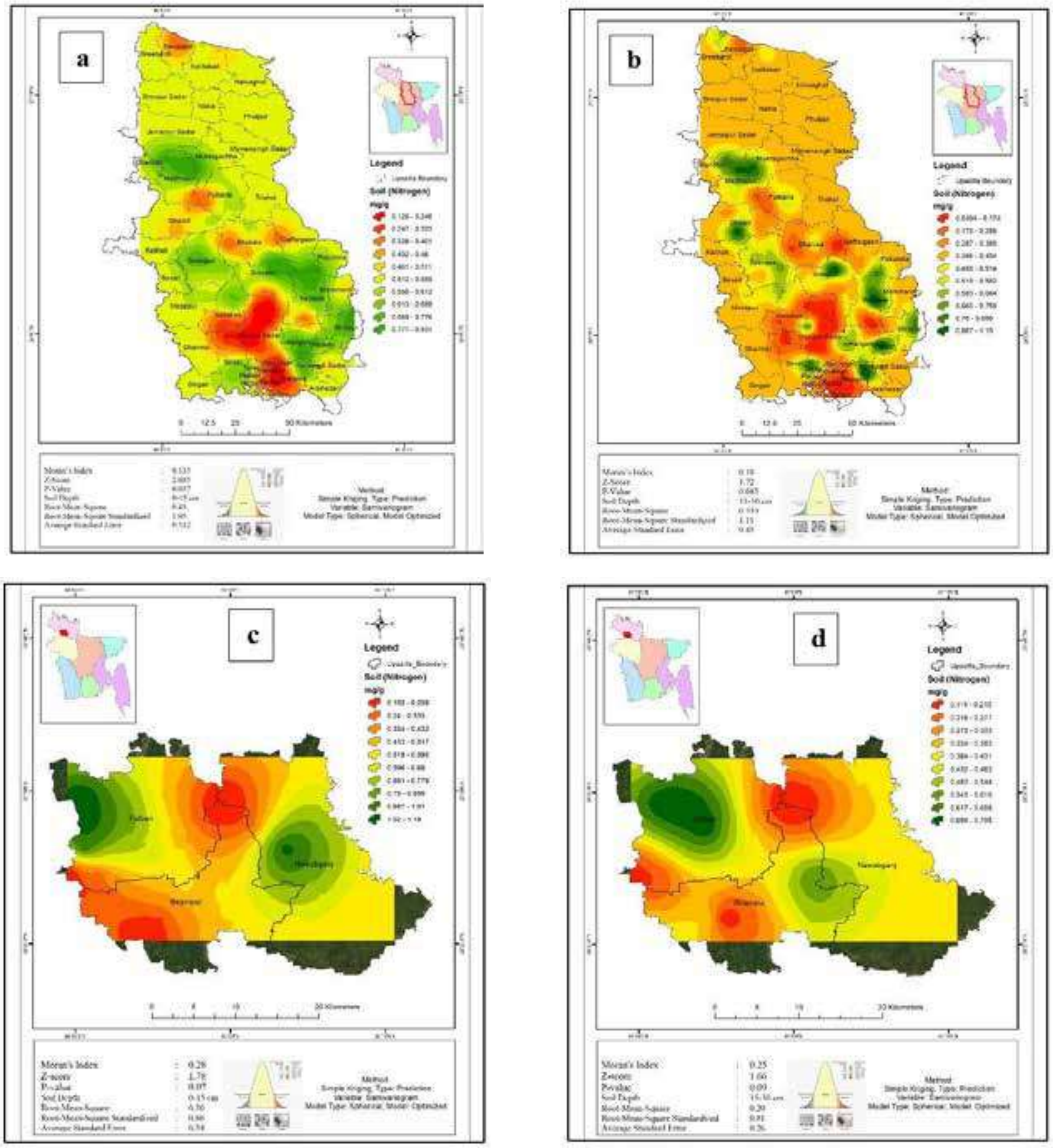

Nutrient maps of Nitrogen a) 0-15 cm, b) 15-30 cm for the Central part and c) 0-15 cm, d) 15-30 cm for the North part.

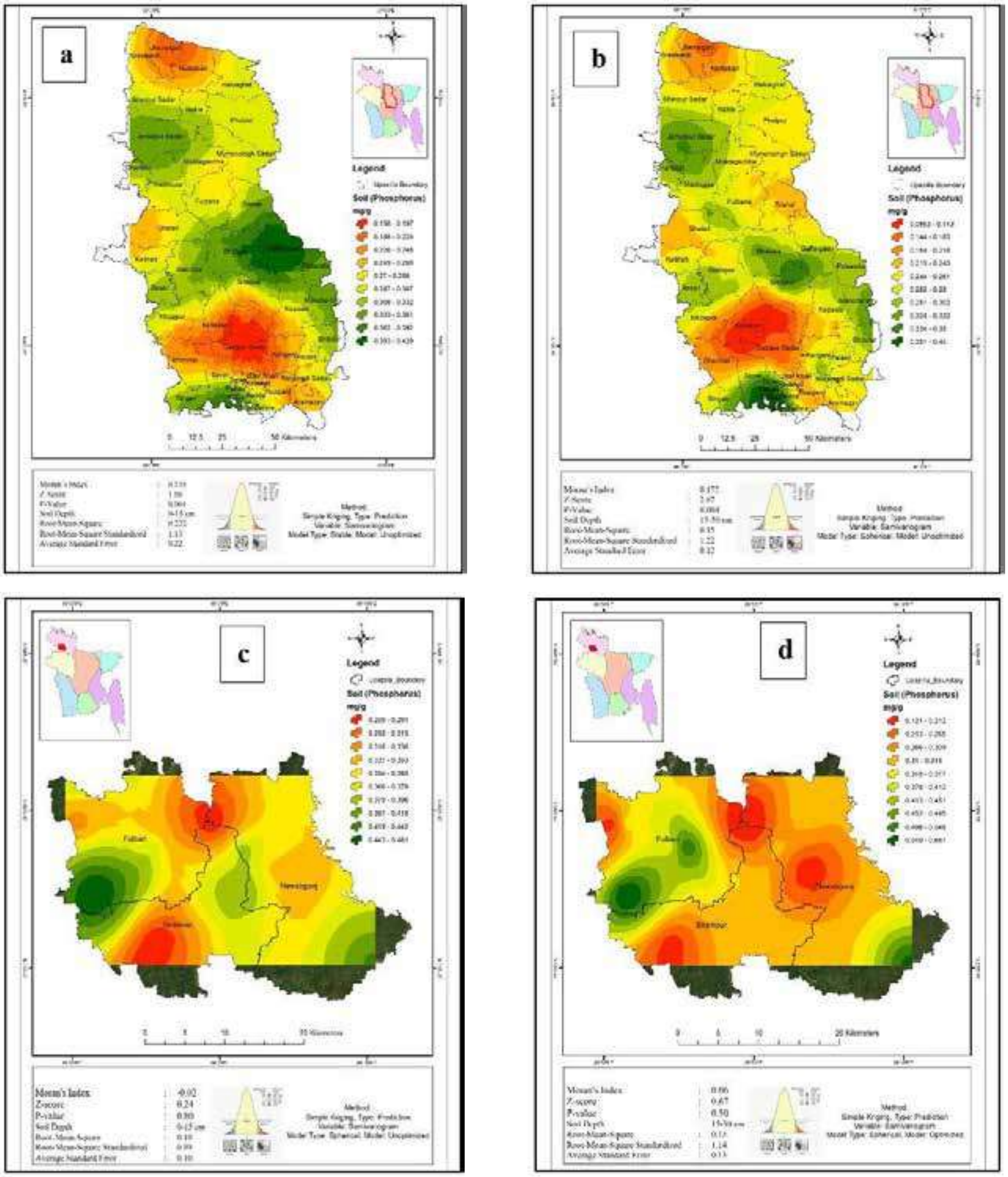

Nutrient maps of Phosphorus a) 0-15 cm, b) 15-30 cm for the Central part and c) 0-15 cm, d) 15-30 cm for the North part.

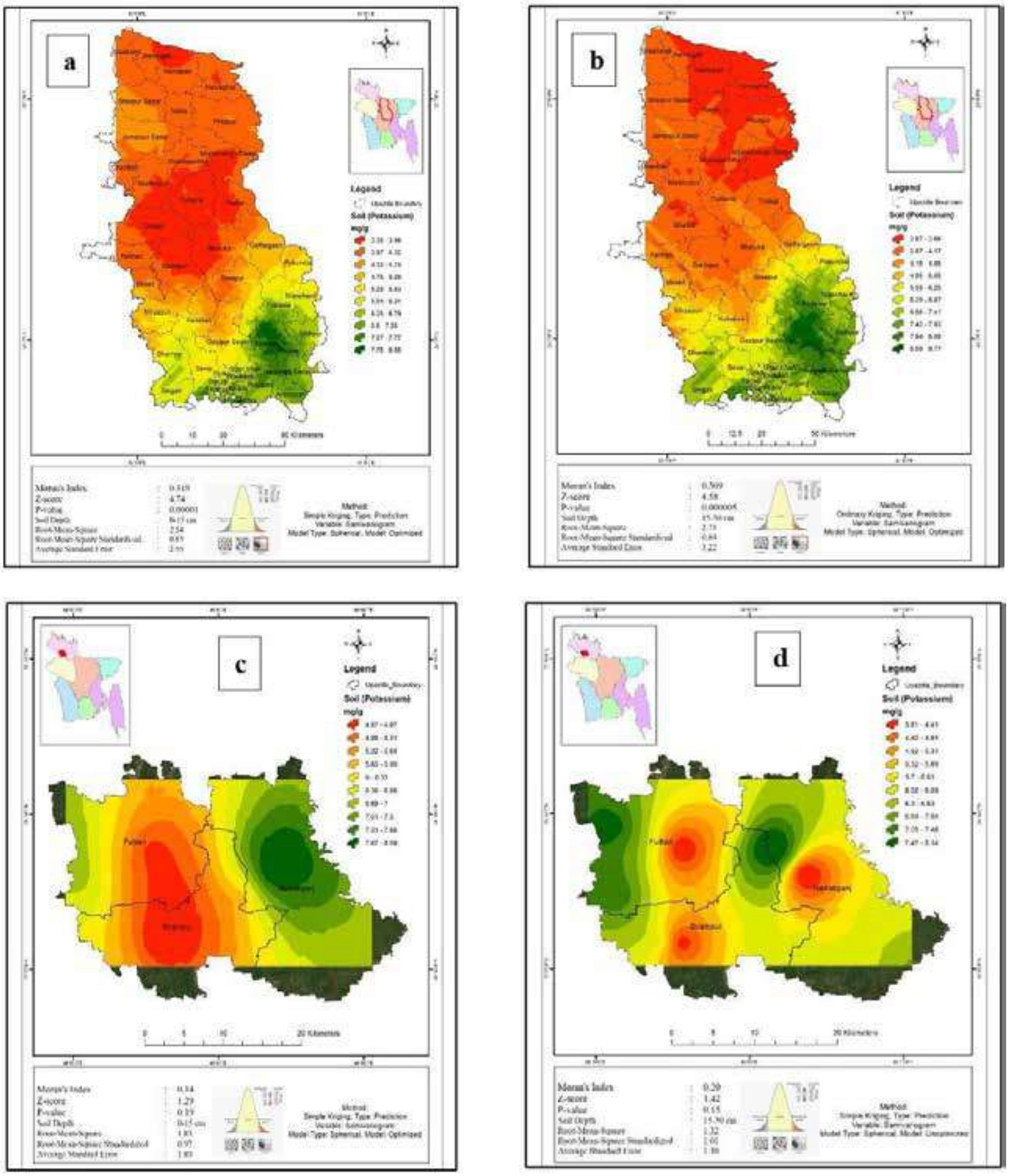

Nutrient maps of Potassium a) 0-15 cm, b) 15-30 cm for the Central part and c) 0-15 cm, d) 15-30 cm for the North part.

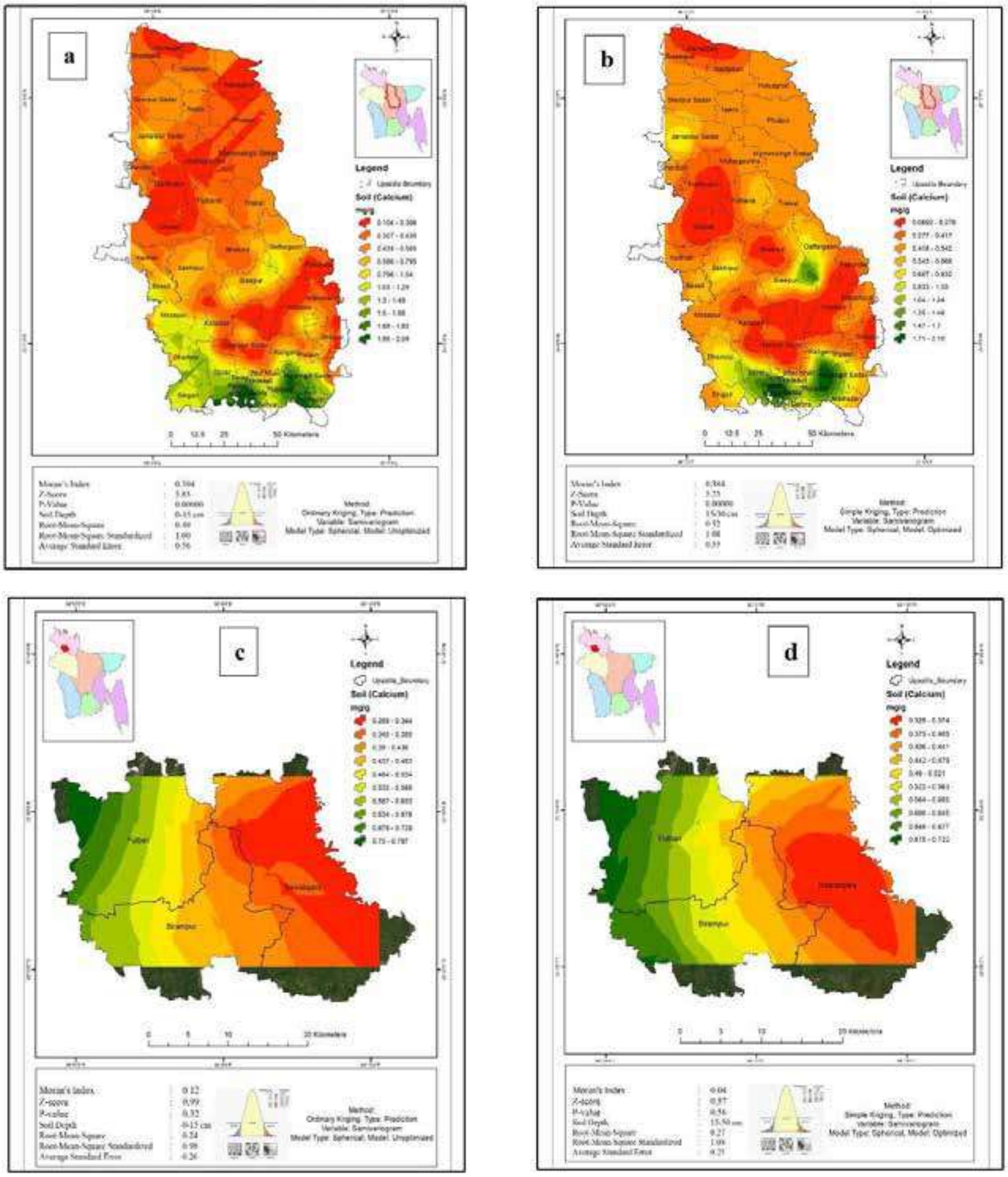

Nutrient maps of Calcium a) 0-15 cm, b) 15-30 cm for the Central part and c) 0-15 cm, d) 15-30 cm for the North part.

Individual Tree detection from Ultra-High resolution UAV(Unmanned Ariel Vehicle) image to monitor plantation survive rate: A case study from SUFAL plantation site.

by

Md. Tauhidor Rahaman

Forester, RIMS Unit, Banabhaban, Agargaon, Dhaka

CHAPTER I

INTRODUCTION

Forest Department under the ministry of Environment, Forest and Climate Change is implementing a project titled 'Sustainable Forest And Livelihood (SUFAL) Project'. The World Bank has funded for the project. The project has provision for innovation grant which are in line with the project objectives. In response to call for concept note and submission of full research proposal, the SUFAL project has awarded research titled **"(Individual Tree Detection from ultra high-resolution UAV (Unmanned Ariel Vehicle) image to monitor plantation survive rate, A case study from SUFAL Plantation site)"**. The duration of the project is 1 year 10 months starting from 29th September 2021 to 29th June 2023 and cost of the project is BDT 46,41,051/-. The project is extended up to September 2023. The formal agreement between researcher and SUFAL PMU was signed on 29th September 2021.

Automatic seedling detection and count using drone technology marks a groundbreaking transformation in plantation monitoring. Conventional plantation monitoring relies on manual surveys, which are labor-intensive, time-consuming, and prone to human error, leading to inconsistent survival assessments (Kattenborn et al., 2014; Shafri et al., 2011). These conventional approaches often result in inconsistencies in seedling survival assessments, making it challenging for forest managers to accurately evaluate plantation health and plan necessary interventions.

High-resolution satellite imagery can significantly enhance plantation monitoring. Satellite- based monitoring, while offering broad coverage, faces challenges such as high costs, limited availability of very high-resolution (VHR) imagery, and persistent cloud cover (Hyyppa et al., 2016; Wallace et al., 2012). However, monitoring first and second-year seedlings requires ultra- high-resolution (0.5m resolution) data, such as WorldView-3 (Korom, A., et al., 2014). Even with such data, detecting first-year seedlings, which range in height from 10 cm to 1.0 m with minimal canopy cover, remains challenging. Using satellite imagery for plantation monitoring is particularly difficult due to the high cost and limited availability of very high-resolution (VHR) images (<0.5m). These images must be ordered in large scenes covering several square kilometers, making it impractical to acquire data for specific plantation areas (e.g., 20, 50, 100, or 500 hectares) scattered across different locations. Furthermore, repeated monitoring over multiple years becomes increasingly expensive due to the high cost of image procurement for each monitoring cycle. Additionally, in the early stages of plantation growth, the seedling canopy may not even span 0.5 meters, limiting the effectiveness of VHR satellite imagery for individual seedling detection. While satellite images can provide a broad overview of plantation areas, accurately identifying, counting, and monitoring individual seedlings remains a significant challenge.

In contrast, recent advancements in Unmanned Aerial Vehicles (UAVs) and Machine Learning (ML) have revolutionized this field by enabling cost-effective, high-resolution data acquisition (2– 5 cm/pixel) and automated analysis (Diaz-Varela et al., 2014; Laliberte & Rango, 2011). UAVs paired with Structure from Motion (SfM) photogrammetry allow flexible, frequent monitoring and generate 3D reconstructions of plantation sites (Quan, 2010; Fisher et al., 2014). Object-Based Image Analysis (OBIA) and Deep Learning (DL) further enhance automation by segmenting and classifying individual trees from UAV imagery (Hentz et al., 2018; Torres-Sánchez et al (2015)., 2015). For instance, Faster R-CNN models have achieved 91.61% accuracy in detecting trees in complex environments like coal mine afforestation areas (Luo et al., 2022), while SSD and RetinaNet offer efficient one-stage detection frameworks (Fromm, 2019).

On the contrary, drones equipped with high-resolution cameras can capture detailed aerial imagery of plantation sites with resolutions as fine as 2–5 cm per pixel. Advanced ML algorithms can analyze these images to automatically detect, count, and geolocate every live seedling with remarkable accuracy. This capability eliminates the need for labor-intensive fieldwork, providing a seamless and scalable solution for monitoring large plantation areas. The automated system not only determines the total number of live seedlings but also creates geo-referenced data, allowing precise tracking of individual trees over time.

One of the major benefits of drone-based plantation monitoring is its ability to analyze seedling distribution and survival patterns. By mapping out areas with high seedling mortality, AI-driven analysis can pinpoint locations that require replanting. This targeted vacancy-filling approach ensures better resource allocation and maximizes plantation success rates. Furthermore, AI driven very high-resolution drone image can generate digital seedling density maps using GIS, which provide insights into growth patterns and highlight potential stress factors affecting tree survival.

The integration of AI, ML, VHR orthomosaic, and digital twins overlay in Google Earth Pro not only enhances accuracy but also streamlines the entire decision-making process for forest managers. Instead of relying on periodic field visits, which can be costly and inefficient, forestry officials can access real-time data remotely. Platforms such as Google Earth Pro or other GIS- based applications allow them to visualize high-resolution geospatial data, enabling efficient monitoring and strategic planning. This level of automation significantly reduces dependence on traditional field surveys, saving time and resources while improving overall plantation outcomes.

Moreover, adopting drone-based AI solutions contributes significantly to large-scale afforestation and reforestation initiatives. By optimizing tree survival rates and ensuring better management of plantation resources, this technology supports global efforts to enhance carbon sequestration, mitigate climate change, and promote biodiversity conservation. The widespread adoption of this high-tech monitoring system by forest departments and restoration practitioners could revolutionize how plantations are managed, making tree-planting efforts more data-driven, efficient, and sustainable. Ultimately, this advanced approach could have the potential to replace conventional monitoring systems, ushering in a new era of precision forestry that ensures long- term environmental and ecological benefits.

This technology has been successfully adopted by several developed countries, including Spain, Brazil, Indonesia, the Netherlands, Malaysia, and Germany, to monitor commercial plantations such as palm, olive, and rubber trees (Csillik et al., 2018; Liu et al., 2021). These plantations generally feature wider spacing and more uniform row and column arrangements, with most being over five or six years old, resulting in broader canopy covers compared to the smaller seedlings found in early plantation stages. However, the conditions in these countries differ significantly from those in Bangladesh, where challenges such as tidal fluctuations, dense understory vegetation (including uri-grass and green algae), and non-uniform seedling spacing complicate detection efforts. In Bangladesh, coastal plantations typically have a spacing of 1.5 meters, while terrestrial plantations have a 2-meter spacing, with less uniform row and column arrangements, making the application of this technology more complex. Additionally, some seedlings are scattered across the plantations, and varying amounts of uri-grass, along with the presence of green algae and other understory vegetation, need to be considered for their potential effects on the detection process. Factors such as high and low tide conditions, green algae, and green understory vegetation also require careful evaluation to understand their influence on drone- based automatic seedling detection. Furthermore, parameters like ground sampling distance (GSD), flight height, and shutter speed play crucial roles in determining the effectiveness of this technology. The research aims to identify the optimal conditions necessary for successfully applying these modern technologies in Bangladesh's unique plantation environments.

Developing an optimal detection model requires careful selection of machine learning frameworks such as CNN, R-CNN, SSD, YOLOv3, YOLOv4, and RetinaNet, along with suitable backbone architectures and ground condition parameters tailored to specific sites. These factors are crucial for ensuring precise automatic seedling detection and counting. Fine-tuning the model based on site-specific conditions—such as canopy cover, tidal influences, green algae presence, understory vegetation, and sun angle—significantly enhances detection accuracy and reliability. This approach strengthens automated plantation monitoring, enabling data-driven decision-making for effective forest management.

1.1 Problem Statement:

Traditional plantation monitoring systems face several uncertainties. First, accurately measuring plantation areas is challenging due to difficult accessibility and the presence of mudflats, making it a labor-intensive task. Additionally, a 20m x 20m plot size is assigned for coastal plantation monitoring, with sample plots allocated within the surveyed area at a 1% sampling intensity (25 plots for 100 ha) in the traditional monitoring system. However, no modern technology, such as GIS-based fishnet tools, is used to define random plot locations. As a result, uncertainties in plantation area measurement, insufficient sampling intensity, lack of accuracy, and potential bias could arise. Furthermore, physically delineating plantation boundaries and collecting data from sample plots are often time-consuming and laborious, making precise monitoring a persistent challenge.

On the other hand, acquiring very high-resolution (VHR) satellite images is expensive, as at least one scene covering several square kilometers must be ordered for a specific Area of Interest (e.g., 50/100/200 hectares). Thus, it is not possible to get images for a particular plantation site. Another issue with VHR satellite imagery is the frequent cloud cover, making it difficult to obtain cloud- free images, particularly in Bangladesh.

Both traditional plantation monitoring methods and satellite-based monitoring systems have their drawbacks. These challenges could be addressed and replaced by modern UAV and machine learning-based scientific techniques for more efficient and accurate plantation monitoring.

1.2 Research Question:

Can the integration of UAV (Unmanned Aerial Vehicle) and AI (Artificial Intelligence) technologies serve as a smart and effective tool for plantation monitoring?

1.3 Objectives:

The objectives of the study are:

1. To evaluate the potential of UAV data combined with advanced machine learning techniques for the automatic detection and counting of individual seedling, with the aim of enhancing the success of afforestation programs.
2. To identify and geo-locate areas where seedlings have failed to survive, in order to support targeted vacancy filling efforts.
3. To investigate the impact of various drone flight parameters (e.g., altitude, ground sampling distance, overlap, and sensor type), site-specific factors (e.g., line uniformity, seedling height, canopy density, understory vegetation such as green algae, uri-grass, and shrubs, tide conditions, and sun angle), and different model frameworks (e.g., SSD, CNN, RCNN, YOLOv3, YOLOv4, RetinaNet) on the development of an optimized model for automatic tree counting.

1.4 Rationale:

The Bangladesh Forest Department has pioneered coastal afforestation efforts. Since 1960, it has established more than 20 million hectares of coastal plantation. Conventional plantation assessment methods depend on manual surveys, which are labor-intensive, time-consuming, and prone to human error. These traditional approaches frequently lead to inconsistencies in seedling survival evaluations, making it difficult for forest managers to accurately assess plantation health and implement necessary interventions.

Satellite based plantation monitoring is challenging because of high costs, especially when using very high-resolution satellite imagery (<1 m). Such images are expensive and difficult to obtain for specific plantation sites, requiring large areas to be covered, and repeated monitoring incurs additional costs. Moreover, these images often do not offer the resolution needed to detect and count individual seedlings in early plantation stages.

In contrast, Unmanned Aerial Vehicles (UAVs) equipped with high-resolution cameras (1– 5 cm) provide a more cost-effective solution for monitoring. UAVs can capture detailed images of plantations, enabling precise detection and counting of individual seedlings. This approach reduces reliance on costly satellite imagery and eliminates the need for repeated image procurement. Additionally, using machine learning algorithms alongside UAV data allows for accurate seedling survival rate assessments and identification of areas requiring replanting. The UAV system can address traditional monitoring challenges, such as area measurement uncertainty, insufficient sampling, and bias, thus improving plantation management efficiency and supporting the SUFAL project's goals.

CHAPTER II

LITERATURE REVIEW

Remote sensing data and analysis techniques are valuable tools for plantation inventories, offering significant advantages over traditional field-based surveys. These methods allow for efficient, accurate, and cost-effective collection of spatial data, which is crucial for monitoring plantation health, growth, and yield. As Kattenborn et al. (2014) emphasized, remote sensing techniques, particularly satellite-based sensors, are indispensable for large-scale monitoring of forests and plantations. One of the most widely used types of remote sensing data for such applications is very high resolution (VHR) optical satellite imagery, which has shown promise in accurately classifying and detecting individual trees (Shafri et al., 2011; Korom et al., 2014; Kamiran & Sarker, 2014). This imagery can facilitate manual counting of individual palms or, in some cases, automatically segmenting palm crowns. These capabilities have demonstrated high classification accuracy in numerous studies.

However, while VHR optical data has its advantages, it also presents certain limitations. For instance, the relatively high acquisition cost of VHR imagery and its susceptibility to weather conditions such as cloud cover significantly restricts its usability in routine monitoring. Moreover, continuous access to such high-quality data may be financially and logistically infeasible, especially in regions with frequent cloud cover or where data availability is inconsistent (Shafri et al., 2011). These limitations have driven the search for alternative remote sensing technologies that could provide accurate, dense, and cost-effective data on plantations.

One such promising technology is Light Detection and Ranging (LiDAR), which has gained considerable attention for plantation inventory and monitoring due to its ability to produce precise, accurate, and dense three-dimensional (3D) point clouds (Hyyppa et al., 2008). LiDAR data allows for detailed measurements of tree canopy structure, height, and distribution, which are critical parameters for plantation management. However, despite its high accuracy and capability to generate 3D data, LiDAR also suffers from high costs, making it less accessible for routine monitoring or smaller-scale projects (Kattenborn et al., 2014). These challenges have encouraged the exploration of more affordable and flexible alternatives.

Recent advancements in Unmanned Aerial Vehicle (UAV) technology have opened up new opportunities for plantation monitoring. UAVs offer several advantages, including their ability to capture very high-resolution optical imagery at lower costs compared to traditional satellite imagery (Wallace et al., 2012). UAVs also provide the flexibility of spatial and temporal data acquisition, allowing for frequent monitoring of plantations and enabling real-time analysis. As a result, UAVs have become an increasingly popular tool in precision agriculture and forestry, particularly for detecting and mapping individual trees or plantations (Hung et al., 2012; Wallace et al., 2016).

The integration of UAVs with advanced image processing techniques, such as Structure from Motion (SfM), has further enhanced their utility in plantation inventory tasks. SfM is a photogrammetric technique that reconstructs 3D scenes from a series of overlapping 2D images taken from different perspectives (Quan, 2010; Fisher et al., 2014). This technique has proven effective for generating high-resolution 3D models of plantation landscapes, making it possible to estimate tree heights, canopy structure, and other critical attributes. The use of SfM combined with UAV imagery has the potential to provide an even more detailed understanding of plantation conditions, enabling more precise inventory and management practices.

Another important development in remote sensing for plantation inventory is the application of object-based image analysis (OBIA) techniques, which offer a more sophisticated approach to image classification than traditional pixel-based methods. OBIA involves segmenting an image into meaningful objects based on their spectral, spatial, and contextual properties, and then classifying these objects using various machine learning algorithms (Diaz-Varela et al., 2014). This approach allows for the automatic detection and classification of individual trees or tree species, overcoming some of the limitations of pixel-based methods, such as confusion between similar land cover types. Machine learning models, particularly Region-based Convolutional Neural Networks (RCNN), have been successfully integrated into OBIA workflows to improve the accuracy of tree detection in UAV imagery (Laliberte & Rango, 2011).

RCNN models in particular have shown considerable promise in tree detection. These models work by first generating candidate regions of interest (ROIs) from an image, then applying a neural network to classify the objects within these regions (Ren et al., 2015). In the context of UAV-based plantation inventory, RCNN has proven effective at automatically detecting individual trees, even in complex environments where trees are densely packed or partially obscured by other vegetation (Hentz et al., 2018). This ability to distinguish between different objects in the landscape is crucial for accurate plantation mapping.

Hentz et al. (2018) demonstrated that UAV imagery coupled with VHR data could automatically detect and measure tree positions in Paraná state, Brazil. This approach allowed for significant cost reductions compared to traditional forest inventories or LiDAR surveys (White et al., 2013; Hernandez et al., 2014). Furthermore, a study conducted by Torres-Sánchez et al. (2015) in Jaén Province, Spain, explored the impact of various factors such as sensor type, altitude, focus length, and overlap on the accuracy of VHR data collection and automatic tree detection. Their findings highlighted the importance of optimizing these parameters to achieve the highest possible accuracy when using UAV imagery for tree detection.

A recent study by Luo et al. (2022) focused on individual tree detection in a coal mine afforestation area using improved Faster-RCNN models applied to UAV RGB images. Conducted in the Ulan Mulan River Basin in the Ordos region of China, the study found that the Faster- RCNN-based model was able to automatically detect trees with an impressive 91.61% accuracy. This model was particularly effective in distinguishing trees from surrounding vegetation, a common challenge in natural environments where various types of vegetation overlap.

Another significant advancement in the use of UAVs for plantation monitoring is the application of Convolutional Neural Networks (CNNs), particularly for detecting seedlings and young trees. Fromm (2019) conducted research in the boreal forests of northeastern Alberta, Canada, where CNNs were applied to drone imagery for the automated detection of conifer seedlings. This study explored the influence of factors such as training set size, seedling size, and spatial resolution on detection accuracy. The results showed that Faster-RCNN, a two-stage object detection model, produced higher precision in detecting seedlings compared to other models like SSD and R-FCN. Faster-RCNN works by proposing regions of interest, which are then analyzed by a subsequent network to classify the object and predict its bounding box (Uijlings et al., 2013; Ren et al., 2015).

Two-stage detectors, like Faster-RCNN, are known for their high accuracy and ability to detect overlapping objects, but they come with a trade-off in terms of computational resource requirements and processing time. In contrast, Single Shot Multibox Detectors (SSD) are one-stage detectors that, while less accurate, are more efficient and require fewer computational resources. SSD has proven particularly useful in real-time applications, where speed is critical (Fromm, 2019).

One application of CNNs for tree detection was conducted by Csillik et al. (2018) in Tulare County, California, USA, where they used CNN frameworks to detect citrus trees from UAV imagery. Their study found that CNN-based methods achieved an accuracy of 96.24% and precision of 94.59%. However, they also identified some limitations, such as difficulty distinguishing between small trees and large trees and confusion between weeds and trees at the edges of plantation parcels. Despite these challenges, CNNs remain a powerful tool for detecting trees in plantations, particularly when the trees are of similar size and shape.

Similarly, Liu et al. (2021) conducted research in Malaysia on automatic oil palm tree detection using UAV imagery and deep learning algorithms. The study, which utilized the Faster- RCNN model, reported an accuracy rate of 97.06%, 96.58%, and 97.79% across three different sites. This study underscores the effectiveness of deep learning models in detecting oil palm trees, a crop that is often grown in dense, monocultural plantations.

In Brazil, Zortea et al. (2018) employed CNNs to identify citrus trees in UAV imagery. The study found that the CNN model achieved an overall accuracy of 94% in detecting citrus trees, most of which were of medium size and uniformly distributed across the plantation. This further highlights the suitability of CNNs for detecting specific types of trees in plantations with relatively homogeneous tree characteristics.

In conclusion, the integration of UAVs, advanced image processing techniques like SfM, and machine learning models such as RCNN and CNNs has revolutionized the way plantation inventories are conducted. These technologies provide accurate, cost-effective, and scalable solutions for monitoring plantations, with the ability to automatically detect individual trees, assess plantation health, and optimize management practices. As these technologies continue to evolve, their potential to transform plantation management will only increase, leading to more efficient, sustainable, and data-driven approaches to plantation monitoring.

CHAPTER III

METHODOLOGY

3.1 Study Area:

The study analyzed mangrove and non-mangrove plantation sites under Bangladesh's SUFAL project. Coastal plantation sampling focused on 1-hectare plots in **Bhula Forest Division** (Shoshigonj Beat, Char Zahir Uddin Beat, Betua Bon Kendra) and **Patuakhali Forest Division** (Pokkia Beat, Sadar Golachipa Range). These plots captured key environmental variables—encompassing uri-grass density, green algae, tidal fluctuations, canopy overlap, understory vegetation, and row uniformity—to streamline model training. By prioritizing small- scale, controlled 1-hectare plots, the study balanced computational efficiency with ecological representativeness, enabling scalable application to larger plantations (e.g., 100–500 ha) with comparable conditions.

Table 01: Different Study Site in The SUFAL plantation area in coastal plantation

S/L	Plantation Name	Crown Overlap	Beat	Range	Forest Division	Location
Bhula_1	Shoshigonj One	No	Shoshigonj	Dowlotkh an	Bhula	22.457601 90.891487
Bhula_2	Shoshigonj Two	No	Shoshigonj	Dowlotkh an	Bhula	22.453599 90.892331
Bhula_3	Shoshigonj Three	No	Shoshigonj	Dowlotkh an	Bhula	22.444078 90.891513
Bhula_4	Shoshigonj Four	No	Shoshigonj	Dowlotkh an	Bhula	22.444416 90.894404
Bhula_5	Char Zahiruddin_One	No	Char Zahir Uddin	Dowlotkh an	Bhula	22.450527 90.896981
Bhula_6	Char Zahiruddin_Two	No	Char Zahir Uddin	Dowlotkh an	Bhula	22.455026 90.899761
Bhula_7	Betua_One	No	Betua	Char Fashion	Bhula	22.233246 90.877385
Bhula_8	Betua_Two	No	Betua	Char Fashion	Bhula	22.234098 90.878385
Bhula_9	Betua_Three	No	Betua	Char Fashion	Bhula	22.233667 90.881466
Patoakhal i _1	Sadar_One	Yes	Sadar	Golachipa	Patoakhali	22.142419 90.398651
Patoakhal i _2	Sadar_Two	Yes	Sadar	Golachipa	Patoakhali	22.141131 90.398477
Patoakhal i _3	Sadar_Three	Yes	Sadar	Golachipa	Patoakhali	22.143028 90.399564
Patoakhal i _4	Pokkhia_One	No	Pokkhia	Golachipa	Patoakhali	22.140459 90.401266
Patoakhal i _5	Pokkhia_Two	No	Pokkhia	Golachipa	Patoakhali	22.097698 90.483962
Patoakhal i _6	Pokkhia_Three	No	Pokkhia	Golachipa	Patoakhali	22.098841 90.485048
Patoakhal i _7	Pokkhia_Four	No	Pokkhia	Golachipa	Patoakhali	22.095206 90.478307
Patoakhal i _8	Pokkhia_Five	No	Pokkhia	Golachipa	Patoakhali	22.093542 90.478235
Patoakhal i _9	Pokkhia_Six	No	Pokkhia	Golachipa	Patoakhali	22.091700 90.476475

SUFAL plantation site were chosen from the Balijhuri sadar beat and Tawakucha Beat of Balijhuri Range, Malakucha Beat from Rangtia Range of Mymensingh Forest Division. Mankhali Beat of Hoyaikkhong and Thainkhali Beat of Ukhia Range were chosen for Cox,sBazar South Forest Division for terrestrial plantation area.

Table 02: Different Study Site in The SUFAL plantation area in terrestrial plantation

S/L	Plantation Name	Crown overlap	Beat	Range	Forest Division	Location
Mymen_ 1	Malakucha_1	No	Sadar	Balijhuri	Mymensingh	25.264679 89.951779
Mymen_ 2	Malakucha_2	No	Sadar	Balijhuri	Mymensingh	25.264804 89.951779
Mymen_ 2	Enrichment	No	Sadar	Balijhuri	Mymensingh	25.254817 89.971514
Mymen_ 4	Tawakucha_1	No	Tawakucha	Rangtia	Mymensingh	25.250911 90.001859
Mymen_ 5	Tawakucha_2	No	Tawakucha	Rangtia	Mymensingh	25.250205 90.002603
Mymen_ 6	Tawakucha_3	No	Tawakucha	Rangtia	Mymensingh	25.248767 90.003066
Cox_1	Mankhali_Jhaw _20h_2019- 2020_1	Yes	Mankhali	Hoyaikkhong	CoxBazar South	21.088344 92.123984
Cox_2	Mankhali_Jhaw _20h_2019- 2020_2	Yes	Mankhali	Hoyaikkhong	CoxBazar South	21.086909 92.125084
Cox_3	Mankhali_Jhaw _20h_2019- 2020_3	Yes	Mankhali	Hoyaikkhong	CoxBazar South	21.085244 92.126230
Cox_4	Thainkhali_FGS _220h_2020-21_One	No	ThainKhali	Ukhia	CoxBazar South	21.174070 92.136414
Cox_1	Thainkhali_FGS _220h_2020-21_Two	No	ThainKhali	Ukhia	CoxBazar South	21.172557 92.136811
Cox_5	Thainkhali_FGS _220h_2020-21_Three	No	ThainKhali	Ukhia	CoxBazar South	21.172587 92.134048
Cox_6	Thainkhali_FGS _220h_2020-21_Four	No	ThainKhali	Ukhia	CoxBazar South	21.123318 92.131755
Cox_7	Monkhali_FGS_ 50h_2019-20_One	No	Mankhali	Hoyaikkhong	CoxBazar South	21.122532 92.130470

Table 03: Different plot scenario (*Intensity: No, Moderate and Heavy)

Category	Seedling Av Ht	Uri-Grass	Green Algae	Canopy Over Lap	Understory Vegetation	Plantation Types
A	15 to 30 cm	No	No	No	N/A	Mangrove
B	15 to 30 cm	Moderate	Heavy	No	N/A	Mangrove
C	15 to 30 cm	High	No	No	N/A	Mangrove
D	15 to 30 cm	N/A	N/A	No	No	Terrestrial
E	15 to 30 cm	N/A	N/A	No	Moderate	Terrestrial
F	15 to 30 cm	N/A	N/A	Yes	Heavy	Terrestrial

Image of category **A**: No uri-grass, No green Algae, No canopy overlap, Low tide

Image of category **A**: No uri-grass, No green Algae, No canopy overlap, Low tide

Image of category **B**: Medium uri-grass, Heavy green Algae, No canopy overlap, Low tide

Image of category **C**: Heavy uri-grass, No green algae, no canopy overlap, low tide

Image of category **C**: Heavy uri-grass, No green algae, no canopy overlap, low tide

Image of category **C**: Heavy uri-grass, no green algae, canopy overlap, tidal effect

Image of category **D**: Low understory vegetation, no canopy overlap, green grasses

Image of category **E**: Moderate understory vegetation, canopy overlap

3.2 Methods:

The workflow comprises three sequential stages: (1) UAV-based acquisition of ultra-high- resolution imagery, (2) photogrammetric orthomosaic generation using close-range techniques, and (3) machine learning-driven object detection, geolocation, and geometric feature extraction.

3.2.1 Very high spatial resolution image acquisition:

A DJI Matrice M200 V2 multi-copter drone equipped with a Zenmuse P1 RGB camera (45MP sensor, f/2.8–f/16 aperture) was used for systematic data collection. The camera featured a 0.01° angular vibration range, tilt (-130° to +40°), roll (-55° to +55°), pan (±320°), ISO 100–256,000, mechanical shutter speed (1/2000–1s), and electronic shutter (1/8000–1s).

3.2.1.1 Camera Setting:

Camera settings play a crucial role in ensuring the capture of blur-free, high-quality drone images, which are essential for producing high-resolution orthomosaics. Both automatic and manual camera settings were explored to obtain clear, sharp images, with necessary adjustments made before moving to the Pix4D capture software. The DJI GO application was used to fine-tune the camera settings, allowing for optimal image clarity. Among the various shutter speeds tested, a manual shutter speed of 1/1600 seconds was found to deliver the best results in terms of sharpness and object detection. In addition to shutter speed, white balance, exposure value (EV), and daylight settings were also adjusted to optimize the image quality. The combination of a manual shutter speed with automatic ISO, white balance, and EV settings minimized motion blur, ensuring the clearest possible images for processing. These settings resulted in high-quality images, while keeping file sizes manageable. By balancing these parameters, the best overall image clarity was achieved, making it possible to generate high-quality orthomosaics that accurately represent the area of interest.

3.2.1.2 Automatic Double Grid Flight Mission:

Pix4d capture for DJI Matrice 200 V2 and DJI ground station was used DJI Pantham 4 Pro for flight mission. DJI ground station or Pix4D Capture was used for flight plan. An appropriate camera setting plays vital rule for a good quality image acquisition and Orthophoto creation process. Drone calibration is also important on site before automatic flight. Calibration improves the image alignment process during post analysis. Image capturing speed is another important parameter. High capturing speed can significantly reduce flight time and could save battery life but it could make blur image. Creating a good quality orthophoto from the Blur image is very difficult, some time impossible. In contrast, Low capturing speed ensure blur less image capturing but it increases flight time. Thus, there is a trade of between quality images and battery life.

3.2.1.3 Ground Sampling Distance:

The flight height (H) required to achieve a specific Ground Sampling Distance (GSD) is determined by the camera focal length (Fr), sensor width (Sw), and image width (Dw), and can be calculated using the formula $H = (Dw * Fr) / Sw$ (Zhang et al., 2007). The distance covered on the ground by one image in the width direction, or the footprint width (Dw), is also influenced by the GSD and the image width, as described by the equation $DW = (imW * GSD) / 100$ (Jensen, 2007). Combining these formulas, the flight height needed to achieve a given GSD can be expressed as $H = (imW * GSD * Fr) / (Sw * 100)$ (Zhang et al., 2007). Pix4D Capture software can automatically compute the GSD and flight height, adjusting the GSD based on the flight elevation, which in turn impacts the data resolution. GSD values ranging from 1.5 to 3.5 cm were explored to ensure high-resolution data collection, with the understanding that higher GSD values provide more detailed imagery but result in larger data volumes, longer post-processing times, and shorter flight durations due to higher power consumption. The table demonstrates the relationship between GSD, flight altitude, area covered, and flight time, showing that higher altitudes with larger GSDs allow for more efficient area coverage but lower spatial resolution. For example, at a 0.5 cm GSD and 18 m altitude, the drone covers 1 hectare in 21.5 minutes, prioritizing high resolution for seedling detection, while at a 5.0 cm GSD and 180 m altitude, 40 hectares are covered in the same time, optimizing coverage efficiency. This presents a trade-off between GSD, resolution, area coverage, and flight time, where a 5.0 cm GSD is sufficient for seedling detection. Pix4D Capture's automated mission planning, integrated with CTRL+DJI connectivity, allows for the execution of double-grid missions with varying front and side overlaps (65–85%) to generate high-quality 3D orthomosaics.

Overlap percentages are dynamically adjusted based on factors such as seedling height, canopy density, and ground conditions, ensuring that the final product meets both resolution and efficiency requirements.

3.2.1.4 Image Capturing in different Plantation site

Automatic image has been captured from different plantation site. Seedling age, crown width, urigrass intensity, green algae, line and row uniformity were considered. This will provide the information about different types and stage of coastal plantation scenario.

Table 05: Different parameter of automatic image capture

Name	GSD (cm/px)	Altitude (m)	Overlap (%)	speed	Area (m)	Flight Time (minutes)	Number of Images	Focal Length	Camera Setting
Bhula_1	0.7	25	80	fast	113*109	19.50	369	15mm f/1.7 ASPH	Default automatic
Bhula_2	0.7	25	80	fast	103*117	19.50	314	15mm f/1.7 ASPH	Default automatic
Bhula_3	01	36	80	fast	102*110	9.50	183	15mm f/1.7 ASPH	Default automatic
Bhula_4	0.84	30	80	fast	102*124	16.50	389	15mm f/1.7 ASPH	Default automatic
Bhula_5	0.79	28	80	fast	100*100	16.50	389	15mm f/1.7 ASPH	Default automatic
Bhula_6	0.79	28	75	fast		16.50	327	15mm f/1.7 ASPH	1/1000, manual focus
Bhula_7	0.79	28	75	fast	102*102	12.50	254	15mm f/1.7 ASPH	1/1200, manual focus
Bhula_8	0.62	22	80	fast	102*110	21.00	306	15mm f/1.7 ASPH	1/1600, manual focus
Bhula_9	0.57	20	70	fast	101*101	14.50	305	15mm f/1.7 ASPH	1/1600, manual focus
Patoakhali_1	0.97	35	80	Mediu m	1	14.50	323	15mm f/1.7 ASPH	1/1600, manual focus
Patoakhali_2	0.97	35	80	Mediu m	100*100	14.25	316	15mm f/1.7 ASPH	1/1600, manual focus
Patoakhali_3	0.84	30	80	Mediu m	101*110	15.00	338	15mm f/1.7 ASPH	1/1600, manual focus
Patoakhali_4	0.84	30	80	Mediu m	80*184	19.00	437	15mm f/1.7 ASPH	1/1600, manual focus
Patoakhali_5	0.84	30	80	Mediu m	107*107	14.50	323	15mm f/1.7 ASPH	1/1600, manual focus

Name	GSD (cm/px)	Altitude (m)	Overlap (%)	speed	Area (m)	Flight Time (minutes)	Number of Images	Focal Length	Camera Setting
Patoakhali_6	0.7	25	80	Mediu m	108* 108	19.75	483	15mm f/1.7 ASPH	1/1600, manual focus
Patoakhali_7	0.42	15	63	mediu m	51*2 04	24.07	343	15mm f/1.7 ASPH	1/1600, manual focus
Patoakhali_8	0.42	15	63	mediu m	109* 100	22.75	573	15mm f/1.7 ASPH	1/1600, manual focus
Patoakhali _9	0.97	35	60	mediu m	101* 101	14.50	294	15mm f/1.7 ASPH	1/1600, manual focus
Mymensing h_1	0.97	35	60	mediu m	101* 101	14.50	294	15mm f/1.7 ASPH	Malakuc ha_1
Mymensing h_2		36	80	mediu m	105* 136	13.50	319	15mm f/1.7 ASPH	Malakuc ha_2
Mymensing h_3		36	80	mediu m	103* 108	10:47	247	15mm f/1.7 ASPH	Enrichme nt
Mymensing h_4	1.0	36	80	mediu m	100* 101	10:15	221	15mm f/1.7 ASPH	Tawakuc ha_1
Mymensing h_5	0.97	35	80	mediu m	108* 94	9.75	223	15mm f/1.7 ASPH	Tawakuc ha_2
Mymensing h_6	1.0	36	80	mediu m	100* 102	14.75	284	15mm f/1.7 ASPH	Default automatic
Mymensing h_7	0.97	35	80	mediu m	101* 109	11.25	258	15mm f/1.7 ASPH	Default automatic
Mymensing h_8	0.97	35	80	mediu m	101* 109	11:13	258	15mm f/1.7 ASPH	Default automatic
Cox_1	0.97	35	80	mediu m	100* 100	14.25	350	Aperture: f/2.2	Default automatic
Cox_2	0.97	35	80	mediu m	100* 100	14.50	328	Aperture: f/2.2	Default automatic
Cox_3	0.97	35	80	mediu m	100* 100	14.15	312	Aperture: f/2.2	Default automatic
Cox_4	0.97	35	80	mediu m	100* 100	13.75	326	Aperture: f/2.2	Default automatic
Cox_1	0.84	30	80	mediu m	100* 100	15.15	412	Aperture: f/2.2	Default automatic
Cox_5	0.84	30	80	mediu m	100* 100	15.20	409	Aperture: f/2.2	Default automatic
Cox_6	0.84	30	80	mediu m	100* 100	15.09	421	Aperture: f/2.2	Default automatic
Cox_7	0.84	30	80	mediu m	100* 100	14.80	400	Aperture: f/2.2	Default automatic

3.2.2 Post data analysis (Ortho mosaic creation)

Photogrammetric processing was conducted using Agisoft Metashape Professional Edition (Agisoft LLC, St. Petersburg, Russia) to generate point clouds, orthophotos, and Digital Elevation Models (DEM) for each plantation plot across different sites. Captured images were first uploaded and carefully inspected to remove unnecessary or low-quality images that could affect the accuracy of the results. The processing workflow involved several key steps: uploading camera positions, aligning images, creating and optimizing a mesh, building a dense point cloud, and ultimately generating the final orthomosaic. This comprehensive process ensures the creation of high-quality, accurate geospatial data for plantation monitoring.

Once the photogrammetric processing was completed, the system generated an automatic report that included valuable details such as the number of images used, flying altitude, ground resolution, and coverage area. Additionally, it included information on camera stations, tie points, and focal length, as well as essential camera calibration data, including calibration coefficients and the correlation matrix. The report also provided the camera location data (X, Y, Z) along with the estimated error levels, and specifications related to the DEM. These processing parameters helped ensure the accuracy and precision of the resulting point clouds, orthophotos, and DEM, which are crucial for detailed analysis of the plantation sites. System generated automatic report for all the plots are attached in the Appendix-II.

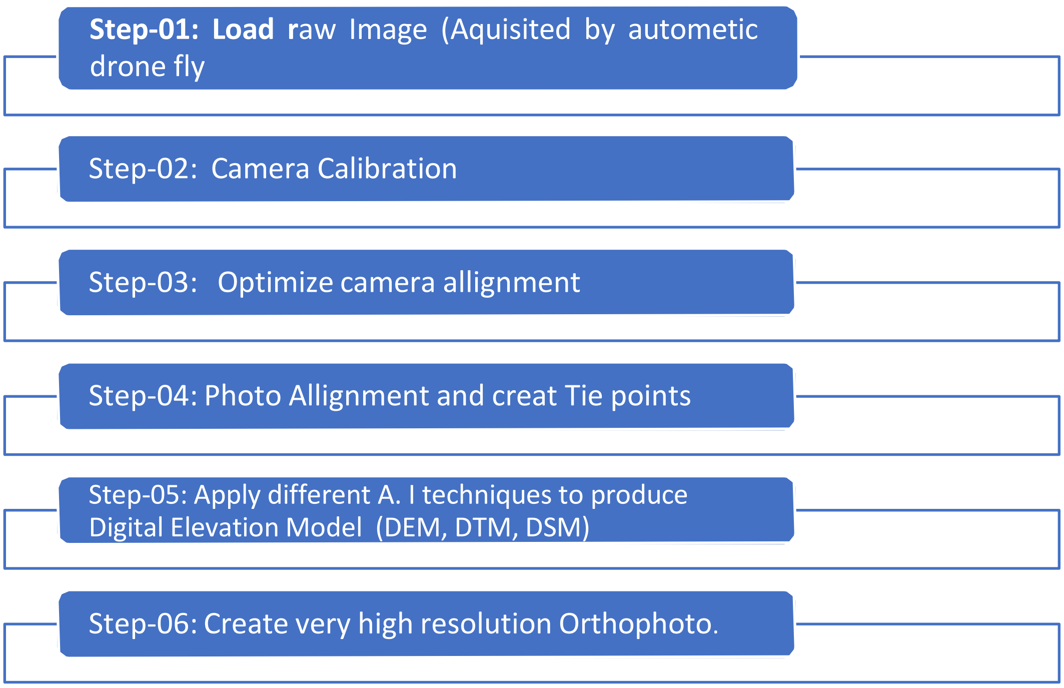

Figure-1: *Flow chart to generate DEM and Orthophoto from raw drone images*

3.3 Object Based Image analysis (OBIA) procedure:

The study employed a Deep Learning (DL) algorithm structured into four primary phases: image segmentation, image classification, computing, and geostatistics, integrating Artificial Intelligence (AI) and Machine Learning (ML) techniques for the detection of individual seedlings from high-resolution drone orthophotos. Deep learning, a subset of machine learning rooted in artificial neural networks and representation learning, was specifically applied for precise feature extraction and classification, significantly enhancing the accuracy of seedling identification. The growing prominence of deep-learning (DL) algorithms in remote sensing has been driven by their ability to automatically extract meaningful features from vast datasets and perform effectively with extensive training samples (Kussul et al., 2017; Liu et al., 2018). While AI, ML, and DL techniques have been applied in geoscience and remote sensing for several decades (Estes et al., 1986; Myneni et al., 1995), their usage has become more widespread in recent years due to their ability to address common challenges in remote sensing applications, such as classification and segmentation, with improved accuracy

(Ball et al., 2017; Zhang et al., 2016; Kamilaris et al., 2018; Han et al., 2017). Notably, deep-learning techniques, which include various neural network architectures and both supervised and unsupervised feature-learning algorithms, are especially valuable in agricultural applications, including plant enumeration and identification (Li et al., 2016).

Recent advancements in the application of Convolutional Neural Networks (CNNs) have further highlighted the efficacy of DL for high-resolution imagery segmentation. CNNs, hierarchical architectures trained on large-scale datasets, are highly effective in performing object recognition and detection tasks (Hu et al., 2015). For example, Guirado et al. (2017) demonstrated that CNNs outperformed traditional Object-Based Image Analysis (OBIA) methods in detecting scattered shrubs from Google Earth images, requiring less human intervention and offering better model transferability. Similarly, Li et al. (2016) utilized CNNs to detect and count oil palm trees in Malaysia from QuickBird satellite imagery, achieving over 96% accuracy and surpassing other state-of-the-art methods, such as local maxima, template matching, and artificial neural networks. In a more detailed study, Chen et al. (2017) applied fully convolutional networks to count apples and oranges in an unstructured environment, further illustrating the versatility of CNNs. Wang et al. (2018) and Sa et al. (2016) also implemented Faster Region-based CNN (Faster R-CNN) algorithms for detecting mango fruit flowers and identifying fruits like sweet peppers and melons, respectively.

Deep-learning architectures, including Deep Neural Networks (DNNs), Recurrent Neural Networks (RNNs), and CNNs, have found broad applications in diverse fields such as climate science and object detection (Ciresan et al., 2012; Krizhevsky et al., 2012; Google, 2017). The primary advantage of deep learning lies in its ability to progressively extract higher-level features from raw input data by utilizing multiple layers. In image processing, for instance, lower layers detect basic features like edges, while deeper layers identify more complex human-interpretable concepts, such as shapes or colors (Deng, 2014). This hierarchical approach, which is fundamental to DL models like CNNs, RNNs, and Faster R-CNN, allows the input data to be transformed into increasingly abstract representations, ultimately enabling accurate tasks such as object detection and classification (Bengio & Yoshua, 2009; Bengio et al., 2013; LeCun et al., 2015).

The study encountered several challenges across different sites, including the presence of green algae and uri-grass, which were often found in conjunction with seedlings. In some cases, the true color (RGB band) of both the seedlings and algae appeared remarkably similar, making it difficult for machine learning models to distinguish between them. To address this, various neural network architectures, such as CNN, R-CNN, SSD, YOLOv3, YOLOv4, and RetinaNet, were tested with different parameters to identify the most effective detection model. Additionally, the study sites presented further complications, such as the presence of Uri-Grass—coastal grass species with similar heights to the seedlings. Some seedlings had heights ranging from 15 cm to over 2 meters, and their crown sizes varied significantly. The overlapping of seedling crowns, particularly during the construction of the R-CNN model, further complicated the task. To overcome these obstacles, multiple deep learning techniques and parameters were explored to optimize the detection model and ensure accurate differentiation between the seedlings, algae, and uri-grass.

Deep learning models, which can be integrated with software tools like ArcGIS Pro, have enabled the automation of feature extraction from aerial imagery, dramatically reducing the time required for manual digitization of objects. Traditional methods of manually extracting objects from imagery could take weeks or even years, depending on the size of the dataset. However, with advancements in computing power and deep learning tools in platforms like ArcGIS Pro, it is now possible to train models to identify and extract features from imagery in a fraction of the time. Deep learning, as a form of machine learning that relies on multiple layers of nonlinear processing, allows for the efficient identification and pattern recognition of features within images. These capabilities have made deep learning an essential tool in object detection, object classification, and image classification applications, particularly in remote sensing contexts (Bengio et al., 2013; Hinton, 2009).

During the study, various deep learning models and their backbones, including ResNet50, ResNet101, ResNet152, Darknet53, CSPDarknet, and TIMM:DENSENET121, were tested to identify the most effective combination for detecting coastal plantation seedlings. Key parameters, such as batch size, validation techniques, and the number of epochs, were adjusted to optimize model performance. After extensive testing, the best-fitting model was identified: the R-CNN model with the ResNet50 backbone, batch size 4, and validation set of 10. This configuration proved most effective in automatically detecting and counting seedlings in coastal plantation areas where seedling crowns were not overlapped, and there was minimal interference from green algae or uri-grass. A detailed description of each model, backbone, and the tested parameters can be found in the Appendix III, while a graphical representation of the model configurations is provided in Figure 3.

In conclusion, the application of deep learning algorithms in this study has demonstrated significant potential for the automation and accuracy of seedling detection in complex remote sensing environments. By leveraging powerful neural networks such as CNNs, R-CNNs, and Faster R-CNNs, the study successfully overcame the challenges posed by similar visual characteristics of different objects (seedlings, algae, and uri-grass) and variations in seedling height and crown size. Furthermore, the integration of deep learning models with ArcGIS Pro has streamlined the process of identifying and classifying objects in high-resolution imagery, marking a significant advancement in remote sensing and agricultural applications. This study highlights the growing importance of deep learning techniques in the analysis of remotely sensed data and sets the stage for further research into optimizing and applying these models to other ecological and environmental monitoring tasks.

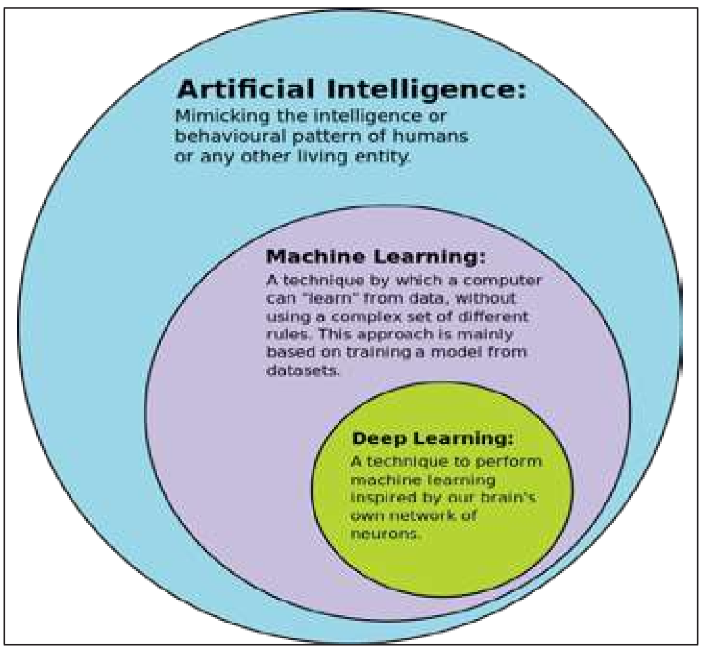

Figure 02: Deep Learning System illustration

3.3.1. Modules Effectiveness Evaluation

Different Machine Learning were tested to find best fitted model with high precision and low omission/commission error. Mask R-CNN and Pascal data frame were explored with R-CNN model (Wang, D., and He, D., 2022), Yolov3 model (Cong, P., *et al*. 2022), Yolov4 model (Zhang, C., 2022), SSD model (Ahmed.,D.,*et al*., 2023) and retina Net model. Different backbone of those model was also being explored to figure out best fitted model. ResNet50, ResNet101, ResNet152, Darknet53, CSPDarknet, TIMM:DENSENET121 backbone were explored with different "Batch", "Validation" and "Epoch". The best fitted Model, Backbone, Batch and validations are described the **Table 06** R-CNN model with ResNet50 backbone, batch 4 and validation 10 provide best fitted model to automatically detect and count costal plantation seedling where seedling crown is not overlapped, no green algae, no uri-grass or limited uri grass. The details of the different models, backbone and other parameter could be found in Figure 3 And details description of each models could found in **appendix III.**

3.3.2 Target detection model comparison

Table 05 demonstrate that ResNet50 backbone has more precision than ResNet 101 and ResNet 152 in R-CNN model construction process. Thus, the backbone is selected and compare R-CNN model with Yolov3, Yolov4, SSD and Retina Net model to ensure best fitted model.

Table 06: Different Backbone comparison of R-CNN model

Study site	Model	Backbone	Batch	Validation	Model Precision
Bhula Final4	R-CNN	ResNet50	4	10	0.844
Bhula Final4	R-CNN	ResNet101	4	10	0.45
Bhula Final4	R-CNN	ResNet152	4	10	0.50

R-CNN model was tested with Yolov3 (He, K.,2017),3 Yolov4 (Li, Y., 2019), SSD (Liu, W.,2016), Retina Net with different backbone for a particular site to understand which model provide more precision. **Table 07** describe different model precision. It has been recorded that R- CNN model has more precision than others. The detail model comparison for all site could be found figure 03.

Table 07: Different Model Comparison

Study site	Meta Data Format	Model	Backbone	Model Precision	Model Accuracy (%)
Bhula Final4	Mask R-CNN	R-CNN	RseNet50,Bat ch 8	0.86	99.01
Bhula Final4	Mask R-CNN	R-CNN	RseNet50	0.844	95.65
Bhula Final4	Pascal	Yolov3	Darknet53	Did not worked	N/A
Bhula Final4	Pascal	Yolov4	CSPDarknet5 3	0.76	87.3
Bhula Final4	Pascal	SSD	Densenet121	0.72	79.5
Bhula Final4	Pascal	Retina Net	TIMM:DENSE NET121	0.44	72.2

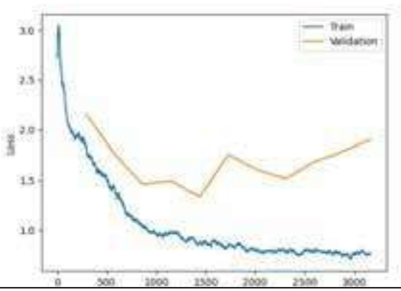	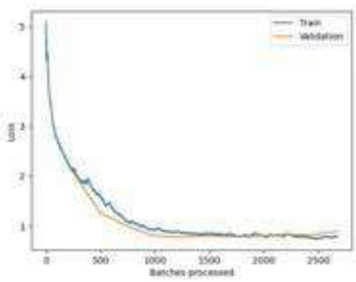	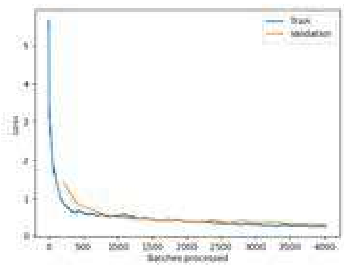
Over fitted R-CNN Model with 0.19 precision (False Positive)	Under fitted R-CNN Model with 0.5 precision (False Negative)	Best fitted R-CNN Model with 0.92 precision
Figure 03A	Figure 03B	Figure 03 C

The **Train Learning Curve** and **Validation Learning Curve** were analyzed to evaluate model performance and determine whether the model was over fitted, under fitted, or optimally fitted. **Figure 3A** illustrates an over fitted model, where excessive false positives and significant deviation indicate poor generalization to new data. In contrast, **Figure 3B** represents an under fitted model, where high false negatives suggest an inadequate learning process, resulting in missed seedling detections. The optimized model, shown in **Figure 3C**, achieved a precision of **0.92**, demonstrating a well-balanced performance with minimal errors. This refinement effectively mitigated false detections while ensuring accurate and reliable seedling identification. These findings emphasize the critical role of **model parameter tuning, environmental factor consideration, and deep learning architecture selection** in enhancing automated afforestation monitoring. Different model, backbone summery for each plot could found in **Table 08** and details could be found on **Appendix III.**

CHAPTER IV

RESULT AND DISCUSSION

4.1. Deep Learning-Based Automatic Seedling Detection Model

The deep learning-based automatic seedling detection model was developed using the Region- Based Convolutional Neural Network (R-CNN) with optimized thresholds and parameters. A detailed description of the model construction process and accuracy assessments is provided in Appendix III. The optimized models demonstrated high accuracy in detecting mang rove seedlings, indicating their potential applicability in large-scale seedling monitoring for afforestation programs. Once drone imagery is collected and converted into an orthomosaic, these models can be effectively deployed for automated seedling detection and counting, significantly improving efficiency over manual counting methods.

4.1.1 Key Outputs of the UAV based Deep Learning Approach

The deep learning-based approach provided several key outputs, including:

- **High-Resolution Digital Twins (0.5–1.5 cm resolution):** After systematically capturing drone data, Agisoft Metashape was used to process the images and generate point clouds. These point clouds were then utilized to create high-resolution orthomosaics with a resolution ranging from 0.5 to 1.5 cm. The resulting orthomosaics can be visualized in Google Earth Pro (in .kml format), offering decision-makers an accurate and detailed representation of plantation conditions. Additionally, Digital Elevation Model (DEM) was derived for each plot to support further analysis. **Appendix II** provides an automatic plot report, which includes detailed plot-wise information.
- **Automated Seedling Detection:** Once the optimal deep learning model was developed, it detected and counted individual seedlings. This automated process eliminates sampling biases and enables precise assessment of seedling survival rates. **Appendix I** includes a plot-wise comparison of automatic versus manual seedling detection, highlighting the model's accuracy.
- **Seedling Density Maps:** Density map generated for grids of 10m × 10m, 20m × 20m, or other desired size. These maps highlight areas of high and low survival rates, allowing targeted vacancy filling to enhance plantation success

Figures 4–9 illustrate various aspects of the deep learning model, including high-resolution imagery, R-CNN-based automatic counting, manual seedling counting in ArcGIS, and a comparative analysis of automatic vs. manual counting. A 10m × 10m grid-based seedling density map is also provided. Figure 4: High-resolution orthophoto of a coastal plantation. Figure 5: R- CNN-based automatic seedling counting. Figure 6: Manual seedling counting using ArcGIS. Figure 7: Comparison of automatic vs. manual seedling counting. Figure 8: 10m × 10m live seedling density map. Figure 9: Accuracy Assessment: Automatic model-based counting Vs. Manual counting.

Figure 04: Very High Resolution Orthophoto

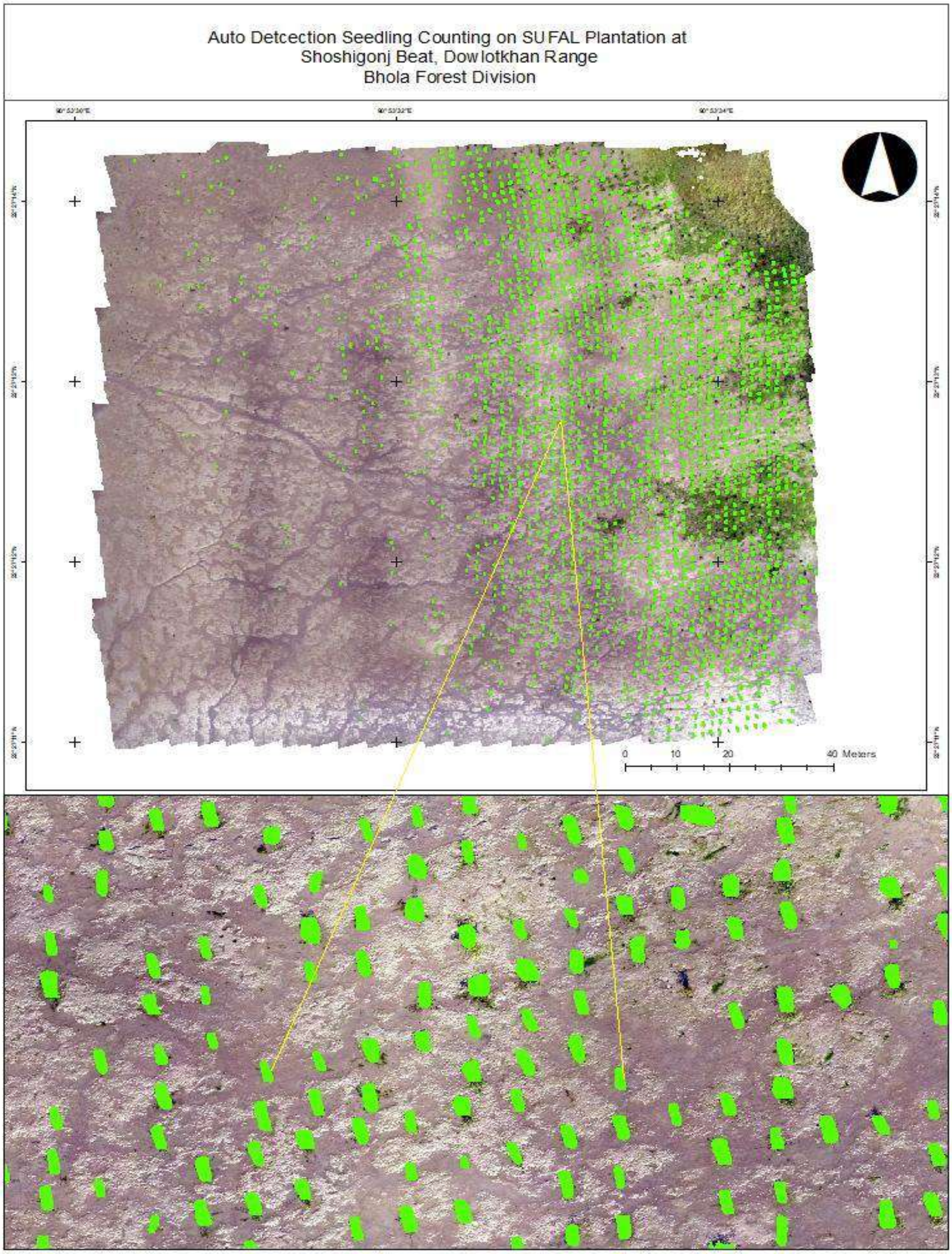

Figure-05: RCNN Model based Automatic seedling counting

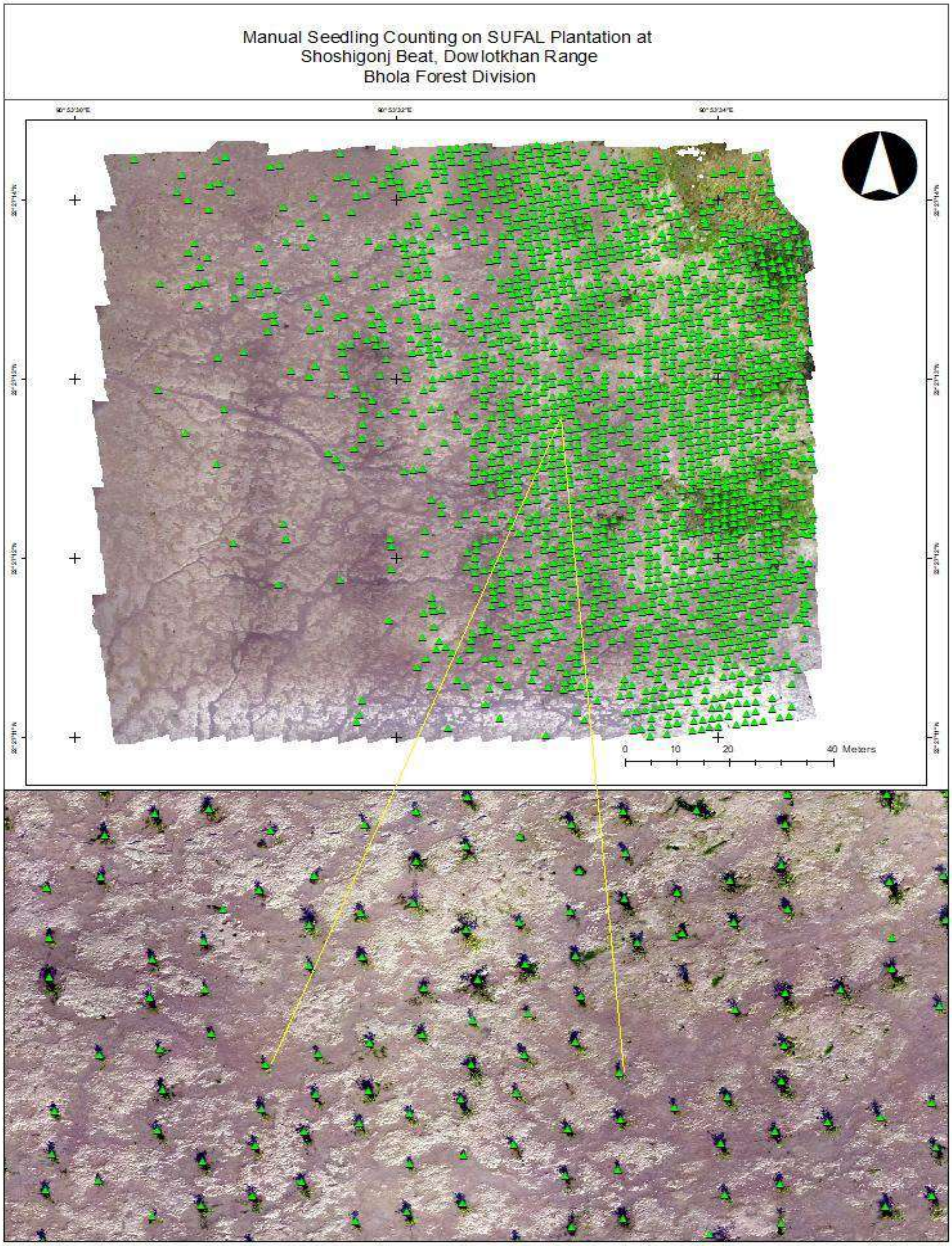

Figure-06: Manual Seedling counting in Arc GIS

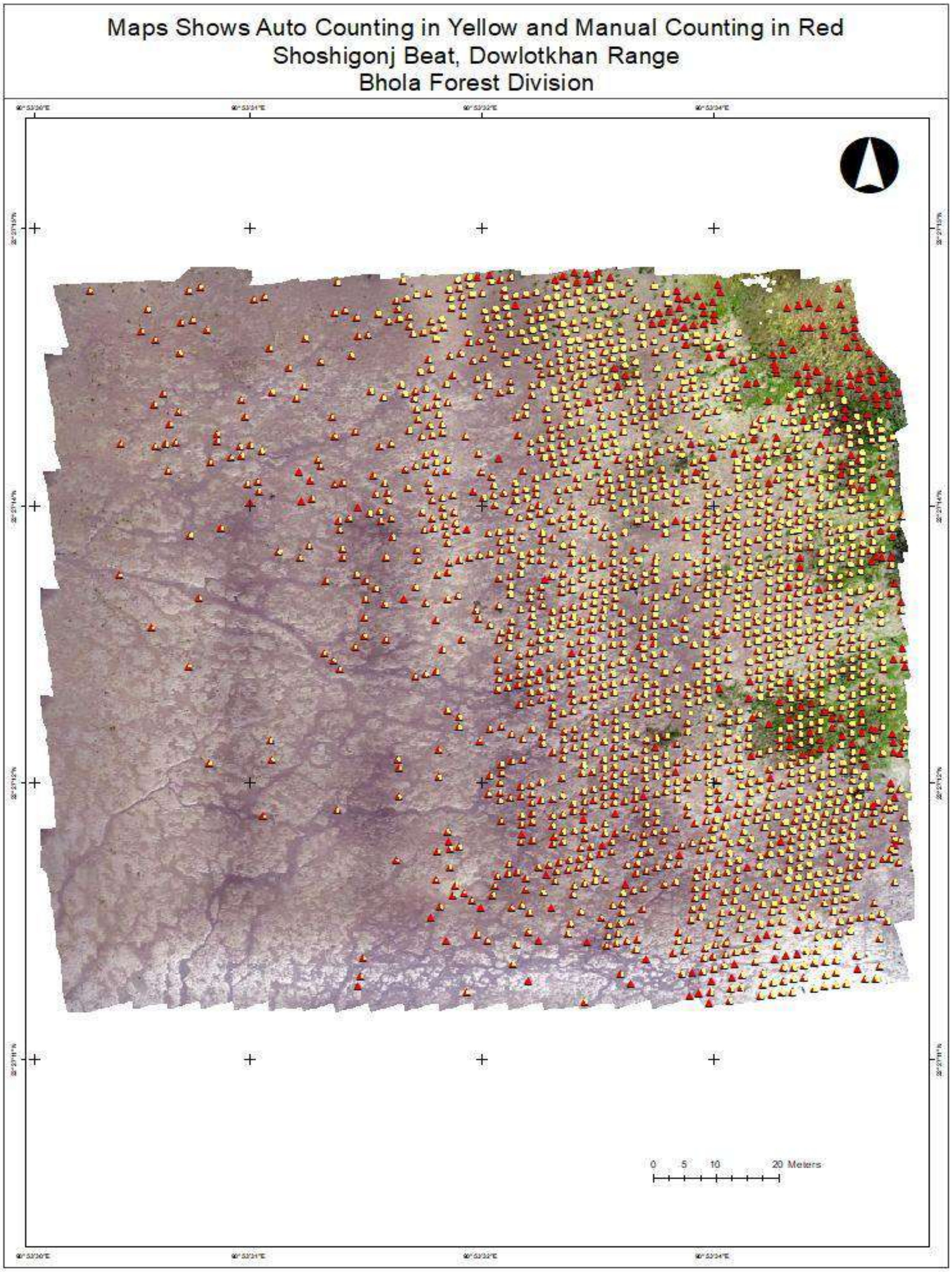

Figure-07: Automatic counting Vs Manual counting

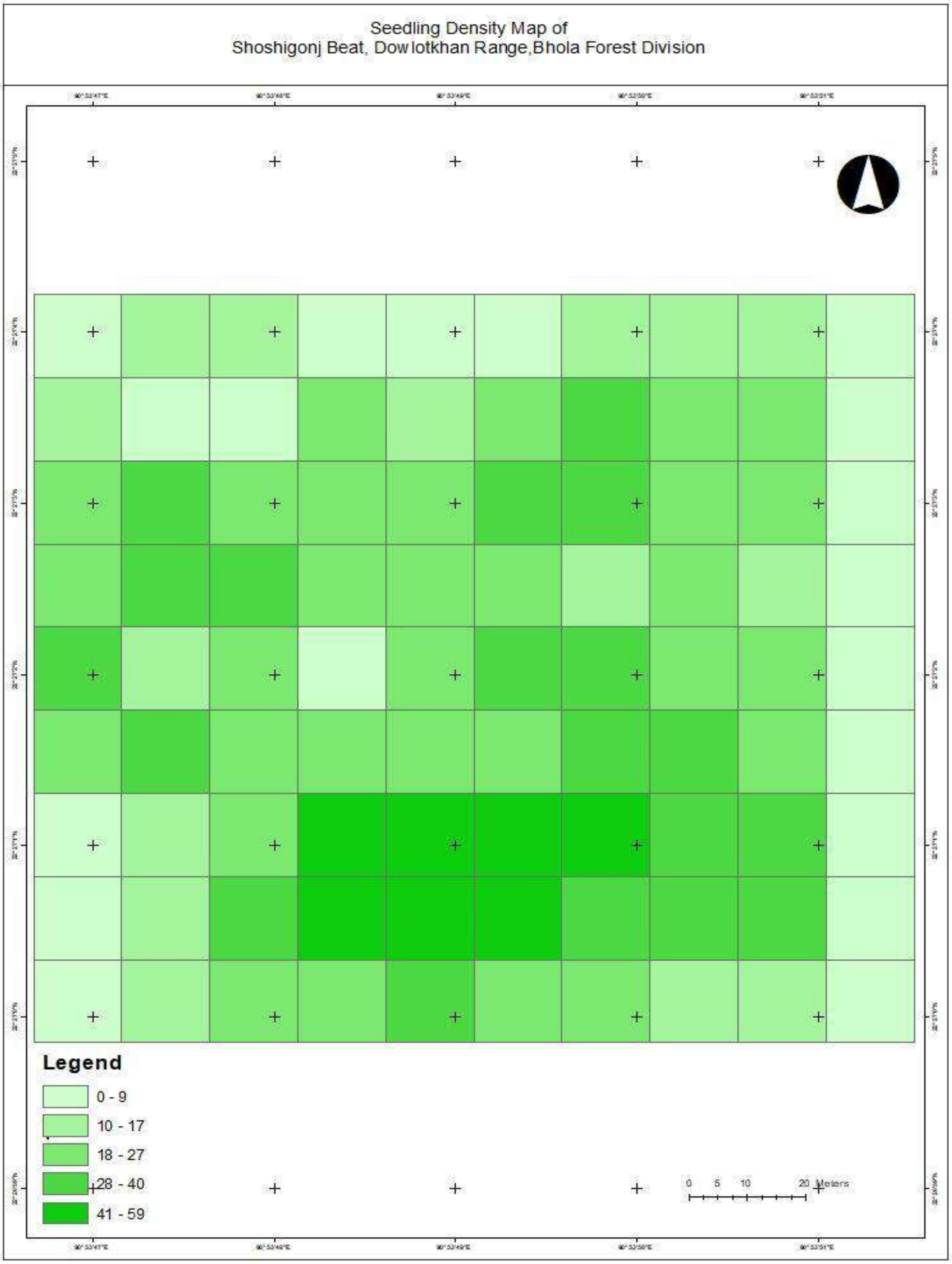

Figure-08: 10m X 10m live seedling density map

4.2 Model Accuracy and Comparative Assessment:

A comparative assessment of automatic and manual seedling counting was conducted to evaluate model accuracy. The analysis considered false negatives and false positives to determine the model's reliability in seedling detection. The best-performing model achieved an overall accuracy of **99.1%** for coastal plantations. The R-CNN model detected **3,187 seedlings**, compared to **3,216 seedlings counted manually**, resulting in **29 false negatives** and **zero false positives**. The model demonstrated high reliability in seedling detection, with optimal performance under favorable environmental conditions.

Key factors influencing model performance included:

- **Optimal ground conditions:** Best results were obtained in areas with minimal uri-grass, low green algae presence, and negligible crown overlap. Line uniformity did not affect model performance.
- **Flight parameters:** The most accurate detections were achieved under low-tide conditions, with drone flights conducted at **40 meters' altitude**, using a **nadir camera angle**, a **shutter speed of 1/1600**, and a **medium image capture speed**.
- **Seedling shadows:** The presence of shadows enhanced detection accuracy by improving contrast between seedlings and the background.

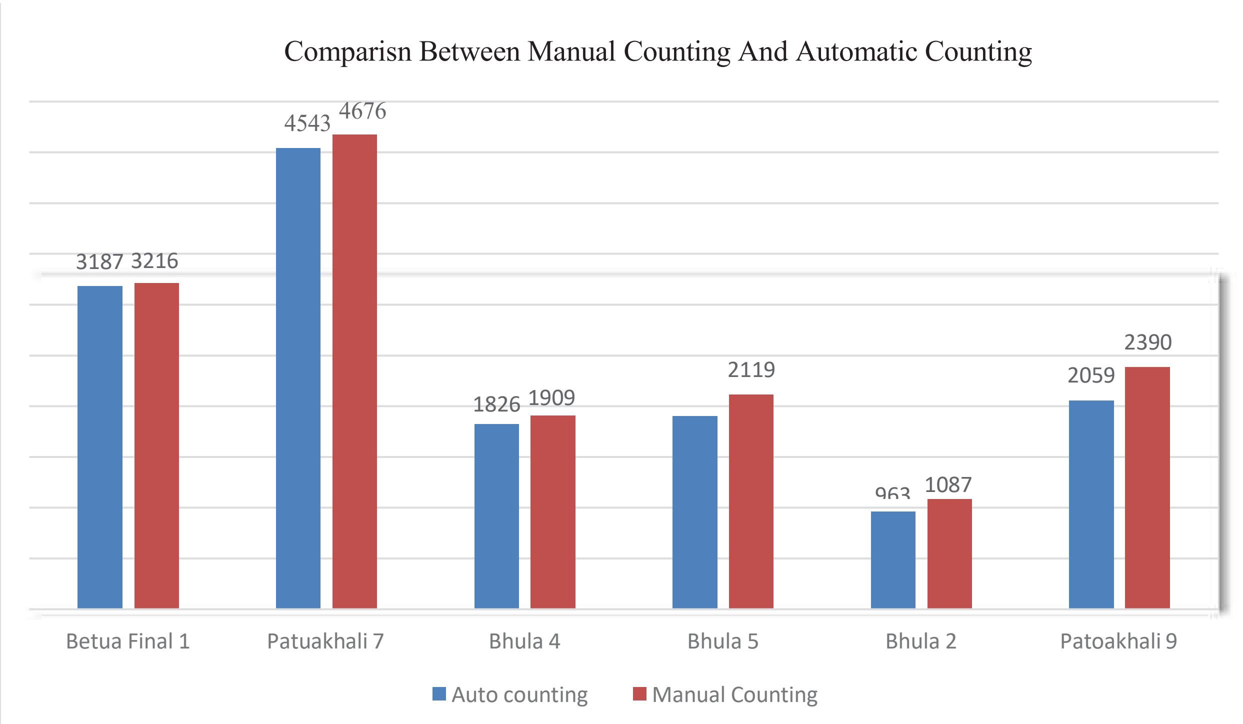

Figure 9: Automatic counting Vs Manual counting of seedling

4.3 Model Performance Across Different Plantation Scenario:

Model performance varied significantly across plantation categories due to environmental factors (Table 9):

- **Category A** (no uri-grass, no green algae, low tide, no canopy overlap) achieved **99.1%** accuracy for Betua Final 1 plot and 97.15% for Patuakhali 7 plot.
- **Category B** (moderate uri-grass, heavy green algae, low tide, no canopy overlap) maintained high accuracy (**95.65%** for Bhula_4, **90.0%** for Bhula_5).
- **Category C** (high uri-grass, closed canopy, mixed tidal conditions) faced challenges, with accuracy dropping to **86.2–88.6%**.

Table 08: Best fitted model accuracy and favorable parameter for coastal Plantation

Name	Category	Model	Auto counting	Manual Counting	False Positive	False Negative	Overall Accuracy %
Betua Final 1	A	RCNN	3187	3216	0	29	99.1
Patuakhali 7	A	RCNN	4543	4676	0	133	97.15
Bhula 4	B	RCNN	1826	1909	0	83	95.65
Bhula 5	B	RCNN	1907	2119	0	212	90.0
Bhula 2	C	RCNN	963	1087		124	88.6
Patoakhali 9	C	RCNN	2059	2390	0	331	86.2

4.4 Challenges in Terrestrial Plantation Monitoring:

Unlike coastal plantations, terrestrial plantations posed significant challenges for deep learning- based seedling detection. The primary issue was **dense understory vegetation**, which led to classification errors due to the high similarity in color, height, and shape between seedlings and surrounding vegetation. Additionally, factors such as **closer spacing (2m), canopy overlap, and high understory density** negatively impacted model performance.

Various deep learning models, including R-CNN, SSD, YOLOv3, and RetinaNet, were evaluated using different batch sizes (4, 6, 8, 12) and validation percentages (10% and 15%). The results demonstrated poor accuracy, with high rates of false positives and false negatives for two sites, while failing to detect seedlings entirely in the remaining plots (see Table 10). For example, at the Malakucha 1 site, the model achieved 79% accuracy but produced significant errors, detecting 2,330 seedlings compared to the manual count of 2,281, with 487 false positives and 989 false negatives. At the Malakucha 2 site, where understory vegetation was sparse, the model detected 919 seedlings with 49.9% accuracy. However, the model performed poorly in areas with dense understory vegetation, failing to detect seedlings effectively. Moreover, it was unable to automatically detect seedlings in the remaining terrestrial plantation sites, underscoring a major limitation.

Table 09: Best fitted model accuracy and favorable parameter for terrestrial Plantation

Model Accuracy for Automatic Seedling Detection in Terrestrial Plantation								
Name	**Category**	**Site Description**	**Model**	**Auto counting**	**Manual Counting**	**False Positive**	**False Negative**	**Overall Accuracy**
Malakucha 1		Line and row is uniform, covered with lots of green understory vegetation	RCNN	2330	2281	487	989	79
Malakucha 2		Line and row is uniform, covered with lots of green understory vegetation	RCNN	919	1841	117	357	49.9
Jhau Plantation		Line and row is uniform, canopy overlapped and ground cover is sand	RCNN	160	2281	00	2121	7
Thainkhali 1		Line and row is uniform, covered with lots of green understory vegetation	RCNN	00	1600	00	1600	00
Thainkhali 2		Line and row is uniform, covered with lots of green understory vegetation	RCNN	00	1528	00	1528	00

Figure 10 provides a comprehensive overview of plot-wise environmental factors and their impact on seedling detection accuracy. It details key variables such as the presence and density of uri- grass, the extent of green algae coverage, understory vegetation conditions, and sun angle (which affects seedling shadow formation). Additionally, the figure compares automatic seedling counts generated by the deep learning model with manual seedling counts conducted on the ground, offering insights into the model's accuracy across different plots. By presenting these factors side by side, Figure 10 highlights the environmental challenges that influence the performance of automated detection systems, such as spectral similarities between seedlings and surrounding vegetation, as well as the impact of shadows and obstructions. This visual representation underscores the importance of considering site-specific conditions when deploying UAV-based monitoring tools and provides a foundation for refining AI models to improve accuracy in diverse plantation environments.

Figure 10: Plot wise automatic seedling detection accuracy.

Location	Green Understory	Urigrass	Green algae	Shadow	Deceted Count Result	Manual Count	False Positive	Accuracy
Bhola_2	No	No	Yes	No	330	1087	-757	30.4
Bhola_2	No	No	Yes	No	0	1087	-1087	0.0
Bhola_4	No	No	Yes	No	1544	2191	-647	70.5
Bhola_4	No	No	Yes	No	1717	2191	-474	78.4
Bhola_4	No	No	No	Moderate	1826	2191	-365	83.3
Betua_F1	No	No	Yes	Moderate	2705	3216	-511	84.1
Betua_F1	No	No	Yes	Moderate	3187	3216	-29	99.1
Bhula Final4	No	no	no	Moderate			0	
Bhula Final4	No	no	no	Moderate			0	
Bhula Final4	No	no	no	Moderate			0	
Bhula Final4	No	no	no	Moderate			0	
Bhula Final4	No	no	no	Moderate	1826	1909	-83	95.7
Bhula Final4	No	no	no	Moderate			0	
Bhula Final4	No	no	no	Moderate			0	
Bhula Final4	No	no	no	Moderate			0	
Cox's Bazar_Jhaw_1	No	no	no	no			0	
Cox's Bazar_Jhaw_2	No	No	No	None	71		71	
Malakucha_1	Moderate	No	Yes	None	160	2281	-2121	7.0
Malakucha_1	Moderate	No	Yes	None	121	2281	-2160	5.3
Malakucha_1	Moderate	No	Yes	None	2330	2281	49	102.1
Malakucha_1	Moderate	No	Yes	None	121	2281	-2160	5.3
Malakucha_2	Moderate	No	Yes	None	919	1841	-922	49.9
Malakucha_2	Moderate	No	Yes	None	645	1841	-1196	35.0
Malakucha_2	Moderate	No	Yes	None	532	1841	-1309	28.9
Pathoakhali_1	No	Yes	No	None	42	3851	-3809	1.1
Pathoakhali_1	No	Yes	No	None	6	3851	-3845	0.2
Pathoakhali_1	No	Yes	No	None		3851	-3851	0.0
Pathoakhali_1	No	Yes	No	None	19	3851	-3832	0.5
Pathoakhali_3	No	Yes	No	None	14	3679	-3665	0.4
Pathoakhali_3	No	Yes	No	None		3679	-3679	0.0
Pathoakhali_5	No	Yes	No	No	51	3128	-3077	1.6
Pathoakhali_5	No	Yes	No	No	1	3128	-3127	0.0
Pathoakhali_6	No	Yes	No	No	1420	2280	-860	62.3
Pathoakhali_6	No	Yes	no	No	240	2280	-2040	10.5
Pathoakhali_6	No	Yes	NO	No	579	2280	-1701	25.4
Pathoakhali_6	No	Yes	no	No	498	2280	-1782	21.8
Pathoakhali_7	No	No	No	Moderate	4543	4676	-133	97.2
Pathoakhali_7	No	No	No	Moderate	135	4676	-4541	2.9
Pathokhali_9	No	No	No	Modearte	2059	2390	-331	86.2
Pathokhali_9	No	No	NO	Modearte	6	2390	-2384	0.3
Pathokhali_9	No	No	No	Modearte	294	2390	-2096	12.3
Pathokhali_9	No	No	No	Modearte	1996	2390	-394	83.5
Pathokhali_9	No	No	No	Modearte	1354	2390	-1036	56.7
Pathokhali_9	No	No	No	Modearte	1969	2390	-421	82.4
Patoakhali8	No	no	no	Moderate	Problem	3811	#VALUE!	#VALUE!
Patoakhali8	No	No	No	Moderate	1091	3811	-2720	28.6
Patoakhali8	No	no	no	Moderate	3185	3811	-626	83.6
Patoakhali8	No	no	No	Moderate	930	3811	-2881	24.4
Patoakhali8	No	no	No	Moderate	3193	3811	-618	83.8
Thainkhali_1	Heavy	No	No	None	0	1528	-1528	0.0
Thainkhali_2	Heavy	No	No	None	0	1976	-1976	0.0
Thainkhali_2	Heavy	No	No	None	0	1976	-1976	0.0
Thainkhali_3	Heavy	No	No	None	0	993	-993	0.0
Thainkhali_3	Heavy	No	No	None	0	993	-993	0.0
Thainkhali_3	Heavy	No	No	None	0	993	-993	0.0
Thainkhali_4	Heavy	No	No	None	0	1600	-1600	0.0
Pathuakhali_2	No	Yes	No	None	0	0	0	#DIV/0!
Bhola_1	No				0	0	0	#DIV/0!
Bhola_2	No	No	Yes	Moderarte	963	1087	-124	88.6
Bhola_3	No	Yes	No	None			0	#DIV/0!
BholFinal_5	No	yes	Yes	Moderate	1907	2119	-212	90.0

4.5 Discussion:

Previous studies on tree detection using deep learning have reported high accuracy for mature trees. For instance, Mohan et al. (2017) achieved **97.55% accuracy** in individual tree detection in Jackson, Wyoming, USA, with an omission and commission error of 2.45%. Similarly, Torres- Sánchez et al. (2015) reported **95% accuracy** using Object-Based Image Analysis (OBIA) for olive, palm, and eucalyptus trees, where wider spacing (5–10m) and large crowns facilitated detection.

However, seedling detection in Bangladesh was more complex due to **small tree height, canopy overlap, high understory density, presence of uri-grass, green algae, and tidal fluctuations**. The model's limitations were evident in areas with:

1. **High uri-grass or green algae coverage**, leading to misclassification due to similar RGB reflectance.
2. **Tidal fluctuations**, particularly during high tide, which affected image clarity and point cloud construction process.
3. **Dense understory vegetation**, which made it difficult to differentiate seedlings from other vegetation.

   Uri-grass, Green algae had significant impact on detection due to its seasonal presence, which alters reflectance patterns in RGB images. Future research should focus on optimizing detection models by integrating **multispectral or hyperspectral imaging** to improve differentiation between seedlings and surrounding vegetation.

CHAPTER V

Conclusion and Recommendation

This study demonstrates the potential of UAV-based machine learning techniques for automated seedling detection and plantation monitoring, offering a transformative approach to afforestation initiatives. By leveraging deep learning models such as R-CNN, YOLOv3, YOLOv4, SSD, and RetinaNet, the research systematically evaluated the accuracy, efficiency, and applicability of AI- driven monitoring systems. The optimized R-CNN-based model, with a precision of 99.1%, emerged as the most effective, accurately detecting and geolocating seedlings while minimizing false positives and false negatives. The findings underscore the superiority of drone-based monitoring over traditional manual surveys, providing a more efficient, scalable, and cost-effective solution. High-resolution orthomosaics (2–5 cm) enabled the generation of precise seedling density maps, facilitating targeted vacancy filling and improved resource allocation. However, model performance was influenced by environmental factors such as tidal conditions, understory vegetation, uri-grass density, and canopy overlap, which posed challenges, particularly in terrestrial plantation settings. Seasonal variations also played a critical role, with optimal data collection requiring low tide conditions to avoid waterlogging, which obscures seedling height and causes scatter reflectance, degrading orthomosaic quality. Additionally, the presence of green algae and uri-grass during certain seasons necessitated careful timing of drone flights to ensure accurate detection.

Despite these advancements, limitations remain. The misclassification of seedlings due to similar spectral signatures with surrounding vegetation highlights the need for further refinement of AI models. The use of RGB cameras in the study resulted in difficulties distinguishing seedlings from green understory vegetation, a challenge that could be addressed by integrating multispectral imaging or LiDAR-equipped UAVs to provide additional spectral and structural data. Furthermore, optimizing flight parameters—such as altitude, shutter speed, nadir angles, and flying speed—proved crucial for achieving high model accuracy. For instance, a slower flying speed and proper camera focus were essential to avoid blurry images, which compromise orthomosaic quality and seedling detection. A ground sampling distance (GSD) of 5 cm was found to be sufficient for automatic seedling detection, balancing resolution and flight efficiency. Future research should focus on developing adaptive AI models fine-tuned for diverse plantation environments, incorporating multispectral and LiDAR technologies to overcome classification challenges. Expanding the study to include long-term monitoring and growth prediction would further enhance plantation management strategies. By refining these techniques, UAV-based machine learning can significantly contribute to precision forestry, carbon sequestration initiatives, and sustainable afforestation programs, reinforcing its role as a transformative tool in global reforestation efforts. Decision-makers are encouraged to adopt these modern, scientific, and precise tools to replace traditional monitoring systems, particularly in coastal plantations, where they can directly contribute to climate change mitigation by enhancing carbon sequestration potential.

References:

Ahmed, D., *et al.,* (2023). 'Machine Vision-Based Crop-Load Estimation UsingYOLOv8', arXiv preprint arXiv:2304.13282, 2023.

Ball, J.E., Anderson, D.T., and Chan, C.S., (2017). Comprehensive survey of deep learning in remote sensing: Theories, tools, and challenges for the community. JARS 11, 042609. [CrossRef]

Bengio, Yoshua (2009). "Learning Deep Architectures for AI". Foundations and Trends in Machine Learning. 2 (1): 1–127. CiteSeerX 10.1.1.701.9550. doi:10.1561/2200000006.

S2CID 207178999. Archived from the original (PDF) on 4 March 2016. Retrieved 3 September 2022.

Bengio, *et al.,* (2013). "Representation Learning: A Review and New Perspectives". IEEE Transactions on Pattern Analysis and Machine Intelligence. 35 (8): 1798–1828.

Chen, S.W., Shivakumar, S.S., Dcunha, S., Das, J., Okon, E., Qu, C., Taylor, C.J., Kumar, V. (2017). Counting Apples and Oranges With Deep Learning: A Data-Driven Approach. IEEE Robot. Autom. Lett. 2, 781–788.

Csillik, O., Cherbini, J., Johnson, R., Lyons, A., and Kelly, M., (2018). Identification of Citrus Trees from Unmanned Aerial Vehicle Imagery Using Convolutional Neural Networks

Ciresan, *et al*., (2012). "Multi-column deep neural networks for image classification". 2012 IEEE Conference on Computer Vision and Pattern Recognition. pp. 3642–3649. arXiv:1202.2745. doi:10.1109/cvpr.2012.6248110. ISBN 978-1-4673-1228-8. S2CID 2161592.

Cong, P., Zhou, J., Li, K. S., and Feng,H., (2022). 'Citrus Tree Crown Segmentation of Orchard Spraying RobotBased on RGB-D Image and Improved Mask R-CNN', Applied Sciences, vol. 13, no. 1, p. 164.

Deng, L.; Yu, D. (2014). "Deep Learning: Methods and Applications" (PDF). Foundations and Trends in Signal Processing. **7** (3–4): 1–199.

Diaz-Varela, R. A., *et al.*,(2014). Automatic identification of agricultural terraces through object oriented asnalysis of very high resolution DSM and multispectral imegerty obtained from Unmanned Ariel Vehicle. J Environ Manage.2014;134:117–126.doi:10.1016/j. jenvman.2014.01.006PMID:244733454.

Estes, J.E., Sailer, C., and Tinney, L.R., (1986). Applications of artificial intelligence techniques to remote sensing, 38, 133–141. [CrossRef]

Fisher,R.B., *et al.,* (2014). Dictionary of computer vision and image processing, 2nd Ed.

Chichester.

Fromm, M., *et al.,* (2019). Automated Detection of Conifer Seedlings in Drone Imagery Using Convolutional Neural Networks.

Guirado, E., Tabik, S., Alcaraz-Segura, D., Cabello, J., Herrera, F., (2017). Deep-Learning Convolutional Neural Networks for scattered shrub detection with Google Earth Imagery.

Google., (2017). "Google's AlphaGo AI wins three-match series against the world's best Go player". TechCrunch. 25 May 2017. Archived from the original on 17 June 2018. Retrieved 17 June 2023.

Hernández-Clemente, R., *et al.*, (2014). A novel methodology to estimate single-tree biophysical parameters from 3D digital imagery compared to aerial laser scanner data. Remote Sens 6: 11627-11648. https://doi.org/10.3390/rs61111627.

Hentz, A. M. K., *et al.* (2018). Estimating forest uniformity in Eucalyptus spp. and Pinus taeda L. stands using field measurements and structure from motion point clouds generated from unmanned aerial vehicle (UAV) data collection. Forest Systems, Volume 27, Issue 2, e005.

Hentz, M., et al. (2018). UAV data with VHR to automatically detect and measure tree position in Paraná State, Brazil.

He, K.; Gkioxari, G.; Dollár, P.; Girshick, R. Mask r-cnn. In Proceedings of the IEEE International Conference on Computer Vision, Venice, Italy, 22–29 October 2017; pp. 2961–2969.

Hung,C., Bryson, M., and Sukkarieh, S. (2012). Multi-class predictive template for tree crown detection. ISPRS J Photogr Remote Sens 68: 170-183.

Hu, F., Xia, G.S., Hu, J., Zhang, L., (2015). Transferring Deep Convolutional Neural Networks for the Scene Classification of High-Resolution Remote Sensing Imagery. Remote Sens. 7, 14680–14707.

Hyyppa, J., *et al.*, (2016). Evaluating the performance of high-altitude aerial image-based digital surface models in detecting individual tree crowns in mature boreal forests. Forests 7 (7): 143. https://doi.org/10.3390/f7070143.

Hinton, G.E. (2009). "Deep belief networks". *Scholarpedia*. **4** (5): 5947.

Kamilaris, A., and Prenafeta-Boldú, F.X., (2018). Deep learning in agriculture: A survey. Comput.

Electron. Agric. 147, 70–90. [CrossRef]

Jensen, J. R. (2007). "Remote sensing of the environment: An earth resource perspective." Pearson Prentice Hall.

Kattenborna, T., (2014). Automatic single palm tree detection in plantations using UAV photogrammetric point clouds.

Kamiran, N., and Starker, M.L.R., (2014). Exploring the Potential of High Resolution Remote Sensing Data for Mapping Vegetation and the Age Groups of Oil Palm Plantation. OP Conference Series: Earth and Environmental Science, 18, 012181.

Korom, A., *et al.*, (2014). Extracting oil palm crown from WorldView-2 satellite image. IOP Conference Series: EarthandEnvironmentalScience18(1),012188.

Krizhevsky, *et. al.,* (2012),. "ImageNet Classification with Deep Convolutional Neural Networks" (PDF). NIPS 2012: Neural Information Processing Systems, Lake Tahoe, Nevada. Archived (PDF) from the original on 2017-01-10. Retrieved 21-05-23.

Kussul, N., Lavreniuk, M., Skakun, S., Shelestov, A., (2017). Deep Learning Classification of Land Cover and Crop Types Using Remote Sensing Data. IEEE Geosci. Remote Sens.

Lett.14, 778–782. [CrossRef]

Laliberte, A., and Rango, A., (2011). Image processing and classification procedures for analysis of sub-decimeter imagery acquired with a unmanned aircraft over a ride rangelands. GIScience Remote sens.2011;48:4-23.

LeCun, Yann; Bengio, Yoshua; Hinton, Geoffrey (2015). "Deep learning". Nature. 521 (7553): 436–444.

Liu, W.; Anguelov, D.; Erhan, D.; Szegedy, C.; Reed, S.; Fu, C. and Berg, A.C., (2016). Ssd: Single shot multi box detector. In Proceedings of the European Conference on Computer Vision, Amsterdam, The Netherlands, 11–14 October 2016; Springer: Cham, Sweitzerland, 2016; pp. 21–37

Li, Y.; Chen, Y.; Wang, and N.; Zhang, Z. (2019) Scale-aware trident networks for object detection. In Proceedings of the IEEE/CVF International Conference on Computer Vision, Seoul, Korea, 27–28 October 2019; pp. 6054–6063.

Li, W., *et al.*, (2016). A Deep Learning Based Oil Palm Tree Detection and Counting for High- Resolution Remote Sensing Images. Remote Sens. 9, 22. [CrossRef]

Liu, T., Abd-Elrahman, A., Morton, J., Wilhelm, V. L., (2018). Comparing fully convolutional networks, random forest, support vector machine, and patch-based deep convolutional neural networks for object-based wetland mapping using images from small unmanned aircraft system. GISci. Remote Sens. 55, 243–264. [CrossRef]

Luo, M., *et al.,* (2022). Individual Tree Detection in Coal Mine Afforestation Area Based on Improved Faster RCNN in UAV RGB Images.

Lucieer, A., *et al.*, (2012). Using a micro-uav for ultra-high resolution multi-sensor observations of Antarctic moss beds. International Archives of the Photogrammetry, Remote Sensing and Spatial Information Sciences, XXXIX-B1, pp. 429433.

Luo, M., Tian, Y., Zhang, S., Huang, L., Wang, H., and Liu, Z., (2022). Individual Tree Detection in Coal Mine Afforestation Area Based on Improved Faster RCNN in UAV RGB Images.

Mohan, M. *et al*., (2017). Individual Tree Detection from Unmanned Aerial Vehicle (UAV) Derived Canopy Height Model in an Open Canopy Mixed Conifer Forest.

Myneni, R.B., *et al.,* (1995) Optical remote sensing of vegetation: Modeling, caveats, and algorithms. Remote Sens. Environ.1995, 51, 169–188. [CrossRef]

Quan, L., (2010) Image based modeling. Springer, NY, 257 pp. https://doi.org/10.1007/978-1-4419-6679-7

Redmon, J.; Farhadi, A. (2018). Yolov3: An incremental improvement.

Ren, S., He, K., Girshick, R., Sun, J., (2015). Faster R-CNN: Towards Real-Time Object Detection with Region Proposal Networks. In Proceedings of the NIPS 2015, Montreal, QC, Canada, 7–12 December 2015.

Sa, I., Ge, Z., Dayoub, F., Upcroft, B., Perez, T., McCool, C., (2016). DeepFruits: A Fruit Detection System Using Deep Neural Networks. Sensors 16, 1222. [CrossRef]

Shafri, H. Z. *et al.,* (2012). Application of LiDAR and optical data for oil palm plantation management in Malaysia. SPIE Asia Pacific Remote Sensing, 85(2), 608. 852608-852608).

Shafri, H. Z., *et al.,* (2011). Semi-automatic detection and counting of oil palm trees from high spatial resolution airborne imagery. International Journal of Remote Sensing, 32(8), pp. 2095-2115.

Torres-Sánchez, J., *et al.*, (n.d). High-Throughput3-DMonitoringof Agricultural-Tree Plantations with Unmanned Aerial Vehicle (UAV) Technology.

Uijlings, J.R.R., van de Sande, K.E.A., Gevers, T.; Smeulders, A.W.M. (2013). Selective Search for Object Recognition. Int. J. Comput. Vis. **2013**, 104, 154–171.

Wallace L., *et al.*, (2012). Development of a UAV-LiDAR system with application to forest inventory. Remote Sens 4: 1519-1543.

Wallace L., *et al.*, (2016). Assessment of forest structure using two UAV techniques: A comparison of airborne laser scanning and structure from motion (SfM) point clouds. Forests 7: 1-16 D.

Wang and He,D., (2022). 'Fusion of Mask RCNN and attention mechanism for instance segmentation of applesunder complex background', Comput Electron Agric, vol. 196, p. 106864

Wang, Z., Underwood, J., Walsh, K.B., (2018). Machine vision assessment of mango orchard flowering. Comput. Electron. Agric. 151, 501–511. [CrossRef]

White, J.C., (2013.) The utility of image-based point clouds for forest inventory: A comparison with airborne laser scanning. Forests 4: 518-536.

Wu,W., Liu, H., Li, L., Long, Y., Wang, X., Wang, Z., Li, J., and Chang, Y., (2021) Application of local fully Convolutional Neural Network combined with YOLO v5 algorithm in small target detection of remote sensing image. PLoS ONE 2021, 16, e0259283.

Xinni Liu, Kamarul Hawari Ghazali, Fengrong Han & Izzeldin Ibrahim Mohamed (2021) Automatic Detection of Oil Palm Tree from UAV Images Based on the Deep Learning Method, Applied Artificial Intelligence, 35:1, 13-24, DOI:10.1080/08839514.2020.1831226

Yu, J. and Zhang, W., (2021). Face mask wearing detection algorithm based on improved YOLO-v4. Sensors 2021, 21, 3263.

Zhang, L., Zhang, L., and Du, B., (2016). Deep Learning for Remote Sensing Data: A Technical Tutorial on the State of the Art. IEEE Geosci. Remote Sens. Mag. 4, 22–40. [CrossRef]

Zhang, C., *et al.*,(2022) 'Multi-species individual tree segmentation and identification based on improved mask R-CNN and UAV imagery in mixed forests', Remote Sens (Basel), vol. 14, no. 4, p. 874

Zortea, M., *et al.,* (2022). Automatic Citrus Tree Detection from UAV Images based on Convolutional Neural Networks.

Zhang, L., Lin, Z., & Wang, L. (2007). "Automatic extraction of high-resolution airborne LiDAR data." International Journal of Remote Sensing, 28(2), 339–351.

Annexure

Research Proposal Evaluation Committee (RPEC)

Serial No.	Name and Designation	Rank
01	Mr. Gobinda Roy, Project Director, Sustainable Forests and Livelihoods (SUFAL) Project, Bana Bhaban, Agargaon, Dhaka-1207.	Convener
02	Conservator of Forests, Wildlife & Nature Conservation Circle, Dhaka.	Member
03	Director, Bangladesh Wildlife Center, Gazipur.	Member
04	Professor Dr. Golam Rakkibu, Forestry and Wood Technology Discipline, Khulna University, Khulna.	Member
05	Dr. Noor Jahan Sarkar, Professor (Retd.), Department of Zoology, University of Dhaka, Dhaka.	Member
06	Dr. Md. Mahabubar Rahman, Divisional Officer, Silviculture Genetics Department, Bangladesh Forest Research Institute, Chittagong.	Member
07	Deputy Project Director-1, Sustainable Forests and Livelihoods (SUFAL) Project, Bana Bhaban, Agargaon, Dhaka.	Member-Secretary

Grant Review Committee (GRC)

Serial No.	Name and Designation	GRC Rank
01	Mr. Md. Amir Hosain Chowdhury, Chief Conservator of Forests, Forest Department, Bangladesh	Chairperson
02	Dr. Rafiqul Haider, Director, Bangladesh Forest Research Institute (BFRI), Chattogram	Member
03	Prof. Dr. Mohammed Mostafa Feeroz, Pro-vice chancellor (education), Jahangirnagar University.	Member
04	Professor Dr. A.Z.M Manzoor Rashid, Department of Forestry and Environmental Science, Shahjalal University of Science and Technology (SUST), Sylhet.	Member
05	DCCF, Planning Wing, Forest Department. Bana Bhaban, Agargaon, Dhaka-1207	Member
06	DCCF, Education and Training Wing, Forest Department, Bana Bhaban, Agargaon, Dhaka-1207.	Member
07	DCCF, Forest Management Wing, Forest Department, Bana Bhaban, Agargaon, Dhaka-1207.	
08	Mr. Gobinda Roy, Project Director, Sustainable Forest and Livelihood (SUFAL) Project, Bana Bhaban, Agargaon, Dhaka-1207.	Member-Secretary

Forestry Related Research Review Council (FRRRC)

Serial No.	Name and Designation	Rank
01	Md. Rakibul Hasan Mukul, Deputy Chief Conservator of Forests, Social Forestry Wing, Bana Bhaban, Agargaon, Dhaka	Convener
02	Dr. Mohammed Kamal Hossain, Professor (Retd.), Institute of Forest and Environmental Sciences, Chattogram University, Chattogram.	Member
03	Dr. Mohammad Al-Amin, Professor, Institute of Forest and Environmental Sciences, Chattogram University, Chattogram.	Member
04	Dr. Kazi Saiful Islam, Professor, Department of Urban and Rural Planning, Khulna University.	Member

Serial No.	Name and Designation	Rank
05	Dr. Saleh Ahmed Khan, Professor, Department of Botany, Jahangir Nagar University, Savar, Dhaka	Member
06	Dr. A.Z.M Monzoor Rashid, Professor, Department of Forestry and Environmental Science, Shahjalal University of Science and Technology, Sylhet.	Member
07	Mr. Mohammad Yosuf, Deputy Project Director-1, Sustainable Forest and Livelihood (SUFAL) Project, Ban Bhawan, Agargaon, Dhaka.	Member-Secretary

Wildlife Related Research Review Council (WRRRC)

Serial No.	Name and Designation	Rank
01	Mr. Md. Jahidul Kabir, Deputy Chief Conservator of Forests, Education and Training Wing, Bana Bhaban, Agargaon, Dhakap	Convener
02	Dr. Noor Jahan Sarkar, Professor (Retd.), Department of Zoology, University of Dhaka.	Member
03	Dr. Monirul Hasan Khan, Professor and Head of Department, Department of Zoology, Jahangirnagar University.	Member
04	Dr. Md. Zakir Hossain Hawlader, Professor, Biotechnology and Molecular Biology, University of Dhaka.	Member
05	Dr. Md. Shamsul Alam, Professor, Department of Fisheries Biology and Genetics, Bangladesh Agricultural University, Mymensingh.	Member
06	Mr. Md. Sanaullah Patwary, Conservator of Forests, Wildlife and Nature Conservation Area, Bana Bhaban, Agargaon, Dhaka.	Member
07	Mr. Md. Abdullah Abraham Hossain, Deputy Project Director-3, Sustainable Forests and Livelihoods (SUFAL) Project, Bana Bhaban, Agargaon, Dhaka	Member-Secretary

Deliverable Review and Comments Giving Committee

Serial No.	Name and Designation	Rank
01	Mr. Mohammad Yousuf, Deputy Project Director-1, Sustainable Forests and Livelihoods (SUFAL) Project, Bana Bhaban, Agargaon, Dhaka.	Chairperson
02	Mr. Ishtiaq Uddin Ahmad, Project Management Specialist, Sustainable Forests and Livelihoods (SUFAL) Project, Bana Bhaban, Agargaon, Dhaka.	Member
03	Mr. Md. Safiul Alam Chowdhury, Senior Monitoring & Evaluation Specialist, Sustainable Forests and Livelihoods (SUFAL) Project, Bana Bhaban, Agargaon, Dhaka.	Member
04	Mr. Md. Abdul Mabud, Senior Collaborative Forest Management Specialist, Sustainable Forests and Livelihoods (SUFAL) Project, Bana Bhaban, Agargaon, Dhaka.	Member
05	Dr. Md. Jahangir Hossain, Senior Livelihoods Specialist, Sustainable Forests and Livelihoods (SUFAL) Project, Bana Bhaban, Agargaon, Dhaka.	Member
06	Mr. Md. Mahbubur Rahman, Deputy Project Director-2, Sustainable Forests and Livelihoods (SUFAL) Project, Bana Bhaban, Agargaon, Dhaka.	Member
07	Mr. Md. Mehedi Hasan Khan, Assistant Project Director-3, Sustainable Forests and Livelihoods (SUFAL) Project, Bana Bhaban, Agargaon, Dhaka.	Member-Secretary

গণপ্রজাতন্ত্রী বাংলাদেশ সরকার

বন অধিদপ্তর